NEUTRINO MIXING, OSCILLATIONS AND DECOHERENCE IN ASTROPHYSICS AND COSMOLOGY

by

Chiu Man Ho

B.S. in Physics, The Chinese University of Hong Kong, 2000

M.Phil. in Physics, The Chinese University of Hong Kong, 2002

Submitted to the Graduate Faculty of
the Department of Physics and Astronomy in partial fulfillment
of the requirements for the degree of

Doctor of Philosophy

University of Pittsburgh

2007

UNIVERSITY OF PITTSBURGH

PHYSICS AND ASTRONOMY DEPARTMENT

This dissertation was presented

by

Chiu Man Ho

It was defended on

June 8th, 2007

and approved by

Daniel Boyanovsky, Professor, Department of Physics and Astronomy

Richard Holman, Professor, Department of Physics

Arthur Kosowsky, Associate Professor, Department of Physics and Astronomy

Adam Leibovich, Assistant Professor, Department of Physics and Astronomy

Donna Naples, Associate Professor, Department of Physics and Astronomy

Vittorio Paolone, Associate Professor, Department of Physics and Astronomy

Dissertation Director: Daniel Boyanovsky, Professor, Department of Physics and Astronomy

NEUTRINO MIXING, OSCILLATIONS AND DECOHERENCE IN ASTROPHYSICS AND COSMOLOGY

Chiu Man Ho, PhD

University of Pittsburgh, 2007

This thesis focuses on a finite-temperature field-theoretical treatment of neutrino oscillations in hot and dense media. By implementing the methods of real-time non-equilibrium field theory, we study the dynamics of neutrino mixing, oscillations, decoherence and relaxation in astrophysical and cosmological environments. We first study neutrino oscillations in the early universe in the temperature regime prior to the epoch of Big Bang Nucleosynthesis (BBN). The dispersion relations and mixing angles in the medium are found to be helicity-dependent, and a resonance like the Mikheyev-Smirnov-Wolfenstein (MSW) effect is realized. The oscillation time scales are found to be longer near a resonance and shorter for off-resonance high-energy neutrinos. We then investigate the space-time propagation of neutrino wave-packets just before BBN. A phenomenon of "*frozen coherence*" is found to occur if the longitudinal dispersion catches up with the progressive separation between the mass eigenstates, before the coherence time limit has been reached. However, the transverse dispersion occurs at a much shorter scale than all other possible time scales in the medium, resulting in a large suppression in the transition probabilities from electron-neutrino to muon-neutrino. We also explore the possibility of charged lepton mixing as a consequence of neutrino mixing in the early Universe. We find that charged leptons, like electrons and muons, can mix and oscillate resonantly if there is a large lepton asymmetry in the neutrino sector. We study sterile neutrino production in the early Universe via active-sterile oscillations. We provide a quantum field theoretical reassessment of the quantum Zeno suppression on the active-to-sterile transition probability and its time average. We determine the *complete* conditions for quantum Zeno suppression. Finally, we examine the interplay between neutrino mixing, oscillations and equilibration in a thermal medium, and the corresponding non-equilibrium dynamics.

TABLE OF CONTENTS

LIST OF FIGURES

PREFACE

It is my honor to be a graduate student of Prof. Daniel Boyanovsky. I learn a great deal of physics, either directly related to my research topic or not, through his lectures and discussions with him. I thank him for his great patience as well as his willingness to teach and discuss. Also, I thank him for encouraging me to broaden my knowledge in different areas of physics. I am grateful for the inspirations, enlightenments and unlimited support from him!

I thank Arthur Kosowsky for teaching me a great deal of astrophysics and cosmology in his classes and group meetings. I also thank him for giving me many invaluable advice and support whenever I need help.

I thank Richard Holman, Adam Leibovich and Ira Rothstein for teaching me a great deal of quantum field theory, particle physics and/or string theory. Their lectures have been very inspiring to me.

I thank Vincent Liu for teaching me a great deal of condensed matter physics.

I thank Hector de Vega, my collaborator, for his hospitality and generosity during my visit in Paris.

I also thank Donna Naples and Vittorio Paolone for raising many interesting questions during my committee meetings.

Furthermore, I would like to thank my parents, my sister and brothers for their love, help and care, far away from United States.

Lastly, and also most importantly, I have to thank my wife Qing Yang for her love, concern, understanding and support. Meeting her in Pittsburgh would be the most romantic and touching story in my memory, and marrying her is the best decision I have ever made in my life!

This work was supported in part by the Andrew Mellon Predoctoral Fellowship, Zaccheus Daniel Predoctoral Fellowship and the National Science Foundation.

1.0 INTRODUCTION

In this beginning chapter, we first give an overview on the current treatment of active and sterile neutrinos in hot and dense media. Then we explain the motivations of this work and provide a brief outline and summary to the thesis.

Readers who prefer getting the main ideas of this thesis are suggested to read the abstract and this introduction chapter first. To learn the main results in each chapter without absorbing into the technical details, they are encouraged to read the summary chapter at the end of this thesis. Interested readers can continue to read the main text of Chapters 2-10 for fun.

1.1 OVERVIEW: NEUTRINOS IN PARTICLE PHYSICS, ASTROPHYSICS AND COSMOLOGY

The Standard Model of particle physics is a well-tested theory that unifies the weak and electromagnetic interactions of elementary particles. In this model, neutrinos are introduced as massless particles. However, by the time of the 2002 Nobel Prize in Physics on "the pioneering detection of cosmic neutrinos", a wealth of experimental data have confirmed that neutrinos are massive and that different flavors of neutrinos can mix and oscillate [1, 2, 3, 4, 5]. Thus, after almost four decades of the prescient suggestion that neutrinos may oscillate [6, 7], neutrino oscillation has now become the first indisputable hint of *new physics* beyond the Standard Model. Increasing effort is devoted to probe into this new physics. While accelerator and reactor experiments measure the mass-squared difference of neutrinos, the current cosmological observations suggest that the sum of the masses of all neutrino species has to be smaller than roughly 1 eV [8].

Neutrinos are the bridge between particle physics, nuclear physics, astrophysics and cosmology [9, 10, 11, 12, 13, 14]. The astrophysical and cosmological systems serve as excellent "laboratories"

to explore the properties of neutrinos under conditions not accessible in terrestrial high energy experiments. Meanwhile, comprehension of neutrino physics, a crucial part of particle physics, is indispensable for understanding the universe.

In addition to the three active neutrinos in the Standard Model, an extra *light* neutrino has been proposed in order to explain the LSND anomaly [15, 16], if it is interpreted along with the solar and atmospheric neutrino data as arising from vacuum neutrino oscillations. However, the limit on the number of active light neutrinos from the Z^0 decay width suggests that a fourth neutrino must be sterile, namely without weak interactions.

Sterile neutrinos are ubiquitous in extensions beyond Standard Model [9, 10, 11, 12]. They are emerging as plausible cold or warm dark matter candidates [17, 18, 19, 20, 21, 22, 23, 24, 25, 26, 27, 28, 29, 30]. They may also be the potentially important ingredients in stellar collapse [31, 32] and primordial nucleosynthesis [33, 34], and may provide an explanation to pulsar "kicks" via asymmetric neutrino emission [35, 36, 37].

Being weak interaction singlets, sterile neutrinos can only be produced via active-sterile mixing and oscillations. Hence any assessment on the possibility of sterile neutrinos as dark matter candidates or their role in supernovae must begin with understanding their production mechanism.

Recently, the MiniBooNE collaboration [38] has reported results in contradiction with those from LSND [15, 16] which suggested a fourth sterile neutrino in $\Delta m^2 \sim 1$ eV^2 range. Although the MiniBooNE results hint at an excess of events below 475 MeV, the analysis distinctly rules out a fourth *light* sterile neutrino with mass scale $\Delta m^2 \sim 1$ eV^2. However, a recent analysis [39] suggests that while $(3+1)$ schemes are strongly disfavoured, $(3+2)$ neutrino schemes provide a good fit to both the LSND and MiniBooNE data, including the low energy events. This is due to the possibility of CP violation in $(3+2)$ schemes, although significant tension remains.

Furthermore, sterile neutrinos as dark matter candidates would require masses in the keV range[17, 18, 19, 20, 21, 22, 23, 25, 27, 28]. This means that the MiniBooNE result does not actually rule out the possibility of a heavier variety of sterile neutrinos as dark matter candidates. The radiative decay of keV neutrinos would contribute to the X-ray background [21, 40]. Analysis from the X-ray background in clusters can provide constraints on the masses and mixing angles of sterile neutrinos [25, 41, 42, 43], and recently it has been suggested that precision laboratory experiments on β decay in tritium may be sensitive to keV neutrinos [44].

Neutrino mixing and oscillations in extreme conditions of high temperature and density play a fundamental role in astrophysics and cosmology [14, 27, 45, 46, 47, 48, 49]. It is now widely

accepted that the resonant flavor mixing due to the Mikheyev-Smirnov-Wolfenstein (MSW) effect in the sun can provide a concrete explanation to the solar neutrino problem [50, 51]. During Big Bang Nucleosynthesis (BBN), neutrino oscillations may cause distortions in the electron-neutrino abundance, which may affect the neutron-to-proton ratio and hence the mass fraction of ^{4}He due to BBN [14]. An important aspect of neutrino oscillations is lepton number violation, leading to the suggestion that the observed baryon asymmetry may actually originate from the lepton sector. This possibility is known as leptogenesis [52, 53, 54]. The dynamical aspects of neutrino oscillations in hot and dense media are crucial to the explosion mechanism of core-collapse supernovae [13, 55, 56], and the formation, evolution and cooling of neutron stars [46, 47, 48].

The *non-equilibrium dynamics* of neutrino mixing, oscillations and equilibration is of substantial relevance within all the settings mentioned above. Neutrino mixing and oscillations introduce a novel aspect to the description of flavor equilibration. This is because neutrinos are produced as "flavor eigenstates" in weak interaction vertices, but propagate as a linear superposition of mass eigenstates. The neutrino mixing matrix is off-diagonal in the neutrino flavor basis while collisional processes due to weak interactions are flavor diagonal. This leads to a competition between production, propagation and relaxation, resulting in a rich and complex dynamics. Therefore, in a hot and dense medium where neutrino interactions cannot be neglected, collisional processes must be studied on the same footing as the dynamics of oscillations.

Neutrino propagation in a cold medium has been first studied in [50] wherein the refractive index of electron neutrinos was obtained. The early studies of neutrino propagation focused on the neutrino dispersion relations and damping rates in the temperature regime relevant for stellar evolution or BBN [14, 57]. The matter effects of neutrino oscillations in the early universe have been investigated in [14, 57, 58, 59]. A consistent calculation of the neutrino dispersion relations in a hot and dense medium, implementing the techniques of quantum field theory at finite temperature, was provided in [57].

Pioneering work on the dynamics of neutrino mixing and oscillations in a medium was cast in terms of the 2×2 Bloch-type equations akin to a spin in a magnetic field [9, 10, 11, 50, 58, 60]. This is a single-particle quantum-mechanical description, wherein the dynamical evolution is described in terms of an effective Hamiltonian for a two-level system. Another early approach relies on a Wigner-Weisskopf effective Hamiltonian for the quantum-mechanical states in the medium [61]. For the single-particle states, the equation of motion for neutrino oscillations has been derived from the underlying field theory in the relativistic limit [13, 62], which was then extended to a kinetic

description of mixing and oscillations in a medium [12, 58, 63, 64, 65, 66].

In all of the approaches mentioned above, the medium effects are always input into the single-particle equation of motion or Schrodinger-like single-particle wavefunctions, after computing the self-energy contributions from charged and neutral currents in a medium with charged leptons, neutrinos and hadrons or quarks. These have been implemented to study the evolution of the neutrino distribution functions in supernovae [32, 67, 68] and the early universe [14, 59, 69, 70, 71, 72], as well as to study the relic neutrino asymmetry [73].

1.2 MOTIVATIONS

The above discussion highlights that the non-equilibrium dynamics of neutrino mixing and oscillations in a hot and dense medium is mostly studied within the framework of a single-particle description. However, a single-particle formulation is inadequate in a hot and dense medium where collective many-body effects may be predominant. In a recent study, the validity of the single-particle picture that underlies the kinetic equations for neutrinos in a medium has been critically re-examined [74].

While the kinetic approach in principle yields the time evolution of the distribution functions [58, 65, 66], it usually invokes a variety of approximations. This includes neglecting interference between particles and antiparticles by restricting the Hamiltonian [65] or introducing some time averaging, and restriction to single-particle state evolution [66]. For a thorough discussion of the kinetic approach to mixing and oscillations, as well as the approximations involved, the reader is referred to [14, 63, 75].

Furthermore, numerical studies of sterile neutrinos as possible dark matter candidates [17, 20, 76, 77, 78] usually rely on a semi-phenomenological approach which inputs an effective production rate in terms of a time averaged transition probability [76, 77].

The main point in the above discussion is to highlight that there is a lack of consistency in the current approach to study neutrino mixing and oscillations in a medium — the results of a quantum field-theoretical calculation of the index of refraction or relaxation rates in the medium are input into a single-particle quantum-mechanical description of mixing and oscillations based on Bloch-type equations. This is at best

a semi-phenomenological approach.

There are many fundamental reasons to study neutrino mixing and oscillations in hot and dense media at a deeper level: (i) Neutrino mixing is the first indisputable experimental evidence of physics beyond the Standard Model; (ii) The MSW resonance in the sun can provide a concrete explanation to the solar neutrino problem [50, 51]; (iii) BBN is particularly sensitive to the spectrum and oscillations of electron-neutrinos [14]; (iv) Leptogenesis in the early universe may be the relevant mechanism for the observed baryon asymmetry [52, 53, 54]; (v) Just like the cosmic microwave background (CMB), there is a cosmic neutrino background left over from the Big Bang; (vi) Dynamical aspects of neutrino oscillations are crucial to the explosion mechanism of core-collapse supernovae [13, 55, 56], and the formation, evolution and cooling of neutron stars [46, 47, 48]; (vii) Sterile neutrinos produced in the early universe via active-sterile mixing may be plausible cold or warm dark matter candidates [17, 18, 19, 20, 21, 22, 23, 24, 25, 26, 27, 28, 29, 30].

Unlike cosmic rays and photons, neutrinos will not be absorbed or obscured when they traverse through the intergalactic medium. Due to their weak interactions with other particles, they serve as an excellent probe to dense astrophysical sources such as supernovae, neutron stars, black holes, gamma ray bursts (GRB) and active galactic nuclei (AGN). On the other hand, neutrinos from the forthcoming supernova explosion will provide remarkable tests to particle physics. Ultra-High Energy (UHE) neutrinos from black holes, GRB and AGN may even probe the existence of extra dimensions [79] and the possibility of Lorentz and CPT violations [80, 81]. These high energy neutrinos may be observable with IceCube [82].

In our view, the proper understanding of collective phenomena in hot and dense media requires a systematic and consistent treatment by implementing the methods of quantum field theory at finite temperature and density. Furthermore, the dynamical evolution of neutrino mixing and oscillations requires a non-equilibrium formulation of quantum field theory specially suited to study the real-time evolution as an initial value problem [83, 84, 85, 86, 87].

Motivated by the fundamental role of neutrinos in particle physics, astrophysics and cosmology, this thesis is devoted to providing a full finite-temperature field-theoretical treatment of neutrino oscillations in hot and dense media. We study the dynamics of

neutrino mixing, oscillations, decoherence and relaxation in astrophysical and cosmological environments, by implementing the methods of real-time non-equilibrium field theory.

This thesis establishes a systematic and consistent framework for studying the non-equilibrium dynamics of neutrinos in hot and dense media. The main ingredients in this program are the quantum density matrix and the effective Dirac equation that includes all the self-energy corrections from the medium. We obtain the retarded neutrino propagator from which we extract the quasiparticle poles. The decoherence as well as relaxation of the neutrino quasiparticles due to collisions are manifestly described by the imaginary parts of the quasiparticle poles instead of putting in by hand semi-phenomenologically.

Furthermore, we explore some new and novel implications of neutrino mixing and oscillations in astrophysics and cosmology, within our theoretically sound framework.

1.3 BRIEF SUMMARY OF MAIN RESULTS

The main results of this thesis are as follows:

- In Chapter 2, we first study the time evolution of the distribution functions for hot and dense gases of two flavor Dirac neutrinos as a consequence of flavor mixing and dephasing, in the absence of weak interactions. This is achieved by obtaining the time evolution of the flavor density matrix directly from quantum field theory at finite temperature and density.

  We find that the dynamics of neutrino oscillations features a hierarchy of time scales. The shorter time scales are associated with the interference between particle and *antiparticle* states, while the longer time scales emerge from the interference between particle states (or antiparticle states) of different masses. In the degenerate case, an initial flavor asymmetry will relax towards an the asymptotic limit via dephasing resulting from the oscillations between flavor modes that are not Pauli blocked, with a power law proportional to the inverse of time.
- In Chapter 3, we study neutrino oscillations in the early universe by implementing finite-temperature field theory. Particularly, we are interested in the temperature regimes that are relevant for Big Bang Nucleosynthesis (BBN). We focus on two flavors of Dirac neutrinos; however, the formulation is general.

We show that the medium dispersion relations and mixing angles are both energy and helicity dependent, and a resonance like the Mikheyev-Smirnov-Wolfenstein (MSW) resonance is realized. The oscillation time scale in the medium is longer as compared to that in the vacuum near a resonance, but much shorter for off resonance high energy neutrinos for which the medium mixing angle becomes vanishingly small.

- In Chapter 4, we investigate the space-time evolution of "flavor" neutrino wave-packets at finite temperature and density prior to BBN. We implement non-equilibrium field theory methods and linear response to study the space-time evolution directly from the effective Dirac equation in the medium.

  We find that there exists a coherence time limit beyond which the two mass eigenstates cease to overlap and so neutrino oscillation is exponentially suppressed. But a novel phenomenon of "frozen coherence" can occur if the longitudinal dispersion catches up with the progressive separation between the two mass eigenstates in the medium, before the coherence time limit has been reached. However, the transverse dispersion occurs at a much shorter scale than all other possible time scales in the medium, resulting in a large suppression in the transition probabilities from electron-neutrino to muon-neutrino, on a time scale much shorter than the Hubble time.

- In Chapter 5, we explore the possibility of large charged lepton mixing as a consequence of neutrino mixing in the early universe. We state the general criteria for charged lepton mixing, critically re-examine aspects of neutrino equilibration.

  We show that it is the off-diagonal elements in the charged-current self-energy that are responsible for the charged lepton mixing. For a large lepton asymmetry in the neutrino sector, there could be a resonant charged lepton mixing in the temperature range $T \sim 5\,\mathrm{GeV}$. In this regime, the electromagnetic damping rate is of the same order as the charged lepton oscillation frequency, suggesting a substantial transition probability during equilibration.

- In Chapter 6, we study sterile neutrino production in the early universe via active-sterile oscillations. We provide a quantum field theoretical reassessment of the quantum Zeno suppression on the active-to-sterile transition probability and its time average.

  We derive the the active-to-sterile transition probability:

$$P_{a\to s}(t) = \frac{\sin^2 2\theta_m}{4}\left[e^{-\Gamma_1 t} + e^{-\Gamma_2 t} - 2\,e^{-\frac{1}{2}(\Gamma_1+\Gamma_2)t}\,\cos\left(\Delta E t\right)\right],$$

where ΔE is the oscillation frequency, $\Gamma_1 = \Gamma_{aa}\cos^2\theta_m$ and $\Gamma_2 = \Gamma_{aa}\sin^2\theta_m$ are the two relaxation rates associated with the propagating modes in the medium, with $\Gamma_{aa} \propto G_F^2 kT^4$ being the active neutrino scattering rate and θ_m the mixing angle in the medium. We point out that the *complete* conditions for quantum Zeno suppression on $P_{a\to s}(t)$ are: (i) $\Gamma_{aa} \ll \Delta E$, and (ii) $\Gamma_1 \approx \Gamma_2$. While the oscillatory term in $P_{a\to s}(t)$ is suppressed on the decoherence time scale $\tau_{\rm dec} = 2/\Gamma_{aa}$, at very high or low temperatures, this is not the relevant time scale for the suppression of the transition probability, but either $1/\Gamma_1$ or $1/\Gamma_2$ whichever is longer.

- In Chapter 7, we learn a quantum kinetic description based on the non-equilibrium effective action and implement it for studying the abundance of a particle species in a thermalized plasma. A specific model of a bosonic field in interaction with two thermalized heavier bosonic fields is studied.

  As a consequence of off-shell corrections to the particle abundance, we find substantial departures from the usual Bose-Einstein prediction in both high temperature limit, and the low temperature but large momentum limit. In the latter case, the particle abundance is exponentially suppressed but larger than the Bose-Einstein result.

- In Chapter 8, we examine the interplay between neutrino mixing, oscillations and equilibration in a thermal medium. The non-equilibrium dynamics is studied in a field theory of flavored neutral mesons that effectively models two flavors of mixed neutrinos, in interaction with other mesons that represent a thermal bath of hadrons or quarks and charged leptons.

  We find that the dispersion relations and mixing angles of the "neutrino" quasiparticles are of the same form as those of neutrinos in the medium, and the relaxation rates are obtained as well. At the time much longer than the two time scales for relaxation, the two-point function of the "neutrino" fields becomes time-translational invariant, reflecting the approach to equilibrium. The equilibrium density matrix is found to be nearly diagonal in the basis of eigenstates of an effective Hamiltonian that includes self-energy corrections in the medium, with perturbatively small off-diagonal elements.

- In Chapter 9, we investigate the production of a sterile species from active-sterile neutrino mixing in a thermalized medium, within the effective model developed in Chapter 8. The quantum kinetic equations for the distribution functions and coherences are obtained from two independent methods, namely the non-equilibrium effective action and the quantum master equation.

We prove that the quantum kinetic equations derived via the non-equilibrium effective action and the quantum master equation are identical up to the leading order in perturbative quantities. We show that if the initial density matrix is off-diagonal in the basis of the propagating modes in the medium, the off-diagonal coherences are damped out on the decoherence time scale. The damping of these off-diagonal coherences leads to an equilibrium reduced density matrix diagonal in the basis of propagating modes in the medium. The "neutrino" distribution functions reach equilibrium on the relaxation time scales associated with the quasiparticle modes in the medium. We have also argued that the simple phenomenological rate equation used in numerical studies of sterile neutrino production in the early universe has severe shortcomings, due to the time average of an overly simplified transition probability in the medium.

- In Chapter 10, we study the CMB power spectra for different *families* of single-field new and chaotic inflation models in which the inflaton potential has general degree $(2n)$ of the scalar field. Under the effective field theory approach to inflation, we investigate the dependence of the scalar spectral index n_s, tensor-to-scalar ratio r on the degree of the inflaton potential, and confront them to the WMAP3 and large scale structure (LSS) data. This chapter has nothing to do with neutrinos, but serves as a way to learn more about cosmology.

  We show in general that fourth degree potentials ($n = 2$) provide the best fit to the data, and the window of consistency with the WMAP3 and LSS data narrows with growing n. While we take $N_e = 50$ as the number of e-foldings before the end of inflation, extrapolations to arbitrary values of N_e can be done with a simple scaling relation. For the new inflationary scenarios, small-field inflation yields $r < 0.16$ while large-field inflation yields $r > 0.16$. The family of chaotic models feature $r \geq 0.16$. We conclude that a measurement of $r < 0.16$ (for $N_e = 50$) distinctly rules out the chaotic scenarios and favors small-field new inflationary models.
- In Chapter 11, we give an extended summary of the main results in each chapter.

2.0 OSCILLATIONS AND EVOLUTION OF A HOT AND DENSE GAS OF FLAVOR NEUTRINOS: A FREE FIELD THEORY STUDY

2.1 INTRODUCTION

In the presence of flavor mixing, individual flavor number is not conserved and a density matrix that is diagonal in the flavor Fock basis will evolve in time and develop off diagonal elements.

Hence time evolution of a dense or hot neutrino gas has to be studied as a quantum mechanical initial value problem: an initial density matrix which is diagonal in the flavor basis is evolved in time with the full Hamiltonian with flavor mixing. In this chapter we focus on studying precisely the time evolution of a dense or hot flavor neutrino gas in the simplest case of *free field theory*. Our goal is to study the evolution of an initially prepared density matrix which is diagonal in the flavor basis and describes a quantum gas of flavor neutrinos at finite density or finite temperature. We undertake the study of the dynamics in *free field theory* as a prelude towards a complete understanding of oscillation phenomena in weak interactions. The first step of any systematic program must be the understanding at the simplest level. As will be detailed below, studying the dynamics of oscillations and mixing in a dense and/or hot medium even at the level of free field theory reveals a wealth of subtle and important phenomena which leads to a firmer understanding of the validity of the various approximations as well as highlighting the potential corrections.

The problem that we study can be stated succinctly as follows: Consider that at a given initial time we have a "box" that contains a hot or dense gas of flavor neutrinos with a given single particle distribution consistent with Fermi-Dirac statistics , how does this *ensemble* evolve in time? How do the populations of flavor neutrinos evolve in time? How do flavor neutrinos *propagate* in the medium?

While our ultimate goal is to study the evolution in the presence of the weak interactions, we begin our study in this simplest free field theory case and the case of two flavors with the following

goals in mind

- To study the evolution directly from the underlying quantum field theory *without* making any approximations. This study will clarify the nature of the various approximations invoked in the literature and exhibit the potential corrections.

- By keeping the full evolution, the different time scales will emerge thus paving the way to providing a firmer understanding of coherence effects as well as the time averaging implied by several approximations.

- A first principle derivation of kinetic equations and or Boltzmann equations require the propagators for the fields[88] in the medium. Thus the study of the evolution in free field theory is the starting point for a systematic treatment of oscillations and collisions in a medium with a neutrino background.

- As it will become clear below, the study of even the simple free field theory case reveals a wealth of phenomena as a consequence of flavor mixing, which to the best of our knowledge has not been recognized and explored fully before in the case of finite temperature and density. The full quantum field theory treatment unambiguously reveals all the complexities associated with flavor mixing and allows a systematic implementation of several approximations which clarify the regime of validity of the single particle description and provide an understanding of the corrections.

Our study is organized as follows: in section 2.2 the theory corresponding to two flavors of neutrinos as well as the density matrix that describes an initial state of flavor neutrinos is presented. In this section we address the quantization aspects and point out the source of subtle mixing phenomena between particles and *antiparticles*, confirming previous results in the literature[89]. In sections 2.3 and 2.4 we study the evolution of the flavor asymmetry as well as that of the individual distribution functions focusing on the emergence of a hierarchy of scales and extracting the asymptotic long time dynamics as well as the phenomenon of flavor pair production via oscillations. In section 2.5 we present the "effective" field theory that describes the long-time dynamics and discuss its regime of validity. In this section we obtain the Feynman propagators and discuss their non-equilibrium aspects. In section 2.6 we discuss the regime of validity of the several approximations as well as caveats in the formulation and present our conclusions.

2.2 NEUTRINO MIXING AND FLAVOR DENSITY MATRIX

We focus our attention on the evolution of *Dirac* neutrinos postponing the case of Majorana neutrinos for further discussion elsewhere. Furthermore, we restrict the discussion to the case of two flavors which provides the simplest scenario. Most of the results can be extrapolated to the case of three active flavors including the case of sterile neutrinos, but for the subtleties associated with CP violating phases which of course are of great interest but will not be addressed here. We will call the flavors the electron and muon neutrino, but the results apply more broadly to active-sterile oscillations.

Consider the Dirac neutrino fields with the Lagrangian density given by

$$\mathcal{L} = \bar{\nu}_e(x)(i\partial\!\!\!/)\nu_e(x) + \bar{\nu}_\mu(x)(i\partial\!\!\!/)\nu_\mu(x) + \begin{pmatrix} \bar{\nu}_e(x) & \bar{\nu}_\mu(x) \end{pmatrix} \begin{pmatrix} m_e & m_{e\mu} \\ m_{e\mu} & m_\mu \end{pmatrix} \begin{pmatrix} \nu_e(x) \\ \nu_\mu(x) \end{pmatrix}, \tag{2.1}$$

where $m_{e\mu}$ is the mixing and we have absorbed a potential phase into a field redefinition. The mass matrix can be diagonalized by introducing a rotation matrix such that

$$\begin{pmatrix} \nu_e(x) \\ \nu_\mu(x) \end{pmatrix} = \begin{pmatrix} C & S \\ -S & C \end{pmatrix} \begin{pmatrix} \psi_1(x) \\ \psi_2(x) \end{pmatrix}, \tag{2.2}$$

where for simplicity of notation we defined

$$C \equiv \cos\theta \; ; \; S \equiv \sin\theta \tag{2.3}$$

where θ is the mixing angle. The diagonalized mass matrix then reads

$$\begin{pmatrix} M_1 & 0 \\ 0 & M_2 \end{pmatrix} = \begin{pmatrix} C & -S \\ S & C \end{pmatrix} \begin{pmatrix} m_e & m_{e\mu} \\ m_{e\mu} & m_\mu \end{pmatrix} \begin{pmatrix} C & S \\ -S & C \end{pmatrix}. \tag{2.4}$$

In the mass eigenstate basis, the Lagrangian density becomes

$$\mathcal{L} = \bar{\psi}_1(x)(i\partial\!\!\!/ - M_1)\psi_1(x) + \bar{\psi}_2(x)(i\partial\!\!\!/ - M_2)\psi_2(x). \tag{2.5}$$

In what follows, we reserve the latin label $i = 1, 2$ for the fields associated with the mass eigenstates ψ and the greek label $\alpha = e,\, \mu$ for the fields associated with the flavor eigenstates ν.

Upon quantization in a volume V, the flavor field operators $\nu_\alpha(x)$ at time $t = 0$ are written as

$$\nu_\alpha(\vec{x}) = \frac{1}{\sqrt{V}} \sum_{\vec{k}} \nu_\alpha(\vec{k})\, e^{i\vec{k}\cdot\vec{x}},$$
$$\nu_\alpha(\vec{k}) = \sum_{\lambda} \left(\alpha^{(\alpha)}_{\vec{k},\lambda} U^{(\alpha)}_{\vec{k},\lambda} + \beta^{(\alpha)\dagger}_{-\vec{k},\lambda} V^{(\alpha)}_{-\vec{k},\lambda} \right) \tag{2.6}$$

where the index λ refers to the Dirac spin index and we have kept the same notation for the field and its spatial Fourier transform to avoid cluttering of notation. A flavor Fock representation is defined by choosing the spinors U and V respectively. In principle these spinors can be chosen to be the positive and negative energy solutions of a Dirac equation with an arbitrary mass, in what follows we will choose these to be $m_e; m_\mu$, namely the masses of the flavor eigenstates in the *absence of mixing*. While we consider this to be a physically motivated choice, it is by no means unique and different alternatives have been discussed in the literature[89, 90, 91].

Thus the spinors U and V are chosen to be solutions of the following Dirac equations

$$\gamma^0(\vec{\gamma}\cdot\vec{k} + m_\alpha)\, U^{(\alpha)}_{\vec{k},\lambda} = \omega_\alpha(k)\, U^{(\alpha)}_{\vec{k},\lambda}$$
$$\gamma^0(\vec{\gamma}\cdot\vec{k} + m_\alpha)\, V^{(\alpha)}_{-\vec{k},\lambda} = -\omega_\alpha(k)\, V^{(\alpha)}_{-\vec{k},\lambda} \tag{2.7}$$
$$\omega_\alpha(k) = \sqrt{k^2 + m_\alpha^2} \tag{2.8}$$

The Dirac spinors U and V, are normalized as follows (no sum over the index α)

$$U^{(\alpha)\dagger}_{\vec{k},\lambda} U^{(\alpha)}_{\vec{k},\lambda'} = V^{(\alpha)\dagger}_{\vec{k},\lambda} V^{(\alpha)}_{\vec{k},\lambda'} = \delta_{\lambda,\lambda'}\ ;\ U^{(\alpha)\dagger}_{\vec{k},\lambda} V^{(\alpha)}_{-\vec{k},\lambda'} = 0. \tag{2.9}$$

and the creation and annihilation operators $\alpha_{\vec{k},\lambda}; \beta_{\vec{k},\lambda}$ obey the usual canonical anticommutation relations.

On the other hand, upon quantization the field operators $\psi_i(x)$ associated with mass eigenstates at time $t = 0$ are given by

$$\psi_i(\vec{x}) = \frac{1}{\sqrt{V}} \sum_{k} \psi_i(\vec{k})\, e^{i\vec{k}\cdot\vec{x}}$$
$$\psi_i(\vec{k}) = \sum_{\lambda} \left(a^{(i)}_{\vec{k},\lambda} F^{(i)}_{\vec{k},\lambda} + b^{(i)\dagger}_{-\vec{k},\lambda} G^{(i)}_{-\vec{k},\lambda} \right). \tag{2.10}$$

where the spinors F, G are now solutions of the following Dirac equations

$$\gamma^0(\vec{\gamma}\cdot\vec{k}+M_i)\,F^{(i)}_{\vec{k},\lambda} = E_i(k)\,F^{(i)}_{\vec{k},\lambda}$$
$$\gamma^0(\vec{\gamma}\cdot\vec{k}+M_i)\,G^{(i)}_{-\vec{k},\lambda} = -E_i(k)\,G^{(i)}_{-\vec{k},\lambda} \tag{2.11}$$
$$E_i(k) = \sqrt{k^2+M_i^2} \tag{2.12}$$

with the normalization conditions (no sum over the label i)

$$F^{(i)\dagger}_{\vec{k},\lambda}F^{(i)}_{\vec{k},\lambda'} = G^{(i)\dagger}_{\vec{k},\lambda}G^{(i)}_{\vec{k},\lambda'} = \delta_{\lambda,\lambda'}\ ;\ F^{(i)\dagger}_{\vec{k},\lambda}G^{(i)}_{-\vec{k},\lambda'} = 0. \tag{2.13}$$

Similarly, the operators a and b satisfy usual canonical anticommutation relations.

2.2.1 Hamiltonian and Charges

The total free field Hamiltonian for mixed neutrinos in the diagonal (mass) basis is given by

$$H = \sum_{\vec{k},i}\left[\bar{\psi}_i(\vec{k})(\vec{\gamma}\cdot\vec{k}+M_i)\psi_i(\vec{k})\right] = \sum_{\vec{k},\lambda,i}\left(a^{(i)\dagger}_{\vec{k},\lambda}a^{(i)}_{\vec{k},\lambda} + b^{(i)\dagger}_{\vec{k},\lambda}b^{(i)}_{\vec{k},\lambda} - 1\right)E_i(k), \tag{2.14}$$

Therefore the time evolution of the operators a, b is given by

$$\begin{aligned} a^{(i)}_{\vec{k},\lambda}(t) &= a^{(i)}_{\vec{k},\lambda}e^{-iE_i(k)t} \\ b^{(i)}_{\vec{k},\lambda}(t) &= b^{(i)}_{\vec{k},\lambda}e^{-iE_i(k)t}. \end{aligned} \tag{2.15}$$

The free field Lagrangian density (2.1) is invariant under independent phase transformations of the fields $\psi_{1,2}$, hence the individual $U(1)$ charges

$$Q_i = \int d^3x\ \psi_i^\dagger(\vec{x},t)\psi_i(\vec{x},t) = \sum_{\vec{k},\lambda}\left[a^{(i)\dagger}_{\vec{k},\lambda}a^{(i)}_{\vec{k},\lambda} - b^{(i)\dagger}_{\vec{k},\lambda}b^{(i)}_{\vec{k},\lambda} + 1\right] \tag{2.16}$$

are time independent.

The discussion that follows will focus on describing a statistical density matrix which is *diagonal* in the flavor basis and describes a hot and or dense ensemble of flavor neutrinos. This discussion requires the *flavor* Hamiltonian which is obtained from the Lagrangian density (2.1) for vanishing mixing $m_{e\mu} = 0$, namely

$$H_f = H_e + H_\mu = \sum_{\vec{k},\alpha}\left[\bar{\nu}_\alpha(\vec{k})(\vec{\gamma}\cdot\vec{k}+m_\alpha)\nu_\alpha(\vec{k})\right] = \sum_{\vec{k},\lambda,\alpha}\left(\alpha^{(\alpha)\dagger}_{\vec{k},\lambda}\alpha^{(\alpha)}_{\vec{k},\lambda} + \beta^{(\alpha)\dagger}_{\vec{k},\lambda}\beta^{(\alpha)}_{\vec{k},\lambda} - 1\right)\omega_\alpha(k), \tag{2.17}$$

The flavor Hamiltonian above is invariant under independent phase transformations of the flavor fields ν_α, thus the individual flavor charges commute with H_f

$$q_\alpha = \int d^3x\, \nu_\alpha^\dagger(\vec{x})\nu_\alpha(\vec{x}) = \sum_{\vec{k}} \nu_\alpha^\dagger(\vec{k})\nu_\alpha(\vec{k}) = \sum_{\vec{k},\lambda}\left[\alpha^{(\alpha)\dagger}_{\vec{k},\lambda}\alpha^{(\alpha)}_{\vec{k},\lambda} - \beta^{(\alpha)\dagger}_{\vec{k},\lambda}\beta^{(\alpha)}_{\vec{k},\lambda} + 1\right] \tag{2.18}$$

Using the transformation law (2.2) between flavor and mass eigenstates it is straightforward to find that the total charges are the same, namely

$$\sum_{i,\vec{k}} \psi_i^\dagger(\vec{k},t)\psi_i(\vec{k},t) = \sum_{\alpha,\vec{k}} \nu_\alpha^\dagger(\vec{k},t)\nu_\alpha(\vec{k},t) \Rightarrow Q_1 + Q_2 = q_e + q_\mu \tag{2.19}$$

2.2.2 Density matrix and time evolution

As stated in the introduction, our focus and goal is to study the time evolution of the distribution function of flavor neutrinos, at the level of free field theory at this stage. The question that we posed in the introduction and address here is the following: consider that at some given time the gas of flavor neutrinos and antineutrinos are described by a quantum statistical ensemble with a Fermi-Dirac distribution function with a fixed chemical potential for each flavor, namely

$$n^{(\alpha)}(k) = \frac{1}{e^{\beta(\omega_\alpha(k)-\mu_\alpha)}+1}\;;\; \bar{n}^{(\alpha)}(k) = \frac{1}{e^{\beta(\omega_\alpha(k)+\mu_\alpha)}+1} \tag{2.20}$$

with $\beta = 1/T$ and μ_α the chemical potential for each flavor.

Such an ensemble is described by a quantum statistical density matrix which is *diagonal* in the Fock space of flavor eigenstates and is given by

$$\hat{\rho} = \hat{\rho}^{(e)} \otimes \hat{\rho}^{(\mu)} \tag{2.21}$$

with the flavor density matrices

$$\hat{\rho}^{(\alpha)} = e^{-\beta(H_\alpha - \mu_\alpha q_\alpha)} \tag{2.22}$$

Hence the initial distribution functions are given by

$$\begin{aligned}
\langle \alpha^{(\alpha)\dagger}_{\vec{k},\lambda}\alpha^{(\alpha)}_{\vec{k},\lambda}\rangle &= \mathrm{Tr}\hat{\rho}^{(\alpha)}\alpha^{(\alpha)\dagger}_{\vec{k},\lambda}\alpha^{(\alpha)}_{\vec{k},\lambda} = n^{(\alpha)}(k) \\
\langle \beta^{(\alpha)\dagger}_{\vec{k},\lambda}\beta^{(\alpha)}_{\vec{k},\lambda}\rangle &= \mathrm{Tr}\hat{\rho}^{(\alpha)}\beta^{(\alpha)\dagger}_{\vec{k},\lambda}\beta^{(\alpha)}_{\vec{k},\lambda} = \bar{n}^{(\alpha)}(k)
\end{aligned} \tag{2.23}$$

In the expressions above we have assumed that the distribution of flavor neutrinos are spin independent, of course a spin dependence of the distribution function can be incorporated in the description.

Although we have stated the problem in terms of a gas flavor neutrinos in thermal equilibrium with Fermi-Dirac distributions, this restriction can be relaxed to arbitrary non-equilibrium single particle distributions consistent with Fermi-Dirac statistics. Regardless of the initial distributions the ensuing time evolution with the full Hamiltonian with mixing will be *out of equilibrium*.

2.2.3 Cold degenerate case:

The case of a cold, degenerate gas of neutrinos is described by the zero temperature limit but fixed chemical potential of the density matrix (2.21) with (2.22). In this limit the individual flavor neutrino gases form Fermi seas "filled up" to the Fermi momentum $k_F^{(\alpha)}$. Consider the case of a positive chemical potential corresponding to a degenerate gas of neutrinos without antineutrinos at zero temperature, the degenerate ground state is given by

$$|FS>=|FS>^{(e)}\otimes|FS>^{(\mu)} \tag{2.24}$$

with

$$|FS>^{(\alpha)}=\prod_{\vec{k}}^{k_F^{(\alpha)}}\alpha^{(\alpha)\dagger}_{\vec{k},\uparrow}\alpha^{(\alpha)\dagger}_{\vec{k},\downarrow}|0>^{(\alpha)} \tag{2.25}$$

with the flavor vacuum state $|0>^{(\alpha)}$ annihilated by the destruction operators $\alpha^{(\alpha)}_{\vec{k},\lambda};\beta^{(\alpha)}_{\vec{k},\lambda}$. The initial density matrix in this case is that of a pure state

$$\hat{\rho}=|FS><FS| \tag{2.26}$$

the distribution function of flavor neutrinos is given by

$$n^{(\alpha)}(k)=\Theta(k_F^{(\alpha)}-k)\ ,\ \bar{n}^{(\alpha)}(k)=0 \tag{2.27}$$

and the chemical potential is $\mu_\alpha=\omega_\alpha(k_F)$. The Fermi momentum is as usual given by

$$k_F^{(\alpha)}=\left(3\pi^2\mathcal{N}^{(\alpha)}\right)^{1/3}\Rightarrow k_F^{(\alpha)}(eV)=6.19\left(\frac{\mathcal{N}^{(\alpha)}}{10^{15}\,\mathrm{cm}^{-3}}\right)^{1/3} \tag{2.28}$$

with $\mathcal{N}^{(\alpha)}$ the neutrino density for each flavor. Although the zero temperature limit is described by a pure state, this state is a truly *many body* state

An important *many body* aspect of the situation under consideration can be gleaned by studying how the creation and annihilation operators of mass eigenstates act on the state $|FS>$. Consider for example the action of the annihilation operator $a^{(1)}_{\vec{k},\lambda}$ on the state, to understand this question we must first obtain $a^{(1)}_{\vec{k},\lambda}$ in terms of the creation and annihilation operators of flavor eigenstates. ¿From equation (2.10) and the relation between fields given by (2.2) we find

$$a^{(1)}_{\vec{k},\lambda} = F^{(1),\dagger}_{\vec{k},\lambda}\left[C\nu_e(\vec{k}) - S\nu_\mu(\vec{k})\right] \tag{2.29}$$

and the expansion for the flavor fields given by (2.7) clearly indicates that if $k < k^{\mu}_F < k^{e}_F$, for example, then $a^{(1)}_{\vec{k},\lambda}|FS>$ is a superposition of states with an electron neutrino "hole", an electron *antineutrino*, a muon neutrino "hole" and a muon *antineutrino*. The antiparticle components of the wave function $a^{(1)}_{\vec{k},\lambda}|FS>$ is a result of the non-vanishing overlap between the positive energy spinors for mass eigenstates and the *negative* energy spinors for flavor eigenstates[89].

2.2.4 Time evolution

Within the framework of free field theory of mixed neutrinos, the time evolution is completely determined by the *total Hamiltonian* H given by eqn. (2.14).

In the Schroedinger picture the density matrix evolves in time with the full Hamiltonian as follows

$$\hat{\rho}(t) = e^{-iHt}\hat{\rho}(0)e^{iHt} \tag{2.30}$$

Since the full Hamiltonian H does not commute with H_e, H_μ because of the flavor mixing, the density matrix does not commute with the Hamiltonian and therefore evolves in time. This is the statement that the initial density matrix (2.21) describes an ensemble *out of equilibrium* when flavor neutrinos are mixed.

Our goal is to obtain the time evolution of the distribution functions for flavor neutrinos and antineutrinos, namely

$$n^{(\alpha)}(\vec{k},t) = \mathrm{Tr}\hat{\rho}^{(\alpha)}(t)\,\alpha^{(\alpha)\dagger}_{\vec{k},\lambda}\alpha^{(\alpha)}_{\vec{k},\lambda} = \mathrm{Tr}\hat{\rho}^{(\alpha)}(0)\,\alpha^{(\alpha)\dagger}_{\vec{k},\lambda}(t)\alpha^{(\alpha)}_{\vec{k},\lambda}(t) \tag{2.31}$$

and similarly for the antineutrino distribution function. The *initial* distribution functions $n^{(\alpha)}(\vec{k},0) = n^{(\alpha)}(\vec{k})$ (and similarly for antineutrinos) given by equations (2.23) or (2.20) for the case of an initial thermal distribution.

It is more convenient to describe the time evolution in the Heisenberg picture wherein the density matrix does not depend on time and the Heisenberg field operators carry the time dependence as made explicit in eqn. (2.36).

The free fields associated with the mass eigenstates ψ_i evolve in time with the usual time dependent phases multiplying the creation and annihilation operators, namely

$$\psi_i(\vec{k},t) = e^{iHt}\psi_i(\vec{k},0)e^{-iHt} = \sum_{\lambda}\left(a^{(i)}_{\vec{k},\lambda}\, e^{-iE_i(k)t}\, F^{(i)}_{\vec{k},\lambda} + b^{(i)\dagger}_{-\vec{k},\lambda}\, e^{iE_i(k)t}\, G^{(i)}_{-\vec{k},\lambda}\right) \tag{2.32}$$

The time evolution of the fields associated with flavor eigenstates, namely ν_α is not so simple:

$$\nu_\alpha(\vec{k},t) = e^{iHt}\nu_\alpha(\vec{k},0)e^{-iHt} = \sum_{\lambda}\left(\alpha^{(\alpha)}_{\vec{k},\lambda}(t)U^{(\alpha)}_{\vec{k},\lambda} + \beta^{(\alpha)\dagger}_{-\vec{k},\lambda}(t)V^{(\alpha)}_{-\vec{k},\lambda}\right) \tag{2.33}$$

where the time dependent operators $\alpha^{(\alpha)}_{\vec{k},\lambda}(t); \beta^{(\alpha)\dagger}_{-\vec{k},\lambda}(t)$ can be obtained by writing the flavor fields in terms of the mass eigenstate fields using eqn. (2.2) and projecting out the components using the orthogonality property given by eqn. (2.9), leading for example to

$$\begin{aligned}
\alpha^{(e)}_{\vec{k},\lambda}(t) &= U^{(e)\dagger}_{\vec{k},\lambda}\left[C\psi_1(\vec{k},t) + S\psi_2(\vec{k},t)\right] \\
\beta^{(e)\dagger}_{-\vec{k},\lambda}(t) &= V^{(e)\dagger}_{-\vec{k},\lambda}\left[C\psi_1(\vec{k},t) + S\psi_2(\vec{k},t)\right]
\end{aligned} \tag{2.34}$$

The expression (2.34) reveals several subtle aspects which are highlighted by considering in detail for example the time evolution of the operator that creates electron neutrinos (a similar analysis holds for the muon neutrinos and their respective antiparticles)

$$\begin{aligned}
\alpha^{(e)\dagger}_{\vec{k},\lambda}(t) &= \sum_{\lambda'}\left\{\left(C\, a^{(1)\dagger}_{\vec{k},\lambda'}\, e^{iE_1(k)t}\, F^{(1)\dagger}_{\vec{k},\lambda'}U^{(e)}_{\vec{k},\lambda} + S\, a^{(2)\dagger}_{\vec{k},\lambda'}\, e^{iE_2(k)t}\, F^{(2)\dagger}_{\vec{k},\lambda'}U^{(e)}_{\vec{k},\lambda}\right) + \right. \\
&\left.\left(C\, b^{(1)}_{-\vec{k},\lambda'}\, e^{-iE_1(k)t}\, G^{(1)\dagger}_{-\vec{k},\lambda'}U^{(e)}_{\vec{k},\lambda} + S\, b^{(2)}_{-\vec{k},\lambda'}\, e^{-iE_2(k)t}\, G^{(2)\dagger}_{-\vec{k},\lambda'}U^{(e)}_{\vec{k},\lambda}\right)\right\}
\end{aligned} \tag{2.35}$$

It is a simple and straightforward exercise using the completeness and orthogonality of the respective spinor wavefunctions, to show that the creation and annihilation operators of flavor states indeed fulfill the canonical anticommutation relations. A Fock representation of flavor states

is therefore consistent and moreover *needed* to describe a quantum statistical ensemble of flavor neutrinos.

The first line in the above expression shows that the annihilation operator for electron corresponds to the expected combination of creation operators for mass eigenstates multiplied by the cosine and sine of the mixing angle, but also multiplied by the overlap of the different spinor wavefunctions. Furthermore, the electron creation operator also involves the *annihilation* of antiparticles associated with the mass eigenstates, a feature recognized in ref.[89]. There are two important consequences of the *exact* relation (7.183):

- The amplitude for creating a mass eigenstate out of the vacuum of mass eigenstates by an electron neutrino creation operator is not only given by the cosine or sine (respectively) of the mixing angle, but also by the overlap of the spinor wave functions $F^{(i)\dagger}_{\vec{k},\lambda'} U^{(e)}_{\vec{k},\lambda}$.
- The electron neutrino creation operator *destroys* antiparticle mass eigenstates. While this aspect is not relevant when the electron neutrino creation operator acts on the *vacuum* of mass eigenstates, it becomes relevant in a medium where both particles and antiparticles states are populated.

These aspects, which were also highlighted in references[89, 90, 91] will be at the heart of the subtle many body aspects of neutrino mixing which contribute to the time evolution of the distribution functions studied below.

The time dependent distribution functions are obtained by taking the trace with the initial density matrix

$$n^{(\alpha)}(\vec{k},t) = \mathrm{Tr}\hat{\rho}^{(\alpha)}(0)\, \alpha^{(\alpha)\dagger}_{\vec{k},\lambda}(t)\, \alpha^{(\alpha)}_{\vec{k},\lambda}(t) \tag{2.36}$$

and similarly for the other distribution functions. One can use the expression (7.183) for the time evolution of the Heisenberg field operator (and the equivalent for the hermitian conjugate), however in order to compute the time evolved distribution function we would need to compute the expectation value of bilinears of the field operators ψ_i in the *flavor diagonal density matrix* $\hat{\rho}(0)$. To do this we would have to re-write the creation and annihilation operators $a^{(i)}_{\vec{k},\lambda}; b^{(i)}_{\vec{k},\lambda}$; etc. in the expression (7.183) back in terms of the creation and annihilation operators $\alpha^{(\alpha)}_{\vec{k},\lambda}; \beta^{(\alpha)}_{\vec{k},\lambda}$; etc.. This is obviously a rather cumbersome method. A more systematic manner to carry out this program is presented below.

Using the expressions (2.17,2.18) we find the following identities

$$\frac{1}{2}\langle\bar{\nu}_\alpha(\vec{k},t)\,\gamma^0\,\nu_\alpha(\vec{k},t)\rangle = n^{(\alpha)}(\vec{k},t) - \bar{n}^{(\alpha)}(\vec{k},t) + 1 \tag{2.37}$$

$$\frac{1}{2\omega_\alpha(k)}\langle\bar{\nu}_\alpha(\vec{k},t)\,(\vec{\gamma}\cdot\vec{k}+m_\alpha)\,\nu_\alpha(\vec{k},t)\rangle = n^{(\alpha)}(\vec{k},t) + \bar{n}^{(\alpha)}(\vec{k},t) - 1 \tag{2.38}$$

Thus the computation of the distribution functions or combinations of them requires to find general expressions of the form

$$< \bar{\nu}_e(\vec{k},t)\,\mathcal{O}\,\nu_e(\vec{k},t) >= \mathcal{O}_{fg} < [\bar{\nu}_e(\vec{k},t)]_f[\nu_e(\vec{k},t)]_g > . \tag{2.39}$$

where the Dirac indices f, g are summed over and the averages are in the flavor diagonal density matrix (2.21,2.22).

Since the time evolution of the fields ψ_i is that of usual free Dirac field in terms of positive and negative frequency components, we write

$$\psi_{(i)}(\vec{k},t) = \left(\Lambda_+^{(i)}(\vec{k})\,e^{-iE_it} + \Lambda_-^{(i)}(\vec{k})\,e^{iE_it}\right)\psi_{(i)}(\vec{k},0). \tag{2.40}$$

where we have introduced the positive and negative frequency projector operators $\Lambda_+(k)$ and $\Lambda_-(k)$ respectively which are given by

$$\Lambda_+^{(i)}(\vec{k}) = \sum_\lambda F^{(i)}_{\vec{k},\lambda}F^{(i)\dagger}_{\vec{k},\lambda} = \left(\frac{\not{k}_{(i)}+M_i}{2E_i}\right)\gamma^0, \tag{2.41}$$

$$\Lambda_-^{(i)}(\vec{k}) = \sum_\lambda G^{(i)}_{-\vec{k},\lambda}G^{(i)\dagger}_{-\vec{k},\lambda} = \gamma^0\left(\frac{\not{k}_{(i)}-M_i}{2E_i}\right) \tag{2.42}$$

$$\not{k}_{(i)} = \gamma^0E_i(k) - \vec{\gamma}\cdot\vec{k} \tag{2.43}$$

These projection operators have the following properties,

$$\Lambda_+^{(i)\dagger}(\vec{k}) = \Lambda_+^{(i)}(\vec{k}) \;\;;\;\; \Lambda_-^{(i)\dagger}(\vec{k}) = \Lambda_-^{(i)}(\vec{k}), \tag{2.44}$$

$$\Lambda_+^{(i)}(\vec{k})\,\Lambda_-^{(i)}(\vec{k}) = 0 \;\;;\;\; \Lambda_-^{(i)}(\vec{k})\,\Lambda_+^{(i)}(\vec{k}) = 0, \tag{2.45}$$

$$\Lambda_+^{(i)}(\vec{k}) + \Lambda_-^{(i)}(\vec{k}) = 1. \tag{2.46}$$

We can now write the time evolution of the flavor fields in a rather simple manner by using the relations between the fields given by (2.2) and the inverse relation which allows to write $\psi_i(\vec{k},0)$ in (2.40) back in terms of $\nu_\alpha(\vec{k},0)$. We find

$$\psi_1(\vec{k},t) = \gamma^0 F_1(\vec{k},t)[C\nu_e(\vec{k},0) - S\nu_\mu(\vec{k},0)] \quad (2.47)$$

$$\bar{\psi}_1(\vec{k},t) = [C\bar{\nu}_e(\vec{k},0) - S\bar{\nu}_\mu(\vec{k},0)]\tilde{F}_1(\vec{k},t)\gamma^0 \quad (2.48)$$

$$\psi_2(\vec{k},t) = \gamma^0 F_2(\vec{k},t)[C\nu_\mu(\vec{k},0) + S\nu_e(\vec{k},0)] \quad (2.49)$$

$$\bar{\psi}_2(\vec{k},t) = [C\bar{\nu}_\mu(\vec{k},0) + S\bar{\nu}_e(\vec{k},0)]\tilde{F}_2(\vec{k},t)\gamma^0 \quad (2.50)$$

where we have introduced the following time evolution kernels

$$F_j(\vec{k},t) = \gamma^0[\Lambda_+^{(j)}(\vec{k})e^{-iE_j(k)t} + \Lambda_-^{(j)}(\vec{k})e^{iE_j(k)t}], \quad (2.51)$$

$$\tilde{F}_j(\vec{k},t) = F_j(\vec{k},-t)\gamma^0 \;\; ; \;\; j = 1,2. \quad (2.52)$$

After straightforward algebra using the mixing transformation (2.2) and equations (2.47-2.50) we find the following result for the time evolution of the flavor fields

$$\nu_e(k,t) = T_{ee}(\vec{k},t)\nu_e(\vec{k},0) + T_{e\mu}(\vec{k},t)\nu_\mu(\vec{k},0), \quad (2.53)$$

$$\bar{\nu}_e(k,t) = \bar{\nu}_e(\vec{k},0)\tilde{T}_{ee}(\vec{k},t) + \bar{\nu}_\mu(\vec{k},0)\tilde{T}_{e\mu}(\vec{k},t), \quad (2.54)$$

$$\nu_\mu(\vec{k},t) = T_{\mu\mu}(\vec{k},t)\nu_\mu(\vec{k},0) + T_{\mu e}(\vec{k},t)\nu_e(\vec{k},0), \quad (2.55)$$

$$\bar{\nu}_\mu(\vec{k},t) = \bar{\nu}_\mu(\vec{k},0)\tilde{T}_{\mu\mu}(\vec{k},t) + \bar{\nu}_e(\vec{k},0)\tilde{T}_{\mu e}(\vec{k},t), \quad (2.56)$$

where the time evolution operators are given by

$$T_{ee}(\vec{k},t) = \gamma^0\left[C^2F_1(\vec{k},t) + S^2F_2(\vec{k},t)\right], \quad (2.57)$$

$$T_{\mu\mu}(\vec{k},t) = \gamma^0\left[C^2F_2(\vec{k},t) + S^2F_1(\vec{k},t)\right], \quad (2.58)$$

$$T_{e\mu}(\vec{k},t) = T_{\mu e} = CS\gamma^0\left[F_2(\vec{k},t) - F_1(\vec{k},t)\right] \quad (2.59)$$

$$\tilde{T}_{\alpha\beta}(\vec{k},t) = \gamma^0 T_{\alpha\beta}(\vec{k},-t)\gamma^0, \quad (2.60)$$

Furthermore since the initial density matrix is flavor diagonal, we find the following expectation values

$$< [\bar{\nu}_e(\vec{k},t)]_f[\nu_e(\vec{k},t)]_g > = < [\bar{\nu}_e(\vec{k},0)]_r[\nu_e(\vec{k},0)]_s > [\tilde{T}_{ee}(\vec{k},t)]_{rf}[T_{ee}(\vec{k},t)]_{gs}$$
$$+ < [\bar{\nu}_\mu(\vec{k},0)]_r[\nu_\mu(\vec{k},0)]_s > [\tilde{T}_{e\mu}(\vec{k},t)]_{rf}[T_{e\mu}(\vec{k},t)]_{gs}, \quad (2.61)$$

and similarly for the muon neutrino fields, where $< \cdots >$ stands for the trace with the initial density matrix.

A noteworthy feature of the above *exact* expressions is that the time evolution of the flavor neutrino fields *mix positive and negative frequency* components of the mass eigenstates. Namely a flavor neutrino state is a linear combination of particles and *antiparticles* of mass eigenstates. Thus a wave packet of flavor neutrinos will necessarily mix positive and negative frequencies of mass eigenstates. This mixing between particles and antiparticles is a consequence of the fact that a flavor eigenstate is a squeezed state of mass eigenstates and viceversa[89].

A simple calculation yields the following expectation values in the initial density matrix

$$
\begin{aligned}
< [\bar{\nu}_\alpha(\vec{k},0)]_r [\nu_\alpha(\vec{k},0)]_s > &= \left[\sum_\lambda < \alpha^{(\alpha)\dagger}_{\vec{k},\lambda} \alpha^{(\alpha)}_{\vec{k},\lambda} > [\bar{U}^{(\alpha)}_{\vec{k},\lambda}]_r [U^{(\alpha)}_{\vec{k},\lambda}]_s \right. \\
&\quad \left. + \sum_\lambda < \beta^{(\alpha)\dagger}_{-\vec{k},\lambda} \beta^{(\alpha)}_{-\vec{k},\lambda} > [\bar{V}^{(\alpha)}_{-\vec{k},\lambda}]_r [V^{(\alpha)}_{-\vec{k},\lambda}]_s \right] \qquad (2.62) \\
&= n^{(\alpha)}(k) \left(\frac{\not{k}_\alpha + m_\alpha}{2\omega_\alpha(k)} \right)_{sr} + (1 - \bar{n}^{(\alpha)}(k)) \left[\gamma^0 \frac{\not{k}_\alpha - m_\alpha}{2\omega_\alpha(k)} \gamma^0 \right]_{sr} \qquad (2.63) \\
&\equiv [N_\alpha(\vec{k})]_{sr} \\
\not{k}_\alpha &= \gamma^0 \omega^\alpha(k) - \vec{\gamma} \cdot \vec{k} \qquad (2.64)
\end{aligned}
$$

where $n^\alpha(k); \bar{n}^\alpha(k)$ are given by the expressions (2.20) and there are no flavor off-diagonal matrix elements at $t = 0$ because the initial density matrix is flavor diagonal.

Combining all the above results, we find the final compact form for the time dependent expectation values in eqn. (2.39), namely

$$
< \bar{\nu}_e(\vec{k},t)\, \mathcal{O}\, \nu_e(\vec{k},t) >= Tr \left[N_e(\vec{k}) \tilde{T}_{ee}(\vec{k},t)\, \mathcal{O}\, T_{ee}(\vec{k},t) \right] + Tr \left[N_\mu(\vec{k}) \tilde{T}_{e\mu}(\vec{k},t)\, \mathcal{O}\, T_{e\mu}(\vec{k},t) \right] \qquad (2.65)
$$

2.2.4.1 Exact time evolution of distribution functions The exact time evolution (in free field theory) of flavor neutrinos is given by

$$
n^{(e)}(k,t) \equiv I^{(e)}(k,t) + J^{(e)}(k,t), \qquad (2.66)
$$

where $I^{(e)}(k,t)$ and $J^{(e)}(k,t)$ are given by

$$I^{(e)}(k,t) = \frac{1}{4\omega_e(k)} Tr\left[N_e(k)\tilde{T}_{ee}(\vec{k},t)\gamma^0(\not{k}_e + m_e)\gamma^0 T_{ee}(\vec{k},t)\right], \tag{2.67}$$

$$J^{(e)}(k,t) = \frac{1}{4\omega_e(k)} Tr\left[N_\mu(\vec{k})\tilde{T}_{e\mu}(\vec{k},t)\gamma^0(\not{k}_e + m_e)\gamma^0 T_{e\mu}(\vec{k},t)\right]. \tag{2.68}$$

$$\bar{n}^{(e)}(k,t) = 1 - \bar{I}^{(e)}(k,t) - \bar{J}^{(e)}(k,t), \tag{2.69}$$

where $\bar{I}^{(e)}(k,t)$ and $\bar{J}^{(e)}(k,t)$ are given by

$$\bar{I}^{(e)}(k,t) = \frac{1}{4\omega_e(k)} Tr\left[N_e(\vec{k})\tilde{T}_{ee}(\vec{k},t)(\not{k}_e - m_e)T_{ee}(\vec{k},t)\right], \tag{2.70}$$

$$\bar{J}^{(e)}(k,t) = \frac{1}{4\omega_e(k)} Tr\left[N_\mu(\vec{k})\tilde{T}_{e\mu}(\vec{k},t)(\not{k}_e - m_e)T_{e\mu}(\vec{k},t)\right]. \tag{2.71}$$

For the muon neutrinos and antineutrinos

$$n^{(\mu)}(k,t) = I^{(\mu)}(k,t) + J^{(\mu)}(k,t) \tag{2.72}$$

where $I^{(\mu)}(k,t)$ and $J^{(\mu)}(k,t)$ are given by

$$I^{(\mu)}(k,t) = \frac{1}{4\omega_\mu(k)} Tr\left[N_\mu(\vec{k})\tilde{T}_{\mu\mu}(\vec{k},t)\gamma^0(\not{k}_\mu + m_\mu)\gamma^0 T_{\mu\mu}(\vec{k},t)\right], \tag{2.73}$$

$$J^{(\mu)}(k,t) = \frac{1}{4\omega_\mu(k)} Tr\left[N_e(\vec{k})\tilde{T}_{\mu e}(\vec{k},t)\gamma^0(\not{k}_\mu + m_\mu)\gamma^0 T_{\mu e}(\vec{k},t)\right]. \tag{2.74}$$

$$\bar{n}^{(\mu)}(k,t) = 1 - \bar{I}^{(\mu)}(k,t) - \bar{J}^{(\mu)}(k,t), \tag{2.75}$$

where $\bar{I}^{(\mu)}(k,t)$ and $\bar{J}^{(\mu)}(k,t)$ are given by

$$\bar{I}^{(\mu)}(k,t) = \frac{1}{4\omega_\mu(k)} Tr\left[N_\mu(\vec{k})\tilde{T}_{\mu\mu}(\vec{k},t)(\not{k}_\mu - m_\mu)T_{\mu\mu}(\vec{k},t)\right], \tag{2.76}$$

$$\bar{J}^{(\mu)}(k,t) = \frac{1}{4\omega_\mu(k)} Tr\left[N_e(\vec{k})\tilde{T}_{\mu e}(\vec{k},t)(\not{k}_\mu - m_\mu)T_{\mu e}(\vec{k},t)\right]. \tag{2.77}$$

The calculation of the traces is simplified by the observation that all of the different terms that enter in the trace, such as $N_\alpha(\vec{k}); \tilde{T}_{\alpha,\alpha'}(\vec{k},t)\gamma^0; \gamma^0 T_{\alpha,\alpha'}(\vec{k},t)$ can be written in the form

$$\gamma^0 A_0(\vec{k},t) - \vec{\gamma}\cdot\vec{A}(\vec{k},t) + B(\vec{k},t) \equiv \not{A}(\vec{k},t) + B(\vec{k},t) \tag{2.78}$$

where the coefficient functions $A_0(\vec{k},t); \vec{A}(\vec{k},t); B(\vec{k},t)$ can be read off each individual term. Thus the traces in the terms above can be calculated by using the standard formulae for the traces of two and four Dirac matrices.

2.2.5 Fast and slow time scales

While the exact compact expressions above describe the full time evolution and provide a set of closed form expressions, they hide the fact that there two *widely different* time scales. These different time scales can be revealed by unravelling the different contributions to the distribution functions as follows. Consider the expectation value on the right hand side of eqn. (2.39) for the case of the electron neutrino

$$\begin{aligned} < [\bar{\nu}_e(\vec{k},t)]_f [\nu_e(\vec{k},t)]_g > &= C^2 < [\bar{\psi}_1(\vec{k},t)]_f [\psi_1(\vec{k},t)]_g > + S^2 < [\bar{\psi}_2(\vec{k},t)]_f [\psi_2(\vec{k},t)]_g > \\ &+ CS < [\bar{\psi}_1(\vec{k},t)]_f [\psi_2(\vec{k},t)]_g + [\bar{\psi}_2(\vec{k},t)]_f [\psi_1(\vec{k},t)]_g > \end{aligned} \tag{2.79}$$

the case of the muon neutrino can be obtained from the expression above by replacing $S \to C; C \to -S$.

By writing each one of the fields ψ_i in terms of the positive and negative frequency contributions which evolve in time with the phases $e^{\mp i E_i(k) t}$ respectively, it is clear that in the products $\bar{\psi}_i(\vec{k},t)\,\psi_i(\vec{k},t)$ there is a contribution that does not depend on time and terms that oscillate in time with the phases $e^{\mp 2 i E_i(k) t}$. These oscillatory terms arise from the interference between particles and antiparticles akin to *zitterbewegung* in principle do not vanish when the density matrix is diagonal in the flavor basis. In the general expectation values in eqn (2.39) these oscillatory terms will multiply the matrix elements of the form $\bar{F}^{(i)}_{\vec{k},\lambda}\mathcal{O}G^{(i)}_{-\vec{k},\lambda}$, thus if these matrix elements do not vanish, these oscillatory terms are present. In the second line in eqn. (2.79) a similar argument shows that there are two types of oscillatory terms, $e^{\mp i(E_1(k)+E_2(k))t}$ and $e^{\mp i(E_1(k)-E_2(k))t}$. The former arise from the interference between the particle and antiparticle states of different masses, while the latter from interference between particle states of different masses (or antiparticle).

The combined analysis from solar neutrinos and KamLAND[92] suggest that for two flavor mixing $M_1^2 - M_2^2 = \Delta M^2 \sim 7 \times 10^{-5}(eV)^2$ and cosmological constraints from WMAP[8] suggest that the average mass of neutrinos is $\bar{M} \lesssim 0.23eV$. Therefore even in the non-relativistic limit with $k \ll M_i$ the ratio $|E_1(k) - E_2(k)|/(E_1(k) + E_2(k)) < 10^{-4}$ and certainly much smaller in the relativistic limit $k \gg M_i$. Hence because of the near degeneracy, or in the relativistic limit for any value of the masses, there are two widely different time scales of evolution for the flavor distribution functions. The longest one corresponding to the interference between particle states (or antiparticle states) of different masses while the shortest one corresponds to the interference between particle and antiparticle states of equal or different masses. This point will be revisited below.

The evolution of the flavor (lepton) *asymmetry* highlights these time scales clearly and is studied below.

2.3 DEGENERATE GAS OF NEUTRINOS: EVOLUTION OF FLAVOR ASYMMETRY

The results obtained above are general and valid for any temperature and chemical potential (density). In this section we focus on understanding the time evolution of the flavor asymmetry $n^{(\alpha)}(k,t) - \bar{n}^{(\alpha)}(k,t)$ in the case of a cold, degenerate gas of flavor neutrinos. From equations (2.37) and (2.79) we find

$$\begin{aligned} n^{(e)}(\vec{k},t) - \bar{n}^{(e)}(\vec{k},t) &= \frac{C^2}{2} < \psi_1^\dagger(\vec{k},t)\psi_1(\vec{k},t) > + \frac{S^2}{2} < \psi_2^\dagger(\vec{k},t)\psi_2(\vec{k},t) > -1 \\ &+ \frac{CS}{2} < \psi_1^\dagger(\vec{k},t)\psi_2(\vec{k},t) + \psi_2^\dagger(\vec{k},t)\psi_1(\vec{k},t) > \qquad (2.80) \\ n^{(\mu)}(\vec{k},t) - \bar{n}^{(\mu)}(\vec{k},t) &= \frac{S^2}{2} < \psi_1^\dagger(\vec{k},t)\psi_1(\vec{k},t) > + \frac{C^2}{2} < \psi_2^\dagger(\vec{k},t)\psi_2(\vec{k},t) > -1 \\ &- \frac{CS}{2} < \psi_1^\dagger(\vec{k},t)\psi_2(\vec{k},t) + \psi_2^\dagger(\vec{k},t)\psi_1(\vec{k},t) > \qquad (2.81) \end{aligned}$$

The first line of the expressions above is time independent because the overlap between positive and negative frequency components vanishes, and the time dependence arises solely from the interference between different mass eigenstates. The time dependent terms (second lines in the above expressions) are opposite for the two flavors realizing the fact that the total charge of mass eigenstates equals that of flavor eigenstates and is time independent (see eqn. (2.19)).

Furthermore the expectation values $< \psi_i^\dagger(\vec{k},t)\,\psi_i(\vec{k},t) >$ (no sum on i) are time independent (in the case of free field theory under consideration) since the interference term between positive and negative frequency spinors vanishes. The time dependence is completely encoded in the contribution that mixes the mass eigenstates.

Therefore the time dependence of the flavor asymmetry is completely determined by the quantity

$$\chi(\vec{k},t) \equiv \frac{CS}{2} < \left(\psi_1^\dagger(\vec{k},t)\psi_2(\vec{k},t) + \psi_2^\dagger(\vec{k},t)\psi_1(\vec{k},t)\right) > . \tag{2.82}$$

Using equations (2.47)- (2.50), it follows that

$$\chi(\vec{k},t) = \frac{C^2S^2}{2}\,Tr\left[\,[N_e(\vec{k}) - N_\mu(\vec{k})][\tilde{F}_1(\vec{k},t)F_2(\vec{k},t) + \tilde{F}_2(\vec{k},t)F_1(\vec{k},t)]\,\right], \tag{2.83}$$

The computation of the traces is simplified by writing

$$\begin{aligned}
F_j(k,t) &= \not{P}_j(t) + M_j(t) && (2.84)\\
P_j^0(t) &= \cos(E_j(k)t), && (2.85)\\
\vec{P}_j(t) &= \frac{i\vec{k}}{E_j(k)}\sin(E_j(k)t), && (2.86)\\
M_j(t) &= -\frac{iM_j}{E_j(k)}\sin(E_j(k)t). && (2.87)
\end{aligned}$$

and similarly we write

$$\begin{aligned}
N_\alpha(k) &= \not{Q}_\alpha + \widetilde{M}_\alpha && (2.88)\\
\not{Q}_\alpha &= \gamma^0 Q_\alpha^0 - \vec{\gamma}\cdot\vec{Q}_\alpha, && (2.89)\\
Q_\alpha^0 &= \frac{1}{2}\left[n^{(\alpha)}(k) + 1 - \bar{n}^{(\alpha)}(k)\right], && (2.90)\\
\vec{Q}_\alpha &= \frac{\vec{k}}{2\omega_\alpha(k)}\left[n^{(\alpha)}(k) - 1 + \bar{n}^{(\alpha)}(k)\right], && (2.91)\\
\widetilde{M}_\alpha &= \frac{m_\alpha}{2\omega_\alpha(k)}\left[n^{(\alpha)}(k) - 1 + \bar{n}^{(\alpha)}(k)\right]. && (2.92)
\end{aligned}$$

For further convenience, we define

$$\Delta\not{Q} = \not{Q}_e - \not{Q}_\mu, \quad ; \quad \Delta\widetilde{M} = \widetilde{M}_e - \widetilde{M}_\mu, \tag{2.93}$$

in terms of which we obtain

$$\chi(\vec{k},t) = \frac{C^2S^2}{2}\,Tr\Big[(\Delta\not{Q}+\Delta\widetilde{M})(\not{P}_1(-t)+M_1(-t))\gamma^0(\not{P}_2(t)+M_2(t)) + (\Delta\not{Q}+\Delta\widetilde{M})(\not{P}_2(-t)+M_2(-t))\gamma^0(\not{P}_1(t)+M_1(t))\Big]. \tag{2.94}$$

After some lengthy but straigthforward algebra we find

$$\chi(\vec{k},t) = \chi(\vec{k},0) - 2C^2S^2\,\Big[\Big(n^{(e)}(k)-\bar{n}^{(e)}(k)\Big)-\Big(n^{(\mu)}(k)-\bar{n}^{(\mu)}(k)\Big)\Big] \Bigg[\left(1-\frac{k^2+M_1M_2}{E_1(k)E_2(k)}\right)\sin^2\left(\frac{E_1(k)+E_2(k)}{2}\,t\right) + \left(1+\frac{k^2+M_1M_2}{E_1(k)E_2(k)}\right)\sin^2\left(\frac{E_1(k)-E_2(k)}{2}\,t\right)\Bigg], \tag{2.95}$$

where $\chi(\vec{k},0)$ is given by

$$\chi(\vec{k},0) = 2C^2S^2\,\Big[\Big(n^{(e)}(k)-\bar{n}^{(e)}(k)\Big)-\Big(n^{(\mu)}(k)-\bar{n}^{(\mu)}(k)\Big)\Big]. \tag{2.96}$$

The expression (2.95) for the time dependence of the flavor asymmetry clearly shows that neutrino mixing results in a time evolution of the flavor asymmetry *unless* the flavor asymmetry for both flavors is the same. This is obviously a consequence of Pauli blocking: if the neutrino states are occupied up to the same momentum electron neutrinos cannot transform into an (occupied) muon neutrino state and viceversa.

In the case of a cold, degenerate gas of flavor neutrinos (we assume here both chemical potentials to be positive) is given by

$$n^{(\alpha)}(k) \to \Theta(k_F^{(\alpha)}-k)\;;\;\bar{n}^{(\alpha)}(k)\to 0 \tag{2.97}$$

If the chemical potential is different for the different flavors, the expression above shows that each wavevector mode will evolve with a different frequency and as a consequence of free field evolution there is no mode mixing. The important question is what is the time evolution of the *total charge* which is the integral of the flavor asymmetry over all momenta. This time evolution will be a result of the *dephasing* through the oscillations between different modes that are not Pauli blocked.

We now proceed to study analytically and numerically the time evolution of the flavor charge densities q_α/V with q_α given by eqn. (2.18) and V the volume. We begin by defining

$$\bar{M} \equiv \frac{M_1 + M_2}{2} \;\; ; \;\; \Delta M^2 \equiv M_1^2 - M_2^2, \tag{2.98}$$

so that M_1 and M_2 can be written in terms of $\bar{M}$ and ΔM^2 as

$$M_1 = \bar{M}\left(1 + \frac{\Delta M^2}{4\bar{M}^2}\right) \;\; ; \;\; M_2 = \bar{M}\left(1 - \frac{\Delta M^2}{4\bar{M}^2}\right). \tag{2.99}$$

We take the following as representative values for the two flavor case[1, 2] $\bar{M} \simeq 0.25\ eV$ and $\Delta M^2 \simeq 7 \times 10^{-5} (eV)^2$. In what follows we assume that $k_F^e > k_F^\mu$ and introduce dimensionless variables by taking k_F^e as the common scale, the opposite limit for the Fermi momenta can be obtained simply from the results below. Hence we define

$$q = \frac{k}{k_F^e} \; ; \; q_r = \frac{k_F^\mu}{k_F^e} \; ; \; \tau = k_F^e t, \tag{2.100}$$

$$\bar{m} = \frac{\bar{M}}{k_F^e} \;\; ; \;\; \delta m^2 = m_1^2 - m_2^2 = \frac{M_1^2 - M_2^2}{(k_F^e)^2} \tag{2.101}$$

$$m_1 = \bar{m}\left(1 + \frac{\Delta M^2}{4\bar{M}^2}\right) \; ; \; m_2 = \bar{m}\left(1 - \frac{\Delta M^2}{4\bar{M}^2}\right); \tag{2.102}$$

$$\varepsilon_1 = \sqrt{q^2 + m_1^2} \; ; \; \varepsilon_2 = \sqrt{q^2 + m_2^2}. \tag{2.103}$$

Hence, in terms of $\mathcal{N}^{(\alpha)} = (k_F^\alpha)^3/3\pi^2$ (see eqn. (2.28)), we find that the time evolution of the flavor charge densities are given by

$$\frac{q_e(t)}{V} = \mathcal{N}^{(e)} - 6C^2 S^2 \mathcal{N}^{(e)} \Big(I_f(\tau) + I_s(\tau) \Big) \tag{2.104}$$

$$\frac{q_\mu(t)}{V} = \mathcal{N}^{(\mu)} + 6C^2 S^2 \mathcal{N}^{(e)} \Big(I_f(\tau) + I_s(\tau) \Big) \tag{2.105}$$

where

$$I_f(\tau) = \int_{q_r}^{1} dq\, q^2 \left(1 - \frac{q^2 + m_1 m_2}{\varepsilon_1 \varepsilon_2}\right) \sin^2\left[\frac{\varepsilon_1 + \varepsilon_2}{2}\,\tau\right] \tag{2.106}$$

$$I_s(\tau) = \int_{q_r}^{1} dq\, q^2 \left(1 + \frac{q^2 + m_1 m_2}{\varepsilon_1 \varepsilon_2}\right) \sin^2\left[\frac{\varepsilon_1 - \varepsilon_2}{2}\,\tau\right] \tag{2.107}$$

We have separated the contributions from the fast ($I_f(\tau)$) and slow ($I_s(\tau)$) time scales as discussed in section (2.2.5) above. In particular, as discussed above the term that oscillates with the *sum* $\varepsilon_1+\varepsilon_2$ is a consequence of the overlap between particles and antiparticles. The pre-factors that multiply the sine functions in equations (2.106,2.107) arise from the overlap between *particle-antiparticle* spinors in (2.106) and particle-particle, anti-particle-anti-particle spinors in (2.107). The overlap between particle and antiparticle spinors is non-vanishing for different masses. Similar contributions from the overlap between particle and antiparticle states of different masses have been found in the studies of refs.[89, 90, 91].

Since the mass eigenstates are almost degenerate or alternatively for any values of the masses in the relativistic limit we find

$$\begin{aligned}\frac{q^2+m_1m_2}{\varepsilon_1\varepsilon_2} &= 1-\frac{\bar{m}^2q^2}{\bar{\varepsilon}^4}\left(\frac{\Delta M^2}{4\bar{M}^2}\right)^2+\mathcal{O}\left(\left(\frac{\Delta M^2}{4\bar{M}^2}\right)^4\right)\\ \bar{\varepsilon} &= \sqrt{q^2+\bar{m}^2}\end{aligned} \tag{2.108}$$

with $\frac{\Delta M^2}{4\bar{M}^2}\sim 3\times 10^{-4}$. Therefore the coefficient that results from the overlap between the particle and antiparticle spinors of different mass is given by

$$1-\frac{q^2+m_1m_2}{\varepsilon_1\varepsilon_2}=\mathcal{O}\left(\frac{\Delta M^2}{4\bar{M}^2}\frac{\bar{M}}{E(k)}\right)^2 \tag{2.109}$$

and the coefficient that results from the overlap between particle-particle or anti-particle-anti-particle of *different* masses is

$$1+\frac{q^2+m_1m_2}{\varepsilon_1\varepsilon_2}=2+\mathcal{O}\left(\frac{\Delta M^2}{4\bar{M}^2}\frac{\bar{M}}{E(k)}\right)^2 \tag{2.110}$$

where $E(k)$ is an energy scale.

Therefore the coefficient of the oscillatory term in $I_f(\tau)$ is a factor at least of order $\left(\frac{\Delta M^2}{4\bar{M}^2}\right)^2\sim 10^{-7}$ smaller than that of $I_s(\tau)$. Furthermore it is clear that the interference terms between particle and antiparticle average out on a time scale $t_f\lesssim 1/\bar{M}$ whereas the particle-particle contributions evolve on a much slower time scale $t_s\sim\bar{M}/\Delta M^2\gg t_f$.

However, despite the fact that the coefficients of the oscillatory terms in $I_s(\tau)$ and $I_f(\tau)$ differ by several orders of magnitude, the fact that the time evolution of $I_s(\tau)$ is much slower allows for a time scale within which both contributions are *comparable*. This can be gleaned from the following argument.

The integrals for $I_s(\tau)$ and $I_f(\tau)$ are dominated by the region $q \sim 1$. Consider an intermediate time scale so that the argument of the oscillatory function in $I_f(\tau)$ is of order one, but the argument of the oscillatory function in $I_s(\tau)$ is $\ll 1$. The contribution to the integral in $I_f(\tau)$ is of order $\bar{m}^2 \left(\frac{\Delta m^2}{4\bar{m}^2}\right)^2$ while the contribution to the integral $I_s(\tau)$ is of order $2(\delta m^2 \tau^2)$. Therefore, it is clear that even when the prefactor of its oscillatory term is small, the integrand of $I_f(\tau)$ will be *larger than* that of $I_s(\tau)$ in the time domain during which

$$\bar{m}^2 \left(\frac{\delta m^2}{4\bar{m}^2}\right)^2 > (\delta m^2 \tau)^2 \Longrightarrow \tau \lesssim 1/\bar{m} \tag{2.111}$$

In the opposite limit, for $\tau >> 1/\bar{m}$ the dynamics is completely dominated by $I_s(\tau)$.

Fig. (2.1) below displays the early time evolution of $I_s(\tau)$ and $I_f(\tau)$ for $0 \leq \tau \lesssim 1/\bar{m}$. It is clear from this figure that $I_f(\tau)$ averages out to its asymptotic value on a short time scale $\tau \sim 1$ ($t \sim 1/k_F$) and that $I_s(\tau)$ begins to dominate the dynamics on time scales $\tau \gtrsim 1/\bar{m}$ as discussed above. In the case of Fig.(2.1), with $k_F^e >> \bar{M}$ the time scale of averaging is $t \sim 1/k_F^e$, but for $k_F << \bar{M}$ it would be of order $1/\bar{M}$.

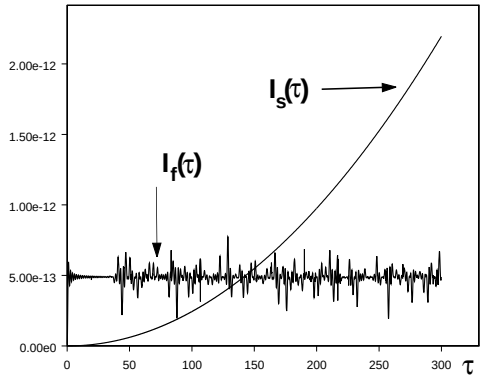

Figure 2.1: $I_s(\tau)$ and $I_s(\tau)$ for $k_F^e = 100\ eV$; $k_F^\mu = 0$; $\bar{M} = 0.25\ eV$; $\Delta M^2 \simeq 7 \times 10^{-5} (eV)^2$ vs. τ. For these values $1/\bar{m} = 400$.

In terms of dimensionful quantities the inequality obtained in eqn. (2.111) above translates into $t < 1/\bar{M}$. With the current estimate $\bar{M} \sim 0.25$ eV the analysis above suggests that the particle-antiparticle interference is dynamically relevant during time scales $t \lesssim 10^{-15}\ s$ although this time scale is comparable to the expansion time scale at the time of the electroweak phase transition, it

is far shorter than the time scales relevant either for primordial nucleosynthesis or for dynamical processes during the collapse of supernovae or neutron star cooling.

While the behavior of $I_s(\tau)$ and $I_f(\tau)$ as a function of τ must in general be studied numerically, the long time limit can be extracted analytically.

The asymptotic long time behavior of $I_s(\tau)$ and $I_f(\tau)$ is determined by the end points of their integrands, in particular for momenta near the Fermi surface. Two relevant cases yield the following results

- **Relativistic Limit: max**$(k_F^e, k_F^\mu) \gg M_1, M_2$

$$\begin{aligned} I_s(\tau) &= \frac{1}{2}\int_{q_r}^1 dq\, q^2 \left(1+\frac{q^2+m_1m_2}{\varepsilon_1\varepsilon_2}\right) + \frac{2}{\delta m^2\tau}\left\{\sin\left(\frac{\delta m^2}{2}\tau\right) - q_r^4 \sin\left(\frac{\delta m^2\tau}{2q_r}\right)\right\} \\ &\quad +\mathcal{O}\left(\frac{1}{(\delta m^2\tau)^2}\right) \qquad (2.112) \\ I_f(\tau) &= \frac{1}{2}\int_{q_r}^1 dq\, q^2 \left(1-\frac{q^2+m_1m_2}{\varepsilon_1\varepsilon_2}\right) - \frac{1}{8\tau}(m_1-m_2)^2\left[\sin(2\tau) - \sin 2q_r\tau\right] \\ &\quad +\mathcal{O}\left(\frac{1}{\tau^2}\right) \qquad (2.113) \end{aligned}$$

  where δm^2 is defined by equation (2.100) along with the other dimensionless variables.

- **Non-Relativistic limit:** $k_F^e, k_F^\mu \ll M_1, M_2$

$$\begin{aligned} I_s(\tau) &= \frac{1}{2}\int_{q_r}^1 dq\, q^2 \left(1+\frac{q^2+m_1m_2}{\varepsilon_1\varepsilon_2}\right) + \frac{m_1m_2}{(m_1-m_2)\,\tau}\left\{\sin\left[(m_1-m_2)(1-\frac{1}{2m_1m_2})\tau\right] - \right. \\ &\quad \left. q_r \sin\left[(m_1-m_2)(1-\frac{q_r^2}{2m_1m_2})\tau\right]\right\} + \mathcal{O}\left(\frac{1}{\tau^{\frac{3}{2}}}\right) \quad ; \quad \text{for} \quad \frac{(m_1-m_2)\tau}{m_1m_2} \gg 1 \\ I_s(\tau) &= \frac{1}{2}\int_{q_r}^1 dq\, q^2 \left(1+\frac{q^2+m_1m_2}{\varepsilon_1\varepsilon_2}\right)\left[1-\cos[(m_1-m_2)\tau]\right]; \ \text{for} \frac{(m_1-m_2)\tau}{m_1m_2} \ll 1 \qquad (2.114) \end{aligned}$$

$$\begin{aligned} I_f(\tau) &= \frac{1}{2}\int_{q_r}^1 dq\, q^2 \left(1-\frac{q^2+m_1m_2}{\varepsilon_1\varepsilon_2}\right) - \frac{(m_1-m_2)^2}{m_1m_2(m_1+m_2)\,\tau}\left\{\sin\left[(m_1+m_2)(1+\frac{1}{2m_1m_2})\tau\right] - \right. \\ &\quad \left. q_r^3 \sin\left[(m_1+m_2)(1+\frac{q_r^2}{2m_1m_2})\tau\right]\right\} + \mathcal{O}\left(\frac{1}{\tau^2}\right) \quad ; \quad \text{for} \quad \frac{(m_1+m_2)\tau}{m_1m_2} \gg 1 \\ I_f(\tau) &= \frac{1}{2}\int_{q_r}^1 dq\, q^2 \left(1-\frac{q^2+m_1m_2}{\varepsilon_1\varepsilon_2}\right)\left[1-\cos[(m_1+m_2)\tau]\right] \quad ; \quad \text{for} \quad \frac{(m_1+m_2)\tau}{m_1m_2} \ll 1 \qquad (2.115) \end{aligned}$$

In both cases, the flavor asymmetry density at asymptotically long time is given by

$$\frac{1}{V}(q_e(t) - q_\mu(t)) \to \left[\mathcal{N}^{(e)} - \mathcal{N}^{(\mu)}\right]\cos^2(2\theta) + \mathcal{O}(1/t) \qquad (2.116)$$

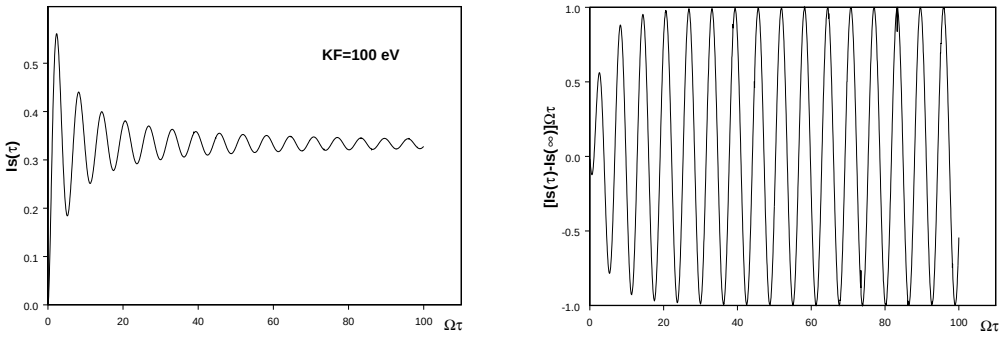

Figure 2.2: $I_s(\tau)$ and $[I_s(\tau) - I_s(\infty)] \times (\Omega\tau)$ for $k_F^e = 100\ eV$; $k_F^\mu = 0$; $\bar{M} = 0.25\ eV$; $\Delta M^2 \simeq 7 \times 10^{-5} (eV)^2$ vs. $\Omega\tau$, with $\Omega = \delta m^2 = 7 \times 10^{-9}$.

The power law fall-off is a consequence of dephasing between different flavor modes that are not Pauli blocked. Fig.(2.2) displays the slow contribution $I_s(\tau)$ and its asymptotic limit given by eqn. (2.112) in the relativistic case.

2.4 DISTRIBUTION FUNCTIONS OF NEUTRINOS AND ANTINEUTRINOS

The distribution functions are given by equations (2.66)-(2.77) for which after lengthy but straightforward algebra we find the following expressions

$$I^{(e)}(k,t) = n^{(e)}(k) - 2n^{(e)}(k)\mathcal{A}(k,t) - \frac{k^2}{\omega_e^2(k)}\left[n^{(e)}(k) - \left(1 - \bar{n}^{(e)}(k)\right)\right]\mathcal{B}(k,t) \tag{2.117}$$

$$\begin{aligned} J^{(e)}(k,t) \;=\; & \left[\frac{C^2S^2(M_1-M_2)^2 + M_1M_2 + k^2}{\omega_e(k)\omega_\mu(k)}\left(n^{(\mu)}(k) - [1 - \bar{n}^{(\mu)}(k)]\right)\right. \\ & \left. + \left(n^{(\mu)}(k) + [1 - \bar{n}^{(\mu)}(k)]\right)\right]\mathcal{A}(k,t) \\ & - \frac{k^2}{\omega_e(k)\omega_\mu(k)}\left[n^{(\mu)}(k) - \left(1 - \bar{n}^{(\mu)}(k)\right)\right]\mathcal{C}(k,t) \end{aligned} \tag{2.118}$$

where $n^{(e)}(k)$ and $\bar{n}^{(e)}(k)$ are the initial distribution functions given by eqn. (2.20) and

$$\mathcal{A}(k,t) = C^2S^2\left[\left(1-\frac{k^2+M_1M_2}{E_1(k)E_2(k)}\right)\sin^2\left(\frac{E_1(k)+E_2(k)}{2}\,t\right)+\right. \tag{2.119}$$

$$\left.\left(1+\frac{k^2+M_1M_2}{E_1(k)E_2(k)}\right)\sin^2\left(\frac{E_1(k)-E_2(k)}{2}\,t\right)\right] \tag{2.120}$$

$$\mathcal{B}(k,t) = C^4S^4(M_1-M_2)^2\left[\frac{1}{E_1(k)}\sin(E_1(k)t)-\frac{1}{E_2(k)}\sin(E_2(k)t)\right]^2 \tag{2.121}$$

$$\mathcal{C}(k,t) = C^2S^2(M_1-M_2)^2\left[\frac{C^2S^2}{E_1^2(k)}\sin^2(E_1(k)t)+\frac{C^2S^2}{E_2^2(k)}\sin^2(E_2(k)t)\right.$$

$$\left.-\frac{2C^2S^2-1}{E_1(k)E_2(k)}\sin(E_1(k)t)\sin(E_2(k)t)\right]. \tag{2.122}$$

The expressions for $\bar{I}^{(e)}(k,t)$ and $\bar{J}^{(e)}(k,t)$ are obtained from those for $I^{(e)}(k,t)$ and $J^{(e)}(k,t)$ above by the replacement

$$n^{(e)}(k) \longleftrightarrow [1-\bar{n}^{(e)}(k)]\ ;\ n^{(\mu)}(k) \longleftrightarrow [1-\bar{n}^{(\mu)}(k)] \tag{2.123}$$

Finally the expressions for $I^{(\mu)}(k,t); \bar{I}^{(\mu)}(k,t); J^{(\mu)}(k,t); \bar{J}^{(\mu)}(k,t)$ are obtained from those for the electron neutrino by the replacement

$$n^{(e)}(k) \longleftrightarrow n^{(\mu)}(k)\ ;\ \bar{n}^{(e)}(k) \longleftrightarrow \bar{n}^{(\mu)}(k)\ ;\ \omega_e(k) \longleftrightarrow \omega_\mu(k)\ ;\ C^2 \longleftrightarrow S^2 \tag{2.124}$$

These dynamical factors $\mathcal{A}(k,t); \mathcal{B}(k,t); \mathcal{C}(k,t)$ are determined by the time evolution while their pre-factors in the expressions for the distribution functions are determined by the initial state. The dynamical factors clearly reveal again the different time scales. Terms that feature the contributions $e^{\pm 2iE_{(1,2)}t}; e^{\pm i(E_1+E_2)t}$ arise from particle-antiparticle interference and their contribution is proportional to $\left(\Delta M^2/\bar{M}^2\right)$ and those that feature $e^{\pm i(E_1-E_2)t}$ arise from particle-particle (or anti-particle- anti-particle) interference. We can find the asymptotic distribution functions at long time by averaging the oscillatory terms over a time scale *longer than the longest* scale $\sim \bar{M}/\Delta M^2$. This time averaging procedure leads to

$$\overline{\mathcal{A}(k,t)} = C^2S^2 \tag{2.125}$$

$$\overline{\mathcal{B}(k,t)} = \overline{\mathcal{C}(k,t)} = \frac{1}{2}C^4S^4(M_1-M_2)^2\left[\frac{1}{E_1^2(k)}+\frac{1}{E_2^2(k)}\right] \tag{2.126}$$

The above expressions are exact and therefore valid for any value of the neutrino masses M_1, M_2. However, the most recent compilation[2, 92] of data suggests that in the two flavor case the mass

eigenstates are almost degenerate with $\Delta M^2 \sim 7 \times 10^{-5}\ (eV)^2$ and the most recent cosmological constraint from WMAP[8] suggests that the average value of the mass $\bar{M}$ is $\lesssim 0.25\ (eV)$. In terms of the $\bar{M}$ and ΔM^2 introduced in eqn. (2.98), we find

$$m_e = \bar{M}\left[1 + \frac{\Delta M^2}{4\bar{M}^2}\cos(2\theta)\right]\ ;\ m_\mu = \bar{M}\left[1 - \frac{\Delta M^2}{4\bar{M}^2}\cos(2\theta)\right] \tag{2.127}$$

In terms of the small ratio $\Delta M^2/\bar{M}^2 \sim 10^{-3}$ we find the average of the distribution functions over the longest time scale to be given by

$$\begin{aligned}
n^{(e)}_{av}(k) &= n^{(e)}(k) - 2C^2S^2\left(n^{(e)}(k) - n^{(\mu)}(k)\right) - \mathcal{R}[k, n^{(\alpha)}, \bar{n}^{(\alpha)}] && (2.128)\\
\bar{n}^{(e)}_{av}(k) &= \bar{n}^{(e)}(k) - 2C^2S^2\left(\bar{n}^{(e)}(k) - \bar{n}^{(\mu)}(k)\right) - \mathcal{R}[k, n^{(\alpha)}, \bar{n}^{(\alpha)}] && (2.129)\\
n^{(\mu)}_{av}(k) &= n^{(\mu)}(k) + 2C^2S^2\left(n^{(e)}(k) - n^{(\mu)}(k)\right) - \mathcal{R}[k, n^{(\alpha)}, \bar{n}^{(\alpha)}] && (2.130)\\
\bar{n}^{(\mu)}_{av}(k) &= \bar{n}^{(\mu)}(k) + 2C^2S^2\left(\bar{n}^{(e)}(k) - \bar{n}^{(\mu)}(k)\right) - \mathcal{R}[k, n^{(\alpha)}, \bar{n}^{(\alpha)}] && (2.131)
\end{aligned}$$

with

$$\begin{aligned}
\mathcal{R}[k, n^{(\alpha)}, \bar{n}^{(\alpha)}] &= \frac{k^2\bar{M}^2}{\bar{E}^4(k)}\left(\frac{\Delta M^2}{4\bar{M}^2}\right)^2 C^2S^2\left[4C^2S^2(n^{(e)}(k) + \bar{n}^{(e)}(k) - 1) + (n^{(\mu)}(k) + \bar{n}^{(\mu)}(k) - 1)\right]\\
&\quad + \mathcal{O}\left(\left(\frac{\Delta M^2}{4\bar{M}^2}\right)^3\right) && (2.132)\\
\bar{E}(k) &= \sqrt{k^2 + \bar{M}^2} && (2.133)
\end{aligned}$$

The term $\mathcal{R}[k, n^{(\alpha)}, \bar{n}^{(\alpha)}]$ arises from the overlap between particle and antiparticle spinors which features the small quantity $\left(\frac{\Delta M^2}{4M^2}\right)$.

Flavor pair production and normal ordering:

The expressions (2.128-2.131) with that for the corrections given by eqn. (2.132) point out an important and subtle aspect of the dynamics of mixing. Consider that the initial density matrix is the flavor *vacuum*, namely set $n^{(e)}(k) = \bar{n}^{(e)}(k) = n^{(\mu)}(k) = \bar{n}^{(\mu)}(k) = 0$. The asymptotic limit of the distribution functions (2.128-2.131) is given to lowest non trivial order in the ratio $\Delta M^2/\bar{M}^2$ by

$$\begin{aligned}
n^{(e)}(k,\infty) = \bar{n}^{(e)}(k,\infty) = n^{(\mu)}(k,\infty) = \bar{n}^{(\mu)}(k,\infty) = &\quad \frac{k^2\bar{M}^2}{4\bar{E}^4(k)}\left(\frac{\Delta M^2}{4\bar{M}^2}\right)^2 \sin^2(2\theta)(1 + \sin^2(2\theta)) +\\
&\mathcal{O}\left(\left(\frac{\Delta M^2}{4\bar{M}^2}\right)^3\right) && (2.134)
\end{aligned}$$

This result clearly indicates that the time evolution results in the creation of particle-antiparticle pairs of electron and muon neutrinos. This is of course a consequence of the non-vanishing overlap between positive and negative energy spinors which results in that a destruction operator for flavor neutrinos develops a component corresponding to a *creation* operator of antineutrinos during time evolution, and viceversa. In leading order in the degeneracy, the typical momentum of the pair created is $k \sim \bar{M}$ therefore these are typically low momentum pairs of flavor neutrinos.

Furthermore a remarkable aspect of this pair production process via neutrino mixing is that the distribution function of the produced particles falls off very *slowly* at high energies, namely $n_{prod}(k,\infty) \propto 1/k^2$. As a result there is a *divergent* number of pairs produced as a consequence of mixing and time evolution. Since the particles and antiparticles are produced in pairs, the flavor charge vanishes, but the individual distribution functions feature a contribution from the pair production process. A normal ordering prescription must be appended to subtract the infinite number of particles created, however unlike normal ordering in the usual free field theory, which subtracts a constant, in the case of mixing such normal ordering requires a subtraction of a *distribution function*.

This is a novel and subtle phenomenon, *flavor pair production* which is a direct many particle consequence of mixing and oscillations. Since this phenomenon is a consequence of the interference between particle and antiparticle states is suppressed by the small quantity $(\Delta M^2/\bar{M})^2$.

Regardless of whether this phenomenon of flavor pair production has any bearing on the cosmology and or astrophysics of neutrinos, it is a genuine many body aspect inherent to the field theory of neutrino mixing that deserves to be studied in its own right as a fundamental aspect of the field theory of mixing.

Off-diagonal densities: Even when the initial density matrix is diagonal in the flavor basis and therefore there are no off-diagonal *initial* correlations, these develop upon time evolution as a consequence of flavor mixing. Following the same steps described above for the distribution functions, we find the off-diagonal density to be given by the following expression

$$
\begin{aligned}
& < \nu_e^\dagger(\vec{k},t)\nu_\mu(\vec{k},t) > \\
= \; & -2\frac{C^2-S^2}{CS}\left[\left(n^{(e)}(k)-\bar{n}^{(e)}(k)\right)-\left(n^{(\mu)}(k)-\bar{n}^{(\mu)}(k)\right)\right]\mathcal{A}(k,t) \\
& +iCS\sin\left[(E_1(k)-E_2(k))\,t\right]\times \\
& \left\{\frac{1}{\omega_e(k)}\left[n^{(e)}(k)-\left(1-\bar{n}^{(e)}(k)\right)\right]\left[(E_1(k)+E_2(k))-(M_1-M_2)\left(\frac{S^2M_1}{E_1(k)}-\frac{C^2M_2}{E_2(k)}\right)\right]\right. \\
& \left.-\frac{1}{\omega_\mu(k)}\left[n^{(\mu)}(k)-\left(1-\bar{n}^{(\mu)}(k)\right)\right]\left[(E_1(k)+E_2(k))-(M_1-M_2)\left(\frac{C^2M_1}{E_1(k)}-\frac{S^2M_2}{E_2(k)}\right)\right]\right\} \\
& +iCS\sin\left[(E_1(k)+E_2(k))\,t\right]\times \\
& \left\{\frac{1}{\omega_e(k)}\left[n^{(e)}(k)-\left(1-\bar{n}^{(e)}(k)\right)\right]\left[(E_1(k)-E_2(k))-(M_1-M_2)\left(\frac{S^2M_1}{E_1(k)}+\frac{C^2M_2}{E_2(k)}\right)\right]\right. \\
& \left.-\frac{1}{\omega_\mu(k)}\left[n^{(\mu)}(k)-\left(1-\bar{n}^{(\mu)}(k)\right)\right]\left[(E_1(k)-E_2(k))-(M_1-M_2)\left(\frac{C^2M_1}{E_1(k)}+\frac{S^2M_2}{E_2(k)}\right)\right]\right\}
\end{aligned}
\tag{2.135}
$$

with $\mathcal{A}(k,t)$ given by eqn. (2.119). The expressions for the distribution functions and the off-diagonal density can be simplified by expanding the coefficients of the oscillatory functions up to leading order in the small quantity $\left(\Delta M^2/\bar{M}^2\right)$. We find

$$
n^{(e)}(k,t) = n^{(e)}(k) - (n^{(e)}(k)-n^{(\mu)}(k))2C^2S^2\left[1-\cos[(E_1(k)-E_2(k))t]\right] + \mathcal{O}\left(\frac{\Delta M^2}{4\bar{M}^2}\right)^2 \tag{2.136}
$$

the other distribution functions may be found from the expression above by the replacements in eqns. (2.123,2.124). Their time averages over the long time scale coincides with the leading expressions in eqns. (2.128-2.131). The off-diagonal density simplifies to the following expression

$$
\begin{aligned}
& < \nu_e^\dagger(\vec{k},t)\nu_\mu(\vec{k},t) > \\
= \; & -2SC\left\{2(C^2-S^2)\left[\left(n^{(e)}(k)-\bar{n}^{(e)}(k)\right)-\left(n^{(\mu)}(k)-\bar{n}^{(\mu)}(k)\right)\right]\sin^2\left[(E_1(k)-E_2(k))\,\frac{t}{2}\right]\right. \\
& \left.-i\left[\left(n^{(e)}(k)+\bar{n}^{(e)}(k)\right)-\left(n^{(\mu)}(k)+\bar{n}^{(\mu)}(k)\right)\right]\sin\left[(E_1(k)-E_2(k))\,t\right]\right\}+\mathcal{O}\left(\frac{\Delta M^2}{4\bar{M}^2}\right)^2
\end{aligned}
\tag{2.137}
$$

The terms of $\mathcal{O}\left(\frac{\Delta M^2}{4\bar{M}^2}\right)^2$ again involve terms that oscillate with the sum of the frequencies corresponding to particle-antiparticle interference as well as terms that oscillate with the difference

of the frequencies arising from the overlap of the particle (or antiparticle) spinor wavefunctions for different masses. The analysis that was presented for the same type of contributions in $I_s(\tau); I_f(\tau)$ above highlight that the particle-antiparticle interference becomes subdominant on time scales $t > 1/\bar{M}$. Hence the first terms $\mathcal{O}\left(\frac{\Delta M^2}{4M^2}\right)^0$ in the approximations (2.136, 2.137) determine the dynamics of the distribution functions and the off-diagonal correlator in leading order in the small ratio $\frac{\Delta M^2}{4M^2}$ for $t >> 1/\bar{M}$.

2.4.1 Equilibrated gas of mass eigenstates

Although we have focused on the case in which the initial density matrix is diagonal in the flavor basis, for completeness we now study the case in which the initial density matrix describes an ensemble of *mass eigenstates* in equilibrium. Therefore this initial density matrix is diagonal in the mass basis and commutes with the Hamiltonian. This situation thus describes a state of equilibrium in which the occupation numbers do not evolve in time (in the non-interacting theory). In this case we find

$$\begin{aligned} < [\bar{\psi}_i(\vec{k},0)]_r [\psi_i(\vec{k},0)]_s > &= n^{(i)}(k) \left(\frac{\not{k}_i + M_i}{2E_i(k)}\right)_{sr} + \left(1 - \bar{n}^{(i)}(k)\right) \left[\gamma^0 \frac{\not{k}_i - M_i}{2E_i(k)} \gamma^0\right]_{sr} \quad (2.138) \\ &\equiv [N_i(\vec{k})]_{sr} \\ \not{k}_i &= \gamma^0 E_i(\vec{k}) - \vec{\gamma}\cdot\vec{k} \quad (2.139) \end{aligned}$$

where $n^{(i)}(k)$ are the occupation numbers of mass eigenstates assumed to depend only on the energy. Just as we did in our previous analysis it proves convenient to write the above correlator in the following form

$$\begin{aligned} N_i(\vec{k}) &= \not{Q}_i + \tilde{M}_i \quad (2.140) \\ \not{Q}_i &= \gamma^0 Q_i^0 - \vec{\gamma}\cdot\vec{Q}_i, \quad (2.141) \\ Q_i^0 &= \frac{1}{2}\left[n^{(i)}(k) + \left(1 - \bar{n}^{(i)}(k)\right)\right], \quad (2.142) \\ \vec{Q}_i &= \frac{\vec{k}}{2E_i(k)}\left[n^{(i)}(k) - \left(1 - \bar{n}^{(i)}(k)\right)\right], \quad (2.143) \\ \tilde{M}_i &= \frac{M_i}{2E_i(k)}\left[n^{(i)}(k) - \left(1 - \bar{n}^{(i)}(k)\right)\right]. \quad (2.144) \end{aligned}$$

Since the density matrix commutes with the full Hamiltonian, the distribution functions of the

flavor eigenstates do not depend on time. Following the procedure detailed above we find the following results

$$
\begin{aligned}
n^{(e)}(k) &= \frac{C^2}{2}\left[\left(1+\frac{k^2+m_eM_1}{\omega_e(k)E_1(k)}\right)n^{(1)}(k)+\left(1-\frac{k^2+m_eM_1}{\omega_e(k)E_1(k)}\right)\left(1-\bar{n}^{(1)}(k)\right)\right] \\
&\quad +\frac{S^2}{2}\left[\left(1+\frac{k^2+m_eM_2}{\omega_e(k)E_2(k)}\right)n^{(2)}(k)+\left(1-\frac{k^2+m_eM_2}{\omega_e(k)E_2(k)}\right)\left(1-\bar{n}^{(2)}(k)\right)\right] \qquad (2.145) \\
\bar{n}^{(e)}(k) &= 1-\frac{C^2}{2}\left[\left(1-\frac{k^2+m_eM_1}{\omega_e(k)E_1(k)}\right)n^{(1)}(k)+\left(1+\frac{k^2+m_eM_1}{\omega_e(k)E_1(k)}\right)\left(1-\bar{n}^{(1)}(k)\right)\right] \\
&\quad -\frac{S^2}{2}\left[\left(1-\frac{k^2+m_eM_2}{\omega_e(k)E_2(k)}\right)n^{(2)}(k)+\left(1+\frac{k^2+m_eM_2}{\omega_e(k)E_2(k)}\right)\left(1-\bar{n}^{(2)}(k)\right)\right] \qquad (2.146)
\end{aligned}
$$

Using the relations given by eqn. (2.127) we find to leading order in $\Delta M^2/\bar{M}^2$

$$
\begin{aligned}
n^{(e)}(k) &= C^2n^{(1)}(k)+S^2n^{(2)}(k)+\mathcal{O}\left(\frac{\Delta M^2}{4\bar{M}^2}\right)^2 \qquad (2.147) \\
n^{(\mu)}(k) &= S^2n^{(1)}(k)+C^2n^{(2)}(k)+\mathcal{O}\left(\frac{\Delta M^2}{4\bar{M}^2}\right)^2 \\
\bar{n}^{(e)}(k) &= C^2\bar{n}^{(1)}(k)+S^2\bar{n}^{(2)}(k)+\mathcal{O}\left(\frac{\Delta M^2}{4\bar{M}^2}\right)^2 \\
\bar{n}^{(\mu)}(k) &= S^2\bar{n}^{(1)}(k)+C^2\bar{n}^{(2)}(k)+\mathcal{O}\left(\frac{\Delta M^2}{4\bar{M}^2}\right)^2 \qquad (2.148)
\end{aligned}
$$

2.5 "EFFECTIVE" (FREE) FIELD THEORY DESCRIPTION

Let us summarize the lessons learned in the analysis of the previous section in order to establish a set of criteria with which to develop an effective description of the dynamics in the case in which the mass eigenstates are nearly degenerate as confirmed by the experimental situation or in the relativistic case.

- For nearly degenerate mass eigenstates there is a hierarchy of scales determined by i) k_F or temperature (T), ii) the average mass $\bar{M}$ and iii) the mass difference M_1-M_2. The experimental situation seems to confirm the near degeneracy with $|M_1-M_2|\ll\bar{M}$, therefore at least two scales are widely separated. Furthermore *if* k_F and or T (temperature) are such that $k_F;T\gg\bar{M}$ which describes a relativistic case, then all three scales are widely separated with the hierarchy $k_F,T\gg\bar{M}\gg|M_1-M_2|$. The dynamics studied above reveals all three scales.

- The time evolution of the distribution functions, flavor asymmetry and off-diagonal correlators all feature terms that oscillate with the frequencies $E_1(k) + E_2(k)$, $2E_{1,2}(k)$, and also terms which oscillate with the difference $E_1(k) - E_2(k)$. The former arise from the interference between particle and antiparticle states of equal or different masses and determine the short time scales $t \lesssim 1/\bar{M}$, while the latter arise from interference between particle states (or antiparticle states) of different masses and determine the long time scales $t \gtrsim \bar{M}/\Delta M^2$. The terms that oscillate with the fast time scales average out on these fast scales and their coefficients are of order $\Delta M^2/\bar{M}^2$ and hence small in the nearly degenerate case. These coefficients result from the overlap between positive and negative energy spinors of slightly different masses. The coefficients of the terms that oscillate on the long time scale are of $\mathcal{O}(1)$ and result from the overlap between positive energy spinors (or between negative energy spinors) of different masses.

- The contributions to the distribution functions and off-diagonal correlators from the terms with fast and slow oscillations are *comparable* within the short time scale $t \lesssim 1/\bar{M}$ but for times longer than this scale the contributions from the terms with fast oscillations are suppressed with respect to those with slow oscillations at least by $\mathcal{O}\left(\frac{\Delta M^2}{4\bar{M}^2}\right)^2$.

We seek to obtain a description of the oscillation dynamics on scales much larger than $1/\bar{M}$ when the contribution from the fast oscillations have averaged out to quantities that are proportional to powers of the small ratio $\frac{\Delta M^2}{4\bar{M}^2}$ and can therefore be neglected in the nearly degenerate case.

In the nearly degenerate case $\Delta M^2/\bar{M}^2 \ll 1$ the masses $m_e, m_\mu, M_1, M_2 \sim \bar{M}$ (see eqns. (2.99),(2.127)), thus in order to isolate the leading order terms as well as to understand corrections in the degeneracy parameter $\Delta M^2/\bar{M}^2$ it proves convenient to expand the positive and negative energy spinors in terms of this small parameter. A straightforward computation in the standard Dirac representation of the Dirac gamma matrices leads to the following result for the flavor positive and negative energy spinors (see eqn. (2.6))

$$\begin{aligned} U^{(\alpha)}_{\vec{k},\lambda} &= \left[1 \pm \frac{\Delta M^2}{4\bar{M}^2}\frac{\bar{M}}{\bar{E}(k)}\cos(2\theta)\left(\frac{\gamma^0\bar{E}(k) - \bar{M}}{2\bar{E}(k)}\right) + \mathcal{O}\left(\frac{\Delta M^2}{4\bar{M}^2}\right)^2\right]\mathcal{U}_{\vec{k},\lambda} \\ V^{(\alpha)}_{-\vec{k},\lambda} &= \left[1 \mp \frac{\Delta M^2}{4\bar{M}^2}\frac{\bar{M}}{\bar{E}(k)}\cos(2\theta)\left(\frac{\gamma^0\bar{E}(k) + \bar{M}}{2\bar{E}(k)}\right) + \mathcal{O}\left(\frac{\Delta M^2}{4\bar{M}^2}\right)^2\right]\mathcal{V}_{\vec{k},\lambda} \end{aligned} \tag{2.149}$$

with

$$\bar{E}(k) = \sqrt{k^2 + \bar{M}^2} \tag{2.150}$$

and the upper sign corresponds to $\alpha = e$ and the lower sign to $\alpha = \mu$. The spinors $\mathcal{U}_{\vec{k},\lambda}$, $\mathcal{V}_{\vec{k},\lambda}$ are positive and negative energy solutions respectively of the Dirac equation with mass $\bar{M}$ with unit normalization. Similarly for the positive and negative energy spinors associated with the mass eigenstates $F^{(i)}_{\vec{k},\lambda}; G^{(i)}_{-\vec{k},\lambda}$ (see eqn. (2.10)), we find

$$\begin{aligned} F^{(i)}_{\vec{k},\lambda} &= \left[1 \pm \frac{\Delta M^2}{4\bar{M}^2}\frac{\bar{M}}{\bar{E}(k)}\left(\frac{\gamma^0\bar{E}(k) - \bar{M}}{2\bar{E}(k)}\right) + \mathcal{O}\left(\frac{\Delta M^2}{4\bar{M}^2}\right)^2\right]\mathcal{U}_{\vec{k},\lambda} \\ G^{(i)}_{-\vec{k},\lambda} &= \left[1 \mp \frac{\Delta M^2}{4\bar{M}^2}\frac{\bar{M}}{\bar{E}(k)}\left(\frac{\gamma^0\bar{E}(k) + \bar{M}}{2\bar{E}(k)}\right) + \mathcal{O}\left(\frac{\Delta M^2}{4\bar{M}^2}\right)^2\right]\mathcal{V}_{\vec{k},\lambda} \end{aligned} \tag{2.151}$$

with the same spinors $\mathcal{U}_{\vec{k},\lambda}; \mathcal{V}_{\vec{k},\lambda}$, where the upper sign corresponds to $i = 1$ and the lower sign to $i = 2$.

It is clear from the approximations (2.149) and (2.151) that the overlap between positive and negative energy spinors of different masses is $\mathcal{O}\left(\frac{\Delta M^2}{4\bar{M}^2}\right)^2$. For times much larger than the fast time scale, the corrections to the spinors are subdominant and can be neglected and the fields associated with the flavor and mass eigenstates are expanded as

$$\nu_\alpha(\vec{k},t) = \sum_\lambda \left(\alpha^{(\alpha)}_{\vec{k},\lambda}(t)\,\mathcal{U}_{\vec{k},\lambda} + \beta^{(\alpha)\dagger}_{-\vec{k},\lambda}(t)\,\mathcal{V}_{-\vec{k},\lambda}\right) + \mathcal{O}\left(\frac{\Delta M^2}{4\bar{M}^2}\right) \tag{2.152}$$

$$\psi_i(\vec{k},t) = \sum_\lambda \left(a^{(i)}_{\vec{k},\lambda}\,\mathcal{U}_{\vec{k},\lambda}\,e^{-iE_i(k)t} + b^{(i)\dagger}_{-\vec{k},\lambda}\,\mathcal{V}_{-\vec{k},\lambda}\,e^{iE_i(k)t}\right) + \mathcal{O}\left(\frac{\Delta M^2}{4\bar{M}^2}\right). \tag{2.153}$$

We can now find the relation between the creation and annihilation operators of flavor states and those of mass eigenstates by using eqn. (2.2), to leading order in the degeneracy parameter we find

$$\alpha^{(e)}_{\vec{k},\lambda}(t) = Ca^{(1)}_{\vec{k},\lambda}\,e^{-iE_1(k)t} + Sa^{(2)}_{\vec{k},\lambda}\,e^{-iE_2(k)t} \tag{2.154}$$

$$\alpha^{(\mu)}_{\vec{k},\lambda}(t) = Ca^{(2)}_{\vec{k},\lambda}\,e^{-iE_2(k)t} - Sa^{(1)}_{\vec{k},\lambda}\,e^{-iE_1(k)t} \tag{2.155}$$

where we have neglected terms of $\mathcal{O}\left(\frac{\Delta M^2}{4\bar{M}^2}\right)$, and similar relations hold for the annihilation operators of the respective antiparticles $\beta^{(\alpha)}_{\vec{k},\lambda}(t)$. It is clear that the approximations leading to the relations

(2.154) and (2.155) are more generally valid not only in the nearly degenerate case but also in the relativistic case $k \gg M_{1,2}$ regardless of the value of the mass difference, since in this case the common spinors are those of massless Dirac fermions in all cases.

In this approximation, the evolution equation for the Heisenberg operators $\alpha^{(\alpha)}_{\vec{k},\lambda}(t)$ does *not* follow directly from any Dirac equation, but can be obtained straightforwardly by taking time derivatives of these operators in eqns. (2.154,2.155) and using the relations (2.154,2.155) to re-write the result in terms of the operators themselves. In the leading order approximation particles and antiparticles do not mix since the overlap between the spinors $\mathcal{U}_{\vec{k},\lambda}$ and $\mathcal{V}_{-\vec{k},\lambda}$ vanishes (in free field theory) and a straightforward calculation leads to the following equations of motion

$$i\frac{d}{dt}\begin{pmatrix} \alpha^{(e)}_{\vec{k},\lambda}(t) \\ \alpha^{(\mu)}_{\vec{k},\lambda}(t) \end{pmatrix} = \left[\bar{E}(k)\begin{pmatrix} 1 & 0 \\ 0 & 1 \end{pmatrix} - \Omega(k)\begin{pmatrix} -\cos(2\theta) & \sin(2\theta) \\ \sin(2\theta) & \cos(2\theta) \end{pmatrix}\right]\begin{pmatrix} \alpha^{(e)}_{\vec{k},\lambda}(t) \\ \alpha^{(\mu)}_{\vec{k},\lambda}(t) \end{pmatrix} \tag{2.156}$$

with

$$\bar{E}(k) = \frac{1}{2}(E_1(k)+E_2(k)) = \sqrt{k^2+\bar{M}^2} + \mathcal{O}\left(\frac{\Delta M^2}{4\bar{M}^2}\right) \tag{2.157}$$

$$\Omega(k) = \frac{1}{2}(E_1(k)-E_2(k)) = \frac{\Delta M^2}{4\bar{E}(k)} + \mathcal{O}\left(\frac{\Delta M^2}{4\bar{M}^2}\right) \tag{2.158}$$

and a similar equation of motion for the annihilation operators for flavor antiparticles $\beta^{(\alpha)}_{\vec{k},\lambda}(t)$. These equations of motion look to be the familiar ones for neutrino oscillations[4, 9, 10, 11, 12, 50, 60, 62], but these are equations for the Heisenberg field operators, rather than for the single particle wave-functions. Once the time evolution of the operators is found, we can find the time evolution of *any multiparticle state*. Furthermore the regime of validity of these equations is more general, they are valid *either* in the nearly degenerate case $\Delta M^2/\bar{M}^2 \ll 1$ for any value of the momentum, or in the relativistic limit for arbitrary value of the masses provided that $k \gg M_1, M_2$.

Inverting the relation between the operators for flavor and mass states at the initial time, namely writing the operators $a^{(i)}_{\vec{k},\lambda}$ in terms of $\alpha^{(\alpha)}_{\vec{k},\lambda}(0)$ using eqns. (2.154, 2.155) at $t=0$, we find (again to leading order)

$$\alpha^{(e)}_{\vec{k},\lambda}(t) = \alpha^{(e)}_{\vec{k},\lambda}(0)\left[C^2e^{-iE_1(k)t} + S^2e^{-iE_2(k)t}\right] + SC\ \alpha^{(\mu)}_{\vec{k},\lambda}(0)\left[e^{-iE_2(k)t} - e^{-iE_1(k)t}\right] \tag{2.159}$$

$$\alpha^{(\mu)}_{\vec{k},\lambda}(t) = \alpha^{(\mu)}_{\vec{k},\lambda}(0)\left[C^2e^{-iE_2(k)t} + S^2e^{-iE_1(k)t}\right] + SC\ \alpha^{(e)}_{\vec{k},\lambda}(0)\left[e^{-iE_2(k)t} - e^{-iE_1(k)t}\right] \tag{2.160}$$

For the antiparticle operators we find the same equations with $\alpha^{(\alpha)}_{\vec{k},\lambda} \to \beta^{(\alpha)}_{\vec{k},\lambda}$.

The Heisenberg field operators given by eqns. (2.159,2.160) (and the equivalent for the antiparticle operators) are the solutions of the equations of motion (2.156).

The time evolution of the distribution functions in an initial density matrix that is diagonal in the flavor basis follows from a straightforward calculation using the above time evolution. We find

$$\begin{aligned} n^{(e)}(k,t) &= \langle \alpha^{(e)\dagger}_{\vec{k},\lambda}(t)\alpha^{(e)}_{\vec{k},\lambda}(t)\rangle \\ &= n^{(e)}(k) - \frac{1}{2}\sin^2(2\theta)\left(n^{(e)}(k) - n^{(\mu)}(k)\right)\left[1-\cos[(E_1(k)-E_2(k))t]\right] \quad (2.161) \\ n^{(\mu)}(k,t) &= \langle \alpha^{(\mu)\dagger}_{\vec{k},\lambda}(t)\alpha^{(\mu)}_{\vec{k},\lambda}(t)\rangle \\ &= n^{(\mu)}(k) + \frac{1}{2}\sin^2(2\theta)\left(n^{(e)}(k) - n^{(\mu)}(k)\right)\left[1-\cos[(E_1(k)-E_2(k))t]\right] \quad (2.162) \end{aligned}$$

The distribution functions for antiparticles to leading order is obtained from the above results by the replacements $n^{(\alpha)} \to \bar{n}^{(\alpha)}$. A straightforward calculation following the above steps leads to the result

$$\begin{aligned} & < \nu^\dagger_e(\vec{k},t)\nu_\mu(\vec{k},t) > \\ = & -\sin(2\theta)\Bigg\{2\cos(2\theta)\left[\left(n^{(e)}(k)-\bar{n}^{(e)}(k)\right)-\left(n^{(\mu)}(k)-\bar{n}^{(\mu)}(k)\right)\right]\sin^2\left[(E_1(k)-E_2(k))\,\frac{t}{2}\right] \\ & -i\left[\left(n^{(e)}(k)+\bar{n}^{(e)}(k)\right)-\left(n^{(\mu)}(k)+\bar{n}^{(\mu)}(k)\right)\right]\sin\left[(E_1(k)-E_2(k))\,t\right]\Bigg\} \quad (2.163) \end{aligned}$$

The results (2.161) and (2.163) reproduce the leading order expressions found in the previous section, eqns. (2.136,2.137). Thus this "effective" free field theory description reproduces the leading order results either in the nearly degenerate case $\Delta M^2 \ll \bar{M}^2$ or in the relativistic case. Furthermore either the effective equations of motion (2.156) or alternatively the time evolution (2.159,2.160) (and those for antiparticles) lead to a set of closed evolution equations for *bilinears*. These are most conveniently written by introducing a fiducial spin $\overrightarrow{S} = (S_x, S_y, S_z)$ with the following components

$$\begin{aligned} S_x(\vec{k},\lambda;t) &= i\left(\alpha^{(\mu)\dagger}_{\vec{k},\lambda}(t)\alpha^{(e)}_{\vec{k},\lambda}(t) - \alpha^{(e)\dagger}_{\vec{k},\lambda}(t)\alpha^{(\mu)}_{\vec{k},\lambda}(t)\right) \quad (2.164) \\ S_y(\vec{k},\lambda;t) &= \left(\alpha^{(\mu)\dagger}_{\vec{k},\lambda}(t)\alpha^{(e)}_{\vec{k},\lambda}(t) + \alpha^{(e)\dagger}_{\vec{k},\lambda}(t)\alpha^{(\mu)}_{\vec{k},\lambda}(t)\right) \quad (2.165) \\ S_z(\vec{k},\lambda;t) &= \left(\alpha^{(e)\dagger}_{\vec{k},\lambda}(t)\alpha^{(e)}_{\vec{k},\lambda}(t) - \alpha^{(\mu)\dagger}_{\vec{k},\lambda}(t)\alpha^{(\mu)}_{\vec{k},\lambda}(t)\right) \quad (2.166) \end{aligned}$$

and a fiducial magnetic field $\overrightarrow{B} = (B_x, B_y, B_z)$ with components

$$\overrightarrow{B}(k) = 2\Omega(k)(0, -\sin(2\theta), \cos(2\theta)) \tag{2.167}$$

in terms of which the equations for the bilinears are akin to the Bloch equations for a spin $\overrightarrow{S}$ precessing in the magnetic field $\overrightarrow{B}$ namely

$$\frac{d\ \overrightarrow{S}(\vec{k}, \lambda; t)}{dt} = \overrightarrow{S}(\vec{k}, \lambda; t) \times \overrightarrow{B}(k) \tag{2.168}$$

The antiparticle operators obey independently a similar set of equations. To leading order in $\Delta M^2/\bar{M}^2$ there is no mixing between particles and antiparticles (suppressed by *two* powers of this small ratio), therefore the number of electron plus muon neutrinos is conserved independently of that for antineutrinos, namely

$$\frac{d}{dt}\left(\alpha^{(e)\dagger}_{\vec{k},\lambda}(t)\alpha^{(e)}_{\vec{k},\lambda}(t) + \alpha^{(\mu)\dagger}_{\vec{k},\lambda}(t)\alpha^{(\mu)}_{\vec{k},\lambda}(t)\right) = 0 \tag{2.169}$$

and similarly for the operators $\beta^{(\alpha)}_{\vec{k},\lambda}$. The set of equations above, for Heisenberg operators is akin to the equations of motion for the "single particle" density matrix obtained in ref.[69], which are equivalent to those investigated in refs.[66, 67, 70, 71, 73].

In the study of synchronized oscillations[69, 71, 73, 72], a self-consistent Hartree-Fock approximation is introduced which leads to a Bloch equation like (2.168) but where the magnetic field $\overrightarrow{B}$ acquires a correction from the self-consistent Hartree terms which arise from forward scattering off neutrinos in the medium.

This effective formulation neglects the dynamics of flavor pair production discussed above since such phenomenon is suppressed by two powers of the small ratio $\Delta M^2/\bar{M}^2$.

2.5.1 Propagators: non-equilibrium correlation functions

While the set of equations of motion (2.156) and (2.168) are reminiscent of those for the single particle wave functions and the single particle density matrix, in fact there is more information in the "effective" free field theory description afforded by the *operator* equations (2.156) and (2.168) combined with the field expansion (2.152). In particular, inserting the solution of the equations of motion (2.159, 2.160) (and the similar ones for the antiparticles) into the expansion (2.152) for the field operators allow us to obtain *any* correlation function in the free field theory at equal *or different times*. These are the building blocks of any systematic perturbative expansion of processes

of weak interactions. In particular the Feynman propagators, which are an essential ingredient in *any* calculation that involves neutrinos are given by

$$\mathcal{S}^F_{(\alpha,\alpha')}(\vec{x}-\vec{x}';t,t') = -i\int \frac{d^3k}{(2\pi)^3} e^{i\vec{k}\cdot(\vec{x}-\vec{x}')} \left[\langle \nu_{(\alpha)}(\vec{k},t)\bar{\nu}_{(\alpha')}(\vec{k},t')\rangle \Theta(t-t') - \langle \bar{\nu}_{(\alpha')}(\vec{k},t')\nu_{(\alpha)}(\vec{k},t)\rangle \Theta(t'-t)\right] \tag{2.170}$$

where the expectation values are in the initial density matrix, which is taken to be diagonal in the flavor basis in the present discussion.

The correlation (Wightmann) functions that enter in the Feynman propagator are found by using the leading order expansion (2.152) with the time evolution of the creation and annihilation operators given by eqns. (2.159,2.160) and similar ones for $\beta^{(\alpha)}_{\vec{k},\lambda}(t)$. With the purpose of highlighting the fast and slow time scales in the propagators, it is convenient to introduce the following functions that evolve on the slow time scale

$$f_k(t) = \cos[\Omega(k)t] - i\ \cos(2\theta)\sin[\Omega(k)t] \tag{2.171}$$

$$g_k(t) = i\ \sin(2\theta)\sin[\Omega(k)t] \tag{2.172}$$

in terms of which the Heisenberg creation and annihilation operators of flavor states are written as follows

$$\alpha^{(e)}_{\vec{k},\lambda}(t) = e^{-i\bar{E}(k)t}\left[\alpha^{(e)}_{\vec{k},\lambda}(0)f_k(t) + \alpha^{(\mu)}_{\vec{k},\lambda}(0)g_k(t)\right] \tag{2.173}$$

$$\alpha^{(\mu)}_{\vec{k},\lambda}(t) = e^{-i\bar{E}(k)t}\left[\alpha^{(\mu)}_{\vec{k},\lambda}(0)f^*_k(t) + \alpha^{(e)}_{\vec{k},\lambda}(0)g_k(t)\right] \tag{2.174}$$

and similarly for the antiparticle Heisenberg operators $\beta^{(\alpha)}_{\vec{k},\lambda}(t)$.

A straighforward calculation of the Wightman functions yields the following results

$$\begin{aligned}\langle \nu_{(e)}(\vec{k},t)\bar{\nu}_{(e)}(\vec{k},t')\rangle = {} & \left(\frac{\not{k}+\bar{M}}{2\bar{E}(k)}\right) e^{-i\bar{E}(k)(t-t')}\left[(1-n^{(e)}(k))f_k(t)f^*_k(t') + (1-n^{(\mu)}(k))g_k(t)g^*_k(t')\right] + \\ & \left(\gamma^0\frac{\not{k}-\bar{M}}{2\bar{E}(k)}\gamma^0\right) e^{i\bar{E}(k)(t-t')}\left[\bar{n}^{(e)}(k)f^*_k(t)f_k(t') + \bar{n}^{(\mu)}(k)g^*_k(t)g_k(t')\right]\end{aligned} \tag{2.175}$$

$$\begin{aligned}\langle \bar{\nu}_{(e)}(\vec{k},t')\nu_{(e)}(\vec{k},t)\rangle = {} & \left(\frac{\not{k}+\bar{M}}{2\bar{E}(k)}\right) e^{-i\bar{E}(k)(t-t')}\left[n^{(e)}(k)f_k(t)f^*_k(t') + n^{(\mu)}(k)g_k(t)g^*_k(t')\right] + \\ & \left(\gamma^0\frac{\not{k}-\bar{M}}{2\bar{E}(k)}\gamma^0\right) e^{i\bar{E}(k)(t-t')}\left[(1-\bar{n}^{(e)}(k))f^*_k(t)f_k(t') + (1-\bar{n}^{(\mu)}(k))g^*_k(t)g_k(t')\right]\end{aligned} \tag{2.176}$$

where

$$\not{k} \equiv \gamma^0 \bar{E}(k) - \vec{\gamma}\cdot\vec{k} \tag{2.177}$$

The Wightman function for the muon neutrino is obtained from that of the electron by the replacement $n^{(e)}(k), \bar{n}^{(e)}(k) \to n^{(\mu)}(k), \bar{n}^{(\mu)}(k)$, *and* $f_k \longleftrightarrow f_k^*$. The off-diagonal Wightman functions are given by

$$\begin{aligned}
\langle \nu_{(\mu)}(\vec{k},t)\bar{\nu}_{(e)}(\vec{k},t')\rangle &= \left(\frac{\not{k}+\bar{M}}{2\bar{E}(k)}\right) e^{-i\bar{E}(k)(t-t')}\left[(1-n^{(\mu)}(k))f_k^*(t)g_k^*(t') + (1-n^{(e)}(k))f_k^*(t')g_k(t)\right] + \\
&\left(\gamma^0\frac{\not{k}-\bar{M}}{2\bar{E}(k)}\gamma^0\right) e^{i\bar{E}(k)(t-t')}\left[\bar{n}^{(\mu)}(k)g_k(t')f_k(t) + \bar{n}^{(e)}(k)g_k^*(t)f_k(t')\right] \qquad (2.178) \\
\langle \bar{\nu}_{(e)}(\vec{k},t')\nu_{(\mu)}(\vec{k},t)\rangle &= \left(\frac{\not{k}+\bar{M}}{2\bar{E}(k)}\right) e^{-i\bar{E}(k)(t-t')}\left[n^{(\mu)}(k)f_k^*(t)g_k^*(t') + n^{(e)}(k)f_k^*(t')g_k(t)\right] + \\
&\left(\gamma^0\frac{\not{k}-\bar{M}}{2\bar{E}(k)}\gamma^0\right) e^{i\bar{E}(k)(t-t')}\left[(1-\bar{n}^{(\mu)}(k))g_k(t')f_k(t) + (1-\bar{n}^{(e)}(k))g_k^*(t)f_k(t')\right] \qquad (2.179)
\end{aligned}$$

the other off-diagonal Wightmann function is obtained from the one above by replacing $n^{(e)} \longleftrightarrow n^{(\mu)}$ *and* $f_k \longleftrightarrow f_k^*$.

We have specifically separated the "fast" evolution, encoded in the exponentials $e^{i\pm\bar{E}(k)(t-t')}$ and the "slow" evolution encoded in the functions $f_k; g_k$ which oscillate with the small frequency $\Omega(k) \sim \Delta M^2/2\bar{E}(k)$. We emphasize that the propagators above are functions not only of the difference $(t-t')$ but also of the *sum* $(t+t')$ which reveals a truly *non-equilibrium* evolution. The manifest lack of time translational invariance reflects the fact that the density matrix which is diagonal in the flavor representation *does not commute* with the time evolution operator.

The discussion at the beginning of this section points out that these propagators are valid on time scales $t, t' \gg 1/\bar{M}$, for which the corrections arising from the interference between particle and antiparticle can be neglected. Therefore the correlation functions obtained from the effective field theory must be understood as being averaged over the fast time scales and their validity is restricted to slow time scales.

The *free field theory* propagators obtained above provide the main ingredients to carry out a study of the weak interactions in a neutrino background in a loop expansion.

2.6 CONCLUSIONS

Our focus was to study the evolution of a dense and or hot gas of flavor neutrinos as a consequence of oscillations and mixing. The goal was to establish an understanding of the dynamics directly from the underlying quantum field theory, beginning with the simplest case of free field theory and restricted to the two flavor case.

Such study leads to a deeper understanding of the various approximations invoked in the literature as well as recognizing the potential corrections. Even at the level of free field theory, which must be the starting point of any program to study the physics of oscillations and mixing in the weak interactions, this study reveals a wealth of dynamical phenomena that has not been explored before within the context of neutrino oscillations in a medium with neutrinos at finite density and temperature.

Our results can be summarized as follows:

- A hierarchy of time scales emerges associated with different interference phenomena. Oscillations on fast time scales $t < 1/\bar{M}$ are associated with the interference between particles and antiparticles while oscillations on slow time scales $t > \bar{M}/\Delta M^2$ arise from the interference between particle (or antiparticle) states with different masses. Observationally the situation for two flavors is that of near degeneracy, which entails that these time scales are widely separated. Furthermore in the relativistic limit with typical energy $\bar{E} \gg M_1, M_2$ there is an even shorter time scale $t \sim 1/\bar{E}$.
- The terms that oscillate on fast scales feature coefficients that are determined by the overlap of positive and negative frequency wave functions of different masses. In the relativistic limit or in the case of near degeneracy as suggested by the recent observations, these terms are of order $(\Delta M^2/\bar{M}^2)^2 \sim 10^{-6}$ (or smaller in the relativistic case), while the coefficients of terms that oscillate on the slow scales are of $\mathcal{O}(1)$ in terms of this ratio. During the short time scales both contributions are comparable, but for $t >> 1/\bar{M}$ the contribution from the overlap between particle and antiparticle states becomes subdominant being at least a factor $(\Delta M^2/\bar{M}^2)^2 \sim 10^{-6}$ smaller than the oscillations on the slow time scale. For the values of $\bar{M}$ consistent with the recent bounds[8] the scale for fast oscillations is $\sim 10^{-15}s$ these are clearly too fast for relevant processes during BBN or neutrino processes in astrophysics, but may be relevant for early universe cosmology. Of course this possibility requires further and deeper studies.

- An initial flavor asymmetry relaxes to equilibrium via dephasing between modes that are not Pauli blocked with a power law $1/t$ on slow time scales $t > k_F/\Delta m^2$ in the relativistic case $k_F >> \bar{M}$. We have obtained exact as well as approximate expressions for the time evolution of the distribution functions and off diagonal densities and discussed their asymptotic behavior, all of which display Pauli blocking between different flavors (see eqns. (2.128-2.131). For completeness we have also studied the case of an equilibrated gas of mass eigenstates which describes a situation of equilibrium in absence of interactions. The non-equilibrium oscillation dynamics leads to the production of particle-antiparticle pairs of flavored neutrinos with typical momenta $k \sim \bar{M}$. Since this phenomenon is a direct consequence of the overlap between particle and antiparticle states the pair yield is suppressed by the factor $(\Delta M^2/\bar{M}^2)^2$.
- The wide separation between the different time scales allows to describe the dynamics on the longer time scales in terms of an "effective" theory. In this effective description the Heisenberg creation and annihilation field operators for flavor neutrinos and antineutrinos obey the familiar Bloch type equations and the spinor structure is common to both flavors as well as the mass eigenstates. This effective description allows to obtain in a simple manner the dynamics of the distribution functions, off diagonal correlation functions and the *non-equilibrium* propagators, all of which must be understood as an average over the fast time scales and valid only on the slow scales.

While we have focused on the evolution of a gas of flavor neutrinos as an *initial value problem* we have not discussed how the initial state is "prepared". This is an important aspect of the physics of neutrino mixing and the weak interactions, since weak interactions only produce flavor states the initial state (or density matrix) must be "prepared" by weak interaction processes that occur on time scales much shorter than those in which such state will relax either via collisions or by oscillations. Clearly we have nothing to say yet on this aspect which deserves a thorough study.

Another aspect that deserves attention is that of the corrections to the "effective" theory described above. These corrections entail powers of the ratios that are small either in the nearly degenerate case or in the relativistic limit. In perturbation theory in the weak interactions, these "small" corrections could conceivably be comparable to perturbative corrections in G_F the Fermi coupling, in which case the terms neglected in the effective theory must be kept on the same footing as the contributions in the weak coupling in the perturbative expansion. Clearly such possibility must be evaluated for the particular situation under consideration.

While we have focused on the dynamics in free field theory, the results will likely be valid in

the interacting case in the case of a low density neutrino gas (or low temperatures). Under these circumstances the corrections to the evolution equations associated with forward scattering off the neutrino background (mean field), which is of order G_F would be much smaller than $\Delta M^2/\bar{M}$ and the free field theory results for the evolution of the asymmetry may very well be valid.

3.0 NEUTRINO OSCILLATIONS IN THE EARLY UNIVERSE

3.1 INTRODUCTION

The full quantum field theory treatment of neutrino mixing in hot and or dense media has not yet received the same level of attention as the more familiar single particle treatment, which however, is not suited when collective many body phenomena become relevant as is typically the case in extreme environments.

Previous quantum field theory studies[14, 57, 93, 94] address either the dispersion relations *or* mixing phenomena under restrictive approximations to lowest order in g^2/M_W^2.

In this chapter, we provide a systematic quantum field theory study of neutrino propagation and oscillations in the early Universe *directly in real time*. Because in the early Universe the lepton asymmetries are expected to be typically of the same order of the baryon asymmetry $\eta_B/\eta_\gamma \sim 10^{-9}$ a consistent description of neutrino propagation and oscillations requires to include corrections non-local in space-time of order g^2/M_W^4 in the dispersion relations[57] *and mixing angles*. We focus our study on the case of two flavors of Dirac neutrinos, taken to be the electron and muon neutrinos, this study can be generalized to more flavors or to Majorana-Dirac mass matrices without any conceptual difficulty.

Our main goals are:

- To provide a systematic and consistent study of the real time dynamics of neutrino oscillation and mixing directly in quantum field theory in conditions of temperature and lepton/neutrino asymmetries applicable to the early Universe prior to the nucleosynthesis era. This is achieved by formulating an initial value problem via linear response and implementing real time field theory methods at finite temperature and density.
- We obtain the dispersion relations and in-medium mixing angles including the *non local* contributions from the neutrino self-energies up to order g^2/M_W^4. Namely we carry out an expansion

of the one-loop self-energy in frequency and momentum to lowest order in $(\omega, k)/M_W$. We find a new contribution which cannot be interpreted as the usual effective potential. These contributions are necessary since the typical asymmetries in the early Universe are very small and these non-local (in space-time) contributions can be of the same order or larger than the local contributions.

- We obtain the in-medium Dirac spinors for both helicities and study the evolution of oscillations and mixing for *both* helicity components directly in real time.
- Two different temperature regimes are studied in detail: i) $m_e \ll T \ll m_\mu$, ii) $m_e, m_\mu \ll T \ll M_W$. The first regime is just prior to big bang nucleosynthesis. Lepton and hadron (proton and neutrons in nuclear statistical equilibrium) or quark asymmetries are included in the one-loop self-energy. We assess in detail the temperature and energy regime for which a resonance in the mixing angle is available in the medium. The second temperature regime is above the QCD phase transition and we include two flavor of (light quarks) with their respective asymmetries. In this regime the mixing angle becomes small. In both cases we also study the mixing and oscillations of positive helicity as well as right handed neutrinos, which are typically neglected in the literature. We also obtain the loop corrections to the *oscillation frequencies* thereby providing a complete description of oscillation and mixing that includes corrections to both the mixing angle and the oscillation frequencies.
- We obtain general oscillation formulae derived directly from the real time evolution in quantum field theory. These formulae reveal the limit in which the usual quantum mechanical single particle description is reliable as well as the corrections to them.

Main Approximations:

Since our study relies on a one-loop self-energy computation including leptons and neutrinos, the inclusion of a neutrino background must necessarily imply some approximations for consistency.

We do not *yet* consider absorptive contributions, which in the temperature regime studied here are of two-loop order, postponing the study of the interplay between oscillations and relaxation to a forthcoming article.

Since we obtain the non-local (in space-time) contributions from the one-loop self energy we must address the issue of the neutrino propagators in the neutral current contributions. Because of mixing, the neutrino propagator in the flavor basis, in which the weak interactions are diagonal, does not correspond to the propagation of mass eigenstates and in principle the non-equilibrium

propagators obtained in ref.[95] must be used. The question of equilibration of a neutrino gas with mixing is one of time scales: the weak interactions are diagonal in the flavor basis, therefore weak processes tend to equilibrate *flavor* neutrinos with a typical weak interaction relaxation rate at high temperature [57] $\Gamma \sim G_F^2\, T^5$. Oscillations, on the other hand mix flavors and tend to redistribute flavor neutrinos into mass eigenstates of energy E on a time scale $\tau_{osc} \sim E/\delta M^2$. Combined fitting of the solar and KamLAND data yield [92] $|\delta M^2| \approx 7.9 \times 10^{-5}\,(eV)^2$, therefore considering $E \sim T$, we find $\Gamma\ \tau_{osc} \sim 10\ (0.1\,T/\mathrm{MeV})^6$. This comparison of time scales suggests that for $T \gtrsim 10\,\mathrm{MeV}$ neutrinos are equilibrated *as flavor eigenstates*. Flavor eigenstates created at local weak interaction vertices will reach thermal equilibrium on time scales far shorter than those required for oscillations into mass eigenstates for temperatures larger than $\sim 10\,\mathrm{MeV}$. Since in a loop integral the typical momenta are of order T, and *assuming* the validity of this estimate, we consider the neutrino propagators in the neutral current self-energy loop to be diagonal in the flavor basis, massless and in thermal equilibrium.

For temperatures $T \lesssim 10\,\mathrm{MeV}$ and certainly below freeze out $T < 1\,\mathrm{MeV}$ a full kinetic description that includes oscillations and expansion[14, 59] is required. The study of the kinetic equations will be the subject of forthcoming work. In this article we restrict our study to the temperature regime $T \gtrsim 10\,\mathrm{MeV}$.

We also *assume* that the lepton and neutrino asymmetries are of the same order as the baryon asymmetry, namely $L_i = (n_i - \bar{n}_i)/n_\gamma \sim 10^{-9}$. For a relativistic species the asymmetry is proportional to $\xi_i\ (1 + \xi_i^2/\pi^2)$ with $\xi_i \equiv \mu_i/T$, therefore under this assumption $\xi_i \sim 10^{-9}$ and we can safely neglect the contribution to the chemical potential in the non-local (in space-time) terms of order g^2/M_W^4.

This chapter is organized as follows: in section 3.2 we obtain the equations of motion for initially prepared neutrino wavepackets by implementing the methods of non-equilibrium field theory and linear response. In section 3.3 we obtain the one-loop self-energy contributions from charged and neutral currents. Section 3.4 is devoted to obtaining the dispersion relations, mixing angles and oscillation time scales in the medium and a study of the possibility of resonances. In section 3.5 we study the real time evolution of neutrino wavepackets as an initial value problem. Section 3.6 presents our conclusions, summarizes our results and presents some conjectures and further questions. The detailed calculation of the self-energy is presented in Appendix A.

3.2 EFFECTIVE DIRAC EQUATION FOR NEUTRINO PROPAGATION IN A MEDIUM

The propagation of a neutrino in a medium is determined by the effective Dirac equation which includes the self-energy corrections. Its solution yields the real time evolution as *an initial value problem*. The correct framework to study the dynamics is the real time formulation of field theory in terms of the closed-time-path integral[83, 84, 85, 86, 87]. In this section we implement this method combined with linear response to obtain the effective equation of motion for an *expectation value* of the neutrino field. The main concept in this approach is the following, consider coupling an external c-number Grassman source to the neutrino field and switching this source adiabatically up to time $t = 0$. This source induces an expectation value of the neutrino field, after switching-off the external source at $t = 0$, the expectation value evolves in time as a solution of the effective Dirac equation in the medium with the initial condition determined by the source term.

The main ingredient in this program is the retarded self-energy which enters in the effective Dirac equation. The real-time formulation of field theory directly leads to causal and retarded equations of motion. It is important to highlight the difference with the S-matrix approach which describes transition amplitudes from in to out states, the real time formulation yields the equations of motion for an *expectation* value and these are fully causal[83, 84, 85, 86, 87].

The self-energy is obtained in the unitary gauge in which only the correct physical degrees of freedom contribute and is manifestly unitary[96]. Previous calculations of the neutrino self-energy in covariant gauges (one of which is the unitary gauge) have proven that although the self-energy does depend on the gauge parameter, the dispersion relations are gauge-invariant [97].

As mentioned above we restrict our discussion to the case of two flavors of Dirac neutrinos, namely the electron and muon neutrinos. The subtle CP violating phases associated with the case of three active neutrinos will not be considered here. However, the method can be generalized to three active neutrinos, sterile neutrinos or even Majorana neutrinos without any conceptual difficulty and will be postponed for further discussion elsewhere.

For Dirac neutrinos, mixing and oscillations can be implemented by a minimal extension of the standard model adding a Dirac mass matrix to the standard model Lagrangian which is off-diagonal in the flavor basis. The relevant part of the Lagrangian density is given by

$$\mathcal{L} = \mathcal{L}^0_\nu + \mathcal{L}^0_W + \mathcal{L}^0_Z + \mathcal{L}_{CC} + \mathcal{L}_{NC}, \tag{3.1}$$

where $\mathcal{L}^0_\nu$ is the free field neutrino Lagrangian minimally modified to include a Dirac mass matrix

$$\mathcal{L}^0_\nu = \overline{\nu}_a \left(i \partial\!\!\!/ \, \delta_{ab} - M_{ab} \right) \nu_b \tag{3.2}$$

with a, b being the flavor indexes. For two flavors of Dirac neutrinos the mass matrix M_{ab} is given by

$$\mathbb{M} = \begin{pmatrix} m_{ee} & m_{e\mu} \\ m_{e\mu} & m_{\mu\mu} \end{pmatrix} , \tag{3.3}$$

$\mathcal{L}^0_{W,Z}$ are the free field lagrangian densities for the vector bosons in the unitary gauge, namely

$$\mathcal{L}^0_W = -\frac{1}{2} \left(\partial_\mu W^+_\nu - \partial_\nu W^+_\mu \right) \left(\partial^\mu W^{-\,\nu} - \partial^\nu W^{-\,\mu} \right) + M^2_W \, W^+_\mu \, W^{-\,\mu} , \tag{3.4}$$

$$\mathcal{L}^0_Z = -\frac{1}{4} \left(\partial_\mu Z_\nu - \partial_\nu Z_\mu \right) \left(\partial^\mu Z^\nu - \partial^\nu Z^\mu \right) + \frac{1}{2} M^2_Z \, Z_\mu \, Z^\mu , \tag{3.5}$$

and the charged and neutral current interaction lagrangian densities are given by

$$\mathcal{L}_{CC} = \frac{g}{\sqrt{2}} \left[\overline{\nu}_a \, \gamma^\mu \, L \, l_a \, W^+_\mu + \bar{l}_a \gamma^\mu \, L \, \nu_a \, W^-_\mu \right] , \tag{3.6}$$

$$\mathcal{L}_{NC} = \frac{g}{2 \cos\theta_w} \left[\overline{\nu}_a \, \gamma^\mu \, L \, \nu_a \, Z_\mu + \overline{f}_a \, \gamma^\mu \, (g^V_a - g^A_a \, \gamma^5) \, f_a \, Z_\mu \right] . \tag{3.7}$$

where $L = (1 - \gamma^5)/2$ is the left-handed chiral projection operator, $g^{V,A}$ are the vector and axial vector couplings for quarks and leptons, l stands for leptons and f generically for the fermion species with neutral current interactions.

For two flavors, the diagonalization of the free field Dirac Lagrangian for neutrinos, (3.2) is achieved by a unitary transformation to mass eigenstates. Considering, flavor and mass eigenstates doublets respectively

$$\begin{pmatrix} \nu_e \\ \nu_\mu \end{pmatrix} \quad , \quad \begin{pmatrix} \nu_1 \\ \nu_2 \end{pmatrix} ,$$

related by unitary transformation

$$\begin{pmatrix} \nu_e \\ \nu_\mu \end{pmatrix} = U \begin{pmatrix} \nu_1 \\ \nu_2 \end{pmatrix} , \tag{3.8}$$

with the unitary transformation given by the 2×2 matrix

$$U = \begin{pmatrix} \cos\theta & \sin\theta \\ -\sin\theta & \cos\theta \end{pmatrix} , \tag{3.9}$$

where θ is the *vacuum* mixing angle.

In the basis of mass eigenstates (ν_1, ν_2) the mass matrix M_{ab} becomes diagonal

$$\begin{pmatrix} M_1 & 0 \\ 0 & M_2 \end{pmatrix} .$$

The elements $m_{ee}, m_{\mu\mu}$ and $m_{e\mu}$ in the mass matrix (3.3) are related to the vacuum mixing angle θ and masses of the propagating mass eigenstates M_1 and M_2 as follows

$$m_{ee} = C^2\, M_1 + S^2\, M_2 \;;\quad m_{\mu\mu} = S^2\, M_1 + C^2\, M_2 \;;\quad m_{e\mu} = -(M_1 - M_2)\, C\, S \;, \tag{3.10}$$

where $C = \cos\theta$ and $S = \sin\theta$.

For later convenience, we introduce

$$\overline{M} = \frac{M_1 + M_2}{2} \quad ; \quad \delta M^2 = M_1^2 - M_2^2 \tag{3.11}$$

The current value for the average of the vacuum masses obtained by WMAP[8] and oscillation parameters from the combined fitting of the solar and KamLAND data are [92]:

$$\overline{M} \approx 0.25\,(eV) \quad ; \quad |\delta M^2| \approx 7.9 \times 10^{-5}\,(eV)^2 \;; \quad \tan^2\theta \approx 0.40 \;. \tag{3.12}$$

For these values of the masses and more generally if there is an almost degeneracy in the hierarchy of neutrino masses the ratio

$$\frac{|\delta M^2|}{\overline{M}^{\,2}} \ll 1 \;. \tag{3.13}$$

The smallness of this ratio in the nearly degenerate case will lead to important simplifications.

Our goal is to obtain the effective Dirac equation for neutrinos propagating in the medium and extract the in-medium mixing angles, propagation frequencies and the wave functions of the propagating modes in the medium. The real-time effective Dirac equation in the medium is derived from linear response by implementing the methods of non-equilibrium quantum field theory described in [87].

Following this approach, we introduce an external Grassmann-valued source that couples linearly to the neutrino field via the lagrangian density

$$\mathcal{L}_S = \overline{\nu}_a\, \eta_a + \overline{\eta}_a\, \nu_a \;. \tag{3.14}$$

whence the total lagrangian density is given by $\mathcal{L} + \mathcal{L}_S$. The external source induces an expectation value for the neutrino field which, in turn, obeys the effective equation of motion with self-energy modifications from the thermal medium [87].

To study the dynamics of the system, it is the *expectation values* rather than the in-out S-matrix elements that are necessary[84]. This requires a generating function for the real-time correlation functions. Denoting generically by Φ the fields (fermions, or gauge bosons), a path integral representation of this generating functional is given by

$$\mathcal{Z}[j^+, j^-] = \int D\Phi^+ \, D\Phi^- e^{i \int (\mathcal{L}[\Phi^+, j^+] - \mathcal{L}[\Phi^-, j^-])} \,, \tag{3.15}$$

and the path integrations over the fields $\Phi^\pm$ will be taken along the forward $(+)$ and backward $(-)$ time branches, in the presence of the sources $j^\pm$ [83, 84, 85, 86, 87]. Here, the sources $j^\pm$ are coupled linearly to the fields $\Phi^\pm$ and thus the real-time correlation functions can be obtained from the functional derivatives of this generating functional with respect to these sources. Functional derivatives with respect to j^+ and j^- give the time-ordered and anti-time-ordered correlation functions respectively.

The sources $j^\pm$ are introduced to compute the real-time correlation functions and will be set to zero after the calculations. However, the external Grassman source η and hence the expectation value induced to the neutrino field will remain the same along both time branches $(\pm)$. For further discussions on the general method, see references [83, 85, 86, 87].

The equation of motion for the expectation value of the neutrino field induced by the external Grassman source is derived by shifting the field

$$\nu_a^\pm = \psi_a + \Psi_a^\pm \quad , \quad \psi_a = \langle \nu_a^\pm \rangle \quad , \quad \langle \Psi_a^\pm \rangle = 0 \,, \tag{3.16}$$

and imposing $\langle \Psi_a^\pm \rangle = 0$ order by order in the perturbation theory [85, 86, 87]. Carrying out this implementation up to one-loop order, we find the following equation of motion

$$\Big(i \not{\partial} \, \delta_{ab} - M_{ab} + \Sigma_{ab}^{tad} \, L \Big) \, \psi_b(\vec{x}, t) + \int d^3x' \int dt' \, \Sigma_{ab}^{ret}(\vec{x} - \vec{x}', t - t') \, \psi_b(\vec{x}', t') = -\eta_a(\vec{x}, t), \tag{3.17}$$

where $\Sigma_{ab}^{ret}(\vec{x} - \vec{x}', t - t')$ is the real-time retarded self-energy given by the exchange one-loop contributions, the first two diagrams displayed in Fig. 3.1 and $\Sigma_{ab}^{tad} \, L$ is the tadpole contribution from the last two diagrams in Fig. 3.1. The expectation value of the neutrino field in the medium describes a beam or wave-packet of test neutrinos, namely these are neutrinos that are injected in the medium, for example by the decay of a neutron or any other heavy particle, but have not (yet) thermalized with the plasma. This is precisely the manner in which linear response leads to a study of real-time phenomena.

Due to the translational invariance of the medium in thermal equilibrium, the retarded self-energy is simply a function of $\vec{x} - \vec{x}'$ and $t - t'$. Hence, the equation can be written in frequency

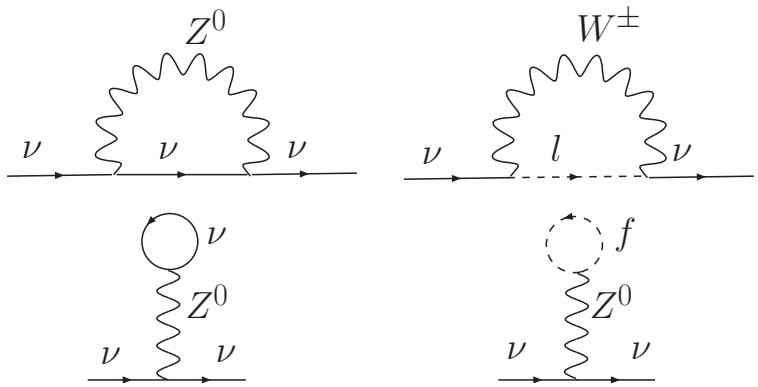

Figure 3.1: One-loop diagrams contributing to the neutrino self-energy.

and momentum space by introducing the space-time Fourier transform of the expectation value and the source

$$\psi_a(\vec{x},t) = \frac{1}{\sqrt{V}}\sum_{\vec{k}}\int d\omega\; \psi_a(\vec{k},\omega)\; e^{i\vec{k}\cdot\vec{x}}\; e^{-i\omega\, t} \quad , \quad \eta_a(\vec{x},t) = \frac{1}{\sqrt{V}}\sum_{\vec{k}}\int d\omega\; \eta_a(\vec{k},\omega)\; e^{i\vec{k}\cdot\vec{x}}\; e^{-i\omega\, t}. \tag{3.18}$$

Furthermore, due to the rotational invariance of the thermal medium, implies that all physical quantities depend on $|\vec{k}| \equiv k$.

We have argued in the introduction that for temperatures $T \gtrsim 10\,\mathrm{MeV}$ the relaxation via the weak interaction is faster than the time scales of (vacuum) oscillations. The validation of this assumption requires a deeper study of the interplay between neutrino oscillations and damping processes in the medium including the two-loop self-energy, which will be the subject of a forthcoming article. *Assuming* the validity of this estimate, the neutrinos in the loop are in thermal equilibrium as flavor eigenstates and at the temperatures of interest we consider them massless. Under this assumption, the self-energy is diagonal in the flavor basis

As a result, the effective Dirac equation for neutrino oscillations in the medium is obtained as

$$\left[\left(\gamma^0\,\omega - \vec{\gamma}\cdot\vec{k}\right)\delta_{ab} - M_{ab} + \Sigma^{tad}_{ab}\,L + \Sigma_{ab}(\omega,k)\,L\right]\;\psi_b(\omega,k) = -\eta_a(\omega,k)\,, \tag{3.19}$$

with

$$\Sigma(\omega,k) = \Sigma_W(\omega,k) + \Sigma_Z(\omega,k) \;\; ; \;\; \Sigma^{tad} = \Sigma^{\nu_e\,tad} + \Sigma^{\nu_\mu\,tad} + \Sigma^{f\,tad}\,, \tag{3.20}$$

where $\Sigma^{f\,tad}$ is the total tadpole contribution from all fermions other than neutrinos in the loop.

The details of the calculation of the self-energy are presented in Appendix A.

3.3 ONE-LOOP SELF-ENERGIES

3.3.1 Charged and Neutral Currents

From Eqs.(A.28)-(A.32) in the Appendix, we found that the self-energy $\Sigma_{W,Z}(\omega,k)$ can be written in the dispersive form

$$\Sigma_{W,Z}(\omega,k) = \int \frac{dk_0}{\pi}\, \frac{Im\,\Sigma_W(k_0,k)}{k_0-\omega-i\epsilon}. \tag{3.21}$$

with

$$\begin{aligned} Im\,\Sigma_W(k_0,k) = \frac{g^2\pi}{2}\int \frac{d^3p}{(2\pi)^3}\frac{1}{4\,W_q\,\omega_p}\Big\{ & [1-N_f(\omega_p)+N_b(W_q)]\;\mathcal{Q}(\vec{p},\vec{q})\,\delta(k_0-\omega_p-W_q)+ \\ & +\left[1-\bar{N}_f(\omega_p)+N_b(W_q)\right]\;\mathcal{Q}(-\vec{p},-\vec{q})\,\delta(k_0+\omega_p+W_q) \\ & +[N_f(\omega_p)+N_b(W_q)]\;\mathcal{Q}(\vec{p},-\vec{q})\,\delta(k_0-\omega_p+W_q) \\ & +\left[\bar{N}_f(\omega_p)+N_b(W_q)\right]\;\mathcal{Q}(-\vec{p},\vec{q})\,\delta(k_0+\omega_p-W_q)\Big\}\,, \end{aligned} \tag{3.22}$$

where we have defined

$$\begin{aligned} & Q^\mu(\vec{p},\vec{q}) = p^\mu + 2\,q^\mu\,\frac{W_q\,\omega_p-\vec{q}\cdot\vec{p}}{M_W^2}\,, \\ & q^\mu = (\,W_q\,,\vec{k}-\vec{p}\,) \quad,\quad \omega_p=\sqrt{|\vec{p}\,|^2+m_f^2} \quad,\quad W_q=\sqrt{|\,\vec{k}-\vec{p}\,|^2+M_W^2}\,. \end{aligned} \tag{3.23}$$

The corresponding contribution from neutral currents can be obtained from the above expression by setting

$$\frac{g}{\sqrt{2}}\to\frac{g}{2\cos\theta_w} \quad,\quad M_W\to M_Z=\frac{M_W}{\cos\theta_w}\,, \tag{3.24}$$

with θ_w being the Weinberg angle.

In the limit $T\ll M_{W,Z}$, the abundance of vector bosons is exponentially suppressed, hence we neglect the terms that feature $N_b(W_q)$. The imaginary part of the one-loop self-energy vanishes on the neutrino mass shell at one-loop level. A non-vanishing damping rate (non-vanishing imaginary part of the self-energy at the neutrino mass shell) at temperatures $T\ll M_W$ arises at two-loop level. Thus we focus solely on $Re\,\Sigma_W(k_0,k)$ when studying the dispersion relation and propagation of neutrinos in the medium.

The form of $Im\,\Sigma_W(k_0,k)$ suggests that $Re\,\Sigma_W(\omega,k)$ can be written as

$$Re\,\Sigma_W(\omega,k) = \gamma^0\;\sigma_W^0(\omega,k) - \vec{\gamma}\cdot\widehat{\mathbf{k}}\;\sigma_W^1(\omega,k), \tag{3.25}$$

where $\sigma_W^0(\omega,k)$ and $\sigma_W^1(\omega,k)$ can be obtained by taking traces on both sides.

Dropping the $T=0$ part and using the dispersive representation (3.21), we find that for any fermion f in the loop,

$$\sigma^0_W(\omega,k) = -\frac{g^2}{2}\int \frac{d^3p}{(2\pi)^3}\frac{1}{4\,W_q\,\omega_p}\quad\left\{\quad N_f(\omega_p)\left[\frac{Q_0(\vec{p},\vec{q})}{W_q+\omega_p-\omega}+\frac{Q_0(\vec{p},-\vec{q})}{W_q-\omega_p+\omega)}\right]\right.$$
$$\left.-\bar{N}_f(\omega_p)\left[\frac{Q_0(\vec{p},\vec{q})}{W_q+\omega_p+\omega}+\frac{Q_0(\vec{p},-\vec{q})}{W_q-\omega_p-\omega}\right]\quad\right\}, \tag{3.26}$$

$$\sigma^1_W(\omega,k) = -\frac{g^2}{2}\int \frac{d^3p}{(2\pi)^3}\frac{1}{4\,W_q\,\omega_p}\quad\left\{\quad N_f(\omega_p)\left[\frac{\widehat{\mathbf{k}}\cdot\vec{Q}(\vec{p},\vec{q})}{W_q+\omega_p-\omega}+\frac{\widehat{\mathbf{k}}\cdot\vec{Q}(\vec{p},-\vec{q})}{W_q-\omega_p+\omega}\right]\right.$$
$$\left.+\bar{N}_f(\omega_p)\left[\frac{\widehat{\mathbf{k}}\cdot\vec{Q}(\vec{p},\vec{q})}{W_q+\omega_p+\omega}+\frac{\widehat{\mathbf{k}}\cdot\vec{Q}(\vec{p},-\vec{q})}{W_q-\omega_p-\omega}\right]\quad\right\}. \tag{3.27}$$

In the thermalized medium with temperature T, the dominant loop momenta is of order $p\sim T$, therefore we neglect the neutrino masses since $T\gtrsim 3-5\,\mathrm{MeV}$. The self-energy is expanded in a power series in the external frequency and momentum ω,k, we refer to terms of the form $\omega/M_W\;;\;k/M_W$ as non-local terms (in space-time) since they represent gradient expansions in configuration space. Furthermore, we will neglect the contribution from leptons with masses $m_f\gg T$ since these will be exponentially suppressed, but we calculate the self-energies up the order $(g^2/M^4_{W,Z})(m_f/T)^2$ for leptons with masses $m_f\ll T$ and all higher order terms will be dropped. A straightforward but lengthy calculation gives

$$\begin{aligned}
\sigma^0_W(\omega,k) &= -\frac{3\,G_F}{\sqrt{2}}(n_f-n_{\bar{f}})+\frac{7\,\pi^2}{15\,\sqrt{2}}\frac{G_F\,\omega\,T^4}{M^2_W}\;,\\
\sigma^1_W(\omega,k) &= -\frac{7\,\pi^2}{45\,\sqrt{2}}\,\frac{G_F\,k\,T^4}{M^2_W}\left[1-\frac{30}{7\,\pi^2}\left(\frac{m_f}{T}\right)^2\right]\;,
\end{aligned} \tag{3.28}$$

where $G_F=\sqrt{2}\,\frac{g^2}{8\,M^2_W}$ is the Fermi constant, and $n_f-n_{\bar{f}}$ is the particle-antiparticle number density difference for any fermion f defined as

$$n_f-n_{\bar{f}} = 2\int\frac{d^3p}{(2\pi)^3}\left[N_f(\omega_p)-\bar{N}_f(\omega_p)\right]\;. \tag{3.29}$$

The contribution to $\sigma^1_W(\omega,k)$ of order g^2/M^2_W vanishes as a consequence of the isotropy of the equilibrium distribution functions. In calculating the non-local (in space-time) terms proportional to $\omega/M_W\;;\;k/M_W$ we have neglected the chemical potentials under the assumption that all asymmetries (leptons and neutrinos) are of the same order as the baryon asymmetry, in which case $\mu/T\sim 10^{-9}$ where μ is the chemical potential for the corresponding species.

In ref.[57] the equivalent to σ^0 is quoted as the coefficient b_L, but no equivalent to σ^1 was provided there, this is a difference between our results and those of ref.[57]. The contribution

$\sigma^1(\omega, k)$ is *new* it *cannot* be identified with an "effective potential" (which is proportional to γ^0) and it will be a source of helicity dependence on frequencies and mixing angles which has not been appreciated in the literature.

To obtain the corresponding expressions for the neutral current interactions, we can simply apply the replacement eq.(3.24).

3.3.2 Tadpole

As we mentioned in section 3.2, the path integrations over the fields $\Phi^{\pm}$ have to be taken along both forward (+) and backward (−) time branches in the presence of the sources $j^{\pm}$. However, the fermion loop of the tadpole diagram corresponds to the coincidence limit of the propagator, and in this limit all four real time propagators coincide[87]. Thus, to derive the correlation function, we only need the source j^{+}. Correspondingly, upon functional derivative with respect to j^{+}, only the time-ordered propagator $iS^{++}(p)$ will be required, where p is the 4-momentum through the loop.

The computation of the tadpole diagram is simplified by writing $iS^{++}(p)$ as

$$i\, S^{++}(p) = i\, (\not{p} + m) \left[\frac{1}{p^2 - m^2 + i\epsilon} + i\, \Gamma(p) \right] , \tag{3.30}$$

where $\Gamma(p)$ is given by

$$\Gamma(p) = 2\, \pi\, \delta(p^2 - m^2)\, \left[\theta(p_0)\, N_f(|p_0|) + \theta(-p_0)\, \bar{N}_f(|p_0|) \right] . \tag{3.31}$$

Since the 4-momentum through the Z boson propagator is zero, the tadpole diagram with any fermion f through the loop is given by

$$-i\, \Sigma^{f\, tad} = \left(\frac{i\, g}{2\, \cos\theta_w} \right)^2 \gamma^{\mu}\, \frac{i g_{\mu\nu}}{M_Z^2}\, (-1) \int \frac{d^4p}{(2\pi)^4}\, Tr \left[\gamma^{\nu}\, (g^V - g^A \gamma^5)\, i\, S^{++}(p) \right] , \tag{3.32}$$

where the values of g^V and g^A for all the fermions are listed in the following table:

Particles	g^V	g^A
ν_e, ν_μ, ν_τ	$\frac{1}{2}$	$\frac{1}{2}$
e, μ, τ	$-\frac{1}{2} + 2\sin^2\theta_w$	$-\frac{1}{2}$
p	$\frac{1}{2} - 2\sin^2\theta_w$	$\frac{1}{2}$
n	$-\frac{1}{2}$	$-\frac{1}{2}$
u, c, t	$\frac{1}{2} - \frac{4}{3}\sin^2\theta_w$	$\frac{1}{2}$
d, s, b	$-\frac{1}{2} + \frac{2}{3}\sin^2\theta_w$	$-\frac{1}{2}$

Evaluation of the integral in eq.(3.32) gives the result

$$\Sigma^{f\,tad} = \frac{2\,G_F\,g^V}{\sqrt{2}}\,(n_f - n_{\bar{f}})\,\gamma^0\ , \tag{3.33}$$

Writing $\Sigma^{f\,tad}(\omega,k)$ in the same form as (3.25), we obtain

$$\sigma^0_{tad} = \frac{2\,G_F\,g^V}{\sqrt{2}}\,(n_f - n_{\bar{f}}) \quad , \quad \sigma^1_{tad} = 0\ . \tag{3.34}$$

and tadpoles with quark loops acquire an extra factor 3 from color. We see that the tadpole contribution is finite and proportional to $n_f - n_{\bar{f}}$. This is the signature of a CP asymmetric medium. It is customary and convenient to express $n_f - n_{\bar{f}}$ in terms of its relative abundance to the photons in the universe. At any temperature T, the photon number density in the universe is given by

$$n_\gamma = \frac{2}{\pi^2}\,\zeta(3)\,T^3\ . \tag{3.35}$$

and the particle-antiparticle asymmetry for any fermion species f is defined as

$$L_f = \frac{n_f - n_{\bar{f}}}{n_\gamma}\ . \tag{3.36}$$

The magnitude of the observed baryon asymmetry is $L_B \simeq 10^{-9}$. Since $B-L$ is conserved in the standard model, it is natural to expect that the lepton asymmetries should be of the same order as L_B. Although there is no a priori reason to expect the neutrino asymmetries to be of the same order, we will henceforth *assume* that all the lepton and neutrino asymmetries $L_e,\ L_\mu,\ L_{\nu_e}$ and L_{ν_μ} are of the order of the baryon asymmetry $\sim 10^{-9}$.

The next step is to compute the contributions from the one-loop exchange diagrams. We focus on two different temperature regimes, $m_e \ll T \ll m_\mu$ in which only the electron is ultrarelativistic and $m_e,\ m_\mu \ll T \ll M_W$ in which both leptons are ultrarelativistic.

3.3.2.1 $\mathbf{m_e \ll T \ll m_\mu}$ This temperature limit is interesting because it is the energy scale right above BBN. The efficiency of BBN is sensitive to the amount of electron neutrinos which, in turn, depends on the detailed dynamics of neutrino oscillations. As it will be discussed below in detail, in the temperature regime $T \gtrsim 5\,\mathrm{MeV}$ the non-local (in space-time) terms proportional to ω, k from the exchange diagrams (both charged and neutral currents) dominate the contributions of the lepton and neutrino asymmetries *assuming* all of them to be of order 10^{-9}.

In the temperature limit with $m_e \ll T \ll m_\mu$, the contribution from μ leptons to the exchange one loop diagram is exponentially suppressed and we neglect it. Apart from electrons and neutrinos,

the thermal background does contain protons and neutrons in nuclear statistical equilibrium since for $T \gtrsim 1\,\mathrm{MeV}$ the weak interactions lead to equilibration on time scales shorter than the Hubble time scale via the reactions

$$n \leftrightarrow p + e^- + \bar{\nu}_e \quad , \quad p + \bar{\nu}_e \leftrightarrow n + e^+ \quad , \quad p + e^- \leftrightarrow n + \nu_e \; . \tag{3.37}$$

In the basis of flavor eigenstates, the total one-loop self-energy contribution is of the form

$$Re\,\Sigma(\omega, k) = [\gamma^0 \mathbb{A}(\omega) - \vec{\gamma}\cdot\widehat{\mathbf{k}}\,\mathbb{B}(k)]\,L \tag{3.38}$$

where $\mathbb{A}(\omega, k)$ and $\mathbb{B}(\omega, k)$ are 2×2 diagonal matrices in the neutrino flavor basis given by

$$\mathbb{A}(\omega) = \begin{pmatrix} A_e(\omega) & 0 \\ 0 & A_\mu(\omega) \end{pmatrix} \; ; \;\; \mathbb{B}(k) = \begin{pmatrix} B_e(k) & 0 \\ 0 & B_\mu(k) \end{pmatrix}, \tag{3.39}$$

Extracting non-local terms (in space-time) up to $\mathcal{O}(\omega/T)\,, \mathcal{O}(k/T)$ we find the following matrix elements,

$$\begin{aligned} A_e(\omega) &= -\frac{3\,G_F}{\sqrt{2}}\,L_e\,n_\gamma + \frac{7\,\pi^2}{15\,\sqrt{2}}\,\frac{G_F\,\omega\,T^4}{M_W^2} - \frac{3\,G_F}{2\,\sqrt{2}}\,L_{\nu_e}\,n_\gamma + \frac{7\,\pi^2}{30\,\sqrt{2}}\,\frac{G_F\,\omega\,T^4}{M_Z^2} \\ &\quad + \frac{G_F}{\sqrt{2}}\,L_{\nu_e}\,n_\gamma + \frac{G_F}{\sqrt{2}}\,L_{\nu_\mu}\,n_\gamma + \frac{2\,G_F}{\sqrt{2}}(-\frac{1}{2} + 2\,\sin^2\,\theta_w)\,L_e\,n_\gamma \\ &\quad + \frac{2\,G_F}{\sqrt{2}}(\frac{1}{2} - 2\,\sin^2\theta_w)\,L_p\,n_\gamma - \frac{G_F}{\sqrt{2}}\,L_n\,n_\gamma, \end{aligned} \tag{3.40}$$

$$\begin{aligned} A_\mu(\omega) &= -\frac{3\,G_F}{2\,\sqrt{2}}\,L_{\nu_\mu}\,n_\gamma + \frac{7\,\pi^2}{30\,\sqrt{2}}\,\frac{G_F\,\omega\,T^4}{M_Z^2} \\ &\quad + \frac{G_F}{\sqrt{2}}\,L_{\nu_e}\,n_\gamma + \frac{G_F}{\sqrt{2}}\,L_{\nu_\mu}\,n_\gamma + \frac{2\,G_F}{\sqrt{2}}(-\frac{1}{2} + 2\,\sin^2\theta_w)\,L_e\,n_\gamma \\ &\quad + \frac{2\,G_F}{\sqrt{2}}(\frac{1}{2} - 2\,\sin^2\theta_w)\,L_p\,n_\gamma - \frac{G_F}{\sqrt{2}}\,L_n\,n_\gamma \; , \end{aligned} \tag{3.41}$$

$$B_e(k) = -\frac{7\,\pi^2}{45\,\sqrt{2}}\,\frac{G_F\,k\,T^4}{M_W^2}\left[1 - \frac{30}{7\,\pi^2}\left(\frac{m_e}{T}\right)^2\right] - \frac{7\,\pi^2}{90\,\sqrt{2}}\,\frac{G_F\,k\,T^4}{M_Z^2}\;, \tag{3.42}$$

$$B_\mu(k) = -\frac{7\,\pi^2}{90\,\sqrt{2}}\frac{G_F\,k\,T^4}{M_Z^2}. \tag{3.43}$$

We purposely displayed the individual terms in the above expressions to highlight that the first line in $A_{e,\mu}(\omega)$ as well as the expressions for $B_{e,\mu}(k)$ arise from the exchange diagrams (the two top diagrams in fig.3.1), while the second and third lines in $A_{e,\mu}(\omega)$ arise from the tadpole diagrams (bottom two diagrams in fig.3.1). We have assumed that the flavor neutrinos are in thermal equilibrium and have consistently neglected neutrino masses. The correction term $(m_e/T)^2$ is displayed so that one can estimate the error incurred when this term is dropped for $T >> m_e$,

the error is less than 1% for $T \gtrsim 5\,\mathrm{MeV}$. In what follows we will neglect this contribution in the temperature range of interest for this section.

Charge neutrality requires that $L_e = L_p$, hence

$$\Sigma^{e\,tad} + \Sigma^{p\,tad} = 0\ . \tag{3.44}$$

Therefore, the expressions for A_e and A_μ simplify to the following:

$$A_e(\omega) = \frac{G_F\ n_\gamma}{\sqrt{2}}\left[-\mathcal{L}_e + \frac{7\ \pi^4}{60\ \zeta(3)}\ \frac{\omega\ T}{M_W^2}\left(2+\cos^2\theta_w\right)\right], \tag{3.45}$$

$$A_\mu(\omega) = \frac{G_F\ n_\gamma}{\sqrt{2}}\left[-\mathcal{L}_\mu + \frac{7\ \pi^4}{60\ \zeta(3)}\ \frac{\omega\ T}{M_W^2}\cos^2\theta_w\right], \tag{3.46}$$

$$B_e(k) = -\frac{G_F\ n_\gamma}{\sqrt{2}}\frac{7\ \pi^4}{180\ \zeta(3)}\ \frac{k\ T}{M_W^2}\left(2+\cos^2\theta_w\right)\ , \tag{3.47}$$

$$B_\mu(k) = -\frac{G_F\ n_\gamma}{\sqrt{2}}\frac{7\ \pi^4}{180\ \zeta(3)}\ \frac{k\ T}{M_W^2}\cos^2\theta_w\ . \tag{3.48}$$

where

$$\begin{aligned} -\mathcal{L}_e &= -\frac{1}{2}\ L_{\nu_e} + L_{\nu_\mu} - 3\ L_e - L_n \\ -\mathcal{L}_\mu &= -\frac{1}{2} L_{\nu_\mu} + L_{\nu_e} - L_n \end{aligned} \tag{3.49}$$

Where in the temperature regime $m_e \ll T \ll m_\mu$ we consistently neglected the muon contribution to the non-local terms proportional to ω, k in the exchange diagrams.

The above expressions also reveal the importance of the temperature region $T \gtrsim 5\,\mathrm{MeV}$. *Assuming* that all asymmetries are of the same order as the baryon asymmetry, namely $L_i \sim 10^{-9}$, we see that for $\omega \sim k \sim T$ the factor $T^2/M_W^2 \gg 10^{-9}$ for $T \gtrsim 5\,\mathrm{MeV}$.

We will discuss below that in this region there is also a resonance in the mixing angle in agreement with the results in[59].

3.3.2.2 $\mathbf{m_e, m_\mu \ll T \ll M_W}$ This temperature region is important because the non-local contributions are much larger than that of the lepton and neutrino asymmetries, assuming *both* to be of the same order $\sim 10^{-9}$ and are the *same* for both leptons if their masses are neglected. Therefore, if the contribution from the lepton and neutrino asymmetries is neglected, *and* terms of $\mathcal{O}(m_e^2/T^2)\,;\,\mathcal{O}(m_\mu^2/T^2)$ are neglected, the matrices $\mathbb{A}, \mathbb{B}$ become proportional to the identity. In this case the mixing angle would be the same as in the vacuum. We will see however, that keeping

terms of $\mathcal{O}(m_e^2/T^2)$; $\mathcal{O}(m_\mu^2/T^2)$ leads to a very different result, namely the vanishing of the mixing angle for negative helicity neutrinos or positive helicity antineutrinos in this temperature range.

For $T \gg m_\mu \sim 100\,\mathrm{MeV}$ the temperature is larger than the critical temperature for deconfinement in QCD $T_c \sim 160\mathrm{MeV}$. Therefore, the medium contains free quarks but no nucleons. Since both u and d quarks have masses smaller than 10 MeV, their masses can be neglected. We only include in our description the two lightest quark degrees of freedom consistently with keeping only a weak doublet. We also assume that there is vanishing strangeness in the medium.

As a result, the corresponding $A_{e,\mu}(\omega), B_{e,\mu}(k)$ are now given by

$$\begin{aligned}
A_e(\omega) &= -\frac{3\,G_F}{\sqrt{2}}\,L_e\,n_\gamma + \frac{7\,\pi^2}{15\,\sqrt{2}}\frac{G_F\,\omega\,T^4}{M_W^2} - \frac{3\,G_F}{2\sqrt{2}}\,L_{\nu_e}\,n_\gamma + \frac{7\,\pi^2}{30\,\sqrt{2}}\frac{G_F\,\omega\,T^4}{M_Z^2} \\
&\quad + \frac{G_F}{\sqrt{2}}\,L_{\nu_e}\,n_\gamma + \frac{G_F}{\sqrt{2}}\,L_{\nu_\mu}\,n_\gamma \\
&\quad + \frac{2\,G_F}{\sqrt{2}}(-\frac{1}{2} + 2\,\sin^2\theta_w)\,L_e\,n_\gamma + \frac{2\,G_F}{\sqrt{2}}(-\frac{1}{2} + 2\,\sin^2\theta_w)\,L_\mu\,n_\gamma \\
&\quad + \frac{6\,G_F}{\sqrt{2}}(\frac{1}{2} - \frac{4}{3}\,\sin^2\theta_w)\,L_u\,n_\gamma + \frac{6\,G_F}{\sqrt{2}}(-\frac{1}{2} + \frac{2}{3}\,\sin^2\theta_w)\,L_d\,n_\gamma\,, \qquad (3.50) \\
A_\mu(\omega) &= -\frac{3\,G_F}{\sqrt{2}}\,L_\mu\,n_\gamma + \frac{7\,\pi^2}{15\,\sqrt{2}}\frac{G_F\,\omega\,T^4}{M_W^2} - \frac{3\,G_F}{2\,\sqrt{2}}\,L_{\nu_\mu}\,n_\gamma + \frac{7\,\pi^2}{30\,\sqrt{2}}\frac{G_F\,\omega\,T^4}{M_Z^2} \\
&\quad + \frac{G_F}{\sqrt{2}}\,L_{\nu_e}\,n_\gamma + \frac{G_F}{\sqrt{2}}\,L_{\nu_\mu}\,n_\gamma \\
&\quad + \frac{2\,G_F}{\sqrt{2}}(-\frac{1}{2} + 2\,\sin^2\theta_w)\,L_e\,n_\gamma + \frac{2\,G_F}{\sqrt{2}}(-\frac{1}{2} + 2\,\sin^2\theta_w)\,L_\mu\,n_\gamma \\
&\quad + \frac{6\,G_F}{\sqrt{2}}(\frac{1}{2} - \frac{4}{3}\,\sin^2\theta_w)\,L_u\,n_\gamma + \frac{6\,G_F}{\sqrt{2}}(-\frac{1}{2} + \frac{2}{3}\,\sin^2\theta_w)\,L_d\,n_\gamma\,, \qquad (3.51) \\
B_e(k) &= -\frac{7\,\pi^2}{45\,\sqrt{2}}\frac{G_F\,k\,T^4}{M_W^2}\left[1 - \frac{30}{7\,\pi^2}\left(\frac{m_e}{T}\right)^2\right] - \frac{7\,\pi^2}{90\,\sqrt{2}}\frac{G_F\,k\,T^4}{M_Z^2}\,, \qquad (3.52) \\
B_\mu(k) &= -\frac{7\,\pi^2}{45\,\sqrt{2}}\frac{G_F\,k\,T^4}{M_W^2}\left[1 - \frac{30}{7\,\pi^2}\left(\frac{m_\mu}{T}\right)^2\right] - \frac{7\,\pi^2}{90\,\sqrt{2}}\frac{G_F\,k\,T^4}{M_Z^2}\,. \qquad (3.53)
\end{aligned}$$

Charge neutrality of the medium leads to the constraint $4\,L_u - L_d - 3\,L_e = 0$, which leads to the following simplified expressions:

$$\begin{aligned}
A_e(\omega) &= \frac{G_F\,n_\gamma}{\sqrt{2}}\left[\,\widetilde{-\mathcal{L}_e} + \frac{7\,\pi^4}{60\,\zeta(3)}\,\frac{\omega\,T}{M_W^2}\left(2 + \cos^2\theta_w\right)\right], \qquad (3.54) \\
A_\mu(\omega) &= \frac{G_F\,n_\gamma}{\sqrt{2}}\left[-\widetilde{\mathcal{L}_\mu} + \frac{7\,\pi^4}{60\,\zeta(3)}\,\frac{\omega\,T}{M_W^2}\left(2 + \cos^2\theta_w\right)\right], \qquad (3.55) \\
B_e(k) &= -\frac{G_F\,n_\gamma}{\sqrt{2}}\frac{7\,\pi^4}{180\,\zeta(3)}\frac{k\,T}{M_W^2}\left[2 + \cos^2\theta_w - \frac{60}{7\,\pi^2}\left(\frac{m_e}{T}\right)^2\right], \qquad (3.56) \\
B_\mu(k) &= -\frac{G_F\,n_\gamma}{\sqrt{2}}\frac{7\,\pi^4}{180\,\zeta(3)}\frac{k\,T}{M_W^2}\left[2 + \cos^2\theta_w - \frac{60}{7\pi^2}\left(\frac{m_\mu}{T}\right)^2\right], \qquad (3.57)
\end{aligned}$$

where

$$-\widetilde{\mathcal{L}_e} = -\frac{1}{2}\, L_{\nu_e} + L_{\nu_\mu} - 3\, L_e + (1 - 4\, \sin^2\theta_w)(2\, L_e - L_\mu) - (1 - 8\sin^2\theta_w) L_u - 2\, L_d \,, \tag{3.58}$$

$$-\widetilde{\mathcal{L}_\mu} = -\frac{1}{2}\, L_{\nu_\mu} + L_{\nu_e} - 3\, L_\mu + (1 - 4\, \sin^2\theta_w)(2\, L_e - L_\mu) - (1 - 8\, \sin^2\theta_w) L_u - 2\, L_d \,. \tag{3.59}$$

In the limit when $T \gg m_{e,\mu}$ both leptons become ultrarelativistic and a CP-symmetric medium becomes flavor blind to the weak interactions. In this case we must keep terms of $\mathcal{O}(m_{e,\mu}/T)$ to understand the nature of oscillations and mixing.

3.4 DISPERSION RELATIONS, MIXING ANGLES AND RESONANCES IN THE MEDIUM

The neutrino dispersion relations and mixing angles in the medium are obtained by diagonalizing the homogeneous effective Dirac equation in the medium, namely by setting $\eta(\omega, k) = 0$ in eq.(3.19). Using the results obtained above, the homogeneous Dirac equation in frequency and momentum becomes

$$\left[\gamma^0\, \omega \mathbb{1} - \vec{\gamma}\cdot\widehat{\mathbf{k}}\, k \mathbb{1} - \mathbb{M} + \left(\gamma^0 \mathbb{A}(\omega) - \vec{\gamma}\cdot\widehat{\mathbf{k}}\, \mathbb{B}(k)\right) L\right]\, \psi(\omega, k) = 0 \,, \tag{3.60}$$

where $\mathbb{1}$ is the 2×2 identity matrix in the flavor basis in which the field $\psi(\omega, k)$ is given by

$$\psi(\omega, k) = \begin{pmatrix} \nu_e(\omega, k) \\ \nu_\mu(\omega, k) \end{pmatrix} \,, \tag{3.61}$$

with $\nu_e(\omega, k)$ and $\nu_\mu(\omega, k)$ each being a 4-component Dirac spinor.

If we multiply the effective Dirac equation (3.60) by the chiral projectors R and L respectively from the left, we obtain

$$\left(\gamma^0\, \mathbb{W} - \vec{\gamma}\cdot\widehat{\mathbf{k}}\, \mathbb{K}\right) \psi_L - \mathbb{M}\, \psi_R = 0 \,, \tag{3.62}$$

$$\left(\gamma^0\, \omega\, \mathbb{1} - \vec{\gamma}\cdot\widehat{\mathbf{k}}\, k\, \mathbb{1}\right) \psi_R - \mathbb{M}\, \psi_L = 0 \,, \tag{3.63}$$

where we have defined the flavor matrices

$$\mathbb{W} = \omega \mathbb{1} + \mathbb{A} \quad , \quad \mathbb{K} = k\, \mathbb{1} + \mathbb{B} \,. \tag{3.64}$$

The set of equations (3.62) and (3.63) couple ψ_L and ψ_R together. To solve the equations, we first multiply (3.62) by $\left(\gamma^0\,\omega - \vec{\gamma}\cdot\widehat{\mathbf{k}}\,k\right)\mathbb{1}$ from the left and use eq.(3.63) to obtain an equation for ψ_L which can be written in terms of the helicity operator $\hat{h}(\widehat{\mathbf{k}}) = \gamma^0\vec{\gamma}\cdot\widehat{\mathbf{k}}\,\gamma^5$, as follows

$$\left[\omega\,\mathbb{W} - k\,\mathbb{K} + \hat{h}(\widehat{\mathbf{k}})(\omega\mathbb{K} - \mathbb{W}k) - \mathbb{M}^2\right]\psi_L = 0\,, \tag{3.65}$$

and the right handed component is given by

$$\psi_R(\omega,k) = \mathbb{M}\,\gamma^0\,\frac{[\omega + \hat{h}(\widehat{\mathbf{k}})\;k]}{\omega^2 - k^2}\;\psi_L(\omega,k)\,. \tag{3.66}$$

It is convenient to separate the Dirac and flavor structure to simplify the study. This is achieved most economically in the chiral representation of the Dirac matrices, in which

$$\gamma^0 = \begin{pmatrix} 0 & -\mathbb{1} \\ -\mathbb{1} & 0 \end{pmatrix}\;\;;\;\;\gamma^5 = \begin{pmatrix} \mathbb{1} & 0 \\ 0 & -\mathbb{1} \end{pmatrix}\,, \tag{3.67}$$

$$\vec{\gamma}\cdot\widehat{\mathbf{k}} = \begin{pmatrix} 0 & \vec{\sigma}\cdot\widehat{\mathbf{k}}\,\mathbb{1} \\ -\vec{\sigma}\cdot\widehat{\mathbf{k}}\,\mathbb{1} & 0 \end{pmatrix}\;\;;\;\;\hat{h}(k) = \vec{\sigma}\cdot\widehat{\mathbf{k}}\begin{pmatrix} \mathbb{1} & 0 \\ 0 & \mathbb{1} \end{pmatrix}\,, \tag{3.68}$$

and by introducing the two component Weyl spinors $v^{(h)}(\widehat{\mathbf{k}})$ eigenstates of helicity,

$$\vec{\sigma}\cdot\widehat{\mathbf{k}}\,v^{(h)}(\widehat{\mathbf{k}}) = h\,v^{(h)}(\widehat{\mathbf{k}})\;\;;\;\;h = \pm 1\,. \tag{3.69}$$

These spinors are normalized so that

$$\left(v^{(h)}(\widehat{\mathbf{k}})\right)^\dagger v^{(h')}(\widehat{\mathbf{k}}) = \delta_{h,h'}\,. \tag{3.70}$$

In terms of these helicity eigenstates, a general flavor doublet of left (L) and right (R) handed Dirac spinors can be written

$$\psi_L = \sum_{h=\pm 1}\begin{pmatrix} 0 \\ v^{(h)}\otimes\varphi^{(h)} \end{pmatrix}\,, \tag{3.71}$$

and

$$\psi_R = \sum_{h=\pm 1}\begin{pmatrix} v^{(h)}\otimes\xi^{(h)} \\ 0 \end{pmatrix}\,, \tag{3.72}$$

where $\varphi^{(h)}$; $\xi^{(h)}$ are flavor doublets. We have purposely left the arguments unspecified because this expansion will be used in real time as well as for the Fourier and Laplace transforms respectively. We need both positive and negative helicity eigenstates because the four independent degrees of freedom for each flavor are positive and negative energy and positive and negative helicity.

Projecting eq. (3.65) onto the helicity eigenstates $v^{(h)}(\widehat{\mathbf{k}})$ we obtain an equation for the flavor doublet $\varphi^{(h)}(\omega,k)$, namely

$$\left[(\omega^2-k^2)\mathbb{1}+(\omega-hk)(\mathbb{A}+h\mathbb{B})-\mathbb{M}^2\right]\varphi^{(h)}(\omega,k)=0\,. \tag{3.73}$$

Projecting eq. (3.66) onto helicity eigenstates yields the relation

$$\xi^{(h)}(\omega,k)=-\mathbb{M}\,\frac{(\omega+h\,k)}{\omega^2-k^2}\,\varphi^{(h)}(\omega,k)\,. \tag{3.74}$$

Writing the doublet $\varphi^{(h)}(\omega,k)$ in the flavor basis as

$$\varphi^{(h)}(\omega,k)=\begin{pmatrix}\nu_e^{(h)}(\omega,k)\\ \nu_\mu^{(h)}(\omega,k)\end{pmatrix}\,, \tag{3.75}$$

leads to the following matrix form for Eq.(3.73)

$$\begin{pmatrix}a^{(h)} & b\\ b & c^{(h)}\end{pmatrix}\begin{pmatrix}\nu_e^{(h)}\\ \nu_\mu^{(h)}\end{pmatrix}=0\,, \tag{3.76}$$

where the matrix elements in the flavor basis are given by

$$a^{(h)} = \omega^2-k^2+(\omega-hk)(A_e+hB_e)-\frac{1}{2}\,(M_1^2+M_2^2)-\frac{1}{2}\,(M_1^2-M_2^2)\,\cos(2\theta)\,, \tag{3.77}$$

$$b = \frac{1}{2}\,(M_1^2-M_2^2)\sin(2\theta)\,, \tag{3.78}$$

$$c^{(h)} = \omega^2-k^2+(\omega-hk)(A_\mu+hB_\mu)-\frac{1}{2}\,(M_1^2+M_2^2)+\frac{1}{2}\,(M_1^2-M_2^2)\,\cos(2\theta)\,. \tag{3.79}$$

Let us introduce a doublet of mass eigenstates in the medium

$$\chi^{(h)}(\omega,k)=\begin{pmatrix}\nu_1(\omega,k)\\ \nu_2(\omega,k)\end{pmatrix}\,, \tag{3.80}$$

related to the flavor doublet $\varphi^{(h)}(\omega,k)$ by a unitary transformation $U_m^{(h)}$ with

$$U_m^{(h)}=\begin{pmatrix}\cos\theta_m^{(h)} & \sin\theta_m^{(h)}\\ -\sin\theta_m^{(h)} & \cos\theta_m^{(h)}\end{pmatrix}\,, \tag{3.81}$$

$$\varphi^{(h)}(\omega,k)=U_m^{(h)}\,\chi^{(h)}(\omega,k)\;\;;\;\;\xi^{(h)}(\omega,k)=U_m^{(h)}\,\zeta^{(h)}(\omega,k)\,. \tag{3.82}$$

The mixing angle in the medium for states with helicity h, $\theta_m^{(h)}$ is obtained by requiring that the unitary transformation eq.(3.81) diagonalizes the matrix equation eq.(3.76). The eigenvalue equation in diagonal form is given by

$$\left\{\omega^2-k^2+\frac{1}{2}\,S_h(\omega,k)-\frac{1}{2}\,(M_1^2+M_2^2)-\frac{1}{2}\,\delta\,M^2\,\Omega_h(\omega,k)\begin{pmatrix}1 & 0\\ 0 & -1\end{pmatrix}\right\}\chi^{(h)}(\omega,k)=0\,, \tag{3.83}$$

where $S_h(\omega,k)$, δM^2, Δ_h and $\Omega_h(\omega,k)$ are respectively given by

$$
\begin{aligned}
S_h(\omega,k) &= (\omega - hk)\left[A_e(\omega) + A_\mu(\omega) + h\ B_e(k) + h\ B_\mu(k)\right]\ , && (3.84)\\
\delta M^2 &= M_1^2 - M_2^2\ , && (3.85)\\
\Delta_h(\omega,k) &= (\omega - hk)\left[A_e(\omega) - A_\mu(\omega) + h\ B_e(k) - h\ B_\mu(k)\right] && (3.86)\\
\Omega_h(\omega,k) &= \left[\left(\cos 2\theta - \frac{\Delta_h(\omega,k)}{\delta M^2}\right)^2 + \sin^2 2\theta\right]^{\frac{1}{2}} && (3.87)
\end{aligned}
$$

The mixing angle in the medium is determined by the relation

$$
\tan[2\theta_m^{(h)}] = \frac{2\ b}{c^{(h)} - a^{(h)}} = \frac{\delta M^2\ \sin(2\theta)}{\delta M^2\ \cos(2\theta) - \Delta_h(\omega,k)}\ , \tag{3.88}
$$

or alternatively by the more familiar relation

$$
\sin 2\theta_m^{(h)} = \frac{\sin 2\theta}{\left[\left(\cos 2\theta - \frac{\Delta_h(\omega,k)}{\delta M^2}\right)^2 + \sin^2 2\theta\right]^{\frac{1}{2}}} \tag{3.89}
$$

We note that the neutrino mass eigenvalues as well as the mixing angle depends on k as well as the **helicity eigenvalue** h. This is one of the novel results which has not been obtained before simply because only left handed negative helicity neutrinos were considered in the literature [5, 9, 45, 50, 51, 56].

The right handed components are obtained from the left handed ones by performing the unitary transformation eq.(3.81) on eq.(3.74). The relation (3.74) leads to the following expressions

$$
\zeta^{(h)}(\omega,k) = -\frac{\omega + h\,k}{\omega^2 - k^2}\ \overline{M}\left[\mathbb{1} + \frac{\delta M^2}{4\overline{M}^2}\begin{pmatrix} \overline{C} & \overline{S} \\ \overline{S} & -\overline{C}\end{pmatrix}\right]\chi^{(h)}(\omega,k)\ , \tag{3.90}
$$

where $\overline{M} = \frac{1}{2}(M_1 + M_2)$ and

$$
\overline{C} = \cos\left[2\ \theta_m^{(h)} - 2\ \theta\right] \quad , \quad \overline{S} = \sin\left[2\ \theta_m^{(h)} - 2\ \theta\right]\ . \tag{3.91}
$$

3.4.1 Eigenvectors and dispersion relations

Eq.(3.83) has the following eigenvectors in the basis of mass eigenstates:

$$\chi_1^{(h)}(\omega,k) = \nu_1^{(h)}(\omega,k)\begin{pmatrix}1\\0\end{pmatrix}, \tag{3.92}$$

$$\zeta_1^{(h)}(\omega,k) = -\nu_1^{(h)}(\omega,k)\,\frac{\omega+h\,k}{\omega^2-k^2}\,\overline{M}\left[\begin{pmatrix}1\\0\end{pmatrix}+\frac{\delta M^2}{4\,\overline{M}^2}\begin{pmatrix}\overline{C}\\ \overline{S}\end{pmatrix}\right], \tag{3.93}$$

and

$$\chi_2^{(h)}(\omega,k) = \nu_2^{(h)}(\omega,k)\begin{pmatrix}0\\1\end{pmatrix}, \tag{3.94}$$

$$\zeta_2^{(h)}(\omega,k) = -\nu_2^{(h)}(\omega,k)\,\frac{\omega+h\,k}{\omega^2-k^2}\,\overline{M}\left[\begin{pmatrix}0\\1\end{pmatrix}+\frac{\delta M^2}{4\,\overline{M}^2}\begin{pmatrix}\overline{S}\\ -\overline{C}\end{pmatrix}\right] \tag{3.95}$$

The corresponding doublets in the flavor basis can be obtained by the unitary transformation eq.(3.81).

The eigenvalues are found in perturbation theory consistently up to $\mathcal{O}(G_F)$ by writing

$$\omega_a^{(h)}(k,\pm) = \pm\left[E_a(k)+\delta\omega_a^{(h)}(k,\pm)\right] \quad , \quad a=1,2 \tag{3.96}$$

with

$$E_{1,2}(k) = \sqrt{k^2+M_{1,2}^2} \tag{3.97}$$

We find,

$$\delta\omega_1^{(h)}(k,\pm) = -\frac{1}{4E_1(k)}\left\{S_h(\pm E_1(k),k)-\delta M^2\left[\left[\left(\cos 2\theta-\frac{\Delta_h(\pm E_1(k),k)}{\delta M^2}\right)^2+\sin^2 2\theta\right]^{\frac{1}{2}}-1\right]\right\} \tag{3.98}$$

$$\delta\omega_2^{(h)}(k,\pm) = -\frac{1}{4E_2(k)}\left\{S_h(\pm E_2(k),k)+\delta M^2\left[\left[\left(\cos 2\theta-\frac{\Delta_h(\pm E_2(k),k)}{\delta M^2}\right)^2+\sin^2 2\theta\right]^{\frac{1}{2}}-1\right]\right\} \tag{3.99}$$

It is important to highlight that whereas the mixing angle only depends on Δ_h, the medium corrections to the frequencies also depend on S_h. This is important because even when in the case when the matrices $\mathbb{A}$, $\mathbb{B}$ become proportional to the identity, in which case $\Delta_h = 0$ and the mixing angle in the medium coincides with that of the vacuum, the frequencies and in particular the oscillation frequency still receives medium corrections.

3.4.2 Resonances

The condition for resonant oscillations is that the mixing $\tan[2\theta_m^{(h)}]$ reaches a maximum (infinity) as a function of a parameter, temperature, density or energy. From eq. (3.88) a resonance takes place when

$$\frac{\Delta_h(\omega,k)}{\delta M^2} = \cos 2\theta \tag{3.100}$$

where $\omega = \omega_a^{(h)}(k,\pm)$ correspond to the dispersion relations for the propagating modes in the medium, given by eq.(3.96). To leading order in G_F the in-medium dispersion relation can be approximated by the free field dispersion relation $\omega_a^{(h)}(k,\pm) \approx \pm\sqrt{k^2+M_{1,2}^2}$. The relativistic limit is warranted because the neutrino momenta in the plasma is $k \gg M_{1,2} \sim$ eV. Furthermore, under the assumption that the hierarchy of vacuum mass eigenstates is nearly degenerate, namely $|\delta M^2/\overline{M}^2| \ll 1$, as seems to be supported by the experimental data, the dispersion relations can be further approximated as follows

$$\omega_a^{(h)}(k,\pm) \approx \lambda k\left(1+\frac{\overline{M}^2}{2k^2}\right) \quad ; \quad \lambda = \pm 1 \tag{3.101}$$

It is convenient to introduce the following notation

$$\mathcal{L}_9 = 10^9\,(\mathcal{L}_e - \mathcal{L}_\mu) \tag{3.102}$$

$$\delta_5 = 10^5\left(\frac{\delta M^2}{\mathrm{eV}^2}\right) \tag{3.103}$$

If the lepton and neutrino asymmetries are of the same order of the baryon asymmetry, then $0.2 \lesssim |\mathcal{L}_9| \lesssim 0.7$ and the fitting from solar and KamLAND data suggests $|\delta_5| \approx 8$. Using the approximations leading to eq. (3.101) the ratio $\Delta_h/\delta M^2$ can be written compactly from eq.(3.86).

We study separately the cases $m_e \ll T \ll m_\mu$ and $m_e, m_\mu \ll T \ll M_W$.

3.4.2.1 $\mathbf{m_e \ll T \ll m_\mu}$

- **case I**: $\omega = k + \frac{\overline{M}^2}{2k}$, $h=-1$, *positive energy, negative helicity neutrinos*:

$$\frac{\Delta_h}{\delta M^2} \approx \frac{4}{\delta_5}\left(\frac{0.1\,T}{\mathrm{MeV}}\right)^4 \frac{k}{T}\left[-\mathcal{L}_9 + \left(\frac{2\,T}{\mathrm{MeV}}\right)^2 \frac{k}{T}\right]. \tag{3.104}$$

  Where we have neglected $\frac{\overline{M}^2}{k^2}$. For fixed temperature, the resonance condition eq.(3.100) is fulfilled for the value of neutrino momentum given by

$$k = \frac{(\mathrm{MeV})^2}{8T}\left\{\mathcal{L}_9 + \left[\mathcal{L}_9^2 + 16\,\delta_5\,\cos 2\theta\left(\frac{200\,\mathrm{MeV}}{T}\right)^2\right]^{\frac{1}{2}}\right\}. \tag{3.105}$$

Hence, for $\delta_5 \cos 2\theta > 0$, there is always a resonance. *If* $|\mathcal{L}_9| \lesssim 1$, then for neutrino momenta such that $\sqrt{Tk} > 1\,\mathrm{MeV}$ the non-local term dominates over the asymmetry and the resonance occurs for $k \sim 25\ \sqrt{\delta_5\ \cos 2\theta}\ (\mathrm{MeV})^3/T^2$. For example, if $T \sim 10$ MeV, the resonance occurs for $k \sim 1$ MeV. If $\delta_5 \cos 2\theta < 0$ there can also be a resonance provided

$$\frac{|\mathcal{L}_9|\,T}{200\,\mathrm{MeV}} > 4\sqrt{|\delta_5\ \cos 2\theta|}. \tag{3.106}$$

However this inequality requires a large value of $|\mathcal{L}_9|$, for example for $T \sim 10$MeV it requires that $|\mathcal{L}_9| \gtrsim 140$.

- **case II**: $\omega = k + \frac{\overline{M}^2}{2k}$, $h = 1$, *positive energy, positive helicity neutrinos:*

$$\frac{\Delta_h}{\delta M^2} \approx \frac{10^{-16}}{\delta_5}\left(\frac{T}{\mathrm{MeV}}\right)^2\ \left(\frac{\overline{M}}{\mathrm{eV}}\right)^2\left[-\mathcal{L}_9\ \frac{T}{k} + 2\left(\frac{T}{\mathrm{MeV}}\right)^2\right] \tag{3.107}$$

Where we have neglected terms of higher order in $\frac{\overline{M}^2}{k^2}$. Because $\overline{M} \sim 1\,\mathrm{eV}$ and $100\,\mathrm{MeV} \gg T \gg 1\,\mathrm{MeV}$ a resonance would only be available for $k \sim 10^{-16}\,\mathrm{MeV}$ which is not a relevant range of momenta for neutrinos in the plasma. Therefore, positive helicity neutrinos mix with the *vacuum mixing angle*.

- **case III**: $\omega = -k - \frac{\overline{M}^2}{2k}$, $h = -1$, *positive energy, negative helicity anti-neutrinos:*

$$\frac{\Delta_h}{\delta M^2} \approx \frac{10^{-16}}{\delta_5}\left(\frac{T}{\mathrm{MeV}}\right)^2\ \left(\frac{\overline{M}}{\mathrm{eV}}\right)^2\left[\mathcal{L}_9\ \frac{T}{k} + 2\left(\frac{T}{\mathrm{MeV}}\right)^2\right]. \tag{3.108}$$

Again in this expression we have neglected higher order terms in $\frac{\overline{M}^2}{k^2}$. A conclusion similar to that of case II above holds in this case. No resonance is available for relevant values of neutrino momenta within the temperature range in which these results are valid. For the cases II and III the ratio $|\Delta_h/\delta M^2| \ll 1$ for all relevant values of the neutrino momentum within the temperature range in which these results are valid. Therefore, negative helicity *antineutrinos* mix with the vacuum mixing angle, just as positive helicity neutrinos.

- **case IV**: $\omega = -k - \frac{\overline{M}^2}{2k}$, $h = 1$, *positive energy, positive helicity anti-neutrinos:*

$$\frac{\Delta_h}{\delta M^2} \approx \frac{4}{\delta_5}\left(\frac{0.1\,T}{\mathrm{MeV}}\right)^4\ \frac{k}{T}\left[\mathcal{L}_9 + \left(\frac{2\,T}{\mathrm{MeV}}\right)^2\ \frac{k}{T}\right]. \tag{3.109}$$

Where we have neglected higher order terms in $\frac{\overline{M}^2}{k^2}$. The position of the resonance in this case is obtained from that in case I above by the replacement $\mathcal{L}_9 \to -\mathcal{L}_9$, namely for fixed temperature the resonance condition is fulfilled at the value of k given by

$$k = \frac{(\mathrm{MeV})^2}{8T}\left\{-\mathcal{L}_9 + \left[\mathcal{L}_9^2 + 16\,\delta_5\ \cos 2\theta\left(\frac{200\,\mathrm{MeV}}{T}\right)^2\right]^{\frac{1}{2}}\right\}. \tag{3.110}$$

Again in the temperature range $1\,\mathrm{MeV} \ll T \ll 100\,\mathrm{MeV}$ there is a resonance if $\delta_5 \cos 2\theta > 0$ (assuming that $|\delta_5 \cos 2\theta| \sim 1$).

Just as in case I, *if* $|\mathcal{L}_9| \lesssim 1$ the non-local term dominates over the asymmetry contribution for $\sqrt{Tk} \gtrsim 1\,\mathrm{MeV}$ and the resonance occurs for $k \sim 25\sqrt{\delta_5 \cos 2\theta}\,(\mathrm{MeV})^3/T^2$.

Cases III and IV reveal an interesting feature: *only* the asymmetry contribution changes sign between neutrinos and antineutrinos whereas the non-local (in space-time) term *remains the same*.

Together these expressions confirm that *if* the lepton and neutrino asymmetries are of the same order as the baryon asymmetry, namely $0.2 \lesssim |\mathcal{L}_9| \lesssim 0.7$, then the non-local terms from the exchange diagrams dominate the self-energy for $T \gtrsim 3-5\,\mathrm{MeV}$ unless the neutrino in the plasma has a momentum k such that $\sqrt{kT} \ll 0.5\,\mathrm{MeV}$.

In summary, for $m_e \ll T \ll m_\mu$ resonances occur in cases I and IV when $h\,\lambda < 0$ (λ is the sign of the energy eigenvalue). For $h\,\lambda > 0$ (cases II and III) no resonance is available for neutrino momenta $k \sim T \sim$ few MeV and mixing angle in the medium coincides with the vacuum value.

3.4.2.2 $\mathbf{m_e, m_\mu \ll T \ll M_W}$ We use $m_\mu \approx 106\,\mathrm{MeV}$ and find the following simple expressions

- **case I**: $\omega = k + \frac{\overline{M}^2}{2k}$, $h = -1$, *positive energy, negative helicity neutrinos*:

$$\frac{\Delta_h}{\delta M^2} \approx \frac{0.4 \times 10^{12}}{\delta_5} \left(\frac{T}{\mathrm{GeV}}\right)^4 \frac{k}{T} \left[4.83\,\frac{k}{T} + 10^{-3}\mathcal{L}_9\right] \tag{3.111}$$

  In this case no resonance is available but for neutrinos with extremely low energy and not relevant for the plasma. For example for $T \sim$ GeV only neutrinos with energy of a few eV would be potentially resonant, but this momentum range is not a relevant one for neutrinos in the plasma. For neutrinos with energy larger than a few *keV* the mixing angle effectively vanishes. Therefore, we conclude that in this temperature regime the mixing angle in the medium for negative helicity neutrinos vanishes.

- **case II**: $\omega = k + \frac{\overline{M}^2}{2k}$, $h = 1$, *positive energy, positive helicity neutrinos*:

$$\frac{\Delta_h}{\delta M^2} \approx -\frac{10^{-7}}{\delta_5} \left(\frac{T}{\mathrm{GeV}}\right)^2 \frac{T}{k} \left(\frac{\overline{M}}{\mathrm{eV}}\right)^2 \left[4.83\,\frac{k}{T} - 10^{-3}\mathcal{L}_9\right] \tag{3.112}$$

  It is clear that for the relevant regime of neutrino momenta in the plasma $|\Delta_h/\delta M^2| \ll 1$. Hence the mixing angle in the medium coincides with the vacuum mixing angle. Thus the conclusion in this case is similar to that in the case described by eq. (3.107), namely positive helicity neutrinos undergo oscillations in the medium with the *vacuum* mixing angle.

- **case III**: $\omega = -k - \frac{\overline{M}^2}{2k}$, $h = -1$, *positive energy, negative helicity anti-neutrinos*:

$$\frac{\Delta_h}{\delta M^2} \approx -\frac{10^{-7}}{\delta_5}\left(\frac{T}{\text{GeV}}\right)^2 \frac{T}{k}\left(\frac{\overline{M}}{\text{eV}}\right)^2 \left[4.83\,\frac{k}{T} + 10^{-3}\mathcal{L}_9\right] \tag{3.113}$$

  The result in this case is similar to that of case II above, negative helicity *antineutrinos* oscillate in the medium with the vacuum mixing angle.

- **case IV**: $\omega = -k - \frac{\overline{M}^2}{2k}$, $h = 1$, *positive energy, positive helicity anti-neutrinos*:

$$\frac{\Delta_h}{\delta M^2} \approx \frac{0.4\times 10^{12}}{\delta_5}\left(\frac{T}{\text{GeV}}\right)^4 \frac{k}{T}\left[4.83\,\frac{k}{T} - 10^{-3}\mathcal{L}_9\right] \tag{3.114}$$

  The conclusion in this case is similar to that of the case described by eq. (3.111) above, the mixing angle effectively vanishes and oscillations of positive helicity *antineutrinos* are suppressed in the medium in this temperature range.

Taken together the above analysis reveals that there is a resonance in the oscillation of negative helicity neutrinos and positive helicity antineutrinos (that is $h\,\lambda < 0$) in the temperature range $m_e \ll T \ll m_\mu$ with a typical neutrino momentum $k \sim T \sim$ few MeV. For $m_e, m_\mu \ll T \ll M_W$ the mixing angle for negative helicity neutrinos and positive helicity antineutrinos (that is $h\,\lambda < 0$) effectively vanishes in the medium, and in both temperature ranges positive helicity neutrinos and negative helicity antineutrinos undergo oscillations in the medium with the vacuum mixing angle. We cannot yet conclude that positive helicity neutrinos and negative helicity antineutrinos are sterile, before studying the corrections to the oscillation frequencies.

3.4.3 Oscillation frequencies and time scales

The oscillation time scale in the medium is given by

$$\tau_m^{(h)}(k,\lambda) = \frac{1}{\left|\omega_1^{(h)}(k,\lambda) - \omega_2^{(h)}(k,\lambda)\right|} = \frac{1}{\left|E_1(k) - E_2(k) + \delta\omega_1^{(h)}(k,\lambda) - \delta\omega_2^{(h)}(k,\lambda)\right|}\,, \tag{3.115}$$

where $E_{1,2}(k) = \sqrt{k^2 + M_{1,2}^2}$ and $\lambda = +1$ and $\lambda = -1$ correspond to neutrino and antineutrinos respectively.

The vacuum oscillation time scale is

$$\tau_v(k) = \frac{1}{|\,E_1(k) - E_2(k)|}\,, \tag{3.116}$$

therefore, in order to understand the loop corrections to the oscillations time scales, it is convenient to study the ratio

$$\frac{\tau_v(k)}{\tau_m^{(h)}(k,\lambda)} = \left| 1 + \frac{\delta\omega_1^{(h)}(k,\lambda) - \delta\omega_2^{(h)}(k,\lambda)}{E_1(k) - E_2(k)} \right| . \tag{3.117}$$

Typical neutrino momenta in the plasma are ultrarelativistic, hence we approximate

$$E_1(k) - E_2(k) \approx \frac{\delta M^2}{2k} = \frac{\delta_5}{2} \frac{10^{-11}\,\mathrm{eV}}{(k/\mathrm{MeV})} . \tag{3.118}$$

furthermore to leading order in G_F we replace $\omega_a^{(h)}(k,\lambda) \approx \lambda k$ in the arguments of $A_{e,\mu}(\omega)$.

The term $\delta\omega_1^{(h)}(k,\lambda) - \delta\omega_2^{(h)}(k,\lambda)$ represents the correction to the vacuum oscillation time scale due to the medium effect. While the general form of these corrections are cumbersome, we can extract simplified expressions in three relevant limits.

- **I Resonant case:** $\frac{\Delta_h(\lambda E_{1,2},k)}{\delta M^2} \approx \cos 2\theta$:

  In section 3.4.2 above we found that resonant flavor oscillations can occur only for $\lambda = +1, h = -1$ and $\lambda = -1, h = +1$. In both these cases we obtain,

$$\begin{aligned} \delta\omega_1^{(h)}(k,\lambda) - \delta\omega_2^{(h)}(k,\lambda) &= -\frac{\delta M^2}{8k^2}\Big[A_e(k) + A_\mu(k) + B_e(k) + B_\mu(k)\Big] \\ &\quad -\frac{\delta M^2}{2k^2}\left(1 + \frac{\overline{M}^2}{2k^2}\right) k\,(1 - \sin 2\theta) . \end{aligned} \tag{3.119}$$

- **II vanishing mixing angle :** $\left|\frac{\Delta_h(\lambda E_{1,2},k)}{\delta M^2}\right| \gg 1$:

  In this limit, $\theta_m^{(h)} \sim 0$ and neutrino flavor mixing is suppressed. In section 3.4.2 above, we found that this occurs only for $\lambda = +1, h = -1$ or $\lambda = -1, h = +1$. Furthermore, $\Delta_h(\lambda E_{1,2}, k)$ is always positive definite in both temperature limits considered here $m_e \ll T \ll m_\mu$ and $m_e, m_\mu \ll T \ll M_W$.

  In this case we obtain

$$\begin{aligned} \delta\omega_1^{(h)}(k,\lambda) - \delta\omega_2^{(h)}(k,\lambda) &= -\frac{\delta M^2}{8k^2}\Big[A_e(k) + A_\mu(k) + B_e(k) + B_\mu(k)\Big] \\ &\quad + \mathrm{sign}\,(\delta M^2)\Big[A_e(k) - A_\mu(k) - B_e(k) + B_\mu(k)\Big] . \end{aligned} \tag{3.120}$$

- **III vacuum mixing:** $\left|\frac{\Delta_h(\lambda E_{1,2},k)}{\delta M^2}\right| \ll 1$:

  In this limit $\theta_m^{(h)} \approx \theta$. In section 3.4.2 above we found that this case occurs for $\lambda = +1, h = +1$ or $\lambda = -1, h = -1$. In both these cases we find

$$\begin{aligned}\delta\omega_1^{(h)}(k,\lambda) - \delta\omega_2^{(h)}(k,\lambda) &= -\frac{\delta M^2}{8k^2}\Big[A_e(k) + A_\mu(k) + B_e(k) + B_\mu(k)\Big] \\ &\quad -\frac{\overline{M}^2}{4k^2}\cos 2\theta\Big[A_e(k) - A_\mu(k) + B_e(k) - B_\mu(k)\Big]\,. \quad (3.121)\end{aligned}$$

We now study these simplified expressions in the different regimes of temperature and for the different helicities components. The most relevant cosmological regime corresponds to momenta of the order of the temperature, hence we will focus on the regime in which the non-local (in space-time) contributions from the exchange diagrams dominate over the lepton-neutrino asymmetries. Taken together these simplifications allow us to study the relevant cosmological range of neutrino energies in a clear manner.

3.4.3.1 $\mathbf{m_e \ll T \ll m_\mu}$

- **case I**: $\omega_{1,2}(k,\lambda) = \lambda\,(k + \frac{M_{1,2}^2}{2k})$; $\lambda = +1, h = -1$ and $\lambda = -1, h = +1$:

  As observed in section (3.4.2) the non-local terms become dominant for $\sqrt{Tk} \geq 1$MeV which is of course consistent with the ultrarelativistic limit $\overline{M}^2/2k^2 \ll 1$. Furthermore in the temperature range of interest in this study, the factors $A_{e,\mu}(k)$ and $B_{e,\mu}(k)$ are of the order $G_F k T^4/M_W^2 \sim 10^{-9}(T/\mathrm{GeV})^4\, k \ll k$. Therefore, near the resonance which occurs when $T^2 k \sim 25\,\sqrt{\delta_5 \cos 2\theta}\,\mathrm{MeV}^3$, the expression (3.119) simplifies to

$$\delta\omega_1^{(h)}(k,\lambda) - \delta\omega_2^{(h)}(k,\lambda) \approx -\frac{\delta M^2}{2k}\,(1 - \sin 2\theta)\,. \quad (3.122)$$

  The ratio of the oscillation time scales (3.117) becomes

$$\frac{\tau_v(k)}{\tau_m^{(h)}(k,\lambda)} \sim |\sin 2\,\theta| < 1 \quad (3.123)$$

  Therefore, for small *vacuum* mixing angle there is a considerable *slow down* of oscillations. Resonant flavor mixing in the medium occurs on *longer* time scales than in the vacuum.

For large neutrino energy, well outside the resonance region for $T^2 k \gg 25\sqrt{|\delta_5 \cos 2\theta|}\,\mathrm{MeV}^3$, eq. (3.104) indicates that $|\Delta_h(\lambda E_{1,2}, k)/\delta M^2| \gg 1$. In this high energy regime we find that

$$\delta\omega_1^{(h)}(k,\lambda) - \delta\omega_2^{(h)}(k,\lambda) \approx \mathrm{sign}\,(\delta M^2)\left[A_e(k) - A_\mu(k) - B_e(k) + B_\mu(k)\right] \quad (3.124)$$

$$= \mathrm{sign}\,(\delta M^2)\,\frac{28\,\pi^2}{45\,\sqrt{2}}\,\frac{G_F\,k\,T^4}{M_W^2} \quad (3.125)$$

$$\simeq 7.9\times 10^{-15}\,\mathrm{eV}\;\mathrm{sign}(\delta M^2)\frac{k}{\mathrm{MeV}}\,\left(\frac{T}{\mathrm{MeV}}\right)^4 \quad (3.126)$$

therefore neutrino oscillations are suppressed by a vanishingly small mixing angle and the ratio of time scales (3.117) becomes

$$\frac{\tau_v(k)}{\tau_m^{(h)}(k,\lambda)} \sim \left|1 + \frac{10^{-3}}{|\delta_5|}\left(\frac{k\,T^2}{\mathrm{MeV}^3}\right)^2\right|. \quad (3.127)$$

A considerable *speed-up* of oscillations occurs for $k\,T^2 \gtrsim 100\,\mathrm{MeV}^3$ since then $\tau_m^{(h)}(k,\lambda) \ll \tau_v(k)$. In this case, off-resonance flavor mixing is suppressed not only by a small mixing angle in the medium but also by a rapid decoherence and dephasing of the oscillations.

- **case II**: $\omega_{1,2}(k,\lambda) = \lambda\,(k + \frac{M_{1,2}^2}{2k})$; $\lambda = +1, h = +1$ and $\lambda = -1, h = -1$:

The results of section 3.4.2 (see eq. (3.107)) indicate that in this case $|\Delta_h(\lambda E_{1,2}, k)/\delta M^2| \ll 1$, corresponding to the mixing angle in the medium being the same as in the vacuum. As a result,

$$\delta\omega_1^{(h)}(k,\lambda) - \delta\omega_2^{(h)}(k,\lambda) \approx -\frac{\overline{M}^2}{4\,k^2}\cos 2\,\theta\left[A_e(k) - A_\mu(k) + B_e(k) - B_\mu(k)\right] \quad (3.128)$$

$$= -\frac{\overline{M}^2}{4\,k^2}\,\cos 2\theta\,\frac{14\,\pi^2}{45\,\sqrt{2}}\,\frac{G_F\,k\,T^4}{M_W^2} \quad (3.129)$$

$$\simeq -6.1\times 10^{-29}\,\mathrm{eV}\;\cos 2\theta\left(\frac{k}{\mathrm{MeV}}\right)^{-1}\left(\frac{T}{\mathrm{MeV}}\right)^4. \quad (3.130)$$

and the ratio of time scales (3.117) becomes

$$\frac{\tau_v(k)}{\tau_m^{(h)}(k,\lambda)} \simeq \left|1 - \frac{10^{-17}\cos 2\theta}{\delta_5}\left(\frac{T}{\mathrm{MeV}}\right)^4\right| \approx 1 \quad (3.131)$$

Therefore, for positive helicity neutrinos and negative helicity *antineutrinos* medium oscillations are the same as vacuum oscillations both in the mixing angle as well as in the oscillation time scales. In this regime of temperature positive helicity neutrinos and antineutrinos are sterile in the sense that these do not interact with the medium.

3.4.3.2 $\mathbf{m_e, m_\mu \ll T \ll M_W}$

- **case I**: $\omega_{1,2}(k,\lambda) = \lambda(k + \frac{M_{1,2}^2}{2k})$; $\lambda = +1, h = -1$ and $\lambda = -1, h = +1$:

This case describes negative helicity neutrinos and positive helicity antineutrinos. Eq. (3.111) indicates that in this case, $|\Delta_h(\lambda E_{1,2}, k)/\delta M^2| \gg 1$ corresponding to vanishing mixing angle in the medium. Therefore, we obtain

$$\begin{aligned}
\delta\omega_1^{(h)}(k,\lambda) - \delta\omega_2^{(h)}(k,\lambda) &\approx \text{sign}\,(\delta M^2)\left[A_e(k) - A_\mu(k) - B_e(k) + B_\mu(k)\right] && (3.132)\\
&= \text{sign}(\delta M^2)\,\frac{2\,G_F\,k\,T^2}{3\,\sqrt{2}}\,\left(\frac{m_\mu}{M_W}\right)^2 && (3.133)\\
&\simeq 9.6\times 10^{-6}\,\text{eV}\,\text{sign}(\delta M^2)\left(\frac{k}{\text{MeV}}\right)\left(\frac{T}{\text{GeV}}\right)^2 . && (3.134)
\end{aligned}$$

and the ratio of time scales is given by

$$\frac{\tau_v(k)}{\tau_m^{(h)}(k,\lambda)} \simeq \left|1 + \frac{10^{12}}{|\delta_5|}\left(\frac{kT}{\text{GeV}^2}\right)^2\right| \gg 1 \qquad (3.135)$$

Hence there is a considerable *speed-up* in the oscillation time scale in the medium. Again, in this case oscillations are strongly suppressed not only by a vanishingly small mixing angle but also by the rapid dephasing in the medium.

- **case II**: $\omega_{1,2}(k,\lambda) = \lambda\,(k + \frac{M_{1,2}^2}{2k})$; $\lambda = +1, h = +1$ and $\lambda = -1, h = -1$:

This case describes positive helicity neutrinos negative helicity *antineutrinos*. Eq. (3.112) shows that in this case $|\Delta_h(\lambda E_{1,2}, k)/\delta M^2| \ll 1$, the mixing angle in the medium is the same as in the vacuum. We find for this case

$$\begin{aligned}
\delta\omega_1^{(h)}(k,\lambda) - \delta\omega_2^{(h)}(k,\lambda) &\approx -\frac{\overline{M}^2}{4k^2}\cos 2\theta\left[A_e(k) - A_\mu(k) + B_e(k) - B_\mu(k)\right] && (3.136)\\
&= \frac{\overline{M}^2}{4\,k^2}\,\cos 2\theta\,\frac{2\,G_F\,k\,T^2}{3\,\sqrt{2}}\left(\frac{m_\mu}{M_W}\right)^2 && (3.137)\\
&\simeq 1.5\times 10^{-19}\,\text{eV}\,\cos 2\theta\left(\frac{k}{\text{MeV}}\right)^{-1}\left(\frac{T}{\text{GeV}}\right)^2 . && (3.138)
\end{aligned}$$

where we have taken $\overline{M} \sim 1\,\text{eV}$. The ratio of time scales in this case is given by

$$\frac{\tau_v(k)}{\tau_m^{(h)}(k,\lambda)} \sim \left|1 + \frac{3\times 10^{-8}\cos 2\theta}{\delta_5}\left(\frac{T}{\text{GeV}}\right)^2\right| \approx 1 \qquad (3.139)$$

Again in this temperature regime we find that positive helicity neutrinos and negative helicity *antineutrinos* are *almost* "sterile" in the sense that neither the mixing angle nor the oscillation time scales receive substantial loop corrections. Thus the combined analysis of mixing angle and propagation frequencies in the medium in the temperature regime under consideration indicates that in medium corrections for positive helicity neutrinos and negative helicity antineutrinos are very small. These degrees of freedom are effectively sterile in that their dynamics is (almost) the same as in the vacuum.

3.5 LAPLACE TRANSFORM AND REAL-TIME EVOLUTION

The main purpose to obtain the Dirac equation in real time is to study the oscillations of neutrinos in the medium as an initial value problem. As described in section 3.2 this is achieved by adiabatically switching the sources $\eta, \overline{\eta}$ from $t = -\infty$ and switching them off at $t = 0$. The adiabatic switching on of the sources induces an expectation value, which evolves in the absence of sources for $t > 0$, after the external source has been switched off. It is convenient to write the effective Dirac eq. (3.17) in terms of spatial Fourier transforms. Using the results of the appendix (A.3) we find

$$\left[\left(i\gamma^0\frac{\partial}{\partial t} - \vec{\gamma}\cdot\vec{k}\right)\,\delta_{ab} - M_{ab} + \Sigma^{tad}_{ab}L\right]\,\psi_b(\vec{k},t) + \int_{-\infty}^{t} dt'\,\Sigma_{ab}(\vec{k},t-t')\,L\,\psi_b(\vec{k},t') = -\eta_a(\vec{k},t), \tag{3.140}$$

where the results of appendix (A.3) yield

$$\Sigma(\vec{k},t-t') = i\int_{-\infty}^{\infty}\frac{dk_0}{\pi}\,\mathrm{Im}\Sigma(\vec{k},k_0)\,e^{-ik_0(t-t')} \quad , \quad \Sigma(\vec{k},k_0) = \Sigma_W(\vec{k},k_0) + \Sigma_Z(\vec{k},k_0) \tag{3.141}$$

For an external Grassmann valued source adiabatically switched on at $t = -\infty$ and off at $t = 0$

$$\eta_a(\vec{k},t) = \eta_a(\vec{k},0)\,e^{\epsilon\,t}\,\theta(-t) \quad , \quad \epsilon \to 0^+ \,. \tag{3.142}$$

It is straightforward to confirm that the solution of the Dirac eq. (3.140) for $t < 0$ is given by

$$\psi_a(\vec{k},t<0) = \psi_a(\vec{k},0)\,e^{\epsilon\,t}\,. \tag{3.143}$$

Inserting this ansatze into the equation (3.140) it is straightforward to check that it is indeed a solution with a linear relation between $\psi_a(\vec{k},0)$ and $\eta_a(\vec{k},0)$. This relation can be used to obtain $\psi_a(\vec{k},0)$ from $\eta_a(\vec{k},0)$, or alternatively, for a given initial value of the field at $t = 0$ to find the source $\eta_a(\vec{k},0)$ that prepares this initial value. For $t > 0$ the source term vanishes, the non-local

integral in eq.(3.140) can be split into an integral from $t=-\infty$ to $t=0$ plus an integral from $t=0$ to t. In the first integral corresponding to $t<0$ we insert the solution eq.(3.143) and obtain the following equation valid for $t>0$

$$\begin{aligned}&\left[\left(i\gamma^0\frac{\partial}{\partial t}-\vec{\gamma}\cdot\vec{k}\right)\,\delta_{ab}-M_{ab}+\Sigma^{tad}_{ab}L\right]\,\psi_b(\vec{k},t)+\int_0^t dt'\,\Sigma_{ab}(\vec{k},t-t')\,L\,\psi_b(\vec{k},t')\\ =\;&-\int_{-\infty}^{+\infty}\frac{dk_0}{\pi}\,\frac{\mathrm{Im}\Sigma_{ab}(\vec{k},k_0)}{k_0}\,e^{-ik_0t}\,L\,\psi_b(\vec{k},0).\end{aligned}\tag{3.144}$$

This equation can be solved by Laplace transform. Introduce the Laplace transforms

$$\widetilde{\psi}(\vec{k},s)=\int_0^\infty dt\;e^{-st}\;\psi(\vec{k},t)\quad,\quad\widetilde{\Sigma}(\vec{k},s)=\int_0^\infty dt\;e^{-st}\;\Sigma(\vec{k},t)=\int_{-\infty}^{+\infty}\frac{dk_0}{\pi}\,\frac{\mathrm{Im}\Sigma(\vec{k},k_0)}{k_0-is}\;,\tag{3.145}$$

where we have used eq.(3.141) to obtain the Laplace transform of the self-energy, which leads to the analyticity relation (see Eq. (3.21)),

$$\widetilde{\Sigma}(\vec{k},s)=\Sigma(\vec{k},\omega=is-i\epsilon)\;.\tag{3.146}$$

In terms of Laplace transforms the equation of motion becomes the following algebraic equation

$$\begin{aligned}&\left[\left(i\gamma^0 s-\vec{\gamma}\cdot\vec{k}\right)\,\delta_{ab}-M_{ab}+\Sigma^{tad}_{ab}\,L+\widetilde{\Sigma}_{ab}(\vec{k},s)\,L\right]\,\widetilde{\psi}_b(\vec{k},s)\\ &=i\left\{\gamma^0\,\delta_{ab}+\frac{1}{is}\left[\widetilde{\Sigma}_{ab}(\vec{k},s)-\widetilde{\Sigma}_{ab}(\vec{k},0)\right]\,L\right\}\psi_b(\vec{k},0)\;.\end{aligned}\tag{3.147}$$

Consistently with the expansion of the self-energy in frequency and momentum up to order ω/M_W, and using eq.(3.146), we replace the expression in the bracket in eq.(3.147) by

$$\frac{1}{is}\left[\widetilde{\Sigma}_{ab}(\vec{k},s)-\widetilde{\Sigma}_{ab}(\vec{k},0)\right]\Big|_{s=0}=\frac{\partial\Sigma(\vec{k},\omega)}{\partial\omega}\Big|_{\omega=0}\equiv\Sigma'(\vec{k},0)\;.\tag{3.148}$$

Using the representation (3.38) for the real part of the self-energy, the eq. (3.147) can be written as

$$\left[\left(\gamma^0\,i\,s-\vec{\gamma}\cdot\vec{k}\right)\,\mathbb{1}-\mathbb{M}+\gamma^0\widetilde{\mathbb{A}}(s)\,L-\vec{\gamma}\cdot\widehat{\mathbf{k}}\,\mathbb{B}(k)\,L\right]\,\widetilde{\psi}_b(\vec{k},s)=i\,\gamma^0\left[\mathbb{1}+\mathbb{A}'(0)\,L\right]\,\psi_b(\vec{k},0)\;,\tag{3.149}$$

where

$$\widetilde{\mathbb{A}}(s)=\mathbb{A}(\omega=is)\quad;\quad\mathbb{A}'(0)=\frac{d\,\mathbb{A}}{d\omega}\Big|_{\omega=0}\;.\tag{3.150}$$

The real time evolution is obtained by the inverse Laplace transform,

$$\psi(\vec{k},t)=\int_\Gamma\frac{ds}{2\pi i}\;\widetilde{\psi}(\vec{k},s)\;e^{st}\;,\tag{3.151}$$

where Γ is the Bromwich contour in the complex s plane running parallel to the imaginary axis to the right of all the singularities of the function $\widetilde{\psi}(\vec{k},s)$ and closing on a large semicircle to the left.

We now follow the same steps as in section 3.4, namely projecting onto right and left components and onto helicity eigenstates. After straightforward manipulations we arrive at the following set of equations

$$\left[-(s^2+k^2)\ \mathbb{1}+(is-\hat{h}(\widehat{\mathbf{k}})k)(\widetilde{\mathbb{A}}+\hat{h}(\widehat{\mathbf{k}})\mathbb{B})-\mathbb{M}^2\right]\widetilde{\psi}_L(\vec{k},s)=i\,\gamma^0\,\mathbb{M}\,\psi_R(\vec{k},0)+i(is-\hat{h}(\widehat{\mathbf{k}})k)\,\mathbb{D}\,\psi_L(\vec{k},0)\ , \tag{3.152}$$

where $\mathbb{D}=\mathbb{1}+\mathbb{A}'(0)$, and

$$\widetilde{\psi}_R(\vec{k},s)=-\frac{is+\hat{h}(\widehat{\mathbf{k}})k}{s^2+k^2}\left[\mathbb{M}\,\gamma^0\,\widetilde{\psi}_L(\vec{k},s)+i\,\psi_R(\vec{k},0)\right]\ . \tag{3.153}$$

We now follow the same steps as above to separate the Dirac and flavor structures by introducing the flavor doublets $\widetilde{\varphi}(\vec{k},s)$, $\widetilde{\xi}(\vec{k},s)$ which are the Laplace transform of the flavor doublets $\varphi(\vec{k},t)$, $\xi(\vec{k},t)$ introduced in the expansion of the Dirac spinors in eqs.(3.71)-(3.72), projecting onto the Weyl spinors eigenstates of helicity, the above equations become

$$\left[-(s^2+k^2)\mathbb{1}+(is-hk)(\widetilde{\mathbb{A}}+h\mathbb{B})-\mathbb{M}^2\right]\widetilde{\varphi}^{(h)}(\vec{k},s)=-i\,\mathbb{M}\,\xi^{(h)}(\vec{k},0)+i\,(is-hk)\,\mathbb{D}\,\varphi^{(h)}(\vec{k},0)\ , \tag{3.154}$$

$$\widetilde{\xi}^{(h)}(\vec{k},s)=-\frac{is+hk}{s^2+k^2}\left[-\mathbb{M}\,\widetilde{\varphi}^{(h)}(\vec{k},s)+i\,\xi^{(h)}(\vec{k},0)\right]\ . \tag{3.155}$$

The solution to eq. (3.154) is obtained as

$$\widetilde{\varphi}^{(h)}(\vec{k},s)=\widetilde{\mathbb{S}}^{(h)}(k,s)\left[-i\mathbb{M}\,\xi^{(h)}(\vec{k},0)+i(i\,s-h\,k)\mathbb{D}\,\varphi^{(h)}(\vec{k},0)\right], \tag{3.156}$$

where the propagator is given by

$$\widetilde{\mathbb{S}}^h(k,s)=\frac{1}{\alpha_h^2(k,s)-\beta_h^2(k,s)}\begin{pmatrix}\alpha_h(k,s)+\beta(k,s)\cos 2\theta_m^{(h)} & -\beta_h(k,s)\sin 2\theta_m^{(h)}\\ -\beta_h(k,s)\sin 2\theta_m^{(h)} & \alpha_h(k,s)-\beta_h(k,s)\cos 2\theta_m^{(h)}\end{pmatrix}, \tag{3.157}$$

in which it will prove convenient to introduce the following quantities

$$\alpha_h(k,s)=\left[\omega^2-k^2+\frac{1}{2}\,S_h(\omega,k)-\frac{1}{2}\,(M_1^2+M_2^2)\right]_{\omega=is-i\epsilon}\ , \tag{3.158}$$

$$\beta_h(k,s)=\frac{1}{2}\,\delta M^2\left[\left(\cos 2\theta-\frac{\Delta_h(\omega,k)}{\delta M^2}\right)^2+\sin^2 2\theta\right]^{\frac{1}{2}}\Bigg|_{\omega=is-i\epsilon}\ . \tag{3.159}$$

The inverse Laplace transform eq.(4.8) can be done straightforwardly, the singularities of $\widetilde{\varphi}^{(h)}(\vec{k},s)$ in the complex s plane are determined by the singularities of the propagator $\widetilde{\mathbb{S}}^{(h)}(k,s)$.

Up to the order in weak interactions considered here, these singularities are isolated poles along the imaginary axis at the positions $s = -i\,\omega_a^{(h)}(k,\pm)$ given by eq. (3.96)-(3.99). As a relevant example of the real time evolution, let us consider that the initial state corresponds to a wave-packet of left-handed electron neutrinos of arbitrary helicity h, with no muon neutrinos. This could, for example, be the case relevant for nucleosynthesis in which a neutron beta decays at the initial time. In this case

$$\varphi^{(h)}(\vec{k},0) = \nu_e^{(h)}(\vec{k}) \begin{pmatrix} 1 \\ 0 \end{pmatrix} \quad , \quad \xi^{(h)}(\vec{k},0) = \begin{pmatrix} 0 \\ 0 \end{pmatrix} \, , \tag{3.160}$$

and we find

$$\widetilde{\varphi}^{(h)}(\vec{k},s) = \nu_e^{(h)}(\vec{k}) \, \frac{i(i\,s - h\,k)[1+A_e'(0)]}{\alpha_h^2(k,s) - \beta_h^2(k,s)} \begin{pmatrix} \alpha_h(k,s) + \beta_h(k,s)\,\cos(2\theta_m^{(h)}) \\ -\beta_h(k,s)\,\sin(2\theta_m^{(h)}) \end{pmatrix} \, , \tag{3.161}$$

$$\widetilde{\xi}^{(h)}(\vec{k},s) = -\nu_e^{(h)}(\vec{k}) \, \frac{i[1+A_e'(0)]}{\alpha_h^2(k,s) - \beta_h^2(k,s)} \, \mathbb{M} \begin{pmatrix} \alpha_h(k,s) + \beta_h(k,s)\,\cos(2\theta_m^{(h)}) \\ -\beta_h(k,s)\,\sin(2\theta_m^{(h)}) \end{pmatrix} \, . \tag{3.162}$$

In order to avoid cluttering the notation, we have not included the frequency argument in the mixing angle in the medium $\theta_m^{(h)}$ but such dependence should be understood throughout.

The term $[\alpha_h(k,s) - \beta_h(k,s)]^{-1}$ features poles at $s = -i\omega_1(k,\pm)$ and the term $[\alpha_h(k,s) + \beta_h(k,s)]^{-1}$ features poles at $s = -i\omega_2(k,\pm)$.

We neglect terms of order $G_F\ T^4/M_W^2 \sim (T/M_W)^4 \ll 1$ since in the regime in which the approximations are valid $T \ll M_W$. The residues of these poles are respectively $2\,\omega_{1,2}(k,\pm)$ and the inverse Laplace transform yield within these approximations,

$$\begin{aligned} \varphi^{(h)}(\vec{k},t) \;=\; & \nu_e^{(h)}(\vec{k}) \sum_{\lambda=\pm} \left[\frac{\omega_1^{(h)}(k,\lambda) - h\,k}{4\,\omega_1^{(h)}(k,\lambda)} \begin{pmatrix} 1 + C_{1,\lambda}^{(h)} \\ -S_{1,\lambda}^{(h)} \end{pmatrix} e^{-i\omega_1^{(h)}(k,\lambda)\,t} \right. \\ & \left. + \frac{\omega_2^{(h)}(k,\lambda) - h\,k}{4\,\omega_2^{(h)}(k,\lambda)} \begin{pmatrix} 1 - C_{2,\lambda}^{(h)} \\ S_{2,\lambda}^{(h)} \end{pmatrix} e^{-i\omega_2^{(h)}(k,\lambda)\,t} \right] , \end{aligned} \tag{3.163}$$

$$\begin{aligned} \xi^{(h)}(\vec{k},t) \;=\; & -\nu_e^{(h)}(\vec{k}) \sum_{\lambda=\pm} \left[\frac{\mathbb{M}}{4\,\omega_1^{(h)}(k,\lambda)} \begin{pmatrix} 1 + C_{1,\lambda}^{(h)} \\ -S_{1,\lambda}^{(h)} \end{pmatrix} e^{-i\omega_1^{(h)}(k,\lambda)\,t} \right. \\ & \left. + \frac{\mathbb{M}}{4\,\omega_2^{(h)}(k,\lambda)} \begin{pmatrix} 1 - C_{2,\lambda}^{(h)} \\ S_{2,\lambda}^{(h)} \end{pmatrix} e^{-i\omega_2^{(h)}(k,\lambda)\,t} \right] . \end{aligned} \tag{3.164}$$

For economy of notation, we introduce the following shorthand

$$C_{a,\lambda}^{(h)} \equiv \cos\left[2\theta_m^{(h)}(\omega_a^{(h)}(k,\lambda))\right] \quad , \quad S_{a,\lambda}^{(h)} \equiv \sin\left[2\theta_m^{(h)}(\omega_a^{(h)}(k,\lambda))\right] \tag{3.165}$$

for $a = 1, 2$, helicity components $h = \pm$ and positive and energy components $\lambda = \pm$.

The above expressions yield a direct comparison with the usual oscillation formulae in the literature. To leading order we set $\omega_{1,2}(k,\lambda) \approx \lambda k\ (1+M^2_{1,2}/2k^2)$ in the prefactors in the expressions above thereby neglecting terms of order G_F. Since the dependence of the mixing angle on the frequency and momentum appears at order G_F, we can set $\omega_{1,2}(k,\lambda) \approx \lambda\, k$ in the argument of the mixing angles, therefore to leading order $C^{(h)}_{1,\lambda} = C^{(h)}_{2,\lambda} \equiv C^{(h)}_{\lambda}$ and $S^{(h)}_{1,\lambda} = S^{(h)}_{2,\lambda} \equiv S^{(h)}_{\lambda}$. With these approximations, for an initial left handed electron state of helicity $h = \mp$ we find

$$\begin{aligned}
\varphi^-(\vec{k},t) &= \nu_e^-(\vec{k})\Bigg[\frac{1}{2}\begin{pmatrix} 1+C^-_+ \\ -S^-_+ \end{pmatrix} e^{-i\omega_1^-(k,+)\,t} + \frac{1}{2}\begin{pmatrix} 1-C^-_+ \\ S^-_+ \end{pmatrix} e^{-i\omega_2^-(k,+)\,t} \\
&+ \frac{M_1^2}{8k^2}\begin{pmatrix} 1+C^-_- \\ -S^-_- \end{pmatrix} e^{i\omega_1^-(k,-)\,t} + \frac{M_2^2}{8k^2}\begin{pmatrix} 1-C^-_- \\ S^-_- \end{pmatrix} e^{i\omega_2^-(k,-)\,t}\Bigg]\,, \qquad (3.166)
\end{aligned}$$

$$\begin{aligned}
\varphi^+(\vec{k},t) &= \nu_e^+(\vec{k})\Bigg[\frac{M_1^2}{8k^2}\begin{pmatrix} 1+C^+_+ \\ -S^+_+ \end{pmatrix} e^{-i\omega_1^+(k,+)\,t} + \frac{M_2^2}{8k^2}\begin{pmatrix} 1-C^+_+ \\ S^+_+ \end{pmatrix} e^{-i\omega_2^+(k,+)\,t} \\
&+ \frac{1}{2}\begin{pmatrix} 1+C^+_- \\ -S^+_- \end{pmatrix} e^{i\omega_1^+(k,-)\,t} + \frac{1}{2}\begin{pmatrix} 1-C^+_- \\ S^+_- \end{pmatrix} e^{i\omega_2^+(k,-)\,t}\Bigg]\,. \qquad (3.167)
\end{aligned}$$

The exponentials $e^{\mp i\omega(k)\,t}$ correspond to positive energy $(-)$ neutrino and positive energy $(+)$ antineutrino components respectively. Therefore, the expressions above reveal that for negative helicity the relevant components in the relativistic limit correspond to positive energy neutrinos, while for positive helicity they correspond to positive energy *antineutrinos*.

The upper component of the expressions above correspond to wavepackets of negative and positive helicity respectively for a left handed electron neutrino, namely $\nu_e^{\mp}(\vec{k},t)$ while the lower components correspond to a left handed *muon* neutrino, namely $\nu_\mu^{\mp}(\vec{k},t)$.

For the right handed components ξ the leading order can be obtained by setting $\mathbb{M} \approx \overline{M}\,\mathbb{1}$ thereby neglecting terms of order $\delta M^2/\overline{M}^2$. This approximation yields,

$$\begin{aligned}
\xi^{\mp}(\vec{k},t) &= -\nu_e^{\mp}(\vec{k})\,\frac{\overline{M}}{4\,k}\Bigg[\begin{pmatrix} 1+C^{\mp}_+ \\ -S^{\mp}_+ \end{pmatrix} e^{-i\omega_1^{\mp}(k,+)\,t} + \begin{pmatrix} 1-C^{\mp}_+ \\ S^{\mp}_+ \end{pmatrix} e^{-i\omega_2^{\mp}(k,+)\,t} \\
&- \begin{pmatrix} 1+C^{\mp}_- \\ -S^{\mp}_- \end{pmatrix} e^{i\omega_1^{\mp}(k,-)\,t} - \begin{pmatrix} 1-C^{\mp}_- \\ S^{\mp}_- \end{pmatrix} e^{i\omega_2^{\mp}(k,-)\,t}\Bigg]\,. \qquad (3.168)
\end{aligned}$$

The upper and lower components correspond to wavepackets for right handed negative and positive helicity electron and muon neutrinos respectively.

From the expression (3.166) we can read off the probability for relativistic left handed, negative helicity electron and muon neutrinos as a function of time,

$$|\nu^-_{e,L}(\vec{k},t)|^2 = |\nu^-_e(\vec{k})|^2\left\{1-\sin^2[2\,\theta^-_m(k)]\;\sin^2\left(\frac{1}{2}\,\Delta\omega^-(k,+)\,t\right)+\mathcal{O}\left(\frac{M^2_{1,2}}{k^2}\right)\right\}\,, \quad (3.169)$$

$$|\nu^-_{\mu,L}(\vec{k},t)|^2 = |\nu^-_e(\vec{k})|^2\left\{\sin^2[2\,\theta^-_m(k)]\;\sin^2\left(\frac{1}{2}\,\Delta\omega^-(k,+)\,t\right)+\mathcal{O}\left(\frac{M^2_{1,2}}{k^2}\right)\right\}\,. \quad (3.170)$$

The probability for left handed relativistic *positive* helicity electron and muon antineutrinos as a function of time are read off from eq.(3.167)

$$|\nu^+_{e,L}(\vec{k},t)|^2 = |\nu^+_e(\vec{k})|^2\left\{1-\sin^2[2\,\theta^+_m(-k)]\;\sin^2\left(\frac{1}{2}\,\Delta\omega^+(k,-)\,t\right)+\mathcal{O}\left(\frac{M^2_{1,2}}{k^2}\right)\right\} \quad (3.171)$$

$$|\nu^+_{\mu,L}(\vec{k},t)|^2 = |\nu^+_e(\vec{k})|^2\left\{\sin^2[2\,\theta^+_m(-k)]\;\sin^2\left(\frac{1}{2}\,\Delta\omega^+(k,-)\,t\right)+\mathcal{O}\left(\frac{M^2_{1,2}}{k^2}\right)\right\}\,, \quad (3.172)$$

where

$$\Delta\omega^\pm(k,\pm)=\frac{\delta M^2}{2k}+\delta\omega^\pm_1(k,\pm)-\delta\omega^\pm_2(k,\pm)\,. \quad (3.173)$$

The corrections $\delta\omega^\pm_a(k,\pm)$ had been studied in detail in section 3.4.3 above. Finally, eq. (3.168) determines the probabilities of finding *right handed* positive and negative helicities neutrinos as a function of time. This equation makes manifest that this probability is suppressed by a factor $\overline{M}/k$ with respect to the left handed component, indeed it is the mass term that is responsible for generating a right handed component from a left handed one and must therefore be suppressed by one power of the ratio M/k. For a typical neutrino momentum $k \gtrsim 1\,\mathrm{MeV}$ this suppression factor is of order 10^{-6}. Eqs.(3.163)-(3.164) provide a complete field theoretical description of oscillations in *real time*. Eqs.(3.169)-(3.170) are obviously reminiscent of the familiar oscillation equations obtained in the simplified quantum mechanical two level system, however there are some important aspects that must be highlighted, namely, the field theoretical formulation introduced here led directly to these oscillation formulae in terms of the mixing angles in the medium and the correct oscillation frequencies that include the quantum loop corrections. Furthermore, the oscillation formulae obtained above reveal the nature of the approximations and allow a consistent inclusion of higher order effects as well as describe the oscillation of *all* helicity components as well as the dynamics of the right handed component. The usual oscillation formula obtained within the single particle quantum mechanical description emerge cleanly in suitable limits and the nature of the corrections is readily manifest.

3.6 CONCLUSIONS

In this chapter, we provided a systematic treatment of neutrino oscillations and mixing directly from quantum field theory in real time in a regime of temperature and density relevant for early Universe cosmology prior to big bang nucleosynthesis. While we have focused on two flavors (electron and muon) of Dirac neutrinos the formulation can be generalized straightforwardly to more flavors and to Majorana-Dirac mass matrices.

We have obtained the medium corrections to the dispersion relations and mixing angles of propagating neutrinos. Implementing methods from real time non-equilibrium quantum field theory at finite temperature and density we have systematically obtained the equations of motion for the neutrino field and studied the real time evolution as an initial value problem. The major advantage of this approach, as compared to the usual approach based on single particle quantum mechanics is that it consistently and systematically includes the medium corrections to the dispersion relations and mixing angles *directly* into the real time evolution and treats left and right handed fields and both helicity components on equal footing. We have argued that collisional relaxation yields thermalization of neutrinos in *flavor eigenstates* for temperature $T \gtrsim 5 - 10\,\mathrm{Mev}$ for which the relaxation time scale via weak interactions is shorter than the oscillation time scale. Assuming the validity of this argument, we obtained the neutrino self-energies up to one-loop including the asymmetries from leptons, neutrinos, hadrons and quarks, as well as non-local (in space-time) terms arising from the expansion of the self-energy loop in the external frequency and momentum. We have consider these non-local terms up to leading order in ω/M_W ; k/M_W since these terms are of the same order of or larger than the contribution from the asymmetries for $T \gtrsim 5\,\mathrm{MeV}$ *if* all asymmetries are of the same order as the baryon asymmetry. This is yet another indication that this is an important temperature regime in the early Universe.

Our main results are summarized as follows:

- Implementing the methods from non-equilibrium real-time field theory at finite temperature and density we obtained the equations of motion for the neutrino fields in linear response. This formulation includes consistently the self-energy loop corrections to the dispersion relations and mixing angles in the medium and treat left and right handed fields with both helicity components on equal footing.
- We have focused on a temperature regime prior to nucleosynthesis $T \gtrsim 5 - 10\,\mathrm{MeV}$ in which we argued that neutrinos are thermalized as flavor eigenstates. We studied two different tem-

perature regimes: $m_e \ll T \ll m_\mu$ within which we have shown that there is the possibility of resonant oscillations of test neutrinos, and $m_e, m_\mu \ll T \ll M_W$ within which the mixing angle for active neutrinos effectively vanishes.

- An expansion of the self-energy in terms of the neutrino frequency and momentum is carried out to lowest order in ω/M_W ; k/M_W thus extracting the leading *non-local* (in space-time) contributions. We find a *new* contribution which cannot be identified with an effective potential. The mixing angles and propagation frequencies in the medium are found to be *helicity dependent*.
- If the lepton and quark asymmetries are of the same order as the baryon asymmetry in the early Universe, we have shown that the non-local (in space-time) terms in the self-energies dominate over the asymmetry for typical energies of neutrinos in the plasma for $T \gtrsim 3 - 5\,\mathrm{MeV}$.
- The oscillation time scale in the medium is *slowed-down* near the resonance, becoming substantially *longer* than in the vacuum for small vacuum mixing angle. For high energy neutrinos off-resonance the mixing angle becomes vanishingly small and the oscillation time scale *speeds-up* as compared to the vacuum. At high temperature, in the region $T \gg m_e, m_\mu$ the mixing angle for active neutrinos effectively vanishes and there is a considerable *speed-up* of oscillations, which are then suppressed by a vanishingly small mixing angle and a rapid dephasing.
- We have obtained the general equations of motion for initially prepared wave packets of neutrinos of arbitrary chirality and helicity. These equations reduce to the familiar oscillation formulae for ultrarelativistic negative helicity neutrinos, but with the bonus that they consistently include the mixing angles and the oscillation frequencies in the medium. These equations not only yield the familiar ones but also quantify the magnitude of the corrections. Furthermore these equations also describe the evolution of right handed neutrinos (of either helicity) which is a consequence of a non-trivial mass matrix and usually ignored in the usual formulation.

4.0 SPACE-TIME PROPAGATION OF NEUTRINO WAVE-PACKETS AT HIGH TEMPERATURE AND DENSITY

4.1 INTRODUCTION

In 1981, Kayser[98] first pointed out subtle but important caveats in the vacuum oscillation formula obtained from the standard plane wave treatment, which result from assuming a definite neutrino momentum for different mass eigenstates. He showed that knowledge of momentum allows experiments to distinguish different neutrino mass eigenstates, essentially destroying the oscillation pattern. He then proposed a wave-packet treatment of neutrino oscillations, in which the neutrino momentum is spread out. Since then, the wave-packet approach has been studied by many authors in both quantum mechanical [9, 10, 99, 100, 101, 102, 103] and field theoretical [104, 105, 106, 107, 108] frameworks, including the study of oscillations of neutrinos produced and detected in crystals[109].

The quantum mechanical approach usually refers to the intermediate wave-packet model in which each propagating mass eigenstate of neutrino is associated with a wave-packet [100]. This model eliminates some of the problems in the plane wave treatment although several conceptual questions remaining unsettled[99]. See [108] and references therein for detailed descriptions of these issues. A field theoretical approach is the external wave-packet model [104] in which the oscillating neutrino is represented by an internal line of a Feynman diagram, while the source and the detector are respectively described by in-coming and out-going wave-packets. A recent review[108] presents the different approaches, summarizes their advantages and caveats and includes the dispersion of wave packets in the study.

An important physical consequence of the wave-packet description of neutrino evolution is the concept of the coherence length beyond which neutrino oscillations vanish. A "flavor neutrino" wave-packet is a linear superposition of wave-packets of mass eigenstates. The different mass

states entail a difference in the group velocity and an eventual separation of the wave-packets associated with mass eigenstates. This separation results in a progressive loss of coherence as overlaps between the wave packets dimishes. See for example[102] for an early explanation. In an actual source-detector experimental setup, the observation time is usually not measured and is commonly integrated out in a wave-packet treatment[102]. This leads to a localization term in the vacuum oscillation formula, which states that neutrino oscillations are suppressed if the spatial uncertainty is much larger than the oscillation length[102].

The coherence of neutrino oscillations in matter has been studied within a geometrical representation in [101], but the medium oscillation formula was not derived. While most of the studies focus on reproducing the standard vacuum oscillation formula, a consistent study of neutrino mixing and propagation in a medium *in real time* has not yet emerged.

While in the vacuum the space-time propagation can be studied in the wave-packet approach by focusing on the space-time evolution of initially prepared single particle "flavor states", the study of the space-time evolution in a medium at finite temperature and density requires a density matrix description.

To the best of our knowledge, a full finite temperature field theoretical treatment of the space-time propagation of neutrino wave-packets in a medium including medium corrections and dispersion dynamics has not yet been offered. We consider this study an important aspect of the program to study the non-equilibrium evolution of neutrinos in the early Universe. Detailed studies have shown that neutrino oscillations and self-synchronization lead to flavor equilibration before BBN[32, 71, 110, 111, 112], beginning at a temperature of $T \sim 30MeV$ with complete flavor equilibration among all flavors at $T \sim 2MeV$ [111]. If neutrinos are produced in the form of spatially localized wave-packets rather than extended plane waves before BBN, the two mass eigenstates separate progressively during propagation due to the small difference in group velocities. A significant amount of neutrino oscillations, which are crucial for "flavor equalization" requires that the two mass eigenstates overlap appreciably throughout their propagation, namely the coherence time scale should be sufficiently large to ensure that "flavor equilibration" through oscillations is effective. Therefore, it is important to pursue a full field theoretical study of neutrino wave-packet propagation in the medium directly in *real time* to determine the relevant time scales for coherence to be maintained and to identify the processes that contribute to its loss.

In this chapter, we study the space-time evolution of neutrino wave packets in extreme environments at high temperature and density, conditions that prevail in the early Universe or during

supernovae explosions. Our goals are the following:

- To provide a consistent and systematic non-equilibrium field-theoretical formulation to study the space-time evolution of initially prepared neutrino wave packets at finite temperature and density. This goal requires a treatment of the space-time evolution in terms of the density matrix, which goes beyond the usual treatment in terms of single particle states. To achieve this goal we implement a recently developed method[113] to study non-equilibrium aspects of neutrino propagation in a medium as an *initial value problem* in linear response. This method yields the effective Dirac equation of motion for the expectation value of the neutrino field induced by an external source. The effective Dirac equation in the medium includes self-energy contributions from charged and neutral currents up to one loop.
- To assess the different time scales associated with wave-packet dispersion, coherence and oscillations including the medium effects, in particular near possible resonances in the in-medium mixing angles. This is achieved by solving the effective Dirac equation in the medium, which includes self-energy corrections, as an initial value problem. The initial wave-packet configuration is "prepared" by an external source term in linear response. This method also allows to assess corrections from the *energy dependence of the mixing angles in the medium* upon the wave-packet dynamics.
- The space-time evolution of the initially prepared wave packet, including dispersive effects allows an assessment of the competition between the progressive loss of coherence in the wave-packet dynamics by the separation of mass eigenstates, collisional decoherence and cosmological expansion. While our study only includes the self-energy from charged and neutral currents up to one-loop, the final result allows us to include results available in the literature[14, 57, 58, 59] to understand the effects of collisional decoherence and cosmological expansion when there is a separation of time scales.
- We focus our study within the context of early Universe cosmology, in particular in the temperature regime just prior to BBN where there is a possibility for resonant transitions[14, 57, 58, 59, 113]. Of particular interest are the medium modifications of the dispersion relations, wave-packet dispersion, oscillation and coherence time scales in this temperature and energy regime.

Since we study the propagation of neutrino wave-packets in a medium, aspects associated with the source-detector measurement processes are not well-defined or relevant in this case. Conse-

quently, in contrast to most studies in the literature, *we do not integrate in time* as is the case for a description of experiments in the vacuum [102]. Therefore, our study of propagation is both in *space and time*.

This chapter is organized as follows. In section 4.2, we obtain the effective Dirac equation of neutrino in a thermal medium implementing the methods of non-equilibrium field theory and linear response[113]. In this section we obtain the in-medium dispersion relations and mixing angles. In section 4.3, we develop the general formulation to study the space-time propagation of neutrino wave-packet. In this section we discuss the different time scales associated with dispersion, oscillations and coherence. In section 4.4 we compare the different time scales with the Hubble and collisional relaxation time scales and discuss the impact of the different scales upon the space-time evolution of the neutrino wave-packets, coherence and oscillations. We present our conclusions in section 4.5.

4.2 EFFECTIVE DIRAC EQUATION OF NEUTRINOS IN A MEDIUM AND LINEAR RESPONSE

The study of the evolution of neutrino wave packets in the vacuum typically involves a description of the experimental production and detection of these wave packets. We study the space-time evolution of wave packets in a medium as an *initial value problem*. This is achieved in *linear response* by coupling an external source term which induces an expectation value of the neutrino field in the density matrix, after this source is switched off the expectation value evolves in time. The propagation of this initial state is described by the effective Dirac equation in the medium, which includes the self-energy corrections. This is the familiar linear response approach to studying the evolution out of equilibrium in condensed matter systems. The correct framework to implement this program is the real-time formulation of field theory in terms of the closed-time-path integral [83, 85, 87].

We restrict our study to the case of two Dirac flavor neutrinos, while the formulation is general and can treat $1-2$ or $1-3$ mixing on equal footing, for convenience we will refer to electron and muon neutrino mixing. The current value for $\overline{M}$ obtained by WMAP [8] and the oscillation

parameters from the combined fitting of the solar and KamLAND data are [92] respectively:

$$\overline{M} \approx 0.25\,(eV) \;\; ; \;\; |\delta M^2_{12}| \approx 7.9 \times 10^{-5}\,(eV)^2 \; ; \;\; \tan^2\theta_{12} \approx 0.40 \; . \tag{4.1}$$

For atmospheric neutrinos, analysis from SuperKamiokande, CHOOZ and atmospheric neutrino data yield,

$$|\delta M^2_{13}| \approx (1.3 - 3.0) \times 10^{-3}\,(eV)^2 \; ; \;\; \sin^2\theta_{13} < 0.067 \; (3\sigma) \; . \tag{4.2}$$

4.2.1 Linear response:

The medium is described by an *ensemble* of states, and the description is in terms of a density matrix. Therefore the question of space-time evolution is more subtle, while in the vacuum one can consider preparing an initial *single particle* state and evolving it in time, such a consideration is not available in a medium, and the question of time evolution *must* be formulated differently, namely in terms of expectation values of the relevant operators in the density matrix.

In equilibrium the neutrino field *cannot* have an expectation value in the density matrix. The usual method in many body theory to study the non-equilibrium evolution of single quasiparticle states is the method of linear response: an external source is coupled to the field which develops an expectation value in the density matrix induced by the source. The expectation value of this field obeys the equation of motion with medium corrections. Upon switching-off the external source, the expectation value evolves in time as a solution of the effective equations of motion in the medium. For a detailed description of this method in non-equilibrium quantum field theory see refs.[85, 87, 113]. The external sources η_a in the Lagrangian density (3.1) induce an expectation value of the neutrino field

$$\psi_a = \langle \nu_a \rangle = \mathrm{Tr}\,\hat{\rho}\,\nu_a \tag{4.3}$$

where $\hat{\rho}$ is the full density matrix of the medium. In linear response this expectation value is linear in the external source and obeys the effective Dirac equation of motion in the medium[87]. It is most conveniently written in terms of the spatial Fourier transforms of the fields, sources and self-energies $\psi_a(\vec{k},t), \eta_a(\vec{k},t), \Sigma(\vec{k},t-t')$ respectively. The one loop self-energies with neutral and charged current contributions had been obtained in refs.[57, 58, 113], and the effective Dirac equation in the medium up to one loop has been obtained in the real time formulation in ref.[113].

It is given by

$$\left[\left(i\gamma^0\frac{\partial}{\partial t}-\vec{\gamma}\cdot\vec{k}\right)\,\delta_{ab}-M_{ab}+\Sigma^{tad}_{ab}L\right]\,\psi_b(\vec{k},t)+\int_{-\infty}^{t}dt'\Sigma_{ab}(\vec{k},t-t')\,L\,\psi_b(\vec{k},t')=-\eta_a(\vec{k},t),\;\;(4.4)$$

where L is the projector on left handed states, $\Sigma^{tad}_{ab}L$ is the (local) tadpole contribution from the neutral currents and $\Sigma_{ab}(\vec{k},t-t')$ is the spatial Fourier transform of the (retarded) self energy which includes both neutral and charged current interactions, and whose spectral representation is given by

$$\Sigma(\vec{k},t-t')=i\int_{-\infty}^{\infty}\frac{dk_0}{\pi}\,\mathrm{Im}\Sigma(\vec{k},k_0)\,e^{-ik_0(t-t')}\;\;;\;\;\Sigma(\vec{k},k_0)=\Sigma_W(\vec{k},k_0)+\Sigma_Z(\vec{k},k_0)\qquad(4.5)$$

where we have separated the charged and neutral current contributions respectively.

It is obvious that Eq. (4.4) takes exactly the same form as Eq. (3.140). Thus, following the same laplace transform procedures as we did in section 3.5, the equation of motion becomes the following algebraic equation

$$D_{ab}(\vec{k},s)\,\widetilde{\psi}_b(\vec{k},s)=i\left(\gamma^0\,\delta_{ab}+\frac{1}{is}\left[\widetilde{\Sigma}_{ab}(\vec{k},s)-\widetilde{\Sigma}_{ab}(\vec{k},0)\right]\,L\right)\psi_b(\vec{k},0)\qquad(4.6)$$

where $D(\vec{k},s)\equiv D(\vec{k},\omega=is-i\epsilon)$ is the analytic continuation of the Dirac operator in frequency and momentum space

$$D_{ab}(\vec{k},\omega)=\left[\left(\gamma^0\omega-\vec{\gamma}\cdot\vec{k}\right)\,\delta_{ab}-M_{ab}+\Sigma^{tad}_{ab}\,L+\Sigma_{ab}(\vec{k},\omega)\,L\right]\qquad(4.7)$$

The full space-time evolution of an initial state is determined by

$$\psi_a(\vec{x},t)=\int d^3k\,e^{i\vec{k}\cdot\vec{x}}\int_\Gamma\frac{ds}{2\pi i}\,D^{-1}_{ab}(\vec{k},s)\,(i\gamma^0)\psi_b(\vec{k},0)\,e^{st}\;,\qquad(4.8)$$

where Γ is the Bromwich contour in the complex s plane running parallel to the imaginary axis to the right of all the singularities of the function $\widetilde{\psi}(\vec{k},s)$ and closing on a large semicircle to the left. We have simplified the expression for the eqn. (4.8) by discarding a perturbatively small correction to the amplitude of $\mathcal{O}(G_F)$, given by the self-energy corrections on the right hand side of eqn. (3.147). Therefore the space-time evolution is completely determined by the singularities of the function $\widetilde{\psi}(\vec{k},s)$ in the complex s-plane. Up to one loop order and for temperatures well below the mass of the vector bosons, the only singularities are simple poles along the imaginary

axis, corresponding to the dispersion relations of the propagating modes in the medium. In this temperature range absorptive processes emerge at the two loop level, consequently these are of $\mathcal{O}(G_F^2)$ and are neglected in the one loop analysis presented here. The integral along the Bromwich contour in the complex s-plane can now be written

$$\int_\Gamma \frac{ds}{2\pi i}\, D^{-1}_{ab}(\vec{k},s)\,(i\gamma^0)\psi_b(\vec{k},0)\,e^{st} = \int_{-\infty}^{\infty}\frac{d\omega}{2\pi}\, D^{-1}_{ab}(\vec{k},\omega)\,(i\gamma^0)\psi_b(\vec{k},0)\,e^{-i\omega\, t} \tag{4.9}$$

where the frequency integral is performed along a line parallel to but slightly below the real ω axis closing counterclockwise in the upper half plane.

The one loop contributions to the self-energy for $\omega, k, T \ll M_W$ were obtained in reference[57, 58, 113] and found to be of the form[113]

$$\Sigma^{tad}_{ab} + \Sigma_{ab}(\vec{k},\omega) = \gamma^0 \mathbb{A}(\omega) - \vec{\gamma}\cdot\widehat{\mathbf{k}}\,\mathbb{B}(k) \tag{4.10}$$

where $\mathbb{A}(\omega)$ and $\mathbb{B}(k)$ are 2×2 diagonal matrices in the neutrino flavor basis.[1]. To lowest order in $k/M_W\,;\omega/M_W$ these matrices are found to be[14, 57, 58, 113]

$$\mathbb{A}(\omega) = \begin{pmatrix} A_e(\omega) & 0 \\ 0 & A_\mu(\omega) \end{pmatrix}\;;\quad \mathbb{B}(k) = \begin{pmatrix} B_e(k) & 0 \\ 0 & B_\mu(k) \end{pmatrix}, \tag{4.11}$$

where the entries $A_e(\omega)$, $A_\mu(\omega)$, $B_e(k)$ and $B_\mu(k)$ can be read off from the results of section 3.3. Also, see the reference[113], as well as [14, 57, 58, 59].

4.2.2 Dispersion relations and mixing angles in the medium

The simple poles of the integrand in (4.9) are the solutions of the homogeneous Dirac equation (3.60). Following the same procedures as we did in section 3.4, the propagating modes in the medium are found by diagonalizing (3.60). This can be done by performing a unitary transformation $\varphi^{(h)}(\omega,k) = U^{(h)}_m\;\chi^{(h)}(\omega,k)$ where

$$U^{(h)}_m = \begin{pmatrix} \cos\theta^{(h)}_m & \sin\theta^{(h)}_m \\ -\sin\theta^{(h)}_m & \cos\theta^{(h)}_m \end{pmatrix}\quad;\quad \chi^{(h)}(\omega,k) = \begin{pmatrix} \nu^{(h)}_1(\omega,k) \\ \nu^{(h)}_2(\omega,k) \end{pmatrix}, \tag{4.12}$$

[1] The equivalence with the notation of ref.[57] is (see eqn. (2) in ref.[57]): $a_{NR} = \mathbb{B}(k)/k\;;\; b_{NR} = \mathbb{A}(\omega) - \omega\,\mathbb{B}(k)/k$.

and a similar transformation for the right handed doublet $\xi^{(h)}(\omega,k)$, with the medium mixing angle $\theta_m^{(h)}$ depending on h,k and ω. Upon diagonalization, the eigenvalue equation is given by [113]

$$\left\{\omega^2-k^2+\frac{1}{2}\,S_h(\omega,k)-\frac{1}{2}\,(M_1^2+M_2^2)-\frac{1}{2}\,\delta\,M^2\,\Omega_h(\omega,k)\begin{pmatrix}1&0\\0&-1\end{pmatrix}\right\}\chi^{(h)}(\omega,k)=0\;, \quad (4.13)$$

where $S_h(\omega,k)$, $\Delta_h(\omega,k)$ and $\Omega_h(\omega,k)$ are respectively given by

$$\begin{aligned} S_h(\omega,k) &= (\omega-hk)\,[A_e(\omega)+A_\mu(\omega)+h\;B_e(k)+h\;B_\mu(k)]\;, && (4.14)\\ \Delta_h(\omega,k) &= (\omega-hk)\,[A_e(\omega)-A_\mu(\omega)+h\;B_e(k)-h\;B_\mu(k)]\;, && (4.15)\\ \Omega_h(\omega,k) &= \left[\left(\cos 2\theta-\frac{\Delta_h(\omega,k)}{\delta M^2}\right)^2+\sin^2 2\theta\right]^{\frac{1}{2}}\;. && (4.16)\end{aligned}$$

This requires the matrix elements in $U_m^{(h)}$ to be of the following form

$$\sin 2\theta_m^{(h)}(\omega,k)=\frac{\sin 2\theta}{\Omega_h(\omega,k)}\;;\quad \cos 2\theta_m^{(h)}(\omega,k)=\frac{\cos 2\theta-\frac{\Delta_h(\omega,k)}{\delta M^2}}{\Omega_h(\omega,k)}. \quad (4.17)$$

The dispersion relations $\omega_a^{(h)}(k,\lambda)$ for the propagating modes in the medium are found in perturbation theory consistently up to $\mathcal{O}(G_F)$ by writing [113]

$$\omega_a^{(h)}(k,\lambda)=\lambda\left[E_a(k)+\delta\omega_a^{(h)}(k,\lambda)\right]\quad,\quad a=1,2\;\;;\;\;\lambda=\pm \quad (4.18)$$

where $E_a(k)=\sqrt{k^2+M_a^2}$, and $\delta\omega_a^{(h)}(k,\lambda)$ are found to be

$$\delta\omega_a^{(h)}(k,\lambda)=-\frac{1}{4E_a(k)}\left\{S_h(\lambda E_a(k),k)+(-1)^a\,\delta M^2\;(\,\Omega_h(\lambda E_a(k),k)-1\,)\right\}. \quad (4.19)$$

For relativistic neutrinos with $k\gg M_a$ the dispersion relations $\omega_a(k)\;\;;\;\;a=1,2$ for the different cases are given to leading order in G_F by

- **Positive energy, negative helicity neutrinos**, $\lambda=+1,h=-1$:

$$\omega_a(k)=k+\frac{M_a^2}{2k}-\frac{1}{4k}\left[S_-(k,k)+(-1)^a\delta M^2\Big(\Omega_-(k,k)-1\Big)\right]. \quad (4.20)$$

- **Positive energy, positive helicity neutrinos**, $\lambda = +1, h = +1$:

$$\omega_a(k) = k + \frac{M_a^2}{2k} - \frac{1}{4k}\left[S_+(k,k) + (-1)^a \delta M^2 \Big(\Omega_+(k,k) - 1\Big)\right] \;\; ; \;\; \omega - h\,k \approx \frac{\overline{M}^2}{2k} \tag{4.21}$$

  where we have neglected corrections of order $\delta M^2/\overline{M}^2$.

- **Negative energy, negative helicity neutrinos**, $\lambda = -1, h = -1$:

$$\omega_a(k) = -k - \frac{M_a^2}{2k} + \frac{1}{4k}\left[S_-(-k,k) + (-1)^a \delta M^2 \Big(\Omega_-(-k,k) - 1\Big)\right] \;\; ; \;\; \omega - h\,k \approx \frac{\overline{M}^2}{2k} \tag{4.22}$$

  where we have again neglected corrections of order $\delta M^2/\overline{M}^2$.

- **Negative energy, positive helicity neutrinos**, $\lambda = -1, h = +1$:

$$\omega_a(k) = -k - \frac{M_a^2}{2k} + \frac{1}{4k}\left[S_+(-k,k) + (-1)^a \delta M^2 \Big(\Omega_+(-k,k) - 1\Big)\right]. \tag{4.23}$$

  In the above expressions the $\Omega_\pm$ are given by eqn. (4.16).

  The vacuum and medium oscillation time scales are respectively defined as

$$T_{vac} \;\; = \;\; \frac{2\pi}{E_1 - E_2} \;\; ; \;\; T_{med} = \frac{2\pi}{\omega_1^{(h)}(k,\lambda) - \omega_2^{(h)}(k,\lambda)}, \tag{4.24}$$

In the relativistic case when $k \gg M_a$, we find

$$T_{vac} \approx \frac{4\pi k}{\delta M^2} \;\; ; \;\; T_{med} \approx \frac{4\pi k}{\delta M^2\, \Omega_h(\lambda\, k, k)} \tag{4.25}$$

leading to the relation

$$\frac{T_{med}}{T_{vac}} = \frac{\sin 2\theta_m^{(h)}(\omega,k)}{\sin 2\theta} \tag{4.26}$$

4.3 SPACE-TIME PROPAGATION OF A NEUTRINO WAVE-PACKET.

We now have all the ingredients necessary to study the space-time evolution of a initial wave packet by carrying out the integrals in eqn. (4.8). For this purpose it is convenient to write

$\psi(\vec{k},0) = \psi_R(\vec{k},0) + \psi_L(\vec{k},0)$ and expand the right and left-handed components in the helicity basis as in Eq. (3.71) and Eq. (3.72), namely

$$\psi_L(\vec{k},0) = \sum_{h=\pm 1} \begin{pmatrix} 0 \\ v^{(h)} \otimes \varphi^{(h)}(\vec{k},0) \end{pmatrix} \;\; ; \;\; \psi_R(\vec{k},0) = \sum_{h=\pm 1} \begin{pmatrix} v^{(h)} \otimes \xi^{(h)}(\vec{k},0) \\ 0 \end{pmatrix} \tag{4.27}$$

where

$$\varphi^{(h)}(\vec{k},0) = \begin{pmatrix} \nu_{eL}^{(h)}(\vec{k},0) \\ \nu_{\mu L}^{(h)}(\vec{k},0) \end{pmatrix} \;\; ; \;\; \xi^{(h)}(\vec{k},0) = \begin{pmatrix} \nu_{eR}^{(h)}(\vec{k},0) \\ \nu_{\mu R}^{(h)}(\vec{k},0) \end{pmatrix} \tag{4.28}$$

The general initial value problem requires to furnish initial conditions for the four components above. However, an inhomogeneous neutrino state is produced by a weak interaction vertex, which produces left handed neutrinos, suggesting to set $\nu_{eR}^{(h)}(\vec{k},0) = 0; \nu_{\mu R}^{(h)}(\vec{k},0) = 0$. Without loss of generality let us consider an initial state describing an inhomogeneous wave-packet of *electron neutrinos* of arbitrary helicity, thus $\nu_{eL}^{(h)}(\vec{k},0) \neq 0; \nu_{\mu L}^{(h)}(\vec{k},0) = 0$.

In the cases of interest neutrinos are relativistic with typical momenta $k \gg \overline{M}$. Following the real time analysis described in detail in ref.[113] in the relativistic case we find

$$\varphi^{(h)}(\vec{k},t) = \frac{1}{2}\,\nu_{eL}^{(h)}(\vec{k},0) \left[\begin{pmatrix} 1+\mathcal{C}_{-h}^{(h)} \\ -\mathcal{S}_{-h}^{(h)} \end{pmatrix} e^{-i\omega_1^{(h)}(k,-h)\,t} + \begin{pmatrix} 1-\mathcal{C}_{-h}^{(h)} \\ \mathcal{S}_{-h}^{(h)} \end{pmatrix} e^{-i\omega_2^{(h)}(k,-h)\,t} + \mathcal{O}\Big(\frac{\overline{M}^2}{k^2}\Big) \right], \tag{4.29}$$

$$\begin{aligned} \xi^{(h)}(\vec{k},t) \;\; = \;\; & \frac{1}{2}\,\nu_{eL}^{(h)}(\vec{k},0) \left(\frac{h\,\overline{M}}{2\,k}\right) \Bigg\{ \begin{pmatrix} 1+\mathcal{C}_{-h}^{(h)} \\ -\mathcal{S}_{-h}^{(h)} \end{pmatrix} e^{-i\omega_1^{(h)}(k,-h)\,t} + \begin{pmatrix} 1-\mathcal{C}_{-h}^{(h)} \\ \mathcal{S}_{-h}^{(h)} \end{pmatrix} e^{-i\omega_2^{(h)}(k,-h)\,t} \\ & - \begin{pmatrix} 1+\cos 2\theta \\ -\sin 2\theta \end{pmatrix} e^{-i\omega_1^{(h)}(k,h)\,t} - \begin{pmatrix} 1-\cos 2\theta \\ \sin 2\theta \end{pmatrix} e^{-i\omega_2^{(h)}(k,h)\,t} + \mathcal{O}\Big(\frac{\overline{M}}{k}\Big) \Bigg\}, \end{aligned} \tag{4.30}$$

where $\varphi^{(h)}(\vec{k},t)$ and $\xi^{(h)}(\vec{k},t)$ are the flavor doublets corresponding to the left-handed and right-handed neutrinos with helicity h respectively. The upper component corresponds to the electron neutrino $\nu_e^{(h)}(\vec{k},t)$ while the lower component corresponds to the muon neutrinos $\nu_\mu^{(h)}(\vec{k},t)$. The factors $\mathcal{C}_\lambda^{(h)}(k)$ and $\mathcal{S}_\lambda^{(h)}(k)$ are defined as

$$\mathcal{C}_\lambda^{(h)}(k) = \cos\Big[2\theta_m^{(h)}(\lambda k)\Big] \;\; ; \;\; \mathcal{S}_\lambda^{(h)}(k) = \sin\Big[2\theta_m^{(h)}(\lambda k)\Big] \; . \tag{4.31}$$

The suppression factor M/k in the right handed component (4.30) is of course a consequence of the chirality flip transition from a mass term in the relativistic limit. For relativistic neutrinos and more specifically for neutrinos in the medium prior to BBN with $k \sim T \sim$ few MeV the right handed component is negligible as expected.

The one-loop computation of the self-energy performed above does not include absorptive processes such as collisions of neutrinos with leptons (or hadrons) in the medium. Such absorptive part will emerge in a two loops calculation and is of $\mathcal{O}(G_F^2)$. While we have not calculated these contributions it is clear from the analysis what it should be expected: the frequencies $\omega_{1,2}(k)$ are the "exact" dispersion relations of the single particle poles of the Dirac propagator in the medium. At two loops the self energy will feature an imaginary part with support on the mass shell of these single particle states. The imaginary part of the self-energy evaluated at these single particle energies yield the *width* of the single quasi-particle states $\Gamma_1(k); \Gamma_2(k)$ and the oscillatory exponentials in the expressions above are replaced as follows

$$e^{-i\omega_a(k)\,t} \to e^{-\Gamma_a(k)\,t}\, e^{-i\omega_a(k)\,t} \quad ; \quad a = 1, 2 \tag{4.32}$$

While our one loop calculation does not include the damping rates Γ_a we will invoke results available in the literature[14, 57, 58, 59] to estimate the collisional relaxation time scales (see section 4.4).

The corresponding fields for the left-handed and right-handed component neutrinos in configuration space are obtained by performing the spatial Fourier transform

$$\varphi^{(h)}(\vec{r}, t) = \int \frac{d^3\vec{k}}{(2\pi)^3}\; \varphi^{(h)}(\vec{k}, t)\; e^{i\vec{k}\cdot\vec{r}}, \tag{4.33}$$

$$\xi^{(h)}(\vec{r}, t) = \int \frac{d^3\vec{k}}{(2\pi)^3}\; \xi^{(h)}(\vec{k}, t)\; e^{i\vec{k}\cdot\vec{r}}. \tag{4.34}$$

For an arbitrary initial configuration these integrals must be done numerically, but analytic progress can be made by assuming an initial Gaussian profile, describing a wave-packet in momentum space centered at a given momentum, $\vec{k}_0$ with a width σ. While the width could generally depend on helicity we will consider the simpler case in which it is the same for both helicities.

Namely, we consider

$$\nu_{eL}^{(h)}(\vec{k},0) = \nu_{eL}^{(h)}(0)\left(\frac{\pi}{\sigma^2}\right)^{\frac{3}{2}} \exp\left[-\frac{(\vec{k}-\vec{k}_0)^2}{4\sigma^2}\right], \tag{4.35}$$

where $\nu_{eL}^{(h)}(0)$ is an arbitrary amplitude and assume that wave packet is narrow in the sense that $\sigma \ll k_0$. In the limit $\sigma \to 0$ the above wave-packet becomes $\nu_{eL}^{(h)}(0)\delta^3(\vec{k}-\vec{k}_0)$. In the opposite limit of large σ the wave packet describes an inhomogeneous distribution spatially localized within a distance $\approx 1/\sigma$. For a narrow wave packet the momentum integral can be carried out by expanding the integrand in a series expansion around k_0 keeping up to quadratic terms.

4.3.1 Integrals

The typical integrals are of the form

$$I(\vec{r},t) = \left(\frac{\pi}{\sigma^2}\right)^{\frac{3}{2}} \int \frac{d^3k}{(2\pi)^3}\mathcal{A}(k)\, \exp\left[-\frac{(\vec{k}-\vec{k}_0)^2}{4\sigma^2} + i\vec{k}\cdot\vec{r} - i\omega(k)\,t\right] \tag{4.36}$$

where $\mathcal{A}$ stands for the factors $(1 \pm \mathcal{C})\,;\mathcal{S}$ in eqns. (4.29,4.30), and $\omega(k)$ are the general dispersion relations obtained above. The computation of these integrals is simplified by noticing that for any function $F(k)$ the expansion around $\vec{k}_0$ up to quadratic order is given by

$$F(k) = F(k_0) + F'(k_0)\,\widehat{\mathbf{k}}_0\cdot(\mathbf{k}-\mathbf{k}_0) + \frac{1}{2}\left(F''(k_0)\,P_{ij}^{\parallel}(\widehat{\mathbf{k}}_0) + \frac{F'(k_0)}{k_0}\,P_{ij}^{\perp}(\widehat{\mathbf{k}}_0)\right)(\mathbf{k}-\mathbf{k}_0)_i(\mathbf{k}-\mathbf{k}_0)_j + \cdots \tag{4.37}$$

where

$$P_{ij}^{\parallel}(\widehat{\mathbf{k}}) = \widehat{\mathbf{k}}_i\widehat{\mathbf{k}}_j \quad ; \quad P_{ij}^{\perp}(\widehat{\mathbf{k}}) = \delta_{ij} - \widehat{\mathbf{k}}_i\widehat{\mathbf{k}}_j \tag{4.38}$$

The result of the integration can be written more compactly by introducing the following quantities

$$\begin{aligned}
\sigma_{\parallel}^2(t) &= \sigma^2\,\frac{\left(1 - i\,\frac{t}{\tau_{\parallel}}\right)}{\left[1+\frac{t^2}{\tau_{\parallel}^2}\right]} \equiv \Phi_{\parallel}(t)\left(1 - i\,\frac{t}{\tau_{\parallel}}\right) \\
\sigma_{\perp}^2(t) &= \sigma^2\,\frac{\left(1 - i\,\frac{t}{\tau_{\perp}}\right)}{\left[1+\frac{t^2}{\tau_{\perp}^2}\right]} \equiv \Phi_{\perp}(t)\left(1 - i\,\frac{t}{\tau_{\perp}}\right)
\end{aligned} \tag{4.39}$$

where we have introduced the perpendicular and parallel dispersion time scales given respectively by

$$\tau_\perp = \frac{k_0}{2\sigma^2 v_g} \quad ; \quad \tau_\parallel = \frac{1}{2\sigma^2 \omega''(k_0)} = \gamma^2 \tau_\perp \,. \tag{4.40}$$

It will be seen in detail below that these two time scales are indeed associated with the spreading of the wave packet in the transverse and longitudinal directions.

The group velocity v_g and effective Lorentz factor[2] γ are given by

$$\vec{v}_g = \omega'(k_0)\,\widehat{\mathbf{k}}_0 \quad ; \quad \gamma^2 = \frac{v_g}{k_0 \omega''(k_0)} \tag{4.41}$$

The transverse and longitudinal coordinates are

$$\vec{X}_\parallel(t) = \widehat{\mathbf{k}}_0 \left(\vec{r}\cdot\widehat{\mathbf{k}}_0 - v_g t\right) \quad ; \quad \vec{X}_\perp = \vec{r} - \widehat{\mathbf{k}}_0 \left(\vec{r}\cdot\widehat{\mathbf{k}}_0\right) \tag{4.42}$$

and in terms of these variables we finally find

$$I(\vec{r},t) = \left[\frac{\sigma_\parallel(t)\sigma_\perp^2(t)}{\sigma^3}\right] \mathcal{A}(k_0;\vec{r},t)\; e^{i\left(\vec{k}_0\cdot\vec{r} - \Psi(\vec{r},t)\,t\right)}\; e^{-\;\Phi_\perp(t)\vec{X}_\perp^2 + \Phi_\parallel(t)\vec{X}_\parallel^2(t)} \tag{4.43}$$

where the phase

$$\Psi(\vec{r},t) \;\;=\;\; \omega(k_0) + \frac{\Phi_\perp(t)}{\tau_\perp}\,X_\perp^2 + \frac{\Phi_\parallel(t)}{\tau_\parallel}\,X_\parallel^2(t) \tag{4.44}$$

and

$$\begin{aligned}\mathcal{A}(k_0;\vec{r},t) \;\;=\;\;& \mathcal{A}(k_0) + 2\,i\,\mathcal{A}'(k_0)\sigma_\parallel^2(t)\,\widehat{\mathbf{k}}_0\cdot\vec{X}_\parallel(t) \\ & + \mathcal{A}''(k_0)\sigma_\perp^2(t)\,\left(1 - 2\sigma_\perp^2(t)\vec{X}_\perp^2\right) + \frac{\mathcal{A}'(k_0)}{k_0}\sigma_\parallel^2(t)\left(1 - 2\sigma_\parallel^2(t)\,\vec{X}_\parallel^2(t)\right)\end{aligned} \tag{4.45}$$

Neglecting the prefactor $\mathcal{A}(k_0;\vec{r},t)$ we see that

$$|I(\vec{r},t)|^2 \propto \left[\left(1+\frac{t^2}{\tau_\parallel^2}\right)\left(1+\frac{t^2}{\tau_\perp^2}\right)^2\right]^{-\frac{1}{2}} e^{-2\;\Phi_\perp(t)\vec{X}_\perp^2 + \Phi_\parallel(t)\vec{X}_\parallel^2(t)} \tag{4.46}$$

describes a wave-packet moving in the direction parallel to the momentum $\vec{k}_0$ with the group velocity v_g and dispersing both along the perpendicular and parallel directions. The expressions for $\Phi_\perp(t)$ and $\Phi_\parallel(t)$ given by eqn. (4.39) clearly show that the dispersion time scales along the

[2]For the usual dispersion relation $\omega(k) = \sqrt{k^2 + M^2}$ it is straightforward to confirm that $\gamma^2 = (1 - v_g^2)^{-1}$

parallel direction and transverse directions are given by $\tau_\parallel, \tau_\perp$ respectively and $\tau_\parallel$ displays the time dilation factor γ. The wave packet is localized in space within a distance of order $1/\sqrt{\Phi(t)} \propto 1/\sqrt{\sigma}$ in either direction. Small σ localizes the wave packet in momentum space while large σ the wave packet is spatially localized. For large σ the integrals must necessarily be performed numerically.

This discussion highlights that the derivative terms in the prefactor $\mathcal{A}(k_0; \vec{r}, t)$, which are a consequence of the *momentum dependence of the mixing angles* correspond to an expansion in the ratio σ/k_0. This can be understood from the following argument: $\mathcal{A} \sim (1 \pm \mathcal{C}), \mathcal{S}$, hence its derivatives with respect to momentum are of the form $f(k)\Delta'$ with $f(k)$ being smooth and bounded functions of $\mathcal{O}(1)$, while Δ is at most of the form $\Delta_0 k + \Delta_1 k^2$ in the relativistic limit, (see eqn. (4.15)) therefore $\Delta' \approx \Delta/k$. These derivatives multiply powers of $\sigma_{\perp,\parallel} X_{\perp,\parallel}$, and the exponential damping in I restricts these contributions to the range $|\sigma_{\perp,\parallel} X_{\perp,\parallel}| \approx 1$. Therefore in the narrow packet approximation $\sigma \ll k_0$ the higher order derivative terms are suppressed by powers of $\sigma/k_0 \ll 1$. We have invoked this narrow packet approximation to carry out the momentum integral, therefore consistently with this approximation we will only keep the first derivative term, which is of $\mathcal{O}(\sigma/k_0)$ and neglect the higher order derivatives, which are of higher order in this ratio. Namely in the analysis that follows we approximate

$$|\mathcal{A}(k_0; \vec{r}, t)|^2 \approx |\mathcal{A}(k_0)|^2 \left[1 + 4\,\frac{\mathcal{A}'(k_0)}{\mathcal{A}(k_0)}\Phi_\parallel(t)\,\widehat{\mathbf{k}}_0 \cdot \vec{X}_\parallel(t)\,\frac{t}{\tau_\parallel}\right] \tag{4.47}$$

In this manner we consistently keep the lowest order corrections arising from the *momentum dependence of the mixing angles in the medium*.

We now have all the ingredients for our analysis of the space time evolution. The above general expressions for the time evolution of initially prepared wave-packets, eqns. (4.29,4.30) combined with the dispersion relations obtained in section (4.2.2) provide a solution to the most general case. We focus our discussion on the case of the early Universe, in which the typical neutrino energies are $\sim$ MeV. With (active) neutrino masses in the range $M_a \sim$ eV and $\delta M^2 \sim 10^{-5} - 10^{-3}$ it is clear from the results above that the amplitude of the right handed component is suppressed by a factor $\overline{M}/k \sim 10^{-6}$ and the medium corrections to the dispersion relations for positive energy neutrinos with positive helicity and negative energy neutrinos with negative helicity are suppressed by a factor $\overline{M}^2/k^2$ with respect to the opposite helicity assignement. Therefore in what follows we focus our discussion to the case of left handed negative helicity neutrinos (and positive helicity antineutrinos).

4.3.2 Space-time evolution and oscillations

We now focus on describing the evolution of negative helicity neutrinos or positive helicity antineutrinos.

The initial state considered above corresponds to a wave-packet of electron neutrinos at $t = 0$ but no muon neutrinos. The lower component of the flavor spinor in eqn. (4.29,4.33) describes the wave-packet of the muon neutrino at any arbitrary time. We begin by studying the transition probability from an initial electron neutrino wave packet of negative helicity to a muon neutrino wave packet.

Using the results obtained in the previous section for the integrals in the narrow packet approximation we find the transition probability

$$\begin{aligned}
\mathcal{P}_{e\to\mu}(\vec{r},t) &= |\nu^{(h)}_{\mu\,L}(\vec{r},t)|^2 \\
&= \frac{1}{4}\,|\nu^{(h)}_{eL}(\vec{k},0)|^2 |\mathcal{S}(k_0)|^2 \left[1 + 4\,\frac{\mathcal{S}'(k_0)}{\mathcal{S}(k_0)}\overline{\Phi}_{\parallel}(t)\,\widehat{\mathbf{k}}_0\cdot\vec{X}_{\parallel}(t)\,\frac{t}{\overline{\tau}_{\parallel}}\right]\times \\
&\quad \left[|I_1(\vec{r},t)|^2 + |I_2(\vec{r},t)|^2 - 2\,|I_1(\vec{r},t)|\,|I_2(\vec{r},t)|\,\cos\left[(\Psi_1(\vec{r},t) - \Psi_2(\vec{r},t))\;t\right]\right] \quad (4.48)
\end{aligned}$$

where $\mathcal{S} = \sin\left[2\theta^{(h)}_m(\pm k)\right]$ and $I_{1,2}(\vec{r},t)$; $\Psi_{1,2}$ correspond to the integrals and phases given by eqn. (4.43,4.44) with the frequencies $\omega_{1,2}(k)$ for negative helicity given by eqns. (4.20). In the expression above we have taken a common *prefactor* by neglecting the differences between the group velocities and the masses, taking $v_g = 1$, and $\overline{\Phi}_{\parallel}, \overline{\tau}_{\parallel}$ correspond to $\Phi_{\parallel}, \tau_{\parallel}$ with a mass $\overline{M}$. We focus our attention on the interference term which is the space-time manifestation of the oscillation phenomenon and features the oscillatory cosine function. The amplitude of the oscillation, $|I_1(\vec{r},t)I_2(\vec{r},t)|$ describes the product of two wavepackets of the form given by eqn. (10.13).

It is convenient to write the product $|I_1\,I_2|$ in the following form

$$|I_1(\vec{r},t)\,I_2(\vec{r},t)| \approx \left[\left(1+\frac{t^2}{\tau^2_{\parallel}}\right)\left(1+\frac{t^2}{\tau^2_{\perp}}\right)^2\right]^{-\frac{1}{2}} e^{-\left(\Phi_{\perp,1}(t)+\Phi_{\perp,2}(t)\right)\vec{X}^2_{\perp}}\, e^{-\Phi_{CM}(t)\vec{X}^2_{CM}(t)}\, e^{-\Phi_R(t)X^2_R(t)} \quad (4.49)$$

where we have introduced the center of mass (CM) and relative (R) variables

$$\vec{X}_{CM} = \widehat{\mathbf{k}}_0 \left(\vec{r} \cdot \widehat{\mathbf{k}}_0 - v_{CM}(t)\, t \right) \quad ; \quad v_{CM}(t) = \frac{\Phi_{\parallel 1}(t)\, v_{g\,1} + \Phi_{\parallel 2}(t)\, v_{g\,2}}{\Phi_{\parallel 1}(t) + \Phi_{\parallel 2}(t)} \tag{4.50}$$

$$\vec{X}_R = \vec{X}_{\parallel 1} - \vec{X}_{\parallel 2} = -\left(\vec{v}_{g\,1} - \vec{v}_{g\,2}\right) t \tag{4.51}$$

$$\Phi_{CM} = \Phi_{\parallel 1} + \Phi_{\parallel 2} \quad ; \quad \Phi_R = \frac{\Phi_{\parallel 1}\, \Phi_{\parallel 2}}{\Phi_{\parallel 1} + \Phi_{\parallel 2}} \tag{4.52}$$

The integral (4.49) describes the product of two gaussian wave packets spreading in the transverse and longitudinal directions and separating in the longitudinal direction because of the difference in group velocities, made explicit by the term $\Phi_R(t) X_R^2(t)$.

The first two terms in eqn. (4.48) describe the incoherent sum of the probabilities associated with separated wave packets of propagating mode eigenstates , in the third, interference term, the product $|I_1||I_2|$ is the overlap between these two wave-packets that are slowly separating because of different group velocities. As discussed above a two loop calculation of the self-energies will lead to a quasiparticle *width* and a damping rate Γ_a for the individual quasiparticle modes of frequency $\omega_a(k)$, the discussion leading up to eqn. (4.32) suggests that the integrals

$$|I_a(\vec{r}, t)| \to e^{-\Gamma_a(k)\, t}\, |I_a(\vec{r}, t)| \,. \tag{4.53}$$

4.3.2.1 Coherence and "freeze-out"

Since $\vec{X}_R = (\vec{v}_{g\,2} - \vec{v}_{g\,1})t$ does not depend on position, the overlap between the separating wave packets becomes vanishingly small for $t >> t_{coh}$ where the coherence time scale t_{coh} is defined by

$$\Phi_R(t_{coh})(\vec{v}_{g\,2} - \vec{v}_{g\,1})^2\, t_{coh}^2 = 1 \tag{4.54}$$

Before we engage in an analysis of the different cases, it is important to recognize that there are several dimensionless small ratios: i) $\sigma/k_0 \ll 1$ describes narrow wave-packets, this approximation was implemented in the calculation of the integrals, ii) $\overline{M}/k \ll 1$ in the relativistic limit with $k \sim$ MeV for example in the early Universe near the epoch of BBN or for supernovae, iii) $\delta M^2/\overline{M}^2 \ll 1$ describes a nearly degenerate hierarchy of neutrino masses. Since in the relativistic limit $v_{1\,g} - v_{2\,g} \sim \delta M^2/k^2$ we can neglect the difference in the masses in $\Phi_\parallel$ and write $\Phi_{\parallel 1} \sim \Phi_{\parallel 2} \sim \overline{\Phi}_\parallel$ where the masses are replaced by the mean mass $\overline{M}$ given by eqn. (3.11), and similarly for $\Phi_\perp$. Therefore to leading order in small quantities we can replace Φ_R above by $\overline{\Phi}_\parallel/2$ leading to

$$\Phi_{CM}(t) = 2\,\overline{\Phi}_\parallel(t) = \frac{2\,\sigma^2}{1 + \frac{t^2}{\overline{\tau}_\parallel^2}} \quad ; \quad v_{CM} = \frac{1}{2}(v_{g\,1} + v_{g\,2}) \tag{4.55}$$

where $\overline{\tau}_{\|}$ is given by eqn. (4.40) for $\overline{M}$, and

$$\frac{1}{2}\overline{\Phi}_{\|}(t)X_R^2(t) = \frac{\left(\frac{t}{t_c}\right)^2}{1+\left(\frac{t}{\overline{\tau}_{\|}}\right)^2} \tag{4.56}$$

where we have introduced the time scale

$$t_c = \frac{\sqrt{2}}{\sigma|v_{g\,2} - v_{g\,1}|} \tag{4.57}$$

The coherence time scale is the solution of the equation

$$\frac{\left(\frac{t_{coh}}{t_c}\right)^2}{1+\left(\frac{t_{coh}}{\overline{\tau}_{\|}^2}\right)^2} = 1 \tag{4.58}$$

The expression (4.56) reveals a remarkable feature: for $t \gg \overline{\tau}_{\|}$ the overlap between the separating wave-packets saturates to a *time independent value*

$$\frac{1}{2}\overline{\Phi}_{\|}(t)X_R^2(t) \to \left(\frac{\overline{\tau}_{\|}}{t_c}\right)^2 . \tag{4.59}$$

This effect has been recognized in ref.[108] and results from the longitudinal dispersion catching up with the separation of the wave packets. This phenomenon is relevant only in the case when $t_c > \overline{\tau}_{\|}$ in which case the overlap of the separating wave packets "freezes" and the packets maintain coherence for the remainder of their evolution. There are two distinct possibilities:

$$t_c \ll \overline{\tau}_{\|} \quad \textbf{: (a)} \tag{4.60}$$

$$t_c \gg \overline{\tau}_{\|} \quad \textbf{: (b)} \tag{4.61}$$

In case **(a)** we can approximate

$$\frac{1}{2}\overline{\Phi}_{\|}(t)X_R^2(t) \approx \left(\frac{t}{t_c}\right)^2 \tag{4.62}$$

since during the time interval in which the separating packets maintain coherence $t \ll t_c \ll \overline{\tau}_{\|}$ and in this case the relevant coherence time scale is t_c.

In case **(b)** the "freeze out" of coherence results and the long time limit of the overlap between the wave packets in the longitudinal direction remains large and determined by eqn. (4.59).

However, while this "freezing of coherence" phenomenon in the longitudinal direction ensues in this regime, by the time when the coherence freezes $t \sim \overline{\tau}_{\|}$ the wave packet has spread dramatically

in the *transverse* direction. This is because of the enormous Lorentz time dilation factor in the longitudinal direction which ensures that $t \sim \overline{\tau}_{\parallel} \gg \tau_{\perp}$ (see eqn. (4.40)). The large spreading in the transverse direction entails a large suppression of the transition probability

$$\mathcal{P}_{e\to\mu}(\vec{r}, t \sim \overline{\tau}_{\parallel}) \propto \left(\frac{\tau_{\perp}}{\overline{\tau}_{\parallel}}\right)^2 \sim \frac{1}{\gamma^4} \sim \left(\frac{\overline{M}}{k_0}\right)^4 . \tag{4.63}$$

For $\overline{M} \sim$ eV and $k_0 \sim$ MeV the above ratio is negligible. Therefore while the phenomenon of freezing of coherence is remarkable and fundamentally interesting, it may not lead to important consequences because the transition probability is strongly suppressed in this regime. Therefore in the time scale during which the transition probability is non-negligible, namely $t \ll \overline{\tau}_{\parallel}$ the overlap integral can be simplified to

$$e^{-\frac{1}{2}\overline{\Phi}_{\parallel}(t)X_R^2(t)} \approx e^{-\left(\frac{t}{t_c}\right)^2} . \tag{4.64}$$

4.3.2.2 Effective oscillation frequency Another aspect of the interference term is the *effective time dependent oscillation frequency* $\Psi_1(\vec{r}, t) - \Psi_2(\vec{r}, t)$ where the Ψ_a are given by eqn. (4.44) for the frequencies $\omega_a(k)$ of the propagating modes. The spatio-temporal dependence of this effective phase is a consequence of the dispersion of the inhomogeneous configurations, encoded in the functions Φ and results in a *drift* of the oscillation frequency, a result that confirms a similar finding in the vacuum case in ref.[114]. Because of the exponential fall off of the amplitudes the maximum value of the *drift* contribution is achieved for $\Phi_{\perp,a}X_{\perp}^2 \sim 1$; $\Phi_{\parallel,a}X_{\parallel,a}^2(t) \sim 1$, namely in front and back of the center of the wave-packets, both in the transverse and the longitudinal directions. Furthermore, because of the Lorentz dilation factor, $\tau_{\parallel} \gg \tau_{\perp}$ for relativistic neutrinos. Therefore we can approximate the effective oscillation frequencies as

$$\Psi_1 - \Psi_2 \sim \omega_1(k) - \omega_2(k) + \frac{2\sigma^2}{k_0}(v_{g,1} - v_{g,2}) \tag{4.65}$$

The dispersion relations and mixing angles obtained above along with the the results (4.29,4.30), yield the complete space-time evolution for wave-packets with initial conditions corresponding to an electron neutrino. Rather than studying the general case, we focus on three different situations which summarize the most general cases,i) $\Delta_h/\delta M^2 \ll 1$ corresponding to the case of vacuum oscillations, ii) $\Delta_h/\delta M^2 \sim \cos 2\theta$ corresponding to a resonance in the medium, and iii) $\Delta_h/\delta M^2 \gg 1$ corresponding to the case a hot and or dense medium in which oscillations are suppressed.

4.3.3 $\Delta_h/\delta M^2 \ll 1$: vacuum oscillations

We study this case not only to compare to results available in the literature, but also to establish a "benchmark" to compare with the results with medium modifications. Beuthe [108] has studied the propagation of neutrino wave-packets in the vacuum case including dispersion and in ref.[114] an effective frequency similar to (4.44) has been found for wave-packets propagating in the vacuum. In this case for positive energy, negative helicity neutrinos with $a = 1, 2$

$$\omega_a(k_0) \sim k_0 + \frac{M_a^2}{2k_0} \quad ; \quad v_{g,a} \sim 1 - \frac{M_a^2}{2k_0^2} \quad ; \quad \omega_a''(k_0) \sim \frac{M_a^2}{k_0^3} \tag{4.66}$$

leading to the vacuum time scales

$$t_{c,v} = \frac{2\sqrt{2}k_0^2}{\sigma|\delta M^2|} \tag{4.67}$$

$$\overline{\tau}_{\parallel} = \frac{k_0^3}{2\sigma^2 \overline{M}^2} \tag{4.68}$$

In the case when

$$\left|\frac{k_0}{\sigma}\frac{\delta M^2}{4\overline{M}^2}\right| \gg 1 \tag{4.69}$$

the vacuum coherence time is given by

$$t_{c,v} = \overline{\tau}_{\parallel}\left|\frac{\sigma}{k_0}\frac{4\overline{M}^2}{\delta M^2}\right| = \frac{2k_0^2}{\sigma|\delta M^2|} \ll \overline{\tau}_{\parallel} \tag{4.70}$$

and the overlap between the separating wave-packets vanishes well before the packets disperse appreciably along the longitudinal direction. On the other hand, in the case when

$$\left|\frac{k_0}{\sigma}\frac{\delta M^2}{4\overline{M}^2}\right| \ll 1 \tag{4.71}$$

the spreading of the wave packets catches up with the separation and the overlap between them freezes when $t \equiv t_{f,v} = \overline{\tau}_{\parallel} = k_0^3/2\sigma^2\overline{M}^2$. With $|\delta M^2|/4\overline{M}^2 \sim 10^{-4}$ for solar or $\sim 10^{-3}$ for atmospheric neutrinos the phenomenon of "freezing" of the overlap and the survival of coherence is available for

$$1 \ll \frac{k_0}{\sigma} \ll \frac{4\overline{M}^2}{|\delta M^2|} \tag{4.72}$$

which is well within the "narrow wave packet" regime. However, as discussed above, when the coherence freezes the transition probability has been strongly suppressed by transverse dispersion.

Therefore during the time scale during which the transition probability is non-negligible we can approximate the exponent in (4.49)

$$\frac{1}{2}\overline{\Phi}_{\parallel}(t)X_R^2(t) \sim \left(\frac{t}{t_{c,v}}\right)^2 \tag{4.73}$$

The effective oscillation frequency is given by eqn. (4.65) which becomes

$$\Psi_1 - \Psi_2 \sim \frac{\delta M^2}{2k}\left(1 - \frac{2\sigma^2}{k_0^2}\right) \tag{4.74}$$

while the corrections tend to diminish the oscillation frequency, these are rather small in the narrow packet approximation.

4.3.4 Medium effects: near resonance

In refs.[14, 57, 58, 59, 113] it was established that if the lepton asymmetries are of the order of the baryon asymmetry $\eta \sim 10^{-9}$ there is the possibility of a resonance for the temperature range $m_e \ll T \ll m_\mu$ for positive energy negative helicity neutrinos with $\omega(k) \sim k + \overline{M}^2/2k \;\; ; \;\; h = -1$ or positive energy positive helicity antineutrinos with $\omega(k) \sim -k - \overline{M}^2/2k \;\; ; \;\; h = 1$ respectively. It is convenient to introduce the following notation

$$\mathcal{L}_9 = 10^9\,(\mathcal{L}_e - \mathcal{L}_\mu) \tag{4.75}$$

$$\delta_5 = 10^5\left(\frac{\delta M^2}{\mathrm{eV}^2}\right) \tag{4.76}$$

If the lepton and neutrino asymmetries are of the same order of the baryon asymmetry, then $0.2 \lesssim |\mathcal{L}_9| \lesssim 0.7$ and the fitting from solar and KamLAND data suggests $|\delta_5| \approx 8$. In this temperature regime we find[113] for positive energy, negative helicity neutrinos

$$\frac{\Delta_-(k,k)}{\delta M^2} \approx \frac{4}{\delta_5}\left(\frac{0.1\,T}{\mathrm{MeV}}\right)^4 \frac{k}{T}\left[-\mathcal{L}_9 + \left(\frac{2\,T}{\mathrm{MeV}}\right)^2 \frac{k}{T}\right]. \tag{4.77}$$

and for positive energy positive helicity antineutrinos

$$\frac{\Delta_+(-k,k)}{\delta M^2} \approx \frac{4}{\delta_5}\left(\frac{0.1\,T}{\mathrm{MeV}}\right)^4 \frac{k}{T}\left[\mathcal{L}_9 + \left(\frac{2\,T}{\mathrm{MeV}}\right)^2 \frac{k}{T}\right]. \tag{4.78}$$

In the above expressions we have neglected terms of order $\frac{\overline{M}^2}{k^2}$. With $k \sim T$ and in the temperature regime just prior to BBN with $T \sim$ few MeV the lepton asymmetry contribution $\mathcal{L}$ is much smaller than the momentum dependent contribution and will be neglected in the analysis

that follows, therefore we refer to $\Delta_h(\lambda k, k)$ and $S_h(\lambda k, k)$ as $\Delta(k)$ and $S(k)$ respectively since these are independent of h, λ in this regime. In this temperature regime we find for both cases (negative helicity neutrinos and positive helicity antineutrinos) the following simple expressions

$$\Delta(k) \approx \frac{56\pi^2}{45\sqrt{2}} \frac{G_F k^2 T^4}{M_W^2} \quad ; \quad S(k) \approx \Delta(k)(1+\cos^2\theta_w). \tag{4.79}$$

A resonance is available when $\Delta(k_0) \sim \delta M^2 \cos 2\theta$, which may occur in this temperature regime for $k_0 \sim T \sim 3.6\,\text{MeV}$[14, 57, 58, 59, 113] for large mixing angle (θ_{12}) or $k \sim T \sim 7\,\text{MeV}$ for small mixing angle (θ_{13}). Near the resonance the in-medium dispersion relations and group velocities are given by

$$\omega_a(k) \approx k + \frac{M_a^2}{2k} - \frac{\delta M^2}{4k}\left\{(1+\cos^2\theta_w)\cos 2\theta + (-1)^{a-1}(1-\sin 2\theta)\right\} \tag{4.80}$$

$$v_{g,a} \approx 1 - \frac{M_a^2}{2k^2} + \frac{\delta M^2}{4k^2}\left\{(1+\cos^2\theta_w)\cos 2\theta + (-1)^{a-1}(1-\sin 2\theta)\right\} \tag{4.81}$$

Again we focus our discussion on the interference terms in the transition probability (4.48), in particular the medium modifications to the oscillation frequencies and coherence time scales. To assess these we note the following (primes stand for derivatives with respect to k):

$$\Omega(k)|_{res} = \sin 2\theta \quad ; \Omega^{'}(k)|_{res} = 0 \quad ; \quad \Omega^{''}(k)|_{res} = \frac{4}{k^2}\frac{\cos^2\theta}{\sin 2\theta} \tag{4.82}$$

which when combined with equation (4.20) yield

$$\omega_1(k) - \omega_2(k) = \frac{\delta M^2}{2k}\sin 2\theta \quad ; \quad v_{g,1} - v_{g,2} \approx -\frac{\delta M^2}{2k^2}\sin 2\theta \tag{4.83}$$

We also note that near the resonance

$$\sin' 2\theta_m(k) \propto \cos 2\theta_m \approx 0\,, \tag{4.84}$$

therefore the corrections arising from the energy dependence of the mixing angle in the transition probability (4.48) become *vanishingly small*. The transverse and longitudinal dispersion time scales are given by

$$\tau_{a\perp} = \frac{k_0}{2\sigma^2 v_{g,a}} \quad ; \quad \tau_{a\parallel} \approx \overline{\tau}_{\parallel}\left[1 - (-1)^{a-1}\frac{\delta M^2}{2\overline{M}^2}\frac{1+\cos^2 2\theta}{\sin 2\theta}\right] \quad ; \quad \overline{\tau}_{\parallel} = \frac{k_0^3}{2\sigma^2\overline{M}^2}. \tag{4.85}$$

Therefore in the medium near the resonance, the argument of the exponential that measures the overlap between the separating wave packets is given by

$$\frac{1}{2}\overline{\Phi}_{\parallel}(t)X_R^2(t) \sim \left(\frac{k_0}{\sigma}\frac{\delta\, M^2}{4\,\overline{M}^2}\,\sin 2\theta\right)^2 \frac{t^2}{\overline{\tau}_{\parallel}^2+t^2} = \frac{\left(\frac{t}{t_{c,m}}\right)^2}{1+\left(\frac{t}{\overline{\tau}_{\parallel}}\right)^2} \tag{4.86}$$

where

$$t_{c,m} = \frac{2k_0^2}{\sigma|\delta\, M^2|\sin 2\theta} = \frac{t_{c,v}}{\sin 2\theta}\,. \tag{4.87}$$

The effective oscillation frequency (4.65) is given by

$$\Psi_1 - \Psi_2 \sim \frac{\delta M^2}{2k}\sin 2\theta\left(1-\frac{2\sigma^2}{k_0^2}\right) \tag{4.88}$$

which when compared to the vacuum result (4.74) confirms the relation between the vacuum and in-medium oscillation time scales (4.26) since near the resonance $\sin 2\theta_m \sim 1$.

We conclude that the main effects from the medium near the resonance are an increase in the coherence and in the oscillation time scale $T = 2\pi/|\Psi_1 - \Psi_2|$ by a factor $1/\sin 2\theta$. For solar neutrino mixing with $\sin 2\theta_{12} \sim 0.9$ the increase in these time scales is at best a 10% effect, but it becomes much more pronounced in the case of atmospheric neutrino mixing since $\sin 2\theta_{13} \ll 1$.

4.3.4.1 $\Delta_h/\delta M^2 \gg 1$ oscillation suppression by the medium. In the temperature or momentum regime for which $\Delta_h/\delta M^2 \gg 1$ the expression for the in-medium mixing angles (4.17) reveals that $\cos 2\theta_m \to -1$. In this case the in-medium mixing angle reaches $\theta_m \to \pi/2$ and the transition probability $\mathcal{P}_{e\to\mu}$ vanishes. Eqn. (4.29) shows that in this case an electron neutrino wavepacket of negative helicity propagates as an eigenstate of the effective Dirac Hamiltonian in the medium with a dispersion relation

$$\omega_2(k) \sim vk + \frac{M_2^2}{2k} \quad ; \quad v = \left[1 - \frac{14}{45\sqrt{2}}\frac{G_F T^4}{M_W^2}\left(1+\text{sign}(\delta M^2)+\cos^2\theta_w\right)\right] \tag{4.89}$$

where we have used eqn. (4.79) for the case when the momentum dependent contribution is much larger than the asymmetries. The in-medium correction to the group velocity being proportional to

$$\frac{G_F T^4}{M_W^2} \sim 10^{-21}\left(\frac{T}{\text{MeV}}\right)^4 \tag{4.90}$$

is negligible in the temperature regime in which the calculation is reliable, namely for $T \ll M_W$.

4.4 TIME SCALES IN THE RESONANCE REGIME

There are several important time scales that impact on the dynamics of wave-packets in the medium as revealed by the discussions above, but also there are two more relevant time scales that are pertinent to a plasma in an expanding Universe: the Hubble time scale $t_H \sim 1/H$ which is the cooling time scale $T(t)/\dot{T}(t)$ and the collisional relaxation time scale $t_{rel} = 1/\Gamma$ with Γ the weak interaction collision rate. Neither t_H nor t_{rel} has been input explicitly in the calculations above which assumed a medium in equilibrium and considered self-energy corrections only up to $\mathcal{O}(G_F)$. The damping factor that leads to the decoherence from neutral and charged current interactions has been studied in detail in references[14, 57, 58, 59] and we take this input from these references in order to compare this time scale for damping and decoherence to the time scales for the space-time evolution of the wave packets obtained above at the one-loop level.

In the temperature regime $1\,\mathrm{MeV} \leq T \leq 100\,\mathrm{MeV}$ the Hubble time scale is[115]

$$t_H \sim 0.6 \left(\frac{T}{\mathrm{MeV}}\right)^{-2} s \tag{4.91}$$

and the collisional rate is estimated to be[14, 57, 58, 59]

$$\Gamma \sim 0.25\, G_F^2 T^5 \sim 0.25 \times 10^{-22} \left(\frac{T}{\mathrm{MeV}}\right)^{5} \mathrm{MeV} \Rightarrow t_{rel} \sim 1.6 \left(\frac{T}{\mathrm{MeV}}\right)^{-5} s \tag{4.92}$$

In order to determine the relevant time scales an estimate of the momentum spread of the initial wavepacket σ is needed. For example, for neutrinos in the LSND experiment, the momentum spread of the stopped muon is estimated to be about $0.01 MeV$ [106]. An estimate of the momentum spread in the medium can be the inverse of the mean-free path of the charged lepton associated with the neutrino[9]. This mean free path is determined by the electromagnetic interaction, in particular large angle scattering, which can be simply estimated from one-photon exchange to be $\lambda_{mf} \sim (\alpha_{em}^2 T)^{-1}$. This estimate yields

$$\sigma \sim \alpha_{em}^2 T \sim 10^{-4} \left(\frac{T}{\mathrm{MeV}}\right) (\mathrm{MeV})\,. \tag{4.93}$$

For neutrinos in the neutrinosphere of a core-collapse supernovae, the estimate for σ is also $\sim 10^{-2}\,\mathrm{MeV}$[9]. We will take a value $\sigma \sim 10^{-3}\,\mathrm{MeV}$ in the middle of this range as representative to obtain order of magnitude estimates for the time scales, but it is straightforward to modify the estimates if alternative values of σ can be reliably established.

We now consider the large mixing angle (LMA) case to provide an estimate of the different time scales, but a similar analysis holds for the case of small vacuum mixing (SMA) by an appropriate change of $k_0; T$. Taking $k_0 \sim T \sim 3.6\,\mathrm{MeV}$, $\sigma \sim 10^{-3}\mathrm{MeV}$, $|\delta M^2| \sim 8 \times 10^{-5}(\mathrm{eV})^2$, $\overline{M} \sim 0.25eV$ we obtain the following time scales near the resonance region:

i) **oscillation time scales:**

$$T_{vac} = \frac{4\pi k_0}{|\delta M^2|} \sim 3.8 \times 10^{-4}\, s \;\; ; \;\; T_{med} = \frac{T_{vac}}{\sin 2\theta} \tag{4.94}$$

ii) **dispersion and coherence time scales:**

$$\tau_\perp \sim \frac{k_0}{2\sigma^2} \sim 1.2 \times 10^{-15}\, s \;\; ; \;\; \overline{\tau}_\parallel \sim \frac{k_0^3}{2\sigma^2 \overline{M}^2} \sim 0.25\, s \tag{4.95}$$

$$t_{c,v} = \frac{2k_0^2}{\sigma|\delta M^2|} \sim 0.21\, s \;\; ; \;\; t_{c,m} = \frac{t_{c,v}}{\sin 2\theta} \tag{4.96}$$

iii) **expansion and collisional relaxation time scales:**

$$t_H \sim 4.6 \times 10^{-2}\, s \;\; ; \;\; t_{rel} \sim 2.8 \times 10^{-3}\, s \tag{4.97}$$

For small vacuum mixing angle (θ_{13}) the above results are modified by taking $k_0 \sim T \sim 7\,\mathrm{MeV}$.

In the resonance region the in-medium coherence time scale is of the same order as the Hubble time (for LMA) or much longer (for SMA) and and there is a large temperature variation during the coherence time scale. However, the decoherence of the wave packets occurs on much shorter time scales determined by the collisional relaxation scale and the coherence time scale is not the relevant one in the medium near the resonance.

Decreasing the momentum spread of the initial wave packet σ *increases* the dispersion and coherence time scales, with the dispersion scales increasing faster. The medium effects are manifest in an increase in the oscillation and the coherence time scales by a factor $1/\sin 2\theta$. This effect is more pronounced for $1-3$ mixing because of a much smaller mixing angle. It is clear from the comparison between the coherence time scale in the medium $t_{c,m}$ and the relaxational (collisional) time scale t_{rel} that unless σ is substantially *larger* than the estimate above, by at least one order of magnitude in the case of $1-2$ mixing, or even more for $1-3$ mixing, collisions via neutral and charge currents is the main source of decoherence between the separating wave-packets near the resonance. However, increasing σ will decrease the transverse dispersion time scale thus leading to greater suppression of the amplitude of the wave packets through dispersion. Furthermore, for large mixing angle $\sin 2\theta \sim 1$ the oscillation scale is *shorter* than the collisional decoherence time scale via the weak interactions t_{rel}, therefore allowing several oscillations before the wave packets decohere,

and because the oscillation scale is much smaller than the Hubble scale the evolution is adiabatic over the scale t_{rel}. But for small mixing angle the opposite situation results and the transition probability is suppressed by collisional decoherence, furthermore for small enough mixing angle there is a breakdown of adiabaticity. However, the strongest suppression of the survival $\mathcal{P}_{e\to e}$ as well as the transition $\mathcal{P}_{e\to\mu}$ probabilities (equally) is the *transverse* dispersion of the wave packets, on a time scale many orders of magnitude *shorter* than the decoherence $t_{c,m}$ and the collisional t_{rel} time scales. Unless σ^2 is within the same order of magnitude of $|\delta M^2|$ the transverse dispersion occurs on time scales much faster than any of the other relevant time scales and the amplitude of the wave-packets is suppressed well before any oscillations or decoherence by any other process can occur. Clearly a better understanding of the initial momentum spread is necessary for a full assessment of the oscillation probability in the medium.

4.5 CONCLUSIONS

In this chapter, we implemented a non-equilibrium quantum field theory method that allows to study the space-time propagation of neutrino wave-packets directly from the effective Dirac equation in the medium. The space-time evolution is studied as an initial value problem with the full density matrix via linear response. The method systematically allows to obtain the space-time evolution of left and right handed neutrino wave packets.

A "flavor neutrino" wave packet evolves in time as a linear superposition of wave-packets of "exact" (quasi) particle states in the medium, described by the poles of the Dirac propagator *in the medium*. These states propagate in the medium with different group velocities and the slow separation between these packets causes their overlap to diminish leading to a loss of spatial and temporal coherence. However, the time evolution of the packets also features *dispersion* as a result of the momentum spread of the wave packets[108].

The space time dynamics feature a rich hierarchy of time scales that depend on the initial momentum spread of the wave packet: the transverse and longitudinal dispersion time scales $\tau_\perp \ll \tau_\parallel$ which are widely separated by the enormous Lorentz time dilation factor $\approx (k/\overline{M})^2$ with $\overline{M}$ the average neutrino mass, and a coherence time scale $t_{c,m}$ that determines when the overlap of the wave packets becomes negligible. The dynamics also displays the phenomenon of "freezing of coherence" which results from the competition between the separation and spreading of the wave

packet along the direction of motion (longitudinal). For time scales larger than $\tau_{\|}$ the overlap of the wave-packets freezes, with a large overlap in the case when $t_{c,m} \gg \tau_{\|}$, which occurs for a wide range of parameters.

We have focused on studying the space-time propagation in the temperature and energy regime in which there is a resonance in the mixing angle in the medium, prior to BBN[14, 57, 58, 59, 113]. Our main results are summarized as follows:

- Both the coherence and oscillation time scales are enhanced in the medium with respect to the vacuum case by a factor $1/\sin 2\theta$ near the resonance, where θ is the vacuum mixing angle.
- There are small corrections to the oscillation formula from the wave-packet treatment, but these are suppressed by two powers of the ratio of the momentum spread of the initial packet to the main momentum.
- There are also small corrections to the space-time evolution from the energy dependence of the mixing angle, but these are negligible near the resonance region.
- The spreading of the wave-packet leads to the phenomenon of "freezing of coherence" which results from the competition between the longitudinal dispersion and coherence time scales. This phenomenon is a result of the longitudinal spreading of the wave-packets "catching up" with their separation. Substantial coherence remains frozen for $t_{c,m} \gg \tau_{\|}$.
- We have compared the wide range of time scales present in the early Universe when the resonance is available for $T \sim 3.6$MeV[14, 57, 58, 59, 113] for large mixing angle. *Assuming* that the initial momentum spread of the wave-packet is determined by the large angle scattering mean free path of charged leptons in the medium[9], we find the following hierarchy between the transverse dispersion $\tau_{\perp}$, oscillation T_{med}, collisional relaxation t_{rel}, Hubble t_H, in-medium coherence $t_{c,m}$ and longitudinal dispersion $\tau_{\|}$ time scales respectively: for large vacuum mixing angle $\sin 2\theta \sim 1$:

$$\tau_{\perp} \ll T_{med} < t_{rel} < t_H \ll t_{c,m} \lesssim \tau_{\|} \tag{4.98}$$

and for small mixing angle $\sin 2\theta \ll 1$

$$\tau_{\perp} \ll t_{rel} \lesssim T_{med} < t_H \ll t_{c,m} \lesssim \tau_{\|}\,. \tag{4.99}$$

The rapid transverse dispersion is responsible for the main suppression of both the persistent and transition probabilities making the amplitudes extremely small on scales much shorter than any of the other scales. Only a momentum spread $\sigma \sim \sqrt{|\delta M|^2}$ will make the transverse

dispersion time scale comparable with the oscillation and relaxation ones. Clearly a better assessment of the momentum spread of wave-packets in the medium is required to provide a more reliable estimate of the wave-packet and oscillation dynamics.

5.0 CHARGED LEPTON MIXING AND OSCILLATIONS FROM NEUTRINO MIXING IN THE EARLY UNIVERSE

5.1 INTRODUCTION

While there is a large body of work on the study of neutrino mixing in hot and dense environments, much less attention has been given to the possibility of mixing and oscillation of *charged leptons*. Charged lepton number non-conserving processes, such as $\mu \to e\,\gamma; \mu \to 3\,e$ mediated by massive mixed neutrinos have been studied in the vacuum in refs.[116, 117, 118]. For Dirac neutrinos the transition probabilities for these processes are suppressed by a factor m_a^4/M_W^4[116, 117, 118]. The WMAP[8] bound on the neutrino masses $m_a < 1\,\mathrm{eV}$ yields typical branching ratios for these processes $B \lesssim 10^{-41}$ making them all but experimentally unobservable.

In this chapter, we explore the possibility of *charged lepton mixing* in the early Universe at high temperature and density. In section 5.2 we discuss the general arguments for charged lepton mixing as a result of neutrino mixing and establish the necessary conditions for this mixing to be substantial. We suggest that large neutrino chemical potentials may lead to substantial charged lepton mixing.

Without oscillations BBN and CMB provide a stringent constraint on the neutrino chemical potentials[21, 119] ξ_α, with $-0.01 \leq \xi_e \leq 0.22\,,\ |\xi_{\mu,\tau}| \leq 2.6$. Detailed studies[32, 71, 110, 111, 112] show that oscillations and self-synchronization lead to flavor equilibration before BBN, beginning at a temperature $T \sim 30\,\mathrm{MeV}$[111] with complete flavor equilibration among the chemical potentials at $T \sim 2\,\mathrm{MeV}$[110, 111]. Thus *prior to flavor equalization* for $T > 30\,\mathrm{MeV}$ there *could* be large neutrino asymmetries consistent with the BBN and CMB bounds in the absence of oscillations. We study whether this possibility could lead to charged lepton mixing focusing on two flavors of Dirac neutrinos corresponding to e, μ and for simplicity in the temperature regime where both are ultrarelativistic, with $m_\mu \ll T \ll M_W$.

In section 5.3 we discuss general arguments within the realm of reliability of perturbation theory suggesting that the equilibrium state is described by a density matrix nearly diagonal in the mass basis. In this section we also discuss caveats and subtleties in the kinetic approach to neutrino equilibration in the literature and argue that results on the equilibrium state are in agreement with the interpretation of an equilibrium density matrix diagonal in the mass basis. Our *main and only assumption* is that for $T > 30\,\mathrm{MeV}$ neutrinos are in equilibrium and the density matrix is nearly diagonal in the mass basis, with distribution functions of mass eigenstates that feature different and large chemical potentials. While this is not the *only*, it is *one* possible scenario for substantial charged lepton mixing that can be explored systematically.

In section 5.4 we explore charged lepton mixing in lowest order in perturbation theory as a consequence of large asymmetries in the equilibrium distribution functions of mass eigenstates. In this section we also critically discuss possible caveats and suggest a program to include non-perturbative corrections in a systematic expansion.

Finally, in section 5.5 we summarize the main aspects and results of the article.

5.2 CHARGED LEPTON MIXING: THE GENERAL ARGUMENT

Charged lepton mixing is a consequence of neutrino mixing in the charged current contribution to the charged lepton self energy. This can be seen as follows: consider the one-loop self energy for the charged leptons. The off-diagonal self-energy $\Sigma_{e\mu}$ is depicted in fig. (5.1) for the case of electron-muon mixing. The internal line in fig. (5.1) (a) is a neutrino propagator off-diagonal in the flavor basis, which is non-vanishing if neutrinos mix. In Fermi's effective field theory obtained by integrating out the vector bosons the effective interaction that gives rise to charged lepton mixing is

$$H_{eff} = \frac{2G_F}{\sqrt{2}} \left[\overline{e}_L \gamma_\mu \nu_{eL}\right] \left[\overline{\nu}_{\mu L} \gamma_\mu \mu_L\right] . \tag{5.1}$$

A simple Hartree-like factorization yields

$$\frac{2G_F}{\sqrt{2}} \overline{e}_L \gamma_\mu < \nu_{eL} \overline{\nu}_{\mu L} > \gamma^\mu \mu_L \equiv \overline{e}_L \, \Sigma_{e\mu} \, \mu_L \tag{5.2}$$

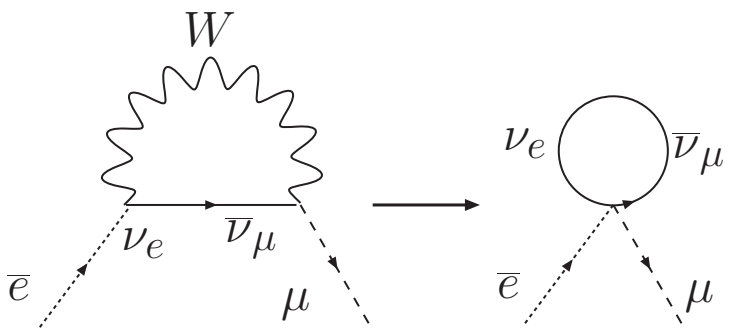

Figure 5.1: Off diagonal charged lepton self energy: (a) one loop W-boson exchange, (b) self-energy in the effective Fermi theory.

where the brackets stand for average in the density matrix of the system. Eqn. (5.2) gives the charged-lepton mixing part of the self energy as

$$\Sigma_{e\mu} = \frac{2G_F}{\sqrt{2}}\,\gamma^\mu < \nu_{eL}\overline{\nu}_{\mu L} > \gamma_\mu\,. \tag{5.3}$$

The Fermi effective field theory contribution to the self-energy is depicted in fig. (5.1) (b).

The focus of this chapter is to study two aspects that emerge from this observation:

- **Mixing:** The propagating modes in the medium are determined by the poles of the full propagator with a self-energy that includes radiative corrections in the medium. The full self-energy for the charged leptons is a 2×2 matrix (in the simple case of two flavors), and eqn. (5.3) yields the off-diagonal matrix element in the flavor basis. This is precisely the main study in this article: we obtain the charged lepton propagator including radiative corrections in the medium up to one loop in the electromagnetic and weak interactions. Neutrino mixing leads to off diagonal components of the propagator in the charged lepton flavor basis. We find the dispersion relation of the true propagating modes in the medium by diagonalization of the *full* propagator including one loop radiative corrections. The true propagating modes in the medium are *admixtures* of electron and muon states: this is precisely what we identify as *mixing*. The results given by equations (5.2,5.3) state *quite generally* that electron and muon states are mixed whenever *the neutrino propagator is off-diagonal in the flavor basis*. We highlight that this is *precisely* the condition for *flavor neutrino oscillations* since the propagator yields the transition amplitude

from an initial to a final state. Therefore we state quite generally that provided flavor neutrinos oscillate, namely if the neutrino propagator is *off diagonal in the flavor basis*, charged leptons associated with these flavor neutrinos will mix. The true propagating modes of charged leptons are linear superpositions of the charged leptons associated with the flavor neutrinos. We emphasize these statements because even though they are a straightforward consequence of flavor neutrino mixing, this precise point, and its consequences, have not been previously addressed in the literature.

- **Oscillations:** Consider the decays $W \to \nu_e\, e$ or neutron beta decay $n \to p\, e\, \overline{\nu}$ in the medium. The electron produced in the medium at the decay vertex propagates *as a linear combination* of the true propagating modes in the medium, each with a different dispersion relation. Upon time evolution this linear superposition will have non-vanishing overlap with a muon state yielding a typical oscillation pattern. We study this *oscillation* between the electron and muon charged lepton by considering the evolution of an electron wave-packet produced locally at the decay vertex. These oscillations are akin to the typical oscillation between flavor neutrino states and are a consequence of the one loop radiative correction depicted in fig.(5.1) with neutrinos in the medium. The transition probability from an initial electron to a muon packet oscillates in time. While in the case of almost degenerate neutrinos oscillations are associated with *macroscopic quantum coherence* because the oscillation lengths are macroscopically large, this is not a necessary condition for oscillations, which occur whenever the initial state is a linear superposition of the propagating modes. The example of neutron beta decay gives a precise meaning to the statement of charged lepton mixing: in the decay of the neutron the charged lepton that is produced is identified with the electron. This is the initial state, which in a medium will propagate as a linear combination of the propagating modes with an oscillatory probability of finding a muon. These oscillations are *fundamentally different* from the space-time oscillations possibly associated with quantum entanglement and discussed in references[120].

Eqn. (5.3) generally states that there is charged lepton mixing when the density matrix is *off diagonal* in the flavor basis. This is equivalent to the statement of neutrino mixing. A simple example of a density matrix off diagonal in the flavor basis is $\hat{\rho} = |0_m >< 0_m|$ with $|0_m >$ being the vacuum state in absence of weak interactions but with a neutrino Hamiltonian with an off diagonal mass matrix in the flavor basis. This is the interaction picture vacuum of the standard

model augmented by a neutrino mass matrix with flavor mixing. In the two flavor case with

$$\nu_e(\vec{x},t) = \cos\theta\,\nu_1(\vec{x},t) + \sin\theta\,\nu_2(\vec{x},t)\ ,\ \nu_\mu(\vec{x},t) = \cos\theta\,\nu_2(\vec{x},t) - \sin\theta\,\nu_1(\vec{x},t) \tag{5.4}$$

with $\nu_{1,2}(\vec{x},t)$ the fields associated with the mass eigenstates,

$$< 0_m|\nu_e(\vec{x},t)\overline{\nu}_\mu(\vec{x}',t')|0_m >= \cos\theta\sin\theta\left[< 0_m|\nu_2(\vec{x},t)\overline{\nu}_2(\vec{x}',t')|0_m > - < 0_m|\nu_1(\vec{x},t)\overline{\nu}_1(\vec{x}',t')|0_m >\right] . \tag{5.5}$$

If the propagators for the mass eigenstates only differ in the masses, this difference leads to a very small self-energy. In a medium the flavor off diagonal expectation value (5.3) could be enhanced by temperature and or density. Therefore the *general* criterion for substantial charged lepton mixing in a medium hinges on just one aspect: a large off diagonal matrix element $< \nu_{eL}\overline{\nu}_{\mu L} >$. One possible case for which this condition is fulfilled is *if* the density matrix is nearly diagonal in the *mass basis* with large chemical potentials for the different mass eigenstates.

We emphasize that this is only *one* condition for substantial charged lepton mixing and by no means unique, the analysis above shows that the most general condition is simply that $< \nu_{eL}\overline{\nu}_{\mu L} >$ be large.

In the general case a full solution of a kinetic equation should yield the value of $< \nu_{eL}\overline{\nu}_{\mu L} >$. *If* an equilibrium state of mixed neutrinos is described by a density matrix nearly diagonal in the mass basis with distribution functions for the different mass eigenstates with large and different chemical potentials, then simple expressions for the equilibrium propagators allow an assessment of the charged lepton mixing self energy. Can this be the case?.

5.3 ON NEUTRINO EQUILIBRATION

5.3.1 Equilibration in the mass basis

A system is in equilibrium if

$$[\hat{\rho}, H] = 0\,, \tag{5.6}$$

where $\hat{\rho}$ is the density matrix of the system and H the total Hamiltonian $H = H_0 + H_{int}$ with H_0 the Hamiltonian in the absence of weak interactions but with a mass matrix and $H_{int} = H_{NC} + H_{CC}$. In the absence of weak interactions, an equilibrium density matrix $\hat{\rho}_0$ commutes with H_0, therefore it is diagonal in the *mass basis*. The equilibrium density matrix cannot have off-diagonal matrix

elements in the mass basis because these oscillate in time. Of course without interactions the system will not reach an equilibrium state, however, as is the usual assumption in statistical mechanics, provided the interactions are sufficiently weak but lead to an equilibrium state, an *almost* free gas of particles in equilibrium is a suitable description, and the canonical density matrix in such case is of the form $\hat{\rho}_0 = e^{-H_0/T}$ (the grand canonical could also include a chemical potential for conserved quantities). Examples of this are abundant, a ubiquitous one is the cosmic microwave background radiation: the Planck distribution function describes free photons in equilibrium, although photons reach equilibrium by undergoing collisions with charged particles in a plasma with cross sections much larger than those of neutrinos.

Consider how the density matrix is modified from the "free field" form by "switching on" the weak interactions in perturbation theory. A perturbative expansion in the interaction picture of H_0 begins by writing the interaction vertices in terms of neutrino fields in the *mass basis*. Neglecting sterile neutrinos, neutral current interaction vertices are diagonal and only the charge current interactions induce off-diagonal correlations in the mass basis. Let us write the full density matrix as $\hat{\rho} = \hat{\rho}_0 + \delta\hat{\rho}$ where $\delta\hat{\rho}$ has a perturbative expansion in the weak coupling. The equilibrium condition leads to the following identity

$$[\delta\hat{\rho}, H_0] = -[\hat{\rho}_0, H_{int}] - [\delta\hat{\rho}, H_{int}] \tag{5.7}$$

Taking matrix elements in the mass eigenstates of H_0 the solution of eqn. (5.7) for the matrix elements of $\delta\hat{\rho}$ in the mass basis can be found in a perturbative expansion. The matrix elements of $\delta\hat{\rho}$ may feature non-vanishing off diagonal correlations in the mass basis as a result of charged current vertices which mix different mass eigenstates. However, a perturbative solution for the matrix elements of eqn. (5.7) in the mass basis would at most result in off diagonal correlations which are *perturbatively* small. Namely, the equilibrium density matrix is nearly diagonal in the mass basis.

Expanding the field operators associated with the mass eigenstates in terms of Fock creation and annihilation operators of mass eigenstates, the spatial Fourier transform of the field operators is given by

$$\nu_i(\vec{k}, 0) = \sum_{\lambda} a_i(\vec{k}, \lambda)\, \mathcal{U}_i(\vec{k}, \lambda) + b_i^{\dagger}(-\vec{k}, \lambda)\, \mathcal{V}_i(-\vec{k}, \lambda) \quad ; \quad i = 1, 2 \tag{5.8}$$

where the spinors $\mathcal{U}, \mathcal{V}$ are orthonormalized positive and negative energy solutions solutions of the Dirac equation with mass m_i. If the density matrix is diagonal in the mass basis, then

$\langle a_i^\dagger(\vec{k})\, a_j(\vec{k})\rangle \propto \delta_{ij}$ and the distribution functions for the mass eigenstates are $\langle a_i^\dagger(\vec{k})\, a_i(\vec{k})\rangle$; $\langle b_i^\dagger(\vec{k})\, b_i(\vec{k})\rangle$ for neutrinos and antineutrinos of mass i respectively. Switching on the *neutral current interaction* which is diagonal in the mass basis (provided there are no sterile neutrinos) will lead to the equilibration of neutrinos and the equilibrium distribution functions will be the usual Fermi-Dirac with a possible chemical potential. The *charged current interactions* yield vertices that are off-diagonal in the mass basis and induce cross correlations of the form $\langle a_i^\dagger\, a_j\rangle$ with $i \neq j$. In free field theory this equal time correlation function, if non-vanishing, oscillates with a time dependence $e^{i(\omega_k^i - \omega_k^j)\, t}$, however, in equilibrium there cannot be a time dependence of these off diagonal correlations as the following argument shows

$$\langle a_i^\dagger(t)\, a_j(t)\rangle = \mathrm{Tr}\left(\hat{\rho} e^{iHt} a_i^\dagger(0)\, a_j(0) e^{-iHt}\right) = \mathrm{Tr}\left(\hat{\rho} a_i^\dagger(0)\, a_j(0)\right) \tag{5.9}$$

where we used eqn. (5.6). Either the charged current interactions that generate these off-diagonal correlations *exactly* cancel the free field time dependence for all values of momentum k or, more likely, they lead to the decay of these off diagonal correlations to asymptotically perturbatively small expectation values as expected from the general arguments following eqn. (5.7).

This observation leads to the conclusion that *if* the perturbative expansion is reliable, the weak interactions lead to an equilibrium state described by a density matrix which is nearly diagonal in the mass basis but for possible perturbatively small off-diagonal elements. In perturbation theory the *equilibrium* distribution functions are diagonal in the mass basis and may feature a chemical potential for each mass eigenstate. Weak interaction vertices involve the flavor fields, but these are linear combinations of the fields that create and annihilate mass eigenstates, the true in-out states. Consider a far off-equilibrium initial state with a population of vector bosons (or neutrons) and no neutrinos, the decay of the vector bosons (or neutrons) results in the creation of a linear superposition of mass eigenstates, which propagate independently after production. Collisional processes via the weak interaction lead to the decoherence of the mass eigenstates and ultimately to a state of *equilibrium* in which equal time expectation values in the density matrix cannot depend on time. Neutral and charged current interactions yield different relaxational dynamics: in the mass basis the neutral current interaction is diagonal and relaxation processes via neutral currents lead to equilibration in the mass basis. Charged currents feature both diagonal and off-diagonal contributions in the mass basis, the diagonal ones yield relaxation dynamics similar to the neutral current interaction. The off diagonal contributions induce correlations between different mass eigenstates, but also lead to the relaxation of these off diagonal correlations. These two types

of processes leading to relaxation dynamics for diagonal and off-diagonal correlations in the mass basis are akin to the different processes that lead to the relaxation times T_1 (diagonal) and T_2 (transverse) in spin systems in nuclear magnetic resonance[121]. These concepts are manifest in Stodolsky's effective Bloch equation description of neutrino oscillations in a medium with a damping coefficient in the "transverse" direction[122] whose inverse is the equivalent of the T_2 relaxation time in spin systems.

By the above arguments this asymptotic equilibrium density matrix must be nearly diagonal in the mass basis at least within the realm of reliability of perturbation theory. Equilibrium correlation functions of operators at different times must be functions of the time difference. Of particular relevance to the discussion below is the flavor off diagonal propagator $\langle \nu_e(\vec{k},t)\overline{\nu}_\mu(\vec{k},t')\rangle$. Writing the flavor fields as linear combinations of the fields $\nu_{1,2}$ this correlation function in the equilibrium density matrix diagonal in the mass basis is to zeroth order in the perturbation

$$\langle \nu_e(\vec{k},t)\,\overline{\nu}_\mu(\vec{k},t')\rangle = -\cos\theta\sin\theta\left[\langle \nu_1(\vec{k},t-t')\,\overline{\nu}_1(\vec{k},0)\rangle - \langle \nu_2(\vec{k},t-t')\,\overline{\nu}_2(\vec{k},0)\rangle\right]. \tag{5.10}$$

Mixed correlators of $\nu_{1,2}$ *cannot* be functions of the time difference because of the different masses lead to a dependence on $t+t'$. As a simple but relevant example, consider the density matrix for the *vacuum*

$$\hat{\rho} = |0><0| \tag{5.11}$$

where $|0>$ is the exact ground state of H. This state can be constructed systematically in perturbation theory from the ground state $|0_m>$ of the Hamiltonian H_0 in absence of weak interactions, namely the interaction picture ground state in the basis of mass eigenstates,

$$|0>=|0_m> + \sum_n |n_m> \frac{< n_m|H_{int}|0_m>}{-E_n} + \cdots . \tag{5.12}$$

where $|n_m>$ are Fock eigenstates of H_0 ("mass eigenstates") with energy E_n. Writing the full density matrix as $\hat{\rho} = |0_m><0_m| + \delta\hat{\rho}$ one can find $\delta\hat{\rho}$ systematically in perturbation theory. The off-diagonal flavor propagator

$$\begin{aligned} S_{e\mu}(\vec{k},t-t') &= <0|\nu_e(\vec{k},t)\overline{\nu}_\mu(\vec{k},t')|0>=<0_m|\nu_e(\vec{k},t)\overline{\nu}_\mu(\vec{k},t')|0_m> + \mathcal{O}(g)+\cdots \\ &= \cos\theta\sin\theta\left[<0_m|\nu_2(\vec{k},t)\overline{\nu}_2(\vec{k},t')|0_m> - <0_m|\nu_1(\vec{k},t)\overline{\nu}_1(\vec{k},t')|0_m>\right] + \mathcal{O}(g)+\cdots . \end{aligned} \tag{5.13}$$

This propagator is the lowest order intermediate state in the process $W\,e \to W\,\mu$, and is also the internal fermion line, along with W-vector boson exchange in the off-diagonal self-energy contribution for charged leptons, see fig.(5.1). This simple example also leads to conclude that if there is

an equilibrium state for which the equal time "distribution function" $< \nu_e(\vec{k})\overline{\nu}_\mu(\vec{k}) > \neq 0$ then the *unequal* time correlation function

$$\mathcal{S}_{e\mu}(\vec{k}, t-t') = < \nu_e(\vec{k},t)\overline{\nu}_\mu(\vec{k},t') > = \cos\theta\sin\theta\left[< \nu_2(\vec{k},t)\overline{\nu}_2(\vec{k},t') > - < \nu_1(\vec{k},t)\overline{\nu}_1(\vec{k},t') >\right] \neq 0 \tag{5.14}$$

As it will become clear below, this is the correlation function that describes the charged lepton mixing. These arguments rely on the validity of the perturbative expansion and require revision in the case where perturbation theory in the mass basis must be reassessed. In section (5.4.3) we discuss this possibility and propose a method to re-arrange the perturbative expansion.

5.3.2 On the kinetic approach

Early kinetic approaches to the dynamics of oscillating neutrinos in thermal environments were proposed by Dolgov[14, 59, 124], Stodolsky[122] and Manohar[123]. Dolgov[124] introduced density matrices in flavor space, whereas Stodolsky[122] and Manohar[123] used a single particle density matrix of flavor states leading to Bloch-like equations and a similar description was studied in ref.[58]. Stodolsky argued that decoherence between flavor states emerged from a "transverse" relaxation akin to the relaxation time T_2 in nuclear magnetic resonance[121]. A Boltzmann equation for mixing and decoherence was established by Raffelt, Sigl and Stodolsky[125] in terms of a "matrix of densities" in the *nonrelativistic domain* instead of the density matrix. In this approach the field operators for different flavors were truncated to only the annihilation operators and obtained a Boltzmann equation in a perturbative expansion. A fully relativistic treatment was presented in ref.[126] introducing "matrices of densities" defined by the expectation value of bilinears of creation and annihilation operators of flavor states. A quantum kinetic description of oscillating neutrinos was presented in ref.[66] with an approach similar to those of refs.[122, 125] in terms of single particle flavor states.

All of the approaches to the kinetic description of oscillating neutrinos in a medium in one way or another use the notion of flavor Fock states, either in terms of single particle flavor neutrino states or by expanding field operators in terms of creation and annihilation Fock operators for flavor states. However, flavor states and the precise definition of Fock operators associated with these states are very subtle and controversial[1, 89, 90, 91, 127, 128].

Precisely, what are flavor states? While in the literature there is no precise definition of a "flavor state", a proper definition of such state should begin by expanding the flavor field operator

in terms of Fock creation and annihilation operators. In such an expansion the spatial Fourier transform of the flavor neutrino field operator, for example the electron neutrino at $t = 0$, is given by

$$\nu_e(\vec{k}, 0) = \sum_s \alpha_e(\vec{k}, s)\mathcal{U}_e(\vec{k}, s) + \beta_e^\dagger(-\vec{k}, s)\mathcal{V}_e(-\vec{k}, s) \tag{5.15}$$

where the spinors $\mathcal{U}_e$; $\mathcal{V}_e$ are orthonormalized positive and negative frequency solutions of a Dirac operator with *some mass* and define a basis. A Fock state of an electron neutrino *can* be defined by

$$|\nu_e(\vec{k}, s)\rangle = \alpha_e^\dagger(\vec{k}, s)|0_m\rangle \tag{5.16}$$

where $|0_m\rangle$ is the vacuum of the non-interacting theory, namely the vacuum of mass eigenstates. However, the expansion (5.15) requires a definite basis corresponding to a definite choice of the Dirac spinors $\mathcal{U}, \mathcal{V}$, which can be chosen to be solutions of a Dirac operator for any arbitrary mass. Each possible choice of mass gives a different definition of "particle". One possible choice is zero mass[126], another choice would be the diagonal elements of the mass matrix in the flavor basis[129] or masses m_1 to the electron neutrino and m_2 to the muon neutrino[89]. Any of these choices is just as good and physically motivated but obviously arbitrary. The creation and annihilation operators are extracted by projection[129], for example $\alpha_e^\dagger(\vec{k}, s) = \nu_e^\dagger(\vec{k}, 0)\mathcal{U}_e(\vec{k}, s)$. Writing the electron neutrino field operator as a linear combination of the field operators that create and annihilate mass eigenstates one finds

$$\begin{aligned}\alpha_e^\dagger(\vec{k}, s) = \quad & \cos\theta \left[\sum_\lambda a_1^\dagger(\vec{k}, \lambda)\, \mathcal{U}_1^\dagger(\vec{k}, \lambda)\mathcal{U}_e(\vec{k}, s) + b_1(-\vec{k}, \lambda)\, \mathcal{V}_1^\dagger(-\vec{k}, \lambda)\mathcal{U}_e(\vec{k}, s)\right] + \\ & \sin\theta \left[\sum_\lambda a_2^\dagger(\vec{k}, \lambda)\, \mathcal{U}_2^\dagger(\vec{k}, \lambda)\mathcal{U}_e(\vec{k}, s) + b_2(-\vec{k}, \lambda)\, \mathcal{V}_2^\dagger(-\vec{k}, \lambda)\mathcal{U}_e(\vec{k}, s)\right]\end{aligned} \tag{5.17}$$

The transformation between the set of "flavor" operators and those that create and annihilate mass eigenstates is unitary and the scalar products of the spinors yield generalized Bogoliubov coefficients. It is clear that there is no single choice of spinor $\mathcal{U}_e$ that will make

$$\begin{aligned}&\mathcal{U}_1^\dagger(\vec{k}, \lambda)\mathcal{U}_e(\vec{k}, s) = 1\,;\, \mathcal{U}_2^\dagger(\vec{k}, \lambda)\mathcal{U}_e(\vec{k}, s) = 1 \\ &\mathcal{V}_1^\dagger(-\vec{k}, \lambda)\mathcal{U}_e(\vec{k}, s) = 0\,;\, \mathcal{V}_2^\dagger(-\vec{k}, \lambda)\mathcal{U}_e(\vec{k}, s) = 0\end{aligned} \tag{5.18}$$

A surprising result of the above identification is that the annihilation operator $\alpha_e(\vec{k}, s)$ *creates a linear combination of antineutrino mass eigenstates* out of the vacuum $|0_m>$[89, 90, 91, 128, 129].

This observation indicates that *any* choice of the solutions for the spinors $\mathcal{U}_e, \mathcal{V}_e$ to define a flavor Fock creation operator leads to $|\nu_e\rangle \neq \cos\theta|\nu_1\rangle + \sin\theta|\nu_2\rangle$. A possible definition of flavor

Fock states would be to *define* the flavor vacuum $|0_f>$ as the state annihilated by the flavor annihilation operators (defined for example for zero mass states) and to construct a Fock Hilbert space out of this vacuum by successive application of flavor Fock creation operators. However, while there is a formal unitary transformation that relates the flavor and mass Fock operators via the Bogoliubov coefficients, such transformation is *not* unitarily implementable in the infinite dimensional Hilbert space[89], in particular $< 0_f|0_m >= 0$. Finally one can simply *define* flavor states as

$$|\nu_e > \equiv \cos\theta|\nu_1 > + \sin\theta|\nu_2 > \ . \tag{5.19}$$

However, because of the ambiguities with the definition of flavor Fock creation-annihilation operators discussed above these single particle states are *indirectly* related to the flavor *fields* $\nu_{e,\mu}(\vec{x},t)$ that enter in the standard model Lagrangian. Furthermore, this *single particle* definition does not yield any information on a Fock representation of many particle flavor states. A quantum statistical description of a neutrino gas is intrinsically a *many body* description, the total wave function of an n-fermion system must be completely antisymmetric under pairwise exchange. The second quantized Fock representation allows a systematic treatment of the many particle aspects, in particular in quantum statistical mechanics a *distribution* function is an expectation value of Fock number operator in the density matrix. Therefore simply *defining* flavor states as in eqn.(5.19) does not yield a complete information on the many particle nature of a neutrino gas. A systematic study of the many particle aspect of the dynamical evolution of a dense gas of flavor neutrinos with a physically motivated definition of flavor states even in the non-interacting theory was presented in ref.[129] wherein subtle but important effects associated with the non-trivial Bogoliubov coefficients in the dynamics were studied. Another subtlety emerges when a chemical potential is assigned to "flavor states", a chemical potential is a thermodynamic variable conjugate to a conserved particle number. Even in the free theory, in absence of weak interactions, flavor number is not conserved if neutrinos mix and as a result a chemical potential for flavor neutrinos is not a well defined quantity even for free mixed neutrinos. Dynamical aspects associated with this issue were also studied in ref.[129].

A counter argument to this critique would hinge on the fact that neutrino masses are small on the relevant energy scales and mass differences are even smaller, therefore one can *approximately* take all of the Dirac spinors to be *practically* massless. Of course if all spinors $\mathcal{U},\mathcal{V}$ for mass and flavor eigenstates are taken to be massless the overlaps (5.18) yield $\mathcal{U}^\dagger\mathcal{U} = 1; \mathcal{U}^\dagger\mathcal{V} = 0$ and eqn. (5.19) becomes an identity. This point will become relevant below.

While this approximation may be justified, it glosses over the main conceptual aspects and avoids the fundamental question of what precisely is a *distribution function* of flavor states. Such function includes information over all scales, it yields the average occupation for *all values of the momenta*, not just the high energy limit.

The main point of this discussion is that there are subtleties and caveats in the kinetic description based on "flavor states" or flavor matrix of densities, which involve Fock operators for flavor states. While these subtleties and caveats may not invalidate the broad aspects of the kinetic results, they cloud the interpretation of the equilibrium state of neutrinos.

To highlight this point consider an equilibrium situation in which $n_{e\mu}(\vec{k}) \equiv < \nu_e^\dagger(\vec{k})\nu_\mu(\vec{k}) >= 0$, for a density matrix diagonal in the mass basis this means

$$\cos\theta \sin\theta \left[< \nu_1^\dagger(\vec{k})\nu_1(\vec{k}) > - < \nu_2^\dagger(\vec{k})\nu_2(\vec{k}) > \right] = 0 \Rightarrow < \nu_1^\dagger(\vec{k})\nu_1(\vec{k}) >=< \nu_2^\dagger(\vec{k})\nu_2(\vec{k}) > \tag{5.20}$$

which in turn leads to the result

$$n_{ee} =< \nu_e^\dagger(\vec{k})\nu_e(\vec{k}) >=< \nu_\mu^\dagger(\vec{k})\nu_\mu(\vec{k}) >= n_{\mu\mu} \tag{5.21}$$

These conditions of "flavor equalization" are the *same* as those obtained in ref.[59] for the equilibrium solution of the kinetic equations, although in that reference one active and one sterile neutrino were studied. The condition (5.20) is *consistent* with identical chemical potentials for the mass eigenstates in the limit $m_1 = m_2 = 0$. As discussed above, it is precisely taking $m_1 = m_2 = 0$ that yields the correspondence between the definition of the flavor states (5.19) and the relation between the flavor and mass eigenstates *fields* when all spinors are taken to be massless. This is also the approximation used in ref.[126] where flavor fields are expanded in the basis of *massless* spinors. These are precisely the approximations invoked in the kinetic approach and correspond to neglecting the neutrino masses. Restoring neutrino masses the off diagonal correlation in the mass basis would be $n_{e\mu}(k) \propto (m_1^2 - m_2^2)/k^2$. Thus an interpretation of the kinetic results is that the equilibrium state is described by a density matrix diagonal in the mass basis with *equal chemical potential* for the mass eigenstates with an off diagonal correlation $n_{e\mu} \propto (m_1^2 - m_2^2)/k^2$ which is *neglected* in the kinetic approach.

Thus the equilibrium solution of the kinetic equation in ref.[59](see eqn. (12) in this reference) can be interpreted as a *confirmation* of the statement of equilibration in the mass basis when the neutrino masses are neglected, although in the "flavor" formulation of the kinetic equations this information is not readily available.

The discussion in the previous section based on general aspects of the full density matrix and a systematic perturbative expansion avoids the caveats associated with the intrinsic ambiguities in the definition of flavor states and suggests that equilibration leads to a density matrix nearly diagonal in the *mass basis*.

Quantum Zeno effect: References[122, 130, 131] discuss the fascinating phenomenon of the Quantum Zeno effect or "Turing's paradox"[122]. In the case of neutrino mixing, this effect arises when the scattering rate is larger than the oscillation rate. Since neutrinos are produced in weak interaction vertices as "flavor eigenstates" when rapid collisions via the weak interactions which are diagonal in the flavor basis prevent oscillations, the states are effectively "frozen" in the flavor basis[122]. This situation *may* be expected at high temperature. An order of magnitude estimate reveals that such a possibility is *not* available in the case under consideration, with a large difference in the neutrino asymmetries. The argument is the following: the oscillation frequency is given by

$$\Omega \sim \frac{\delta m^2}{k}\left[\Big(\cos 2\theta - \frac{V(k)}{\delta m^2}\Big)^2 + \Big(\sin 2\theta\Big)^2\right]^{\frac{1}{2}} , \tag{5.22}$$

where the matter potential

$$V(k) \approx k\, G_F T^3 L\ , \tag{5.23}$$

and L is the neutrino asymmetry *difference* between the two generations of neutrinos. Our study relies on the possibility of large asymmetries, namely $L \sim 1$. The decay rates are of the order

$$\Gamma \approx G_F^2 T^5\ . \tag{5.24}$$

The "quantum zeno effect" would operate provided $\Gamma >> \Omega$. Even if $V(k) >> \delta m^2$ which can occur at high temperatures, the oscillation frequency

$$\Omega \sim G_F T^3\, L \tag{5.25}$$

and $\frac{\Gamma}{\Omega} \sim G_F T^2/L << 1$ under the assumptions invoked in this article, namely: i) $L \sim 1$, ii) perturbation theory is valid in Fermi's effective field theory. A reversal of this bound would entail a breakdown of the perturbative expansion, and of the Fermi effective field theory. In perturbation theory the bound is even stronger if $\delta m^2 >> V(k)$. Thus we conclude that, under the conditions studied in this article, the quantum Zeno effect is not effective in "freezing" the states in the flavor basis and that oscillations and relaxation may indeed result in a density matrix which is off diagonal in the flavor basis.

5.3.3 Main assumptions

After the above discussion on the general aspects of equilibration and the kinetic approach, we are in position to clearly state our main assumptions. These are the following:

- For $T >> 1\,\mathrm{MeV}$ the electromagnetic and weak interaction rates ensure that leptons are in equilibrium in the early Universe, namely their distribution functions are time independent.
- The results from the kinetic approach in refs.[111] indicate that for $T >> 30\,\mathrm{MeV}$ neutrino oscillations are suppressed and *flavor* equilibration via oscillations is *not* operational. Therefore for $T >> 30\,\mathrm{MeV}$ neutrinos are in equilibrium, and there could be large asymmetries in the neutrino sector consistent with the BBN and CMB bounds in the *absence* of oscillations.
- The arguments presented above lead us to *assume* that the equilibrium state of the neutrino gas is described by a density matrix which is nearly diagonal in the mass basis, and allow the distribution functions of mass eigenstates to feature different chemical potentials. As per the discussion above, this is consistent with the interpretation of the equilibrium state *after* equalization of the chemical potentials discussed after eqn. (5.20).

  Equation (5.14) entails that the equilibrium off-diagonal flavor propagator does not vanish. The numerical study in ref.[111] shows that flavor equilibration with $|\xi_\nu| \lesssim 0.07$ is established but for $T \sim 2\,\mathrm{MeV}$, well below the scale of interest in our study, clearly leaving open the possibility, which we assume here, of large asymmetries in the neutrino sector at a temperature much higher than that of flavor equalization. In summary: the combination of the general arguments suggesting that the equilibrium density matrix is nearly diagonal in the mass basis, at least within the framework of perturbation theory, along with the results of the kinetic approach lead us to *assume* that at high temperature $T \gtrsim 30\,\mathrm{MeV}$ neutrinos are in equilibrium, the density matrix is nearly diagonal in the mass basis and there could be large asymmetries for the different mass states consistent with the bounds in absence of oscillations. Equilibration of mass eigenstates implies that the neutrino propagators in the mass basis only depend on the time difference (translational invariance in time) and are determined by the equilibrium distribution functions, the off-diagonal flavor propagator is given by eqn.(5.14).

The *dynamics* that leads to equilibration and the mechanism by which substantial chemical potentials emerge is of course very important and require a much deeper and detailed investigation as well as an understanding of initial conditions for lepton asymmetries. A consistent study should address the subtleties and caveats associated with the notion of flavor states or Fock operators. Such

program is certainly beyond the scope and focus of this article. Here we study the consequences of this assumption in a perturbative expansion in the mass basis up to one loop order, namely up to leading order in the weak and electromagnetic interactions. In order to explore the main possible consequences of neutrino equilibration with large asymmetries within a simpler setting, we focus on the regime of temperature much larger than the charged lepton masses.

We emphasize, that our main observation, namely that charged leptons mix if neutrinos mix is one of *principle* and of a general nature. Our purpose is to study the potentially novel broad aspects of charged lepton mixing under these circumstances in the simplest scenario, postponing a more detailed analysis to a future study.

5.4 EXPLORING THE CONSEQUENCES

In perturbation theory in the electroweak interactions, the self-energy is computed in the basis of mass eigenstates, hence it is off-diagonal in the flavor basis if neutrinos are in equilibrium as mass eigenstates in the absence of oscillations. Including the electromagnetic self-energy, and introducing the charged lepton spinor fields ν_α with $\alpha\,,\,\beta = e,\mu$ the effective Dirac equation in the medium for the space-time Fourier transforms of these fields is the following[113]

$$\left[\left(\gamma^0\,\omega - \vec{\gamma}\cdot\vec{k}\right)\delta_{\alpha\,\beta} - \mathbb{M}_{\alpha\,\beta} + \Sigma^{em}_{\alpha\,\beta}(\omega,k) + \widetilde{\Sigma}^{NC}_{\alpha\,\beta}(\omega,k) + \Sigma^{NC}_{\alpha\,\beta}(\omega,k)\,L + \Sigma^{CC}_{\alpha\,\beta}(\omega,k)\,L\right]\,\psi_\beta(\omega,k) = 0, \tag{5.26}$$

where $\mathbb{M} = \mathrm{diag}(M_e, M_\mu)$ is the charged lepton mass matrix and $L = (1-\gamma^5)/2$.

5.4.1 Electromagnetic self-energy

The leading electromagnetic contribution to the charged lepton self-energy $\Sigma^{em}_{\alpha\,\beta}(\omega,k)$ for temperatures much larger than the lepton masses is dominated by one-photon exchange in the hard-thermal loop approximation[132, 133]. As discussed below, the temperature region of interest for substantial charged-lepton mixing is $T \sim$ Gev, therefore we will neglect corrections of order $M_e^2/T^2; M_\mu^2/T^2 \ll 10^{-2}$ (which already multiply one power of α) to leading order.

Quark-lepton chemical equilibrium may lead to charged lepton chemical potentials as large as those for neutrinos, therefore we allow for arbitrary charged lepton chemical potentials with the possibility that $\mu_{e,\mu}/T \sim \mathcal{O}(1)$. The self-energy $\Sigma^{em}_{\alpha\,\beta}(\omega,k)$ is diagonal in flavor space $\Sigma^{em}(\omega,k) =$

diag $\left(\Sigma_e^{em}(\omega,k),\Sigma_\mu^{em}(\omega,k)\right)$. The matrix elements are given by $(f=e,\mu)$ [132, 133]

$$\Sigma_f^{em}(\omega,k)=-\gamma^0\left[\frac{m_f^2}{k}Q_0\left(\frac{\omega}{k}\right)-i\Gamma\right]+\vec{\gamma}\cdot\widehat{\mathbf{k}}\,\frac{m_f^2}{k}\left(\frac{\omega}{k}\,Q_0\left(\frac{\omega}{k}\right)-1\right)\quad;\quad Q_0(x)=\frac{1}{2}\ln\frac{x+1}{x-1}\tag{5.27}$$

with

$$m_f^2=\frac{\pi}{2}\,\alpha\,T^2\,[1+D(\xi_f)]\quad;\quad f=e,\mu.\tag{5.28}$$

The function

$$D(\xi_f)=\frac{4}{\pi^2}\int_0^\infty xdx\left[\frac{1}{e^{x-\xi_f}+1}-\frac{1}{e^x+1}\right]\quad;\quad \xi_f=\frac{\mu_f}{T}\tag{5.29}$$

is monotonically increasing with $-0.196\leq D(\xi)\leq 0.4,$ for $-1\leq\xi\leq 1$.

The leading order damping rate Γ in Σ^{em} emerges from threshold infrared divergences associated with the emission and absorption of soft, transverse magnetostatic photons[134, 135] and is insensitive to the masses for temperature larger than the mass of the charged leptons. In an abelian plasma transverse photons do not acquire a magnetic mass and are only screened *dynamically* by Landau damping[133, 134, 135]. Detailed work in high temperature QED plasmas[133, 134, 135] reveals that the exchange of soft magnetostatic photons yields an anomalous damping of fermionic excitations, which can be accurately described by the damping rate given by

$$\Gamma=\alpha T\,\ln\left(\frac{\omega_p}{\alpha T}\right).\tag{5.30}$$

The plasma frequency ω_p is determined by the photon polarization fermion loop with all relativistic fermionic species: for $T\sim$ GeV with electron, muon and three light quark degrees of freedom we find to leading logarithimic order

$$\Gamma=\alpha T\ln\left(\frac{8\pi}{3e}\right)\sim 3.3\,\alpha T.\tag{5.31}$$

A collisional contribution to the charged lepton damping rate Γ is of order $\alpha^2 T$[134] and will be neglected to leading order in α.

5.4.2 Charged and neutral currents self-energy

As depicted in fig. (5.1) to lowest order in perturbation theory in the interaction picture of H_0, there is a flavor off-diagonal contribution to the charged lepton self energy, $\Sigma_{e,\mu}$ given by a W-boson exchange and an internal off-diagonal fermion propagator $<\overline{\nu}_e(\vec{x},t)\nu_\mu(\vec{x}',t')>$. In the mass basis this propagator is given by eqn. (5.14) and the general form of the corresponding self energy

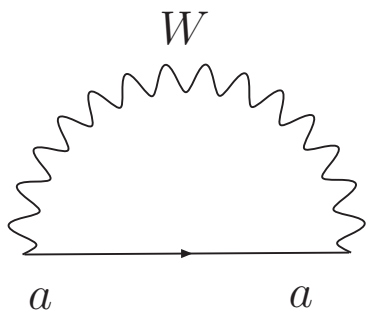

Figure 5.2: Charged current self energy $\Sigma_a(\omega, k)$ with $a = 1, 2$ corresponding to mass eigenstate neutrinos in the fermion line. The external lines correspond to e, μ charged leptons with frequency ω and momentum k.

contribution is depicted in fig.5.2 where the internal fermion line corresponds to a mass eigenstate neutrino ν_a in equilibrium with chemical potential $\mu_a = T\,\xi_a$.

We focus on the temperature regime $T \ll M_W$ and obtain the charged current contribution to the self-energy up to leading order in a local expansion in the frequency and momentum of the external leptons neglecting terms proportional to $m_a/M_W \lesssim 10^{-17}$. The general expressions for charged and neutral current self-energies are given in references[57, 113] where we refer the reader for more details.

Denoting by $\Sigma_a^{CC}(\omega, k)$ the one-loop charged current self-energy with internal neutrino line corresponding to a mass eigenstate ν_a displayed in fig.5.2, the matrix $\Sigma_{\alpha,\beta}^{CC}(\omega, k)$ in eqn. (5.26) has the following entries

$$\begin{aligned}
\Sigma_{e,e}^{CC} &= C^2\,\Sigma_1 + S^2\,\Sigma_2 \\
\Sigma_{\mu,\mu}^{CC} &= S^2\,\Sigma_1 + C^2\,\Sigma_2 \\
\Sigma_{e,\mu}^{CC} &= \Sigma_{\mu,e}^{CC} = -CS\,(\Sigma_1 - \Sigma_2)
\end{aligned} \tag{5.32}$$

consistently with a perturbative calculation in the mass basis to lowest order in the weak interactions $C = \cos\theta\,;\, S = \sin\theta$ and θ is the neutrino vacuum mixing angle. A fit to the solar and KamLAND[92] data yields $\tan^2\theta \approx 0.40$.

The off diagonal element $\Sigma_{e,\mu}^{CC}$ in eqn. (5.32) is responsible for charged lepton mixing. The flavor off-diagonal propagator in this self-energy is precisely given by eqn. (5.14). The form of this

off-diagonal self-energy makes clear that there is mixing provided $\theta \neq 0, \pi/2$ *and* $\Sigma_1 - \Sigma_2 \neq 0$. The calculation of the self-energy $\Sigma^{CC}_{e,\mu}$ in the *vacuum* is standard: it is performed in the interaction picture of the true basis of in-out states, these are *mass eigenstates*. In this case the difference of the self-energies is determined solely by the neutrino mass difference, therefore in the vacuum $\Sigma^{CC}_{e,\mu} \propto G_F \Delta m^2 \sim 10^{-27}$ and the mixing between charged leptons is negligible.

The main point of our study is that in the medium in equilibrium with large neutrino asymmetries for the mass eigenstates, charged lepton mixing may be substantial. The propagating modes in the medium are determined by the poles of the exact propagator. An off diagonal self-energy $\Sigma_{e\mu}$ entails that the charged lepton propagating modes are admixtures of electron and muon degrees of freedom. We now study this possibility in detail when the temperature is much larger than the lepton masses. We focus on this case for simplicity in order to extract the main features of the phenomenon and to highlight the main steps in the calculation.

We are only interested in the real part of the self-energies since at this order the imaginary part vanishes on the charged lepton mass shells. From the results obtained in[113], for any loop with a lepton with mass m in the high temperature limit $T \gg m$ we obtain

$$Re\,\Sigma(\omega,k) = \gamma^0\,\sigma^0(\omega,k) - \vec{\gamma}\cdot\widehat{\mathbf{k}}\,\sigma^1(\omega,k). \tag{5.33}$$

For $M_{W,Z} \gg T, \omega, k$ we find

$$\sigma^0(\omega,k) = -\frac{3\,g\,G_F\,n_\gamma}{\sqrt{2}}L + \frac{7\,\pi^2}{15\,\sqrt{2}}\frac{g\,G_F\,\omega\,T^4}{M_B^2}\,I\,, \tag{5.34}$$

$$\sigma^1(\omega,k) = -\frac{7\,\pi^2}{45\,\sqrt{2}}\,\frac{g\,G_F\,k\,T^4}{M_B^2}\,I\,, \tag{5.35}$$

where g is the appropriate factor for charged or neutral currents, L is the asymmetry for the corresponding lepton and $M_B = M_{W,Z}$ for charged or neutral currents, $n_\gamma = 2\,\zeta(3)\,T^3/\pi^2$, and

$$I = \frac{120}{7\pi^4}\int_0^\infty \frac{x^3}{e^{x-\xi}+1}\,dx\,. \tag{5.36}$$

The neutrino asymmetries are given by $L_a = (\pi^2/12\zeta(3))(\xi_a + \xi_a^3/\pi^2)$. In the absence of oscillations the combined analysis from CMB and BBN yield an upper bound on the asymmetry parameters $|\xi_e| \lesssim 0.1, |\xi_\mu| \sim 1$ for *flavor neutrinos*[21, 119] which we *assume* to imply a similar bound on the asymmetries for the mass eigenstates, ξ_a. The validity of this assumption in free field theory is confirmed by the analysis in ref.[129]. From (5.32) and the above results the following general form for the charged and neutral current self-energies is obtained

$$Re\,\Sigma(\omega,k) = \frac{3\,G_F\,n_\gamma}{2\sqrt{2}}\,[\gamma^0\mathbb{A}(\omega) - \vec{\gamma}\cdot\widehat{\mathbf{k}}\,\mathbb{B}(k)] \tag{5.37}$$

where $\mathbb{A}(\omega,k)$ and $\mathbb{B}(\omega,k)$ are 2×2 matrices in the charged lepton flavor basis given by

$$\mathbb{A}(\omega)=\begin{pmatrix} A_{ee}(\omega) & A_{e\mu}(\omega) \\ A_{e\mu}(\omega) & A_{\mu\mu}(\omega)\end{pmatrix}\;;\;\; \mathbb{B}(k)=\begin{pmatrix} B_{ee}(k) & B_{e\mu}(k) \\ B_{e\mu}(k) & B_{\mu\mu}(k)\end{pmatrix}. \tag{5.38}$$

where the matrix elements are given by

$$A^{CC}_{ee}(\omega) = -\left[L_+ + \cos 2\theta\, L_- - \frac{7\,\pi^4}{90\,\zeta(3)}\frac{\omega\,T}{M_W^2}\,(I_+ + \cos 2\theta\, I_-)\right] \tag{5.39}$$

$$A^{CC}_{\mu\mu}(\omega) = -\left[L_+ - \cos 2\theta\, L_- - \frac{7\,\pi^4}{90\,\zeta(3)}\frac{\omega\,T}{M_W^2}\,(I_+ - \cos 2\theta\, I_-)\right] \tag{5.40}$$

$$A^{CC}_{e\mu}(\omega) = \sin 2\theta\left[L_- - \frac{7\,\pi^4}{90\,\zeta(3)}\frac{\omega\,T}{M_W^2}\,I_-\right] \tag{5.41}$$

and

$$B^{CC}_{ee}(k) = -\frac{7\pi^4}{270\,\zeta(3)}\,\frac{k\,T}{M_W^2}(I_+ + \cos 2\theta\, I_-) \tag{5.42}$$

$$B^{CC}_{\mu\mu}(k) = -\frac{7\pi^4}{270\,\zeta(3)}\,\frac{k\,T}{M_W^2}(I_+ - \cos 2\theta\, I_-) \tag{5.43}$$

$$B^{CC}_{e\mu}(k) = \frac{7\pi^4}{270\,\zeta(3)}\,\frac{k\,T}{M_W^2}\sin 2\theta\, I_-\,, \tag{5.44}$$

where we have introduced $L_\pm = L_1 \pm L_2, I_\pm = I_1 \pm I_2$. The neutral current contributions are flavor diagonal and given by

$$A^{NC}_{ee}(\omega) = -(1-4\,\sin^2\theta_w)\left[\mathcal{L}_e - \frac{7\,\pi^4}{90\,\zeta(3)}\frac{\omega\,T}{M_W^2}\,\cos^2\theta_w\, I_e\right] - \frac{4}{3}\sum_f g_f^v\, L_f \tag{5.45}$$

$$A^{NC}_{\mu\mu}(\omega) = -(1-4\,\sin^2\theta_w)\left[\mathcal{L}_\mu - \frac{7\,\pi^4}{90\,\zeta(3)}\frac{\omega\,T}{M_W^2}\,\cos^2\theta_w\, I_\mu\right] - \frac{4}{3}\sum_f g_f^v\, L_f \tag{5.46}$$

$$\widetilde{A}^{NC}_{ee}(\omega) = -4\,\sin^4\theta_w\left[\mathcal{L}_e - \frac{7\,\pi^4}{90\,\zeta(3)}\frac{\omega\,T}{M_W^2}\,\cos^2\theta_w\, I_e\right] + \frac{8}{3}\,\sin^2\theta_w\sum_f g_f^v\, L_f \tag{5.47}$$

$$\widetilde{A}^{NC}_{\mu\mu}(\omega) = -4\,\sin^4\theta_w\left[\mathcal{L}_\mu - \frac{7\,\pi^4}{90\,\zeta(3)}\frac{\omega\,T}{M_W^2}\,\cos^2\theta_w\, I_\mu\right] + \frac{8}{3}\,\sin^2\theta_w\sum_f g_f^v\, L_f\,, \tag{5.48}$$

and

$$B^{NC}_{ee}(k) = -\frac{7\pi^4}{270\,\zeta(3)}\,\frac{k\,T}{M_W^2}(1-4\,\sin^2\theta_w)\,\cos^2\theta_w\, I_e \tag{5.49}$$

$$B^{CC}_{\mu\mu}(k) = -\frac{7\pi^4}{270\,\zeta(3)}\,\frac{k\,T}{M_W^2}(1-4\,\sin^2\theta_w)\,\cos^2\theta_w\, I_\mu \tag{5.50}$$

$$\widetilde{B}^{NC}_{ee}(k) = \frac{4\,\sin^4\theta_w\; B^{NC}_{ee}(k)}{(1-4\,\sin^2\theta_w)}\;\;;\;\; \widetilde{B}^{NC}_{\mu\mu}(k) = \frac{4\,\sin^4\theta_w\; B^{NC}_{\mu\mu}(k)}{(1-4\,\sin^2\theta_w)}\,, \tag{5.51}$$

where g_f^v , L_f are the vector coupling and asymmetry of fermion species f, θ_w is the Weinberg angle and $\mathcal{L}_{e,\mu}$ are the *charged* lepton asymmetries. The non-vanishing off-diagonal matrix elements $A_{e\mu}^{CC}$, $B_{e\mu}^{CC}$ lead to charged lepton mixing and oscillations. It is convenient to combine the charged leptons into a doublet of Dirac fields

$$\psi(\omega,k) = \begin{pmatrix} \psi_e(\omega,k) \\ \psi_\mu(\omega,k) \end{pmatrix} . \tag{5.52}$$

In the chiral representation the left and right handed components of the Dirac doublet are written as linear combinations of Weyl spinors $v^{(h)}$ eigenstates of the helicity operator $\vec{\sigma}\cdot\widehat{\mathbf{k}}$ with eigenvalues $h = \pm 1$, as follows[113]

$$\psi_L = \sum_{h=\pm 1} \begin{pmatrix} 0 \\ v^{(h)} \otimes \varphi^{(h)} \end{pmatrix} \;\; ; \;\; \nu_R = \sum_{h=\pm 1} \begin{pmatrix} v^{(h)} \otimes \xi^{(h)} \\ 0 \end{pmatrix} \tag{5.53}$$

The left handed doublet

$$\varphi^{(h)}(\omega,k) = \begin{pmatrix} l_e^{(h)}(\omega,k) \\ l_\mu^{(h)}(\omega,k) \end{pmatrix} , \tag{5.54}$$

obeys the following effective Dirac equation in the medium to leading order in α, G_F[113]

$$\left\{ \left[(\omega + i\Gamma)^2 - k^2\right] \mathbb{1} + \frac{3\, G_F\, n_\gamma}{2\sqrt{2}} \left(2\omega\, \widetilde{\mathbb{A}}^{NC} - 2k\, \widetilde{\mathbb{B}}^{NC} + (\omega - hk)(\mathbb{A} + h\mathbb{B}) \right) - \widetilde{\mathbb{M}}^2 \right\} \varphi^{(h)}(\omega,k) = 0 , \tag{5.55}$$

where $\widetilde{\mathbb{M}}^2 = \mathrm{diag}\left(M_e^2 + 2m_e^2, M_\mu^2 + 2m_\mu^2\right)$ where $m_{e,\mu}^2$ are given by eqn. (5.28) and to avoid cluttering of notation $\mathbb{A}$, $\mathbb{B}$ are the *sums* of the charged and neutral current contributions. To leading order the right handed doublet is determined by the relation[113]

$$\xi^{(h)}(\omega,k) = -\mathbb{M}\, \frac{(\omega + h\, k)}{\omega^2 - k^2}\, \varphi^{(h)}(\omega,k) . \tag{5.56}$$

The propagating modes in the medium are found by diagonalization of the above Dirac equation. Let us introduce a doublet of *collective modes* in the medium

$$\chi^{(h)}(\omega,k) = \begin{pmatrix} l_1^{(h)}(\omega,k) \\ l_2^{(h)}(\omega,k) \end{pmatrix} , \tag{5.57}$$

related to the flavor doublet $\varphi^{(h)}(\omega,k)$ by a unitary transformation $U_m^{(h)}$ with

$$U_m^{(h)} = \begin{pmatrix} \cos\theta_m^{(h)} & \sin\theta_m^{(h)} \\ -\sin\theta_m^{(h)} & \cos\theta_m^{(h)} \end{pmatrix} , \tag{5.58}$$

$$\varphi^{(h)}(\omega,k) = U_m^{(h)}\ \chi^{(h)}(\omega,k). \tag{5.59}$$

and a similar transformation for the right handed doublet $\xi^{(h)}(\omega,k)$, where the mixing angle $\theta_m^{(h)}$ depend on h,k and ω. The eigenvalue equation in diagonal form is given by

$$\left\{(\omega+i\Gamma)^2-k^2+\frac{1}{2}\ S_h(\omega,k)-\frac{1}{2}\ (M_e^2+M_\mu^2+2\,m_e^2+2\,m_\mu^2)+\frac{1}{2}\ \Omega_h(\omega,k)\begin{pmatrix}1&0\\0&-1\end{pmatrix}\right\}\chi^{(h)}(\omega,k)=0\ , \tag{5.60}$$

where $S_h(\omega,k)$, $\Delta_h(\omega,k)$ and $\Omega_h(\omega,k)$ are respectively given by

$$\begin{aligned}
S_h(\omega,k) &= \frac{3\ G_F\ n_\gamma}{2\sqrt{2}}\Big\{(\omega-hk)\,[A_{\mu\mu}(\omega)+A_{ee}(\omega)+h(\ B_{ee}(k)+B_{\mu\mu}(k))]+ \\
&\quad 2\omega(\widetilde{A}^{NC}_{\mu\mu}+\widetilde{A}^{NC}_{ee})-2k(\widetilde{B}^{NC}_{\mu\mu}+\widetilde{B}^{NC}_{ee})\Big\}\ , \qquad (5.61)\\
\Delta_h(\omega,k) &= \frac{3\ G_F\ n_\gamma}{2\sqrt{2}}\Big\{(\omega-hk)[\ A_{\mu\mu}(\omega)-A_{ee}(\omega)\ +h(B_{\mu\mu}(\omega)-B_{ee}(\omega))]+ \\
&\quad 2\omega(\widetilde{A}^{NC}_{\mu\mu}-\widetilde{A}^{NC}_{ee})-2k(\widetilde{B}^{NC}_{\mu\mu}-\widetilde{B}^{NC}_{ee})\Big\}\ , \qquad (5.62)\\
\Omega_h(\omega,k) &= \left(\Big[\ \delta\widetilde{M}^2-\Delta_h(\omega,k)\ \Big]^2+[\,2(\omega-hk)(A_{e\mu}+h\,B_{e\mu})\,]^2\right)^{\frac{1}{2}}. \qquad (5.63)
\end{aligned}$$

where $\delta\widetilde{M}^2 = M_\mu^2 - M_e^2 + 2m_\mu^2 - 2m_e^2$. The mixing angle in the medium is determined by the relations

$$\sin 2\theta_m^{(h)} = -\frac{2(\omega-hk)\,(A_{e\mu}+h\,B_{e\mu})}{\Omega_h(\omega,k)}\quad ;\quad \cos 2\theta_m^{(h)} = \frac{\delta\widetilde{M}^2-\Delta_h(\omega,k)}{\Omega_h(\omega,k)}. \tag{5.64}$$

where ω must be replaced by the solution of the eigenvalue equation (5.60) for each collective mode. A remarkable convergence of scales emerges for $T\sim 5\,\mathrm{GeV}$: *if* the neutrino asymmetry $|L_-|\sim 1$ then for nearly thermalized relativistic charged leptons with $\omega\sim -hk$ with $k\sim T$, all of the terms in the expression for $\Omega_h(\omega,k)$ are of the same order, namely, $|\Delta_h(k,k)|\sim |TA_{e\mu}|\sim \delta\widetilde{M}^2$. For relativistic leptons $|\omega|$ can be replaced by k in the arguments of the functions A,B to leading order in α, G_F.

For $M_\mu \ll \omega,k,T \ll M_W$ we find that the leading contribution to Δ_h is given by

$$\Delta_h(\omega,k)\simeq 1.2\,10^{-5}\left(\frac{T}{\mathrm{GeV}}\right)^4\left[\left(\frac{\omega-h\,k}{2T}\right)L_-\ \cos 2\theta-0.29\left(\frac{6.3\omega-h\,k}{7.3T}\right)\Big(\mathcal{L}_\mu-\mathcal{L}_e\Big)\right]\ (\mathrm{GeV}^2)\,, \tag{5.65}$$

where we have used the value $\sin^2\theta_w = 0.23$. A resonance in the mixing angle occurs for $\Delta_h = \delta\widetilde{M}^2$. The typical momentum of a lepton in the plasma is $k \sim T$, therefore in the temperature regime $T \ll M_W$ wherein our calculation is reliable, a resonance is available $\omega_{e,\mu}(k) \sim -h\,k \sim -h\,T$ *if* the neutrino asymmetry is close to the upper bound. Taking the values for $|\xi_a|$ inferred from the upper bounds from combined CMB and BBN data in absence of oscillations[21, 119] and the fit $\tan^2\theta \sim 0.40$ from the combined solar and KamLAND data[92] suggest the upper bound $|L_-\cos 2\theta| \sim 1$. With the asymmetry parameters for the charged leptons $|\xi_f|$ smaller than or of the same order of $|\xi_a|$, resonant mixing may occur in the temperature range $T \sim 5\,\mathrm{GeV}$. Even when the asymmetries from charged leptons do not allow for a resonance or at lower temperature, it is clear that at high temperature and for large neutrino asymmetries such that $L_- \sim 1$ there is a *large mixing angle* because of the convergence of scales. Hence at high temperature and large *differences* in the chemical potential for mass eigenstates, the propagating charged lepton collective excitations in the medium will be large admixtures of $e\,;\mu$ states. Consider a slightly off-equilibrium disturbance in the medium corresponding to an initial state describing an inhomogeneous wave packet of electrons. The real time evolution of this state in the medium has to be studied as an initial value problem. Following the real time analysis presented in ref.[113], we find that if an initial state describes a wave-packet of left handed electrons of helicity h, with amplitude $l_e^h(0;k); k \gg M_\mu$ but no muons, the persistence and transition probabilities are given by

$$P_{e\to e}(t;k) = |l_e^h(0;k)|^2\, e^{-2\Gamma t}\left[1-\sin^2(2\theta_m^h(k))\sin^2\left[\frac{\Omega(k)}{4k}\,t\right]\right] \tag{5.66}$$

$$P_{e\to\mu}(t;k) = |l_e^h(0;k)|^2\, e^{-2\Gamma t}\sin^2(2\theta_m^h(k))\sin^2\left[\frac{\Omega(k)}{4k}\,t\right] \quad ; \quad \Omega(k) = \Omega_h(k,k)\,. \tag{5.67}$$

The exponential prefactor reveals the *equilibration* of the charged lepton distribution with the equilibration rate 2Γ[133, 135]. It is also remarkable that $\Gamma \sim \Omega(k)/k$ in the temperature and energy regime of relevance for the resonance $k \sim T \sim 5\,\mathrm{GeV}$. Therefore we conclude that during the equilibration time scale of charged leptons, there is a substantial transition probability. Collisional contributions are of order $\alpha^2 T$ or $G_F^2 T^5$ for electromagnetic or weak interaction processes leading to collisional relaxation time scales far larger than the oscillation scale for $T \sim 5\,\mathrm{GeV}$.

In the radiation dominated phase for $M_W \gg T$ as discussed here, we find that the ratio of the oscillation to the expansion time scale $H\tau_{osc} \lesssim 10^{-16}(T/\mathrm{GeV})^3 \ll 1$, namely oscillation of mixed charged leptons occur on time scales much shorter than the expansion scale and the cosmological expansion can be considered adiabatic.

5.4.3 Remarks: beyond perturbation theory

We have focused on the high temperature limit to provide a detailed calculation within a simpler scenario, to extract the main aspects of the phenomenon and to highlight the main steps of the calculation. However, it is clear that a similar calculation can be performed at much lower temperature and the point of principle is still valid under the assumption of an equilibrium density matrix diagonal in the mass basis: there *could* be substantial charged lepton mixing if there are large chemical potential differences between the distribution functions of mass eigenstates. As per the discussion above, this is *not* the only scenario that yields substantial charged lepton mixing, the general condition is that the off diagonal self energy $\Sigma_{e\mu}$ in eqn. (5.3) be non-zero (and large). The off diagonal expectation value $< \nu_{eL}\overline{\nu}_{\mu L} >$ must in general be found from the equilibrium solution of a kinetic equation, but with a consistent treatment that avoids the caveats and subtleties discussed in section (5.3.2).

The arguments in favor of an equilibrium density matrix diagonal (or nearly so) in the mass basis, and the specific calculation described above relied on a perturbative expansion in the interaction picture of the unperturbed Hamiltonian H_0 which includes the neutrino mass matrix. There are possible caveats in the validity of perturbation theory, particularly in the case where medium effects lead to large corrections to the *single particle* states. For example, a large "index of refraction" arising from forward scattering with particles in the medium may lead to non-perturbative changes in the properties of the single particle basis. The lowest order contribution to the self-energy from forward scattering has been obtained in ref.[57], these are in general dependent on the energy of the neutrinos. Including these corrections in a perturbative approach entails summing the geometric Dyson series for the one-particle irreducible self energy in the neutrino propagators. This case is akin to the generation of a thermal mass from forward scattering in a scalar ϕ^4 field theory at finite temperature[133], when this thermal mass is larger than the zero temperature mass there is a large modification in the propagating single particle modes in the medium. In the scalar field theory case a self-consistent re-arrangement of the perturbative expansion consists in adding the thermal mass to the *unperturbed* Hamiltonian and at the same time a counterterm in the interaction part. The free single particle propagators now include the thermal mass term, and in order to avoid double counting, the counterterm in the interaction Hamiltonian cancels the contributions that yield the thermal mass corrections systematically order by order in the perturbative expansion. We propose a similar strategy to include the medium modifications to the propagating single particle modes

in the medium. In references[57, 113] it is found that the forward scattering contributions to the effective Hamiltonian in the medium are of the form

$$\delta H = \gamma^0 \mathbb{A}(k) - \vec{\gamma} \cdot \hat{\vec{k}} \, \mathbb{B}(k) \tag{5.68}$$

with $\mathbb{A}(k); \mathbb{B}(k)$ momentum dependent matrices in flavor space, their explicit expressions are given in refs.[57, 113]. A re-arrangement of the perturbative expansion results by writing

$$H = \widetilde{H}_0 + \widetilde{H}_{int} \tag{5.69}$$

where $\widetilde{H}_0 = H_0 + \delta H$ and $\widetilde{H}_{int} = H_{int} + H_c$ where the "counterterm" Hamiltonian $H_c = -\delta H$ systematically cancels the forward scattering corrections to the self-energies consistently in the perturbative expansion. The new "free" Hamiltonian $\widetilde{H}_0$ includes self-consistently the modifications to the propagating single particle states from the in-medium index of refraction. The field operators are now written in the basis of the solutions of the Dirac equation from the new Hamiltonian and finally the interaction is written in terms of these fields. Thus the perturbative expansion is re-organized in terms of the single particle propagating modes in the medium. The main complication in this program is that the mixing angles in the medium which determine the single particle propagating modes, are energy dependent, this introduces a non-locality in the interaction vertices which now become dependent on the energy and momentum flowing into the vertex.

If there is substantial charged lepton mixing, such phenomenon in turn affects the index of refraction for neutrinos in the medium and possibly the equilibration dynamics of neutrinos. A self-consistent treatment of the charged lepton mixing and neutrino mixing and relaxation would be required to understand the dynamical aspects of neutrino and charge lepton equilibration. This task is beyond the goals and focus of this article.

5.5 CONCLUSIONS

In this chapter, we focused on studying the possibility of charged lepton mixing as a consequence of neutrino mixing at high temperature and density in the early Universe. There are three main points in this chapter:

- We establish that a general criterion for charged lepton mixing as a consequence of neutrino mixing is that there must be off diagonal correlation of flavor fields in the density matrix. We

identified *one* possible case in which there could be charged lepton mixing: that the equilibrium density matrix be nearly diagonal in the mass basis. This is the case in the vacuum, but in this case the smallness of the neutrino masses entails that charged lepton mixing is negligible. We argued that this effect can be enhanced in a medium if the density matrix is nearly diagonal in the mass basis with large and different chemical potential for mass eigenstates. While this is not the only case in which charged lepton mixing can occur, it is one in which we can provide a definite calculation to assess charged lepton mixing.

- We have given general arguments to suggest that within the realm of validity of perturbation theory, the equilibrium density matrix must be nearly diagonal in the mass basis. We have critically re-examined the kinetic approach to neutrino mixing and relaxation in a medium at high temperature and density and highlighted several caveats and subtleties with flavor states, and or Fock operators associated with these states that cloud the interpretation of the density matrix. We argue that an equilibrium solution of the kinetic equations describing "flavor equalization"[59] can be interpreted as a confirmation that the density matrix is nearly diagonal in the mass basis. This interpretation leads us to the main and only assumption, namely that *before* "flavor equalization" for $T \gtrsim 30\,\mathrm{MeV}$ neutrinos are in equilibrium, the density matrix is nearly diagonal in the mass basis but with distribution functions for mass eigenstates with large and different chemical potentials in agreement with the bounds from BBN and CMB in absence of oscillations.
- Under this assumption and the validity of perturbation theory we have provided a definite calculation of charged lepton mixing. While the general criterion for charged lepton mixing does not imply that this is the *only* case in which charged leptons mix, it is a scenario that allows a definite calculation to assess the phenomenon in a quantitative manner.

In conclusion, under the assumption that the mass eigenstates of mixed neutrinos in the early Universe are in thermal equilibrium with different chemical potentials for $T >> 30\,\mathrm{MeV}$, *before* oscillations establish the equalization of flavor asymmetries[111] neutrino mixing leads to charged leptons mixing with large mixing angles in the plasma. We explored this possibility by obtaining the leading order contributions to the charged lepton self energies in the high temperature limit. If the upper bounds on the neutrino asymmetry parameters from BBN and CMB without oscillations is assumed along with the fit for the vacuum mixing angle for two generations from the KamLAND data, we find that charged leptons mix resonantly in the temperature range $T \sim 5\,\mathrm{GeV}$ in the early Universe. The electromagnetic damping rate is of the same order as the oscillation frequency in

the energy and temperature regime relevant for the resonance suggesting a substantial transition probability during equilibration. The cosmological expansion scale is much larger than the time scale of charged lepton oscillations. Although we assumed the validity of perturbation theory we recognized possible caveats in the high temperature limit arising from potentially large corrections to the single-particle propagating modes from the in-medium index of refraction. We proposed a re-organization of the perturbative expansion that includes the correct single-particle propagators self-consistently. We have focused on the high temperature limit as a simpler scenario to assess charged lepton mixing, however, the calculation can be performed at lower temperatures with the corresponding technical complications associated with the lepton masses. While at much lower temperatures there is no resonant mixing of charged leptons, the results of the calculation establish a point of principle, namely that for large chemical potential differences in the distribution function of mass eigenstates of neutrinos, the charged lepton propagating modes in the medium will be admixtures of the electron and muon degrees of freedom with non-vanishing mixing angle.

We believe that the phenomenon of charged lepton mixing in a medium warrants a deeper and thorough investigation. Our study also raises relevant questions on the kinetic approach: a consistent description of the kinetics of neutrino oscillation and relaxation avoiding the caveats associated with flavor states and or Fock operators associated with these states. Furthermore, substantial charged lepton mixing also suggests that a dynamical description should include self-consistently both neutrino and charged lepton mixing in a full non-equilibrium treatment. These aspects as well as possible consequences of charged lepton mixing for leptogenesis will be explored elsewhere.

6.0 STERILE NEUTRINO PRODUCTION VIA ACTIVE-STERILE OSCILLATIONS: THE QUANTUM ZENO EFFECT

6.1 INTRODUCTION

Sterile neutrinos couple to standard model active neutrinos through an off diagonal mass matrix, therefore they are produced via active-sterile oscillations. In the hot and dense environment of the early Universe when the scattering rate of active neutrinos off the thermal medium is large, namely a short mean free path, there is a competition between the oscillation length and the mean free path. It is expected that when the oscillation length is much larger than the mean free path, the active to sterile transition probability is hindered because rapid scattering events "freeze" the state to the active flavor state. This phenomenon receives the name of quantum Zeno effect or Turing's paradox, studied early in quantum optical coherence[136] but revisited within the context of neutrino oscillations in a medium in the pioneering work of references[60, 63, 64].

A semiclassical description of sterile neutrino production in the early Universe is achieved with the following semiphenomenological Boltzmann equation[20, 61, 77, 78, 137]

$$\frac{d}{dt} f_s(p,t) \approx \Gamma(a \to s; p)\,[f_a(p;t) - f_s(p;t)] \tag{6.1}$$

where $f_{a,s}$ are the distribution functions for active (a) and sterile (s) neutrinos, d/dt is the total time derivative including the redshift of momenta through the expansion in the early Universe and $\Gamma(a \to s; p)$ is an effective reaction rate. It is determined to be[61, 77]

$$\Gamma(a \to s; p) \approx \frac{\Gamma_{aa}(p)}{2} \left\langle P_{a\to s} \right\rangle \tag{6.2}$$

where $\Gamma_{aa}(p) \sim G_F^2\, p\, T^4$ is the active neutrino reaction rate and $\left\langle P_{a\to s} \right\rangle$ is a time average of the active-sterile transition probability in the medium which in reference[77] is given by

$$\left\langle P_{a\to s} \right\rangle = \Gamma \int_0^\infty P_{a\to s}(t) dt \tag{6.3}$$

where

$$\Gamma = \frac{\Gamma_{aa}}{2} \tag{6.4}$$

is the inverse of the decoherence time scale. Hence the rate that enters in the kinetic equation (6.1) is given by[77]

$$\Gamma(a \to s; p) = \frac{\Gamma_{aa}(p)}{4} \frac{\sin^2 2\theta_m(p) \left(\frac{2\,\Delta E(p)}{\Gamma_{aa}(p)}\right)^2}{\left[1 + \left(\frac{2\,\Delta E(p)}{\Gamma_{aa}(p)}\right)^2\right]} \tag{6.5}$$

where $\theta_m(p), \Delta E(p)$ are the mixing angle and active-sterile oscillation frequency in the medium respectively. The quantum Zeno paradox is manifest in the ratio $2\Delta E(p)/\Gamma_{aa}(p)$ in (6.5): for a relaxation time shorter than the oscillation time scale, or mean free path smaller than the oscillation length, $\Gamma_{aa}(p) \gg \Delta E(p)$ and the active-sterile transition probability is suppressed, with a concomitant reduction of the sterile production rate in the kinetic equation (6.1).

A field theoretic approach to sterile neutrino production near a MSW resonance which focuses primarily on the hadronic contribution and seemingly yields a very different rate has been proposed in reference[138], and more recently it has been observed that quantum Zeno suppression may have important consequences in thermal leptogenesis[12].

Goals: The emerging cosmological and astrophysical importance of sterile neutrinos motivates us to reconsider the dynamical aspects of their production. Most theoretical studies of the production of sterile neutrinos via active-sterile mixing rely on the kinetic description afforded by equation (6.1). While taking this description for *granted*, we focus our attention on the phenomenon of the quantum Zeno suppression of the active-sterile transition probability. We provide a quantum field theoretical understanding of the quantum Zeno suppression in *real time* and a reassessment of the time averaged transition probability $\langle P_{a\to s}\rangle$ by studying the non-equilibrium time evolution of the *full density matrix* and focusing on the dynamics of the quasiparticle propagating modes in the medium, in particular their dispersion relation and widths.

In section (6.2) we draw an analogy with mixing, oscillation and decay in the familiar setting of the neutral kaon system to establish the main observation: that each propagating mode in the medium features a different relaxation rate and the time averaged transition probability depends on *both*. In this section we obtain the general result for the time averaged transition probability $\langle P_{a\to s}\rangle$ in terms of the oscillation frequency and *both* relaxation rates, thereby establishing the main differences with the results available in the literature[20, 77, 78].

In section (6.3) we follow this analysis with a detailed study of the time evolution of the *full quantum field theory density matrix*, obtain the equations of motion for expectation values of the

neutrino fields and provide a detailed calculation of the dispersion relations and widths of the propagating modes (quasiparticles) in the medium up to second order in the weak interactions by obtaining the full neutrino propagator in the medium. In this section we also obtain the active-sterile transition probability $P_{a\to s}(t)$ in terms of the weak interaction scattering rate for active neutrinos and the mixing angle in the medium.

In section (6.4) we discuss in detail the conditions for the quantum Zeno effect, both in real time and in the time-averaged transition probability. In section (6.5) we discuss the implications of our results for the production of sterile neutrinos in the early Universe. In this section we argue that the in the early Universe far away from an MSW resonance the wide separation of the damping scales makes *any* definition of the time averaged transition probability *ambiguous*, and question the validity of the usual rate equation to describe sterile neutrino production in the early Universe far away from MSW resonances.

Section (6.6) presents our conclusions and poses further questions.

6.2 THE QUANTUM MECHANICAL PICTURE: COMPLETE CONDITIONS FOR QUANTUM ZENO SUPPRESSION.

Before we proceed with the quantum field theory study of the time evolution of the *full density matrix* which is pursued in detail in the following sections, it is illuminating to present our main observations on the suppression of the transition probability by interactions with the medium within the simple quantum mechanical picture of "strangeness" oscillations of neutral kaons[139, 140].

The neutral kaon system features many similarities to the case of mixing of two neutrinos in the medium: there are two different widths for the propagating eigenstates, and a time averaged probability is introduced in the study of $K_0 - \bar{K}_0$ oscillation to assess indirect CP violation experimentally[140]. The emergence of *two* relaxation rates for neutrinos propagating in the medium will be studied in the next section with the full quantum field theory density matrix. Of course the neutral kaon system is not *exactly* analog to the case of neutrinos, kaons are decaying single particle states even in the absence of a medium, while neutrinos acquire a relaxation rate (width) as a consequence of elastic and inelastic processes *in the medium*. Nevertheless, in both cases the decay or relaxation rates are determined by the imaginary part of the complex poles of the corresponding propagators.

In this section we explore the dynamical aspects of the presence of two time scales within the simpler quantum mechanical kaon system.

In section 6.3 we study the propagation of neutrinos in the medium from the full quantum field theory density matrix: we obtain the *neutrino propagator in the medium*, show that the complex poles yield two different relaxation rates and provide a complete quantum field theory analysis of the time evolution of flavor off diagonal density matrix elements.

Consider two quantum states labeled as $|\nu_a\rangle; |\nu_s\rangle$ which are linear superposition of propagating modes $|\nu_1\rangle; |\nu_2\rangle$, namely

$$\begin{aligned} |\nu_a\rangle &= \cos\theta|\nu_1\rangle + \sin\theta|\nu_2\rangle \\ |\nu_s\rangle &= \cos\theta|\nu_2\rangle - \sin\theta|\nu_1\rangle \,. \end{aligned} \tag{6.6}$$

(In the neutral kaon system $\theta = \pi/4$).

Let us consider that $|\nu_1\rangle; |\nu_2\rangle$ feature the time evolution of decaying states,

$$|\nu_{1,2}(t)\rangle = |\nu_{1,2}(0)\rangle\, e^{-iE_{1,2}t}\, e^{-\frac{\Gamma_{1,2}}{2}t} \tag{6.7}$$

leading to

$$\begin{aligned} |\nu_a(t)\rangle &= \cos\theta|\nu_1(0)\rangle\, e^{-iE_1 t}\, e^{-\frac{\Gamma_1}{2}t} + \sin\theta|\nu_2(0)\rangle\, e^{-iE_2 t}\, e^{-\frac{\Gamma_2}{2}t} \\ |\nu_s(t)\rangle &= \cos\theta|\nu_2(0)\rangle\, e^{-iE_2 t}\, e^{-\frac{\Gamma_2}{2}t} - \sin\theta|\nu_1(0)\rangle\, e^{-iE_1 t}\, e^{-\frac{\Gamma_1}{2}t} \,. \end{aligned} \tag{6.8}$$

For the familiar case of neutral kaons the states $|\nu_{1,2}>$ correspond to the long and short lived kaon states.

The transition probability $P_{a\to s}(t)$ is given by

$$P_{a\to s}(t) = |\langle\nu_s(0)|\nu_a(t)\rangle|^2 = \frac{\sin^2 2\theta}{2}\, e^{-\Gamma t}\,[\cosh(\gamma t) - \cos(\Delta E t)] \tag{6.9}$$

where

$$\Gamma = \frac{1}{2}\,(\Gamma_1 + \Gamma_2) \quad ; \quad \gamma = \frac{1}{2}\,(\Gamma_1 - \Gamma_2) \quad ; \quad \Delta E = E_1 - E_2 \,. \tag{6.10}$$

The *decoherence* time scale is $1/\Gamma$, since this is the time scale of suppression of the *oscillatory overlap* between the two states.

In section 6.3 we study the time evolution of the full quantum field theory density matrix for neutrinos and obtain the neutrino propagator in the medium. The complex poles of the neutrino propagator yield the dispersion relation and relaxation rates of the propagating modes in the medium. We find that for one active and one sterile neutrino the two propagating modes in the medium feature *different* widths or relaxation rates, $\Gamma_1(k);\Gamma_2(k)$. From the time evolution of flavor off-diagonal density matrix elements we obtain the active-sterile transition probability $P_{a\to s}$ which is similar in form to (6.9) (see eqn. (6.81)). The *quantum Zeno effect* or Turing's paradox[60, 63] arises when the transition probability is suppressed by rapid scattering in the medium.

Sterile neutrinos are produced via the production of the active species and the transition from mixing $a \to s$. The transition probability (6.9), (see also (6.81)) is suppressed by the exponential prefactor which is a consequence of collisions in the medium. This suppression leads to the often quoted condition for quantum Zeno suppression: if collisions in the medium are faster than the oscillation time scale, these hinder the production of sterile neutrinos and the state of the system is "frozen"[20, 60, 63, 77, 78]. According to this condition, if $\Gamma \gg \Delta E$ the oscillation $a \to s$ is strongly suppressed by the decay, in the opposite limit, $\Delta E \gg \Gamma$ there are many oscillations with a substantial transition probability. This argument implicitly assumes that the interaction rates of the propagating modes in the medium are the same, hence that there is only one time scale for relaxation.

However, in general there are *two* different rates Γ_1, Γ_2 for the different propagating eigenstates and we show below that this introduces *substantial modifications* to the necessary conditions for quantum Zeno suppression.

Following the arguments of references[61, 77], a measure of the influence of the $a \to s$ transition probability on the sterile neutrino production rate is obtained from the average of the transition probability on the time scale of the exponential decay of the *coherence*, namely the oscillatory interference term which results from the overlap of the two propagating states. Using the result (6.9) we find instead

$$\left\langle P_{a\to s} \right\rangle \equiv \Gamma \int_0^\infty P_{a\to s}(t)\, dt = \frac{\sin^2 2\theta}{2}\, \frac{\left(\frac{\gamma}{\Gamma}\right)^2 + \left(\frac{\Delta E}{\Gamma}\right)^2}{\left[1-\left(\frac{\gamma}{\Gamma}\right)^2\right]\left[1+\left(\frac{\Delta E}{\Gamma}\right)^2\right]}\,. \tag{6.11}$$

This expression features two remarkable differences with the result (6.5)[77]: the extra terms $(\gamma/\Gamma)^2$ in the numerator and $1-(\gamma/\Gamma)^2$ in the denominator, both are consequence of the fact that the relaxation is determined by *two* time scales Γ_1, Γ_2. Only when these scales are *equal*, namely

when $\gamma = 0$ the result (6.5) often used in the literature is recovered.

This simple analysis leads us to state that the *complete conditions* for quantum Zeno suppression of the transition probability are that *both* $\gamma/\Gamma \ll 1$ *and* $\Delta E/\Gamma \ll 1$. That these are indeed the correct necessary conditions for quantum Zeno suppression can be gleaned from figure (6.1) which displays the transition probability (without the prefactor $\sin^2 2\theta/2$) as a function of time for several values of the ratios $\gamma/\Gamma, \Delta E/\Gamma$ even without performing the time average.

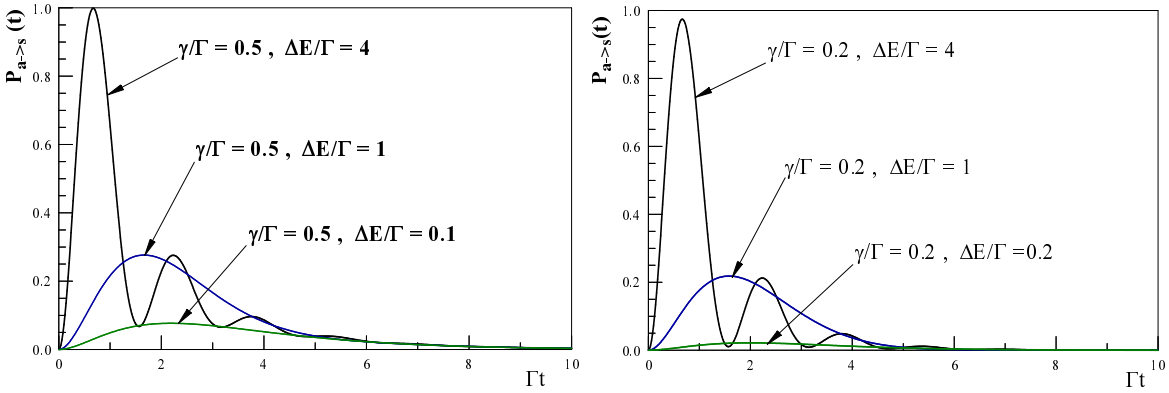

Figure 6.1: The transition probability $P_{a\to s}(t)$ (without the prefactor $\sin^2 2\theta/2$) vs. Γt. The left panel is for $\gamma/\Gamma = 0.5$, $\Delta E/\Gamma = 4, 1, 0.1$, the right panel is for $\gamma/\Gamma = 0.2$, $\Delta E/\Gamma = 4, 1, 0.2$.

The main difference between the result (6.11) and that in reference [77] is that in this reference it has been assumed that $\Gamma_1 = \Gamma_2$, namely $\gamma = 0$, in which case the result (6.11) agrees with that in [77].

Thus it is clear from the above analysis that quantum Zeno suppression is *not* operational when there is a wide separation between the rates, $\Gamma_1 \gg \Gamma_2$ *or* $\Gamma_1 \ll \Gamma_2$, *even when* $\Delta E/\Gamma \ll 1$. The failure of quantum Zeno suppression in these cases is a consequence of the fact that in this limit of wide separation of relaxation scales implies $(\gamma/\Gamma)^2 \sim 1$, which in turn leads to an *enhancement* of the average transition probability because the time integral is dominated by the longest time scale. Such is the case, for example, for the long and short lived kaon states whose lifetimes differ by almost three orders of magnitude.

Although the discussion above focused on the time averaged transition probability, in the following sections we study the quantum Zeno effect and the different time scales directly in real time based on the non-equilibrium time evolution of the *full quantum density matrix*.

6.3 QUANTUM FIELD THEORY TREATMENT IN THE MEDIUM

6.3.1 Non-equilibrium density matrix

In a medium the relevant question is *not* that of the time evolution of a pure quantum state, but more generally that of a density matrix from which expectation values of suitable operators can be obtained.

In order to provide a detailed understanding of the quantum Zeno effect, we need a reliable estimate of the dispersion relations $E_{1,2}(k)$ and the relaxation rates $\Gamma_{1,2}(k)$ in the medium which are determined by the complex poles of the neutrino propagator in the medium.

In this chapter, we obtain these from the study of the real time evolution of the *full density matrix* by implementing the methods of quantum field theory in real time described in references[141, 142, 143, 144, 145, 146]. This is achieved by introducing external (Grassmann) sources that induce an expectation value for the neutrino fields. Upon switching off the sources these expectation values relax towards equilibrium and their time evolution reveals both the correct energy and the relaxation rates[145, 146]. The main ingredient in this program is the active neutrino self-energy which we obtain up to second order in the standard model weak interactions and from which we extract the index of refraction and the widths which determine the dispersion relations and decay rates of the quasiparticle modes in the medium.

We consider a model of one active and one sterile Dirac neutrinos in which active-sterile mixing is included via an off diagonal Dirac mass matrix. The relevant Lagrangian density is given by

$$\mathcal{L} = \mathcal{L}^0_\nu + \mathcal{L}_{Ia}\,, \tag{6.12}$$

where

$$\mathcal{L}^0_\nu = \overline{\nu}\,(i\not{\partial}\,\mathbb{1} - \mathbb{M})\,\nu\,, \tag{6.13}$$

with ν being the neutrino doublet

$$\nu \equiv \begin{pmatrix} \nu_a \\ \nu_s \end{pmatrix}\,, \tag{6.14}$$

and a, s refer to the flavor indexes of the active and sterile neutrinos respectively. The Dirac mass

matrix $\mathbb{M}$ is given by

$$\mathbb{M} = \begin{pmatrix} m_{aa} & m_{as} \\ m_{as} & m_{ss} \end{pmatrix} . \tag{6.15}$$

It can be diagonalized by the unitary transformation that takes flavor into mass eigenstates, namely

$$\begin{pmatrix} \nu_a \\ \nu_s \end{pmatrix} = U(\theta) \begin{pmatrix} \nu_1 \\ \nu_2 \end{pmatrix} , \tag{6.16}$$

with the unitary transformation given by the 2×2 matrix

$$U(\theta) = \begin{pmatrix} \cos\theta & \sin\theta \\ -\sin\theta & \cos\theta \end{pmatrix} . \tag{6.17}$$

In this basis the mass matrix is diagonal

$$\mathbb{M} = \begin{pmatrix} M_1 & 0 \\ 0 & M_2 \end{pmatrix} , \tag{6.18}$$

with the relation

$$m_{aa} = \cos^2\theta M_1 + \sin^2\theta M_2 \;\; ; \;\; m_{ss} = \sin^2\theta M_1 + \cos^2\theta M_2 \;\; ; \;\; m_{as} = \frac{1}{2}(M_2 - M_1)\sin 2\theta \, , \tag{6.19}$$

where θ is the *vacuum* mixing angle. The Lagrangian density $\mathcal{L}_{Ia}$ describes the weak interactions of the active neutrino ν_a with hadrons or quarks and its associated charged lepton. Leptons, hadrons or quarks reach equilibrium in a thermal bath on time scales far shorter than those of neutrinos, therefore in what follows we assume hadrons or quarks and charged leptons to be in thermal equilibrium. Furthermore, in our analysis we will *not* include the non-linearities associated with a neutrino background, such component requires a full non-equilibrium treatment and is not germane to the focus of this study. The Lagrangian density that includes both charged and neutral current interactions can be written in the form

$$\mathcal{L}_{Ia} = \left[\frac{g}{\sqrt{2}} \mathcal{O}_a L \nu_a + G_F \overline{\nu_{La}} \gamma_\mu J^\mu L \nu_a \right] \tag{6.20}$$

where $L = (1-\gamma^5)/2$, $\mathcal{O}_a$ describes the charged current interaction with hadrons or quarks and the charged lepton, and J^μ represents the background current of the bath in equilibrium and describes the neutral current contributions in the limit of the effective Fermi interaction after integrating out the neutral vector boson. In the case of all active species the neutral current yields a contribution

which is the same for all flavors (when the neutrino background is neglected), hence it does not contribute to oscillations and the effective matter potential. In the case in which there are sterile neutrinos, which do not interact with the background directly, the neutral current contribution does contribute to the medium modifications of active-sterile mixing angles and oscillations frequencies.

To study the dynamics in a medium we must consider the time evolution of the *density matrix*. While the usual approach truncates the full density matrix to a 2×2 "flavor" subspace thus neglecting all but the flavor degrees of freedom, and studies its time evolution in terms of Bloch-type equations[60, 77], our study relies instead on the time evolution of the *full quantum field theoretical density matrix*.

The time evolution of the quantum density matrix $\hat{\rho}$ is given by the quantum Liouville equation

$$i\frac{d\hat{\rho}(t)}{dt} = [H, \hat{\rho}(t)] \tag{6.21}$$

where H is the full Hamiltonian with weak interactions. The solution is given by

$$\hat{\rho}(t) = e^{-iHt}\,\hat{\rho}(0)\,e^{iHt} \tag{6.22}$$

from which the time evolution of observables associated with an operator $\mathcal{O}$, namely its expectation value in the time evolved density matrix is given by

$$\langle \mathcal{O}(t) \rangle = \mathrm{Tr}\hat{\rho}(t)\mathcal{O}\,. \tag{6.23}$$

The time evolution of the density matrix requires the unitary time evolution operators that evolve forward (e^{-iHt}) and backward (e^{iHt}) in time. The density matrix elements in the field basis are given by

$$\hat{\rho}(\psi, \psi'; t) = \int \mathcal{D}\phi\mathcal{D}\phi'\,\langle\psi|e^{-iHt}|\phi\rangle\,\hat{\rho}(\phi, \phi'; 0)\,\langle\phi'|e^{iHt}|\psi'\rangle\,, \tag{6.24}$$

the matrix elements of the forward and backward time evolution operators can be handily written as path integrals and the resulting expression involves a path integral along a forward and backward contour in time. This is the Schwinger-Keldysh[141, 142, 143, 144] formulation of non-equilibrium quantum statistical mechanics which yields the correct time evolution of quantum density matrices in field theory. Expectation values of operators are obtained as usual by coupling sources conjugate to these operators in the Lagrangian and taking variational derivatives with respect to these sources. This formulation of non-equilibrium quantum field theory yields all the correlation and Green's function and is undoubtedly more complete than the simpler 2×2 truncation to the flavor degrees

of freedom. Of primary focus for our program in this article is the *neutrino retarded propagator*

$$S_{\alpha\beta}(\vec{x}-\vec{x}';t-t') = -i\Theta(t-t')\Big\langle\big\{\psi_\alpha(\vec{x},t),\overline{\psi}_\beta(\vec{x'},t')\big\}\Big\rangle\,, \tag{6.25}$$

where the flavor indices α,β correspond to either active or sterile and the brackets stand for ensemble average in the full quantum density matrix (6.22). The (complex) poles in complex frequency space of the spatio-temporal Fourier transform of the neutrino propagator yields the dispersion relations and damping rates of the quasiparticle states in the medium. It is not clear if this important information can be extracted from the truncated 2×2 density matrix in flavor space usually invoked in the literature and which forms the basis of the kinetic description (6.1), but certainly the *full quantum field density matrix* does have all the information on the correct dispersion relations and relaxation rates.

A standard approach to obtain the propagation frequencies and damping rates of quasiparticle excitations in a medium is the method of linear response[147]. An external source η is coupled to the field operator ψ to induce an expectation value of this operator in the many body density matrix, the time evolution of this expectation value yields the quasiparticle dynamics, namely the propagation frequencies and damping rates. In linear response

$$\langle\psi_\alpha(\vec{x},t)\rangle = -\int d^3x'dt' S_{\alpha\beta}(\vec{x}-\vec{x}';t-t')\,\eta_\beta(\vec{x}',t')\,, \tag{6.26}$$

where $S(\vec{x}-\vec{x}';t-t')$ is the retarded propagator or Green's function (6.25) and averages are in the full quantum density matrix. We emphasize that the quasiparticle dispersion relations and damping rates are obtained from the complex poles of the spatio-temporal Fourier transform of the retarded propagator in the complex frequency plane[147, 148]. For one active and one sterile neutrino there are two propagating modes in the medium. Up to one loop order $\mathcal{O}(G_F)$ the index of refraction in the medium yields two different dispersion relations[57], hence we *expect* also that the damping rates for these two propagating modes which will be obtained up to $\mathcal{O}(G_F^2)$ will be different. This expectation will be confirmed below with the explicit computation of the propagator up to two-loop order.

Linear response is the standard method to obtain the dispersion relations and damping rates of quasiparticle excitations in a plasma in finite temperature field theory[148]. The linear response relation (6.26) can be inverted to write

$$S^{-1}\langle\psi(\vec{x},t)\rangle = -\eta(\vec{x},t)\,, \tag{6.27}$$

where S^{-1} is the (non-local) differential operator which is the inverse of the propagator, namely the *effective Dirac operator* in the medium that includes self-energy corrections. This allows to study the dynamics as an *initial value problem* and to recognize the quasiparticle dispersion relations and damping rates directly from the time evolution of an initial value problem. This method has been applied to several different problems in quantum field theory out of equilibrium and the reader is referred to the literature for detailed discussions[85, 86, 87, 145, 146].

It is important to highlight that $\langle\psi(\vec{x},t)\rangle$ *is not* a single particle wave function but the expectation value of the quantum field operator in the non-equilibrium density matrix, namely an ensemble average. In contrast to this expectation value, a single particle wave function is defined as $\langle 1|\psi(\vec{x},t)|0\rangle$ where $|0\rangle$ is the vacuum and $|1\rangle$ a Fock state with *one* single particle.

In the present case the initial value problem allows us also to study the time evolution of flavor off diagonal density matrix elements. Consider an external source η_a that induces an initial expectation value only for the active neutrino field ψ_a, such an external source *prepares* the initial density matrix so that at $t = 0$ the active neutrino field operator features a non-vanishing expectation value, while the sterile one has a vanishing expectation value. Upon time evolution the density matrix develops *flavor off diagonal matrix elements* and the *sterile* neutrino field ψ_s develops an expectation value. The solution of the equation of motion (6.27) as an initial value problem allows us to extract precisely the time evolution of $\langle\psi_s\rangle$ from which we unambiguously extract the transition probability in the medium.

6.3.2 Equations of motion in linear response

The linear response approach to studying the non-equilibrium evolution relies on "adiabatically switching on" an external source η that initializes the quantum density matrix to yield an expectation value for the neutrino field(s). Upon switching off the external source the expectation values of the neutrino fields relax to equilibrium. The real time evolution of the expectation values reveals the dispersion relations and damping rates of the propagating quasiparticle modes in the medium. These are determined by the poles of the retarded propagator in the complex frequency plane[147, 148].

The equation of motion for the expectation value of the flavor doublet is obtained by introducing

external Grassmann-valued sources η[85, 86, 87]

$$\mathcal{L}_S = \overline{\nu}\,\eta + \overline{\eta}\,\nu\,, \tag{6.28}$$

shifting the field

$$\nu_\alpha^\pm = \psi_\alpha + \Psi_\alpha^\pm \;\;;\;\; \psi_\alpha = \langle \nu_\alpha^\pm \rangle \;\;;\;\; \langle \Psi_\alpha^\pm \rangle = 0, \tag{6.29}$$

for $\alpha = a, s$, and imposing $\langle \Psi_a^\pm \rangle = 0$ order by order in the perturbation theory [85, 86, 87]. Implementing this program up to two-loop order, we find the following equation of motion

$$\left(i\,\partial\!\!\!/\,\delta_{\alpha\beta} - M_{\alpha\beta} + \Sigma^{tad}_{\alpha\beta} L \right)\, \psi_\beta(\vec{x},t) + \int d^3x' \int_{-\infty}^{t} dt' \Sigma_{\alpha\beta}(\vec{x}-\vec{x}', t-t')\psi_\beta(\vec{x}',t') = -\eta_\alpha(\vec{x},t), \tag{6.30}$$

The self energy contribution $\Sigma^{tad} \propto G_F$ describes the one-loop neutral current contribution to the matter potential in the medium, and Σ^{ret} includes contributions of order G_F but also of order G_F^2. The latter describes the two-loops diagrams with intermediate states of hadrons or quarks and the charged lepton and its spatio-temporal Fourier transform features an imaginary part that yields the relaxation rates of neutrinos in the medium. As shown in ref.[145], the spatial Fourier transform of the retarded self-energy can be written as

$$\Sigma(\vec{k}, t-t') = \frac{i}{\pi} \int_{-\infty}^{\infty} dk_0\, \mathrm{Im}\Sigma(\vec{k},k_0)\, e^{ik_0(t-t')}\,. \tag{6.31}$$

The imaginary part $\mathrm{Im}\Sigma(\vec{k},k_0)$ determines the relaxation rate of the neutrinos in the medium. Since only the active neutrino interacts with the degrees of freedom in the medium, both self-energy contributions are of the form

$$\Sigma = \begin{pmatrix} \Sigma_{aa} & 0 \\ 0 & 0 \end{pmatrix}\,. \tag{6.32}$$

Following ref.[145], we proceed to solve the equation of motion by Laplace transform as befits an initial value problem. Introducing the Laplace transform, the equation of motion becomes (see also ref.[145] for details)

$$\left[\left(i\gamma^0 s - \vec{\gamma}\cdot\vec{k} \right)\, \delta_{\alpha\beta} - M_{\alpha\beta} + \Sigma^{tad}_{\alpha\beta}\, L + \widetilde{\Sigma}_{\alpha\beta}(\vec{k},s)\, L \right] \widetilde{\psi}_\beta(\vec{k},s) = i\left(\gamma^0\, \delta_{\alpha\beta} + \mathcal{O}(G_F) \right) \psi_\beta(\vec{k},0)\,. \tag{6.33}$$

where the Laplace transform of the retarded self energy admits a dispersive representation which follows from eqn.(7.56), namely[145]

$$\widetilde{\Sigma}(\vec{k},s)=\int_{-\infty}^{\infty}\frac{dk_0}{\pi}\frac{\mathrm{Im}\Sigma(\vec{k},k_0)}{k_0-is} \tag{6.34}$$

In what follows we will ignore the perturbative corrections on the right hand side of (6.33) since these only amount to a perturbative multiplicative renormalization of the amplitude, (see ref.[145] for details).

The chiral nature of the interaction constrains the self-energy to be of the form[145]

$$\Sigma^{tad}\,L+\widetilde{\Sigma}(\vec{k},s)\,L=\Big(\gamma^0\mathbb{A}(s;k)-\vec{\gamma}\cdot\hat{\mathbf{k}}\,\mathbb{B}(s;k)\Big)\,L \tag{6.35}$$

where the matrices $\mathbb{A},\mathbb{B}$ are of the form given in eqn. (6.32) with the only matrix elements being $A_{aa};B_{aa}$ respectively. The dispersive form of the self-energy (6.34) makes manifest that for s near the imaginary axis in the complex s-plane

$$\widetilde{\Sigma}(\vec{k},s=-i\omega\pm\epsilon)=\int_{-\infty}^{\infty}\frac{dk_0}{\pi}\mathcal{P}\left[\frac{\mathrm{Im}\Sigma(\vec{k},k_0)}{k_0-\omega}\right]\pm i\,\mathrm{Im}\Sigma(\vec{k},\omega)\,, \tag{6.36}$$

where $\mathcal{P}$ indicates the principal part. This result will be important below.

The solution of the algebraic matrix equation (6.33) is simplified by expanding the left and right handed components of the Dirac doublet $\widetilde{\psi}$ in the helicity basis as

$$\widetilde{\psi}_L=\sum_{h=\pm1}\begin{pmatrix}0\\ v^{(h)}\otimes\widetilde{\varphi}^{(h)}\end{pmatrix}\quad;\quad\widetilde{\psi}_R=\sum_{h=\pm1}\begin{pmatrix}v^{(h)}\otimes\widetilde{\xi}^{(h)}\\ 0\end{pmatrix} \tag{6.37}$$

where the Weyl spinors $v^{(h)}$ are eigenstates of helicity $\vec{\sigma}\cdot\hat{\mathbf{k}}$ with eigenvalues $h=\pm1$ and $\widetilde{\varphi}^{(h)};\widetilde{\xi}^{(h)}$ are flavor doublets with the upper component being the active and the lower the sterile neutrinos.

Projecting the equation of motion (6.33) onto right and left handed components and onto helicity eigenstates, we find after straightforward algebra

$$\left[-(s^2+k^2)\mathbb{1}+(is-hk)(\mathbb{A}(k;s)+h\,\mathbb{B}(k;s))-\mathbb{M}^2\right]\widetilde{\varphi}^{(h)}(\vec{k},s)=i(is-hk)\mathbb{1}\,\varphi^{(h)}(\vec{k},0)-i\mathbb{M}\,\xi^{(h)}(\vec{k},0) \tag{6.38}$$

$$\widetilde{\xi}^{(h)}(\vec{k},s)=-\frac{is+hk}{s^2+k^2}\left[-\mathbb{M}\,\widetilde{\varphi}^{(h)}(\vec{k},s)+i\xi^{(h)}(\vec{k},0)\right] \tag{6.39}$$

where again we have neglected perturbatively small corrections on the right hand side of eqn. (6.38).

It proves convenient to introduce the following definitions,

$$\delta M^2 = M_1^2 - M_2^2 \;\; ; \;\; \overline{M}^{\,2} = \frac{1}{2}(M_1^2 + M_2^2) \tag{6.40}$$

$$S_h(k;s) = (is - hk)(A_{aa}(k;s) + hB_{aa}(k;s)) \tag{6.41}$$

$$\Delta_h(k;s) = \frac{S_h(k;s)}{\delta M^2} \tag{6.42}$$

$$\rho_h(k;s) = \Big[(\cos 2\theta - \Delta_h(k;s))^2 + \sin^2 2\theta\Big]^{\frac{1}{2}} \tag{6.43}$$

$$\cos 2\theta_m^{(h)}(k;s) = \frac{\cos 2\theta - \Delta_h(k;s)}{\rho_h(k;s)} \tag{6.44}$$

$$\sin 2\theta_m^{(h)}(k;s) = \frac{\sin 2\theta}{\rho_h(k;s)} \tag{6.45}$$

in terms of which

$$\begin{aligned} &-(s^2+k^2)\mathbb{1} + (is - hk)(\mathbb{A}(k;s) + h\,\mathbb{B}(k;s)) - \mathbb{M}^2 \\ &= \left(-s^2 - k^2 + \frac{1}{2}S_h(k,s) - \overline{M}^{\,2}\right)\mathbb{1} - \frac{\delta M^2}{2}\,\rho_h(k;s)\begin{pmatrix} \cos 2\theta_m^{(h)}(k;s) & -\sin 2\theta_m^{(h)}(k;s) \\ -\sin 2\theta_m^{(h)}(k;s) & -\cos 2\theta_m^{(h)}(k;s) \end{pmatrix} \end{aligned} \tag{6.46}$$

The solution of the equation (6.38) is given by

$$\widetilde{\varphi}^{(h)}(\vec{k},s) = \widetilde{\mathbb{S}}^{(h)}(k,s)\left[-i\mathbb{M}\,\xi^{(h)}(\vec{k},0) + i(is - hk)\mathbb{1}\,\varphi^{(h)}(\vec{k},0)\right] \tag{6.47}$$

where the propagator $\widetilde{\mathbb{S}}^{(h)}(k,s)$ is given by

$$\widetilde{\mathbb{S}}^{(h)}(k,s) = \frac{1}{[\alpha_h^2(s,k) - \beta_h^2(s,k)]}\left[\alpha_h(s,k)\,\mathbb{1} + \beta_h(s,k)\begin{pmatrix} \cos 2\theta_m^{(h)}(k;s) & -\sin 2\theta_m^{(h)}(k;s) \\ -\sin 2\theta_m^{(h)}(k;s) & -\cos 2\theta_m^{(h)}(k;s) \end{pmatrix}\right] \tag{6.48}$$

where

$$\alpha_h(k;s) = \left[-(s^2+k^2) + \frac{1}{2}\,S_h(k;s) - \overline{M}^{\,2}\right] \tag{6.49}$$

$$\beta_h(k;s) = \frac{\delta M^2}{2}\,\rho_h(k;s)\,. \tag{6.50}$$

The real time evolution is obtained by inverse Laplace transform,

$$\varphi^{(h)}(\vec{k},t) = \int_{\Gamma} \frac{ds}{2\pi i}\, \widetilde{\varphi}^{(h)}(\vec{k},s)\, e^{st}\,, \tag{6.51}$$

where Γ is the Bromwich contour in the complex s plane running parallel to the imaginary axis to the right of all the singularities of the function $\widetilde{\varphi}(\vec{k},s)$ and closing on a large semicircle to the left of the imaginary axis. The singularities of $\widetilde{\varphi}(\vec{k},s)$ are those of the propagator (6.48). *If the particles are asymptotic states and do not decay* these are isolated simple poles along the imaginary axis away from multiparticle cuts. However, in a medium or for decaying states, the isolated poles move into the continuum of the multiparticle cuts and off the imaginary axis. This is the general case of resonances which correspond to poles in the second or higher Riemann sheet and the propagator is a complex function with a branch cut along the imaginary axis in the complex s-plane as indicated by eqn. (6.36). Its analytic continuation onto the physical sheet features the usual Breit-Wigner resonance form and a complex pole and the width determines the damping rate of quasiparticle excitations[85, 86, 87].

It is important and relevant to highlight that the full width or damping rate is the *sum* of all the partial widths that contribute to the damping from different physical processes: decay if there are available decay channels, and in a medium the collisional width and or Landau damping also contribute to the imaginary part of the self-energy on the mass shell. The quasiparticle damping rate is one-half the relaxation rate in the Boltzmann equation for the distribution functions[87, 149].

It is convenient to change the integration variable to $s = -i\omega + \epsilon$ with $\epsilon \to 0^+$ and to write the real time solution (6.51) as follows

$$\varphi^{(h)}(\vec{k},t) = \int_{-\infty}^{\infty} \frac{d\omega}{2\pi}\, \widetilde{\varphi}^{(h)}(\vec{k},s=-i\omega+\epsilon)\, e^{-i\omega\, t}\,, \tag{6.52}$$

Rather than studying the most general cases and in order to simplify the discussion we focus on the cases of relevance for nearly ultrarelativistic neutrinos in the early Universe. Let us consider that initially there are no right handed neutrinos and only active neutrinos of negative helicity are produced, namely $h=-1$, and

$$\varphi^{(-1)}(\vec{k},0) = \begin{pmatrix} \nu_a(\vec{k},0) \\ 0 \end{pmatrix}\,, \tag{6.53}$$

hence

$$\begin{pmatrix} \nu_a(\vec{k},t) \\ \nu_s(\vec{k},t) \end{pmatrix} = i\int_{-\infty}^{\infty} \frac{d\omega}{2\pi}\, e^{-i\omega\, t}\, (\omega + k)\, G(k;\omega) \quad \begin{pmatrix} \nu_a(\vec{k},0) \\ 0 \end{pmatrix} \tag{6.54}$$

where

$$G(k;\omega) \equiv \widetilde{\mathbb{S}}^{(-1)}(k, s = -i\omega + \epsilon) \tag{6.55}$$

and the integral in (6.54) is carried out in the complex ω plane closing along a semicircle at infinity in the lower half plane describing retarded propagation in time.

In order to understand the nature of the singularities of the propagator, we must first address the structure of the self energy, in particular the imaginary part, which determines the relaxation rates. Again we focus on negative helicity neutrinos for simplicity. Upon the analytic continuation $s = -i\omega + \epsilon$ for this case we define

$$S(k,\omega) \equiv S_{h=-1}(k; s = -i\omega + \epsilon) = (\omega + k)\, \frac{1}{4}\, \mathrm{Tr}(\gamma^0 - \vec{\gamma}\cdot\ \hat{\mathbf{k}})\widetilde{\Sigma}_{aa}(\vec{k},s)\Big|_{s=-i\omega+\epsilon} \tag{6.56}$$

From equation (6.36) which is a consequence of the dispersive form (6.34) of the self energy $\widetilde{\Sigma}_{aa}(\vec{k},s)$, it follows that

$$S(k,\omega) = S_R(k,\omega) + iS_I(k,\omega) \tag{6.57}$$

where $S_{R,I}$ are the real and imaginary parts respectively. The real part of the self energy determines the correction to the dispersion relations of the neutrino *quasiparticle* modes in the medium, namely the "index of refraction", while the imaginary part determines the relaxation rate of these quasiparticles.

6.3.3 The self-energy: quasiparticle dispersion relations and widths:

Figure (7.2) shows the one loop contributions of $\mathcal{O}(G_F)$ including the neutral current tadpole diagrams which contribute to the in-medium "index of refraction" for one active species, and the two loop contribution of $\mathcal{O}(G_F^2)$ with intermediate states of hadrons (or quarks) and the associated charged lepton, in the limit of Fermi's effective field theory.

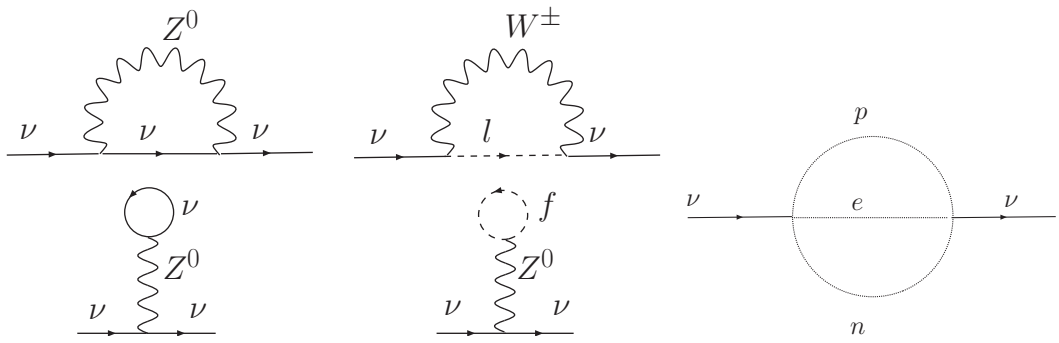

Figure 6.2: Left: one loop contributions to the self energy, the diagrams in the second line yield Σ^{tad}. These contributions are of $\mathcal{O}(G_F)$. Right: two loops contribution of $\mathcal{O}(G_F^2)$ to the self-energy in Fermi's effective field theory limit, with internal lines corresponding to hadrons and the charged lepton, or alternatively quarks and the charged lepton above the QCD phase transition.

In a medium at temperature T the real part of the one-loop contributions to $S(k,\omega)$ is of the form[20, 26, 57, 145]

$$S_R(k,\omega) = (\omega + k)\, G_F T^3 \left[L + \frac{T}{M_W^2} (a\omega + bk) \right] \tag{6.58}$$

where L is a function of the asymmetries of the fermionic species and a, b simple coefficients, all of which may be read from the results in ref.[20, 57, 145]. *Assuming* that all asymmetries are of the same order as the baryon asymmetry in the early Universe $L \sim 10^{-9}$ the term $\propto T/M_W^2$ in (6.58) for $\omega \sim k \sim T$ dominates over the asymmetry term for $T \gtrsim 3\,\mathrm{MeV}$[57, 145] and in what follows we neglect the CP violating terms associated with the lepton asymmetry.

The imaginary part to one loop order is obtained from a Cutkosky cut (discontinuity) of the diagrams with vector boson exchange shown on the left side in figure (6.3) and is determined by the processes $W \to l_a \overline{\nu}_a, Z \to \overline{\nu}_a \nu_a$. Both of these contributions are exponentially suppressed at temperatures $T \ll M_{W,Z}$, hence the one-loop contributions to the imaginary part of $S(k;\omega)$ is *negligible* for temperatures well below the electroweak scale. The two loop contribution to the imaginary part is obtained from the discontinuity cut of the two loop diagram with internal hadron or quark and charged lepton lines in figure (7.2). Some of the processes that contribute to the imaginary part in this order are for example neutron β decay $n \to p + e^+ + \overline{\nu}$ and its inverse, along with scattering processes in the medium. The imaginary part of the on-shell self-energy for

these contributions is proportional to $G_F^2\, k\, T^4$[26, 57] at temperatures $T \ll M_W$. Therefore in this temperature range

$$S_I(k,\omega) \sim (\omega + k)\, G_F^2\, k\, T^4\,. \tag{6.59}$$

The consistency and validity of perturbation theory and of Fermi's effective field theory for scales $\omega, k, T \ll M_W$ entail the following inequality

$$S_I(k,\omega) \ll S_R(k,\omega)\,. \tag{6.60}$$

For example near the neutrino mass shell for ultrarelativistic neutrinos with $\omega \sim k$, assuming $L \sim 10^{-9}$ and discarding this CP violating contribution for $T > 3\,\mathrm{MeV}$ because it is subleading, we find

$$\frac{S_I(k,\omega)}{S_R(k,\omega)} \sim g^2 \tag{6.61}$$

with g the weak coupling. This discussion is relevant for the detailed understanding of the circumstances under which the quantum Zeno effect is operative (see section (6.5) below).

The propagator $G(k;\omega)$ for negative helicity neutrinos is found to be given by

$$G(k;\omega) = \frac{1}{2\beta}\left[\frac{1}{\alpha-\beta} - \frac{1}{\alpha+\beta}\right]\begin{pmatrix} \alpha+\beta\cos 2\theta_m & -\beta\sin 2\theta_m \\ -\beta\sin 2\theta_m & \alpha-\beta\cos 2\theta_m \end{pmatrix}, \tag{6.62}$$

where we have suppressed the arguments for economy of notation, and defined

$$\alpha = \omega^2 - k^2 - \overline{M}^{\,2} + \frac{1}{2}S_R(k,\omega) + \frac{i}{2}S_I(k,\omega)\,, \tag{6.63}$$

$$\beta = \frac{\delta M^2}{2}\left[\left(\cos 2\theta - \frac{S_R(k,\omega)}{\delta M^2} - i\frac{S_I(k,\omega)}{\delta M^2}\right)^2 + \sin^2 2\theta\right]^{\frac{1}{2}}, \tag{6.64}$$

$$\theta_m \equiv \theta_m^{(-1)}(k, s = -i\omega + \epsilon)\,. \tag{6.65}$$

The inequality (6.60) licenses us to write β consistently up to $\mathcal{O}(G_F^2)$ as

$$\beta \simeq \frac{\delta M^2}{2}\rho(k,\omega) - \frac{i}{2}S_I(k,\omega)\cos 2\theta_m\,, \tag{6.66}$$

where

$$\rho(k,\omega) = \left[\left(\cos 2\theta - \frac{S_R(k,\omega)}{\delta M^2}\right)^2 + \sin^2 2\theta\right]^{\frac{1}{2}}. \tag{6.67}$$

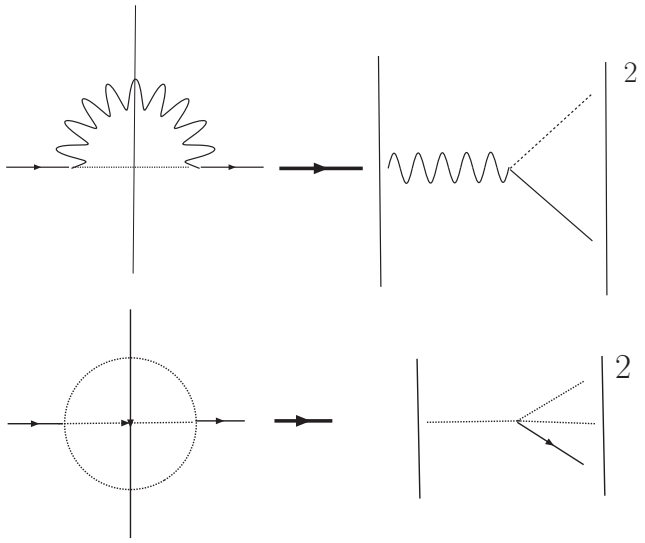

Figure 6.3: Contributions to the imaginary part of the self energy, the vertical line represents a Cutkosky cut. Left: discontinuity from the one loop contributions to the self energy of $\mathcal{O}(G_F)$, from the decay of vector bosons for example $W \to l\overline{\nu}$. Right: discontinuity from the two loops contribution of $\mathcal{O}(G_F^2)$, arising for example from $n \to p + e^+ + \overline{\nu}_e$ or similar processes at the quark level.

Equation (6.62) makes manifest that $G(k;\omega)$ is strongly peaked at the values of ω for which $\alpha = \pm\beta$. These determine the position of the complex poles in the analytic continuation. In the relativistic approximation $k \gg M_{1,2}$ we find the following complex poles:

- For $\alpha = \beta$**:**

$$\omega_1(k) = E_1(k) - i\,\frac{\Gamma_1(k)}{2} \tag{6.68}$$

with

$$E_1(k) \approx k + \frac{1}{2k}\left[\overline{M}^2 + \frac{\delta M^2}{2}\rho(k) - \frac{S_R(k)}{2}\right] \tag{6.69}$$

$$\frac{\Gamma_1(k)}{2} = \frac{\Gamma_{aa}(k)}{2}\cos^2\theta_m(k) \tag{6.70}$$

- For $\alpha = -\beta$**:**

$$\omega_2(k) = E_2(k) - i\frac{\Gamma_2(k)}{2} \tag{6.71}$$

with

$$E_2(k) \approx k + \frac{1}{2k}\left[\overline{M}^2 - \frac{\delta M^2}{2}\rho(k) - \frac{S_R(k)}{2}\right] \tag{6.72}$$

$$\frac{\Gamma_2(k)}{2} = \frac{\Gamma_{aa}(k)}{2}\sin^2\theta_m(k)\,. \tag{6.73}$$

where

$$\rho(k) \equiv \left[\left(\cos 2\theta - \frac{S_R(k,\omega=k)}{\delta M^2}\right)^2 + \sin^2 2\theta\right]^{\frac{1}{2}}, \tag{6.74}$$

$\Gamma_{aa}(k)$ is the standard model result for the scattering rate of the active neutrino species[20, 57, 77, 78]

$$\frac{\Gamma_{aa}(k)}{2} = \frac{S_I(k,\omega=k)}{2k} = \frac{1}{4}\mathrm{Tr}(\gamma^0 - \vec{\gamma}\cdot\ \hat{\mathbf{k}})\mathrm{Im}\Sigma_{aa}(\vec{k},\omega=k) \sim G_F^2\,T^4\,k \tag{6.75}$$

and $\theta_m(k) = \theta_m^{(h=-1)}(k, s=-ik)$ is the mixing angle in the medium for negative helicity neutrinos of energy $\omega \sim k$ in the relativistic limit. The relations (6.70,6.73) are the same as those recently found in reference[146].

Combining all the results we find

$$\begin{pmatrix} \nu_a(\vec{k},t) \\ \nu_s(\vec{k},t) \end{pmatrix} = \left[e^{-iE_1(k)t}\,e^{-\frac{\Gamma_1(k)}{2}t}\,\frac{1}{2}\begin{pmatrix} 1+\cos 2\theta_m(k) & -\sin 2\theta_m(k) \\ -\sin 2\theta_m(k) & 1-\cos 2\theta_m(k) \end{pmatrix} + e^{-iE_2(k)t}\,e^{-\frac{\Gamma_2(k)}{2}t}\,\frac{1}{2}\begin{pmatrix} 1-\cos 2\theta_m(k) & \sin 2\theta_m(k) \\ \sin 2\theta_m(k) & 1+\cos 2\theta_m(k) \end{pmatrix}\right]\begin{pmatrix} \nu_a(\vec{k},0) \\ 0 \end{pmatrix} \tag{6.76}$$

This expression can be written in the following more illuminating manner,

$$\begin{pmatrix} \nu_a(\vec{k},t) \\ \nu_s(\vec{k},t) \end{pmatrix} = U(\theta_m(k))\begin{pmatrix} e^{-iE_1(k)t}\,e^{-\frac{\Gamma_1(k)}{2}t} & 0 \\ 0 & e^{-iE_2(k)t}\,e^{-\frac{\Gamma_2(k)}{2}t} \end{pmatrix} U^{-1}(\theta_m(k))\begin{pmatrix} \nu_a(\vec{k},0) \\ 0 \end{pmatrix}, \tag{6.77}$$

where $U(\theta_m(k))$ is the mixing matrix (6.17) but in terms of the mixing angle in the medium.

In obtaining the above expressions we have neglected perturbative corrections from wave function renormalization and replaced $\omega + k \sim 2k$ thus neglecting terms that are subleading in the relativistic limit, and the imaginary part in ω, which although it is of $\mathcal{O}(G_F^2)$, yields the effective Wigner-Weisskopf approximation[146].

6.3.4 Physical interpretation:

The above results have the following clear physical interpretation. The active (a) and sterile (s) neutrino fields in the medium are linear combinations of the fields associated with the $1, 2$ quasiparticle modes with dispersion relations $E_{1,2}(k)$ and damping rates $\Gamma_{1,2}(k)$ respectively, on the mass shell of the quasiparticle modes the relation between them is the usual one for neutrinos propagating in a medium with an index of refraction, namely

$$\nu_a(\vec{k},t) = \cos\theta_m(k)\ \nu_1(\vec{k},t) + \sin\theta_m(k)\ \nu_2(\vec{k},t) \tag{6.78}$$

$$\nu_s(\vec{k},t) = \cos\theta_m(k)\ \nu_2(\vec{k},t) - \sin\theta_m(k)\ \nu_1(\vec{k},t)\,. \tag{6.79}$$

These relations between the expectation values of flavor fields and the fields associated with the propagating quasiparticle modes in the medium are obtained from the diagonalization of the neutrino propagator on the mass shell of the quasiparticle modes. These are recognized as the usual relations between flavor and "mass" fields in a medium with an index of refraction.

At temperatures much higher than that at which a resonance occurs (and for $k \sim T$) $\theta_m(k) \sim \pi/2$ then $\nu_a \sim \nu_2$, and the active neutrino features a damping rate $\Gamma_2 \sim \Gamma_{aa}$ while the sterile neutrino $\nu_s \sim \nu_1$ with a damping rate $\Gamma_1 = \Gamma_{aa}\cos^2\theta_m(k) \ll \Gamma_{aa}$. In the opposite limit for temperatures much lower than that of the resonance and for very small vacuum mixing angles $\nu_a \sim \nu_1$ and features a damping rate $\Gamma_1 \sim \Gamma_{aa}$ while $\nu_s \sim \nu_2$ with a damping rate $\Gamma_2 \sim \Gamma_{aa}\sin^2\theta \ll \Gamma_{aa}$. Thus it is clear that in both limits the active neutrino has the larger damping rate and the sterile one the smallest one. This physical interpretation confirms that there *must* be two widely different time scales for relaxation in the high and low temperature limits, the *longest time scale* or alternatively the *smallest damping rate* always corresponds to the sterile neutrino. This is obviously in agreement with the expectation that sterile neutrinos are much more weakly coupled to the plasma than the active neutrinos for $\sin 2\theta_m(k) \sim 0$. This analysis highlights that *two time scales* must be expected on physical grounds, not just one, the decoherence time scale, which only determines the suppression of the *overlap* between the propagating states in the mixed neutrino state.

This physical interpretation of the different damping rates is of crucial importance in the description of the transition probability. The *decoherence* time scale corresponds to the time scale for suppression of the overlap between the two quasiparticle modes in the medium, hence it is determined by the *sum* of the individual damping rates. However, the total transition probability $P_{a\to s}(t)$ not only includes the overlap between the two modes but also the probability of each mode

in the mixed state, and these are suppressed by the individual damping rates $\Gamma_{1,2}(k)$, which are widely separated far away of the resonance.

It is important to highlight that the emergence of *two time scales* can be gleaned in the pioneering work on sterile neutrino production of ref.[61] (see eqn. (10) in that reference) obtained within a phenomenological Wigner-Weisskopf approximation. Our quantum field theory study based on the full density matrix and the neutrino propagator in the medium provides a consistent and systematic treatment of propagation in the medium that displays both time scales.

6.4 QUANTUM ZENO EFFECT

6.4.1 Real time interpretation

Consider a density matrix in which the expectation value of the sterile neutrino field *vanishes* at the initial time $t = 0$. Then it is clear from equation (6.76) that flavor off-diagonal density matrix elements develop in time signaling that sterile neutrinos are produced via active-sterile oscillation with amplitude

$$\nu_s(\vec{k},t) = -\frac{1}{2}\sin 2\theta_m(k)\left[e^{-iE_1(k)t}\,e^{-\frac{\Gamma_1(k)}{2}t} - e^{-iE_2(k)t}\,e^{-\frac{\Gamma_2(k)}{2}t}\right]\nu_a(\vec{k},0) \tag{6.80}$$

From the solution (6.80) we can read off the transition probability

$$P_{a\to s}(t) = \frac{\sin^2 2\theta_m(k)}{2}\,e^{-\Gamma(k)t}\left[\cosh(\gamma(k)t) - \cos(\Delta E(k)t)\right] \tag{6.81}$$

which is of the same form as the expression obtained from the quantum mechanical analysis (6.9) with the identification

$$\Gamma(k) = \frac{1}{2}\Big(\Gamma_1(k)+\Gamma_2(k)\Big) = \frac{\Gamma_{aa}(k)}{2} \tag{6.82}$$

$$\gamma(k) = \frac{1}{2}\Big(\Gamma_1(k)-\Gamma_2(k)\Big) = \frac{\Gamma_{aa}(k)}{2}\cos 2\theta_m(k) \tag{6.83}$$

$$\Delta E(k) = E_1(k) - E_2(k) = \frac{\delta M^2}{2\,k}\rho(k) \tag{6.84}$$

For the analysis that follows it is more convenient to write (6.81) in the form

$$P_{a\to s}(t) = \frac{\sin^2 2\theta_m(k)}{4}\left[e^{-\Gamma_1 t} + e^{-\Gamma_2 t} - 2\,e^{-\Gamma(k)t}\cos(\Delta E(k)t)\right]. \tag{6.85}$$

The first two terms are obviously the probabilities for the quasiparticle modes $1, 2$, while the oscillatory term is the usual interference between these but now damped by the factor $e^{-\Gamma(k)t}$. We highlight that the *decoherence* time scale is precisely $\Gamma^{-1}(k) = 2/\Gamma_{aa}(k)$ as anticipated in references[60, 77], namely the *interference* between the two quasiparticle modes is suppressed on this time scale. However, the *total* transition probability is suppressed on this time scale *only* if $\Gamma_1 = \Gamma_2 = \Gamma$, namely near a resonance. In this case

$$P_{a\to s}(t) = \sin^2 2\theta_m(k)\; e^{-\frac{\Gamma_{aa}}{2}\,t}\; \sin^2\left[\frac{\Delta E(k)}{2}\,t\right], \tag{6.86}$$

which is the result quoted in reference[77]. Under these conditions quantum Zeno suppression occurs when $\Gamma(k) \gg \Delta E(k)$ in which case the decoherence time scale is much smaller than the oscillation time scale and the transition probability is suppressed before $a \to s$ oscillations take place.

However, far away on either side of the resonance, although the oscillatory interference term is suppressed on the decoherence time scale Γ^{-1}, the transition probability is *not* suppressed on this scale but on a much longer time scale, determined by the *smaller* of $\Gamma_{1,2}$. Only when $\Gamma_1 = \Gamma_2 = \Gamma$, namely $\gamma = 0$ both the coherence (oscillatory interference term) and the transition probability are suppressed on the decoherence time scale. This phenomenon is displayed in (6.4). This figure shows the transition probability as a function of time without the prefactor $\sin^2 2\theta_m(k)$ since it is not the relevant quantity for quantum Zeno suppression, which only emerges from the competition between the damping and the oscillation time scales.

Even for $\Gamma(k) \gg \Delta E(k)$, claimed in the literature [20, 60] to be the condition for quantum Zeno suppression, the transition probability is substantial on time scales much longer than Γ^{-1} if Γ_1 and Γ_2 are *widely separated*. This situation is depicted in figure (6.5). From this analysis we conclude that the conditions for quantum Zeno suppression of $P_{a\to s}(t)$ are: **(i):** $\Gamma(k) \gg \Delta E(k)$ *and* **(ii):** $\gamma(k) \sim 0$, namely $\Gamma_1(k) \sim \Gamma_2(k)$. These conditions which are obtained from the time dependence of $P_{a\to s}(t)$ are consistent with those found from the simple quantum mechanical example in terms of the time averaged probability (6.11). We then emphasize that it is *not* necessary to average the probability over time to recognize the criteria for the quantum Zeno effect, these can be directly gleaned from the time evolution of the probability as originally proposed[136].

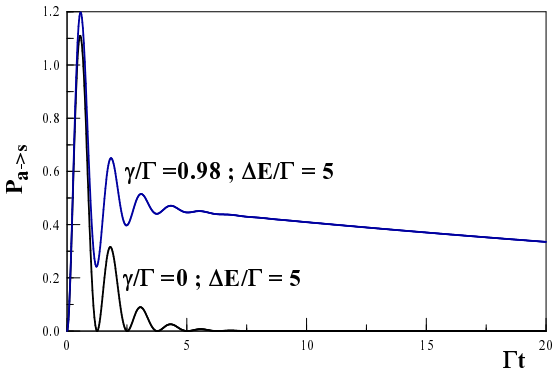

Figure 6.4: The transition probability $P_{a\to s}(t)$ (6.81) (without the prefactor $\sin^2 2\theta_m/2$) vs. Γt. The figure depicts the cases $\cos 2\theta_m(k) = 0.98$ and $\cos 2\theta_m(k) = 0$ respectively, both with $\Delta E/\Gamma = \delta M^2\rho(k)/2k\Gamma = 5$. The scale for suppression of the oscillatory interference is $1/\Gamma$ in both cases.

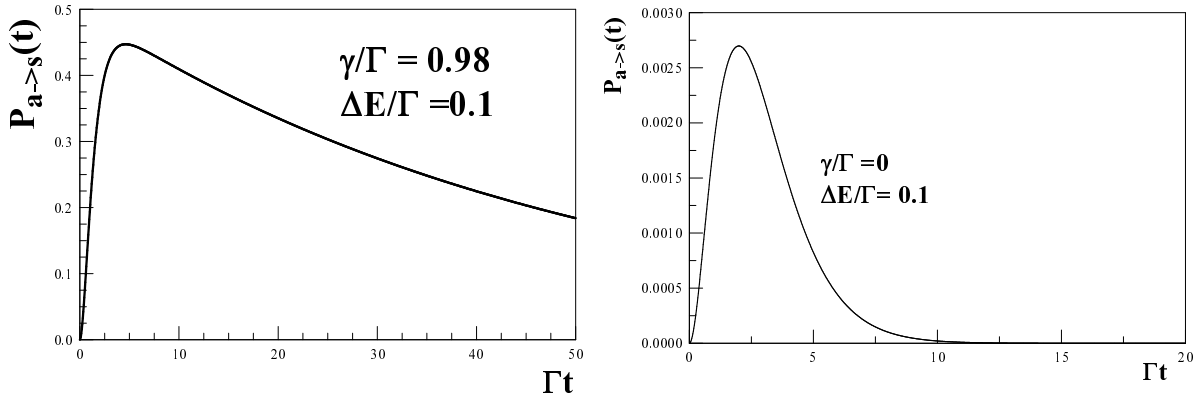

Figure 6.5: The transition probability $P_{a\to s}(t)$ (6.81) (without the prefactor $\sin^2 2\theta_m/2$) vs. Γt in the quantum Zeno limit $\Gamma \gg \Delta E$ for the cases $\cos 2\theta_m(k) = 0.98, 0$ and $\Delta E/\Gamma = \delta M^2\rho(k)/2k\Gamma = 0.1$. The ramp-up time scale is $\sim 1/\Gamma_1 \sim 1/\Gamma$. In the left figure the damping time scale is $\sim 1/\Gamma_2 \sim 50/\Gamma$. The right figure displays the resonant case for which the damping and coherence time scale coincide, when the conditions for quantum Zeno suppression are fulfilled.

6.4.2 High and low temperature limits: assessment of the quantum Zeno condition

In order to establish when the quantum Zeno condition $\Delta E(k)/\Gamma_{aa}(k) \ll 1$ is fulfilled we focus on the cases far away from resonances and, according to the exhaustive analysis of ref.[17, 20] and the constraints from the X-ray background in clusters[41, 42], in the region of parameter space $1\,\mathrm{keV} \lesssim m_s \lesssim 10\,\mathrm{keV}$, $10^{-10} \lesssim \sin^2 2\theta \lesssim 10^{-6}$. We consider $T \gtrsim 3\,\mathrm{MeV}$ for which we can neglect the CP violating asymmetry contribution in (6.58) assuming that it is of the same order as the baryon asymmetry $L \sim 10^{-9}$[57, 145]. In this regime $\delta M^2 \sim m_s^2$, and from (6.58) we find

$$\frac{S_R(k,k)}{\delta M^2} \sim 10^{-14} \left(\frac{T}{\mathrm{MeV}}\right)^6 \left(\frac{k}{T}\right)^2 \left(\frac{\mathrm{keV}}{m_s}\right)^2 \tag{6.87}$$

Taking $k \sim T$ and $m_s \sim 1\,\mathrm{keV}$ the MSW resonance $S_R(k,k)/\delta M^2 = 1$ occurs at $T_{MSW} \sim 215\,\mathrm{MeV}$ (a more precise estimate yields $T \sim 180\,\mathrm{MeV}$[17, 20]). For $T \gg T_{MSW}$ corresponding to $S_R(k,k)/\delta M^2 \gg 1$ the active sterile oscillation frequency becomes

$$\Delta E(k) = \frac{\delta M^2}{2\,k}\rho(k) \sim \frac{S_R(k,k)}{2k} \sim \frac{G_F\,T^4\,k}{M_W^2} \tag{6.88}$$

From the result (6.75) for $\Gamma_{aa}(k)$ we find in the high temperature limit $T \gg T_{MSW}$

$$\frac{2\,\Delta E(k)}{\Gamma_{aa}(k)} \sim \frac{G_F\,T^4\,k}{G_F^2\,T^4\,k\,M_W^2} \sim \frac{1}{g^2} \gg 1 \tag{6.89}$$

where g is the weak coupling. We note that in the high temperature limit the ratio $\Delta E(k)/\Gamma_{aa}(k)$ becomes independent of T, k.

In the low temperature limit $3\,\mathrm{MeV} \lesssim T \ll T_{MSW}$ it follows that $S_R(k,k)/\delta M^2 \ll 1$ and the active-sterile oscillation frequency is

$$\Delta E(k) \sim \frac{m_s^2}{2k} \tag{6.90}$$

hence the ratio

$$\frac{\Delta E(k)}{\Gamma_{aa}(k)} \sim \frac{m_s^2}{G_F^2\,T^4\,k^2} \sim 10^{16} \left(\frac{m_s}{\mathrm{keV}}\right)^2 \left(\frac{T}{\mathrm{MeV}}\right)^{-6} \left(\frac{k}{T}\right)^{-2} \tag{6.91}$$

which for $k \sim T$ can be simplified to

$$\frac{2\,\Delta E(k)}{\Gamma_{aa}(k)} \sim 10^2 \left(\frac{T_{MSW}}{T}\right)^6 \gg 1\,. \tag{6.92}$$

At the MSW resonance $T = T_{MSW}$, $\cos 2\theta_m \sim 0$, $\Delta E(k) = m_s^2 \sin 2\theta / 2k$ and the ratio becomes

$$\frac{2\,\Delta E(k)}{\Gamma_{aa}(k)} \sim 10^2 \sin 2\theta \ll 1 \tag{6.93}$$

for $10^{-5} \lesssim \sin 2\theta \lesssim 10^{-3}$. Therefore at the MSW resonance $\cos 2\theta_m(k) \sim 0$ and *both* conditions for quantum Zeno suppression, $\gamma/\Gamma \ll 1$, $\Delta E/\Gamma \ll 1$ are fulfilled.

6.4.3 Validity of the perturbative expansion:

The quantum Zeno condition $\Gamma_{aa}(k) \gg \Delta E(k)$ requires a consistent assessment of the validity of the perturbative expansion in the standard model and or Fermi's effective field theory. The active neutrino scattering rate $\Gamma_{aa} \propto G_F^2\, k\, T^4$ is a *two loops* result, while to leading order in weak interactions, the index of refraction contribution to the dispersion relation $S_R(k,\omega)$ is of one-loop order[57]. In the high temperature limit when $S_R \gg \delta M^2 \sim m_s^2$ the active-sterile oscillation frequency is

$$\Delta E(k) \sim \frac{|S_R(k,k)|}{2k} \tag{6.94}$$

combining this result with equation (6.75) at high temperature or density where the index of refraction dominates over δM^2, it follows that

$$\frac{\Delta E(k)}{\Gamma_{aa}(k)} \sim \frac{|S_R(k,k)|}{S_I(k,k)} \tag{6.95}$$

for $k \sim T$ the perturbative relation (6.61) suggests that this ratio is $\gtrsim 1/g^2 \gg 1$. An opposite ratio, namely $\Delta E(k)/\Gamma_{aa} \ll 1$ would entail that the two-loop contribution (Γ_{aa}) is *larger* than the one-loop contribution that yields the index of refraction S_R. Thus quantum Zeno suppression at high temperature when the index of refraction dominates the oscillation frequency necessarily implies a breakdown of the strict perturbative expansion. Such potential breakdown of perturbation theory in the standard model or Fermi's effective field theory in the quantum Zeno limit has been already observed in a different context by these authors in ref.[150], and deserves deeper scrutiny. We are currently exploring extensions beyond the standard model in which neutrinos couple to scalar fields motivated by Majoron models, in these extensions the coupling to the scalar (Majoron) provides a different scale that permits to circumvent this potential caveat. We expect to report on our results in a forthcoming article[151].

6.5 IMPLICATIONS FOR STERILE NEUTRINO PRODUCTION IN THE EARLY UNIVERSE:

6.5.1 Time averaged transition probability, production rate and shortcomings of the rate equation

Combining the result (6.11) with (6.81,6.82,6.83) yields the following time averaged transition probability

$$\left\langle P_{a\to s}\right\rangle = \frac{\sin^2 2\theta_m(k)}{2}\ \frac{\cos^2 2\theta_m(k) + \left(\frac{2\Delta E(k)}{\Gamma_{aa}(k)}\right)^2}{\sin^2 2\theta_m(k)\left[1+\left(\frac{2\Delta E(k)}{\Gamma_{aa}(k)}\right)^2\right]} \tag{6.96}$$

We have purposely kept the $\sin^2 2\theta_m(k)$ in the numerator and denominator to highlight the cancelation between this factor arising from the transition probability in the numerator with the factor $1-(\gamma/\Gamma)^2$ arising from the total integrated probability in the denominator. The factor $\cos^2 2\theta_m(k)$ in the numerator and the $\sin^2 2\theta_m(k)$ in the denominator are hallmarks of the presence of the *two different relaxation rates* $\Gamma_1(k),\Gamma_2(k)$, and are responsible for the difference with the result (6.5). The extra factor $\sin^2 2\theta_m(k)$ in the denominator signals an enhancement when $\theta_m(k) = 0,\pi/2$. In the case $\theta_m(k)\sim 0$ the relaxation rate $\Gamma_2(k) \ll \Gamma_1(k)$ whereas for $\theta_m(k)\sim\pi/2$ the opposite holds, $\Gamma_1(k)\ll\Gamma_2(k)$. In either case there is a wide separation between the relaxation rates of the propagating modes in the medium and the longest time scale for relaxation dominates the time integral in (6.96). This is depicted in fig. (6.5).

This is an important difference with the result in [77] wherein it was assumed that $\Gamma_1=\Gamma_2$, in which case $\gamma=0$. For $\theta_m(k)\sim 0,\pi/2$, the ratio $\gamma/\Gamma\sim 1$ leads to an enhancement of the time averaged transition probability. The interpretation of this result should be clear. The probability $P_{a\to s}(t)$ has two distinct contributions, the interference oscillatory term, and the non-oscillatory terms. When one of these non-oscillatory terms features a much longer relaxation time scale, it dominates the integrand at long time after the interference term has become negligible, as shown in figure (6.5). Therefore the time integral receives the largest contribution from the term with the smallest relaxation rate, this is the origin of the factor $1-(\gamma/\Gamma)^2 = \sin^2 2\theta_m(k)$ in the denominator.

Taking the kinetic equation that describes sterile neutrino production (6.1) along with the effective production rate (6.2) **at face value**, the new result (6.96) for the average transition

probability yields the effective production rate

$$\Gamma(a \to s; k) = \frac{\Gamma_{aa}(k)}{4} \frac{\cos^2 2\theta_m(k) + \left(\frac{2\Delta E(k)}{\Gamma_{aa}(k)}\right)^2}{\left[1 + \left(\frac{2\Delta E(k)}{\Gamma_{aa}(k)}\right)^2\right]} \,. \tag{6.97}$$

The result of references[20, 77, 78] is retrieved *only* near an MSW resonance for which $\cos 2\theta_m(k) \approx 0$, in this case the relaxation rates become the same and $\gamma = 0$. However, accounting for *both* relaxation rates $\Gamma_1; \Gamma_2$ yields the new result (6.96,6.97) which is generally very different from the usual one (6.5).

The result (6.97) is suspicious, taking the limit of $\sin 2\theta_m(k) \sim 0$, it still yields a non-vanishing sterile neutrino production rate despite the fact sterile neutrinos decouple from the plasma in this limit. The origin of this result is the **time averaged probability** $\langle P_{a\to s}\rangle$ (6.3) *not in any ambiguity in the calculation of the relaxation rates or in the time dependence of the transition probability* $P_{a\to s}(t)$. The time integral in the averaged expression (6.3) introduces a *denominator* $\sin^2 2\theta_m(k)$ from the longest time scale, and it is this denominator that is responsible for the enhancement. Thus the unreliability of the result (6.97) is a direct consequence of using the time-averaged transition probability (6.3) in the rate equation (6.1).

The real time analysis presented above clearly suggests that far away from an MSW resonance when Γ_1 and Γ_2 differ widely, Γ^{-1} is *not* the relevant time scale for suppression of the transition probability, but the *longest* of Γ_1^{-1} and Γ_2^{-1} therefore the time averaged transition probability (6.3) *cannot be the correct ingredient in the rate equation.* A more suitable definition of the average transition probability under these circumstances should be

$$\langle P_{a\to s}\rangle = \Gamma_{sm} \int_0^\infty P_{a\to s}(t) dt \tag{6.98}$$

where Γ_{sm} is the *smallest of* $\Gamma_{1,2}$. In a non-expanding cosmology this would indeed be the correct definition of an average transition probability, however in the early Universe as the temperature diminishes upon cosmological expansion, Γ_{sm} changes with time crossing from Γ_1 over to Γ_2 at the resonance and the alternative definition (6.98) would imply a "rate" with a sliding averaging time scale that changes rapidly near an MSW resonance. One can instead provide yet another suitable definition of an averaged transition rate

$$\langle P_{a\to s}\rangle = \frac{\Gamma_1 \Gamma_2}{\Gamma_1 + \Gamma_2} \int_0^\infty P_{a\to s}(t) dt \,. \tag{6.99}$$

When the two rates differ widely the prefactor always approximates the smaller one. Since

$$\frac{\Gamma_1\,\Gamma_2}{\Gamma_1+\Gamma_2}=\frac{\Gamma_{aa}}{4}\left[1-\frac{\gamma^2(k)}{\Gamma^2(k)}\right] \tag{6.100}$$

this definition would cancel the enhancement from the $\sin^2 2\theta_m(k)$ in the denominator in (6.96) (still leaving the $\cos^2 2\theta_m(k)$ in the numerator), but it misses the *correct* definition of the average rate by a factor 2, namely by 100%, in the region of the resonance where $\Gamma_1=\Gamma_2=\Gamma_{aa}/2$.

Obviously the ambiguity in properly defining a time averaged transition probability stems from the wide separation of the time scales associated with the damping of the quasiparticle modes, far away from an MSW resonance. Near the resonance both time scales become comparable and there is no ambiguity in the averaging scale. Complicating this issue further is the fact that in the early Universe these time scales are themselves time dependent as a consequence of the cosmological expansion and feature a rapid crossover behavior at an MSW resonance.

6.5.2 Caveats of the kinetic description

It is important to highlight the main *two different* aspects at the origin of the enhanced production rate given by equation (6.97) in the high temperature regime, for $\theta_m(k)\sim\pi/2$: i) the **assumption** of the validity of the usual rate equation in terms of a time-averaged transition probability wherein the relevant time scale for averaging is the decoherence time scale $1/\Gamma$, ii) the result of a complete self-energy calculation that yields *two time scales* which are widely different far away from an MSW resonance, in particular at very high and very low temperatures. The real time study of the transition probability shows that the *oscillatory interference term* is suppressed on the *decoherence* time scale $1/\Gamma$, but also that this is *not* the relevant time scale for the suppression of the transition probability far away from an MSW resonance. The transition probability actually grows during $1/\Gamma$ reaches its maximun on this time scale and remains near this value for a long time interval between $1/\Gamma$ and $1/\Gamma_{sm}$ where Γ_{sm} is the *smaller* of Γ_1,Γ_2. The enhanced rate emerges when *taking for granted* the definition of the time-averaged probability in terms of the decoherence scale but including in this expression the correct form of the transition probability (6.85). As discussed above, alternative definitions of a time-averaged rate could be given, but all of them have caveats when applied to sterile neutrino production in the early Universe.

However, we emphasize, that the underlying physical reason for the enhancement does not call for a simple *redefinition* of the rate but for a full reassessment of the kinetic equation of sterile

neutrino production. The important fact is that the wide separation of scales *prevent* a consistent description in terms of a *rate* in the kinetic equation, a *rate* implies only one relevant time scale for the build-up or relaxation of population, whereas our anaysis reveals two widely different scales that are of the same order only near an MSW resonance.

Kinetic rate equations are generally a Markovian limit of more complicated equations in which the transition probability in general features a *non-linear time dependence* . Only when the non-linear aspects of the time dependence of the transition probability are transients that disappear faster than the scale of build-up or relaxation an average transition probability per unit time, namely a rate, can be defined and the *memory* aspects associated with the time evolution of the transition probability can be neglected. This *is not* the case if there is a wide separation of scales, and under these circumstances the assumptions leading to the kinetic equation (6.1) must be revised and its validity questioned, very likely requiring a reassessment of the kinetic description. This situation becomes even more pressing in the early Universe. In the derivation of the average probability in ref.[77] the rate Γ_{aa} (denoted by τ_0 in that reference) is taken as a constant in the time integral in the average. This is a suitable approximation *if* the integrand falls off in the time scale $1/\Gamma_{aa}$, since this time scale is shorter than the Hubble expansion time scale for $T > 1\,\mathrm{MeV}$. However, if there is a *much longer* time scale, when one of the relaxation rates is very small, as is the case depicted in fig.(6.5), then this approximation cannot be justified and a full time-dependent kinetic description beyond a simple rate equation must be sought.

Thus we are led to conclude that the simple rate equation (6.1) based on the time-averaged transition probability (6.3) is *incorrect* far away from MSW resonances.

An alternative kinetic description based on a production rate obtained from quantum field theory has recently been offered[138] and seems to yield a result very different for the rate equation (6.1) in terms of the time-averaged transition probability. However, this alternative description focuses on the hadronic contribution near the MSW resonance, and as such cannot yet address the issue of the widely separated time scales far away from it. A full quantum field theoretical treatment far away from an MSW resonance which systematically and consistently treats the two widely different time scales is not yet available.

Thus we conclude that while the result for the rate (6.97) is a *direct consequence* of including the correct transition probability $P_{a\to s}(t)$ given by (6.85) into the rate equation (6.1), our field theoretical analysis of the full neutrino propagator in the medium, and the real time evolution of the transition probability, extracted from the *full density matrix* leads us to challenge the validity

of the rate equation to describe sterile neutrino production in the early Universe away from MSW resonances.

6.6 CONCLUSIONS

Motivated by the cosmological importance of sterile neutrinos, we reconsider an important aspect of the kinetics of sterile neutrino production via active-sterile oscillations at high temperature: quantum Zeno suppression of the sterile neutrino production rate.

Within an often used kinetic approach to sterile neutrino production, the production rate involves two ingredients: the active neutrino scattering rate Γ_{aa} and a time averaged active-sterile transition probability $\langle P_{a\to s}\rangle$[20, 61, 76, 77, 78] in the case of one sterile and one active neutrino.

For one active and one sterile neutrino, we establish an analogy with the familiar case of neutral kaon oscillations and argue that in a medium there are two propagating modes with different propagating frequencies and *damping rates*.

Unlike the usual treatment in terms of a truncated 2×2 density matrix for flavor degrees of freedom, we study the dynamics of active-sterile transitions directly from the *full real time evolution of the quantum field density matrix*. Active-sterile transitions are studied as an initial value problem wherein the main ingredient is the *full neutrino propagator in the medium*, obtained directly from the quantum density matrix and includes the self-energy up to two-loops in standard model weak interactions. The correct dispersion relations and damping rates of the quasiparticles modes are obtained from the neutrino propagator in the medium. The transition probability is obtained from the time evolution of the off-diagonal density matrix elements and the solution of the equation of motion for the propagating quasiparticle modes in the medium.

There are three main results from our study:

- **I):** The damping rates of the two different propagating modes in the medium are given by

$$\Gamma_1(k) = \Gamma_{aa}(k)\cos^2\theta_m(k)\,;\,\Gamma_2(k) = \Gamma_{aa}(k)\sin^2\theta_m(k) \tag{6.101}$$

  where $\Gamma_{aa}(k) \propto G_F^2\, k\, T^4$ is the active neutrino scattering rate and $\theta_m(k)$ is the mixing angle in the medium. The dispersion relations are the usual ones with the index of refraction correction[57], plus perturbatively small two-loop corrections of $\mathcal{O}(G_F^2)$. We give a simple physical explanation for this result: for very high temperature when $\theta_m \sim \pi/2$, $\nu_a \sim \nu_2; \nu_s \sim \nu_1$ and

$\Gamma_2 \sim \Gamma_{aa}; \Gamma_1 \ll \Gamma_{aa}$. In the opposite limit of very low temperature and small vacuum mixing angle $\theta_m \sim 0$, $\nu_a \sim \nu_1; \nu_s \sim \nu_2$ and $\Gamma_1 \sim \Gamma_{aa}; \Gamma_2 \ll \Gamma_{aa}$. Thus in either case the sterile neutrino is much more weakly coupled to the plasma than the active one.

- **II):** We study the active-sterile transition probability $P_{a\to s}(t)$ directly in real time from the time evolution of the propagating modes in the medium and the flavor off-diagonal quantum field density matrix elements. The result is given by

$$P_{a\to s}(t) = \frac{\sin^2 2\theta_m(k)}{4}\left[e^{-\Gamma_1(k)\,t} + e^{-\Gamma_2(k)\,t} - 2\,e^{-\Gamma(k)t}\cos(\Delta E(k)t)\right] \;;\; \Gamma(k) = \frac{1}{2}(\Gamma_1(k)+\Gamma_2(k))\,. \tag{6.102}$$

The real time analysis shows that even when $\Gamma(k) \gg \Delta E(k)$, which in the literature [20, 60] is taken to indicate quantum Zeno suppression, we find that the transition probability is substantial on time scales much longer than Γ^{-1} if Γ_1 and Γ_2 are *widely separated*. While the oscillatory interference term is suppressed by the *decoherence* time scale $1/\Gamma(k) = 2/\Gamma_{aa}(k)$ in agreement with the results of [60, 77], at very high or low temperature this is *not* the relevant time scale for the suppression of the transition probability, which is given by $1/\Gamma_{sm}$ with Γ_{sm} the *smaller* between Γ_1, Γ_2. Thus, we obtain the *complete* conditions for quantum Zeno suppression: i) $2\Delta E(k)/\Gamma_{aa} \ll 1$ where $\Delta E(k)$ is the oscillation frequency in the medium, *and* ii) $\Gamma_1 \sim \Gamma_2$. This latter condition is only achieved near an MSW resonance. Furthermore we studied consistently up to second order in standard model weak interactions, in which temperature regime the quantum Zeno condition $\Gamma_{aa}(k) \gg \Delta E(k)$ is fulfilled. We find that for $m_s \sim$ keV and $10^{-5} \lesssim \sin 2\theta \lesssim 10^{-3}$[17, 20, 78] the *opposite* condition, $\Gamma_{aa}(k) \ll \Delta E(k)$ is fulfilled in the high temperature limit $T \gg T_{MSW} \sim 215\,\text{MeV}$, as well as in the *low* temperature regime $3\,\text{MeV} \lesssim T \ll T_{MSW}$. We therefore conclude that the quantum Zeno conditions are *only* fulfilled near an MSW resonance for $T \sim T_{MSW}$.

- **III):** Inserting the result (6.102) into the expressions for the time averaged transition probability (6.3) and the sterile neutrino production rate (6.2) yields an expression for this rate that is *enhanced* at very high or low temperature given by equation (6.97) instead of the result (6.5) often used in the literature. The surprising enhancement at high or low temperature implied by (6.97) originates in *two* distinct aspects: i) the *assumption* of the validity of the rate kinetic equation in terms of a time-averaged transition probability with an averaging time scale determined by the decoherence scale $2/\Gamma_{aa}$, and ii) inserting the result (6.102) into the definition of the time-averaged transition probability. The enhancement is a distinct result of the *fact*

that at very high or low temperatures the decoherence time scale is *not* the relevant scale for suppression of $P_{a\to s}$ but either $1/\Gamma_1$ or $1/\Gamma_2$ whichever is *longer* in the appropriate temperature regime. Our analysis shows that far away from the region of MSW resonance, the transition probability reaches its maximum on time scale $1/\Gamma(k)$, remains near this value during a long time scale $1/\Gamma_{sm} \gg 1/\Gamma$. We have also argued that in the early Universe the definition of a time averaged transition probability is *ambiguous* far away from MSW resonances. Our analysis leads us to conclude that the simple rate equation (6.1) in terms of the production rate (6.2), (6.3) is incorrect far away from MSW resonances.

We emphasize and clarify an important distinction between the results summarized above. Whereas **I** and **II** are solidly based on a consistent and systematic quantum field theory calculation of the neutrino propagator, the correct equations of motion for the quasiparticle modes in the medium and the time evolution of flavor off diagonal quantum density matrix elements, the results summarized in **III** stem from a stated **assumption**, namely the validity of a kinetic description in terms of the time-averaged transition probability (6.3). The enhancement of the sterile production rate arising from this **assumption**, along with the ambiguity in properly defining a time-averaged transition probability in an expanding cosmology in the temperature regime far away from a MSW resonance all but suggest important caveats in the validity of the kinetic description for sterile neutrino production in terms of a simple rate equation in this regime. We also suggest that a deeper understanding of possible quantum Zeno suppression at high temperature requires a reassessment of the validity of the perturbative expansion in the standard model or in Fermi's effective field theory. Further studies of these issues are in progress.

7.0 PARTICLE ABUNDANCE IN A THERMAL PLASMA: QUANTUM KINETICS VERSUS BOLTZMANN EQUATION

7.1 INTRODUCTION

Phenomena out of equilibrium played a fundamental role in the early Universe: during phase transitions, baryogenesis, nucleosynthesis, recombination, particle production, annihilation and freeze out of relic particles, some of which could be dark matter candidates[17, 152, 153]. Of the many different non-equilibrium processes, particle production, annihilation and freeze-out and baryogenesis[152, 154] are non-equilibrium kinetic processes which are mainly studied via the Boltzmann equation[17, 152, 153].

The Boltzmann kinetic equation is also the main approach to study equilibration, thermalization and abundance of a species in a plasma. A thorough formulation of *semiclassical* kinetic theory in an expanding Friedmann-Robertson-Walker cosmology is given in ref.[153].

However the Boltzmann equation is a classical equation for the *distribution function* with an inhomogeneity determined by collision terms which are computed with the S-matrix formulation of quantum field theory. The collision term in the Boltzmann equation is obtained from the transition *probability* per unit time extracted from the asymptotic long time limit of the transition matrix element. This is tantamount to implementing Fermi's golden rule. Potential quantum interference and memory effects are completely ignored in this approach. Furthermore a single particle distribution function, the main ingredient in the Boltzmann equation, is usually defined via some coarse graining procedure. All of these shortcomings of the usual semiclassical Boltzmann equations when extrapolated to the realm of temperatures and density in the Early Universe, suggest that in order to provide a reliable understanding of such delicate processes such as baryo and leptogenesis a full quantum field theory treatment of kinetics may be required[154].

One of the basic predictions of the Boltzmann equation is that the local thermodynamic equilib-

rium solution for the abundance of a particle species is determined by the Bose-Einstein or Fermi-Dirac distribution functions, hence exponentially suppressed at low temperatures (in absence of a chemical potential).

This basic prediction has recently been challenged in a series of articles[155] wherein a surprising result is obtained: the abundance of heavy particles with masses much larger than the temperature is *not* exponentially suppressed as the Boltzmann equation predicts but the suppression is a *power law*. Such result, if correct, can have important consequences for the relic abundance of cold dark matter candidates.

This result, however, has been criticized and scrutinized in detail by several authors[156, 157, 158] who concluded that it is a consequence of the definition of the particle number introduced in ref.[155]. The definition of the *total* number of particles proposed in [155] is based on the non-interacting Hamiltonian for the heavy particle divided by its mass plus counterterms, which purportedly account for renormalization effects. The results of references[156, 157, 158] point out the inherent ambiguity in separating the contribution to the energy density from the particle and that of the bath and the interaction. The ambiguity in the separation of the different contributions to the energy has been studied thoroughly in these references in particular exactly solvable models[156], effective field theory[157] or a consistent treatment of renormalization effects[158].

Understanding the limitations of and corrections to the Boltzmann kinetic description and potential departures from the predicted abundances is important for a deeper assessment of possible mechanisms of baryogenesis as well as for the relic abundance of cold dark matter candidates. In the case of baryogenesis, the applicability and reliability of Boltzmann kinetics in the conditions of temperature and density that prevailed in the early Universe warrants a critical reassessment[154].

While the work in refs.[156, 157, 158] has clarified the shortcomings of the definition of the *total* particle number proposed in[155] explaining the origin of the power law suppression as a consequence of the ambiguity in this definition, what is missing from this discussion is a suitable definition of a *distribution function* and its real time evolution. The Boltzmann equation is a local differential equation that determines the dynamics of the *single particle distribution function*. Therefore in order to clearly assess potential corrections to the equilibrium solutions of the familiar Boltzmann equation a suitable distribution function and its dynamical evolution must be understood.

The definition of the distribution function both in non-relativistic many body theory[159] as well as in relativistic quantum field theory[160, 161] is typically based on a Wigner transform of a two point correlation function, which is not manifestly positive semidefinite. Usual derivations of the

Boltzmann kinetic equation invoke gradient expansions or quasiparticle (on-shell) approximations which lead to Markovian dynamics. Alternative derivations of the kinetic equations[162] which explicitly implement real time perturbation theory often invoke a long time limit and Fermi's Golden rule which enforces energy conservation in the kinetic equation. This is also the case in the dynamical renormalization group approach to quantum kinetics advocated in ref.[163] although this latter method allows one to systematically include off-shell corrections. Whichever method of derivation of the kinetic equation is used, the first step is to *define* a single particle distribution function.

Any definition of the distribution function of particles that *decay* in the vacuum (resonances) is fraught with ambiguities because the spectral representation of such particles is not a sharp delta function but typically a Breit-Wigner distribution. Since these particles decay even in *vacuum* and do not exist as asymptotic states any definition of an operator that "counts" these particles will unavoidably be ambiguous.

In this work, we circumvent this ambiguity by focusing on the study of the quantum kinetics and equilibration dynamics of the distribution functions of particles that are *stable* at zero temperature associated with a field Φ. Stable physical particles are asymptotic states which can be measured and a distribution function for the single particle physical states can be introduced according to the basic assumptions of asymptotic theory. While our ultimate goal is to find a quantum kinetic description for phenomena in the early Universe, in this article we focus on a study in Minkowski space-time as a first step towards that goal.

In this chapter, we provide a framework for non-equilibrium quantum kinetics beyond the usual Boltzmann equation. This non-equilibrium formulation includes off-shell and non-Markovian (memory) processes which are not accounted for in the semiclassical Boltzmann equation and result in modifications of the equilibrium abundances. We focus on the case of a scalar field Φ coupled to other heavier fields for a wide variety of relevant interacting quantum field theories. Here we consider that the *heavier* fields constitute a thermal bath in equilibrium. In order to study the thermalization of the Φ particle as well as the time evolution of its distribution function we consider the case in which the field Φ is coupled to the thermal bath at some initial time t_i. We then obtain the *non-equilibrium* effective action for the field Φ by integrating out the degrees of freedom of the thermal bath to lowest order in the coupling of the field Φ to the heavy sector but in principle to *all orders* in the couplings of the heavy fields amongst themselves.

At zero temperature the Φ-particles are stable because they are the lightest, therefore they are

manifest as asymptotic states. Hence according to asymptotic theory we introduce a definition of an interpolating number operator that counts these particles, for example as those measured by a detector in a collision experiment in the vacuum. At finite temperature the distribution function is the expectation value of this interpolating operator in the statistical ensemble. The real time evolution of this distribution function is completely determined by the non-equilibrium effective action and its asymptotic long time limit determines the abundance of the physical particles Φ in the thermal plasma. The non-equilibrium approach introduced here, borrows from the seminal work on quantum Brownian motion[141, 164, 165, 166] which is adapted to quantum field theory.

After the discussion of the general case, we introduce a specific model in which the scalar field Φ associated with the stable particle couples to two heavier bosonic fields which constitute the thermal bath. At lowest order in the coupling we find that the Φ particle despite being the lightest, acquires a width in the medium as a consequence of the two body decay of the heavier particle and its recombination in the plasma. These processes result in a broadening of its spectral function and corrections to its equilibrium abundance.

This chapter is organized as follows: in section (7.2) we introduce the general form of the interacting quantum field theories considered and develop the formulation in terms of the non-equilibrium effective action. The effective action is obtained to lowest order in the coupling of the field Φ to the heavier fields (the bath) and in principle to *all orders* in the coupling of the bath fields amongst themselves. We show that a stochastic formulation in terms of a Langevin equation emerges naturally. In section (7.3) we introduce the definition of the fully renormalized interpolating number operator and the single particle distribution function based on asymptotic theory. The time evolution of this distribution function is completely determined by the solution of the stochastic Langevin equation.

In section (9.2) we study a specific model in which the Φ field is coupled to two heavy scalar fields with a coupling $g\,\Phi\,\chi_1\,\chi_2$. This interacting quantum field theory provides an excellent testing ground and highlights the main conceptual results. We study the dynamics of the distribution function for the Φ particle up to one loop order. The asymptotic distribution function is studied for a wide range of parameters allowing to extract fairly general conclusions whose validity goes beyond this specific model. In particular we analyze in detail how off-shell effects result in *large* corrections to the usual Bose-Einstein equilibrium abundance. In section (7.5) we obtain the usual Boltzmann quantum kinetic equation and highlight the main assumptions implicit in its derivation. We contrast the predictions for the asymptotic abundance between the non-equilibrium kinetic

formulation and that of the usual quantum kinetic Boltzmann equation, highlighting that memory and off-shell effects are responsible for the differences in the predictions. Our conclusions and a discussion on the cosmological consequences are presented in section (7.6). Appendix B is devoted to the explicit calculation of the self-energy in the specific example studied.

7.2 GENERAL FORMULATION: THE NON-EQUILIBRIUM EFFECTIVE ACTION

We focus on the description of the dynamics of the relaxation of the occupation number of a scalar field Φ which is in interaction with other fields either fermionic or bosonic, collectively written as χ_i, with a Lagrangian density of the form

$$\mathcal{L}[\Phi(x),\chi(x)] = \mathcal{L}_{0,\Phi}[\Phi(x)] + \mathcal{L}_{\chi_i}[\chi_i(x)] + g\Phi\mathcal{O}[\chi_i(x)] \tag{7.1}$$

where $\mathcal{O}[\chi_i]$ stands for an operator non-linear in the fields χ_i and $\mathcal{L}_{0,\Phi}$ is the free field Lagrangian density for the field Φ but $\mathcal{L}_{\chi_i}[\chi_i(x)]$ is the full Lagrangian for the fields χ including interactions amongst themselves. This general form describes several relevant cases:

- Interacting scalars, for example the linear sigma model in the broken symmetry phase. The interaction between the massive scalar and the Goldstone bosons is of the form $\sigma\pi^2$. In this article we focus on the case of a trilinear interaction of the form $\Phi\sum_{ij} g_{ij}\chi_i\chi_j$ where the fields $\chi_{1,2}$ have masses larger than that of the Φ field.
- A Yukawa theory with χ being fermionic fields and Φ a scalar field, with interaction $\Phi\bar{\Psi}\Psi$. This could be generalized to a chiral model.
- A gauge theory in which Φ is the gauge field and χ is either a complex scalar or fermion fields, the interaction being of the form $A^\mu J_\mu$ with J_μ being a bilinear of the fields. In particular this approach has been recently implemented to study photon production from a quark gluon plasma in local thermal equilibrium[167]. This case is particularly relevant for assessing potential distortions in the spectrum of the cosmic microwave background.
- Another possible realization of this situation could be the case in which Φ is a neutrino field in interaction with leptons and (or) quarks which constitute a thermal or dense plasma.
- The case of a self-interacting scalar field in which one mode say with wave vector k is singled out as the "system" and the other modes are treated as a "bath".

In all of these cases the fields χ_i are treated as a bath in equilibrium assuming that the bath fields are sufficiently strongly coupled so as to guarantee their thermal equilibration. These fields will be "integrated out" yielding a reduced density matrix for the field Φ in terms of an effective real-time functional, known as the influence functional[164] in the theory of quantum brownian motion. The reduced density matrix can be represented by a path integral in terms of the non-equilibrium effective action that includes the influence functional. This method has been used extensively to study quantum brownian motion[164, 165, 166] and for preliminary studies of quantum kinetics in the simpler case of a particle coupled linearly to a bath of harmonic oscillators[155, 168].

The models can be generalized further by considering that the interaction between Φ and χ is also polynomial in Φ. However, in this chapter we will consider the simpler case described by (9.2) since it describes a broad range of physically relevant cases, and as will be discussed below this case already reveals a wealth of novel phenomena. As we will discuss in detail below most of the relevant phenomena can be highlighted within this wide variety of models and most of the results will be seen to be fairly general.

The relaxation of the distribution function is an initial value problem, therefore we propose the initial density matrix at a time t_i to be of the form

$$\hat{\rho}(t_i) = \hat{\rho}_{\Phi,i} \otimes \hat{\rho}_{\chi_i,i} \tag{7.2}$$

The initial density matrix of the χ_i fields will be taken to describe state in thermal equilibrium at a temperature $T = 1/\beta$, namely

$$\hat{\rho}_{\chi} = e^{-\beta H_{\chi}} \tag{7.3}$$

where $H_{\chi_i}(\chi_i)$ is the Hamiltonian for the fields χ_i. We will now refer collectively to the set of fields χ_i simply as χ to avoid cluttering of indices.

In the field basis the matrix elements of $\hat{\rho}_{\Phi,i}$ are given by

$$\langle \Phi | \hat{\rho}_{\Phi,i} | \Phi' \rangle = \rho_{\Phi,i}(\Phi; \Phi') \tag{7.4}$$

The density matrix for Φ will represent an initial out of equilibrium state.

The physical situation described by this initial state is that of a field (or fields) in thermal equilibrium at a temperature $T = 1/\beta$, namely a heat bath, which is put in contact with another system, here represented by the field Φ. Once the system and bath are put in contact their mutual interaction will eventually lead to a state of thermal equilibrium. The goal is to study the relaxation

of the field Φ towards equilibrium with the "bath". The initial density matrix of the field Φ will describe a state with few quanta (or the vacuum) initially.

The real time evolution of this initial uncorrelated state will introduce transient evolution, however the long time behavior will be insensitive to this initial transient. Furthermore, we point out that it is important to study the initial transient stage for the following reason. As a particle Φ propagates in the medium it will be screened or dressed by the excitations in the medium and it will propagate as a "quasiparticle". Its distribution function will be shown to become insensitive to the initial conditions on time scales larger than the "quasiparticle" relaxation time.

The strategy is to integrate out the χ fields therefore obtaining the reduced time dependent density matrix for the field Φ, and the non-equilibrium influence functional for this field. Once we obtain the reduced density matrix for the field Φ we can compute expectation values or correlation functions of this field. We will focus on studying the time evolution of the distribution function, or particle number to be defined below.

The time evolution of the initial density matrix is given by

$$\hat{\rho}(t_f) = e^{-iH(t_f - t_i)} \hat{\rho}(t_i) e^{iH(t_f - t_i)} \tag{7.5}$$

Where the total Hamiltonian H is given by

$$H = H_\Phi(\Phi) + H_\chi(\chi) + H_I(\Phi, \chi) \tag{7.6}$$

The calculation of correlation functions is facilitated by introducing currents coupled to the different fields. Furthermore since each time evolution operator in eqn. (9.13) will be represented as a path integral, we introduce different sources for forward and backward time evolution operators, referred to as J^+, J^- respectively. The forward and backward time evolution operators in presence of sources are $U(t_f, t_i; J^+)$, $U^{-1}(t_f, t_i, J^-)$ respectively.

We will only study correlation functions of the Φ field, therefore we carry out the trace over the χ degrees of freedom. Since the currents $J^\pm$ allow us to obtain the correlation functions for any arbitrary time by simple variational derivatives with respect to these sources, we can take $t_f \to \infty$ without loss of generality.

The non-equilibrium generating functional is given by

$$\mathcal{Z}[j^+, j^-] = \mathrm{Tr} U(\infty, t_i; J^+) \hat{\rho}(t_i) U^{-1}(\infty, t_i, J^-) \tag{7.7}$$

Where $J^{\pm}$ stand collectively for all the sources coupled to different fields. Functional derivatives with respect to the sources J^{+} generate the time ordered correlation functions, those with respect to J^{-} generate the anti-time ordered correlation functions and mixed functional derivatives with respect to J^{+}, J^{-} generate mixed correlation functions. Each one of the time evolution operators in the generating functional (7.7) can be written in terms of a path integral: the time evolution operator $U(\infty, t_i; J^{+})$ involves a path integral *forward* in time from t_i to $t = \infty$ in presence of sources J^{+}, while the inverse time evolution operator $U^{-1}(\infty, t_i, J^{-})$ involves a path integral *backwards* in time from $t = \infty$ back to t_i in presence of sources J^{-}. Finally the equilibrium density matrix for the bath $e^{-\beta H_\chi}$ can be written as a path integral along imaginary time with sources J^{β}. Therefore the path integral form of the generating functional (7.7) is given by

$$\mathcal{Z}[j^{+}, j^{-}] = \int D\Phi_i \int D\Phi'_i \, \rho_{\Phi,i}(\Phi_i; \Phi'_i) \int \mathcal{D}\Phi^{\pm} \int \mathcal{D}\chi^{\pm} \mathcal{D}\chi^{\beta} e^{iS[\Phi^{\pm}, \chi^{\pm}; J^{\pm}_{\Phi}; J^{\pm}_{\chi}]} \tag{7.8}$$

with the boundary conditions $\Phi^{+}(\vec{x}, t_i) = \Phi_i(\vec{x})\,;\; \Phi^{-}(\vec{x}, t_i) = \Phi'_i(\vec{x})$.

The non-equilibrium action is given by

$$\begin{aligned} S[\Phi^{\pm}, \chi^{\pm}; J^{\pm}_{\Phi}; J^{\pm}_{\chi}] \;\; &= \;\; \int_{t_i}^{\infty} dt d^3x \, \left[\mathcal{L}_{0,\Phi}(\Phi^{+}) + J^{+}_{\Phi}\Phi^{+} + h\Phi^{+} - \mathcal{L}_{0,\Phi}(\Phi^{-}) - J^{-}_{\Phi}\Phi^{-} - h\Phi^{-} \right] \\ &+ \int_{\mathcal{C}} d^4x \left\{ \mathcal{L}_{\chi}(\chi) + J_{\chi}\chi + g\,\Phi\,\mathcal{O}[\chi] \right\} \end{aligned} \tag{7.9}$$

where $\mathcal{C}$ describes a contour in the complex time plane as follows: along the forward branch $(t_i, +\infty)$ the fields and sources are $\Phi^{+}, \chi^{+}, J^{+}_{\chi}$, along the backward branch (∞, t_i) the fields and sources are $\Phi^{-}, \chi^{-}, J^{-}_{\chi}$ and along the Euclidean branch $(t_i, t_i - i\beta)$ the fields and sources are $\Phi = 0; \chi^{\beta}, J^{\beta}_{\chi}$. Along the Euclidean branch the interaction term vanishes since the initial density matrix for the field χ is assumed to be that of thermal equilibrium. The contour is depicted in fig. (7.1)

The linear term $h\Phi^{\pm}$ is a counterterm that will be required to cancel the linear terms (tadpole) in $\Phi^{\pm}$ in the non-equilibrium effective action. This issue will be discussed below when we obtain the non-equilibrium effective action for the field Φ after integrating out the field(s) χ.

The trace over the degrees of freedom of the χ field with the initial equilibrium density matrix, entail periodic (for bosons) or antiperiodic (for fermions) boundary conditions for χ along the contour $\mathcal{C}$. However, the boundary conditions on the path integrals for the field Φ are given by

$$\Phi^{+}(\vec{x}, t = \infty) = \Phi^{-}(\vec{x}, t = \infty) \tag{7.10}$$

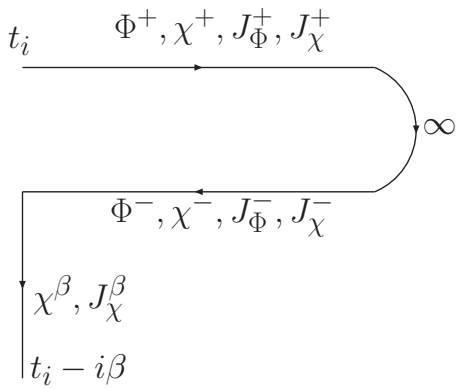

Figure 7.1: Contour in time for the non-equilibrium path integral representation.

and

$$\Phi^+(\vec{x}, t = t_i) = \Phi_i(\vec{x}) \quad ; \quad \Phi^-(\vec{x}, t = t_i) = \Phi_i'(\vec{x}) \tag{7.11}$$

The reason for the different path integrations is that whereas the χ field is traced over with an initial thermal density matrix (since it is taken as the "bath"), the initial density matrix for the Φ field will be specified later as part of the initial value problem. The path integral over χ leads to the influence functional for $\Phi^\pm$[164].

7.2.1 Tracing over the "bath" degrees of freedom

As far as the path integrals over the bath degrees of freedom χ is concerned the fields $\Phi^\pm$ are simply c-number sources. The contour path integral

$$Z[\Phi^\pm] = \int \mathcal{D}\chi^\pm \mathcal{D}\chi^\beta e^{i\int_{\mathcal{C}} d^4x \left\{ \mathcal{L}_\chi(\chi) + J_\chi \chi + g\,\Phi\,\mathcal{O}[\chi] \right\}} \tag{7.12}$$

is the generating functional of correlation functions of the field χ in presence of external c-number sources $\Phi^\pm$ (the sources $J_\chi^\pm$ generate the correlation functions via functional derivatives and are set to zero at the end of the calculation), namely

$$\int \mathcal{D}\chi^\pm \mathcal{D}\chi^\beta e^{i\int_{\mathcal{C}} d^4x \left\{ \mathcal{L}_\chi(\chi) + g\Phi\,\mathcal{O}[\chi] \right\}} = \left\langle e^{ig\int_{\mathcal{C}} d^4x \Phi\,\mathcal{O}[\chi]} \right\rangle_\chi Z[0]. \tag{7.13}$$

Note that the expectation value in the right hand side of eqn. (7.13) is in the equilibrium density matrix of the field χ. The path integral can be carried out in perturbation theory and the result exponentiated to yield the effective action as follows

$$\begin{aligned}\left\langle e^{ig\int_{\mathcal{C}} d^4x\Phi\,\mathcal{O}[\chi]}\right\rangle_\chi &= 1+ig\int_{\mathcal{C}} d^4x\Phi(x)\left\langle\mathcal{O}[\chi](x)\right\rangle_\chi \\ &+\frac{(ig)^2}{2}\int_{\mathcal{C}} d^4x\int_{\mathcal{C}} d^4x'\Phi(x)\Phi(x')\Big\langle\mathcal{O}[\chi](x)\mathcal{O}[\chi](x')\Big\rangle_\chi+\mathcal{O}(g^3)\end{aligned} \tag{7.14}$$

This the usual expansion of the exponential of the connected correlation functions, where this series is identified with

$$\left\langle e^{ig\int_{\mathcal{C}} d^4x\Phi\,\mathcal{O}[\chi]}\right\rangle_\chi = e^{i\,L_{if}[\Phi^+,\Phi^-]}\,, \tag{7.15}$$

and where the *influence functional*[164] $L_{if}[\Phi^+,\Phi^-]$ is given by the following expression

$$L_{if}[\Phi^+,\Phi^-]=g\int_{\mathcal{C}} d^4x\Phi(x)\,\langle\mathcal{O}[\chi](x)\rangle_\chi+i\frac{g^2}{2}\int_{\mathcal{C}} d^4x\int_{\mathcal{C}} d^4x'\Phi(x)\Phi(x')\langle\mathcal{O}[\chi](x)\mathcal{O}[\chi](x')\rangle_{\chi,con}+\mathcal{O}(g^3) \tag{7.16}$$

In detail, the integrals along the contour $\mathcal{C}$ stand for the following:

$$\int_{\mathcal{C}} d^4x\Phi(x)\,\langle\mathcal{O}[\chi](x)\rangle_\chi=\int d^3x\int_{t_i}^{\infty}dt\left[\Phi^+(\vec{x},t)\langle\mathcal{O}[\chi^+](x)\rangle_\chi-\Phi^-(\vec{x},t)\langle\mathcal{O}[\chi^-](x)\rangle_\chi\right] \tag{7.17}$$

$$\begin{aligned}&\int_{\mathcal{C}} d^4x\int_{\mathcal{C}} d^4x'\Phi(x)\Phi(x')\langle\mathcal{O}[\chi](x)\mathcal{O}[\chi](x')\rangle_{\chi,con}\\ =\;&\int d^3x\int_{t_i}^{\infty}dt\int d^3x'\int_{t_i}^{\infty}dt'\Big[\Phi^+(x)\Phi^+(x')\langle\mathcal{O}[\chi^+](x)\mathcal{O}[\chi^+](x')\rangle_{\chi,con}\\ &+\Phi^-(x)\Phi^-(x')\langle\mathcal{O}[\chi^-](x)\mathcal{O}[\chi^-](x')\rangle_{\chi,con}\\ &-\Phi^+(x)\Phi^-(x')\langle\mathcal{O}[\chi^+](x)\mathcal{O}[\chi^-](x')\rangle_{\chi,con}\\ &-\Phi^-(x)\Phi^+(x')\langle\mathcal{O}[\chi^-](x)\mathcal{O}[\chi^+](x')\rangle_{\chi,con}\Big]\end{aligned} \tag{7.18}$$

Since the expectation values above are computed in a thermal equilibrium translational invariant density matrix, it is convenient to introduce the spatial Fourier transform of the composite operator $\mathcal{O}$ in a spatial volume V as

$$\mathcal{O}_{\vec{k}}(t)=\frac{1}{\sqrt{V}}\int d^3x e^{i\vec{k}\cdot\vec{x}}\mathcal{O}[\chi(\vec{x},t)] \tag{7.19}$$

in terms of which we obtain following the correlation functions

$$\langle \mathcal{O}_{\vec{k}}(t)\rangle = \langle \mathcal{O}^{+}_{\vec{k}}(t)\rangle = \langle \mathcal{O}^{-}_{\vec{k}}(t)\rangle = \mathrm{Tr}\, e^{-\beta H_\chi}\, O_{\vec{k}}(t) \tag{7.20}$$

$$\langle \mathcal{O}_{\vec{k}}(t)\mathcal{O}_{-\vec{k}}(t')\rangle = \langle \mathcal{O}^{-}_{\vec{k}}(t)\mathcal{O}^{+}_{-\vec{k}}(t')\rangle = \mathrm{Tr}\, \mathcal{O}_{-\vec{k}}(t')\, e^{-\beta H_\chi}\, O_{\vec{k}}(t) = \mathcal{G}^{>}_{k}(t-t') = \mathcal{G}^{-+}_{k}(t,t') \tag{7.21}$$

$$\langle \mathcal{O}_{-\vec{k}}(t')\mathcal{O}_{\vec{k}}(t)\rangle = \langle \mathcal{O}^{+}_{\vec{k}}(t)\mathcal{O}^{-}_{-\vec{k}}(t')\rangle = \mathrm{Tr}\, O_{\vec{k}}(t)\, e^{-\beta H_\chi}\, \mathcal{O}_{-\vec{k}}(t') = \mathcal{G}^{<}_{k}(t-t') = \mathcal{G}^{+-}_{k}(t,t') = \mathcal{G}^{-+}_{k}(t',t) \tag{7.22}$$

$$\langle T\mathcal{O}_{\vec{k}}(t)\mathcal{O}_{-\vec{k}}(t')\rangle = \mathcal{G}^{>}_{k}(t-t')\Theta(t-t') + \mathcal{G}^{<}_{k}(t-t')\Theta(t'-t) = \mathcal{G}^{++}_{k}(t,t') \tag{7.23}$$

$$\langle \widetilde{T}\mathcal{O}_{\vec{k}}(t)\mathcal{O}_{-\vec{k}}(t')\rangle = \mathcal{G}^{>}_{k}(t-t')\Theta(t'-t) + \mathcal{G}^{<}_{k}(t-t')\Theta(t-t') = \mathcal{G}^{--}_{k}(t,t') \tag{7.24}$$

The time evolution of the operators is determined by the Heisenberg picture of H_χ, namely $\mathcal{O}_{\vec{k}}(t) = e^{iH_\chi(t-t_i)}\mathcal{O}_{\vec{k}}(t_i)e^{-iH_\chi(t-t_i)}$. Because the density matrix for the bath is in equilibrium, the correlation functions above are solely functions of the time difference. These correlation functions are computed *exactly* to *all orders* in the couplings of the bath fields amongst themselves.

These correlation functions are not independent, but obey

$$\mathcal{G}^{++}_{k}(t,t') + \mathcal{G}^{--}_{k}(t,t') - \mathcal{G}^{-+}_{k}(t,t') - \mathcal{G}^{+-}_{k}(t,t') = 0 \tag{7.25}$$

The non-equilibrium effective action is given by

$$L_{eff}[\Phi^+,\Phi^-] = \int_{t_i}^{\infty} dt d^3x\, \left[\mathcal{L}_{0,\Phi}(\Phi^+) + h\Phi^+ - \mathcal{L}_{0,\Phi}(\Phi^-) - h\Phi^-\right] + L_{if}[\Phi^+,\Phi^-] \tag{7.26}$$

where we have set the sources $J^\pm$ for the fields $\Phi^\pm$ to zero.

The choice of counterterm

$$h = -\langle \mathcal{O}(\vec{x},t)\rangle \tag{7.27}$$

cancels the terms linear in $\Phi^\pm$ (tadpole) in the non-equilibrium effective action.

In what follows we take $t_i = 0$ without loss of generality since (i) for $t > t_i$ the total Hamiltonian is time independent and the correlations will be solely functions of $t-t_i$, and (ii) we will be ultimately interested in the limit $t \gg t_i$ when all transient phenomena has relaxed. In terms of the spatial Fourier transform of the fields $\Phi^\pm$ defined as in eqn. (7.19) we find

$$
\begin{aligned}
& iL_{eff}[\Phi^+,\Phi^-] \\
= & \sum_{\vec{k}} \Bigg\{ \frac{i}{2}\int_0^\infty dt \left[\dot{\Phi}^+_{\vec{k}}(t)\dot{\Phi}^+_{-\vec{k}}(t) - (k^2+m^2)\Phi^+_{\vec{k}}(t)\Phi^+_{-\vec{k}}(t) - \dot{\Phi}^-_{\vec{k}}(t)\dot{\Phi}^-_{-\vec{k}}(t) + (k^2+m^2)\Phi^-_{\vec{k}}(t)\Phi^-_{-\vec{k}}(t) \right] \\
& -\frac{g^2}{2}\int_0^\infty dt \int_0^\infty dt' \left[\Phi^+_{\vec{k}}(t)\mathcal{G}^{++}_k(t,t')\Phi^+_{-\vec{k}}(t') + \Phi^-_{\vec{k}}(t)\mathcal{G}^{--}_k(t,t')\Phi^-_{-\vec{k}}(t') \right. \\
& \left. -\Phi^+_{\vec{k}}(t)\mathcal{G}^{+-}_k(t,t')\Phi^-_{-\vec{k}}(t') - \Phi^-_{\vec{k}}(t)\mathcal{G}^{-+}_k(t,t')\Phi^+_{-\vec{k}}(t') \right] \Bigg\} \qquad (7.28)
\end{aligned}
$$

where all the time integrations are in the interval $0 \leq t \leq \infty$.

A similar program has been used recently to study the relaxation of scalar fields[169] as well as the photon production from a quark gluon plasma in thermal equilibrium[167].

7.2.2 Stochastic description: generalized Langevin equation

As it will become clear below, it is more convenient to introduce the Wigner center of mass and relative variables

$$
\Psi(\vec{x},t) = \frac{1}{2}\left(\Phi^+(\vec{x},t) + \Phi^-(\vec{x},t)\right) \quad ; \quad R(\vec{x},t) = \left(\Phi^+(\vec{x},t) - \Phi^-(\vec{x},t)\right) \qquad (7.29)
$$

and the Wigner transform of the initial density matrix for the Φ field

$$
\begin{aligned}
\mathcal{W}(\Psi_i;\Pi_i) &= \int DR_i e^{-i\int d^3x \Pi_i(\vec{x})R_i(\vec{x})} \rho(\Psi_i + \frac{R_i}{2};\Psi_i - \frac{R_i}{2}) \qquad (7.30) \\
\rho(\Psi_i + \frac{R_i}{2};\Psi_i - \frac{R_i}{2}) &= \int D\Pi_i e^{i\int d^3x \Pi_i(\vec{x})R_i(\vec{x})} \mathcal{W}(\Psi_i;\Pi_i) \qquad (7.31)
\end{aligned}
$$

The boundary conditions on the Φ path integral given by (7.11) translate into the following boundary conditions on the center of mass and relative variables

$$
\Psi(\vec{x},t=0) = \Psi_i \quad ; \quad R(\vec{x},t=0) = R_i \qquad (7.32)
$$

furthermore, the boundary condition (7.10) yields the following boundary condition for the relative field

$$
R(\vec{x},t=\infty) = 0. \qquad (7.33)
$$

This observation will be important in the steps that follow. In terms of the spatial Fourier transforms of the center of mass and relative variables (9.22) introduced above, integrating by

parts and accounting for the boundary conditions (7.32), the non-equilibrium effective action (9.20) becomes:

$$\begin{aligned} iL_{eff}[\Psi,R] &= \int_0^\infty dt \sum_{\vec{k}} \left\{ -iR_{-\vec{k}} \left(\ddot{\Psi}_{\vec{k}}(t) + (k^2+m^2)\Psi_k(t) \right) \right\} \\ &- \int_0^\infty dt \int_0^\infty dt' \left\{ \frac{1}{2} R_{-\vec{k}}(t) R_{\vec{k}}(t') \mathcal{K}_k(t-t') + R_{-\vec{k}}(t) i\Sigma_k^R(t-t') \Psi_{\vec{k}}(t') \right\} \\ &+ \int d^3x R_i(\vec{x}) \dot{\Psi}(\vec{x}, t=0) \end{aligned} \tag{7.34}$$

where the last term arises after the integration by parts in time, using the boundary conditions (7.32) and (7.33). The kernels in the above effective Lagrangian are given by (see eqns. (7.21-7.24))

$$\mathcal{K}_k(t-t') = \frac{g^2}{2} \left[\mathcal{G}_k^>(t-t') + \mathcal{G}_k^<(t-t') \right] \tag{7.35}$$

$$i\Sigma_k^R(t-t') = g^2 \left[\mathcal{G}_k^>(t-t') - \mathcal{G}_k^<(t-t') \right] \Theta(t-t') \equiv i\Sigma_k(t-t')\Theta(t-t') \tag{7.36}$$

The term quadratic in the relative variable R can be written in terms of a stochastic noise as

$$\begin{aligned} &\exp\left\{ -\frac{1}{2} \int dt \int dt' R_{-\vec{k}}(t) \mathcal{K}_k(t-t') R_{\vec{k}}(t') \right\} \\ &= \int \mathcal{D}\xi \exp\left\{ -\frac{1}{2} \int dt \int dt' \;\; \xi_{\vec{k}}(t) \mathcal{K}_k^{-1}(t-t') \xi_{-\vec{k}}(t') + i \int dt \;\; \xi_{-\vec{k}}(t) R_{\vec{k}}(t) \right\} \end{aligned} \tag{7.37}$$

The non-equilibrium generating functional can now be written in the following form

$$\begin{aligned} \mathcal{Z} &= \int D\Psi_i \int D\Pi_i \int \mathcal{D}\Psi \mathcal{D}R \mathcal{D}\xi \;\; \mathcal{W}(\Psi_i;\Pi_i) DR_i e^{i\int d^3x R_i(\vec{x})(\Pi_i(\vec{x}) - \Psi(\vec{x},t=0))} \mathcal{P}[\xi] \\ &\exp\left\{ -i \int_0^\infty dt \;\; R_{-\vec{k}}(t) \left[\ddot{\Psi}_{\vec{k}}(t) + (k^2+m^2)\Psi_{\vec{k}}(t) + \int dt' \;\; \Sigma_k^R(t-t')\Psi_{\vec{k}}(t') - \xi_{\vec{k}}(t) \right] \right\} \end{aligned} \tag{7.38}$$

$$\mathcal{P}[\xi] = \exp\left\{ -\frac{1}{2} \int_0^\infty dt \int_0^\infty dt' \;\; \xi_{\vec{k}}(t) \mathcal{K}_k^{-1}(t-t') \xi_{-\vec{k}}(t') \right\} \tag{7.39}$$

The functional integral over R_i can now be done, resulting in a functional delta function, that fixes the boundary condition $\dot{\Psi}(\vec{x}, t=0) = \Pi_i(\vec{x})$.

Finally the path integral over the relative variable can be performed, leading to a functional delta function and the final form of the generating functional given by

$$\mathcal{Z} = \int D\Psi_i D\Pi_i \;\; \mathcal{W}(\Psi_i;\Pi_i) \mathcal{D}\Psi \mathcal{D}\xi \;\; \mathcal{P}[\xi]\, \delta \left[\ddot{\Psi}_{\vec{k}}(t) + (k^2+m^2)\Psi_{\vec{k}}(t) + \int_0^t dt' \;\; \Sigma_k(t-t')\Psi_{\vec{k}}(t') - \xi_{\vec{k}}(t) \right] \tag{7.40}$$

with the boundary conditions on the path integral on Ψ given by

$$\Psi(\vec{x}, t=0) = \Psi_i(\vec{x}) \;\; ; \;\; \dot{\Psi}(\vec{x}, t=0) = \Pi_i(\vec{x}) \tag{7.41}$$

where we have used the definition of $\Sigma_k^R(t-t')$ in terms of $\Sigma_k(t-t')$ given in equation (7.36).

The meaning of the above generating functional is the following: in order to obtain correlation functions of the center of mass Wigner variable Ψ we must first find the solution of the classical *stochastic* Langevin equation of motion

$$\ddot{\Psi}_{\vec{k}}(t) + (k^2+m^2)\Psi_{\vec{k}}(t) + \int_0^t dt'\ \Sigma_k(t-t')\Psi_{\vec{k}}(t') = \xi_{\vec{k}}(t)$$
$$\Psi_{\vec{k}}(t=0) = \Psi_{i,\vec{k}};\quad \dot{\Psi}_{\vec{k}}(t=0) = \Pi_{i,\vec{k}} \tag{7.42}$$

for arbitrary noise term ξ and then average the products of Ψ over the stochastic noise with the Gaussian probability distribution $\mathcal{P}[\xi]$ given by (7.39), and finally average over the initial configurations $\Psi_i(\vec{x});\Pi_i(\vec{x})$ weighted by the Wigner function $\mathcal{W}(\Psi_i,\Pi_i)$, which plays the role of an initial phase space distribution function.

Calling the solution of (9.23) $\Psi_{\vec{k}}(t;\xi;\Psi_i;\Pi_i)$, the two point correlation function, for example, is given by

$$\langle \Psi_{-\vec{k}}(t)\Psi_{\vec{k}}(t')\rangle = \int \mathcal{D}[\xi]\mathcal{P}[\xi]\int D\Psi_i \int D\Pi_i\ \ \mathcal{W}(\Psi_i;\Pi_i)\Psi_{\vec{k}}(t;\xi;\Psi_i;\Pi_i)\Psi_{-\vec{k}}(t';\xi;\Psi_i;\Pi_i) \tag{7.43}$$

We note that in computing the averages and using the functional delta function to constrain the configurations of Ψ to the solutions of the Langevin equation, there is the Jacobian of the operator $d^2/dt^2+(k^2+m^2)+\int dt'\Sigma_k^{ret}(t-t')$ which however, is independent of the field and cancels between numerator and denominator in the averages.

This formulation establishes the connection with a *stochastic* problem and is similar to the Martin-Siggia-Rose[170] path integral formulation for stochastic phenomena. There are two different averages:

- The average over the stochastic noise term, which up to this order is Gaussian. We denote the average of a functional $\mathcal{F}[\xi]$ over the noise with the probability distribution function $P[\xi]$ given by eqn. (7.39) as

$$\langle\langle \mathcal{F}[\xi]\rangle\rangle \equiv \frac{\int \mathcal{D}\xi P[\xi]\mathcal{F}[\xi]}{\int \mathcal{D}\xi P[\xi]}. \tag{7.44}$$

  Since the noise probability distribution function is Gaussian the only necessary correlation functions for the noise are given by

$$\langle\langle \xi_{\vec{k}}(t)\rangle\rangle = 0\ ,\ \langle\langle \xi_{\vec{k}}(t)\xi_{\vec{k}'}(t')\rangle\rangle = \mathcal{K}_k(t-t')\,\delta^3(\vec{k}+\vec{k}') \tag{7.45}$$

and the higher order correlation functions are obtained from Wick's theorem. Because the noise kernel $\mathcal{K}_k(t-t') \neq \delta(t-t')$ the noise is *colored*.

- The average over the initial conditions with the Wigner distribution function $\mathcal{W}(\Psi_i, \Pi_i)$ which we denote as

$$\overline{\mathcal{A}[\Psi_i, \Pi_i]} \equiv \frac{\int D\Psi_i \int D\Pi_i \;\; \mathcal{W}(\Psi_i; \Pi_i)\mathcal{A}[\Psi_i, \Pi_i]}{\int D\Psi_i \int D\Pi_i \;\; \mathcal{W}(\Psi_i; \Pi_i)} \tag{7.46}$$

In what follows we will consider a Gaussian initial Wigner distribution function with vanishing mean values of $\Psi_i; \Pi_i$ with the following averages:

$$\overline{\Psi_{i,\vec{k}}\Psi_{i,-\vec{k}}} = \frac{1}{2W_k}\left[1 + 2\mathcal{N}_{b,k}\right] \tag{7.47}$$

$$\overline{\Pi_{i,\vec{k}}\Pi_{i,-\vec{k}}} = \frac{W_k}{2}\left[1 + 2\mathcal{N}_{b,k}\right] \tag{7.48}$$

$$\overline{\Pi_{i,\vec{k}}\Psi_{i,-\vec{k}} + \Psi_{i,\vec{k}}\Pi_{i,-\vec{k}}} = 0 \tag{7.49}$$

where W_k is a reference frequency. Both W_k and $\mathcal{N}_{b,k}$ characterize the initial gaussian density matrix. Such a density matrix describes a free field theory of particles with frequencies W_k. The averages (7.47,7.48) are precisely the expectation values obtained in a free field Fock state with $\mathcal{N}_{b,k}$ number of free field quanta of momentum k and frequency W_k or a free field density matrix which is diagonal in the Fock representation of a free field with frequency W_k. This can be seem simply by writing the field and canonical momentum in terms of the usual creation and annihilation operators of Fock quanta of momentum k and frequency W_k. While this is a particular choice of initial state, we will see below that the distribution function becomes insensitive to it after a time scale longer than the quasiparticle relaxation time.

The average in the time evolved full density matrix is therefore defined by

$$\langle \cdots \rangle \equiv \overline{\langle\langle \cdots \rangle\rangle} \quad . \tag{7.50}$$

7.2.3 Fluctuation and Dissipation:

From the expression (7.36) for the self-energy and the Wightmann functions (7.21,7.22) which are obtained as averages in the equilibrium density matrix of the χ fields (bath), we now obtain a dispersive representation for the kernels $\mathcal{K}_k(t-t'); \Sigma_k^R(t-t')$. This is achieved by explicitly writing

the expectation value in terms of energy eigenstates of the bath, introducing the identity in this basis, and using the time evolution of the Heisenberg field operators to obtain

$$g^2\mathcal{G}_k^{>}(t-t') = \int_{-\infty}^{\infty} d\omega\ \sigma_{\vec{k}}^{>}(\omega)\ e^{i\omega(t-t')} \tag{7.51}$$

$$g^2\mathcal{G}_k^{<}(t-t') = \int_{-\infty}^{\infty} d\omega\ \sigma_{\vec{k}}^{<}(\omega)\ e^{i\omega(t-t')} \tag{7.52}$$

with the spectral functions

$$\sigma_{\vec{k}}^{>}(\omega) = \frac{g^2}{\mathcal{Z}_b}\sum_{m,n} e^{-\beta E_n}\langle n|\mathcal{O}_{\vec{k}}(0)|m\rangle\langle m|\mathcal{O}_{-\vec{k}}(0)|n\rangle\,\delta(\omega-(E_n-E_m)) \tag{7.53}$$

$$\sigma_{\vec{k}}^{<}(\omega) = \frac{g^2}{\mathcal{Z}_b}\sum_{m,n} e^{-\beta E_m}\langle n|\mathcal{O}_{-\vec{k}}(0)|m\rangle\langle m|\mathcal{O}_{\vec{k}}(0)|n\rangle\,\delta(\omega-(E_m-E_n)) \tag{7.54}$$

where $\mathcal{Z}_b = \mathrm{Tr}\, e^{-\beta H_\chi}$ is the equilibrium partition function of the "bath". Upon relabelling $m \leftrightarrow n$ in the sum in the definition (7.54) we find the KMS relation[171, 172]

$$\sigma_k^{<}(\omega) = \sigma_k^{>}(-\omega) = e^{\beta\omega}\sigma_k^{>}(\omega) \tag{7.55}$$

where we have used parity and rotational invariance in the second line above to assume that the spectral functions only depend of the absolute value of the momentum.

Using the spectral representation of the $\Theta(t-t')$ we find the following representation for the retarded self-energy

$$\Sigma_k^R(t-t') = \int_{-\infty}^{\infty}\frac{dk_0}{2\pi}e^{ik_0(t-t')}\widetilde{\Sigma}^R(k,k_0) \tag{7.56}$$

with

$$\widetilde{\Sigma}^R(k,k_0) = \int_{-\infty}^{\infty} d\omega\frac{[\sigma_k^{>}(\omega)-\sigma_k^{<}(\omega)]}{\omega-k_0+i\epsilon} \tag{7.57}$$

Using the condition (7.55) the above spectral representation can be written in a more useful manner as

$$\widetilde{\Sigma}^R(k,k_0) = -\frac{1}{\pi}\int_{-\infty}^{\infty} d\omega\frac{\mathrm{Im}\widetilde{\Sigma}^R(k,\omega)}{\omega-k_0+i\epsilon}\,, \tag{7.58}$$

where the imaginary part of the self-energy is given by

$$\mathrm{Im}\widetilde{\Sigma}^R(k,\omega) \;=\; \pi\sigma_k^>(\omega)\left[e^{\beta\omega}-1\right] \tag{7.59}$$

and is clearly positive for $\omega > 0$. Equation (7.55) entails that the imaginary part of the retarded self-energy is an odd function of frequency, namely

$$\mathrm{Im}\widetilde{\Sigma}^R(k,\omega) = -\mathrm{Im}\widetilde{\Sigma}^R(k,-\omega)\;. \tag{7.60}$$

The relation (7.59) leads to the following results which will be useful later

$$\sigma_k^>(\omega) \;=\; \frac{1}{\pi}\mathrm{Im}\widetilde{\Sigma}^R(k,\omega)\,n(\omega) \tag{7.61}$$

$$\sigma_k^<(\omega) \;=\; \frac{1}{\pi}\mathrm{Im}\widetilde{\Sigma}^R(k,\omega)\,[1+n(\omega)] \tag{7.62}$$

Similarly from the definitions (7.35) and (7.51,7.52) and the condition (7.55) we find

$$\mathcal{K}_k(t-t') \;=\; \int_{-\infty}^{\infty}\frac{dk_0}{2\pi}e^{ik_0(t-t')}\widetilde{\mathcal{K}}(k,k_0) \tag{7.63}$$

$$\widetilde{\mathcal{K}}(k,k_0) \;=\; \pi\sigma_k^>(k_0)\left[e^{\beta k_0}+1\right] \tag{7.64}$$

whereupon using the condition (7.55) leads to the followint generalized form of the fluctuation-dissipation relation

$$\widetilde{\mathcal{K}}(k,k_0) = \mathrm{Im}\widetilde{\Sigma}^R(k,k_0)\coth\left[\frac{\beta k_0}{2}\right] \tag{7.65}$$

Thus we see that $\mathrm{Im}\widetilde{\Sigma}^R(k,k_0)\,;\,\widetilde{\mathcal{K}}(k,k_0)$ are odd and even functions of frequency respectively.

For further analysis below we will also need the following representation (see eqn. (7.36))

$$\Sigma_k(t-t') = -i\int_{-\infty}^{\infty}e^{i\omega(t-t')}\left[\sigma_k^>(\omega)-\sigma_k^<(\omega)\right]d\omega = \frac{i}{\pi}\int_{-\infty}^{\infty}e^{i\omega(t-t')}\mathrm{Im}\widetilde{\Sigma}^R(k,\omega)d\omega \tag{7.66}$$

whose Laplace transform is given by

$$\widetilde{\Sigma}(k,s) \equiv \int_0^{\infty}dte^{-st}\Sigma_k(t) = -\frac{1}{\pi}\int_{-\infty}^{\infty}\frac{\mathrm{Im}\widetilde{\Sigma}^R(k,\omega)}{\omega+is}d\omega \tag{7.67}$$

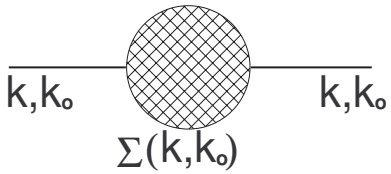

Figure 7.2: Self-energy of Φ to lowest order in g^2 but to all orders in the couplings of the fields χ amongst themselves. The external lines correspond to the field Φ.

This spectral representation, combined with (7.58) lead to the relation

$$\widetilde{\Sigma}^R(k,k_0) = \widetilde{\Sigma}(k, s = ik_0 + \epsilon) \tag{7.68}$$

We highlight that the self-energy $\widetilde{\Sigma}^R(k,k_0)$ as well as the fluctuation kernel $\widetilde{\mathcal{K}}(k,k_0)$ are *to all orders* in the couplings amongst the fields χ but to lowest order, namely $\mathcal{O}(g^2)$ in the coupling between the field Φ and the fields χ. The self-energy is depicted in fig.(7.2).

7.2.4 The solution:

The solution of the Langevin equation (9.23) can be found by Laplace transform. Defining the Laplace transforms

$$\widetilde{\Psi}_{\vec{k}}(s) \equiv \int_0^\infty dt e^{-st} \Psi_{\vec{k}}(t) \tag{7.69}$$

$$\widetilde{\xi}_{\vec{k}}(s) \equiv \int_0^\infty dt e^{-st} \xi_{\vec{k}}(t) \tag{7.70}$$

along with the Laplace transform of the self-energy given by eqn. (7.67) we find the solution

$$\widetilde{\Psi}_{\vec{k}}(s) = \frac{\Pi_{i,\vec{k}} + s\Psi_{i,\vec{k}} + \widetilde{\xi}_{\vec{k}}(s)}{s^2 + \omega_{\vec{k}}^2 + \widetilde{\Sigma}(k,s)} \;\; ; \;\; \omega_k^2 = k^2 + m^2 \tag{7.71}$$

where we have used the initial conditions (7.41). The solution in real time can be written in a more compact manner as follows. Introduce the function $f_k(t)$ that obeys the following equation

of motion and initial conditions

$$\ddot{f}_k(t) + \omega_k^2 \, f_k(t) + \int_0^t dt' \; \Sigma_k(t-t') f_k(t') = 0 \quad ; \quad f(t=0) = 0; \quad \dot{f}_k(t=0) = 1 \tag{7.72}$$

whose Laplace transform is given by

$$\widetilde{f}_k(s) = \frac{1}{s^2 + \omega_k^2 + \widetilde{\Sigma}(k,s)} \tag{7.73}$$

In terms of this auxiliary function the solution of the Langevin equation (9.23) in real time is given by

$$\Psi_k(t;\Psi_i;\Pi_i;\xi) = \Psi_{i,\vec{k}} \; \dot{f}_k(t) + \Pi_{i,\vec{k}} \; f_k(t) + \int_0^t f_k(t-t') \; \xi_{\vec{k}}(t') dt' \tag{7.74}$$

For the study of the number operator below we will also need the time derivative of the solution, given by

$$\dot{\Psi}_k(t;\Psi_i;\Pi_i;\xi) = \Psi_{i,\vec{k}} \; \ddot{f}_k(t) + \Pi_{i,\vec{k}} \; \dot{f}_k(t) + \int_0^t \dot{f}_k(t-t') \; \xi_{\vec{k}}(t') dt' \tag{7.75}$$

where we have used the initial conditions given in eqn. (9.28). From eqn. (7.71) it is clear that the solution (9.28) represents a Dyson resummation of the perturbative expansion.

The real time solution for $f(t)$ is found by the inverse Laplace transform

$$f_k(t) = \int_C \frac{ds}{2\pi i} \frac{e^{st}}{s^2 + \omega_k^2 + \widetilde{\Sigma}(k,s)} \tag{7.76}$$

where C stands for the Bromwich contour, parallel to the imaginary axis in the complex s plane to the right of all the singularities of $\widetilde{f}(s)$ and along the semicircle at infinity for $\mathrm{Re}\, s < 0$. The singularities of $\widetilde{f}(s)$ in the physical sheet are isolated single particle poles and multiparticle cuts along the imaginary axis. Thus the contour can be deformed to run parallel to the imaginary axis with a small positive real part with $s = i\omega + \epsilon \, ; \, -\infty \leq \omega \leq \infty$, returning parallel to the imaginary axis with $s = i\omega - \epsilon \, ; \, \infty > \omega > -\infty$, with $\epsilon = 0^+$ as depicted in fig. (7.3).

From the spectral representations (7.59,7.67)) one finds that $\widetilde{\Sigma}(k, s = i\omega \pm \epsilon) = \mathrm{Re}\widetilde{\Sigma}^R(k,\omega) \pm \mathrm{Im}\widetilde{\Sigma}^R(k,\omega)$ and using that $\mathrm{Im}\widetilde{\Sigma}^R(k,\omega) = -\mathrm{Im}\widetilde{\Sigma}^R(k,-\omega)$ we find the following solution in real time

$$f_k(t) = \int_{-\infty}^{\infty} \sin(\omega t) \, \rho(k,\omega;T) \, d\omega \, , \tag{7.77}$$

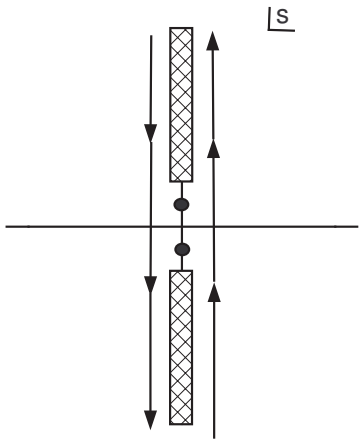

Figure 7.3: General structure of the self-energy in the complex s-plane. The dashed regions correspond to multiparticle cuts namely $\mathrm{Im}\widetilde{\Sigma}^R(k, s = i\omega + \epsilon) \neq 0$. The dots depict isolated poles.

where we have introduced the spectral density

$$\rho(k,\omega;T) = \frac{1}{\pi}\,\frac{\Big[\mathrm{Im}\widetilde{\Sigma}^R(k,\omega;T) + 2\omega\epsilon\Big]}{\Big[\omega^2 - \omega_k^2 - \mathrm{Re}\widetilde{\Sigma}^R(k,\omega;T)\Big]^2 + \Big[\mathrm{Im}\widetilde{\Sigma}^R(k,\omega;T) + 2\omega\epsilon\Big]^2}\;, \tag{7.78}$$

and we have made explicit the temperature dependence of the self-energy.

We have kept the infinitesimal $2\omega\epsilon$ with $\epsilon \to 0^+$ since if there are isolated single particle poles away from the multiparticle cuts for which $\mathrm{Im}\widetilde{\Sigma}^R(k,s) = 0$ then this term ensures that the isolated pole contribution is accounted for, namely

$$\frac{1}{\pi}\,\frac{2\omega\epsilon}{\Big[\omega^2 - \omega_k^2 - \mathrm{Re}\widetilde{\Sigma}^R(k,\omega)\Big]^2 + [2\omega\epsilon]^2} = \mathrm{sign}(\omega)\,\delta\left[\omega^2 - \omega_k^2 - \mathrm{Re}\widetilde{\Sigma}^R(k,\omega)\right]\;. \tag{7.79}$$

The initial condition $\dot{f}_k(t=0) = 1$ leads to the following sum rule

$$\int_{-\infty}^{\infty}\frac{d\omega}{\pi}\,\frac{\omega\,\Big[\mathrm{Im}\widetilde{\Sigma}^R(k,\omega) + 2\omega\epsilon\Big]}{\Big[\omega^2 - \omega_k^2 - \mathrm{Re}\widetilde{\Sigma}^R(k,\omega)\Big]^2 + \Big[\mathrm{Im}\widetilde{\Sigma}^R(k,\omega) + 2\omega\epsilon\Big]^2} = 1 \tag{7.80}$$

7.3 COUNTING PARTICLES: THE NUMBER OPERATOR

In an interacting theory the definition of a particle number requires careful consideration. To begin with, a distinction must be made between physical particles that appear in asymptotic states and can be counted by a detector, from unstable particles or resonances which have a finite lifetime and decay into other particles. Resonances are not asymptotic states, do not correspond to eigenstates of a Hamiltonian and their presence is inferred from virtual contributions to cross sections. In an interacting theory virtual processes turn a bare particle into a physical particle by dressing the bare particle with a cloud of virtual excitations. Physical particles correspond to asymptotic states and are eigenstates of the full (interacting) Hamiltonian with the physical mass. These physical particles correspond to *real* poles in the Green's functions or propagators in the complex frequency plane. In the exact vacuum state, the propagator of the field associated with the physical particles features poles below the multiparticle continuum at the exact frequencies and with a residue given by the wave function renormalization constant Z. The wave function renormalization determines the overlap between the bare and interacting single particle states. Lorentz invariance of the vacuum state entails that the exact frequencies are of the form $\Omega_k = \sqrt{k^2 + m_P^2}$, where m_P is the physical mass and that the wave function renormalization is independent of the momentum k. In asymptotic theory, the spatial Fourier transform of the field operator $\hat{\Phi}_{\vec{k}}(t)$ obeys the (weak) asymptotic condition

$$\hat{\Phi}_{\vec{k}}(t)|0\rangle \;\; \overrightarrow{t \to \infty} \;\; \sqrt{\frac{Z}{2\Omega_k}}\, e^{i\Omega_k\, t}\, a^{\dagger}_{out}|0\rangle \equiv \sqrt{\frac{Z}{2\Omega_k}}\, e^{i\Omega_k\, t}\, |1_{\vec{k}}\rangle\,, \tag{7.81}$$

where $|1_{\vec{k}}\rangle$ is the state with one physical particle.

In a medium at finite temperature there are no asymptotic states, each particle, even when stable in vacuum acquires a width in a medium either by collisional processes (collisional broadening) or other processes such as Landau damping. The width acquired by a physical particle in a medium is a consequence of the interaction between the physical particle and the excitations in the medium. In particular the medium-induced width is necessary to ensure that physical particles relax to a state of thermal equilibrium with the medium. The relaxation rate is a measure of the width of the particle in the medium. Therefore in a medium a physical particle becomes a *quasiparticle* with a medium modification of the dispersion relation and a width.

Thus the question arises as to what particles are "counted" by a definition of a distribution function, namely, a decision must be made to count either physical particles or *quasiparticles*.

One can envisage counting physical particles by introducing a detector in the medium. Such detector must be calibrated so as to "click" every time it finds a particle with given characteristics. A detector that has been calibrated to measure physical particles in a scattering experiment for example, will measure the energy and the momentum (and any other good quantum numbers) of a particle. Every time that the detector measures a momentum $\vec{k}$ and an energy Ω_k determined by the dispersion relation of the physical particle (as well as other available quantum numbers), it counts this "hit" as one particle.

Once this detector has been calibrated in this manner, for example by carrying out a scattering experiment in the vacuum, we can insert this detector in a medium and let it count the physical particles *in the medium*.

Counting *quasiparticles* entails a different calibration of the detector which must account for the properties of the medium in the definition of a quasiparticle. The first obstacle in such calibration is the fact that a quasiparticle does not have a definite dispersion relation because its spectral density features a width, namely a quasiparticle is not associated with a sharp energy but with a continuum distribution of energies. How much of this distribution will be accepted by the detector in its definition of a quasiparticle, will depend on the filtering process involved in accepting a quasiparticle, and so cannot be unique. Therefore statements about measuring a distribution of quasiparticles are somewhat ambiguous.

In this article we focus on the first strategy, by counting only *physical particles*. Hence we *propose* a number operator that "counts" the physical particle states of mass m_P that a detector will measure for example in a scattering experiment at asymptotically long times. Asymptotic theory and the usual reduction formula suggest the following *definition* of an interpolating number operator that counts the number of physical (stable) particles in a state

$$\hat{N}_k(t) = \frac{1}{2\Omega_k\, Z}\left\{\hat{\dot{\Phi}}_{\vec{k}}(t)\hat{\dot{\Phi}}_{-\vec{k}}(t) + \Omega_k^2\hat{\Phi}_{\vec{k}}(t)\hat{\Phi}_{-\vec{k}}(t)\right\} - \mathcal{C}_k \tag{7.82}$$

where Z is the wave function renormalization, namely the residue of the single (physical) particle pole in the exact propagator, $\Omega_k = \sqrt{k^2 + m_P^2}$ is the renormalized physical frequency and the normal ordering constant $\mathcal{C}_k$ will be adjusted so as to include renormalization effects. In free field theory $\Omega_k = \omega_k = \sqrt{k^2 + m^2}\,, Z = 1\,, \mathcal{C}_k = 1/2$. However, in asymptotic theory the field Φ creates a single particle state of momentum k and mass m_P with amplitude $\sqrt{Z}$ out of the exact vacuum.

The quantity $\mathcal{C}_k$ arises from the necessity of redefining the normal ordering for the correct identification of the particle number in an interacting field theory. It will be fixed below by requiring

that the expectation value of $\hat{N}_k(t)$ vanishes in the exact vacuum state at asymptotically long time. Alternatively this constant can be extracted from the equal time limit of the operator product expansion.

The approach that we follow is to consider an initial factorized density matrix corresponding to a tensor product of a density matrix of the field Φ and a thermal bath of the fields χ. This initial state will evolve in time with the full interacting Hamiltonian, leading to transient phenomena which results in the dressing of the bare particles by the virtual excitations. At asymptotically long times the bare particle is fully dressed into the physical particle, and at finite temperature, a quasiparticle. The time evolution of the interpolating number operator will reflect this transient stage and the dynamics of the dressing of the bare into the physical state. Since the thermal bath is stationary, the distribution of physical particles in the bath will be extracted from the asymptotic long time limit of the expectation value of the interpolating Heisenberg number operator $\hat{N}_k(t)$ in the initial state.

The expectation value of $\hat{N}_k(t)$ is related to the real-time correlation functions of the field Φ as follows

$$\langle \hat{N}_k(t) \rangle = \frac{1}{4\Omega_k Z} \left(\frac{\partial}{\partial t} \frac{\partial}{\partial t'} + \Omega_k^2 \right) \left[g_k^>(t,t') + g_k^<(t,t') \right]_{t=t'} - \mathcal{C}_k \tag{7.83}$$

where the non-equilibrium correlation functions are given by

$$\langle \Phi^+_{\vec{k}}(t) \Phi^+_{-\vec{k}}(t') \rangle = g_k^>(t,t')\Theta(t-t') + g_k^<(t,t')\Theta(t'-t) \tag{7.84}$$

$$\langle \Phi^-_{\vec{k}}(t) \Phi^-_{-\vec{k}}(t') \rangle = g_k^>(t,t')\Theta(t'-t) + g_k^<(t,t')\Theta(t-t') \tag{7.85}$$

$$\langle \Phi^-_{\vec{k}}(t) \Phi^+_{-\vec{k}}(t') \rangle = g_k^>(t,t') \tag{7.86}$$

$$\langle \Phi^-_{-\vec{k}}(t') \Phi^+_{\vec{k}}(t) \rangle = g_k^<(t,t') \tag{7.87}$$

In terms of the center of mass field $\Psi_k(t) = (\Phi^+_{\vec{k}}(t) + \Phi^-_{\vec{k}}(t))/2$ introduced above it is straightforward to find that the correlation function in the bracket in (7.83) is given by

$$\langle \Psi_{\vec{k}}(t) \Psi_{-\vec{k}}(t') \rangle = \frac{1}{2} \left[g_k^>(t,t') + g_k^<(t,t') \right] \tag{7.88}$$

and the occupation number can be written in terms of the center of mass Wigner variable introduced in eqn. (9.22) as follows

$$\langle \hat{N}_k(t) \rangle = \frac{1}{2\Omega_k Z} \left[\langle \dot{\Psi}_{\vec{k}}(t) \dot{\Psi}_{-\vec{k}}(t) \rangle + \Omega_k^2 \langle \Psi_{\vec{k}}(t) \Psi_{-\vec{k}}(t) \rangle \right] - \mathcal{C}_k \tag{7.89}$$

where the expectation values are obtained as in eqn. (7.50) and $\Psi_{\vec{k}}(t)$ is the solution of the Langevin equation given by (9.28,7.75).

A straightforward calculation implementing eqn. (7.50) writing the noise in terms of its temporal Fourier transform and using the Fourier representation of the noise kernel (7.63) leads to the following result

$$N_k(t) \equiv \langle \hat{N}_k(t) \rangle = \frac{1}{2\Omega_k Z} \left\{ \frac{1}{2W_k} \left[1 + 2\mathcal{N}_{b,k}\right] \left[\ddot{f}_k^2(t) + (\Omega_k^2 + W_k^2)\ \dot{f}_k^2(t) + \Omega_k^2 W_k^2\ f_k^2(t) \right] + \int_{-\infty}^{\infty} \frac{d\omega}{2\pi} \widetilde{\mathcal{K}}(k,\omega) \left[|\mathcal{F}_k(\omega,t)|^2 + \Omega_k^2 |\mathcal{H}_k(\omega,t)|^2 \right] \right\} - \mathcal{C}_k \tag{7.90}$$

where we have introduced

$$\mathcal{H}_k(\omega,t) = \int_0^t d\tau f_k(\tau) e^{-i\omega\tau} \tag{7.91}$$

$$\mathcal{F}_k(\omega,t) = \int_0^t d\tau \dot{f}_k(\tau) e^{-i\omega\tau} \tag{7.92}$$

$f_k(t)$ is given in eqn. (7.77) and the fluctuation kernel $\widetilde{\mathcal{K}}(k,\omega)$ is given by eqn. (9.27).

The result (7.90) for the time evolution of the distribution function, along with the expressions (7.91,7.92) clearly highlights the *non-Markovian* nature of the evolution. The integrals in time in (7.91,7.92) include *memory* of the past evolution. This is one of the most important aspects that distinguishes the quantum kinetic approach from the usual Boltzmann equation. We will contrast these aspects in section (7.5).

7.3.1 Counting physical particles in a thermal bath

In the vacuum the spectral density of the field Φ which describes a physical particle is depicted in fig. (7.4). It features isolated poles along the real axis in the physical sheet in the complex frequency (ω) plane at the position of the *exact* single particle dispersion relation Ω_k with $|\Omega_k| < |\omega_{th}|$ where ω_{th} is the lowest multiparticle threshold.

As mentioned above, in a medium stable physical particles acquire a width as a consequence of the interactions with physical excitations, and become *quasiparticles*. The width can originate in several different processes such as collisions or Landau damping. The poles move off the physical sheet into the second (or higher) Riemann sheet in the complex ω plane, thus becoming a resonance. This is the statement that there are no asymptotic states in the medium.

The analytic structure of the spectral density at finite temperature is in general fairly complicated. While at zero temperature the multiparticle thresholds are above the light cone $|\omega| > k$,

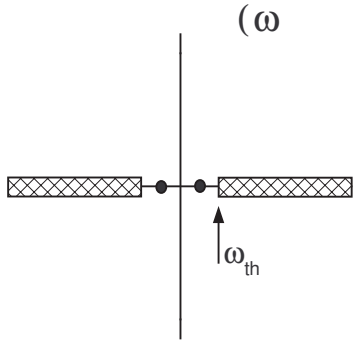

Figure 7.4: Spectral density $\rho_k(\omega, T=0)$ for stable particles. The dots represent the isolated poles at $\pm\Omega_k$ and the shaded regions the multiparticle cuts. ω_{th} is the lowest multiparticle threshold.

at finite temperature (or density) there appear branch cuts with support below the light cone[149, 171, 172, 173]. However a general statement in a medium is that the poles associated with stable particles in vacuum (along the real axis in the physical sheet) move off the physical sheet and the spectral density does not feature isolated poles but only branch cut singularities in the physical sheet, associated with multiparticle processes in the medium.

In perturbation theory the resonance is very close to the real axis (but in the second or higher Riemann sheet) and the width is very small as compared with the position of the resonance. We will study a particular example in the next section.

In perturbation theory the spectral density $\rho(k,\omega,T)$ (7.78) features a sharp peak at the position of the *quasiparticle* "pole" which is determined by

$$\mathcal{W}_k^2(T) - \omega_k^2 - \mathrm{Re}\widetilde{\Sigma}^R(k, \mathcal{W}_k(T); T) = 0 \tag{7.93}$$

Near the quasiparticle "poles" the spectral density is well described by the Breit-Wigner approximation

$$\rho_{BW}(k,\omega;T) \simeq \frac{\mathcal{Z}_k(T)}{2\mathcal{W}_k(T)}\,\frac{1}{\pi}\frac{\mathrm{sign}(\omega)\,\Gamma_k(T)}{(|\omega| - \mathcal{W}_k(T))^2 + \Gamma_k^2(T)}\;, \tag{7.94}$$

where $\mathcal{W}_k(T)$ is determined by eqn. (7.93) and the finite temperature residue and width are given

by

$$\frac{1}{\mathcal{Z}_k(T)} = \left[1 - \frac{1}{2\mathcal{W}_k(T)} \frac{\partial \mathrm{Re}\widetilde{\Sigma}^R(k,\omega;T)}{\partial\omega}\right]_{\omega=\mathcal{W}_k(T)} \tag{7.95}$$

$$\Gamma_k(T) = \mathcal{Z}_k \frac{\mathrm{Im}\widetilde{\Sigma}^R(k,\mathcal{W}_k(T);T)}{2\mathcal{W}_k(T)} \tag{7.96}$$

At zero temperature of the bath, the (quasi) particle dispersion relation $\mathcal{W}_k(T)$ is identified with the dispersion relation of the stable physical particle, namely the "on-shell" pole, the residue $\mathcal{Z}_k(T)$ is identified with the wavefunction renormalization constant Z which is the residue at the on-shell pole for the physical particle, and the width vanishes at zero temperature since the particle is stable in the vacuum, namely

$$\mathcal{W}_k(T=0) = \Omega_k \tag{7.97}$$

$$\mathcal{Z}_k(T=0) = Z \tag{7.98}$$

$$\Gamma_k(T=0) = 0 \tag{7.99}$$

In the Breit-Wigner approximation the real time solution is easily found to be

$$f_k^{BW}(t) \simeq \mathcal{Z}_k(T) \frac{\sin\left[\mathcal{W}_k(T)\,t\right]}{\mathcal{W}_k(T)}\, e^{-\Gamma_k(T)\,t} \tag{7.100}$$

This solution describes the relaxation of single *quasiparticles*, where $\mathcal{W}_k(t)$ is the quasiparticle dispersion relation and $\Gamma_k(T)$ is the quasiparticle decay rate.

The asymptotic long time limit of the distribution function (7.90) is obtained by using the following identities

$$\mathcal{H}_k(\omega,\infty) = \int_0^\infty e^{-i(\omega-i\epsilon)t} f_k(t) dt = \widetilde{f}_k(s = i\omega + \epsilon) \tag{7.101}$$

$$\mathcal{F}_k(\omega,\infty) = \int_0^\infty e^{-i(\omega-i\epsilon)t} \dot{f}_k(t) dt = i\omega \widetilde{f}_k(s = i\omega + \epsilon) \tag{7.102}$$

where $\widetilde{f}_k(s)$ is the Laplace transform of $f_k(t)$ given by eqn. (7.73) and in (7.102) we have integrated by parts, used the initial condition $f_k(0) = 0$ and introduced a convergence factor $\epsilon \to 0^+$. Hence

the expectation value of the interpolating number operator in the asymptotic long-time limit is given by

$$N_k(\infty) = \int_0^\infty \left(\frac{\omega^2 + \Omega_k^2}{2\, Z\, \Omega_k} \right) [1 + 2n(\omega)]\, \rho(k, \omega, T)\, d\omega \; - \mathcal{C}_k \; , \tag{7.103}$$

where $n(\omega)$ is the Bose-Einstein distribution function and we have used the fluctuation-dissipation relation (9.27) as well as eqn. (7.73) which lead to the $\rho(k, \omega, T)$ in (7.103). The dependence of the asymptotic distribution function on the spectral density is a consequence of the fluctuation-dissipation relation (9.27) as well as the *non-Markovian* time evolution as displayed in (7.101,7.102).

The real time solution (7.100) clearly reveals that the asymptotic limit is reached for $t > \tau_k = 1/2\Gamma_k(T)$ where $\Gamma_k(T)$ is the quasiparticle relaxation rate. The distribution function at $t >> \tau_k$ does not depend on the initial distribution $\mathcal{N}_{b,k}$ or the reference frequencies W_k. Therefore at times longer than the quasiparticle relaxation time the distribution function becomes *independent of the initial conditions*. This is to be expected if the state reaches thermal equilibrium with the bath, since in thermal equilibrium there is no memory of the initial conditions or correlations.

The integral term in the asymptotic distribution (7.103) is easily understood as *full thermalization* from the following argument.

Let us consider the correlations functions $g_k^>(t, t'); g_k^<(t, t')$ given by eqns. (7.86,7.87). In *thermal equilibrium* they have the spectral representation

$$g_k^>(t, t') = \int \rho^>(k, \omega; T)\, e^{i\omega(t-t')} d\omega \tag{7.104}$$

$$g_k^<(t, t') = \int \rho^<(k, \omega; T)\, e^{i\omega(t-t')} d\omega \tag{7.105}$$

where

$$\rho^>(k, \omega; T) = \frac{1}{\mathcal{Z}_T} \sum_{m,n} e^{-\beta E_n} \langle n|\Phi_{\vec{k}}(0)|m\rangle\langle m|\Phi_{-\vec{k}}(0)|n\rangle\, \delta(\omega - (E_n - E_m)) \tag{7.106}$$

$$\rho^<(k, \omega; T) = \frac{1}{\mathcal{Z}_T} \sum_{m,n} e^{-\beta E_m} \langle n|\Phi_{-\vec{k}}(0)|m\rangle\langle m|\Phi_{\vec{k}}(0)|n\rangle\, \delta(\omega - (E_m - E_n))\,. \tag{7.107}$$

Where $\mathcal{Z}_T$ is the thermal equilibrium partition function. A straightforward re-labelling of indices leads to the relation

$$\rho^<(k, \omega; T) = \rho^>(k, -\omega; T) = e^{\beta\omega} \rho^>(k, \omega; T) \tag{7.108}$$

The spectral density is given by

$$\rho(k,\omega;T) = \rho^{<}(k,\omega;T) - \rho^{>}(k,\omega;T) \tag{7.109}$$

leading to the relations

$$\rho^{>}(k,\omega;T) = \rho(k,\omega;T)\, n(\omega) \tag{7.110}$$

$$\rho^{<}(k,\omega;T) = \rho(k,\omega;T)\, [1+n(\omega)] \ , \tag{7.111}$$

where $n(\omega) = 1/[e^{\beta\omega}-1]$.

Therefore *in thermal equilibrium* the expectation value of the operator term in eqns. (7.82, 7.83) is given by

$$\frac{1}{4\Omega_k\, Z}\left(\frac{\partial}{\partial t}\frac{\partial}{\partial t'} + \Omega_k^2\right)\left[g_k^{>}(t,t') + g_k^{<}(t,t')\right]_{t=t'} = \int_{-\infty}^{\infty}\left(\frac{\omega^2+\Omega_k^2}{4\, Z\, \Omega_k}\right)[1+2n(\omega)]\ \rho(k,\omega;T)\, d\omega \ , \tag{7.112}$$

which is precisely the integral term in the asymptotic limit given by eqn. (7.103). Therefore the expression (7.103) indicates that the excitations of the field Φ have reached a state of thermal equilibrium with the bath. The normal ordering constant $\mathcal{C}_k$ in (7.103) is a subtraction necessary to redefine normal ordering in the interacting theory and is defined from the operator product expansion to yield vanishing number of particles in the vacuum.

While the asymptotic long time limit can be obtained directly from the spectral representation of the interpolating number operator in the equilibrium state, the real time formulation in terms of the non-equilibrium effective action has two advantages: i) it makes explicit the connection with the fluctuation dissipation relation and clearly states that the equilibrium abundance is determined by the *noise* correlation function of the bath, ii) the real time dynamics clearly shows thermalization on time scales $t > \tau_k$. These statements would not be immediately recognized from the equilibrium spectral representation.

The result (7.103) becomes more illuminating in the *narrow width approximation* where the Breit-Wigner approximation for the spectral density (7.94) is supplemented with the narrow width limit $\Gamma_k(T) \to 0$ which leads to

$$\rho(k,\omega;T) \simeq \frac{\mathcal{Z}_k(T)}{2\mathcal{W}_k(T)}\ \mathrm{sign}(\omega)\delta\left(|\omega| - \mathcal{W}_k(T)\right) \ , \tag{7.113}$$

which in turn leads to the *approximate* result

$$N_k(\infty) \sim \frac{\mathcal{Z}_k(T)}{Z}\left(\frac{\mathcal{W}_k^2(T)+\Omega_k^2}{2\,\mathcal{W}_k(T)\,\Omega_k}\right)\left[\frac{1}{2}+n(\mathcal{W}_k(T))\right]-\mathcal{C}_k \tag{7.114}$$

Obviously the zero temperature pole Ω_k and residue Z and their finite temperature counterparts $\mathcal{W}_k(T), \mathcal{Z}_k(T)$ differ by terms that are of order g^2, namely perturbatively small, therefore in the narrow width approximation, which itself is a result of the weak coupling assumption one could write

$$N_k(\infty) \sim n(\Omega_k)+\left[\frac{1}{2}+\mathcal{O}(g^2)-\mathcal{C}_k\right] \tag{7.115}$$

Thus choosing the normal ordering factor $\mathcal{C}_k = 1/2 + \mathcal{O}(g^2)$ would lead to the conclusion that the physical particles are distributed in the thermal bath with a Bose-Einstein distribution function with the argument being the physical pole frequency (at zero temperature). Furthermore the normal ordering constant $\mathcal{C}_k \sim 1/2$ is identified with the usual normal ordering of the number operator in the free field vacuum.

In order to understand in detail the perturbative correction we have to first decide on what are $\Omega_k, Z, \mathcal{C}_k$. The importance of the perturbative corrections cannot be underestimated, if the temperature of the bath is much smaller than Ω_k the distribution function $n(\Omega_k) \ll 1$ and the perturbative corrections can be of the same order or larger. What should be clear from the above discussion is that in order to make precise the perturbative correction to the abundance, we must specify unambiguously what is being counted.

7.3.1.1 Physical particles in the vacuum The next step is to define $\Omega_k, Z, \mathcal{C}_k$. As it was emphasized above, the number operator that we seek counts physical particles. These are stable excitations off the full vacuum state of the theory and are associated with isolated single particle poles in the spectral density *at zero temperature*.

The zero temperature limit of the asymptotic distribution function (7.103) is

$$N_k(\infty; T=0) = \int_0^\infty \left(\frac{\omega^2+\Omega_k^2}{2\,Z\,\Omega_k}\right)\rho(k,\omega,T=0)\,d\omega-\mathcal{C}_k\ , \tag{7.116}$$

At $T = 0$ the spectral density features the isolated single particle poles away from the multi-particle continuum as depicted in fig. (7.4). The contribution from the single particle poles to the

zero temperature spectral density is given by eqn. (7.79), therefore we write

$$\rho(k,\omega,T=0) = \mathrm{sign}(\omega)\,\frac{Z}{2\Omega_k}\,\delta(\omega-\Omega_k) + \rho_c(k,\omega,T=0)\,, \tag{7.117}$$

where $\rho_c(k,\omega,T=0)$ is the continuum contribution with support for $|\omega| > \omega_{th}$, where ω_{th} is the lowest multiparticle threshold, and the position of the isolated pole satisfies

$$\Omega_k^2 - \omega_k^2 - \mathrm{Re}\widetilde{\Sigma}^R(k,\Omega_k) = 0 \tag{7.118}$$

At zero temperature Lorentz covariance implies that $\Omega_k^2 = k^2 + m_P^2$, where m_P is the pole mass of the physical excitations (asymptotic states).

The residue at the single (physical) particle pole, Z, is given by

$$\frac{1}{Z} = \left[1 - \frac{1}{2\Omega_k}\frac{\partial \mathrm{Re}\widetilde{\Sigma}^R(k,\omega;T)}{\partial\omega}\right]_{\omega=\Omega_k}. \tag{7.119}$$

Introducing the zero temperature form of the spectral density (7.117) in the sum rule (7.80) the following alternative expression is obtained.

$$Z = 1 - 2\int_{\omega_{th}}^{\infty} \omega\,\rho_c(k,\omega,T=0)\,d\omega \tag{7.120}$$

Therefore the asymptotic distribution of particles in the vacuum is given by

$$N_k(\infty;T=0) = \frac{1}{2} + \int_0^{\infty}\left(\frac{\omega^2+\Omega_k^2}{2\,Z\,\Omega_k}\right)\rho_c(k,\omega,T=0)\,d\omega - \mathcal{C}_k\,, \tag{7.121}$$

The normal ordering term $\mathcal{C}_k$ is now fixed by requiring that for $T=0$ the vacuum state has vanishing number of physical excitations. In other words, by requiring $N_k(\infty,T=0)=0$ we are led to

$$\mathcal{C}_k = \frac{1}{2} + \int_0^{\infty}\left(\frac{\omega^2+\Omega_k^2}{2\,Z\,\Omega_k}\right)\rho_c(k,\omega,T=0)\,d\omega. \tag{7.122}$$

We have kept the lower limit in the integral to be $\omega=0$ for further convenience, however $\rho_c(k,\omega,T=0)$ *vanishes* for $|\omega| < \omega_{th}$.

Equations (7.118), (7.119,7.120) and (7.122) determine all of the parameters $\Omega_k, Z, \mathcal{C}_k$ for the proper definition of the distribution function for physical particles.

Hence the distribution function of *physical* excitations in equilibrium with the bath at finite temperature is finally given by the simple expression

$$\mathcal{N}(k,T) \equiv N_k(\infty) = \int_0^\infty \left(\frac{\omega^2+\Omega_k^2}{2\,Z\,\Omega_k}\right)\Big\{\,[1+2n(\omega)]\,\rho(k,\omega,T) - \rho_c(k,\omega,T=0)\Big\}\,d\omega\,-\frac{1}{2}\,, \quad (7.123)$$

This is the final form of the asymptotic distribution function of physical particles in equilibrium in the thermal bath with $\Omega_k = \sqrt{k^2+m_P^2}; Z; \mathcal{C}_k$ given by equations (7.118),(7.119) (or (7.120),(7.122)) respectively.

7.3.2 Renormalization:

In renormalizable theories the wavefunction renormalization constant Z is ultraviolet divergent and the expression for the asymptotic distribution function (7.123) seems to be ambiguous. However proper renormalization as described below shows that the asymptotic abundance is finite.

In general the imaginary part of the self-energy can be written as a sum of a zero temperature and a finite temperature contribution, the latter vanishing at zero temperature, thus we write

$$\mathrm{Im}\widetilde{\Sigma}^R(\omega,k;T) = \mathrm{Im}\widetilde{\Sigma}^R_0(\omega,k) + \mathrm{Im}\widetilde{\Sigma}^R_T(\omega,k) \quad (7.124)$$

Therefore the real part of the self-energy, which is obtained from the imaginary part by a dispersion relation (Kramers-Kronig) can also be written as a sum of a zero temperature plus a finite temperature contribution,

$$\mathrm{Re}\widetilde{\Sigma}^R(\omega,k;T) = -\frac{1}{\pi}\mathcal{P}\int_0^\infty 2k_0\frac{\mathrm{Im}\widetilde{\Sigma}^R(k_0,k;T)}{k_0^2-\omega^2}\,dk_0 \equiv \mathrm{Re}\widetilde{\Sigma}^R_0(\omega,k) + \mathrm{Re}\widetilde{\Sigma}^R_T(\omega,k) \quad (7.125)$$

where $\mathcal{P}$ stands for the principal part of the integral, and we have used the fact that $\mathrm{Im}\widetilde{\Sigma}^R(k_0,k;T)$ is an odd function of k_0. Both $\mathrm{Im}\widetilde{\Sigma}^R_T(\omega,k)$ and $\mathrm{Re}\widetilde{\Sigma}^R_T(\omega,k)$ vanish at $T=0$.

The position of the physical pole is obtained at zero temperature from the relation (7.118),

$$\Omega_k^2 - \omega_k^2 - \mathrm{Re}\widetilde{\Sigma}^R_0(k,\Omega_k) = 0 \quad (7.126)$$

The subtracted real part of the self energy is

$$\mathrm{Re}\widetilde{\Sigma}^R_0(k,\omega) - \mathrm{Re}\widetilde{\Sigma}^R_0(k,\Omega_k) = \Big[1 - Z^{-1}[k,\omega]\Big](\omega^2-\Omega_k^2) \quad (7.127)$$

where

$$Z^{-1}[k,\omega] = 1 + \frac{1}{\pi}\mathcal{P}\int_0^\infty 2k_0 \frac{\mathrm{Im}\widetilde{\Sigma}_0^R(k_0,k)}{(k_0^2-\omega^2)(k_0^2-\Omega_k^2)}\, dk_0 \tag{7.128}$$

As mentioned above, in renormalizable theories $Z[k,\omega]$ is ultraviolet logarithmically divergent, therefore it is convenient to perform yet another subtraction of the integral term in (7.128) as follows,

$$Z^{-1}[k,\omega] = Z^{-1} - \Pi_0(k,\omega)\,, \tag{7.129}$$

where Z is the wavefunction renormalization constant, namely the residue at the pole,

$$Z^{-1} = 1 + \frac{1}{\pi}\mathcal{P}\int_0^\infty 2k_0 \frac{\mathrm{Im}\widetilde{\Sigma}_0^R(k_0,k)}{(k_0^2-\Omega_k^2)^2}\, dk_0\,, \tag{7.130}$$

and $\Pi_0(k,\omega)$ is the real part of the twice subtracted self-energy given by

$$\Pi_0(k,\omega) = -\frac{1}{\pi}(\omega^2-\Omega_k^2)\;\mathcal{P}\int_0^\infty 2k_0 \frac{\mathrm{Im}\widetilde{\Sigma}_0^R(k_0,k)}{(k_0^2-\omega^2)(k_0^2-\Omega_k^2)^2}\, dk_0 \tag{7.131}$$

The two subtractions had been performed on the single particle mass-shell. In a renormalizable theory the integral in the twice subtracted real part of the self energy $\Pi_0(k,\omega)$ is *finite* while the integral in Z^{-1} is logarithmically divergent. However the finite temperature parts do not have primitive divergences since all the primitive divergences are those of the zero temperature theory.

Combining equations (7.150), (7.126), (7.127) and (7.129), the spectral density (7.78) can be written in the following form

$$\rho(k,\omega;T) = \frac{1}{\pi}\,\frac{\Big[\mathrm{Im}\widetilde{\Sigma}^R(k,\omega;T) + 2\omega\epsilon\Big]}{\Big[Z^{-1}(\omega^2-\Omega_k^2) - \widetilde{\Pi}(k,\omega;T)\Big]^2 + \Big[\mathrm{Im}\widetilde{\Sigma}^R(k,\omega;T) + 2\omega\epsilon\Big]^2}\,, \tag{7.132}$$

where

$$\widetilde{\Pi}(k,\omega;T) = (\omega^2-\Omega_k^2)\Pi_0(k,\omega) + \mathrm{Re}\widetilde{\Sigma}_T^R(\omega,k) \tag{7.133}$$

Introducing the *renormalized* real and imaginary part of the self-energy as

$$\widetilde{\Pi}_r(k,\omega;T) = Z\,\widetilde{\Pi}(k,\omega;T) \tag{7.134}$$

$$\mathrm{Im}\widetilde{\Sigma}_r^R(k,\omega;T) = Z\,\mathrm{Im}\widetilde{\Sigma}^R(k,\omega;T) \tag{7.135}$$

the spectral density (7.132) can be written as

$$\rho(k,\omega;T) = Z\,\rho_r(k,\omega;T)\,, \tag{7.136}$$

where

$$\rho_r(k,\omega;T) = \frac{1}{\pi}\,\frac{\left[\mathrm{Im}\widetilde{\Sigma}^R_r(k,\omega;T) + 2\omega\epsilon\right]}{\left[(\omega^2-\Omega_k^2) - \widetilde{\Pi}_r(k,\omega;T)\right]^2 + \left[\mathrm{Im}\widetilde{\Sigma}^R_r(k,\omega;T) + 2\omega\epsilon\right]^2}\,. \tag{7.137}$$

We note that at zero temperature the spectral density $\rho_r(k,\omega;T=0)$ has unit residue at the single physical particle pole.

Since both $\widetilde{\Pi}(k,\omega;T)$ and $\mathrm{Im}\widetilde{\Sigma}^R(k,\omega;T)$ are proportional to g^2, the renormalization of the real and imaginary part of the self-energy in eqns. (7.134),(7.135) is tantamount to the renormalization of the coupling constant[1]

$$g_r = \sqrt{Z}g \tag{7.138}$$

In terms of g_r, both $\widetilde{\Pi}_r(k,\omega;T)$ and $\mathrm{Im}\widetilde{\Sigma}^R_r(k,\omega;T)$ are *finite* since the only counterterms necessary are those of the zero temperature theory. Therefore the equilibrium distribution function can be written solely in terms of renormalized quantities as follows

$$\mathcal{N}(k,T) = \int_0^\infty \left(\frac{\omega^2+\Omega_k^2}{2\,\Omega_k}\right)\Big\{\,[1+2n(\omega)]\,\rho_r(k,\omega,T) - \rho_{r,c}(k,\omega,T=0)\Big\}\,d\omega\;-\frac{1}{2}\,. \tag{7.139}$$

This definition of the asymptotic distribution function is one of the main results of this article.

7.4 THE MODEL

The results obtained in the previous section are general and as mentioned above the quantum kinetic effects that modify the standard Boltzmann suppression of particle abundance in the medium depend on the particular theory under consideration. To highlight the main concepts in a spe-

[1]The coupling g in the Lagrangian already has the proper renormalization of the (composite) operator $\mathcal{O}[\chi]$.

cific scenario, we now consider a theory of three interacting real scalar fields with the following Lagrangian density.

$$\mathcal{L} = \frac{1}{2}\partial_\mu \Phi \partial^\mu \Phi - \frac{1}{2} m^2 \Phi^2 + \sum_{i=1}^{2} \left[\frac{1}{2}\partial_\mu \chi_i \partial^\mu \chi_i - \frac{1}{2} M_i^2 \chi_i^2 \right] - g \Phi \, \chi_1 \, \chi_2 + \mathcal{L}_{int}[\chi_1 \, \chi_2] \tag{7.140}$$

We will assume that the mutual interaction between the fields χ_1 , χ_2 ensures that the fields $\chi_{1,2}$ are in thermal equilibrium at a temperature $T = 1/\beta$. A similar model has been previously studied in ref.[149] for an analysis of the different processes in the medium.

The particles associated with the field Φ will be stable at $T = 0$ provided $m_P < M_1 + M_2$, where m_P is the zero temperature pole mass of the Φ particles. In order to study the emergence of a width for the particles of the field Φ to lowest order in perturbation theory we will consider the case in which $M_1 > m_P + M_2$ (or alternatively $M_2 > m_P + M_1$) in this case the quanta of the field χ_1 can *decay* into those of the field Φ and χ_2. Since the particles $1, 2$ are in a thermal bath in equilibrium the presence of the heavier species (here taken to be that of the field χ_1) in the medium results in a *width* for the excitations of field Φ through the process of decay of the heavier particle into the lighter scalars and its recombination, namely $\chi_1 \leftrightarrow \Phi + \chi_2$. As will be seen in detail below the kinematics for this process is similar to that for Landau damping in the case of massive particles [173].

The relevant quantity is the self-energy of the field Φ which we now obtain to one loop order $\mathcal{O}(g^2)$ in the Matsubara representation. The one-loop self-energy is given by

$$\Sigma(\nu_n, \vec{k}) = -g^2 \int \frac{d^3\vec{p}}{(2\pi)^3} \frac{1}{\beta} \sum_{\omega_m} G^{(0)}_{\chi_1}(\omega_m, \vec{p}) \, G^{(0)}_{\chi_2}(\omega_m + \nu_n, \vec{p} + \vec{k}) \, , \tag{7.141}$$

where ω_m, ν_n are Bosonic Matsubara frequencies. It is convenient to write the Matsubara propagators in the following dispersive form

$$
\begin{aligned}
G^{(0)}_{\chi_1}(\omega_m,\vec{p}) &= \int dp_0 \frac{\rho_1(p_0,\vec{p})}{p_0 - i\omega_m}\,, && (7.142)\\
G^{(0)}_{\chi_2}(\omega_m+\nu_n,\vec{p}+\vec{k}) &= \int dq_0 \frac{\rho_2(q_0,\vec{p}+\vec{k})}{q_0 - i\omega_m - i\nu_n}\,, && (7.143)\\
\rho_1(p_0,\vec{p}) &= \frac{1}{2\omega^{(1)}_{\vec{p}}}[\delta(p_0-\omega^{(1)}_{\vec{p}}) - \delta(p_0+\omega^{(1)}_{\vec{p}})]\,, && (7.144)\\
\rho_2(q_0,\vec{p}+\vec{k}) &= \frac{1}{2\omega^{(2)}_{\vec{p}+\vec{k}}}[\delta(q_0-\omega^{(2)}_{\vec{p}+\vec{k}}) - \delta(q_0+\omega^{(2)}_{\vec{p}+\vec{k}})]\,, && (7.145)\\
\omega^{(1)}_{\vec{p}} &= \sqrt{\vec{p}^2+M_1^2}\,; \quad \omega^{(2)}_{\vec{p}+\vec{k}} = \sqrt{(\vec{p}+\vec{k})^2+M_2^2}\,. && (7.146)
\end{aligned}
$$

This representation allows to carry out the sum over Matsubara frequencies ω_m in a rather straightforward manner[171, 172] which automatically leads to the following dispersive representation of the self-energy

$$
\Sigma(k,\nu_n) = -\frac{1}{\pi}\int_{-\infty}^{\infty} d\omega \frac{\mathrm{Im}\widetilde{\Sigma}^R(k,\omega)}{\omega - i\nu_n} \tag{7.147}
$$

with the imaginary part of the self-energy given by

$$
\mathrm{Im}\widetilde{\Sigma}^R(k,\omega) = \pi g^2 \int \frac{d^3\vec{p}}{(2\pi)^3}\int dp_0 \int dq_0\,[n(p_0)-n(q_0)]\,\rho_1(p_0,\vec{p})\,\rho_2(q_0,\vec{p}+\vec{k})\,\delta(\omega-q_0+p_0) \tag{7.148}
$$

where $n(q)$ are the Bose-Einstein distribution functions. From the representation (7.58) the retarded self-energy follows by analytic continuation, namely

$$
\widetilde{\Sigma}^R(k,k_0) = \Sigma(k,\nu_n = k_0 - i\epsilon) \tag{7.149}
$$

The imaginary part of the self energy can be written as a sum of several different contributions, namely

$$
\mathrm{Im}\widetilde{\Sigma}^R_r(k,\omega;T) = \sigma_0(k,\omega) + \sigma_a(k,\omega;T) + \sigma_b(k,\omega;T)\,, \tag{7.150}
$$

where $\sigma_0(k,\omega)$ is the zero temperature contribution given by

$$
\sigma_0(k,\omega) = \frac{g^2}{32\pi^2}\int \frac{d^3\vec{p}}{\omega^{(1)}_{\vec{p}}\omega^{(2)}_{\vec{p}+\vec{k}}}\left[\delta\left(\omega-\omega^{(1)}_{\vec{p}}-\omega^{(2)}_{\vec{p}+\vec{k}}\right) - \delta\left(\omega+\omega^{(1)}_{\vec{p}}+\omega^{(2)}_{\vec{p}+\vec{k}}\right)\right], \tag{7.151}
$$

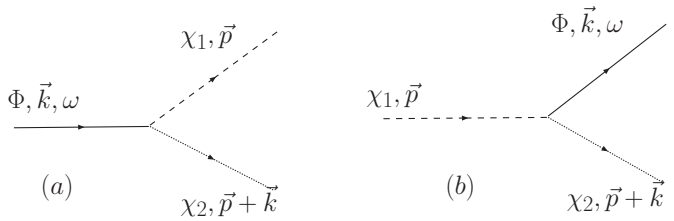

Figure 7.5: Processes contributing to $\sigma_0(k,\omega), \sigma_a(k,\omega)$ (a) and to $\sigma_b(k,\omega)$ (b). The inverse processes are not shown.

and $\sigma_a(k,\omega), \sigma_b(k,\omega)$ are the finite temperature contributions given by

$$\sigma_a(k,\omega;T) = \frac{g^2}{32\pi^2}\int \frac{d^3\vec{p}}{\omega^{(1)}_{\vec{p}}\,\omega^{(2)}_{\vec{p}+\vec{k}}}\left[n(\omega^{(1)}_{\vec{p}}) + n(\omega^{(2)}_{\vec{p}+\vec{k}})\right]\left[\delta\left(\omega - \omega^{(1)}_{\vec{p}} - \omega^{(2)}_{\vec{p}+\vec{k}}\right) - \delta\left(\omega + \omega^{(1)}_{\vec{p}} + \omega^{(2)}_{\vec{p}+\vec{k}}\right)\right], \tag{7.152}$$

$$\sigma_b(k,\omega;T) = \frac{g^2}{32\pi^2}\int \frac{d^3\vec{p}}{\omega^{(1)}_{\vec{p}}\,\omega^{(2)}_{\vec{p}+\vec{k}}}\left[n(\omega^{(2)}_{\vec{p}+\vec{k}}) - n(\omega^{(1)}_{\vec{p}})\right]\left[\delta\left(\omega - \omega^{(1)}_{\vec{p}} + \omega^{(2)}_{\vec{p}+\vec{k}}\right) - \delta\left(\omega + \omega^{(1)}_{\vec{p}} - \omega^{(2)}_{\vec{p}+\vec{k}}\right)\right], \tag{7.153}$$

The processes that contribute to $\sigma_0(k,\omega)$ and $\sigma_a(k,\omega)$ are $\Phi \leftrightarrow \chi_1\,\chi_2$ while the processes that contribute to $\sigma_b(k,\omega)$ are $\chi_{1,2} \leftrightarrow \Phi\,\chi_{2,1}$ depicted schematically in fig. (7.5)

The details of the calculation of the different contributions are relegated to the appendix. The result is summarized as follows:

$$\sigma_0(k,\omega) = \frac{g^2}{16\pi Q^2}\,\mathrm{sign}(\omega)\,\Theta[Q^2-(M_1+M_2)^2\,]\left[(Q^2)^2-2Q^2(M_1^2+M_2^2)+(M_1^2-M_2^2)^2\right]^{\frac{1}{2}}\;;\; Q^2=\omega^2-k^2 \tag{7.154}$$

We have explicitly displayed the fact that the zero temperature contribution to the imaginary part is manifestly Lorentz invariant and solely a function of the invariant mass $Q^2 = \omega^2 - k^2$. The finite temperature contributions are

$$\sigma_a(k,\omega;T) = \frac{g^2}{16\pi k\,\beta}\,\mathrm{sign}(\omega)\,\Theta[Q^2-(M_1+M_2)^2\,]\left[\ln\left(\frac{1-e^{-\beta\omega^+_p}}{1-e^{-\beta\omega^-_p}}\right) + M_1 \leftrightarrow M_2\right] \tag{7.155}$$

$$\sigma_b(k,\omega;T) = \frac{g^2}{16\pi k\,\beta}\,\mathrm{sign}(\omega)\,\Theta[(M_1-M_2)^2-Q^2\,]\left[\ln\left(\frac{1-e^{-\beta|\omega_p^-|}}{1-e^{-\beta|\omega_p^+|}}\right)+M_1\leftrightarrow M_2\right] \tag{7.156}$$

where

$$\omega_p^{\pm} = \frac{|\omega|}{2Q^2}(Q^2+M_1^2-M_2^2)\pm\frac{k}{2Q^2}\left[(Q^2+M_1^2-M_2^2)^2-4Q^2M_1^2\right]^{\frac{1}{2}} \;\;;\;\; Q^2=\omega^2-k^2. \tag{7.157}$$

The real part of the self energy is obtained from the dispersive form (7.58) and can be separated into a zero temperature and a finite temperature part as follows

$$\mathrm{Re}\widetilde{\Sigma}^R(k,\omega;T) = \mathrm{Re}\widetilde{\Sigma}_0^R(k,\omega)+\mathrm{Re}\widetilde{\Sigma}_T^R(k,\omega;T) \tag{7.158}$$

with

$$\mathrm{Re}\widetilde{\Sigma}_0^R(k,\omega) = -\frac{1}{\pi}\mathcal{P}\int_{-\infty}^{\infty}\frac{\sigma_0(k_0,k)}{k_0-\omega}\,dk_0 \tag{7.159}$$

$$\mathrm{Re}\widetilde{\Sigma}_T^R(k,\omega;T) = -\frac{1}{\pi}\mathcal{P}\int_{-\infty}^{\infty}\frac{\sigma_a(k_0,k;T)+\sigma_b(k_0,k;T)}{k_0-\omega}\,dk_0 \tag{7.160}$$

where $\mathcal{P}$ stands for the principal part. We note that both $\sigma_0(k,\omega)$ and $\sigma_a(k,\omega)$ feature the standard two particle threshold above the light cone at the invariant mass $Q^2=(M_1+M_2)^2$ whereas the finite temperature contribution $\sigma_b(k,\omega)$ has support for invariant mass $Q^2\leq(M_1-M_2)^2$ even *below the light cone* and vanishes at $T=0$. In the case of massless particles in the loop this contribution is below the light cone and is identified with Landau damping[171, 173, 172]. In particular at zero temperature the isolated poles are at $Q^2=m_P^2$, hence if $m_P^2<(M_1-M_2)^2$ the physical particle pole is embedded in the multiparticle continuum and moves off the real axis onto the second (or higher) Riemann sheet in the complex frequency plane. Because of this the physical particle acquires a width. The spectral density for the case $m_P^2<(M_1-M_2)^2$ is depicted in fig. (7.6)

7.4.0.1 Zero temperature: $\Omega_k;Z;\mathcal{C}_k$: Using that $\sigma_0(k_0,k)$ is odd in k_0 and that it is solely a function of the invariant $P^2=k_0^2-k^2$ for $k_0>0$, it is straightforward to find the following manifestly Lorentz invariant result

$$\mathrm{Re}\widetilde{\Sigma}_0^R(k,\omega) = -\frac{1}{\pi}\mathcal{P}\int_{(M_1+M_2)^2}^{\infty}\frac{\sigma_0(P^2)}{P^2-Q^2}\,dP^2 \;\;;\;\; Q^2=\omega^2-k^2 \tag{7.161}$$

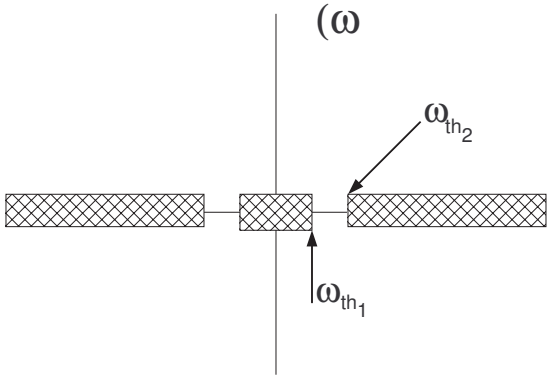

Figure 7.6: Spectral density $\rho(k,\omega,T)$ for $m_P^2 < (M_1-M_2)^2$. The shaded areas are the multiparticle cuts with thresholds $\omega_{th1} = \sqrt{k^2+(M_1-M_2)^2}$ and $\omega_{th2} = \sqrt{k^2+(M_1+M_2)^2}$. The single particle poles at $\Omega_k^2 = k^2 + m_P^2$ moved off the real axis into an unphysical sheet.

where we have explicitly exhibited the two particle threshold in the lower limit. Lorentz invariance requires that the single particle pole features the dispersion relation $\Omega_k^2 = k^2 + m_P^2$, and so the equation that determines the single particle physical poles, namely eqn. (7.118) is given by

$$m_P^2 - m^2 - \mathrm{Re}\widetilde{\Sigma}_0^R(Q^2 = m_P^2) = 0 \tag{7.162}$$

From the results of the previous section (see eqn. (7.130)) the wave function renormalization constant is given by

$$Z^{-1} = 1 + \frac{1}{\pi}\mathcal{P}\int_{(M_1+M_2)^2}^{\infty} \frac{\sigma_0(P^2)}{(P^2-m_P^2)^2}\, dP^2\,, \tag{7.163}$$

Separating the residue at the physical particle pole and following the steps described in section (7.3.2) the renormalized spectral density (7.136,7.137) at zero temperature can now be written in the following simple form

$$\begin{aligned}\rho_r(k,\omega;T=0) &= \frac{1}{\pi}\frac{\left[\sigma_{0,r}(Q^2)+2\omega\epsilon\right]}{\left[(Q^2-m_P^2)\Big(1-\Pi_{0,r}(Q^2)\Big)\right]^2 + \left[\sigma_{0,r}(Q^2)+2\omega\epsilon\right]^2} \\ &= \mathrm{sign}(\omega)\,\delta(\omega^2-\Omega_k^2) + \rho_{c,r}(k,\omega;T=0)\end{aligned} \tag{7.164}$$

where $\sigma_{0,r}(k,\omega) = Z\sigma_0(k,\omega)$ is given by the expression (7.154) but with the coupling constant replaced by the renormalized coupling $Zg^2 = g_r^2$

The continuum contribution is given by

$$\rho_{c,r}(k,\omega;T=0) = \frac{1}{\pi}\frac{\sigma_{0,r}(Q^2)}{\Big[(Q^2-m_P^2)\Big(1-\Pi_{0,r}(Q^2)\Big)\Big]^2 + \Big[\sigma_{0,r}(Q^2)\Big]^2}\ , \tag{7.165}$$

with

$$\Pi_{0,r}(Q^2) = -\frac{1}{\pi}(Q^2-m_P^2)\ \mathcal{P}\int_{(M_1+M_2)^2}^{\infty}\frac{\sigma_{0,r}(P^2)}{(P^2-Q^2)(P^2-m_P^2)^2}\ dP^2 \tag{7.166}$$

where we have made explicit the two particle threshold in the lower limit of the integral.

The *exact* expression for Z given by the sum rule (7.120) coincides with Z given by eqn. (7.163) to lowest order in perturbation theory ($\mathcal{O}(g^2)$).

Up to $\mathcal{O}(g^2)$ we can neglect $\sigma_0(k,\omega)$ as well as $\Pi_{0,r}(k,\omega)$ in the denominator of the continuum contribution (7.165) because $Q^2 \geq (M_1^2+M_2^2) > m_P^2$ and the denominator is never perturbatively small. Therefore to leading order in the coupling we can approximate

$$\rho_{c,r}(k,\omega;T=0) \simeq \frac{1}{\pi}\frac{\sigma_{0,r}(Q^2)}{(Q^2-m_P^2)^2}\ . \tag{7.167}$$

The renormalized spectral function at finite temperature can be separated into the contributions from the different multiparticle cuts,

$$\rho_r(k,\omega,T) = \rho_{I,r}(k,\omega,T) + \rho_{II,r}(k,\omega,T) \tag{7.168}$$

where the contribution with support above the two particle cut is

$$\rho_{I,r}(k,\omega;T) = \frac{1}{\pi}\frac{[\sigma_{0,r}(k,\omega)+\sigma_{a,r}(k,\omega;T)]}{\Big[(Q^2-m_P^2)\Big(1-\Pi_{0,r}(Q^2)\Big) - \mathrm{Re}\widetilde{\Sigma}^R_{T,r}(k,\omega;T)\Big]^2 + \Big[\sigma_{0,r}(Q^2)+\sigma_{a,r}(k,\omega;T)\Big]^2} \tag{7.169}$$

and that which has support below the light cone given by

$$\rho_{II,r}(k,\omega;T) = \frac{1}{\pi}\frac{\sigma_b(k,\omega;T)}{\Big[(Q^2-m_P^2)\Big(1-\Pi_{0,r}(Q^2)\Big) - \mathrm{Re}\widetilde{\Sigma}^R_{T,r}(k,\omega;T)\Big]^2 + \Big[\sigma_{b,r}(k,\omega;T)\Big]^2} \tag{7.170}$$

where again the renormalized quantities are obtained from the unrenormalized ones by replacing $g \to g_r = Zg$.

Since $\rho_{I,r}(k,\omega)$ has support only for $|\omega| > \sqrt{k^2 + (M_1^2 + M_2^2)}$ its denominator is never perturbatively small, therefore to leading order $\mathcal{O}(g^2)$ in the perturbative expansion it can be approximated by

$$\rho_{I,r}(k,\omega;T) \simeq \frac{1}{\pi} \frac{[\sigma_{0,r}(k,\omega) + \sigma_{a,r}(k,\omega;T)]}{(\omega^2 - k^2 - m_P^2)^2} \tag{7.171}$$

For $\rho_{II,r}(k,\omega)$ we must keep the full expression because for $m_P^2 < (M_1 - M_2)^2$ the denominator becomes perturbatively small for $\omega^2 \sim k^2 + m_P^2$. Therefore the final expression for the asymptotic distribution function (7.139) to leading order in the coupling ($\mathcal{O}(g^2)$) is given by

$$\mathcal{N}(k,T) = \mathcal{N}_I(k;T) + \mathcal{N}_{II}(k,T) \tag{7.172}$$

where the different contributions reflect the different multiparticle cuts, namely

$$\mathcal{N}_{II}(k,T) = \int_0^\infty \left(\frac{\omega^2 + \Omega_k^2}{2\,\Omega_k}\right) \Big\{ [1 + 2n(\omega)]\, \rho_{II,r}(k,\omega,T) \Big\}\, d\omega \; - \frac{1}{2} \tag{7.173}$$

$$\mathcal{N}_I(k,T) = \frac{2}{\pi} \int_{\omega_{th}(k)}^\infty \left[\frac{\omega^2 + \Omega_k^2}{2\,\Omega_k(\omega^2 - \Omega_k^2)^2}\right] \Big\{ n(\omega) \Big[\sigma_{0,r}(k,\omega) + \sigma_{a,r}(k,\omega;T)\Big] + \frac{1}{2}\sigma_{a,r}(k,\omega;T) \Big\}\, d\omega\,, \tag{7.174}$$

where $\omega_{th}(k) = \left[k^2 + (M_1 + M_2)^2\right]^{\frac{1}{2}}$ is the two particle cut.

7.4.1 The approach to equilibrium:

Before we study the asymptotic distribution function we address the approach to equilibrium. The time evolution of the (interpolating) number operator $N_k(t)$ given by eqns. (7.90-7.92) is completely determined by the real time evolution of the solution $f_k(t)$ given by eqn. (7.77). For $m_P < |M_1 - M_2|$ the particle acquires a width through the two body decay of the heavier particle in the bath and the particle pole is now embedded in the continuum for $Q^2 < (M_1 - M_2)^2$, which is the relevant part of the spectral density is $\sigma_b(k,\omega,T)$ given in eqn. (7.156). In the Breit Wigner approximation, the spectral density is given by eqns. (7.94,7.93,7.95) with

$$\Gamma_k(T) = \mathcal{Z}_k \frac{\sigma_b(k, \mathcal{W}_k(T), T)}{2\,\mathcal{W}_k(T)} \tag{7.175}$$

The real time evolution of the solution $f_k(t)$ in the Breit-Wigner approximation is given by eqn. (7.100). Figure (7.7) displays both the *exact* solution (7.77) and the Breit-Wigner approximation

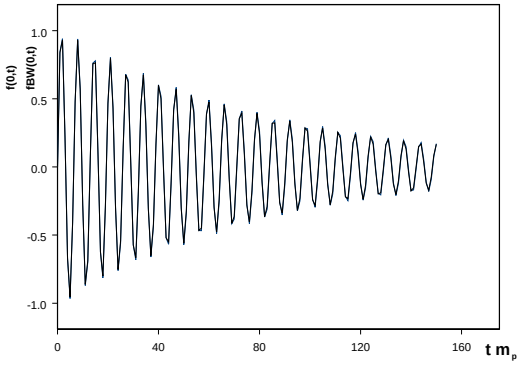

Figure 7.7: The functions $f_{k=0}(t)$ and $f^{BW}_{k=0}(t)$ vs $t\,m_P$ for $g^2/(16\pi^2 m_P^2) = 0.01$ $M_1 = 4m_P$; $M_2 = m_P$; $T = 10m_P$. For these values of the parameters we find numerically: $\mathcal{Z}_0(T) = 0.998$, $\mathcal{W}_0(T) = 0.973m_P$, $\Gamma_0(T) = 0.012m_P$. The exact solution and the Breit-Wigner approximation are indistinguishable.

(7.100) for $k = 0$. The exact and approximate solutions are indistinguishable during the time scale of the numerical evolution as gleaned from this figure.

The asymptotic long time evolution is determined by the behavior of the spectral density near the thresholds and is typically of the form of a power law[174]. However, such asymptotic behavior sets in at very long times, beyond the regime in which our numerical study is trustworthy. It is numerically exceedingly difficult to extract the exponential relaxation from the power laws that dominate at asymptotically long time because the amplitude becomes very small in the weak coupling case.

The main conclusion is that the distribution function approaches thermalization and becomes insensitive to the initial conditions for time scales $t > \tau_k = 1/2\Gamma_k(T)$, where $\Gamma_k(T)$ is the quasiparticle relaxation rate.

7.4.2 The asymptotic distribution function:

In the Breit-Wigner approximation and assuming a very narrow resonance near the physical particle pole

$$\rho_{II,r}(k,\omega,T) \sim \frac{1}{\pi}\frac{\mathrm{sign}(\omega)\,\Gamma_k}{(\omega^2-\Omega_k^2)^2+\Gamma_k^2} \sim \mathrm{sign}(\omega)\delta(\omega^2-\Omega_k^2) \tag{7.176}$$

where in the second term on the right hand side the width has been neglected by assuming a very narrow resonance at Ω_k. Therefore in this narrow width approximation one would expect that the different contributions are given by

$$\mathcal{N}_{II}(k,T) \sim n(\Omega_k) \;\; ; \;\; \mathcal{N}_I(k,T) = \mathcal{O}(g^2) \tag{7.177}$$

where $n(\Omega_k)$ is the Boltzmann distribution function for the stable particle. This rather simple analysis would lead to the conclusion that the corrections to the equilibrium abundance are perturbatively small.

However, even for weakly coupled theories we expect this simple argument to be incorrect both in the high and low temperature regimes. The main reason for this expectation is that the approximation (7.176) suggests that this argument neglects the fact that the spectral density has support for frequencies *smaller* than the position of the physical particle pole (namely for $|\omega| \neq \Omega_k$). From the expression (7.173) it is clear that the region of small ω will lead to a substantial correction since for $\omega \ll T$ the Bose-Einstein distribution function in (7.173) becomes $n(\omega) \sim T/\omega >> 1$, thus the region of $|\omega| < \Omega_k$ and in particular $|\omega| \ll T$ gives a non-trivial contribution to the abundance. The region of spectral density for $|\omega| > \Omega_k$ will yield a much smaller, but non-negligible contribution. Furthermore in the high temperature limit $T \gg k, m_P, M_{1,2}$ the width is expected to become large. This can be gleaned from the expression for $\sigma_b(\omega,k,T)$ in eqn. (7.153), which for $T \gg \omega_p^{1,2}$ is proportional to T. This is clearly a statement that at high temperatures there is a large population of heavy particles which results in a larger number of processes $\chi_1 \leftrightarrow \Phi\,\chi_2$ in the medium, thereby increasing the width of the particle Φ. As the width of the spectral density near the physical particle pole increases, the spectral density has larger support in the small ω region, thereby increasing the off-shell contributions to the abundance. These arguments will be confirmed both analytically and numerically below.

We now study numerically and analytically the asymptotic distribution function to assess precisely the magnitude and origin of the corrections to the equilibrium abundance. The parameter

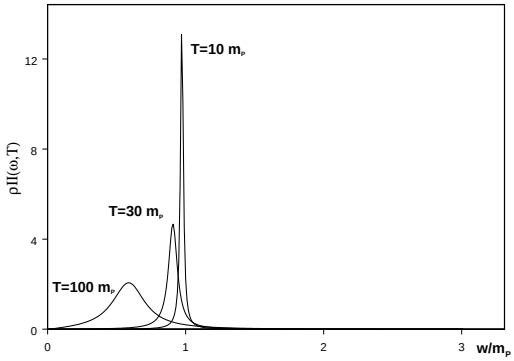

Figure 7.8: The spectral density $\rho_{II}(k=0,\omega,T)$ vs ω/m_P for $g^2/(16\pi^2 m_P^2) = 0.01$ $M_1 = 4m_P$; $M_2 = m_P$ and $T/m_p = 10, 30, 100$ respectively.

space is fairly large, thus we consider separately the cases of small momenta $k \ll m_P, M_1, M_2, T$ and the case of large momenta $k \gg m_P, M_1, M_2, T$ choosing the unit of energy to be the zero temperature pole mass of the particle, m_P and keeping the value of the masses of the heavy fields fixed with $M_1 > M_2 + m_P$.

7.4.2.1 $k = 0$ The limit $k = 0$ of the spectral density can be easily obtained from the expressions given above (7.154-7.156). Of particular importance is the high temperature limit of $\sigma_b(0,\omega,T)$ since this contribution to the spectral density determines the width of the spectral function near the physical particle pole $\Gamma_0(T)$ given by eqn. (7.175).

A straightforward calculation leads to the following result in the limit $T \gg m_P$, $M_{1,2}$,

$$\frac{\sigma_b(0,m_P,T)}{2\,m_P} = \frac{g^2 T}{8\pi^2}\,\frac{\left[m_P^4 + (M_1^2 - M_2^2)^2 - 2m_P^2(M_1^2 + M_2^2)\right]^{\frac{1}{2}}}{\left[(M_1^2 - M_2^2)^2 - m_P^4\right]} \tag{7.178}$$

We note that this expression for the width is *classical* since restoring $g^2 \to g^2\hbar\,; T \to T/\hbar$ the expression above is independent of $\hbar$. This is a consequence of the fact that the high temperature limit is completely determined by the Rayleigh-Jeans part of the Bose-Einstein distribution function. As a result when the temperature is much larger than all mass scales, the width is proportional to T and the spectral density becomes wider, enhancing the off-shell contributions. Fig.

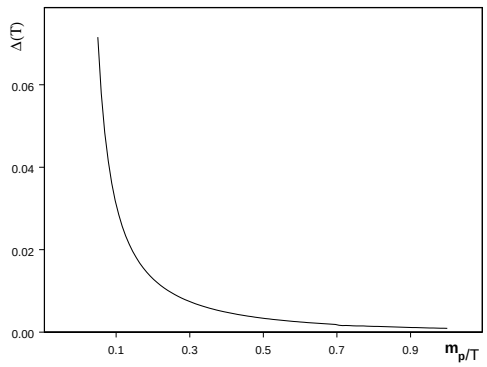

Figure 7.9: The ratio $\Delta(T) = (\mathcal{N}(0,T) - n(m_P))/n(m_P)$ vs m_P/T for $g^2/(16\pi^2 m_P^2) = 0.01$ $M_1 = 4m_P$; $M_2 = m_P$.

(7.8) displays the spectral density for several values of the temperature highlighting the broadening for large temperature. It is clear from this figure that at very high temperatures perturbation theory breaks down in this model since the width can become comparable to the physical mass or the position of the pole. This situation has been previously noticed in a scalar field theory at high temperatures, and a finite temperature renormalization group was introduced to provide a non-perturbative resummation[175].

Restricting ourselves to the regime in temperature within which perturbation theory is still reliable, namely for $\Gamma_0(T) \ll m_P$, we study the departure of the distribution function from the Bose-Einstein form (for $k = 0$) numerically.

Figure (7.9) displays the quantity

$$\Delta(T) = \frac{\mathcal{N}(k=0,T) - n(m_P)}{n(m_P)} \tag{7.179}$$

for a weakly coupled case in the range of temperatures $1 \leq T/m_p \leq 20$ for $M_1 = 4m_P$, $M_2 = m_P$ within which we find numerically that $\Gamma_0(T)/m_P \leq 0.1$ which we use as a reasonable criterion for the validity of perturbation theory (see fig. 7.8).

This figure clearly indicates that even within the high temperature regime where perturbation theory is reliable and the spectral density still features a rather narrow Breit-Wigner peak, there

are substantial departures from the Bose-Einstein form in the equilibrium distribution function. At low temperatures fig. (7.9) clearly displays an exponential suppression and the distribution function essentially becomes the Bose-Einstein distribution. In this limit the width is extremely small and the spectral density is almost a delta function on the physical particle mass shell, and the off-shell effects are perturbatively small.

7.4.2.2 $k \gg T, m_P, M_{1,2}$ In the limit of large momenta several interesting features emerge: i) the width of the spectral density becomes very small, this is a consequence of the fact that there are very few heavy states for large momenta in the heat bath if the momentum is large. The width as a function of k is depicted in fig. (7.10), which displays clearly this behavior. ii) As a function of the variable ω, the position of the peak in the spectral density becomes closer to the threshold for $k \gg m_P, M_{1,2}$. As a result of both these effects the spectral distribution becomes strongly peaked near threshold and the threshold moves to larger values of the frequency, thus leaving behind a larger region of the spectra off-shell for frequencies *smaller* than the position of the peak. The spectral density while small away from the peak is, however, non-vanishing and the fact that there is now a larger region in frequency ω below the (narrow) peak, brings about a competition of scales as can be understood from the following argument. The very narrow peak (almost a delta function at $\omega = \Omega_k \sim k$) leads to a contribution $\mathcal{N}_{II}(k,T) \sim n(\Omega_k)$, which for $k \gg T$ is $\ll 1$. This on-shell contribution competes against the off-shell contributions from integrating the spectral density for $\omega < \Omega_k$ which is also very small because $\sigma_b(k,\omega,T)/\Omega_k^2 \ll 1$ but for $\omega \ll T$ is multiplied by the Bose enhancement factor $\sim T/\omega$. The competition between the "on-shell" contribution $n(\Omega_k)$ and the off-shell contributions is studied numerically.

Fig. (7.11) displays both the Bose-Einstein distribution function $n(\Omega_k)$ and the asymptotic distribution function $\mathcal{N}(k,T)$ in the limit $k \gg T, m_P, M_{1,2}$.

It is clear from this figure that while the distribution function $\mathcal{N}(k,T)$ is strongly suppressed for $k \gg T$ it is *larger* than the Bose-Einstein distribution. The main reason for this enhancement is precisely the competition mentioned above, namely the position of the peak in the spectral density moves towards threshold which for large k corresponds to large values of the frequency ω. Therefore there is a large region in which the spectral density is very small but non-vanishing for $\omega < \Omega_k$. Clearly the part of the spectral density with support for $\omega > \Omega_k$ yields a much smaller contribution to the distribution function. Furthermore, for $\omega \ll T$ the factor $n(\omega) \sim T/\omega \gg 1$ which enhances further the off-shell contributions.

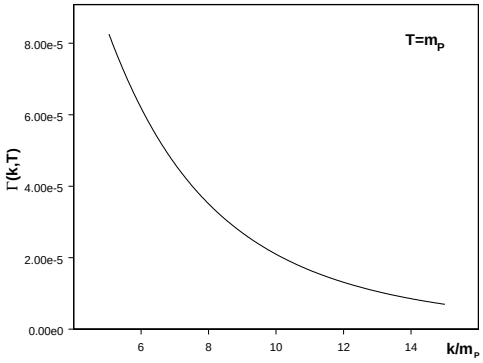

Figure 7.10: The width $\Gamma(k,T)$ in units of m_P vs k/m_P for $k \gg T$ for $T = m_P$ for $g^2/(16\pi^2 m_P^2) = 0.01$ $M_1 = 4m_P$; $M_2 = m_P$.

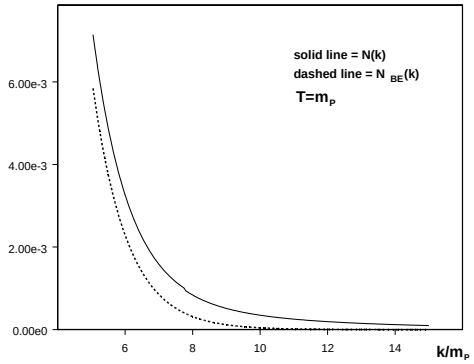

Figure 7.11: The distribution functions $\mathcal{N}(k,T)$ given by eqn. (7.172) (solid line) vs. the Bose-Einstein distribution $N_{BE}(k,T)$ (dashed line) as a function of k/m_P for $T = m_P$; $g^2/(16\pi^2 m_P^2) = 0.01$; $M_1 = 4m_P$; $M_2 = m_P$.

These results in the different regimes can be summarized as follows:

- In the high temperature regime the larger abundance of heavier particles in the bath leads to a broadening of the spectral density. This broadening in turn results in a larger off-shell

contribution to the abundance $\mathcal{N}(k,T)$ and an enhancement of the distribution function over the Bose-Einstein result. The off-shell region of small frequency yields a substantial contribution because of the factor $n(\omega) \sim T/\omega$ in (7.139). In the model considered perturbation theory breaks down at high temperature and the imaginary part on-shell becomes classical. This situation is akin to the case of a self-interacting bosonic field theory studied in ref. [175]. A high temperature renormalization group resummation program such as in ref.[175] may be required to provide a non-perturbative resummation.

- For momenta much larger than the mass scales and the temperature there is also a large enhancement of the distribution function $\mathcal{N}(k,T)$ over the Bose-Einstein result. In this case the spectral density features a very narrow resonance near the position of the physical pole at $\omega \simeq \Omega_k$, which however moves closer to threshold. For large k the off-shell region of support of the spectral density becomes larger and though the spectral density is strongly suppressed, the off-shell contribution from the region $\omega < \Omega_k$ competes with the contribution from the on-shell pole, namely the Bose-Einstein distribution function $n(\Omega_k)$ because for $k >> T$ $n(\Omega_k) \ll 1$. The off-shell contribution from the region $\omega << \Omega_k$ is comparable to or larger than $n(\Omega_k)$ for $k \gg T$ and is enhanced in the region $\omega \ll T$ by the factor $n(\omega) \sim T/\omega$.

While these results may be particular to the model studied, we expect most of these features to be robust and fairly general. In particular at high temperature it is physically reasonable to expect a thermal broadening of the spectral density either from collisions, many-body decays or Landau damping as in the case studied here. Broadening of the spectral function yields a larger contribution from the small ω region which is enhanced further by the factor $n(\omega) \sim T/\omega$ for $\omega \ll T$. Therefore a substantial departure of the distribution function $\mathcal{N}(k,T)$ from the Bose-Einstein distribution is expected at high temperature. A possible breakdown of perturbation theory in the high temperature regime may require the implementation of a non-perturbative resummation procedure akin to that introduced in ref.[175]. At low temperatures, much lower than the mass and momentum scales a departure from simple Bose-Einstein is also expected. In this case even though the spectral function features a sharp and narrow peak at a position very near the physical particle pole, the Bose-Einstein distribution function is very small. Hence the off-shell region $\omega << \Omega_k$ of the spectral function will lead to a substantial contribution which is further enhanced by the factor $n(\omega) \sim T/\omega$ for $\omega \ll T$. Again because the temperature is much smaller than any of the scales, the spectral density will be exponentially suppressed off shell and the equilibrium abundance will reflect this suppression, but just as in the case studied here, may still be larger than the simple Bose-Einstein

abundance. Of course our study within this particular model serves only as a guidance and the details of the enhancement will depend on the theory under consideration, but the main lesson learned here is that the off-shell, small frequency region of the spectral density yields a substantial contribution to the equilibrium abundance in interacting theories.

7.5 BOLTZMANN KINETICS IN RENORMALIZED PERTURBATION THEORY

It is important to understand the origin of the differences between the quantum kinetic equation for the distribution function (7.90) and the usual quantum Boltzmann equation. Therefore in this section we provide a derivation of the quantum Boltzmann equation in *renormalized perturbation theory* to highlight the origin of the different equilibrium abundances. We assume that the bath is in equilibrium just as we did in our derivation of the effective action and the time evolution for the distribution function in the previous sections.

The quantum Boltzmann equation is a differential equation for the single particle distribution function. However, as we have discussed in detail above, the *physical* particles have mass m_P and the Heisenberg field operators create physical particles out of the vacuum with an amplitude determined by the wave function renormalization. Therefore in order to account for the mass and wave function renormalization, and to obtain the kinetic Boltzmann equation for the physical particles it is convenient to re-write the Lagrangian by introducing counterterms, namely

$$\mathcal{L} = \frac{1}{2}\partial_\mu\Phi_r\partial^\mu\Phi_r - \frac{1}{2}m_P^2\Phi_r^2 + \sum_{i=1}^{2}\left[\frac{1}{2}\partial_\mu\chi_i\partial^\mu\chi_i - \frac{1}{2}M_i^2\chi_i^2\right] - g_r\Phi_r\,\chi_1\,\chi_2 + \mathcal{L}_{count} + \mathcal{L}_{int}[\chi_1\,;\,\chi_2] \tag{7.180}$$

$$\mathcal{L}_{count} = \frac{1}{2}(Z-1)\partial_\mu\Phi_r\partial^\mu\Phi_r - \frac{1}{2}\Delta m^2\Phi_r^2 \tag{7.181}$$

where $g_r = \sqrt{Z}g$ and we assume that the renormalization aspects of the fields $\chi_{1,2}$ had already been included in $\mathcal{L}_{int}[\chi_1\,;\,\chi_2]$. The counterterms in (7.181) are treated systematically in perturbation theory along with the cubic interaction. Note that $Z-1\,,\,\Delta m^2$ are both of $\mathcal{O}(g^2)$.

The renormalized field Φ_r is expanded in terms of creation and annihilation operators of physical Fock states,

$$\Phi_r(\vec{x},t) = \frac{1}{\sqrt{V}}\sum_{\vec{k}}\Phi_{\vec{k}}(t)e^{i\vec{k}\cdot\vec{x}} \tag{7.182}$$

$$\Phi_{\vec{k}}(t) = \frac{1}{\sqrt{2\Omega_k}}\left[a_{\vec{k}}\,e^{-i\Omega_k\,t} + a^{\dagger}_{-\vec{k}}\,e^{i\Omega_k\,t}\right] \tag{7.183}$$

and a similar expansion for the bath fields χ_1, χ_2 in terms of creation and annihilation operators and the corresponding frequencies $\omega_k^{(1,2)}$. The total interaction Lagrangian is

$$L_{int} = \frac{g_r}{\sqrt{V}}\sum_{\vec{k}}\sum_{\vec{p}}\Phi_k\,\chi_{1,\vec{p}}\,\chi_{2,-\vec{p}-\vec{k}} + L_{count} \tag{7.184}$$

where L_{count} is the counterterm Lagrangian. The kinetic Boltzmann equation for the occupation number of the Fock quanta of the field Φ is

$$\frac{dN_k}{dt} = \frac{dN_k}{dt}\bigg|_{gain} - \frac{dN_k}{dt}\bigg|_{loss} \tag{7.185}$$

The gain and loss terms are obtained by calculating the transition *probabilities* per unit time for processes that lead to the increase (gain) and decrease (loss) the occupation number, namely $dN_k(t)/dt = dP_k/dt$. Within the framework of the kinetic description such calculation is carried out by implementing Fermi's Golden rule. The processes that lead to the increase or decrease of the population are read-off the interaction and energy conservation emerges as a consequence of taking the long time limit as is manifest in Fermi's Golden rule. The cubic interaction term in L_{int} gives rise to several different processes which are gleaned by expanding the product in terms of the creation and annihilation operators of all the fields involved. The different phases that enter in such terms determine the energy conservation delta functions in Fermi's Golden rule. Some of the processes are depicted in fig. (7.5). When $m_P < M_1, M_2$ the quanta of the field Φ cannot decay into those of the bath fields, however if $M_1 > M_2 + m_P$ (or $M_2 > M_1 + m_P$) the heavier bath field can decay into particles of Φ therefore increasing the population. This process is depicted in fig. (7.5-(b)). The inverse process contributes to the loss term. Let us consider the case $M_1 > M_2 + m_P$ (the case $M_2 > M_1 + m_P$ is similar by $M_2 \leftrightarrow M_1$). The *only process* that leads to the gain in the population by energy conservation is $\chi_1 \to \Phi\,\chi_2$ and consequently the *only* process that leads to the loss of population with energy conservation is the inverse process of annihilation $\Phi\,\chi_2 \to \chi_1$. The calculation of the gain and loss terms is as follows: consider the initial Fock state $|N_{\vec{k}}, n^{(1)}_{\vec{p}}, n^{(2)}_{\vec{p}+\vec{k}}\rangle$ where N is the occupation of particles of Φ and $n^{(1,2)}$ that for the respective bath fields. To lowest

order in the coupling g the interaction from the counterterm Lagrangian does not contribute to the gain or loss, but only to forward scattering since these terms are already of $\mathcal{O}(g^2)$ and the transition probabilities will be at least of (g^3). Thus to lowest order $\mathcal{O}(g^2)$, the gain term arises from the following matrix element

$$\mathcal{M}_{gain} = -\frac{ig_r}{\sqrt{V}}\langle N_{\vec{k}}+1, n^{(1)}_{\vec{p}}-1, n^{(2)}_{\vec{p}+\vec{k}}+1\Big| \int_{-\infty}^{\infty} dt\, \Phi_k(t)\, \chi_{1,\vec{p}}(t)\, \chi_{2,-\vec{p}-\vec{k}}(t)\Big| N_{\vec{k}}, n^{(1)}_{\vec{p}}, n^{(2)}_{\vec{p}+\vec{k}}\rangle \quad (7.186)$$

The limits in the time integral had been extended to $\pm\infty$ according to Fermi's Golden rule which leads to energy conservation. The calculation of this matrix element is straightforward, taking the absolute value squared of this matrix element, summing over $\vec{p}$ and averaging over the occupation numbers of the particles in the bath, which is assumed in equilibrium, one obtains the inclusive transition probability

$$P_{gain} = \frac{2\,t}{2\Omega_k}\frac{g^2}{32\pi^2}\Big(1+N_k\Big)\int \frac{d^3\vec{p}}{\omega^{(1)}_{\vec{p}}\omega^{(2)}_{\vec{p}+\vec{k}}}\, n(\omega^{(1)}_{\vec{p}})\left[1+n(\omega^{(2)}_{\vec{p}+\vec{k}})\right]\delta\left(\Omega_k+\omega^{(2)}_{\vec{p}+\vec{k}}-\omega^{(1)}_{\vec{p}}\right) \quad (7.187)$$

where $n(\omega^{(1,2)}_{\vec{p}})$ are the Bose-Einstein distribution functions since the thermal bath is assumed to remain in equilibrium. To obtain the above expression we have used $\left|2\pi\delta\left(\Omega_k+\omega^{(2)}_{\vec{p}+\vec{k}}-\omega^{(1)}_{\vec{p}}\right)\right|^2 = 2\pi\delta\left(\Omega_k+\omega^{(2)}_{\vec{p}+\vec{k}}-\omega^{(1)}_{\vec{p}}\right)t$ where t is the total interaction time. A similar calculation leads to the total transition probability for the loss process:

$$P_{loss} = \frac{2\,t}{2\Omega_k}\frac{g^2}{32\pi^2}N_k\int \frac{d^3\vec{p}}{\omega^{(1)}_{\vec{p}}\omega^{(2)}_{\vec{p}+\vec{k}}}\left[1+n(\omega^{(1)}_{\vec{p}})\right]n(\omega^{(2)}_{\vec{p}+\vec{k}})\,\delta\left(\Omega_k+\omega^{(2)}_{\vec{p}+\vec{k}}-\omega^{(1)}_{\vec{p}}\right) \quad (7.188)$$

The kinetic equation can now be written in the following form

$$\frac{dN_k}{dt} = (1+N_k)\,\gamma^{>}_k - N_k\,\gamma^{<}_k \quad (7.189)$$

The gain and loss rates are given by

$$\gamma^{>}_k = \frac{2}{2\Omega_k}\frac{g^2}{32\pi^2}\int \frac{d^3\vec{p}}{\omega^{(1)}_{\vec{p}}\omega^{(2)}_{\vec{p}+\vec{k}}}\, n(\omega^{(1)}_{\vec{p}})\left[1+n(\omega^{(2)}_{\vec{p}+\vec{k}})\right]\delta\left(\Omega_k+\omega^{(2)}_{\vec{p}+\vec{k}}-\omega^{(1)}_{\vec{p}}\right) \quad (7.190)$$

$$\gamma^{<}_k = \frac{2}{2\Omega_k}\frac{g^2}{32\pi^2}\int \frac{d^3\vec{p}}{\omega^{(1)}_{\vec{p}}\omega^{(2)}_{\vec{p}+\vec{k}}}\left[1+n(\omega^{(1)}_{\vec{p}})\right]n(\omega^{(2)}_{\vec{p}+\vec{k}})\,\delta\left(\Omega_k+\omega^{(2)}_{\vec{p}+\vec{k}}-\omega^{(1)}_{\vec{p}}\right) \quad (7.191)$$

Since the bath particles are in thermal equilibrium with a Bose-Einstein distribution function the detailed balance condition follows, namely

$$\gamma_k^> = e^{-\beta\,\Omega_k}\,\gamma_k^< \tag{7.192}$$

The solution of the Boltzmann kinetic equation (7.189) is the following

$$N_k(t) = n(\Omega_k) + [N_k(0) - n(\Omega_k)]e^{-\gamma_k\,t} \tag{7.193}$$

where

$$\gamma_k = \gamma_k^< - \gamma_k^> = \frac{2}{2\Omega_k}\,\frac{g^2}{32\pi^2}\int \frac{d^3\vec{p}}{\omega_{\vec{p}}^{(1)}\omega_{\vec{p}+\vec{k}}^{(2)}}\left[n(\omega_{\vec{p}+\vec{k}}^{(2)}) - n(\omega_{\vec{p}}^{(1)})\right]\delta\left(\Omega_k - \omega_{\vec{p}}^{(1)} + \omega_{\vec{p}+\vec{k}}^{(2)}\right) \tag{7.194}$$

Comparing this expression with those for the imaginary part of the self energy given by the expressions (7.150,7.151,7.152,7.153) it is straightforward to see that

$$\gamma_k = 2\,\frac{\mathrm{Im}\tilde{\Sigma}_r^R(k,\Omega_k,T)}{2\Omega_k} \tag{7.195}$$

where

$$\mathrm{Im}\tilde{\Sigma}_r^R(k,\Omega_k,T) = \sigma_{b,r}(k,\Omega_k,T) \tag{7.196}$$

This expression for the relaxation rate should be compared to the decay rate for the single *quasiparticle* Γ_k given by eqn. (7.96,7.100)). Since the quasiparticle residue in perturbation theory is $\mathcal{Z}_k(T) = 1 + \mathcal{O}(g^2)$ and the difference between the quasiparticle frequency $\mathcal{W}_k(T)$ and the single particle frequency Ω_k is of $\mathcal{O}(g^2)$ to leading order in the coupling g, the relaxation rate of the distribution function γ_k and that of the single quasiparticle Γ_k (see eqn. (7.96)) is

$$\gamma_k = 2\Gamma_k + \mathcal{O}(g^4) \tag{7.197}$$

We have provided this derivation of the usual quantum Boltzmann equation and its solution in the case when the bath remains in equilibrium to highlight the similarities and differences with the real time evolution of the distribution function given by eqn. (7.90):

- The derivation above clearly shows that the Fock states that enter in the matrix elements (7.186) are the asymptotic free field Fock states associated with physical particles of mass m_P. This is

similar to the definition of the interpolating number operator (7.82) which is based on the free field asymptotic physical states, and includes both mass and wave-function renormalization.

- By implementing Fermi's golden rule, namely taking the time interval to infinity, thereby enforcing the *on shell delta function*, extracting the linear time dependence and dividing by time to provide a *local* differential equation for the time evolution of the distribution function all memory aspects have been neglected. Namely implementing Fermi's golden rule results in neglecting memory effects, which in turn results in only *on-shell processes* contributing to the rate equation. Contrary to this, the real time evolution of the distribution function (7.90) includes memory effects as is manifest in the time integrals (7.91,7.92) in (7.90). In turn these time integrals keep memory of the past time evolution, and at asymptotically long time lead to the full spectral density as manifest in eqn. (7.103), not just an on-shell delta function. The presence of the full spectral density in the asymptotic distribution includes the off-shell contributions discussed in the previous section. This discussion brings to the fore that one of the main origins of the differences can be traced to memory effects and the fact that the real time evolution of the distribution function (7.90) is *non-Markovian*. The memory of the past time evolution translates in off-shell processes through the full spectral density.
- As emphasized in section (7.2) the expression (7.90) for the quantum kinetic distribution function implies a Dyson-like resummation of the perturbative expansion and includes consistently the renormalization aspects associated with asymptotic single particle states, namely the correct pole mass and the wave function renormalization. The dependence of the asymptotic distribution function on the full spectral density is a consequence of the fluctuation-dissipation relation.

7.6 CONCLUSIONS

Motivated by a critical reassessment of the applicability of Boltzmann kinetics in the early Universe, in this chapter we studied the abundance of physical quanta of a field Φ in a thermal plasma by introducing a quantum kinetic description based on the non-equilibrium effective action for this field. We focused on understanding the equilibrium abundance of *particles that are stable in the vacuum* and interact with *heavier* particles which constitute a thermal bath.

The non-equilibrium effective action is obtained by integrating out the heavy particles to lowest

order in the coupling of the field Φ to the bath but in principle to all orders in the coupling of the heavy fields amongst them. We show that the non-equilibrium effective action leads to a Langevin stochastic description with a Gaussian but colored noise and a non-Markovian self-energy kernel. The correlation function of the noise and the non-Markovian self-energy kernel are related by a generalized fluctuation dissipation relation. The correlation functions are determined by the solution of this Langevin equation which furnishes a Dyson resummation of the perturbative expansion. We introduced a definition of the single physical particle distribution function in terms of a fully renormalized interpolating Heisenberg number operator based on asymptotic theory. The real time evolution of this single particle distribution function is completely determined by the solution of the Langevin equation.

We show that in a heat bath at finite temperature this number operator becomes insensitive to the initial conditions after a time scale $\approx 1/2\,\Gamma_k(T)$, where $\Gamma_k(T)$ is the *single quasiparticle* relaxation rate. We prove that the asymptotic long time limit of this distribution function describes full thermalization of the Φ particle with the thermal bath. The equilibrium distribution function depends on the full spectral density and includes off-shell corrections as a result of the non-Markovian real time evolution (with memory) and the fluctuation-dissipation relation. Its expression is given by eqn. (7.139). We argue that while we obtained the distribution function in the case of a field linearly coupled to a thermal bath of heavier particles, the final form of the distribution function at asymptotically long time is much more generally applicable.

In order to provide a detailed assessment of novel specific features of the distribution function in particular departure from the usual Bose-Einstein distribution, we considered a model in which the thermal bath is described by two heavy bosonic fields $\chi_{1,2}$ coupled to the field Φ as $g\,\Phi\,\chi_1\,\chi_2$, with $M_1 > M_2 + m_p$ and m_p the pole mass of the field Φ. We obtained the real time effective action at one loop level. We find that the in-medium processes of two body decay of the heavier particle, and its recombination, namely $\chi_1 \leftrightarrow \chi_2\Phi$ results in a width for the Φ-particle and a broadening of its spectral density. A detailed study of the single (physical) particle distribution function reveals substantial corrections to the Bose-Einstein distribution at high temperature as well as low temperature but large momentum. At high temperature the spectral density broadens dramatically and the off-shell contributions become very substantial resulting in an enhancement of the abundance with respect to the Bose-Einstein distribution. We found that at very high temperatures, perturbation theory breaks down and a resummation of the perturbative expansion via the renormalization group at finite temperature may be required[175]. This case must be studied

further.

In the limit where the momentum of the particle is much larger than the temperature and the masses, our analysis also reveals a substantial departure from the Bose-Einstein distribution. In this case the spectral density is sharply peaked near the (zero temperature) physical pole mass, but the position of the peak moves to higher energies. As a result, the spectral density features off-shell contributions in a large region of frequencies *smaller* than the position of the peak. The small frequency region is further enhanced by temperature factors and these off shell contributions, while exponentially small, compete with the exponentially small on-shell contribution which yields the Bose-Einstein distribution. As a result the distribution function, while strongly suppressed at high momenta much larger than the temperature (and mass scales), is considerably larger than the Bose-Einstein abundance predicted by the usual Boltzmann equation.

In order to highlight the origin of the enhancement, we derived the Boltzmann equation in *renormalized perturbation theory* up to the same order in the coupling to the bath as the non-equilibrium effective action, which is the basis for the quantum kinetic description. This derivation makes manifest the origin of the discrepancy: the usual Boltzmann equation is based on Fermi's golden rule, which requires taking a long time limit in the transition *probability*. In taking the long time limit and extracting the asymptotic behavior of the transition probability energy conservation is manifest as an on-shell delta function, and all memory effects have been neglected. Furthermore in considering the transition probability in a gain-loss balance equation, interference phenomena have been neglected. As a result the Boltzmann equation neglects off-shell contributions. Precisely these off-shell contributions from the support of the spectral density away from its peak and near the particle mass shell, are responsible for the departure from the Bose-Einstein result. The enhancement over the Bose-Einstein distribution is a consequence of the off-shell support of the spectral density at frequencies *smaller* than the position of the peak.

Although these results were obtained within the particular specific model studied here, the origin of the discrepancies suggests these to be much more general. The spectral density of a particle that is stable at zero temperature features an on-shell delta function below the multiparticle thresholds. However in a medium this peak will be broadened by different processes and the particle becomes a quasiparticle. This unavoidable feature of an interacting particle in a medium results in a broader spectral density with a region of support at frequencies *smaller* than the position of the peak, which leads to a *larger* contribution to the abundance as compared to the Bose-Einstein distribution which is the "on-shell" result.

Cosmological consequences. An important feature of the distribution function (7.139) is that it is exponentially suppressed at low temperatures since all the intermediate states are heavy and therefore exponentially suppressed at low temperatures. Therefore the off-shell contributions are strongly suppressed leading to the conclusion that the low temperature abundance is exponentially suppressed. This is in agreement with the results of refs.[156, 158]. Therefore we do *not* expect the low temperature enhancement of the abundance to be of any practical relevance for cold dark matter candidates.

The consequences for the cosmic microwave background depend on the temperature regime. For temperatures much larger than the electron mass the photons in the plasma propagate as in-medium quasiparticles of two species: longitudinal and transverse plasma excitations (plasmons). The plasma frequency in the high temperature regime is of the order $\omega_{pl} \propto \sqrt{\alpha_{em}}\, T$[171, 172]. The corrections to the dispersion relations (plasma frequency) arise from intermediate states of electron-positron pairs and yield a contribution to the spectral density with support below the light cone. These are Landau damping processes[171, 172] while those that yield the width arise from Compton scattering and pair annihilation and are of higher order. The plasmon width (up to logarithmic corrections) is of order $\Gamma \propto \alpha_{em}^2 T$. Thus the spectral function for photons features support both above and below the light cone, the latter is a result of Landau damping processes[171, 172]. This latter contribution is important because it yields support in the small frequency region which is Bose enhanced. Both the plasma frequency and the width are strong functions of temperature and we expect substantial corrections to the power spectrum of the cosmic microwave background for $T \gg 1$ Mev. However, these potential corrections are observable only indirectly, possibly through nucleosynthesis. For temperatures well below the electron mass the lowest order $\mathcal{O}(\alpha_{em})$ correction to the spectral density arises from an electron loop and an electron-positron loop (we ignore the contribution from protons). The former gives a Landau damping cut below the light cone akin to the contribution (7.153)[171, 172] and the latter gives a two particle cut above the pair-production threshold. Both are off-shell contributions and yield corrections to the spectral density which are proportional to the electron number density (equal to the proton number density) $n_e \sim x_e(\Omega_b h_0^2)(1+z)^3 \times 10^{-5}\mathrm{cm}^{-3}$, with x_e the ionization fraction. The width of the spectral density near the mass shell results from Compton scattering and is of order α_{em}^2. It is approximately given by $\Gamma \sim \sigma_T n_e \sqrt{\frac{k_B T}{m_e}}$ and σ_T is the Thompson scattering cross section. During recombination the ionization fraction diminishes precipitously within a window of redshift $\Delta z \sim 100$ which is the width of the last scattering surface. This rapid vanishing of the ionization fraction and consequently of the (free)

electron density entails that the broadening of the spectrum and the spectral distortions become vanishingly small at the end of recombination. At decoupling the mean free path is comparable to the size of the horizon and the spectral density for photons is basically that of free field theory. Hence recombination erases any observable vestige of spectral distortion through many body processes and spectral broadening, thus there are no observable consequences of these effects in the CMB.

8.0 NON EQUILIBRIUM DYNAMICS OF MIXING, OSCILLATIONS AND EQUILIBRATION: A MODEL STUDY

8.1 INTRODUCTION

Beginning with pioneering work on neutrino mixing in media[60, 124, 176, 177, 178], the study of the dynamical evolution has been typically cast in terms of single particle "flavor states" or matrix of densities that involve either a non-relativistic treatment of neutrinos or consider flavor neutrinos as massless. The main result that follows from these studies is a simplified set of Bloch equations with a semi-phenomenological damping factor (for a thorough review see[26]).

Most of these approaches involve in some form the concept of distribution functions for "flavor states", presumably these are obtained as expectation values of Fock number operators associated with flavor states. However, there are several conceptual difficulties associated with flavor Fock states, still being debated[89, 90, 91, 128, 179, 180, 181, 182].

The importance of neutrino mixing and oscillations, relaxation and equilibration in all of these timely aspects of cosmology and astroparticle physics warrant a deeper scrutiny of the non-equilibrium phenomena firmly based on quantum field theory.

Our ultimate goal is to study the non-equilibrium dynamics of oscillation, relaxation and equilibration directly in the quantum field theory of weak interactions bypassing the ambiguities associated with the definition of flavor Fock states. We seek to understand the nature of the equilibrium state: the *free field Hamiltonian* is diagonal in the mass basis, but the interactions are diagonal in the flavor basis, however, equilibration requires interactions, hence there is a competition between mass and flavor basis, which leads to the question of which is the basis in which the equilibrium density matrix is diagonal. Another goal is to obtain the dispersion relations and the *relaxation rates* of the correct quasiparticle excitations in the medium.

In this chapter, we make progress towards these goals by studying a simpler model of two

"flavored" *mesons* representing the electron and muon neutrinos that mix via an off-diagonal mass matrix and interact with other *mesons* which represent either hadrons (neutrons and protons) or quarks and charged leptons via an interaction vertex that models the charged current weak interaction. The meson fields that model hadrons (or quarks) and charged leptons are taken as a *bath in thermal equilibrium*. In the standard model the assumption that hadrons (or quarks) and charged leptons can be considered as a bath in thermal equilibrium is warranted by the fact that their strong and electromagnetic interactions guarantee faster equilibration rates than those of neutrinos.

This model bears the most relevant characteristics of the standard model Lagrangian augmented by an off diagonal neutrino mass matrix and will be seen to yield a remarkably faithful description of oscillation and relaxational dynamics in a thermal medium at high temperature. It effectively describes the thermalization dynamics of neutrinos in a medium at high temperature such as the early Universe for $T \gtrsim 3\,\mathrm{MeV}$[11, 26, 183].

Furthermore, Dolgov et. al.[184] argue that the spinor nature of the neutrinos is not relevant to describe the dynamics of mixing at high energies, thus we expect that this model captures the relevant dynamics.

An exception is the case of neutrinos in supernovae, a situation in which neutrino degeneracy, hence Pauli blocking, becomes important and requires a full treatment of the fermionic aspects of neutrinos. Certainly the *quantitative* aspects such as relaxation rates must necessarily depend on the fermionic nature. However, we expect that a bosonic model will capture, or at minimum provide a guiding example, of the most general aspects of the non-equilibrium dynamics. The results found in our study lend support to this expectation.

While meson mixing has been studied previously[185], mainly motivated by mixing in the neutral kaon and pseudoscalar η, η' systems, our focus is different in that we study the real time dynamics of oscillation, relaxation and equilibration in a *thermal medium* at high temperature including radiative corrections with a long view towards understanding general aspects that apply to neutrino physics in the high temperature environment of the early Universe.

While neutrino equilibration in the early Universe for $T \gtrsim 3\,\mathrm{MeV}$ prior to BBN is undisputable[11, 26, 183], the main questions that we address in this article are whether the equilibrium density matrix is diagonal in the flavor or mass basis and the relation between the relaxation rates of the propagating modes in the medium.

Strategy: the meson fields that model flavor neutrinos are treated as the "system" while those

that describe hadrons (or quarks) and charged leptons, as the "bath" in thermal equilibrium. An initial density matrix is evolved in time and the "bath" fields are integrated out up to second order in the coupling to the system, yielding a "reduced density matrix" which describes the dynamics of correlation functions solely of system fields (neutrinos). This program pioneered by Feynman and Vernon[164] for coupled oscillators (see also[165, 168]) is carried out in the interacting theory by implementing the closed-time path-integral representation of a time evolved density matrix[141]. This method yields the *real time non-equilibrium effective action*[186] including the self-energy which yields the "index of refraction" correction to the mixing angles and dispersion relations[57] in the medium and the decay and relaxation rates of the quasiparticle excitations. The non-equilibrium effective action thus obtained yields the time evolution of correlation and distribution functions and expectation values in the reduced density matrix[186]. The approach to equilibrium is determined by the long time behavior of the two point correlation function and its equal time limit, the one-body density matrix. The most general aspects of the dynamics of mixing and equilibration are completely determined by the spectral properties of the correlators of the bath degrees of freedom in equilibrium.

In section (8.2) we introduce the model and discuss the ambiguities in defining flavor Fock operators, states and distribution functions. In section (8.3) we obtain the reduced density matrix, the non-equilibrium effective action and the Langevin-like equations of motion for the expectation value of the fields. In section (8.4) we provide the general solution of the Langevin equation. In section (8.5) we obtain the dispersion relations, mixing angles and decay rates of quasiparticle modes in the medium. In this section an effective Weisskopf-Wigner description of the long time dynamics is derived. In section (8.6) we study the approach to equilibrium in terms of the one-body density matrix. In this section we discuss the consequences for "sterile neutrinos". Section (8.7) summarizes our conclusions.

8.2 THE MODEL

We consider a model of mesons with two flavors e , μ in interaction with a "charged current" denoted W and a "flavor lepton" χ_α modeling the charged current interactions in the EW model.

In terms of field doublets

$$\Phi = \begin{pmatrix} \phi_e \\ \phi_\mu \end{pmatrix} \;\; ; \;\; X = \begin{pmatrix} \chi_e \\ \chi_\mu \end{pmatrix} \tag{8.1}$$

the Lagrangian density is

$$\mathcal{L} = \frac{1}{2}\left\{\partial_\mu \Phi^T \partial^\mu \Phi - \Phi^T \mathbb{M}^2 \Phi\right\} + \mathcal{L}_0[W,\chi] + G\, W\, \Phi^T \cdot X + G\phi_e^2\chi_e^2 + G\phi_\mu^2\chi_\mu^2 \tag{8.2}$$

where the mass matrix is given by

$$\mathbb{M}^2 = \begin{pmatrix} M^2_{ee} & M^2_{e\mu} \\ M^2_{e\mu} & M^2_{\mu\mu} \end{pmatrix} \tag{8.3}$$

where $\mathcal{L}_0[W,\chi]$ is the free field Lagrangian density for W, χ which need not be specified. The mesons $\phi_{e,\mu}$ play the role of the flavored neutrinos, $\chi_{e,\mu}$ the role of the charged leptons and W a charged current, for example the proton-neutron current $\overline{p}\gamma^\mu(1 - g_A\gamma_5)n$ or a similar quark current. The coupling G plays the role of G_F. As it will be seen below, we do not need to specify the precise form, only the spectral properties of the correlation function of this current are necessary.

Passing from the flavor to the mass basis for the fields $\phi_{e,\mu}$ by an orthogonal transformation $\Phi = U(\theta)\,\varphi$

$$\begin{pmatrix} \phi_e \\ \phi_\mu \end{pmatrix} = U(\theta) \begin{pmatrix} \varphi_1 \\ \varphi_2 \end{pmatrix} \;\; ; \;\; U(\theta) = \begin{pmatrix} \cos\theta & \sin\theta \\ -\sin\theta & \cos\theta \end{pmatrix} \tag{8.4}$$

where the orthogonal matrix $U(\theta)$ diagonalizes the mass matrix $\mathbb{M}^2$, namely

$$U^{-1}(\theta)\,\mathbb{M}^2\,U(\theta) = \begin{pmatrix} M_1^2 & 0 \\ 0 & M_2^2 \end{pmatrix} \tag{8.5}$$

In the flavor basis $\mathbb{M}$ can be written as follows

$$\mathbb{M}^2 = \overline{M}^{\,2}\,\mathbb{1} + \frac{\delta M^2}{2} \begin{pmatrix} -\cos 2\theta & \sin 2\theta \\ \sin 2\theta & \cos 2\theta \end{pmatrix} \tag{8.6}$$

where we introduced

$$\overline{M}^{\,2} = \frac{1}{2}(M_1^2 + M_2^2) \;\; ; \;\; \delta M^2 = M_2^2 - M_1^2\,. \tag{8.7}$$

8.2.1 Mass and flavor states:

It is convenient to take the spatial Fourier transform of the fields $\phi_\alpha; \varphi_i$ and their canonical momenta $\pi_\alpha = \dot{\phi}_\alpha; \upsilon_i = \dot{\varphi}_i$ with $\alpha = e, \mu$ and $i = 1, 2$ and write (at t=0),

$$\begin{aligned} \phi_\alpha(\vec{x}) &= \frac{1}{\sqrt{V}} \sum_{\vec{k}} \phi_{\alpha,\vec{k}}\, e^{i\vec{k}\cdot\vec{x}} \quad ; \quad \varphi_i(\vec{x}) = \frac{1}{\sqrt{V}} \sum_{\vec{k}} \varphi_{i,\vec{k}}\, e^{i\vec{k}\cdot\vec{x}} \\ \pi_\alpha(\vec{x}) &= \frac{1}{\sqrt{V}} \sum_{\vec{k}} \pi_{\alpha,\vec{k}}\, e^{i\vec{k}\cdot\vec{x}} \quad ; \quad \upsilon_i(\vec{x}) = \frac{1}{\sqrt{V}} \sum_{\vec{k}} \upsilon_{i,\vec{k}}\, e^{i\vec{k}\cdot\vec{x}} \end{aligned} \tag{8.8}$$

in these expressions we have denoted the spatial Fourier transforms with the same name to avoid cluttering of notation but it is clear from the argument which variable is used. The free field Fock states associated with mass eigenstates are obtained by writing the fields which define the mass basis φ_i in terms of creation and annihilation operators,

$$\varphi_{i,\vec{k}} = \frac{1}{\sqrt{2\omega_i(k)}} \left[a_{i,\vec{k}} + a^\dagger_{i,-\vec{k}} \right] \quad ; \quad \upsilon_{i,\vec{k}} = \frac{-i\omega_i(k)}{\sqrt{2\omega_i(k)}} \left[a_{i,\vec{k}} - a^\dagger_{i,-\vec{k}} \right] \tag{8.9}$$

with

$$\omega_i(k) = \sqrt{k^2 + M_i^2} \quad ; \quad i = 1, 2 \tag{8.10}$$

The annihilation ($a_{i,\vec{k}}$) and creation ($a^\dagger_{i,\vec{k}}$) operators obey the usual canonical commutation relations, and the free Hamiltonian in the mass basis is the usual sum of independent harmonic oscillators with frequencies $\omega_i(k)$. One can, in principle, *define* annihilation and creation operators associated with the flavor fields $a_{\alpha,\vec{k}}, a^\dagger_{\alpha,\vec{k}}$ respectively in a similar manner

$$\phi_{\alpha,\vec{k}} = \frac{1}{\sqrt{2\Omega_\alpha(k)}} \left[a_{\alpha,\vec{k}} + a^\dagger_{\alpha,-\vec{k}} \right] \quad ; \quad \pi_{\alpha,\vec{k}} = \frac{-i\Omega_\alpha(k)}{\sqrt{2\Omega_\alpha(k)}} \left[a_{\alpha,\vec{k}} - a^\dagger_{\alpha,-\vec{k}} \right] \tag{8.11}$$

with the annihilation ($a_{\alpha,\vec{k}}$) and creation ($a^\dagger_{\alpha,\vec{k}}$) operators obeying the usual canonical commutation relations. However, unlike the case for the mass eigenstates, the frequencies $\Omega_\alpha(k)$ are *arbitrary*. *Any choice* of these frequencies furnishes a *different* Fock representation, therefore there is an intrinsic ambiguity in defining Fock creation and annihilation operators for the *flavor* fields since these do not have a definite mass. In references[89, 90, 91] a particular assignment of masses has been made, but any other is equally suitable. The orthogonal transformation between the flavor and mass fields eqn. (9.4), leads to the following relations between the flavor and mass Fock operators,

$$a_{e,\vec{k}} = \cos\theta \left[a_{1,\vec{k}}\, \mathbf{A}_{e,1}(k) + a^{\dagger}_{1,-\vec{k}}\, \mathbf{B}_{e,1}(k) \right] + \sin\theta \left[a_{2,\vec{k}}\, \mathbf{A}_{e,2}(k) + a^{\dagger}_{2,-\vec{k}}\, \mathbf{B}_{e,2}(k) \right] \quad (8.12)$$

$$a_{\mu,\vec{k}} = \cos\theta \left[a_{2,\vec{k}}\, \mathbf{A}_{\mu,2}(k) + a^{\dagger}_{2,-\vec{k}}\, \mathbf{B}_{\mu,2}(k) \right] - \sin\theta \left[a_{1,\vec{k}}\, \mathbf{A}_{\mu,1}(k) + a^{\dagger}_{1,-\vec{k}}\, \mathbf{B}_{\mu,1}(k) \right] \quad (8.13)$$

where $\mathbf{A}_{\alpha,i}, \mathbf{B}_{\alpha,i}$ are the generalized Bogoliubov coefficients

$$\mathbf{A}_{\alpha,i} = \frac{1}{2}\left(\sqrt{\frac{\Omega_\alpha(k)}{\omega_i(k)}} + \sqrt{\frac{\omega_i(k)}{\Omega_\alpha(k)}} \right) \;\; ; \;\; \mathbf{B}_{\alpha,i} = \frac{1}{2}\left(\sqrt{\frac{\Omega_\alpha(k)}{\omega_i(k)}} - \sqrt{\frac{\omega_i(k)}{\Omega_\alpha(k)}} \right). \quad (8.14)$$

These coefficients obey the condition

$$\left(\mathbf{A}^2_{\alpha,i} - \mathbf{B}^2_{\alpha,i} \right) = 1 \quad (8.15)$$

which guarantees that the transformation between mass and flavor Fock operators is formally unitary and both sets of operators obey the canonical commutation relations for *any* choice of the frequencies $\Omega_\alpha(k)$. Neglecting the interactions, the ground state $|0>$ of the Hamiltonian is the vacuum annihilated by the Fock annihilation operators of the mass basis,

$$a_{i,\vec{k}}|0> = 0 \;\; \text{for all } i = 1, 2\,, \vec{k}\,. \quad (8.16)$$

In particular the number of *flavor* Fock quanta in the non-interacting ground state, which is the *vacuum* of mass eigenstates is

$$< 0|a^{\dagger}_{e,\vec{k}}\, a_{e,\vec{k}}|0> = \cos^2\theta\, \frac{\left[\Omega_e(k) - \omega_1(k)\right]^2}{4\,\Omega_e(k)\,\omega_1(k)} + \sin^2\theta\, \frac{\left[\Omega_e(k) - \omega_2(k)\right]^2}{4\,\Omega_e(k)\,\omega_2(k)} \quad (8.17)$$

$$< 0|a^{\dagger}_{\mu,\vec{k}}\, a_{\mu,\vec{k}}|0> = \cos^2\theta\, \frac{\left[\Omega_\mu(k) - \omega_2(k)\right]^2}{4\,\Omega_\mu(k)\,\omega_2(k)} + \sin^2\theta\, \frac{\left[\Omega_\mu(k) - \omega_1(k)\right]^2}{4\,\Omega_\mu(k)\,\omega_1(k)} \quad (8.18)$$

namely the non-interacting ground state (the vacuum of mass eigenstates) is a *condensate* of "flavor" states[89, 90, 91] with an average number of "flavored particles" that depends on the arbitrary frequencies $\Omega_\alpha(k)$. Therefore these "flavor occupation numbers" or "flavor distribution functions" are *not* suitable quantities to study equilibration.

Assuming that $\Omega_\alpha(k) \to k$ when $k \to \infty$, in the high energy limit $\mathbf{A} \to 1$; $\mathbf{B} \to 0$ and in this high energy limit

$$a_{e,\vec{k}} \approx \cos\theta\, a_{1,\vec{k}} + \sin\theta\, a_{2,\vec{k}} \;\; ; \;\; a_{\mu,\vec{k}} \approx \cos\theta a_{2,\vec{k}} - \sin\theta a_{1,\vec{k}} \quad (8.19)$$

Therefore, under the assumption that the arbitrary frequencies $\Omega_\alpha(k) \to k$ in the high energy limit, there is an approximate identification between Fock states in the mass and flavor basis in this limit. However, such identification is only *approximate* and only available in the asymptotic regime of large momentum, but becomes ambiguous for arbitrary momenta. In summary the definition of flavor Fock states is ambiguous, the ambiguity may *only* be approximately resolved in the very high energy limit, but it is clear that there is no unique definition of a flavor *distribution function* which is valid for all values of momentum k and that can serve as a definite yardstick to study equilibration. Even the non-interacting ground state features an arbitrary number of flavor Fock quanta depending on the arbitrary choice of the frequencies $\Omega_\alpha(k)$ in the definition of the flavor Fock operators. This is not a consequence of the meson model but a *general* feature in the case of mixed fields with similar ambiguities in the spinor case[182].

We emphasize that while the flavor Fock operators are *ambiguous* and not uniquely defined, there is no ambiguity in the flavor *fields* ϕ_α which are related to the mass fields φ_i via the unitary transformation (9.4). While there is no unambiguous definition of the flavor number operator or distribution function, there is an unambiguous number operator for the Fock quanta in the mass basis $N_i(k) = a^\dagger_{i,\vec{k}}\, a_{i,\vec{k}}$, whose expectation value is the distribution function for mass Fock states.

8.3 REDUCED DENSITY MATRIX AND NON-EQUILIBRIUM EFFECTIVE ACTION

Our goal is to study the equilibration of neutrinos with a bath of hadrons or quarks and charged leptons in thermal equilibrium at high temperature. This setting describes the thermalization of neutrinos in the early Universe prior to BBN, for temperatures $T \gtrsim 3\,\mathrm{MeV}$[11, 26, 183].

We focus on the dynamics of the "system fields", either the flavor fields ϕ_α or alternatively the mass fields φ_i. The strategy is to consider the time evolved full density matrix and trace over the bath degrees of freedom χ, W. It is convenient to write the Lagrangian density (8.2) as

$$\mathcal{L}[\phi_\alpha, \chi_\alpha, W] = \mathcal{L}_0[\phi] + \mathcal{L}_0[W, \chi] + G\phi_\alpha \mathcal{O}_\alpha + G\phi_\alpha^2 \chi_\alpha^2 \tag{8.20}$$

with an implicit sum over the flavor label $\alpha = e, \mu$, where

$$\mathcal{O}_\alpha = \chi_\alpha\, W\,. \tag{8.21}$$

$\mathcal{L}_0[\cdots]$ are the free Lagrangian densities for the fields $\phi_\alpha, \chi_\alpha, W$ respectively. The fields ϕ_α are considered as the "system" and the fields χ_α, W are treated as a bath in thermal equilibrium at a temperature $T \equiv 1/\beta$. We consider a factorized initial density matrix at a time $t_i = 0$ of the form

$$\hat{\rho}(0) = \hat{\rho}_\phi(0) \otimes e^{-\beta H_0[\chi, W]} \tag{8.22}$$

where $H_0[\chi, W]$ is Hamiltonian for the fields χ, W. Although this factorized form of the initial density matrix leads to initial transient dynamics, we are interested in the long time dynamics, in particular in the long time limit. The bath fields χ_α, W will be "integrated out" yielding a reduced density matrix for the fields ϕ_α in terms of an effective real-time functional, known as the influence functional[164] in the theory of quantum brownian motion. The reduced density matrix can be represented by a path integral in terms of the non-equilibrium effective action that includes the influence functional. This method has been used extensively to study quantum brownian motion[164, 165], and quantum kinetics[168, 186].

In the flavor field basis the matrix elements of $\hat{\rho}_\phi(0)$ are given by

$$\langle \phi_\alpha | \hat{\rho}_\phi(0) | \phi'_\beta \rangle = \rho_{\phi;0}(\phi_\alpha; \phi'_\beta) \tag{8.23}$$

or alternatively in the mass field basis

$$\langle \varphi_i | \hat{\rho}_\varphi(0) | \varphi'_j \rangle = \rho_{\varphi;0}(\varphi_i; \varphi'_j)\,. \tag{8.24}$$

The time evolution of the initial density matrix is given by

$$\hat{\rho}(t_f) = e^{-iH(t_f - t_i)} \hat{\rho}(t_i) e^{iH(t_f - t_i)}\,, \tag{8.25}$$

where the total Hamiltonian H is

$$H = H_0[\phi] + H_0[\chi, W] + H_I[\phi, \chi, W]\,. \tag{8.26}$$

The calculation of correlation functions is facilitated by introducing currents coupled to the different fields. Furthermore since each time evolution operator in eqn. (8.25) will be represented as a path integral, we introduce different sources for forward and backward time evolution operators, referred to as J^+, J^- respectively. The forward and backward time evolution operators in presence of sources are $U(t_f, t_i; J^+)$, $U^{-1}(t_f, t_i, J^-)$ respectively.

We will only study correlation functions of the "system" fields ϕ (or φ in the mass basis), therefore we carry out the trace over the χ and W degrees of freedom. Since the currents $J^\pm$

allow us to obtain the correlation functions for any arbitrary time by simple variational derivatives with respect to these sources, we take $t_f \to \infty$ without loss of generality. The non-equilibrium generating functional is given by[168, 186]

$$\mathcal{Z}[j^+, j^-] = \mathrm{Tr} U(\infty, t_i; J^+)\hat{\rho}(t_i)U^{-1}(\infty, t_i, J^-)\,, \tag{8.27}$$

where $J^\pm$ stand collectively for all the sources coupled to different fields. Functional derivatives with respect to the sources J^+ generate the time ordered correlation functions, those with respect to J^- generate the anti-time ordered correlation functions and mixed functional derivatives with respect to J^+, J^- generate mixed correlation functions. Each one of the time evolution operators in the generating functional (8.27) can be written in terms of a path integral: the time evolution operator $U(\infty, t_i; J^+)$ involves a path integral *forward* in time from t_i to $t = \infty$ in presence of sources J^+, while the inverse time evolution operator $U^{-1}(\infty, t_i, J^-)$ involves a path integral *backwards* in time from $t = \infty$ back to t_i in presence of sources J^-. Finally the equilibrium density matrix for the bath $e^{-\beta\, H_0[\chi, W]}$ can be written as a path integral along imaginary time with sources J^β. Therefore the path integral form of the generating functional (8.27) is given by

$$\mathcal{Z}[j^+, j^-] = \int D\Phi_i D\Phi'_i\, \rho_{\Phi,i}(\Phi_i; \Phi'_i) \int \mathcal{D}\Phi^\pm \mathcal{D}\chi^\pm \mathcal{D}W^\pm \mathcal{D}\chi^\beta \mathcal{D}W^\beta\, e^{iS[\Phi^\pm, \chi^\pm, W^\pm; J^\pm_\Phi; J^\pm_\chi; J^\pm_W]} \tag{8.28}$$

with the boundary conditions $\Phi^+(\vec{x}, t_i) = \Phi_i(\vec{x})\,;\, \Phi^-(\vec{x}, t_i) = \Phi'_i(\vec{x})$. The trace over the bath fields χ, W is performed with the usual periodic boundary conditions in Euclidean time.

The non-equilibrium action is given by

$$\begin{aligned} S[\Phi^\pm, \chi^\pm; J^\pm_\Phi; J^\pm_\chi; J^\pm_W] \;=\; & \int_{t_i}^{\infty} dt d^3x \left[\mathcal{L}_0(\phi^+) + J^+_\phi \phi^+ - \mathcal{L}_0(\phi^-) - J^-_\phi \phi^-\right] + \\ & \int_{\mathcal{C}} d^4x \Big\{ \mathcal{L}_0[\chi, W] + J_\chi \chi + J_W\, W + G\, \phi_\alpha\, \mathcal{O}_\alpha + G\phi^2_\alpha \chi^2_\alpha \Big\} \end{aligned} \tag{8.29}$$

where $\mathcal{C}$ describes the following contour in the complex time plane: along the forward branch $(t_i, +\infty)$ the fields and sources are Φ^+, χ^+, J^+_χ, along the backward branch (∞, t_i) the fields and sources are Φ^-, χ^-, J^-_χ and along the Euclidean branch $(t_i, t_i - i\beta)$ the fields and sources are $\Phi = 0; \chi^\beta, J^\beta_\chi$. Along the Euclidean branch the interaction term vanishes since the initial density matrix for the field χ is assumed to be that of thermal equilibrium. This contour is depicted in fig. (8.1)

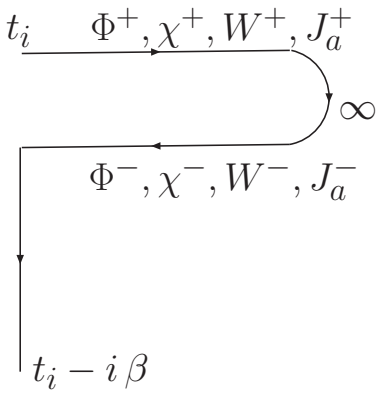

Figure 8.1: Contour in time for the non-equilibrium path integral representation.

The trace over the degrees of freedom of the χ field with the initial equilibrium density matrix, entail periodic boundary conditions for χ, W along the contour $\mathcal{C}$. However, the boundary conditions on the path integrals for the field Φ are given by

$$\Phi^+(\vec{x}, t = \infty) = \Phi^-(\vec{x}, t = \infty) \tag{8.30}$$

and

$$\Phi^+(\vec{x}, t = t_i) = \Phi_i(\vec{x}) \quad ; \quad \Phi^-(\vec{x}, t = t_i) = \Phi_i'(\vec{x}) \tag{8.31}$$

The reason for the different path integrations is that whereas the χ and W fields are traced over with an initial thermal density matrix, the initial density matrix for the Φ field will be specified later as part of the initial value problem. The path integral over χ, W leads to the influence functional for $\Phi^{\pm}$[164].

Because we are not interested in the correlation functions of the bath fields but only those of the "system" fields, we set the external c-number currents $J_\chi = 0; J_W = 0$. Insofar as the bath fields are concerned, the system fields Φ act as an external c-number source, and tracing over the bath fields leads to

$$\int \mathcal{D}\chi^{\pm}\mathcal{D}W^{\pm}\mathcal{D}\chi^{\beta}\mathcal{D}W^{\beta}\, e^{\,i\int_{\mathcal{C}} d^4x\left\{\mathcal{L}_0[\chi,W]+G\,\phi_\alpha\mathcal{O}_\alpha+G\phi_\alpha^2\chi_\alpha^2\right\}} = \left\langle e^{iG\int_{\mathcal{C}} d^4x\phi_\alpha\mathcal{O}_\alpha+\phi_\alpha^2\chi_\alpha^2}\right\rangle_0 \mathrm{Tr}e^{-\beta H^0[\chi,W]}. \tag{8.32}$$

The expectation value in the right hand side of eqn. (8.32) is in the equilibrium free field density matrix of the fields χ, W. The path integral can be carried out in perturbation theory and the result exponentiated to yield the effective action as follows

$$\begin{aligned}\left\langle e^{iG\int_{\mathcal{C}} d^4x\phi_\alpha\mathcal{O}_\alpha+\phi^2_\alpha\chi^2_\alpha}\right\rangle_0 = \quad & 1+iG\int_{\mathcal{C}} d^4x\Big\{\phi_\alpha(x)\left\langle\mathcal{O}_\alpha(x)\right\rangle_0+\phi^2_\alpha(x)\left\langle\chi^2_\alpha(x)\right\rangle_0\Big\} \\ & +\frac{(iG)^2}{2}\int_{\mathcal{C}} d^4x\int_{\mathcal{C}} d^4x'\phi_\alpha(x)\phi_\beta(x')\Big\langle\mathcal{O}_\alpha(x)\mathcal{O}_\beta(x')\Big\rangle_0+\mathcal{O}(G^3)\end{aligned} \tag{8.33}$$

This is the usual expansion of the exponential of the connected correlation functions, therefore this series is identified with

$$\left\langle e^{iG\int_{\mathcal{C}} d^4x\phi_\alpha\mathcal{O}_\alpha+\phi^2_\alpha\chi^2_\alpha}\right\rangle_0 = e^{i\,L_{if}[\phi^+,\phi^-]}\,, \tag{8.34}$$

where $L_{if}[\phi^+,\phi^-]$ is the *influence functional*[164], and $\langle\cdots\rangle_0$ stand for expectation values in the bath in equilibrium. For $\left\langle\chi_\alpha(x)W(x)\right\rangle_0 = 0$ the influence functional is given by

$$L_{if}[\phi^+,\phi^-] = G\int_{\mathcal{C}} d^4x\phi^2_\alpha(x)\left\langle\chi^2_\alpha(x)\right\rangle_0+i\frac{G^2}{2}\int_{\mathcal{C}} d^4x\int_{\mathcal{C}} d^4x'\phi_\alpha(x)\phi_\beta(x')\langle\mathcal{O}_\alpha(x)\mathcal{O}_\beta(x')\rangle_0+\mathcal{O}(G^3)\,. \tag{8.35}$$

In the above result we have neglected second order contributions of the form $G^2\phi^4_\alpha$. These non-linear contributions give rise to interactions between the quasiparticles and *will be neglected* in this article. Here we are primarily concerned with establishing the general properties of the quasiparticles and their equilibration with the bath and not with their mutual interaction. As in the case of mixed neutrinos, the inclusion of a "neutrino" background may lead to the phenomenon of non-linear synchronization[13, 69, 187], but the study of this phenomenon is beyond the realm of this article.

We focus solely on the non-equilibrium effective action up to quadratic order in the "neutrino fields", from which we extract the dispersion relations, relaxation rates and the approach to equilibrium with the bath of the quasiparticle modes in the medium.

The integrals along the contour $\mathcal{C}$ stand for the following expressions:

$$G\int_{\mathcal{C}} d^4x\phi^2_\alpha(x)\left\langle\chi^2_\alpha(x)\right\rangle_0 = V_{\alpha\alpha}\int d^3x\int_{t_i}^{\infty} dt\left[\phi^{2\,+}_\alpha(x)-\phi^{2\,-}_\alpha(x)\right] \tag{8.36}$$

where $V_{\alpha\alpha}$ are the "matter potentials" which are independent of position under the assumption of translational invariance, and time independent under the assumption that the bath is in equilibrium, and

$$\begin{aligned}
&\int_{\mathcal{C}} d^4x \int_{\mathcal{C}} d^4x' \phi_\alpha(x)\phi_\beta(x')\langle \mathcal{O}_\alpha(x)\mathcal{O}_\beta(x')\rangle_0 \\
= &\int d^3x \int_{t_i}^{\infty} dt \int d^3x' \int_{t_i}^{\infty} dt' \Big[\phi^+_\alpha(x)\phi^+_\beta(x')\langle \mathcal{O}^+_\alpha(x)\mathcal{O}^+_\beta(x')\rangle_0 \\
&\quad + \phi^-_\alpha(x)\phi^-_\beta(x')\langle \mathcal{O}^-_\alpha(x)\mathcal{O}^-_\beta(x')\rangle_0 - \phi^+_\alpha(x)\phi^-_\beta(x')\langle \mathcal{O}^+_\alpha(x)\mathcal{O}^-_\beta(x')\rangle_0 \\
&\quad - \phi^-_\alpha(x)\phi^+_\beta(x')\langle \mathcal{O}^-_\alpha(x)\mathcal{O}^+_\beta(x')\rangle_0\Big]
\end{aligned} \tag{8.37}$$

Since the expectation values above are computed in a thermal equilibrium translational invariant density matrix, it is convenient to introduce the spatial Fourier transform of the composite operator $\mathcal{O}$ in a spatial volume V as

$$\mathcal{O}_{\alpha,\vec{k}}(t) = \frac{1}{\sqrt{V}} \int d^3x e^{i\vec{k}\cdot\vec{x}} \mathcal{O}_\alpha(\vec{x},t) \tag{8.38}$$

in terms of which we obtain following the correlation functions

$$\langle \mathcal{O}^-_{\alpha,\vec{k}}(t)\mathcal{O}^+_{\beta,-\vec{k}}(t')\rangle = \mathrm{Tr}\, \mathcal{O}_{\beta,-\vec{k}}(t')\, e^{-\beta H^0[\chi,W]}\, \mathcal{O}_{\alpha,\vec{k}}(t) = \mathcal{G}^>_{\alpha\beta}(k;t-t') \equiv \mathcal{G}^{-+}_{\alpha\beta}(k;t-t') \tag{8.39}$$

$$\langle \mathcal{O}^+_{\alpha,\vec{k}}(t)\mathcal{O}^-_{\beta,-\vec{k}}(t')\rangle = \mathrm{Tr}\, \mathcal{O}_{\alpha,\vec{k}}(t)\, e^{-\beta H_\chi}\, \mathcal{O}_{\beta,-\vec{k}}(t') = \mathcal{G}^<_{\alpha\beta}(k;t-t') \equiv \mathcal{G}^{+-}_{\alpha\beta}(k;t-t') = \mathcal{G}^{-+}_{\beta,\alpha}(k;t'-t) \tag{8.40}$$

$$\langle \mathcal{O}^+_{\alpha,\vec{k}}(t)\mathcal{O}^+_{\beta,-\vec{k}}(t')\rangle = \mathcal{G}^>_{\alpha\beta}(k;t-t')\Theta(t-t') + \mathcal{G}^<_{\alpha\beta}(k;t-t')\Theta(t'-t) \equiv \mathcal{G}^{++}_{\alpha\beta}(k;t-t') \tag{8.41}$$

$$\langle \mathcal{O}^-_{\alpha,\vec{k}}(t)\mathcal{O}^-_{\beta,-\vec{k}}(t')\rangle = \mathcal{G}^>_{\alpha\beta}(k;t-t')\Theta(t'-t) + \mathcal{G}^<_{\alpha\beta}(k;t-t')\Theta(t-t') = \mathcal{G}^{--}_{\alpha\beta}(k;t-t') \tag{8.42}$$

The time evolution of the operators is determined by the Heisenberg picture of $H_0[\chi,W]$. Because the density matrix for the bath is in equilibrium, the correlation functions above are solely functions of the time difference as made explicit in the expressions above. These correlation functions are not independent, but obey

$$\mathcal{G}^{++}_{\alpha\beta}(k;t,t') + \mathcal{G}^{--}_{\alpha\beta}(k;t,t') - \mathcal{G}^{-+}_{\alpha\beta}(k;t,t') - \mathcal{G}^{+-}_{\alpha\beta}(k;t,t') = 0 \tag{8.43}$$

The correlation function $\mathcal{G}^>_{\alpha\beta}$ up to lowest order in the coupling G is given by

$$\mathcal{G}^>_{\alpha\beta}(k;t-t') = \int \frac{d^3p}{(2\pi)^3} \langle W_{\vec{p}+\vec{k}}(t) W_{-\vec{p}-\vec{k}}(t')\rangle \langle \chi_{\vec{p},\alpha}(t)\chi_{-\vec{p},\beta}(t')\rangle \tag{8.44}$$

where the expectation value is in the free field equilibrium density matrix of the respective fields. This correlation function is diagonal in the flavor basis and this entails that all the Green's functions (8.39-8.42) are diagonal in the flavor basis.

The non-equilibrium effective action yields the time evolution of the reduced density matrix, it is given by

$$L_{eff}[\phi^+,\phi^-] = \int_{t_i}^{\infty} dt d^3x \, \left[\mathcal{L}_0(\phi^+) - \mathcal{L}_0(\phi^-)\right] + L_{if}[\phi^+,\phi^-] \tag{8.45}$$

where we have set the sources $J^{\pm}$ for the fields $\phi^{\pm}$ to zero.

In what follows we take $t_i = 0$ without loss of generality since (i) for $t > t_i$ the total Hamiltonian is time independent and the correlations will be solely functions of $t - t_i$, and (ii) we will be ultimately interested in the limit $t \gg t_i$ when all transient phenomena has relaxed. Adapting the methods presented in ref. [186] to account for the matrix structure of the effective action, introducing the spatial Fourier transform of the fields $\phi^{\pm}$ defined as in eqn. (8.38) and the matrix of the matter potentials

$$\mathbb{V} = \begin{pmatrix} V_{ee} & 0 \\ 0 & V_{\mu\mu} \end{pmatrix} \tag{8.46}$$

we find

$$\begin{aligned} iL_{eff}[\phi^+,\phi^-] \;=\; & \sum_{\vec{k}} \Bigg\{ \frac{i}{2}\int_0^{\infty} dt \Big[\dot{\phi}^+_{\alpha,\vec{k}}(t)\dot{\phi}^+_{\alpha,-\vec{k}}(t) - \phi^+_{\alpha,\vec{k}}(t)(k^2\,\delta_{\alpha\beta} + \mathbb{M}^2_{\alpha\beta} + \mathbb{V}_{\alpha\beta})\phi^+_{\beta,-\vec{k}}(t) \\ & -\dot{\phi}^-_{\alpha,\vec{k}}(t)\dot{\phi}^-_{\alpha,-\vec{k}}(t) + \phi^-_{\alpha,\vec{k}}(t)(k^2\,\delta_{\alpha\beta} + \mathbb{M}^2_{\alpha\beta} + \mathbb{V}_{\alpha\beta})\phi^-_{\beta,-\vec{k}}(t) \Big] \\ & -\frac{G^2}{2}\int_0^{\infty} dt \int_0^{\infty} dt' \Big[\phi^+_{\alpha,\vec{k}}(t)\mathcal{G}^{++}_{\alpha\beta}(k;t,t')\phi^+_{\beta,-\vec{k}}(t') + \phi^-_{\alpha,\vec{k}}(t)\mathcal{G}^{--}_{\alpha\beta}(k;t,t')\phi^-_{\beta,-\vec{k}}(t') \\ & -\phi^+_{\alpha,\vec{k}}(t)\mathcal{G}^{+-}_{\alpha\beta}(k;t,t')\phi^-_{\beta,-\vec{k}}(t') - \phi^-_{\alpha,\vec{k}}(t)\mathcal{G}^{-+}_{\alpha\beta}(k;t,t')\phi^+_{\beta,-\vec{k}}(t') \Big] \Bigg\} \end{aligned} \tag{8.47}$$

The "matter potentials" $V_{\alpha\alpha}$ play the role of the index of refraction correction to the dispersion relations[57] and is of first order in the coupling G whereas the contributions that involve $\mathcal{G}$ are of order G^2. As it will become clear below, it is more convenient to introduce the Wigner center of mass and relative variables

$$\Psi_\alpha(\vec{x},t) = \frac{1}{2}\left(\phi^+_\alpha(\vec{x},t) + \phi^-_\alpha(\vec{x},t)\right) \quad ; \quad R_\alpha(\vec{x},t) = \left(\phi^+_\alpha(\vec{x},t) - \phi^-_\alpha(\vec{x},t)\right) \tag{8.48}$$

and the Wigner transform of the initial density matrix for the ϕ fields

$$\mathcal{W}(\Psi^0;\Pi^0) = \int DR_{0,\alpha} e^{-i\int d^3x \Pi_{0,\alpha}(\vec{x})R_{0,\alpha}(\vec{x})} \rho(\Psi^0 + \frac{R^0}{2};\Psi^0 - \frac{R^0}{2}) \tag{8.49}$$

with the inverse transform

$$\rho(\Psi^0+\frac{R^0}{2};\Psi^0-\frac{R^0}{2})=\int D\Pi^0_\alpha e^{i\int d^3x\Pi^0_\alpha(\vec{x})R^0_\alpha(\vec{x})}\mathcal{W}(\Psi^0;\Pi^0) \tag{8.50}$$

The boundary conditions on the ϕ path integral given by (8.31) translate into the following boundary conditions on the center of mass and relative variables

$$\Psi_\alpha(\vec{x},t=0)=\Psi^0_\alpha \;\;;\;\; R_\alpha(\vec{x},t=0)=R^0_\alpha \tag{8.51}$$

furthermore, the boundary condition (8.30) yields the following boundary condition for the relative field

$$R_\alpha(\vec{x},t=\infty)=0. \tag{8.52}$$

This observation will be important in the steps that follow.

The same description applies to the fields in the mass basis. We will treat both cases on equal footing with the notational difference that Greek labels α,β refer to the flavor and Latin indices i,j refer to the mass basis.

In terms of the spatial Fourier transforms of the center of mass and relative variables (8.48) introduced above, integrating by parts and accounting for the boundary conditions (8.51), the non-equilibrium effective action (8.47) becomes:

$$\begin{aligned}
iL_{eff}[\Psi,R] &= \int_0^\infty dt\sum_{\vec{k}}\Big\{-iR_{\alpha,-\vec{k}}\Big(\ddot{\Psi}_{\alpha,\vec{k}}(t)+(k^2\delta_{\alpha\beta}+\mathbb{M}^2_{\alpha\beta}+\mathbb{V}_{\alpha\beta})\Psi_{\beta,\vec{k}}(t)\Big)\Big\} \\
&- \int_0^\infty dt\int_0^\infty dt'\sum_{\vec{k}}\Big\{\frac{1}{2}R_{\alpha,-\vec{k}}(t)\mathcal{K}_{\alpha\beta}(k;t-t')R_{\beta,\vec{k}}(t')+R_{\alpha,-\vec{k}}(t)\,i\Sigma^R_{\alpha\beta}(k;t-t')\Psi_{\beta,\vec{k}}(t')\Big\} \\
&+ i\int d^3xR^0_\alpha(\vec{x})\dot{\Psi}_\alpha(\vec{x},t=0)
\end{aligned} \tag{8.53}$$

where the last term arises after the integration by parts in time, using the boundary conditions (8.51) and (8.52). The kernels in the above effective Lagrangian are given by (see eqns. (8.39-8.42))

$$\mathcal{K}_{\alpha\beta}(k;t-t') = \frac{G^2}{2}\Big[\mathcal{G}^>_{\alpha\beta}(k;t-t')+\mathcal{G}^<_{\alpha\beta}(k;t-t')\Big] \tag{8.54}$$

$$i\Sigma^R_{\alpha\beta}(k;t-t') = G^2\Big[\mathcal{G}^>_{\alpha\beta}(k;t-t')-\mathcal{G}^<_{\alpha\beta}(k;t-t')\Big]\Theta(t-t')\equiv i\Sigma_{\alpha\beta}(k;t-t')\Theta(t-t') \tag{8.55}$$

The term quadratic in the relative variable R can be written in terms of a stochastic noise as

$$\begin{aligned}
&\exp\Big\{-\frac{1}{2}\int dt\int dt' R_{\alpha,-\vec{k}}(t)\mathcal{K}_{\alpha\beta}(k;t-t')R_{\beta\vec{k}}(t')\Big\} \\
&= \int\mathcal{D}\xi\exp\Big\{-\frac{1}{2}\int dt\int dt'\,\xi_{\alpha,\vec{k}}(t)\mathcal{K}^{-1}_{\alpha\beta}(k;t-t')\xi_{\beta,-\vec{k}}(t')+i\int dt\,\xi_{\alpha,-\vec{k}}(t)R_{\alpha,\vec{k}}(t)\Big\}
\end{aligned} \tag{8.56}$$

The non-equilibrium generating functional can now be written in the following form

$$\begin{aligned}\mathcal{Z} &= \int D\Psi^0 \int D\Pi^0 \int \mathcal{D}\Psi\mathcal{D}R\mathcal{D}\xi \;\; \mathcal{W}(\Psi^0;\Pi^0) DR^0 e^{i\int d^3x R_{0,\alpha}(\vec{x})\left(\Pi^0_\alpha(\vec{x}) - \dot{\Psi}_\alpha(\vec{x},t=0)\right)} \mathcal{P}[\xi] \\ &\exp\left\{-i\int_0^\infty dt\, R_{\alpha,-\vec{k}}(t)\left[\ddot{\Psi}_{\alpha,\vec{k}}(t) + (k^2\,\delta_{\alpha\beta} + \mathbb{M}^2_{\alpha\beta} + \mathbb{V}_{\alpha\beta})\Psi_{\beta,\vec{k}}(t)\right.\right. \\ &\left.\left. + \int dt'\,\Sigma^R_{\alpha\beta}(k;t-t')\Psi_{\beta,\vec{k}}(t') - \xi_{\alpha,\vec{k}}(t)\right]\right\} \qquad (8.57)\end{aligned}$$

$$\mathcal{P}[\xi] = \exp\left\{-\frac{1}{2}\int_0^\infty dt\int_0^\infty dt' \;\; \xi_{\alpha,\vec{k}}(t)\mathcal{K}^{-1}_{\alpha\beta}(k;t-t')\xi_{\beta,-\vec{k}}(t')\right\} \qquad (8.58)$$

The functional integral over R^0 can now be done, resulting in a functional delta function, that fixes the boundary condition $\dot{\Psi}_\alpha(\vec{x},t=0) = \Pi^0_\alpha(\vec{x})$. Finally the path integral over the relative variable can be performed, leading to a functional delta function and the final form of the generating functional given by

$$\begin{aligned}\mathcal{Z} &= \int D\Psi^0 D\Pi^0\, \mathcal{W}(\Psi^0;\Pi^0)\mathcal{D}\Psi\mathcal{D}\xi\,\mathcal{P}[\xi]\;\times \\ &\delta\left[\ddot{\Psi}_{\alpha,\vec{k}}(t) + (k^2\,\delta_{\alpha\beta} + \mathbb{M}^2_{\alpha\beta} + \mathbb{V}_{\alpha\beta})\Psi_{\beta,\vec{k}}(t) + \int_0^t dt'\;\Sigma_{\alpha\beta}(k;t-t')\Psi_{\beta,\vec{k}}(t') - \xi_{\alpha,\vec{k}}(t)\right]\end{aligned} \qquad (8.59)$$

with the boundary conditions on the path integral on Ψ given by

$$\Psi_\alpha(\vec{x},t=0) = \Psi^0_\alpha(\vec{x}) \;\;;\;\; \dot{\Psi}_\alpha(\vec{x},t=0) = \Pi^0_\alpha(\vec{x})\,, \qquad (8.60)$$

where we have used the definition of $\Sigma^R_{\alpha\beta}(k;t-t')$ in terms of $\Sigma_{\alpha\beta}(k;t-t')$ given in equation (8.55).

The meaning of the above generating functional is the following: to obtain correlation functions of the center of mass Wigner variable Ψ we must first find the solution of the classical *stochastic* Langevin equation of motion

$$\begin{aligned}&\ddot{\Psi}_{\alpha,\vec{k}}(t) + (k^2\,\delta_{\alpha\beta} + \mathbb{M}^2_{\alpha\beta} + \mathbb{V}_{\alpha\beta})\Psi_{\beta,\vec{k}}(t) + \int_0^t dt'\;\Sigma_{\alpha\beta}(k;t-t')\Psi_{\beta,\vec{k}}(t') = \xi_{\alpha,\vec{k}}(t) \\ &\Psi_{\alpha,\vec{k}}(t=0) = \Psi^0_{\alpha,\vec{k}} \;\;;\;\; \dot{\Psi}_{\alpha,\vec{k}}(t=0) = \Pi^0_{\alpha,\vec{k}}\end{aligned} \qquad (8.61)$$

for arbitrary noise term ξ and then average the products of Ψ over the stochastic noise with the Gaussian probability distribution $\mathcal{P}[\xi]$ given by (8.58), and finally average over the initial configurations $\Psi^0(\vec{x});\Pi^0(\vec{x})$ weighted by the Wigner function $\mathcal{W}(\Psi^0,\Pi^0)$, which plays the role of an initial phase space distribution function.

Calling the solution of (8.61) $\Psi_{\alpha,\vec{k}}(t;\xi;\Psi_i;\Pi_i)$, the two point correlation function, for example,

is given by

$$\langle \Psi_{\alpha,\vec{k}}(t)\Psi_{\beta,-\vec{k}}(t')\rangle = \frac{\int \mathcal{D}[\xi]\mathcal{P}[\xi]\int D\Psi^0\int D\Pi^0\;\; \mathcal{W}(\Psi^0;\Pi^0)\Psi_{\alpha,\vec{k}}(t;\xi;\Psi^0;\Pi^0)\Psi_{\beta,-\vec{k}}(t';\xi;\Psi^0;\Pi^0)}{\int \mathcal{D}[\xi]\mathcal{P}[\xi]\int D\Psi^0\int D\Pi^0\;\; \mathcal{W}(\Psi^0;\Pi^0)} \; . \tag{8.62}$$

In computing the averages and using the functional delta function to constrain the configurations of Ψ to the solutions of the Langevin equation, there is the Jacobian of the operator $(d^2/dt^2 + k^2)\delta_{\alpha\beta} + \mathbb{M}^2 + \mathbb{V} + \int dt' \Sigma^{ret}(k;t-t')$ which however, is independent of the field and the noise and cancels between numerator and denominator in the averages. There are two different averages:

- The average over the stochastic noise term, which up to this order is Gaussian. We denote the average of a functional $\mathcal{F}[\xi]$ over the noise with the probability distribution function $P[\xi]$ given by eqn. (8.58) as

$$\langle\langle \mathcal{F}\rangle\rangle \equiv \frac{\int \mathcal{D}\xi P[\xi]\mathcal{F}[\xi]}{\int \mathcal{D}\xi P[\xi]}. \tag{8.63}$$

  Since the noise probability distribution function is Gaussian the only necessary correlation functions for the noise are given by

$$\langle\langle \xi_{\alpha,\vec{k}}(t)\rangle\rangle = 0 \; , \; \langle\langle \xi_{\alpha,\vec{k}}(t)\xi_{\beta,\vec{k}'}(t')\rangle\rangle = \mathcal{K}_{\alpha\beta}(k;t-t')\,\delta^3(\vec{k}+\vec{k}') \tag{8.64}$$

  and the higher order correlation functions are obtained from Wick's theorem as befits a Gaussian distribution function. Because the noise kernel $\mathcal{K}_{\alpha\beta}(k;t-t') \neq \delta(t-t')$ the noise is *colored*.

- The average over the initial conditions with the Wigner distribution function $\mathcal{W}(\Psi^0,\Pi^0)$ which we denote as

$$\overline{\mathcal{A}[\Psi^0,\Pi^0]} \equiv \frac{\int D\Psi^0\int D\Pi^0\;\; \mathcal{W}(\Psi^0;\Pi^0)\mathcal{A}[\Psi^0,\Pi^0]}{\int D\Psi^0\int D\Pi^0\;\; \mathcal{W}(\Psi^0;\Pi^0)} \tag{8.65}$$

Therefore, the average in the time evolved reduced density matrix implies *two* distinct averages: an average over the initial conditions of the system fields and and average over the noise distribution function. The *total* average is defined by

$$\langle\cdots\rangle \equiv \overline{\langle\langle\cdots\rangle\rangle} \quad . \tag{8.66}$$

Equal time expectation values and correlation functions are simply expressed in terms of the center of mass Wigner variable Ψ as can be seen as follows: the expectation values of the field

$$\langle \phi^+(\vec{x},t)\rangle = \mathrm{Tr}\phi(\vec{x},t)\rho(t) \quad ; \quad \langle \phi^-(\vec{x},t)\rangle = \mathrm{Tr}\rho(t)\phi(\vec{x},t) \tag{8.67}$$

hence the total average (8.66) is given by

$$\langle \phi(\vec{x},t)\rangle = \langle \Psi(\vec{x},t)\rangle \,. \tag{8.68}$$

Similarly the *equal time* correlation functions obey

$$\langle \phi^+(\vec{x},t)\phi^+(\vec{x}',t)\rangle = \langle \phi^+(\vec{x},t)\phi^-(\vec{x}',t)\rangle = \langle \phi^-(\vec{x},t)\phi^+(\vec{x}',t)\rangle = \langle \phi^-(\vec{x},t)\phi^-(\vec{x}',t)\rangle = \langle \Psi(\vec{x},t)\Psi(\vec{x}',t)\rangle \,. \tag{8.69}$$

Therefore the center of mass variables Ψ contain all the information necessary to obtain expectation values and equal time correlation functions.

8.3.1 One body density matrix and equilibration

We study equilibration by focusing on the one-body density matrix

$$\rho_{\alpha\beta}(k;t) = \mathrm{Tr}\rho(0)\phi_\alpha(\vec{k},t)\phi_\beta(-\vec{k},t) = \mathrm{Tr}\rho(t)\phi_\alpha(\vec{k},0)\phi_\beta(-\vec{k},0) \tag{8.70}$$

where

$$\rho(t) = e^{-iHt}\rho(0)e^{iHt} \tag{8.71}$$

is the time evolved density matrix. The time evolution of the one-body density matrix obeys the Liouville-type equation

$$\frac{d}{dt}\rho_{\alpha\beta}(t) = -i\mathrm{Tr}\big[H,\rho(t)\big]\phi_\alpha(\vec{k},0)\phi_\beta(-\vec{k},0)\,. \tag{8.72}$$

If the system reaches equilibrium with the bath at long times, then it is expected that

$$\big[H,\rho(t)\big] \overset{t\to\infty}{\longrightarrow} 0 \tag{8.73}$$

Therefore the asymptotically long time limit of the one-body density matrix yields information on whether the density matrix is diagonal in the flavor or any other basis. Hence we seek to obtain

$$\rho_{\alpha\beta}(k;\infty) = \mathrm{Tr}\rho(\infty)\phi_\alpha(\vec{k},0)\phi_\beta(-\vec{k},0) = \langle \Psi_{\alpha\vec{k}}(\infty)\Psi_{\beta,-\vec{k}}(\infty)\rangle \,. \tag{8.74}$$

and to establish the basis in which it is nearly diagonal. The second equality in eqn. (8.74) follows from eq. (8.69), and the average is defined by eq.(8.66). To establish a guide post, consider the one-body density matrix for the *free* "neutrino fields" in thermal equilibrium, for which the equilibrium density matrix is

$$\rho_{eq} = e^{-\beta H_0[\varphi]} \tag{8.75}$$

where $H_0[\varphi]$ is the free "neutrino" Hamiltonian. This density matrix is *diagonal* in the basis of mass eigenstates and so is the one-body density matrix which in the mass basis is given by

$$\rho_{ij}(k) = \begin{pmatrix} \frac{1}{2\omega_1(k)} \coth\left[\frac{\beta\omega_1(k)}{2}\right] & 0 \\ 0 & \frac{1}{2\omega_2(k)} \coth\left[\frac{\beta\omega_2(k)}{2}\right] \end{pmatrix} \quad ; \quad i,j = 1,2 \tag{8.76}$$

therefore in the flavor basis the one-body density matrix is given by

$$\rho_{\alpha\beta}(k) = U(\theta) \begin{pmatrix} \frac{1}{2\omega_1(k)} \coth\left[\frac{\beta\omega_1(k)}{2}\right] & 0 \\ 0 & \frac{1}{2\omega_2(k)} \coth\left[\frac{\beta\omega_2(k)}{2}\right] \end{pmatrix} U^{-1}(\theta) \quad ; \quad \alpha,\beta = e,\mu \tag{8.77}$$

This simple example provides a guide to interpret the approach to equilibrium. Including interactions there is a competition between the mass and flavor basis. The interaction is diagonal in the flavor basis, while the unperturbed Hamiltonian is diagonal in the mass basis, this of course is the main physical reason behind neutrino oscillations. In the presence of interactions, the correct form of the equilibrium one-body density matrix can only be obtained from the asymptotic long time limit of the time-evolved density matrix.

8.3.2 Generalized fluctuation-dissipation relation

From the expressions (8.54) and (8.55) in terms of the Wightmann functions (8.39,8.40) which are averages in the equilibrium density matrix of the bath fields (χ, W), we obtain a dispersive representation for the kernels $\mathcal{K}_{\alpha\beta}(k;t-t');\Sigma^R_{\alpha\beta}(k;t-t')$. This is achieved by writing the expectation value in terms of energy eigenstates of the bath, introducing the identity in this basis, and using the time evolution of the Heisenberg field operators to obtain

$$G^2\ \mathcal{G}^{>}_{\alpha\beta}(k;t-t') = \int_{-\infty}^{\infty} d\omega\ \sigma^{>}_{\alpha\beta}(\vec{k},\omega)\ e^{i\omega(t-t')} \quad ; \quad G^2\ \mathcal{G}^{<}_{\alpha\beta}(k;t-t') = \int_{-\infty}^{\infty} d\omega\ \sigma^{<}_{\alpha\beta}(\vec{k},\omega)\ e^{i\omega(t-t')} \tag{8.78}$$

with the spectral functions

$$\sigma^{>}_{\alpha\beta}(\vec{k},\omega) = \frac{G^2}{\mathcal{Z}_b}\sum_{m,n} e^{-\beta E_n}\langle n|\mathcal{O}_{\alpha,\vec{k}}(0)|m\rangle\langle m|\mathcal{O}_{\beta,-\vec{k}}(0)|n\rangle\,\delta(\omega-(E_n-E_m)) \tag{8.79}$$

$$\sigma^{<}_{\alpha\beta}(\vec{k},\omega) = \frac{G^2}{\mathcal{Z}_b}\sum_{m,n} e^{-\beta E_m}\langle n|\mathcal{O}_{\beta,-\vec{k}}(0)|m\rangle\langle m|\mathcal{O}_{\alpha,\vec{k}}(0)|n\rangle\,\delta(\omega-(E_m-E_n)) \tag{8.80}$$

where $\mathcal{Z}_b = \mathrm{Tr}\, e^{-\beta H_\chi}$ is the equilibrium partition function of the "bath" and in the above expressions the averages are solely with respect to the bath variables. Upon relabelling $m \leftrightarrow n$ in the sum in the definition (8.80) and using the fact that these correlation functions are parity and rotational invariant[171] and diagonal in the flavor basis we find the KMS relation[171]

$$\sigma^{<}_{\alpha\beta}(k,\omega) = \sigma^{>}_{\alpha\beta}(k,-\omega) = e^{\beta\omega}\sigma^{>}_{\alpha\beta}(k,\omega)\,. \tag{8.81}$$

Using the spectral representation of the $\Theta(t-t')$ we find the following representation for the retarded self-energy

$$\Sigma^R_{\alpha\beta}(k;t-t') = \int_{-\infty}^{\infty}\frac{dk_0}{2\pi}e^{ik_0(t-t')}\widetilde{\Sigma}^R_{\alpha\beta}(k;k_0) \tag{8.82}$$

with

$$\widetilde{\Sigma}^R_{\alpha\beta}(k;k_0) = \int_{-\infty}^{\infty} d\omega\frac{[\sigma^{>}_{\alpha\beta}(k;\omega)-\sigma^{<}_{\alpha\beta}(k;\omega)]}{\omega-k_0+i\epsilon}\,. \tag{8.83}$$

Using the condition (8.81) the above spectral representation can be written in a more useful manner as

$$\widetilde{\Sigma}^R_{\alpha\beta}(k;k_0) = -\frac{1}{\pi}\int_{-\infty}^{\infty} d\omega\frac{\mathrm{Im}\widetilde{\Sigma}^R_{\alpha\beta}(k;\omega)}{\omega-k_0+i\epsilon}\,, \tag{8.84}$$

where the imaginary part of the self-energy is given by

$$\mathrm{Im}\widetilde{\Sigma}^R_{\alpha\beta}(k;\omega) = \pi\sigma^{>}_{\alpha\beta}(k;\omega)\left[e^{\beta\omega}-1\right] \tag{8.85}$$

and is positive for $\omega > 0$. Equation (8.81) entails that the imaginary part of the retarded self-energy is an odd function of frequency, namely

$$\mathrm{Im}\widetilde{\Sigma}^R_{\alpha\beta}(k;\omega) = -\mathrm{Im}\widetilde{\Sigma}^R_{\alpha\beta}(k;-\omega)\,. \tag{8.86}$$

The relation (8.85) leads to the following results which will be useful later

$$\sigma^{>}_{\alpha\beta}(k;\omega) = \frac{1}{\pi}\mathrm{Im}\widetilde{\Sigma}^R_{\alpha\beta}(k;\omega)\,n(\omega) \quad ; \quad \sigma^{<}_{\alpha\beta}(k;\omega) = \frac{1}{\pi}\mathrm{Im}\widetilde{\Sigma}^R_{\alpha\beta}(k;\omega)\,[1+n(\omega)] \tag{8.87}$$

where $n(\omega) = [e^{\beta\omega} - 1]^{-1}$ is the Bose-Einstein distribution function. Similarly from the definitions (8.54) and (8.78) and the condition (8.81) we find

$$\mathcal{K}_{\alpha\beta}(k; t - t') = \int_{-\infty}^{\infty} \frac{dk_0}{2\pi} e^{ik_0(t-t')} \widetilde{\mathcal{K}}_{\alpha\beta}(k; k_0) \tag{8.88}$$

$$\widetilde{\mathcal{K}}_{\alpha\beta}(k; k_0) = \pi\sigma^{>}_{\alpha\beta}(k; k_0) \left[e^{\beta k_0} + 1 \right] \tag{8.89}$$

whereupon using the condition (7.55) leads to the generalized fluctuation-dissipation relation

$$\widetilde{\mathcal{K}}_{\alpha\beta}(k; k_0) = \mathrm{Im}\widetilde{\Sigma}^{R}_{\alpha\beta}(k; k_0) \coth \left[\frac{\beta k_0}{2} \right] . \tag{8.90}$$

Thus we see that $\mathrm{Im}\widetilde{\Sigma}^{R}_{\alpha\beta}(k; k_0)$; $\widetilde{\mathcal{K}}_{\alpha\beta}(k; k_0)$ are odd and even functions of frequency respectively.

For the analysis below we also need the following representation (see eqn. (8.55))

$$\Sigma_{\alpha\beta}(k; t - t') = -i \int_{-\infty}^{\infty} e^{i\omega(t-t')} \left[\sigma^{>}_{\alpha\beta}(k; \omega) - \sigma^{<}_{\alpha\beta}(k; \omega) \right] d\omega = \frac{i}{\pi} \int_{-\infty}^{\infty} e^{i\omega(t-t')} \mathrm{Im}\widetilde{\Sigma}^{R}_{\alpha\beta}(k; \omega) d\omega \tag{8.91}$$

whose Laplace transform is given by

$$\widetilde{\Sigma}_{\alpha\beta}(k; s) \equiv \int_{0}^{\infty} dt e^{-st} \Sigma_{\alpha\beta}(k; t) = -\frac{1}{\pi} \int_{-\infty}^{\infty} \frac{\mathrm{Im}\widetilde{\Sigma}^{R}_{\alpha\beta}(k; \omega)}{\omega + is} d\omega \tag{8.92}$$

This spectral representation, combined with (8.84) lead to the relation

$$\widetilde{\Sigma}^{R}_{\alpha\beta}(k; k_0) = \widetilde{\Sigma}_{\alpha\beta}(k; s = ik_0 + \epsilon) \tag{8.93}$$

The self energy and noise correlation kernels $\widetilde{\Sigma}, \widetilde{\mathcal{K}}$ are diagonal in the flavor basis because the interaction is diagonal in this basis. Namely, in the flavor basis

$$\widetilde{\Sigma}(k, \omega) = \begin{pmatrix} \widetilde{\Sigma}_{ee}(k, \omega) & 0 \\ 0 & \widetilde{\Sigma}_{\mu\mu}(k, \omega) \end{pmatrix} \quad ; \quad \widetilde{\mathcal{K}} = [1 + 2n(\omega)] \, \mathrm{Im}\widetilde{\Sigma}(k, \omega) = \begin{pmatrix} \widetilde{\mathcal{K}}_{ee}(k, \omega) & 0 \\ 0 & \widetilde{\mathcal{K}}_{\mu\mu}(k, \omega) \end{pmatrix} . \tag{8.94}$$

In the *mass* basis these kernels are given by

$$\widetilde{\Sigma} = \frac{1}{2} \left(\widetilde{\Sigma}_{ee} + \widetilde{\Sigma}_{\mu\mu} \right) \mathbb{1} + \frac{1}{2} \left(\widetilde{\Sigma}_{ee} - \widetilde{\Sigma}_{\mu\mu} \right) \begin{pmatrix} \cos 2\theta & \sin 2\theta \\ \sin 2\theta & -\cos 2\theta \end{pmatrix} \tag{8.95}$$

and

$$\widetilde{\mathcal{K}} = \frac{1}{2} \left(\widetilde{\mathcal{K}}_{ee} + \widetilde{\mathcal{K}}_{\mu\mu} \right) \mathbb{1} + \frac{1}{2} \left(\widetilde{\mathcal{K}}_{ee} - \widetilde{\mathcal{K}}_{\mu\mu} \right) \begin{pmatrix} \cos 2\theta & \sin 2\theta \\ \sin 2\theta & -\cos 2\theta \end{pmatrix} . \tag{8.96}$$

8.4 DYNAMICS: SOLVING THE LANGEVIN EQUATION

The solution of the equation of motion (8.61) can be found by Laplace transform. Define the Laplace transforms

$$\widetilde{\Psi}_{\alpha,\vec{k}}(s) = \int_0^\infty dt e^{-st} \Psi_{\alpha;\vec{k}}(t) \;\; ; \;\; \widetilde{\xi}_{\alpha,\vec{k}}(s) = \int_0^\infty dt e^{-st} \xi_{\alpha,\vec{k}}(t) \tag{8.97}$$

along with the Laplace transform of the self-energy given by eqn. (8.92). The Langevin equation in Laplace variable becomes the following algebraic matrix equation

$$\left[(s^2 + k^2)\delta_{\alpha\beta} + \mathbb{M}^2_{\alpha\beta} + \mathbb{V}_{\alpha\beta} + \widetilde{\Sigma}_{\alpha\beta}(k;s) \right] \widetilde{\Psi}_{\beta,\vec{k}}(s) = \Pi_{0,\alpha,\vec{k}} + s\, \Psi_{0,\alpha,\vec{k}} + \widetilde{\xi}_{\alpha,\vec{k}}(s) \tag{8.98}$$

where we have used the initial conditions (8.60). The solution in real time can be written in a more compact manner as follows. Introduce the matrix function

$$\widetilde{G}(k;s) = \left[(s^2 + k^2)\mathbb{1} + \mathbb{M}^2 + \mathbb{V} + \widetilde{\Sigma}(k;s) \right]^{-1} \tag{8.99}$$

and its anti-Laplace transform

$$G_{\alpha\beta}(k;t) = \int_{\mathcal{C}} \frac{ds}{2\pi i} \widetilde{G}_{\alpha\beta}(k;s)\, e^{st} \tag{8.100}$$

where $\mathcal{C}$ refers to the Bromwich contour, parallel to the imaginary axis in the complex s plane to the right of all the singularities of $\widetilde{G}(k;s)$. This function obeys the initial conditions

$$G_{\alpha\beta}(k;0) = 0 \;\; ; \;\; \dot{G}_{\alpha\beta}(k;0) = 1\,. \tag{8.101}$$

In terms of this auxiliary function the solution of the Langevin equation (8.61) in real time is given by

$$\Psi_{\alpha,\vec{k}}(t;\Psi^0;\Pi^0;\xi) = \dot{G}_{\alpha\beta}(k;t)\, \Psi^0_{\beta\vec{k}} + G_{\alpha\beta}(k;t)\, \Pi^0_{\beta,\vec{k}} + \int_0^t G_{\alpha\beta}(k;t')\; \xi_{\beta,\vec{k}}(t-t')dt'\,, \tag{8.102}$$

where the dot stands for derivative with respect to time. In the flavor basis we find

$$\widetilde{G}_f(k;s) = \mathcal{S}(k;s) \left[\Big(s^2 + \overline{\omega}^2(k) + \overline{\Sigma}(k;s) \Big) \mathbb{1} + \frac{\delta M^2}{2} \begin{pmatrix} \cos 2\theta - \Delta(k;s) & -\sin 2\theta \\ -\sin 2\theta & -\cos 2\theta + \Delta(k;s) \end{pmatrix} \right] \tag{8.103}$$

whereas in the mass basis we find

$$\widetilde{G}_m(k;s) = \mathcal{S}(k;s)\left[\Big(s^2+\overline{\omega}^2(k)+\overline{\Sigma}(k;s)\Big)\mathbb{1}+\frac{\delta M^2}{2}\begin{pmatrix} 1-\Delta(k;s)\,\cos 2\theta & \Delta(k;s)\,\sin 2\theta \\ \Delta(k;s)\,\sin 2\theta & -1+\Delta(k;s)\,\cos 2\theta \end{pmatrix}\right] \tag{8.104}$$

where $\overline{M}^2$ and δM^2 were defined by eqn. (9.7) and to simplify notation we defined

$$\overline{\omega}(k) = \sqrt{k^2+\overline{M}^2} \tag{8.105}$$

$$\overline{\Sigma}(k;s) = \frac{1}{2}\Big(\widetilde{\Sigma}_{ee}(k;s)+V_{ee}+\widetilde{\Sigma}_{\mu\mu}(k;s)+V_{\mu\mu}\Big) \tag{8.106}$$

$$\Delta(k;s) = \frac{\widetilde{\Sigma}_{ee}(k;s)+V_{ee}-\widetilde{\Sigma}_{\mu\mu}(k;s)-V_{\mu\mu}}{M_2^2-M_1^2} \tag{8.107}$$

and

$$\mathcal{S}(k;s) = \left[\Big(s^2+\overline{\omega}^2(k)+\overline{\Sigma}(k;s)\Big)^2-\Big(\frac{\delta M^2}{2}\Big)^2\Big[(\cos 2\theta-\Delta(k;s))^2+(\sin 2\theta)^2\Big]\right]^{-1} \tag{8.108}$$

In what follows we define the analytic continuation of the quantities defined above with the same nomenclature to avoid introducing further notation, namely

$$\overline{\Sigma}(k;\omega)\equiv\overline{\Sigma}(k;s=i\omega+\epsilon)\quad;\quad \Delta(k;\omega)\equiv\Delta(k;s=i\omega+\epsilon)\,. \tag{8.109}$$

Their real and imaginary parts are given by

$$\overline{\Sigma}_R(k;\omega) = \frac{1}{2}\left[\Sigma_{R,ee}(k,\omega)+\Sigma_{R,\mu\mu}(k,\omega)+V_{ee}+V_{\mu\mu}\right] \tag{8.110}$$

$$\overline{\Sigma}_I(k;\omega) = \frac{1}{2}\left[\Sigma_{I,ee}(k,\omega)+\Sigma_{I,\mu\mu}(k,\omega)\right] \tag{8.111}$$

$$\Delta_R(k;\omega) = \frac{1}{\delta M^2}\left[\Sigma_{R,ee}(k,\omega)-\Sigma_{R,\mu\mu}(k,\omega)+V_{ee}-V_{\mu\mu}\right] \tag{8.112}$$

$$\Delta_I(k;\omega) = \frac{1}{\delta M^2}\left[\Sigma_{I,ee}(k,\omega)-\Sigma_{I,\mu\mu}(k,\omega)\right] \tag{8.113}$$

We remark that while the matter potential V is of of order G, Σ is of order G^2. Therefore, in perturbation theory

$$\overline{\Sigma}_R(k;\omega) >> \overline{\Sigma}_I(k;\omega)\quad;\quad \Delta_R(k;\omega) >> \Delta_I(k;\omega)\,. \tag{8.114}$$

This inequality also holds in the standard model, where the matter potential is of order G_F[57] while the absorptive part that determines the relaxation rates is of order G_F^2. This perturbative inequality will be used repeatedly in the analysis that follows, and we emphasize that it holds in the correct description of neutrinos propagating in a medium.

8.5 SINGLE PARTICLES AND QUASIPARTICLES

Exact single particle states are determined by the position of the isolated poles of the Green's function in the complex $s-$ plane. Before we study the interacting case, it proves illuminating to first study the *free*, non-interacting case.

8.5.1 Non-interacting case: $G = 0$

To begin the analysis, an example helps to clarify this formulation: consider the non-interacting case $G = 0$ in which $\overline{\Sigma} = 0; \Delta = 0$. In this case $\widetilde{G}_{f,m}(k;s)$ have simple poles at $s = \pm i\omega_1(k)$ and $\pm i\omega_2(k)$ where

$$\omega_i(k) = \sqrt{k^2 + M_i^2} \quad ; \quad i = 1, 2\,. \tag{8.115}$$

Computing the residues at these simple poles we find in the flavor basis

$$G_f(k;t) = \frac{\sin(\omega_1(k)t)}{\omega_1(k)}\,\mathbb{R}^{(1)}(\theta) + \frac{\sin(\omega_2(k)t)}{\omega_2(k)}\,\mathbb{R}^{(2)}(\theta) \tag{8.116}$$

where we have introduced the matrices

$$\mathbb{R}^{(1)}(\theta) = \begin{pmatrix} \cos^2\theta & -\cos\theta\sin\theta \\ -\cos\theta\sin\theta & \sin^2\theta \end{pmatrix} = U(\theta)\begin{pmatrix} 1 & 0 \\ 0 & 0 \end{pmatrix} U^{-1}(\theta) \tag{8.117}$$

$$\mathbb{R}^{(2)}(\theta) = \begin{pmatrix} \sin^2\theta & \cos\theta\sin\theta \\ \cos\theta\sin\theta & \cos^2\theta \end{pmatrix} = U(\theta)\begin{pmatrix} 0 & 0 \\ 0 & 1 \end{pmatrix} U^{-1}(\theta) \tag{8.118}$$

In the mass basis

$$G_m(k;t) = \begin{pmatrix} \frac{\sin(\omega_1(k)t)}{\omega_1(k)} & 0 \\ 0 & \frac{\sin(\omega_2(k)t)}{\omega_2(k)} \end{pmatrix} \tag{8.119}$$

with the relation

$$G_f(k;t) = U(\theta)\, G_m(k;t)\, U^{-1}(\theta) \tag{8.120}$$

and $U(\theta)$ is given by 9.4. Consider for simplicity an initial condition with $\Psi^0 \neq 0; \Pi^0 = 0$ in both cases, flavor and mass. The expectation value of the flavor fields Φ_α in the reduced density matrix (8.66) is given by

$$\left\langle \begin{pmatrix} \Psi_{e,\vec{k}}(t) \\ \Psi_{\mu,\vec{k}}(t) \end{pmatrix} \right\rangle = \left[\cos(\omega_1(k)t)\,\mathbb{R}^{(1)}(\theta) + \cos(\omega_2(k)t)\,\mathbb{R}^{(2)}(\theta)\right] \begin{pmatrix} \Psi^0_{e,\vec{k}} \\ \Psi^0_{\mu,\vec{k}} \end{pmatrix} \tag{8.121}$$

and that for the fields in the mass basis is

$$\left\langle \begin{pmatrix} \Psi_1(k;t) \\ \Psi_2(k;t) \end{pmatrix} \right\rangle = \begin{pmatrix} \Psi^0_{1,\vec{k}} \cos(\omega_1(k)t) \\ \Psi^0_{2,\vec{k}} \cos(\omega_2(k)t) \end{pmatrix} \tag{8.122}$$

These are precisely the solutions of the classical equations of motion in terms of flavor and mass eigenstates, namely

$$\begin{aligned} \phi_e(k;t) &= \cos\theta\,\varphi_1(k;t) + \sin\theta\,\varphi_2(k;t) \\ \phi_\mu(k;t) &= \cos\theta\,\varphi_2(k;t) - \sin\theta\,\varphi_2(k;t) \end{aligned} \tag{8.123}$$

where

$$\varphi_1(k;t) = \varphi_1(k;0)\,\cos\omega_1(k)t \;\;;\;\; \varphi_2(k;t) = \varphi_2(k;0)\,\cos\omega_2(k)t \tag{8.124}$$

for vanishing initial canonical momentum and the initial values are given in terms of flavor fields by

$$\begin{aligned} \varphi_1(k;0) &= \cos\theta\,\phi_e(k;0) - \sin\theta\,\phi_\mu(k;0) \\ \varphi_2(k;0) &= \cos\theta\,\phi_\mu(k;0) + \sin\theta\,\phi_e(k;0) \end{aligned} \tag{8.125}$$

inserting (8.124) with the initial conditions (8.125) one recognizes that the solution (8.121) is the expectation value of the classical equation of motion with initial conditions on the flavor fields and vanishing initial canonical momentum.

It is convenient to separate the positive (particles) and negative (antiparticles) frequency components by considering an initial condition with $\Pi^0_{\alpha,\vec{k}} \neq 0$, in such a way that the time dependence is determined by phases corresponding to the propagation of particles (or antiparticles). Without mixing ($\theta = 0$) this is achieved by choosing the following initial conditions

$$\Pi^0_{\alpha,\vec{k}} = \mp i\Omega_\alpha(k)\,\Psi^0_{\alpha,\vec{k}} \tag{8.126}$$

for particles ($-$) and antiparticles ($+$) respectively, as in eq. (8.11). This choice of initial conditions leads to the result

$$\begin{aligned} &\langle\langle \Psi_{\alpha,\vec{k}}(t) \rangle\rangle \\ &= \left\{ \mathbb{R}^{(1)}_{\alpha\beta}(\theta) \left[\cos(\omega_1(k)t) \mp i\frac{\Omega_\beta(k)}{\omega_1(k)} \sin(\omega_1(k)t) \right] + \mathbb{R}^{(2)}_{\alpha\beta}(\theta) \left[\cos(\omega_2(k)t) \mp i\frac{\Omega_\beta(k)}{\omega_2(k)} \sin(\omega_2(k)t) \right] \right\} \Psi^0_{\beta,\vec{k}} \end{aligned} \tag{8.127}$$

It is clear from (8.127) that no single choice of frequencies $\Omega_\beta(k)$ can lead uniquely to time evolution in terms of single particle/antiparticle phases $e^{\mp i\omega_{1,2}(k)t}$. This is a consequence of the ambiguity in the definition of flavor states as discussed in detail in section (8.2.1). However, for the cases in which $|M_1^2 - M_2^2| \ll (k^2 + \overline{M}^2)$, relevant for relativistic mixed neutrinos, and for $K^0\overline{K}^0$ and $B^0\overline{B}^0$ mixing, the positive and negative frequency components can be *approximately* projected out as follows. Define

$$\overline{\omega}(k) = \sqrt{k^2 + \overline{M}^2} \tag{8.128}$$

in the nearly degenerate or relativistic regime when $|\delta M^2|/\,\overline{\omega}^2(k) \ll 1$

$$\omega_1(k) = \overline{\omega}(k)\left[1 - \frac{\delta M^2}{4\,\overline{\omega}^2(k)} + \mathcal{O}\left(\frac{\delta M^2}{\overline{\omega}^2(k)}\right)^2\right] \;\; ; \;\; \omega_2(k) = \overline{\omega}(k)\left[1 + \frac{\delta M^2}{4\,\overline{\omega}^2(k)} + \mathcal{O}\left(\frac{\delta M^2}{\overline{\omega}^2(k)}\right)^2\right]. \tag{8.129}$$

Taking $\Omega_\beta(k) = \overline{\omega}(k)$ and choosing for example the negative sign (positive frequency component) in (8.127) we find

$$\langle \Psi_{\alpha,\vec{k}}(t)\rangle = \left\{ \mathbb{R}^{(1)}_{\alpha\beta}(\theta)\, e^{-i\omega_1(k)t} + \mathbb{R}^{(2)}_{\alpha\beta}(\theta)\, e^{-i\omega_2(k)t} + \mathcal{O}\left(\frac{\delta M^2}{\overline{\omega}^2(k)}\right)\right\} \Psi^0_{\beta,\vec{k}} \tag{8.130}$$

Consider the following initial condition

$$\Psi^0_{\vec{k}} = \begin{pmatrix} \Psi^0_{e,\vec{k}} \\ 0 \end{pmatrix} \tag{8.131}$$

neglecting the corrections in (8.130) we find

$$|\langle \Psi_{\mu,\vec{k}}(t)\rangle|^2 = \sin^2 2\theta\, \sin^2\left(\frac{\delta M^2}{4\,\overline{\omega}(k)}\, t\right) \Psi^0_{e,\vec{k}} + \mathcal{O}\left(\frac{\delta M^2}{\overline{\omega}^2(k)}\right)^2 \tag{8.132}$$

which is identified with the usual result for the oscillation transition probability $\Psi_e \to \Psi_\mu$ upon neglecting the corrections.

8.5.2 Interacting case: $G \neq 0$

For $G \neq 0$, the self-energy as a function of frequency and momentum is in general complex, the imaginary part arises from multiparticle thresholds. When the imaginary part of the self-energy does not vanish at the value of the frequency corresponding to the dispersion relation of the free

particle states, these particles can decay and no longer appear as asymptotic states. The poles in the Green's function move off the physical sheet into a higher Riemann sheet, the particles now become resonances.

Single particle states correspond to true poles of the propagator (Green's function) in the physical sheet, which are necessarily away from the multiparticle thresholds. This case is depicted in fig. (8.2).

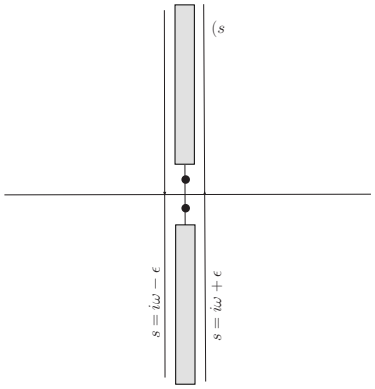

Figure 8.2: Bromwich contour in s-plane, the shaded region denotes the cut discontinuity from multiparticle thresholds across the imaginary axis, the filled circles represent the single particle poles.

Let us consider the Green's function in the flavor basis eqn. (8.103). The single particle poles are determined by the poles of $\mathcal{S}(k;s)$ on the imaginary axis away from the multiparticle cuts. These are determined by the roots of the following equations

$$\Omega_1^2(k) = \overline{\omega}^{\,2}(k) + \overline{\Sigma}_R(k;\Omega_1(k)) - \frac{\delta M^2}{2}\Big[\big(\cos 2\theta - \Delta_R(k;\Omega_1(k))\big)^2 + \big(\sin 2\theta\big)^2\Big]^{\frac{1}{2}} \quad (8.133)$$

$$\Omega_2^2(k) = \overline{\omega}^{\,2}(k) + \overline{\Sigma}_R(k;\Omega_2(k)) + \frac{\delta M^2}{2}\Big[\big(\cos 2\theta - \Delta_R(k;\Omega_2(k))\big)^2 + \big(\sin 2\theta\big)^2\Big]^{\frac{1}{2}} \quad (8.134)$$

along with the conditions

$$\overline{\Sigma}_I(k;\Omega_{1,2}(k)) = 0 \;\; ; \;\; \Delta_I(k;\Omega_{1,2}(k)) = 0 \quad (8.135)$$

where the subscripts R, I refer to the real and imaginary parts respectively. Evaluating the residues at the single particle poles and using that the real and imaginary parts of the self-energies are even

and odd functions of frequency respectively, we find

$$G_f(k;t) = Z_k^{(1)} \frac{\sin(\Omega_1(k)t)}{\Omega_1(k)} \;\; \mathbb{R}^{(1)}\big(\theta_m^{(1)}(k)\big) + Z_k^{(2)} \frac{\sin(\Omega_2(k)t)}{\Omega_2(k)} \;\; \mathbb{R}^{(2)}\big(\theta_m^{(2)}(k)\big) + G_{f,cut}(t) \tag{8.136}$$

where $G_{f,cut}(t)$ is the contribution from the multiparticle cut, the matrices $\mathbb{R}^{(1,2)}$ are given by (9.30,9.31) and $\theta_m^{1,2}(k)$ are the mixing angles *in the medium*

$$\begin{aligned} \cos 2\theta_m^i(k) &= \frac{\cos 2\theta - \Delta_R(\Omega_i(k))}{\Big[\big(\cos 2\theta - \Delta_R(k;\Omega_i(k))\big)^2 + \big(\sin 2\theta\big)^2\Big]^{\frac{1}{2}}} \\ \sin 2\theta_m^i(k) &= \frac{\sin 2\theta}{\Big[\big(\cos 2\theta - \Delta_R(k;\Omega_i(k))\big)^2 + \big(\sin 2\theta\big)^2\Big]^{\frac{1}{2}}} \,. \end{aligned} \tag{8.137}$$

for $i = 1, 2$. The wave function renormalization constants are given by

$$Z_k^{(i)} = \left[1 - \frac{1}{2\omega}\Big(\overline{\Sigma}_R'(k;\omega) - (-1)^i \frac{\delta M^2}{2} \cos 2\theta_m^i(k) \Delta_R'(k;\omega)\Big)\right]^{-1}_{\omega=\Omega^i(k)} \tag{8.138}$$

where the prime stands for derivative with respect to ω. At asymptotically long time the contribution from the cut $G_{f,cut}(t) \sim t^{-\alpha}$ where α is determined by the behavior of the self-energy at threshold[174, 188].

In perturbation theory and in the limit $\overline{\omega}(k)^2 \gg |\delta M^2|$ the dispersion relations (8.133,8.134) can be solved by writing

$$\pm\Omega^i(k) = \pm(\overline{\omega}(k) + \delta\omega_i(k)) \,, \tag{8.139}$$

we find

$$\delta\omega_i(k) = \frac{\overline{\Sigma}_R(k;\overline{\omega}(k))}{2\,\overline{\omega}(k)} + (-1)^i \;\; \frac{\delta M^2}{4\,\overline{\omega}(k)} \, \overline{\varrho}(k) \tag{8.140}$$

where we defined

$$\varrho(k;\omega) = \left[(\cos 2\theta - \Delta_R(k;\omega))^2 + (\sin 2\theta)^2\right]^{\frac{1}{2}} \tag{8.141}$$

and the shorthand

$$\overline{\varrho}(k) = \varrho(k;\omega = \overline{\omega}(k)) \,. \tag{8.142}$$

To leading order in the perturbative expansion and in $\delta M^2/\overline{\omega}^2(k)$ we find $\theta_m^{(1)}(k) = \theta_m^{(2)}(k) = \theta_m(k)$. Gathering these results, we find the dispersion relations and mixing angles in the medium to be

given by the following relations,

$$\Omega_1(k) = \overline{\omega}(k) + \frac{\overline{\Sigma}_R(k;\overline{\omega}(k))}{2\,\overline{\omega}(k)} - \frac{\delta M^2}{4\,\overline{\omega}(k)}\,\overline{\varrho}(k) \tag{8.143}$$

$$\Omega_2(k) = \overline{\omega}(k) + \frac{\overline{\Sigma}_R(k;\overline{\omega}(k))}{2\,\overline{\omega}(k)} + \frac{\delta M^2}{4\,\overline{\omega}(k)}\,\overline{\varrho}(k)\,, \tag{8.144}$$

and

$$\begin{aligned}\cos 2\theta_m(k) &= \frac{\cos 2\theta - \Delta_R(k;\overline{\omega}(k))}{\left[\left(\cos 2\theta - \Delta_R(k;\overline{\omega}(k))\right)^2 + \left(\sin 2\theta\right)^2\right]^{\frac{1}{2}}} \\ \sin 2\theta_m(k) &= \frac{\sin 2\theta}{\left[\left(\cos 2\theta - \Delta_R(k;\overline{\omega}(k))\right)^2 + \left(\sin 2\theta\right)^2\right]^{\frac{1}{2}}}\,.\end{aligned} \tag{8.145}$$

These dispersion relations and mixing angles have exactly the *same form* as those obtained in the field theoretical studies of neutrino mixing in a medium[57, 189].

8.5.3 Quasiparticles and relaxation

Even a particle that is stable in the vacuum acquires a width in the medium through several processes, such as collisional broadening or Landau damping[171]. In this case there are no isolated poles in the Green's function in the physical sheet, the poles move off the imaginary axis in the complex $s-$plane on to a second or higher Riemann sheet. The Green's function now features branch cut discontinuities across the imaginary axis perhaps with isolated regions of analyticity. The inverse Laplace transform is now carried out by wrapping around the imaginary axis as shown in fig. (8.3), and the real time Green's function is given by

$$G_{\alpha\beta}(k;t) = \frac{i}{\pi}\int_{-\infty}^{\infty} d\omega\, e^{i\omega t}\;\; \mathrm{Im}\widetilde{G}_{\alpha\beta}(k;s=i\omega+\epsilon) \tag{8.146}$$

Under the validity of perturbation theory, when the inequality (8.114) is fulfilled we consistently keep terms up to $\mathcal{O}(G^2)$ and find the imaginary part to be given by the following expression

$$\mathrm{Im}\widetilde{G}(k;s=i\omega+\epsilon) = \frac{-\mathbb{A}(D_-\gamma_+ + D_+\gamma_-) + \mathbb{B}(D_+D_- - \gamma_+\gamma_-)}{(D_+^2+\gamma_+^2)(D_-^2+\gamma_-^2)} \tag{8.147}$$

where we have introduced

$$D_\pm(k;\omega) = -\omega^2 + \overline{\omega}_k^2 + \overline{\Sigma}_R(k;\omega) \;\mp \frac{1}{2}\delta M^2 \varrho(k;\omega) \tag{8.148}$$

$$\gamma_\pm(k;\omega) = \frac{1}{2}\left(1 \pm \cos 2\theta_m(\omega,k)\right)\,\Sigma_{I,ee}(k;\omega) + \frac{1}{2}\left(1 \mp \cos 2\theta_m(\omega,k)\right)\,\Sigma_{I,\mu\mu}(k;\omega) \tag{8.149}$$

$\Sigma_{R,I}$ are the real and imaginary parts of the self energy respectively, with

$$\Delta_R(k;\omega) = \frac{1}{\delta M^2}\left[\Sigma_{R,ee}(k;\omega) + V_{ee} - \Sigma_{R,\mu\mu}(k;\omega) - V_{\mu\mu}\right] , \tag{8.150}$$

and

$$\mathbb{A}(k;\omega) = \left[-\omega^2 + \overline{\omega}_k^2 + \overline{\Sigma}_R(k;\omega)\mathbb{1}\right] + \frac{\delta M^2}{2}\begin{pmatrix} \cos 2\theta - \Delta_R(k;\omega) & -\sin 2\theta \\ -\sin 2\theta & -\cos 2\theta + \Delta_R(k;\omega) \end{pmatrix} , \tag{8.151}$$

$$\mathbb{B}(k;\omega) = \begin{pmatrix} \Sigma_{I,\mu\mu}(k;\omega) & 0 \\ 0 & \Sigma_{I,ee}(k;\omega) \end{pmatrix} . \tag{8.152}$$

The denominator in (8.147) features complex zeroes for

$$D_\pm(k;\omega) + \gamma_\pm(k;\omega) = 0 . \tag{8.153}$$

Near these zeroes $\mathrm{Im}\widetilde{G}(k; s = i\omega + \epsilon)$ has the typical Breit-Wigner form for resonances. The dynamical evolution at long times is dominated by the complex poles in the upper half $\omega-$ plane associated with these resonances. In perturbation theory the complex poles of $\mathrm{Im}\widetilde{G}(k; s = i\omega + \epsilon)$ occur at

$$\omega = \pm\Omega_1(k) + i\frac{\Gamma_1(k)}{2} \tag{8.154}$$

and

$$\omega = \pm\Omega_2(k) + i\frac{\Gamma_2(k)}{2} \tag{8.155}$$

where $\Omega_{1,2}(k)$ are given by (8.133,8.134) and

$$\frac{\Gamma_1(k)}{2} = \frac{\gamma_+(k,\Omega_1(k))}{2\,\Omega_1(k)} \approx \frac{\gamma_+(k,\overline{\omega}(k))}{2\,\overline{\omega}(k)} \quad ; \quad \frac{\Gamma_2(k)}{2} = \frac{\gamma_-(k,\Omega_2(k))}{2\,\Omega_2(k)} \approx \frac{\gamma_-(k,\overline{\omega}(k))}{2\,\overline{\omega}(k)} \tag{8.156}$$

These relaxation rates can be written in an illuminating manner

$$\Gamma_1(k) = \Gamma_{ee}(k)\cos^2\theta_m(k) + \Gamma_{\mu\mu}(k)\sin^2\theta_m(k) \tag{8.157}$$

$$\Gamma_2(k) = \Gamma_{\mu\mu}(k)\cos^2\theta_m(k) + \Gamma_{ee}(k)\sin^2\theta_m(k) \tag{8.158}$$

where

$$\Gamma_{\alpha\alpha}(k) = \frac{\Sigma_{I,\alpha\alpha}(k;\overline{\omega}(k))}{\overline{\omega}(k)} \tag{8.159}$$

are the relaxation rates of the flavor fields in *absence* of mixing. These relaxation rates are similar to those proposed within the context of flavor conversions in supernovae[190], or active-sterile oscillations[77, 78, 112].

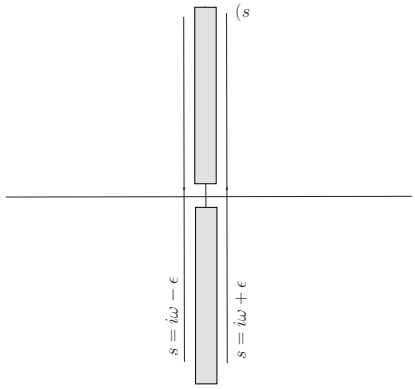

Figure 8.3: Bromwich contour in s-plane, the shaded region denotes the cut discontinuity from multiparticle thresholds across the imaginary axis.

We carry out the frequency integral in (8.146) by approximating the integrand as a sum of two Breit-Wigner Lorentzians near $\omega = \pm\Omega_{1,2}(k)$ with the following result in the flavor basis,

$$G_f(k;t) = Z_k^{(1)}\, e^{-\frac{\Gamma_1(k)}{2}t}\left[\frac{\sin(\Omega_1(k)t)}{\Omega_1(k)}\,\mathbb{R}^{(1)}(\theta_m(k)) - \frac{\widetilde{\gamma}(k)}{2}\,\frac{\cos(\Omega_1(k)t)}{\Omega_1(k)}\,\mathbb{R}^{(3)}(\theta_m(k))\right] + Z_k^{(2)}\, e^{-\frac{\Gamma_2(k)}{2}t}\left[\frac{\sin(\Omega_2(k)t)}{\Omega_2(k)}\,\mathbb{R}^{(2)}(\theta_m(k)) + \frac{\widetilde{\gamma}(k)}{2}\,\frac{\cos(\Omega_2(k)t)}{\Omega_2(k)}\,\mathbb{R}^{(3)}(\theta_m(k))\right] \quad (8.160)$$

where again we have used the approximation $|\delta M^2| \ll \overline{\omega}^{\,2}(k)$ and introduced

$$\mathbb{R}^{(3)}(\theta) = \sin 2\theta \begin{pmatrix} \sin 2\theta & \cos 2\theta \\ \cos 2\theta & -\sin 2\theta \end{pmatrix} = \sin 2\theta\, U(\theta) \begin{pmatrix} 0 & 1 \\ 1 & 0 \end{pmatrix} U^{-1}(\theta) \quad (8.161)$$

and

$$\widetilde{\gamma}(k) = \frac{\Sigma_{I,ee}(k;\overline{\omega}(k) - \Sigma_{I,\mu\mu}(k;\overline{\omega}(k))}{\delta M^2\,\overline{\varrho}(k)}\,. \quad (8.162)$$

Under the assumption that $\Sigma_{R,\alpha,\alpha} \gg \Sigma_{I,\alpha,\alpha}$ it follows that $\widetilde{\gamma}(k) \ll 1$. As in the previous section, we can approximately project the positive frequency component by choosing the initial condition (8.126) with $\Omega_\alpha = \overline{\omega}(k)$, leading to the result

$$\langle \Psi_{\alpha,\vec{k}}(t)\rangle \;=\; e^{-iW(k)t-\frac{\overline{\Gamma}(k)}{2}t}\Bigg\{ Z_k^{(1)}\, e^{i\Delta\omega(k)t-\frac{\Delta\Gamma(k)}{2}t}\,\Big(\mathbb{R}^{(1)}(\theta_m(k)) + i\frac{\widetilde{\gamma}(k)}{2}\,\mathbb{R}^{(3)}(\theta_m(k))\Big)$$
$$+\, Z_k^{(2)}\, e^{-i\Delta\omega(k)t+\frac{\Delta\Gamma(k)}{2}t}\,\Big(\mathbb{R}^{(2)}_{\alpha,\beta}(\theta) - i\frac{\widetilde{\gamma}(k)}{2}\,\mathbb{R}^{(3)}(\theta_m(k))\Big) + \mathcal{O}\left(\frac{\delta M^2}{\overline{\omega}^{\,2}(k)}\right)\Bigg\}\Psi^0_{\beta,\vec{k}} \tag{8.163}$$

where

$$W(k) \;=\; \overline{\omega}(k) + \frac{\overline{\Sigma}_R(k;\overline{\omega}(k))}{4\,\overline{\omega}(k)} \tag{8.164}$$

$$\frac{\overline{\Gamma}(k)}{2} \;=\; \frac{1}{4\overline{\omega}(k)}\Big[\Sigma_{I,ee}(k,\overline{\omega}(k) + \Sigma_{I,\mu\mu}(k,\overline{\omega}(k)\Big] \tag{8.165}$$

$$\Delta\omega(k) \;=\; \frac{\delta M^2\,\overline{\varrho}(k)}{4\,\overline{\omega}(k)} \tag{8.166}$$

$$\frac{\Delta\Gamma(k)}{2} \;=\; \frac{\cos 2\theta_m}{4\;\overline{\omega}(k)}\Big[\Sigma_{I,ee}(k,\overline{\omega}(k) - \Sigma_{I,\mu\mu}(k,\overline{\omega}(k)\Big] \tag{8.167}$$

With the initial condition (8.131) we now find the long time evolution of the transition probability $\Psi_e \to \Psi_\mu$

$$|\langle \Psi_{\mu,\vec{k}}(t)\rangle|^2 \sim \frac{\sin^2 2\theta_m(k)}{4}\Big[e^{-\Gamma_1(k)t} + e^{-\Gamma_2(k)t} - 2\; e^{-\frac{1}{2}(\Gamma_1(k)+\Gamma_2(k))t}\cos\big(2\Delta\omega(k)t\big)\Big]\;\Psi^0_{e,\vec{k}} \tag{8.168}$$

where we have neglected perturbatively small terms by setting $Z^{(i)} \sim 1\;;\;\widetilde{\gamma}(k) \sim 0$ in prefactors. The solution (8.163) can be written in the following illuminating form

$$\langle \Psi_{\alpha,\vec{k}}(t)\rangle = e^{-iW(k)t-\frac{\overline{\Gamma}(k)}{2}t}\,\mathcal{U}\big(\theta_m(k)\big)\begin{pmatrix} Z_k^{(1)}\, e^{i\Delta\omega(k)t-\frac{\Delta\Gamma(k)}{2}t} & 0 \\ 0 & Z_k^{(2)}\, e^{-i\Delta\omega(k)t+\frac{\Delta\Gamma(k)}{2}t}\end{pmatrix}\mathcal{U}^{-1}\big(\theta_m(k)\big)\;\Psi^0_{\beta,\vec{k}} \tag{8.169}$$

where

$$\mathcal{U}\big(\theta_m(k)\big) = \begin{pmatrix} \cos\theta_m(k)\big(1+i\widetilde{\gamma}(k)\big) & \sin\theta_m(k)\big(1-i\widetilde{\gamma}(k)\big) \\ -\sin\theta_m(k) & \cos\theta_m(k)\end{pmatrix} \tag{8.170}$$

$$\mathcal{U}^{-1}\big(\theta_m(k)\big) = \frac{1}{\big(1+i\;\cos\theta_m(k)\;\widetilde{\gamma}(k)\big)}\begin{pmatrix} \cos\theta_m(k) & -\sin\theta_m(k)\big(1-i\widetilde{\gamma}(k)\big) \\ -\sin\theta_m(k) & \cos\theta_m(k)\big(1+i\widetilde{\gamma}(k)\big)\end{pmatrix} \tag{8.171}$$

Obviously the matrix $\mathcal{U}$ is *not unitary*.

8.5.4 Long time dynamics: Weisskopf-Wigner Hamiltonian

A phenomenological description of the dynamics of mixing and decay for neutral flavored mesons, for example $K_0\overline{K}_0$; $B_0\overline{B}_0$ relies on the Weisskopf-Wigner (WW) approximation[191]. In this approximation the time evolution of states is determined by a non-hermitian Hamiltonian that includes in a phenomenological manner the exponential relaxation associated with the decay of the neutral mesons. This approach has received revived attention recently with the possibility of observation of quantum mechanical coherence effects, in particular CP-violation in current experiments with neutral mesons[192]. In ref.[193] a field theoretical analysis of the (WW) approximation has been provided for the $K_0\overline{K}_0$ system.

The form of the solution (8.169) *suggests* that a (WW) approximate description of the asymptotic dynamics in terms of a non-hermitian Hamiltonian is available. To achieve this formulation we separate explicitly the *fast* time dependence via the phase $e^{\mp i\overline{\omega}(k)t}$ for the positive and negative frequency components, writing

$$\Psi_{\vec{k}}(t) = e^{-i\overline{\omega}(k)t}\ \Psi^{+}_{\vec{k}}(t) + e^{i\overline{\omega}(k)t}\ \Psi^{-}_{\vec{k}}(t) \tag{8.172}$$

where $\Psi^{\pm}_{\vec{k}}(t)$ the amplitudes of the flavor vectors that evolve *slowly* in time. The solution for the positive frequency component (8.163) follows from the time evolution of the *slow* component determined by

$$i\frac{d}{dt}\Psi^{+}_{\vec{k}}(t) = \mathcal{H}_w\Psi^{+}_{\vec{k}}(t) \tag{8.173}$$

where the effective *non-hermitian* Hamiltonian $\mathcal{H}$ is given by

$$\mathcal{H}_w = \frac{\delta M^2}{4\,\overline{\omega}(k)}\begin{pmatrix} -\cos 2\theta & \sin 2\theta \\ \sin 2\theta & \cos 2\theta \end{pmatrix} + \frac{\Sigma_R(k;\overline{\omega}(k)) + \mathbb{V}}{2\,\overline{\omega}(k)} - i\,\frac{\Sigma_I(k;\overline{\omega}(k))}{2\,\overline{\omega}(k)} \tag{8.174}$$

with

$$\Sigma_R(k;\overline{\omega}(k)) + \mathbb{V} = \begin{pmatrix} \Sigma_{R,ee}(k;\overline{\omega}(k)) + V_{ee} & 0 \\ 0 & \Sigma_{R,\mu\mu}(k;\overline{\omega}(k)) + V_{\mu\mu} \end{pmatrix} \tag{8.175}$$

$$\Sigma_I(k;\overline{\omega}(k)) = \begin{pmatrix} \Sigma_{I,ee}(k;\overline{\omega}(k)) & 0 \\ 0 & \Sigma_{I,\mu\mu}(k;\overline{\omega}(k)) \end{pmatrix} \tag{8.176}$$

The (WW) Hamiltonian $\mathcal{H}_w$ can be written as

$$\mathcal{H}_w = \left\{\frac{\overline{\Sigma}_R(k;\overline{\omega}(k))}{4\,\overline{\omega}(k)} - i\frac{\overline{\Gamma}(k)}{2}\right\}\mathbb{1} + \frac{\delta M^2\ \overline{\varrho}(k)}{4\ \overline{\omega}(k)}\begin{pmatrix} -(\cos 2\theta_m(k) + i\widetilde{\gamma}(k)) & \sin 2\theta_m(k) \\ \sin 2\theta_m(k) & (\cos 2\theta_m(k) + i\widetilde{\gamma}(k)) \end{pmatrix} \tag{8.177}$$

where we have used the definitions given in equations (9.34,8.142,9.33,9.41,8.165). It is straightforward to confirm that the Wigner-Weisskopf Hamiltonian can be written as

$$\mathcal{H}_w = \mathcal{U}(\theta_m(k)) \begin{pmatrix} \lambda_-(k) & 0 \\ 0 & \lambda_+(k) \end{pmatrix} \mathcal{U}^{-1}(\theta_m(k)) \tag{8.178}$$

where $\mathcal{U}(\theta_m(k))$ is given in (8.170) and using the definitions given in eqn. (8.164-8.167) the *complex* eigenvalues are

$$\lambda_\mp(k) = W(k) - \varpi(k) - i\frac{\overline{\Gamma}(k)}{2} \mp \left(\Delta\omega(k) + i\frac{\Delta\Gamma(k)}{2}\right) \tag{8.179}$$

The solution of the effective equation for the slow amplitudes (8.173) coincides with the long time dynamics given by (8.163) when the wave function renormalization constants are approximated as $Z^{(i)}_{\vec{k}} \sim 1$. Therefore the (WW) description of the time evolution based on the *non-hermitian* Hamiltonian $\mathcal{H}_w$ (8.174) *effectively* describes the evolution of flavor multiplets under the following approximations:

- Only the long-time dynamics can be extracted from the Weisskopf-Wigner Hamiltonian.
- The validity of the perturbative expansion, *and* of the condition $\delta M^2 \ll \varpi(k)^2$.
- Wavefunction renormalization corrections are neglected $Z^{(i)} \sim 1$ and only leading order corrections of order $\widetilde{\gamma}(k)$ are included.

While the Weisskopf-Wigner effective description describes the relaxation of the flavor fields, it misses the stochastic noise from the bath, therefore, it *does not* reliably describe the approach to equilibrium.

8.6 EQUILIBRATION: EFFECTIVE HAMILTONIAN IN THE MEDIUM

As discussed in section 8.3.1 we study equilibration by focusing on the asymptotic long time behavior of the one-body density matrix or equal time correlation function, namely

$$\lim_{t\to\infty} \langle \Psi_{\alpha,\vec{k}}(t)\Psi_{\beta,-\vec{k}}(t)\rangle \,. \tag{8.180}$$

In particular we seek to understand which basis diagonalizes the equilibrium density matrix.

Consider general initial conditions $\Psi^0 \neq 0$ and $\Pi^0 \neq 0$, in which case the flavor field $\Psi_{\alpha,\vec{k}}(t)$ is given by Eq. (8.102) with $G_f(k;t)$ given by eqn. (9.29). For $t \gg \Gamma^{-1}_{1,2}$, the first two contributions to (8.102) which depend on the initial conditions fall-off exponentially as $e^{-\frac{\Gamma_{1,2}}{2}t}$ and *only* the last

term, the convolution with the noise, survives at asymptotically long time, indicating that the equilibrium state is insensitive to the initial conditions as it must be.

To leading order in the perturbative expansion in G, and in the limit $\delta M^2/\overline{\omega}^2(k) \ll 1$, we can approximate $\theta_m^{(1)}(k) \approx \theta_m^{(2)}(k) = \theta_m(k)$, where the effective mixing angle in the medium $\theta_m(k)$ is determined by the relations (9.33). Similarly we can approximate the wave function renormalization constants as $Z^{(1)}(k) \approx Z^{(2)}(k) = Z(k)$ with

$$Z(k) = \left[1 - \frac{1}{2\omega}\Big(\overline{\Sigma}_R^{'}(k;\omega) - (-1)^i \frac{\delta M^2}{2}\cos 2\theta_m(k)\Delta_R^{'}(k;\omega)\Big)\right]^{-1}_{\omega=\overline{\omega}(k)} \tag{8.181}$$

where the prime stands for derivative with respect to ω. Thus, $G_f(k;t)$ and $G_m(k;t)$ are related by

$$G_f(k;t) \approx Z(k)\, U(\theta_m)\, G_m(k;t)\, U^{-1}(\theta_m) \tag{8.182}$$

where $G_m(k;t)$ is given by

$$\begin{aligned} G_m(k;t) = & \begin{pmatrix} \frac{\sin(\Omega_1(k)t)}{\Omega_1(k)}\, e^{-\frac{\Gamma_1(k)}{2}t} & 0 \\ 0 & \frac{\sin(\Omega_2(k)t)}{\Omega_2(k)}\, e^{-\frac{\Gamma_2(k)}{2}t} \end{pmatrix} + \\ & \frac{\widetilde{\gamma}(k)}{2}\, \sin 2\theta_m(k) \left[e^{-\frac{\Gamma_2(k)}{2}t}\frac{\cos(\Omega_2(k)t)}{\Omega_2(k)} - e^{-\frac{\Gamma_1(k)}{2}t}\frac{\cos(\Omega_1(k)t)}{\Omega_1(k)}\right] \begin{pmatrix} 0 & 1 \\ 1 & 0 \end{pmatrix} \end{aligned} \tag{8.183}$$

It is useful to define the quantities $h_m(t,\omega)$ and $\widetilde{\xi}_{\beta,\vec{k}}(\omega)$ as follows

$$h_m(t,\omega) = \int_0^t e^{-i\omega t'}\, G_m(k;t)\, dt' \tag{8.184}$$

and

$$\xi_{\beta,\vec{k}}(t-t') = \int_{-\infty}^{+\infty} e^{i\omega(t-t')}\, \widetilde{\xi}_{\beta,\vec{k}}(\omega)\, d\omega, \tag{8.185}$$

with the noise average in the flavor basis given by

$$\langle\langle\, \widetilde{\xi}_{\rho,\vec{k}}(\omega)\, \widetilde{\xi}_{\sigma,-\vec{k}}(\omega')\, \rangle\rangle = \widetilde{\mathcal{K}}_{\rho\sigma}(k;\omega)\delta(\omega+\omega') = \mathrm{Im}\widetilde{\Sigma}^R_{\rho\sigma}(k;\omega)\coth\left(\frac{\beta\omega}{2}\right)\delta(\omega+\omega')\,. \tag{8.186}$$

We find convenient to introduce

$$\widetilde{\mathcal{K}}_m(k;\omega) = U^{-1}(\theta_m)\, \widetilde{\mathcal{K}}(k;\omega)\, U(\theta_m)\,. \tag{8.187}$$

The approach to equilibrium for $t >> \Gamma_{1,2}^{-1}$ can be established from the unequal time two-point correlation function, given by

$$\lim_{t,t'\to\infty} \langle \Psi_{\alpha,\vec{k}}(t)\Psi_{\beta,-\vec{k}}(t')\rangle = Z^2(k)U(\theta_m)\Bigg\{ \int_{-\infty}^{+\infty} d\omega \; e^{i\omega(t-t')} \; h_m(\infty,\omega)\,\widetilde{\mathcal{K}}_m(k;\omega)\,h_m(\infty,-\omega)\Bigg\}U^{-1}(\theta_m) \tag{8.188}$$

where we have taken the upper limit $t \to \infty$ in (8.185). The fact that the correlation function becomes a function of the *time difference*, namely time translational invariant, indicates that the density matrix commutes with the total Hamiltonian in the long time limit. The one-body density matrix is obtained from (8.188) in the coincidence limit $t = t'$.

Performing the integration over ω, we obtain after a lengthy but straightforward calculation

$$\lim_{t\to\infty} \langle \Psi_{\alpha,\vec{k}}(t)\Psi_{\beta,-\vec{k}}(t)\rangle = Z^2(k)\,U(\theta_m) \begin{pmatrix} \Lambda_{11}(k) & \Lambda_{12}(k) \\ \Lambda_{21}(k) & \Lambda_{22}(k) \end{pmatrix} U^{-1}(\theta_m); \tag{8.189}$$

wherein

$$\Lambda_{11}(k) = \frac{1}{2\,\Omega_1(k)} \coth\left(\frac{\beta\Omega_1(k)}{2}\right) \;\; ; \;\; \Lambda_{22}(k) = \frac{1}{2\,\Omega_2(k)} \coth\left(\frac{\beta\Omega_2(k)}{2}\right), \tag{8.190}$$

and to the leading order of $\delta M^2/\overline{\omega(k)}^2 \ll 1$, we find $\Lambda_{21} = \Lambda_{12}(\Omega_1 \to \Omega_2)$ where

$$\Lambda_{12}(k) \;\; = \;\; \frac{1}{2\,\Omega_1(k)} \coth\left(\frac{\beta\Omega_1(k)}{2}\right) \sin 2\theta_m(k)\, \frac{\widetilde{\gamma}(k)\,\eta(k)}{1+(\,\eta(k)\,)^2} \;\; ; \;\; \eta(k) = \frac{2\Omega_1(k)\,(\,\Gamma_1(k)+\Gamma_2(k)\,)}{\delta M^2 \overline{\varrho}(k)}. \tag{8.191}$$

Since $\widetilde{\gamma}(k) \ll 1$, it is obvious that $\Lambda_{12}(k)$ and $\Lambda_{21}(k)$ are perturbatively small compared with $\Lambda_{11}(k)$ and $\Lambda_{22}(k)$, in either case $\eta(k) \gg 1$ or $\eta(k) \ll 1$. The asymptotic one-body density matrix (8.74) then becomes

$$\rho_{\alpha,\beta}(k;\infty) = U(\theta_m) \begin{pmatrix} \frac{Z}{2\,\Omega_1(k)} \coth\left(\frac{\beta\Omega_1(k)}{2}\right) & \epsilon \\ \epsilon & \frac{Z}{2\,\Omega_2(k)} \coth\left(\frac{\beta\Omega_2(k)}{2}\right) \end{pmatrix} U^{-1}(\theta_m) \;\; ; \;\; \epsilon \lesssim \mathcal{O}(G^2) \tag{8.192}$$

where we neglected corrections of $\mathcal{O}(G^2)$ in the diagonal matrix elements.

Neglecting the perturbative off-diagonal corrections, the one-body density matrix *commutes* with the *effective Hamiltonian in the medium* which in the flavor basis is given by

$$
\begin{aligned}
H_{eff}(k) &= \overline{\omega}(k)\begin{pmatrix} 1 & 0 \\ 0 & 1 \end{pmatrix} + \frac{\delta M^2}{4\,\overline{\omega}(k)}\begin{pmatrix} -\cos 2\theta & \sin 2\theta \\ \sin 2\theta & \cos 2\theta \end{pmatrix} \\
&\quad + \frac{1}{2\overline{\omega}(k)}\begin{pmatrix} \Sigma_{R,ee}(k;\overline{\omega}(k)) + V_{ee} & 0 \\ 0 & \Sigma_{R,\mu\mu}(k;\overline{\omega}(k)) + V_{\mu\mu} \end{pmatrix}
\end{aligned}
\tag{8.193}
$$

this effective in-medium Hamiltonian can be written in a more illuminating form

$$
H_{eff}(k) = U(\theta_m)\begin{pmatrix} \Omega_1(k) & 0 \\ 0 & \Omega_2(k) \end{pmatrix} U^{-1}(\theta_m) \tag{8.194}
$$

where $\Omega_{1,2}(k)$ are the correct propagation frequencies in the medium given by eqn. (9.35,9.36).

This effective Hamiltonian includes the radiative corrections in the medium via the flavor diagonal self-energies (forward scattering) and apart from the term proportional to the identity is identified with the *real part* of the Weisskopf-Wigner Hamiltonian $\mathcal{H}_w$ given by eqn. (8.174). This form highlights that the off-diagonal elements of the one-body density matrix in the basis of *eigenstates of the effective Hamiltonian in the medium* are *perturbatively small*. The unitary transformation $U(\theta_m)$ relates the flavor fields to the fields in the *basis of the effective Hamiltonian in the medium*.

Comparing this result to the free field case in thermal equilibrium, where the one body density matrix in the flavor basis is given by eqn. (8.77), it becomes clear that in the long time limit equilibration is achieved and the one-body density matrix is nearly diagonal in the basis of the *eigenstates of the effective Hamiltonian in the medium* (8.193) with the diagonal elements determined by the distribution function of these eigenstates.

This means that within the realm of validity of perturbation theory, the equilibrium correlation function *is nearly diagonal in the basis of the effective Hamiltonian in the medium*. This result confirms the arguments advanced in [182]. Since the effective action is quadratic in the "neutrino fields" higher correlation functions are obtained as Wick contractions of the two point correlators, hence the fact that the two point correlation function and consequently the one-body density matrix are diagonal in the basis of the eigenstates of the effective Hamiltonian in the medium guarantee that all higher correlation functions are also diagonal in this basis.

8.6.1 On "sterile neutrinos"

The results obtained in the previous sections apply to the case of two "flavored neutrinos" both in interaction with the bath. However, these results can be simply extrapolated to the case of one "active" and one "sterile" neutrino that mix via a mass matrix that is off-diagonal in the flavor basis. By definition a "sterile" neutrino *does not* interact with hadrons, quarks or charged leptons, therefore for this species there are no radiative corrections. Consider for example that the "muon neutrino" represented by ϕ_μ does *not* couple to the bath, but it does couple to the "electron neutrino" solely through the mixing in the mass matrix. Since the interaction is diagonal in the flavor basis, the decoupling of this "sterile neutrino" can be accounted for simply by imposing the following "sterility conditions" for the matter potential $\mathbb{V}$ and the self energies

$$V_{\mu\mu} \equiv 0 \; ; \; \Sigma_{R,\mu\mu} \equiv 0 \; ; \; \Sigma_{I,\mu\mu} \equiv 0 \; . \tag{8.195}$$

All of the results obtained above for the dispersion relations and relaxation rates apply to this case by simply imposing these "sterility conditions". In particular it follows that

$$\Gamma_1(k) = \Gamma_{ee}(k) \cos^2\theta_m(k) \; ; \; \Gamma_2(k) = \Gamma_{ee} \sin^2\theta_m(k) \tag{8.196}$$

where $\Gamma_{ee}(k)$ is the relaxation rate of the *active neutrino* in absence of mixing. This result highlights that in the limit $\theta \to 0$ the in-medium eigenstate labeled "2" is seen to correspond to the sterile state, because in the absence of mixing this state does not acquire a width. However, for non-vanishing vacuum mixing angle, the "sterile neutrino" nonetheless *equilibrates* with the bath as a consequence of the "active-sterile" mixing, which effectively induces a coupling between the "sterile" and the bath[77, 78, 112, 190, 194]. The result for $\Gamma_2(k)$, namely the relaxation rate of the "sterile" neutrino is of the same form as that proposed in refs. [77, 78, 112, 190, 194]. The result for the "sterile" rate $\Gamma_2(k)$ compares to those in these references in the limit in which perturbation theory is valid, namely $\Sigma_{ee}(k)/\delta M^2 \overline{\varrho}(k) \ll 1$ since the denominator in this ratio is proportional to the oscillation frequency in the medium.

8.7 CONCLUSIONS

In this chapter, we studied the non-equilibrium dynamics of mixing, oscillations and equilibration in a model field theory that bears all of the relevant features of the standard model of neutrinos

augmented by a mass matrix off diagonal in the flavor basis. To avoid the complications associated with the spinor nature of the neutrino fields, we studied an interacting model of flavored neutral mesons. Two species of flavored neutral mesons play the role of two flavors of neutrinos, these are coupled to other mesons which play the role of hadrons or quarks and charged leptons, via flavor diagonal interactions that model charged currents in the standard model. These latter meson fields are taken to describe a bath in thermal equilibrium, and the meson-neutrino fields are taken to be the "system". We obtain a reduced density matrix and the non-equilibrium effective action for the "neutrinos" by integrating out the bath degrees of freedom up to second order in the coupling in the full time-evolved density matrix.

The non-equilibrium effective action yields all the information on the particle and quasiparticle modes in the medium, and the approach to equilibrium.

Our main results can be summarized as follows:

- We obtain the dispersion relations, mixing angles and relaxation rates of the two quasiparticle modes in the medium. The dispersion relations and mixing angles are of the same form as those obtained for neutrinos in a medium[57, 189].
- The relaxation rates are found to be

$$\Gamma_1(k) = \Gamma_{ee}(k)\cos^2\theta_m(k) + \Gamma_{\mu\mu}(k)\sin^2\theta_m(k) \tag{8.197}$$

$$\Gamma_2(k) = \Gamma_{\mu\mu}(k)\cos^2\theta_m(k) + \Gamma_{ee}(k)\sin^2\theta_m(k) \tag{8.198}$$

  where

$$\Gamma_{\alpha\alpha}(k) = \frac{\Sigma_{I,\alpha\alpha}(k;\overline{\omega}(k))}{\overline{\omega}(k)} \tag{8.199}$$

  are the relaxation rates of the flavor fields in *absence* of mixing and $\Sigma_{I,\alpha,\alpha}$ are the imaginary parts of the "neutrino" self energy which is diagonal in the flavor basis. These relaxation rates are similar in form to those proposed in refs.[77, 78, 112, 190], within the context of active-sterile conversion or flavor conversion in supernovae.
- The long time dynamics is approximately described by an effective Weisskopf-Wigner approximation with a non-hermitian Hamiltonian. The real part includes the "index of refraction" and the renormalization of the frequencies and the imaginary part is determined by the absorptive part of the second order self-energy and describes the relaxation. While this (WW) approximation describes mixing, oscillations and relaxation, it *does not* capture the dynamics of equilibration.

- For time $t >> \Gamma_{1,2}^{-1}$ the two point function of the neutrino fields becomes time translational invariant reflecting the approach to equilibrium. The asymptotic long time limit of the one-body density matrix reveals that the density matrix is nearly diagonal in the basis of eigenstates of an effective Hamiltonian in the medium (8.193) with perturbatively small off-diagonal corrections in this basis. The diagonal components in this basis are determined by *the distribution function of these eigenstates*.
- "Sterile" neutrinos: these results apply to the case in which only one of the flavored neutrinos is "active" but the other is "sterile". Consider for example that the "muon neutrino" is sterile in the sense that it does not couple to the bath. This sterile degree of freedom is thus identified with the in medium eigenstate "2" because in the absence of mixing $\theta = 0$ its dynamics is completely free. The "sterility" condition corresponds to setting the matter potential $V_{\mu\mu} = 0$ and the self-energy $\Sigma_{\mu\mu} = 0$ with a concomitant change in the dispersion relations. All the results obtained above apply just the same, but with $\Gamma_{\mu\mu}(k) = 0$, from which it follows that $\Gamma_2(k) = \Gamma_{ee}(k) \sin^2 \theta_m(k)$. The final result is that "sterile" neutrinos do thermalize with the bath via "active-sterile" mixing. If the mixing angle in the medium is small, the equilibration time scale for the "sterile neutrino" is much larger than that for the "active" species, but equilibration is eventually achieved nonetheless. This result is a consequence of "active-sterile" oscillations which effectively induces an interaction of the sterile neutrino with the bath[77, 78, 112, 190, 194].

Although the meson field theory studied here describes quite generally the main features of mixing, oscillations and relaxation of neutrinos, a detailed quantitative assessment of the relaxation rates and dispersion relations do require a full calculation in the standard model. Furthermore there are several aspects of neutrino physics that are distinctly associated with their spinorial nature and cannot be inferred from this model. While only the left handed component of neutrinos couple to the weak interactions, a (Dirac) mass term couples the left to the right handed component, and through this coupling the right handed component develops a dynamical evolution. Although the coupling to the right handed component is very small in the ultrarelativistic limit, it is conceivable that non-equilibrium dynamics may lead to a substantial right handed component during long time intervals. The study of this possibility would be of importance in the early Universe because the right handed component may thereby become an "active" one that may contribute to the total number of species in equilibrium in the thermal bath thus possibly affecting the expansion history of the Universe.

Another important fermionic aspect is Pauli blocking which is relevant in the case in which neutrinos are degenerate, for example in supernovae. These aspects will be studied elsewhere.

9.0 PRODUCTION OF A STERILE SPECIES: QUANTUM KINETICS

9.1 INTRODUCTION

The rich and complex dynamics of oscillations, decoherence and damping is of *fundamental* and phenomenological importance not only in neutrino cosmology but also in the dynamics of meson mixing and CP violation[195, 196]. In ref.[184] it was argued that the spinor nature of neutrinos is not relevant to describe the dynamics of mixing and oscillations at high energy which can then be studied within a (simpler) quantum field theory of meson degrees of freedom.

Recently we reported on a study[197] of mixing, decoherence and relaxation in a theory of mesons which provides an accurate description of similar phenomena for mixed neutrinos. This effective theory incorporates interactions that model the medium effects associated with charge and neutral currents for neutrinos and yield a robust picture of the non-equilibrium dynamics of mixing, decoherence and equilibration which is remarkably general. The fermion nature of the distributions and Pauli blocking effects can be simply accounted for in the final result[197]. This study implemented quantum field theory methods to obtain the non-equilibrium effective action for the "neutrino" degrees of freedom. The main ingredient in the time evolution is the *full propagator* for the "neutrino" degrees of freedom in the medium. The complex poles of the propagator yield the dispersion relation and damping rates of quasiparticle modes in the medium. The dispersion relations are found to be the usual ones for neutrinos in a medium with the index of refraction correction from forward scattering. For the case of two flavors, there are *two damping rates* which are widely different away from MSW resonances. The results of this study motivated[198] a deeper scrutiny of the rate equation which is often used to study sterile neutrino production in the early Universe[20, 77, 78].

One of the observations in[198] is that the emergence of *two widely different* damping time scales precludes a reliable kinetic description in terms of a *time averaged transition probability* suggesting

that a simple rate equation to describe sterile neutrino production in the early Universe far away from MSW resonances may not be reliable.

Motivation and goals: The broad potential relevance of sterile neutrinos as warm dark matter candidates in cosmology and their impact in the late stages of stellar collapse warrant a deeper scrutiny of the quantum kinetics of production of the sterile species. Our goal is to provide a quantum field theory study of the non-equilibrium dynamics of mixing, decoherence and damping and to obtain the quantum kinetic equations that determine the production of a sterile species. We make progress towards this goal within a meson model with one active and one sterile degrees of freedom coupled to a bath of mesons in equilibrium discussed in ref.[197]. As demonstrated by the results of ref.[197] this (simpler) theory provides a remarkable effective description of propagation, mixing, decoherence and damping of neutrinos in a medium. While ref.[197] studied the approach to equilibrium focusing on the one body density matrix and single quasiparticle dynamics, in this article we obtain the non-equilibrium effective action, the quantum master equation and the complete set of quantum kinetic equations for the distribution functions and coherences. We also establish a generalization of the active-sterile transition probability based on the quantum master equation. In distinction with a recent quantum field theory treatment[**?**] we seek to understand the quantum kinetics of production not only near MSW resonances, at which both time scales concide[197, 198] but far away from the resonance region where the damping time scales are widely separated[197, 198].

In section (9.2) we introduce the model, obtain the effective action, and the full propagator from which we extract the dispersion relations and damping rates. In section (9.3) we define the active and sterile distribution functions and obtain their quantum kinetic non-equilibrium evolution from the effective action, discussing the various approximations. In section (9.4) we obtain the quantum Master equation for the reduced density matrix, also discussing the various approximations. In this section we obtain the full set of quantum kinetic equations for the populations and coherences and show their equivalence to the results from the effective action. In section (9.5) we study the kinetic evolution of the off-diagonal coherences and introduce a generalization of the active-sterile transition probability *in a medium* directly from the quantum master equation. In section (9.6) we establish the equivalence between the kinetic equations obtained from the quantum master equation and those most often used in the literature in terms of a "polarization vector", along the way identifying the components of this "polarization vector" in terms of the populations of the propagating states in the medium $1, 2$ and the coherences. While this formulation is equivalent to

the quantum kinetic equations obtained from the master equation and effective action, we argue that the latter formulations yield more information, making explicit that the *fundamental* damping scales are the widths of the quasiparticle modes in the medium and allow to define the generalization of the transition probability *in the medium*. We also discuss the shortcomings of the phenomenological rate equations often invoked for numerical studies of sterile neutrino production. Section (9.7) summarizes our conclusions. Appendices C and D elaborate on technical aspects.

9.2 THE MODEL, EFFECTIVE ACTION, AND DISTRIBUTION FUNCTIONS

We consider a model of mesons with two flavors a, s in interaction with a " vector boson" and a "flavor lepton" here denoted as W, χ_a respectively, modeling charged and neutral current interactions in the standard model. This model has been proposed as an effective description of neutrino mixing, decoherence and damping in a medium in ref.[197] to which we refer reader for details. As it will become clear below, the detailed nature of the bath fields W, χ_a is only relevant through their equilibrium correlation functions which can be written in dispersive form.

In terms of the field doublet

$$\Phi = \begin{pmatrix} \phi_a \\ \phi_s \end{pmatrix} \tag{9.1}$$

the Lagrangian density is

$$\mathcal{L} = \frac{1}{2}\left\{\partial_\mu \Phi^T \partial^\mu \Phi - \Phi^T \mathbb{M}^2 \Phi\right\} + \mathcal{L}_0[W,\chi] + G\, W\, \phi_a \chi_a + G\phi_a^2 \chi_a^2 \tag{9.2}$$

where the mass matrix is given by

$$\mathbb{M}^2 = \begin{pmatrix} M^2_{aa} & M^2_{as} \\ M^2_{as} & M^2_{ss} \end{pmatrix} \tag{9.3}$$

and $\mathcal{L}_0[W,\chi]$ is the free field Lagrangian density for W, χ which need not be specified.

The mesons $\phi_{a,s}$ play the role of the active and sterile flavor neutrinos, χ_a the role of the charged lepton associated with the active flavor and W a charged current, for example the proton-neutron current $\overline{p}\gamma^\mu(1 - g_A\gamma_5)n$ or a similar quark current. The coupling G plays the role of G_F. The interaction between the "neutrino" doublet and the W, χ_a fields is of the same form as that studied in ref.[12, 63, 64] for neutral and charged current interactions. As it will be seen below, we do

not need to specify the precise form, only the spectral properties of the correlation function of this current are necessary.

The flavor $\phi_{a,s}$ and the mass basis fields $\varphi_{1,2}$ are related by an orthogonal transformation $\Phi = U(\theta)\,\varphi$

$$\begin{pmatrix} \phi_a \\ \phi_s \end{pmatrix} = U(\theta) \begin{pmatrix} \varphi_1 \\ \varphi_2 \end{pmatrix} \;\; ; \;\; U(\theta) = \begin{pmatrix} \cos\theta & \sin\theta \\ -\sin\theta & \cos\theta \end{pmatrix} \tag{9.4}$$

where the orthogonal matrix $U(\theta)$ diagonalizes the mass matrix $\mathbb{M}^2$, namely

$$U^{-1}(\theta)\,\mathbb{M}^2\,U(\theta) = \begin{pmatrix} M_1^2 & 0 \\ 0 & M_2^2 \end{pmatrix} \tag{9.5}$$

In the flavor basis the mass matrix $\mathbb{M}$ can be written in terms of the vacuum mixing angle θ and the eigenvalues of the mass matrix as

$$\mathbb{M}^2 = \overline{M}^{\,2}\,\mathbb{1} + \frac{\delta M^2}{2} \begin{pmatrix} -\cos 2\theta & \sin 2\theta \\ \sin 2\theta & \cos 2\theta \end{pmatrix} \tag{9.6}$$

where we introduced

$$\overline{M}^{\,2} = \frac{1}{2}(M_1^2 + M_2^2) \;\; ; \;\; \delta M^2 = M_2^2 - M_1^2\,. \tag{9.7}$$

For the situation under consideration with keV sterile neutrinos with small vacuum mixing angle $\theta \ll 1$

$$M_{aa} \sim M_1 \;;\; M_{ss} \sim M_2 \tag{9.8}$$

and in the vacuum

$$\phi_a \sim \phi_1 \;;\; \phi_s \sim \phi_2\,. \tag{9.9}$$

We focus on the description of the dynamics of the "system fields" $\phi_\alpha,\ \alpha = a, s$. The strategy is to consider the time evolved full density matrix and trace over the bath degrees of freedom χ, W. It is convenient to write the Lagrangian density (9.2) as

$$\mathcal{L}[\phi_\alpha, \chi_\alpha, W] = \mathcal{L}_0[\phi] + \mathcal{L}_0[W, \chi] + G\phi_a\mathcal{O}_a + G\phi_a^2\chi_a^2 \tag{9.10}$$

where

$$\mathcal{O}_a = \chi_a\,W\,. \tag{9.11}$$

and $\mathcal{L}_0[\cdots]$ are the free Lagrangian densities for the fields ϕ_α, χ_a, W respectively. The fields ϕ_α are considered as the "system" and the fields χ_a, W are treated as a bath in thermal equilibrium at a temperature $T \equiv 1/\beta$. We consider a factorized initial density matrix at a time $t_0 = 0$ of the form

$$\widehat{\rho}(0) = \rho_\Phi(0) \otimes \rho_B(0) \quad ; \quad \rho_B(0) = e^{-\beta\, H_0[\chi, W]} \tag{9.12}$$

where $H_0[\chi, W]$ is Hamiltonian for the fields χ_a, W in absence of interactions with the neutrino field ϕ_a.

Although this factorized form of the initial density matrix leads to initial transient dynamics, we are interested in the long time dynamics, in particular in the long time limit.

The bath fields χ_α, W will be "integrated out" yielding a reduced density matrix for the fields ϕ_α in terms of an effective real-time functional, known as the influence functional[164] in the theory of quantum brownian motion. The reduced density matrix can be represented by a path integral in terms of the non-equilibrium effective action that includes the influence functional. This method has been used extensively to study quantum brownian motion[164, 165], and quantum kinetics[168, 186] and more recently in the study of the non-equilibrium dynamics of thermalization in a similar model[197]. The time evolution of the initial density matrix is given by

$$\widehat{\rho}(t) = e^{-iH(t-t_0)} \widehat{\rho}(t_0) e^{iH(t-t_0)} \tag{9.13}$$

Where the total Hamiltonian H is

$$H = H_0[\phi] + H_0[\chi, W] + H_I[\phi, \chi, W] \tag{9.14}$$

Denoting all the fields collectively as X to simplify notation, the density matrix elements in the field basis are given by

$$\langle X|\widehat{\rho}(t)|X'\rangle = \int DX_i DX_i' \; \langle X|e^{-iH(t-t_0)}|X_i\rangle \; \langle X_i|\widehat{\rho}(t_0)|X_i'\rangle \; \langle X_i'|e^{iH(t-t_0)}|X'\rangle \, . \tag{9.15}$$

The density matrix elements in the field basis can be expressed as a path integral by using the representations

$$\langle X|e^{-iH(t-t_0)}|X_i\rangle = \int \mathcal{D}X^+ \; e^{i\int_{t_0}^{t} dt \int d^3x \mathcal{L}[X^+]} \quad ; \quad X^+(t_0) = X_i; X^+(t) = X \, . \tag{9.16}$$

Similarly

$$\langle X_i'|e^{iH(t-t_0)}|X'\rangle = \int \mathcal{D}X^- \; e^{-i\int_{t_0}^{t} dt \int d^3x \mathcal{L}[X^-]} \quad ; \quad X^-(t_0) = X_i'; X^-(t) = X' \, . \tag{9.17}$$

Therefore the full time evolution of the density matrix can be systematically studied via the path integral

$$\mathcal{Z} = \int \mathcal{D}X^{+}\mathcal{D}X^{-} e^{i\int_{t_0}^{t} dt \int d^3x \left\{\mathcal{L}[X^{+}]-\mathcal{L}[X^{-}]\right\}} , \tag{9.18}$$

with the boundary conditions discussed above. This representation allows to obtain expectation values or correlation functions $\mathcal{C}(X, X_i, X'_i, X'; t, t')$ which depend on the values of the fields $X_i; X'_i$ through the initial conditions. In order to obtain expectation values or correlation functions in the full time evolved density matrix, the results from the path integral must be averaged in the initial density matrix $\widehat{\rho}(t_0)$, namely

$$\langle \mathcal{C}(X, X'; t, t') \rangle \equiv \int DX_i DX'_i \; \langle X_i | \widehat{\rho}(t_0) | X'_i \rangle \; \mathcal{C}(X, X_i, X'_i, X'; t, t') . \tag{9.19}$$

We will only study correlation functions of the "system" fields ϕ_α, therefore we carry out the trace over the χ_a and W degrees of freedom in the path integral (9.18) systematically in a perturbative expansion in G. The resulting series is re-exponentiated to yield the *non-equilibrium* effective action and the generating functional of connected correlation functions of the fields ϕ_α. This procedure has been explained in detail in references[168, 186] and more recently in [197] within a model similar to the one under consideration. Following the procedure detailed in these references we obtain the non-equilibrium effective action up to order G^2 and quadratic in the fields ϕ_α neglecting higher order non-linearities,

$$\begin{aligned} iL_{eff}[\phi^+, \phi^-] \;\; = \;\; & \sum_{\vec{k}} \left\{ \frac{i}{2} \int dt \Big[\dot{\phi}^{+}_{\alpha,\vec{k}}(t) \dot{\phi}^{+}_{\alpha,-\vec{k}}(t) - \phi^{+}_{\alpha,\vec{k}}(t)(k^2 \mathbb{1} + \mathbb{M}^2 + \mathbb{V}) \phi^{+}_{\beta,-\vec{k}}(t) \right. \\ & \left. - \dot{\phi}^{-}_{\alpha,\vec{k}}(t) \dot{\phi}^{-}_{\alpha,-\vec{k}}(t) + \phi^{-}_{\alpha,\vec{k}}(t)(k^2 \mathbb{1} + \mathbb{M}^2 + \mathbb{V}) \phi^{-}_{-\vec{k}}(t) \Big] \right. \\ & - \frac{G^2}{2} \int dt \int dt' \left[\phi^{+}_{a,\vec{k}}(t) \mathcal{G}^{++}(k; t, t') \phi^{+}_{a,-\vec{k}}(t') + \phi^{-}_{a,\vec{k}}(t) \mathcal{G}^{--}(k; t, t') \phi^{-}_{a,-\vec{k}}(t') \right. \\ & \left. \left. - \phi^{+}_{a,\vec{k}}(t) \mathcal{G}^{+-}(k; t, t') \phi^{-}_{a,-\vec{k}}(t') - \phi^{-}_{a,\vec{k}}(t) \mathcal{G}^{-+}(k; t, t') \phi^{+}_{a,-\vec{k}}(t') \right] \right\} \end{aligned} \tag{9.20}$$

where the *matter potential* is

$$\mathbb{V} = \begin{pmatrix} V_{aa} & 0 \\ 0 & 0 \end{pmatrix} \quad ; \quad V_{aa} = G\langle \chi_a^2 \rangle , \tag{9.21}$$

with the average in the initial bath density matrix. The corresponding one-loop diagram at order G that yields the *matter potential* is depicted in figure (9.1).

The correlation functions $\mathcal{G}(t, t') \sim \langle \mathcal{O}_a(t) \mathcal{O}_a(t') \rangle = \langle W(t) W(t') \rangle \langle \chi_a(t) \chi_a(t') \rangle$ are also determined by averages in the initial equilibrium bath density matrix and their explicit form is given in reference[197] (see also appendix (D)).

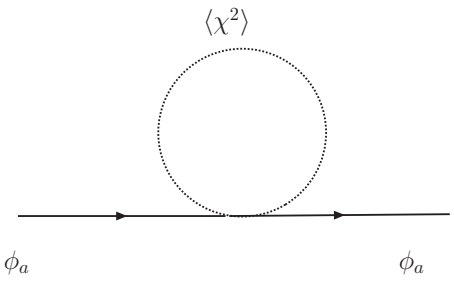

Figure 9.1: One loop self-energy for the active species at order G, corresponding to the matter potential $V_{aa} = G\langle\chi^2\rangle$.

Performing the trace over the bath degrees of freedom the resulting non-equilibrium effective action acquires a simpler form in terms of the Wigner center of mass and relative variables[168, 186, 197]

$$\Psi_\alpha(\vec{x},t) = \frac{1}{2}\left(\phi^+_\alpha(\vec{x},t) + \phi^-_\alpha(\vec{x},t)\right) \;\; ; \;\; R_\alpha(\vec{x},t) = \left(\phi^+_\alpha(\vec{x},t) - \phi^-_\alpha(\vec{x},t)\right) \;\; ; \;\; \alpha = a,s \tag{9.22}$$

and a corresponding Wigner transform of the initial density matrix for the ϕ fields. See ref.[197] for details. The resulting form allows to cast the dynamics of the Wigner center of mass variable as a *stochastic* Langevin functional equation, where the effects of the bath enter through a dissipative kernel and a stochastic noise term, whose correlations obey a generalized fluctuation-dissipation relation[168, 186, 197]. In terms of spatial Fourier transforms the time evolution of the center of mass Wigner field Ψ is given by the following Langevin (stochastic) equation (see derivations and details in refs.[164, 165, 168, 186, 197])

$$\begin{aligned} &\ddot{\Psi}_{\alpha,\vec{k}}(t) + (k^2\,\delta_{\alpha\beta} + \mathbb{M}^2_{\alpha\beta} + \mathbb{V}_{\alpha\beta})\Psi_{\beta,\vec{k}}(t) + \int_0^t dt'\; \Sigma_{\alpha\beta}(k;t-t')\Psi_{\beta,\vec{k}}(t') = \xi_{\alpha,\vec{k}}(t) \\ &\Psi_{\alpha,\vec{k}}(t=0) = \Psi^0_{\alpha,\vec{k}} \;\; ; \;\; \dot{\Psi}_{\alpha,\vec{k}}(t=0) = \Pi^0_{\alpha,\vec{k}} \end{aligned} \tag{9.23}$$

where $\Psi^0_{\alpha,\vec{k}}, \Pi^0_{\alpha,\vec{k}}$ are the initial values of the field and its canonical momentum. The stochastic noise $\xi_{\alpha,\vec{k}}(t)$ is described by a Gaussian distribution function [168, 186, 197]with

$$\langle\xi_{\alpha,\vec{k}}(t)\rangle = 0 \;\; ; \;\; \langle\xi_{\alpha,\vec{k}}(t)\xi_{\beta,-\vec{k}}(t')\rangle = \mathcal{K}_{\alpha,\beta}(k;t-t') \equiv \int_{-\infty}^{\infty}\frac{d\omega}{2\pi}e^{i\omega(t-t')}\widetilde{\mathcal{K}}_{\alpha\beta}(k;\omega) \tag{9.24}$$

and the angular brackets denote the averages with the Gaussian probability distribution function, determined by the averages over the bath degrees of freedom. The retarded self-energy kernel has

the following spectral representation[197]

$$\Sigma_{\alpha\beta}(k;t-t') = \frac{i}{\pi}\int_{-\infty}^{\infty} e^{i\omega(t-t')}\mathrm{Im}\widetilde{\Sigma}_{\alpha\beta}(k;\omega)d\omega \tag{9.25}$$

where the imaginary part in the flavor basis is

$$\mathrm{Im}\widetilde{\Sigma}(k;\omega) = \mathrm{Im}\widetilde{\Sigma}_{aa}(k;\omega)\begin{pmatrix} 1 & 0 \\ 0 & 0 \end{pmatrix}, \tag{9.26}$$

and $\mathrm{Im}\widetilde{\Sigma}_{aa}(k;\omega)$ is obtained from the cut discontinuity in the one-loop diagram in figure (9.2). In this figure the W propagator should be identified with the *full* charged vector boson propagator in the standard model, including a radiative self-energy correction from a quark, lepton or hadron loop.

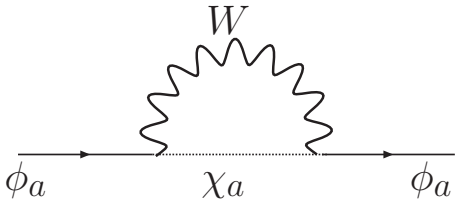

Figure 9.2: One loop self-energy for the active species to order G^2. The cut discontinuity across the $W-\chi$ lines yields the imaginary part $\mathrm{Im}\widetilde{\Sigma}_{aa}(k;\omega)$.

Because the bath fields are in thermal equilibrium, the noise correlation kernel $\widetilde{\mathcal{K}}_{\alpha\beta}(k;\omega)$ in eqn. (9.24) and the absorptive part of the retarded self energy $\mathrm{Im}\widetilde{\Sigma}_{\alpha\beta}(k;\omega)$ obey the generalized fluctuation dissipation relation[168, 186, 197]

$$\widetilde{\mathcal{K}}_{\alpha\beta}(k;\omega) = \mathrm{Im}\widetilde{\Sigma}_{\alpha\beta}(k;\omega)\coth\left[\frac{\beta\omega}{2}\right] \tag{9.27}$$

The solution of the Langevin equation (9.23) is[168, 186, 197]

$$\Psi_{\alpha,\vec{k}}(t) = \dot{G}_{\alpha\beta}(k;t)\,\Psi^0_{\beta,\vec{k}} + G_{\alpha\beta}(k;t)\,\Pi^0_{\beta,\vec{k}} + \int_0^t G_{\alpha\beta}(k;t')\;\xi_{\beta,\vec{k}}(t-t')dt'\,, \tag{9.28}$$

from which is clear that the propagator $G_{\alpha\beta}$ contains all the relevant information for the non-equilibrium dynamics.

In the Breit-Wigner (narrow width) approximation, the matrix propagator $G(k;t)$ in the flavor

basis is given by[197]

$$G(k;t) = \quad Z_k^{(1)}\, e^{-\frac{\Gamma_1(k)}{2}t}\left[\frac{\sin(\Omega_1(k)t)}{\Omega_1(k)}\,\mathbb{R}^{(1)}(\theta_m) - \frac{\widetilde{\gamma}(k)}{2}\,\frac{\cos(\Omega_1(k)t)}{\Omega_1(k)}\,\mathbb{R}^{(3)}(\theta_m)\right] + Z_k^{(2)}\, e^{-\frac{\Gamma_2(k)}{2}t}\left[\frac{\sin(\Omega_2(k)t)}{\Omega_2(k)}\,\mathbb{R}^{(2)}(\theta_m) + \frac{\widetilde{\gamma}(k)}{2}\,\frac{\cos(\Omega_2(k)t)}{\Omega_2(k)}\,\mathbb{R}^{(3)}(\theta_m)\right] \tag{9.29}$$

where $Z_k^{(i)}$ are the residues at the quasiparticle poles and we have introduced the matrices

$$\mathbb{R}^{(1)}(\theta) = \begin{pmatrix} \cos^2\theta & -\cos\theta\sin\theta \\ -\cos\theta\sin\theta & \sin^2\theta \end{pmatrix} = U(\theta)\begin{pmatrix} 1 & 0 \\ 0 & 0 \end{pmatrix} U^{-1}(\theta) \tag{9.30}$$

$$\mathbb{R}^{(2)}(\theta) = \begin{pmatrix} \sin^2\theta & \cos\theta\sin\theta \\ \cos\theta\sin\theta & \cos^2\theta \end{pmatrix} = U(\theta)\begin{pmatrix} 0 & 0 \\ 0 & 1 \end{pmatrix} U^{-1}(\theta) \tag{9.31}$$

$$\mathbb{R}^{(3)}(\theta) = \sin 2\theta \begin{pmatrix} \sin 2\theta & \cos 2\theta \\ \cos 2\theta & -\sin 2\theta \end{pmatrix} = \sin 2\theta\, U(\theta) \begin{pmatrix} 0 & 1 \\ 1 & 0 \end{pmatrix} U^{-1}(\theta)\,. \tag{9.32}$$

From the results of reference[197] to leading order in G, the mixing angle in the medium is determined from the relations

$$\cos 2\theta_m = \frac{\cos 2\theta - \frac{V_{aa}}{\delta M^2}}{\varrho} \quad ; \quad \sin 2\theta_m = \frac{\sin 2\theta}{\varrho}\,, \tag{9.33}$$

where

$$\varrho = \left[\big(\cos 2\theta - \frac{V_{aa}}{\delta M^2}\big)^2 + \big(\sin 2\theta\big)^2\right]^{\frac{1}{2}}. \tag{9.34}$$

The propagating frequencies and widths are given by[197]

$$\Omega_1(k) = \omega_1(k) + \Delta\omega_1(k) \;\; ; \;\; \Gamma_1(k) = \frac{\mathrm{Im}\widetilde{\Sigma}_{aa}(k;\omega_1(k))}{\omega_1(k)}\,\cos^2\theta_m \tag{9.35}$$

$$\Omega_2(k) = \omega_2(k) + \Delta\omega_2(k) \;\; ; \;\; \Gamma_2(k) = \frac{\mathrm{Im}\widetilde{\Sigma}_{aa}(k;\omega_2(k))}{\omega_2(k)}\,\sin^2\theta_m\,, \tag{9.36}$$

where

$$\omega_1^2(k) = k^2 + \overline{M}^2 + \frac{V_{aa}}{2} - \frac{\delta M^2\,\varrho}{2} \tag{9.37}$$

$$\omega_2^2(k) = k^2 + \overline{M}^2 + \frac{V_{aa}}{2} + \frac{\delta M^2\,\varrho}{2} \tag{9.38}$$

are the propagating frequencies (squared) in the medium including the matter potential at order G, namely the index of refraction arising from forward scattering, with $\overline{M}^2\,;\delta M^2$ defined in equation

(9.7). The second order frequency shifts are

$$\Delta\omega_1(k) = -\frac{\cos^2\theta_m}{2\pi\omega_1(k)}\int d\omega\mathcal{P}\left[\frac{\mathrm{Im}\widetilde{\Sigma}_{aa}(k;\omega)}{\omega-\omega_1(k)}\right] \tag{9.39}$$

$$\Delta\omega_2(k) = -\frac{\sin^2\theta_m}{2\pi\omega_2(k)}\int d\omega\mathcal{P}\left[\frac{\mathrm{Im}\widetilde{\Sigma}_{aa}(k;\omega)}{\omega-\omega_2(k)}\right] , \tag{9.40}$$

and[197]

$$\widetilde{\gamma}(k) = \frac{\mathrm{Im}\widetilde{\Sigma}_{aa}(k;\overline{\omega}(k))}{\omega_2^2(k)-\omega_1^2(k)} \;\; ; \;\; \overline{\omega}(k) = \sqrt{k^2+\overline{M}^2}\,. \tag{9.41}$$

The relationship between the damping rates $\Gamma_{1,2}$ and the imaginary part of the self energy is the same as that obtained in the study of neutrinos with standard model interactions in a medium in[198].

To leading order in perturbation theory the denominator in equation (9.41) is $\delta M^2\rho$. When the matter potential dominates (at high temperature in the standard model), $V_{aa} \gg \delta M^2$ and $\delta M^2\rho \sim V_{aa} \propto G \gg \mathrm{Im}\widetilde{\Sigma}_{aa} \propto G^2$, thus in this regime $\widetilde{\gamma} \propto G \ll 1$. For example with active neutrinos with standard model interactions at high temperature, it was argued in ref.[198] that $V_{aa} \propto G_F kT^5/M_W^2$ whereas $\mathrm{Im}\widetilde{\Sigma}_{aa} \sim G_F^2 kT^5$ therefore at high temperature $\widetilde{\gamma} \sim \mathrm{Im}\widetilde{\Sigma}_{aa}/V_{aa} \sim g_w \ll 1$ with g_w the standard model weak coupling.

In the opposite limit, for $\delta M^2 \gg V_{aa} \propto G$ the vacuum mass difference dominates $\rho \sim 1$ and $\widetilde{\gamma} \ll 1$ since $\delta M^2 \gg G \gg G^2$. This analysis is similar to that in ref.[198] and precludes the possibility of "quantum zeno suppression"[20, 60] at high temperature.

The *only* region in which $\widetilde{\gamma}$ *may not be perturbatively small* is near a resonance at which $\rho = |\sin 2\theta|$ and only for very small vacuum mixing angle so that $\delta M^2|\sin 2\theta| \propto G^2$. This situation requires a careful re-examination of the perturbative expansion, and in this case the propagator *cannot* be described as two separate Breit-Wigner resonances because the width of the resonances is of the same order of or larger than the separation between them. Such a possibility would require a complete re-assessment of the dynamics of the propagating modes in the medium as a consequence of the breakdown of the Breit-Wigner (or narrow width) approximation. However, for very small vacuum mixing angle, indeed a distinct possibility for keV sterile neutrinos[20], the MSW resonance is very narrow and in most of the parameter range $\widetilde{\gamma} \ll 1$ and can be safely neglected. This is certainly the case at very high or very low temperature regimes in which $V_{aa} \gg \delta M^2$ or $V_{aa} \ll \delta M^2$ respectively.

In summary, it follows from this discussion that $\widetilde{\gamma}(k) \ll 1$, with the possible exception near an MSW resonance for extremely small vacuum mixing angle[197], and such a case must be studied

in detail non-perturbatively.

Hence, neglecting perturbatively small corrections, the Green's function in the flavor basis can be written as

$$G(k;t) = U(\theta_m(k)) G_m(k;t) U^{-1}(\theta_m(k)) \tag{9.42}$$

with

$$G_m(k;t) = \begin{pmatrix} e^{-\frac{\Gamma_1(k)}{2}t} \ \frac{\sin(\Omega_1(k)t)}{\Omega_1(k)} & 0 \\ 0 & e^{-\frac{\Gamma_2(k)}{2}t} \ \frac{\sin(\Omega_2(k)t)}{\Omega_2(k)} \end{pmatrix} \tag{9.43}$$

This Green's function and the expression for the damping rates $\Gamma_{1,2}$ in eqn. (9.35,9.36) lead to the following physical interpretation. The fields that diagonalize the Green's function on the mass shell, namely $\phi_{1,2}$ are associated with the quasiparticle modes in the medium and describe the propagating excitations in the medium. From eqn. (9.42) these are related to the flavor fields $\phi_{a,s}$ by the unitary transformation

$$\phi_a = \cos\theta_m \phi_1 + \sin\theta_m \phi_2 \ \ ; \ \ \phi_s = \cos\theta_m \phi_2 - \sin\theta_m \phi_1 \, . \tag{9.44}$$

When the matter potential $V_{aa} \gg \delta M^2$, namely when $\theta_m \sim \pi/2$ it follows that $\phi_a \sim \phi_2$ and the damping rate of the active species is $\Gamma_2 \sim \Gamma_{aa}$ while $\phi_s \sim \phi_1$ and the damping rate of the "sterile" species is $\Gamma_1 \sim \Gamma_{aa}\cos^2\theta_m \ll \Gamma_{aa}$, where

$$\Gamma_{aa} \simeq \frac{\mathrm{Im}\widetilde{\Sigma}_{aa}(k;k)}{k} \tag{9.45}$$

is the ultrarelativistic limit of the damping rate of the active species in absence of mixing. In the opposite limit, when the medium mixing angle is small $\theta_m \sim 0$, corresponding to the near-vacuum case, $\phi_a \sim \phi_1$ and the active species has a damping rate $\Gamma_1 \sim \Gamma_{aa}$ while $\phi_s \sim \phi_2$ with $\Gamma_2 \sim \Gamma_{aa}\sin^2\theta_m \ll \Gamma_{aa}$. In both limits the sterile species is weakly coupled to the plasma, active and sterile species become equally coupled near an MSW resonance for $\theta_m \sim \pi/4$.

We emphasize that the relation (9.44) *is not* a relation between wave functions, but between the *fields* associated with the flavor eigenstates (active-sterile) and those associated with the propagating (quasiparticle) excitations in the medium (see section (9.5)).

9.3 QUANTUM KINETICS:

The distribution functions for the active (a) and sterile (s) species are defined in terms of the diagonal entries of the mass matrix in the flavor representation, namely

$$N_\alpha(k;t) = \frac{1}{2W_\alpha(k)}\left[\langle\dot{\phi}_\alpha(\vec{k};t)\dot{\phi}_\alpha(-\vec{k},t)\rangle + W^2_\alpha(k)\langle\phi_\alpha(\vec{k};t)\phi_\alpha(-\vec{k},t)\rangle\right] - \frac{1}{2} \;\; ; \;\; \alpha = a,s \tag{9.46}$$

where

$$W^2_\alpha(k) = k^2 + M^2_{\alpha\alpha}\,. \tag{9.47}$$

The equal time expectation values of Heisenberg field operators are in the initial density matrix, and as shown in references[168, 186, 197] they are the same as the equal time expectation value of the center of mass Wigner variables Ψ, where the expectation value is now in terms of the initial density matrix for the system and the distribution function of the noise which is determined by the thermal bath[168, 186, 197]. Therefore the distribution functions for the active and sterile species are given by

$$N_\alpha(k;t) = \frac{1}{2W_\alpha(k)}\left[\langle\dot{\Psi}_\alpha(\vec{k};t)\dot{\Psi}_\alpha(-\vec{k},t)\rangle + W^2_\alpha(k)\langle\Psi_\alpha(\vec{k};t)\Psi_\alpha(-\vec{k},t)\rangle\right] - \frac{1}{2} \;\; ; \;\; \alpha = a,s \tag{9.48}$$

and the averages are taken over the initial density matrix of the system and the noise probability distribution. This expression combined with eqn.(9.28) makes manifest that the full time evolution of the distribution function is completely determined by the *propagator* $G_{\alpha\beta}(k,t)$ obtained from the solution of the effective equations of motion in the medium[197].

It proves convenient to introduce a *matrix* of distribution functions in terms of a parameter Ω as follows

$$\mathbb{N}_{\alpha\beta}(k,t;\Omega) \equiv \frac{1}{2\Omega}\left[\langle\dot{\Psi}_\alpha(\vec{k};t)\dot{\Psi}_\beta(-\vec{k},t)\rangle + \Omega^2\langle\Psi_\alpha(\vec{k};t)\Psi_\beta(-\vec{k},t)\rangle\right] - \frac{1}{2}\,\delta_{\alpha\beta} \tag{9.49}$$

from which we extract the active and sterile distribution functions from the diagonal elements, namely

$$N_a(k;t) = \mathbb{N}_{a,a}(k,t;W_a(k)) \;\; ; \;\; N_s(k;t) = \mathbb{N}_{s,s}(k,t;W_s(k)) \tag{9.50}$$

and the off-diagonal elements determine off-diagonal correlation functions of the fields and their canonical momenta in the flavor basis.

We consider first the initial density matrix for the system $\widehat{\rho}_\Phi(0)$ to be *diagonal in the flavor basis* with free field correlations

$$\text{Tr } \widehat{\rho}_\Phi(0)\Psi^0_{\alpha,\vec{k}}\Psi^0_{\beta,-\vec{k}} = \frac{1}{2W_\alpha(k)}\,[1+2N_\alpha(k;0)]\,\delta_{\alpha\beta} \tag{9.51}$$

$$\text{Tr } \widehat{\rho}_\Phi(0)\Pi^0_{\alpha,\vec{k}}\Pi^0_{\beta,-\vec{k}} = \frac{W_\alpha(k)}{2}\,[1+2N_\alpha(k;0)]\,\delta_{\alpha\beta} \tag{9.52}$$

$$\text{Tr } \widehat{\rho}_\Phi(0)\Psi^0_{\alpha,\vec{k}}\Pi^0_{\beta,-\vec{k}} = 0 \tag{9.53}$$

with $N_\alpha(k;0)$ being the initial distribution functions for the active and sterile species. Different initial conditions will be studied below.

Following the steps described in appendix (**??**) it is convenient to write $\mathbb{N}(k,t;\Omega) = \mathbb{N}^{(I)}(k,t;\Omega) + \mathbb{N}^{(\xi)}(k,t;\Omega)$ where $\mathbb{N}^{(I)}$ depends on the initial conditions but not on the noise ξ and $\mathbb{N}^{(\xi)}$ depends on the noise ξ but not on the initial conditions. We find

$$\begin{aligned}
&\mathbb{N}^{(I)}(k,t;\Omega) \\
=\;& \mathbb{R}^{(1)}(\theta_m)\,e^{-\Gamma_1 t}\left\{\cos^2(\theta_m)\left[\frac{W_a^2+\Omega_1^2}{2W_a\Omega}\right]\left[\frac{1}{2}+N_a(0)\right]+\sin^2(\theta_m)\left[\frac{W_s^2+\Omega_1^2}{2\Omega W_s}\right]\left[\frac{1}{2}+N_s(0)\right]\right\}\left[\frac{\Omega^2+\Omega_1^2}{2\Omega_1^2}\right] \\
+\;& \mathbb{R}^{(2)}(\theta_m)\,e^{-\Gamma_2 t}\left\{\sin^2(\theta_m)\left[\frac{W_a^2+\Omega_2^2}{2W_a\Omega}\right]\left[\frac{1}{2}+N_a(0)\right]+\cos^2(\theta_m)\left[\frac{W_s^2+\Omega_2^2}{2\Omega W_s}\right]\left[\frac{1}{2}+N_s(0)\right]\right\}\left[\frac{\Omega^2+\Omega_2^2}{2\Omega_2^2}\right] \\
+\;& \mathbb{R}^{(3)}(\theta_m)\,e^{-\frac{1}{2}(\Gamma_1+\Gamma_2)t}\cos\left[(\Omega_1-\Omega_2)t\right]\left[\frac{\Omega^2+\Omega_2\Omega_1}{4\Omega_1\Omega_2}\right]\left\{\frac{(W_a-W_s)}{4\Omega}\left(\frac{\Omega_1\Omega_2}{W_aW_s}-1\right)\right. \\
&\left.+N_a(0)\left(\frac{\Omega_1\Omega_2+W_a^2}{2\Omega W_a}\right)-N_s(0)\left(\frac{\Omega_1\Omega_2+W_s^2}{2\Omega W_s}\right)\right\}-\frac{\mathbb{1}}{2}\,.
\end{aligned} \tag{9.54}$$

We have suppressed the dependence on k to simplify the notation. The contribution from the noise term can be written as

$$\mathbb{N}^{(\xi)}(k,t;\Omega) = \frac{1}{2\Omega}\int\frac{d\omega}{2\pi}U(\theta_m)\Big\{h_m(\omega,t)\mathcal{K}_m(\omega)h_m^*(\omega,t)+\Omega^2 f_m(\omega,t)\mathcal{K}_m(\omega)f_m^*(\omega,t)\Big\}U^{-1}(\theta_m) \tag{9.55}$$

where

$$h_m(\omega,t) = \int_0^t e^{-i\omega t'}G_m(k;t') \;\;;\;\; f_m(\omega,t) = \int_0^t e^{-i\omega t'}\dot{G}_m(k;t') \tag{9.56}$$

and

$$\mathcal{K}_m(\omega) = \text{Im}\widetilde{\Sigma}_{aa}(k;\omega)\;[1+2n(\omega)]\begin{pmatrix}\cos^2(\theta_m) & \cos(\theta_m)\sin(\theta_m)\\ \cos(\theta_m)\sin(\theta_m) & \sin^2(\theta_m)\end{pmatrix} \tag{9.57}$$

After lengthy but straightforward algebra we find

$$\mathbb{N}^{(\xi)}(k,t;\Omega) = \left[\frac{\Omega^2+\Omega_1^2}{2\Omega_1\Omega}\right]\left[\frac{1}{2}+n(\Omega_1(k))\right]\left(1-e^{-\Gamma_1(k)t}\right)\,\mathbb{R}^{(1)}(\theta_m(k)) + \left[\frac{\Omega^2+\Omega_2^2}{2\Omega_2\Omega}\right]\left[\frac{1}{2}+n(\Omega_2(k))\right]\left(1-e^{-\Gamma_2(k)t}\right)\,\mathbb{R}^{(2)}(\theta_m(k)) \tag{9.58}$$

where we have neglected terms proportional to $\widetilde{\gamma}$.

Approximations: In arriving at the expressions (9.54), (9.58), we have made the following approximations:

- **(a)** We have taken $Z_k^{(i)} = 1$ thus neglecting terms which are perturbatively small, of $\mathcal{O}(G^2)$.
- **(b)** We have assumed $\Gamma_i/\Omega_i \ll 1$, which is warranted in perturbation theory and neglected terms proportional to this ratio.
- **(c)** As discussed above, consistently with perturbation theory we have assumed $\widetilde{\gamma}(k) \ll 1$ and neglected terms proportional to it. This corresponds to the interaction rate much smaller than the oscillation frequencies and relies on the consistency of the perturbative expansion.
- **(d)** In oscillatory terms we have taken a time average over the *rapid time scales* $1/\Omega_{1,2}$ replacing $\sin^2(\Omega_{1,2}t) = \cos^2(\Omega_{1,2}t) \to 1/2\,;\, \sin(\Omega_{1,2}t) = \cos(\Omega_{1,2}t) \to 0$.

Ultrarelativistic limit: The above expressions simplify considerably in the *ultrarelativistic limit* in which

$$\Omega \sim W_a(k) \sim W_s(k) \sim \Omega_1(k) \sim \Omega_2(k) \sim k\,, \tag{9.59}$$

and in this limit it follows that

$$\Gamma_1 = \Gamma_{aa}\cos^2\theta_m \;;\; \Gamma_2 = \Gamma_{aa}\sin^2\theta_m \tag{9.60}$$

and Γ_{aa} is the ultrarelativistic limit of the width of the active species in the absence of mixing given by eqn. (9.45). In this limit we obtain the following simple expression for the time evolution of the occupation number *matrix* in the flavor basis (suppressing the k dependence for simplicity)

$$\begin{aligned}\mathbb{N}(t) &= \mathbb{R}^{(1)}(\theta_m)\left[n(\Omega_1) + \left(N_a(0)\cos^2(\theta_m) + N_s(0)\sin^2(\theta_m) - n(\Omega_1)\right)e^{-\Gamma_1 t}\right] \\ &+ \mathbb{R}^{(2)}(\theta_m)\left[n(\Omega_2) + \left(N_a(0)\sin^2(\theta_m) + N_s(0)\cos^2(\theta_m) - n(\Omega_2)\right)e^{-\Gamma_2 t}\right] \\ &+ \frac{1}{2}\,\mathbb{R}^{(3)}(\theta_m)\,e^{-\frac{1}{2}(\Gamma_1+\Gamma_2)t}\,\cos\left[(\Omega_1-\Omega_2)t\right]\left(N_a(0)-N_s(0)\right).\end{aligned} \tag{9.61}$$

It is straightforward to verify that

$$\mathbb{N}(0) = \begin{pmatrix} N_a(0) & 0 \\ 0 & N_s(0) \end{pmatrix} . \tag{9.62}$$

The active and sterile populations are given by the diagonal elements of (9.61), namely

$$\begin{aligned} N_a(t) &= \cos^2(\theta_m)\left[n(\Omega_1) + \Big(N_a(0)\cos^2(\theta_m) + N_s(0)\sin^2(\theta_m) - n(\Omega_1)\Big)\, e^{-\Gamma_1 t}\right] \\ &+ \sin^2(\theta_m)\left[n(\Omega_2) + \Big(N_a(0)\sin^2(\theta_m) + N_s(0)\cos^2(\theta_m) - n(\Omega_2)\Big)\, e^{-\Gamma_2 t}\right] \\ &+ \frac{1}{2}\,\sin^2(2\theta_m)\, e^{-\frac{1}{2}(\Gamma_1+\Gamma_2)t}\,\cos\left[(\Omega_1-\Omega_2)t\right]\Big(N_a(0) - N_s(0)\Big) . \end{aligned} \tag{9.63}$$

$$\begin{aligned} N_s(t) &= \sin^2(\theta_m)\left[n(\Omega_1) + \Big(N_a(0)\cos^2(\theta_m) + N_s(0)\sin^2(\theta_m) - n(\Omega_1)\Big)\, e^{-\Gamma_1 t}\right] \\ &+ \cos^2(\theta_m)\left[n(\Omega_2) + \Big(N_a(0)\sin^2(\theta_m) + N_s(0)\cos^2(\theta_m) - n(\Omega_2)\Big)\, e^{-\Gamma_2 t}\right] \\ &- \frac{1}{2}\,\sin^2(2\theta_m)\, e^{-\frac{1}{2}(\Gamma_1+\Gamma_2)t}\,\cos\left[(\Omega_1-\Omega_2)t\right]\left(N_a(0) - N_s(0)\right) . \end{aligned} \tag{9.64}$$

The oscillatory term which results from the interference of the propagating modes $1, 2$ damps out with a damping factor

$$\frac{1}{2}(\Gamma_1 + \Gamma_2) = \frac{\Gamma_{aa}}{2} \tag{9.65}$$

which determines the *decoherence time scale* $\tau_{dec} = 2/\Gamma_{aa}$. These expressions are one of the main results of this article.

Initial density matrix diagonal in the $1-2$ basis: The above results were obtained assuming that the initial density matrix is diagonal in the flavor basis, if instead, it is diagonal in the basis of the propagating modes in the medium, namely the $1-2$ basis, it is straightforward to find the result

$$\begin{aligned} \mathbb{N}(t) = \quad & U(\theta_m)\Bigg\{ \begin{pmatrix} 1 & 0 \\ 0 & 0 \end{pmatrix} \left[n(\Omega_1) + \Big(N_1(0) - n(\Omega_1)\Big)\, e^{-\Gamma_1 t}\right] \\ & + \begin{pmatrix} 0 & 0 \\ 0 & 1 \end{pmatrix} \left[n(\Omega_2) + \Big(N_2(0) - n(\Omega_2)\Big)\, e^{-\Gamma_2 t}\right]\Bigg\} U^{-1}(\theta_m) . \end{aligned} \tag{9.66}$$

In particular, the active and sterile distribution functions become

$$N_a(t) = \cos^2\theta_m\left[n(\Omega_1)+\Big(N_1(0)-n(\Omega_1)\Big)\,e^{-\Gamma_1 t}\right]+\sin^2\theta_m\left[n(\Omega_2)+\Big(N_2(0)-n(\Omega_2)\Big)\,e^{-\Gamma_2 t}\right] \tag{9.67}$$

$$N_s(t) = \cos^2\theta_m\left[n(\Omega_2)+\Big(N_2(0)-n(\Omega_2)\Big)\,e^{-\Gamma_2 t}\right]+\sin^2\theta_m\left[n(\Omega_1)+\Big(N_1(0)-n(\Omega_1)\Big)\,e^{-\Gamma_1 t}\right]. \tag{9.68}$$

The results summarized by eqns. (9.63-9.68) show that the distribution functions for the propagating modes in the medium, namely the $1,2$ quasiparticles, reach equilibrium with the damping factor $\Gamma_{1,2}$ which is *twice* the damping rate of the quasiparticle modes (see eqn. (9.43)). The interference term is present *only* when the initial density matrix is *off diagonal* in the (1,2) basis of propagating modes in the medium.

If the initial density matrix is off-diagonal in the (1,2) basis, these off diagonal components damp-out within the decoherence time scale τ_{dec}, while the diagonal elements attain the values of the equilibrium distributions on the time scales $1/\Gamma_1, 1/\Gamma_2$.

9.4 THE QUANTUM MASTER EQUATION

The quantum master equation is the equation of motion of the *reduced* density matrix of the system fields in the interaction picture after integrating out the bath degrees of freedom. The first step is to define the interaction picture, for which a precise separation between the free and interaction parts in the Hamiltonian is needed[200]. In order to carry out the perturbative expansion in terms of the eigenstates in the medium, we include the lowest order forward scattering correction, namely the index of refraction into the un-perturbed Hamiltonian. This is achieved by writing the term

$$\phi_a^2\chi^2 = \phi_a^2\langle\chi^2\rangle + \phi_a^2\delta\chi^2 \tag{9.69}$$

where

$$\delta\chi^2 = \chi^2 - \langle\chi^2\rangle \quad ; \quad \langle\delta\chi^2\rangle = 0 \tag{9.70}$$

and the average is performed in the bath density matrix $\rho_B(0) = e^{-\beta H_0[\chi,W]}$. In this manner the quadratic part of the Lagrangian density for the active and sterile fields is

$$\mathcal{L}_0[\phi] = \frac{1}{2}\left\{\partial_\mu\Phi^T\partial^\mu\Phi - \Phi^T(\mathbb{M}^2+\mathbb{V})\Phi\right\} \tag{9.71}$$

where $\mathbb{V}$ is the matter potential given by eqn. (9.21). The unperturbed Hamiltonian for the system fields in the medium is diagonalized by the unitary transformation (9.4) but with the unitary matrix $U(\theta_m)$ with θ_m being the mixing angle in the medium given by equations (9.33,9.34) and φ_1, φ_2 are now the fields associated with the eigenstates of the Hamiltonian in the medium including the index of refraction correction from the matter potential to $\mathcal{O}(G)$ ($\mathcal{O}(G_F)$ in the case of neutrinos with standard model interactions). Introducing creation and annihilation operators for the fields $\varphi_{1,2}$ with usual canonical commutation relations, the unperturbed Hamiltonian *for the propagating modes in the medium including the index of refraction* is

$$H_S[\varphi_{1,2}] = \sum_{\vec{k}} \sum_{i=1,2} \left[a_i^\dagger(\vec{k}) a_i(\vec{k}) \omega_i(k) \right] \tag{9.72}$$

where $\omega_i(k)$ are the propagating frequencies in the medium given in equation (9.37,9.38). The interaction Hamiltonian is

$$H_I = G \int d^3x \left[\phi_a^2 \delta\chi^2 + \phi_a \mathcal{O}_a \right] \tag{9.73}$$

where

$$\phi_a = \cos(\theta_m)\varphi_1 + \sin(\theta_m)\varphi_2 \,. \tag{9.74}$$

This formulation represents a *re-arrangement* of the perturbative expansion in terms of the fields that create and annihilate the propagating modes *in the medium*. The remaining steps are available in the quantum optics literature[200]. Denoting the Hamiltonian for the bath degrees of freedom $H_0[\chi, W] \equiv H_B$ the total Hamiltonian is $H = H_S + H_B + H_I \equiv \overline{H}_0 + H_I$. The density matrix in the interaction picture is

$$\widehat{\rho}_i(t) = e^{i\overline{H}_0 t} \widehat{\rho}(t) e^{-i\overline{H}_0 t} \tag{9.75}$$

where $\widehat{\rho}(t)$ is given by eqn. (9.13) and it obeys the equation of motion

$$\frac{d\widehat{\rho}_i(t)}{dt} = -i \left[H_I(t), \widehat{\rho}_i(t) \right] \tag{9.76}$$

with $H_I(t) = e^{i\overline{H}_0 t} H_I e^{-i\overline{H}_0 t}$ is the interaction Hamiltonian in the interaction picture of $\overline{H}_0$. Iteration of this equation up to second order in the interaction yields[200]

$$\frac{d\widehat{\rho}_i(t)}{dt} = -i \left[H_I(t), \widehat{\rho}_i(0) \right] - \int_0^t dt' \left[H_I(t), \left[H_I(t'), \widehat{\rho}_i(t') \right] \right] + \cdots \tag{9.77}$$

The *reduced* density matrix for the system is obtained from the total density matrix by tracing over the bath degrees of freedom which are assumed to remain in equilibrium[200]. At this stage, several standard approximations are invoked[200]:

- **i): factorization:** the total density matrix is assumed to factorize

$$\widehat{\rho}_i(t) = \rho_{S,i}(t) \otimes \rho_B(0) \tag{9.78}$$

  where it is assumed that the bath remains in equilibrium, this approximation is consistent with obtaining the effective action by tracing over the bath degrees of freedom with an equilibrium thermal density matrix. The correlation functions of the bath degrees of freedom are not modified by the coupling to the system.

- **ii): Markovian approximation:** the memory of the evolution is neglected and in the double commutator in (9.77) $\widehat{\rho}_i(t')$ is replaced by $\widehat{\rho}_i(t)$ and taken out of the integral.

Taking the trace over the bath degrees of freedom yields the quantum master equation for the reduced density matrix,

$$\frac{d\rho_{S,i}(t)}{dt} = -\int_0^t dt' \mathrm{Tr}_B\{ \left[H_I(t), \left[H_I(t'), \widehat{\rho}_i(t)\right]\right] \} + \cdots \tag{9.79}$$

where the first term has vanished by dint of the fact that the matter potential was absorbed into the unperturbed Hamiltonian, namely $Tr_B\rho_B(0)\delta\chi^2 = 0$. This is an important aspect of the interaction picture in the basis of the propagating states *in the medium*. Up to second order we will only consider the interaction term

$$H_I(t) = \sum_{\vec{k}} \left[\cos\theta_m \varphi_{1,\vec{k}}(t) + \sin\theta_m \varphi_{2,\vec{k}}(t)\right] \mathcal{O}_{-\vec{k}}(t) \tag{9.80}$$

where we have written the interaction Hamiltonian in terms of spatial Fourier transforms and the fields are in the interaction picture of $\overline{H}_0$. We neglect non-linearities from the second order contributions of the term $\phi_a^2\delta\chi^2$, the non-linearities associated with the neutrino background are included in the forward scattering corrections accounted for in the matter potential. The quartic non-linearities are associated with active "neutrino-neutrino" elastic scattering and are not relevant for the production of the sterile species.

The next steps are: i) writing out explicitly the nested commutator in (9.79) yielding four different terms, ii) taking the trace over the bath degrees of freedom yielding the correlation functions of the bath operators $Tr_B\mathcal{O}(t)\mathcal{O}(t')$ (and $t \leftrightarrow t'$) and, iii) carrying out the integrals in the variable t'. While straightforward these steps are lengthy and technical and are relegated to appendix (D). Two further approximations are invoked[200],

- **iii): the "rotating wave approximation":** terms that feature rapidly varying phases of the form $e^{\pm 2i\omega_{1,2}t}; e^{\pm i(\omega_1+\omega_2)t}$ are averaged out in time leading to their cancellation. This ap-

proximation also has a counterpart in the effective action approach in the averaging of rapidly varying terms, see the discussion after equation (9.58).

- **iv): the Wigner Weisskopf approximation:** time integrals of the form

$$\int_0^t e^{-i(\omega-\Omega)\tau} d\tau \approx -i\mathcal{P}\left[\frac{1}{\omega-\Omega}\right] + \pi\delta(\omega-\Omega) \tag{9.81}$$

where $\mathcal{P}$ stands for the principal part. The Markovian approximation **(ii)** when combined with the Wigner-Weisskopf approximation is equivalent to approximating the propagators by their narrow width Breit-Wigner form in the effective action.

All of these approximations **i)- iv)** detailed above are standard in the derivation of quantum master equations in the literature[200].

The quantum master equation is obtained in appendix (D), it features diagonal and off-diagonal terms in the $1-2$ basis and is of the Lindblad form[200] which ensures that the trace of the reduced density matrix is a constant of motion as it must be, because it is consistently derived from the full Liouville evolution (9.13). We now focus on the ultrarelativistic case $\omega_1(k) \sim \omega_2(k) \sim k$ which leads to substantial simplifications and is the relevant case for sterile neutrinos in the early Universe, we also neglect the second order corrections to the propagation frequencies. With these simplifications we obtain,

$$\begin{aligned}
\frac{d\rho_{S,i}}{dt} &= \left\{ \sum_{j=1,2} \sum_{\vec{k}} -\frac{\Gamma_j(k)}{2} \Big[[1+n(\omega_j(k))] \Big(\rho_{S,i} a_j^\dagger(\vec{k}) a_j(\vec{k}) + a_j^\dagger(\vec{k}) a_j(\vec{k}) \rho_{S,i} - 2 a_j(\vec{k}) \rho_{S,i} a_j^\dagger(\vec{k}) \Big) \right. \\
&+ n(\omega_j(k)) \Big(\rho_{S,i} a_j(\vec{k}) a_j^\dagger(\vec{k}) + a_j(\vec{k}) a_j^\dagger(\vec{k}) \rho_{S,i} - 2 a_j^\dagger(\vec{k}) \rho_{S,i} a_j(\vec{k}) \Big) \Big] \\
&- \sum_{\vec{k}} \frac{\widetilde{\Gamma}(k)}{2} \Big\{ \Big[\Big(1+n(\omega_1(k)) \Big) \Big(a_2^\dagger(k;t) a_1(k;t) \rho_{S,i} + \rho_{S,i} a_1^\dagger(k;t) a_2(k;t) - a_2(k;t) \rho_{S,i} a_1^\dagger(k;t) \\
&- a_1(k;t) \rho_{S,i} a_2^\dagger(k;t) \Big) + n(\omega_1(k)) \Big(a_2(k;t) a_1^\dagger(k;t) \rho_{S,i} + \rho_{S,i} a_1(k;t) a_2^\dagger(k;t) - a_2^\dagger(k;t) \rho_{S,i} a_1(k;t) \\
&- a_1^\dagger(k;t) \rho_{S,i} a_2(k;t) \Big) \Big] \\
&+ \Big[\Big(1+n(\omega_2(k)) \Big) \Big(a_1^\dagger(k;t) a_2(k;t) \rho_{S,i} + \rho_{S,i} a_2^\dagger(k;t) a_1(k;t) - a_1(k;t) \rho_{S,i} a_2^\dagger(k;t) \\
&- a_2(k;t) \rho_{S,i} a_1^\dagger(k;t) \Big) + n(\omega_2(k)) \Big(a_1(k;t) a_2^\dagger(k;t) \rho_{S,i} + \rho_{S,i} a_2(k;t) a_1^\dagger(k;t) - a_1^\dagger(k;t) \rho_{S,i} a_2(k;t) \\
&- a_2^\dagger(k;t) \rho_{S,i} a_1(k;t) \Big) \Big] \Big\} ,
\end{aligned} \tag{9.82}$$

where

$$\Gamma_1(k) = \Gamma_{aa}(k)\cos^2\theta_m \quad , \quad \Gamma_2(k) = \Gamma_{aa}(k)\sin^2\theta_m$$
$$\widetilde{\Gamma}(k) = \frac{1}{2}\sin 2\theta_m \Gamma_{aa}(k) \quad ; \quad \Gamma_{aa}(k) = \frac{\mathrm{Im}\Sigma_{aa}(k,k)}{k} \tag{9.83}$$

and the interaction picture operators are given in eqn. (D.8). The expectation value of any system's operator A is given by

$$\langle A\rangle(t) = \mathrm{Tr}\rho_{i,S}(t)A(t) \tag{9.84}$$

where $A(t)$ is the operator in the interaction picture of $\overline{H}_0$, thus the time derivative of this expectation value contains two contributions

$$\frac{d}{dt}\langle A\rangle(t) = \mathrm{Tr}\dot{\rho}_{i,S}(t)A(t) + \mathrm{Tr}\rho_{i,S}(t)\dot{A}(t)\,. \tag{9.85}$$

The distribution functions for active and sterile species is defined as in equation (9.48) with the averages defined as in (9.84), namely

$$N_\alpha(k;t) = \mathrm{Tr}\rho_{i,S}(t)\left[\frac{\dot{\phi}_\alpha(\vec{k};t)\dot{\phi}_\alpha(-\vec{k},t)}{2W_\alpha(k)} + \frac{W_\alpha(k)}{2}\,\phi_\alpha(\vec{k};t)\phi_\alpha(-\vec{k},t)\right] - \frac{1}{2}\,, \tag{9.86}$$

where the fields are in the interaction picture of $\overline{H}_0$. The active and sterile fields are related to the fields that create and annihilate the propagating modes in the medium as

$$\phi_a(\vec{k}) = \cos\theta_m\varphi_1(\vec{k}) + \sin\theta_m\varphi_2(\vec{k}) \quad ; \quad \phi_s(\vec{k}) = \cos\theta_m\varphi_2(\vec{k}) - \sin\theta_m\varphi_1(\vec{k})\,. \tag{9.87}$$

In the interaction picture of $\overline{H}_0$

$$\varphi_j(\vec{k},t) = \frac{1}{\sqrt{2\omega_j(k)}}\left[a_j(\vec{k})\;e^{-i\omega_j(k)t} + a_j^\dagger(-\vec{k})\;e^{i\omega_j(k)t}\right] \tag{9.88}$$

where $\omega_j(k)$ are the propagation frequencies in the medium up to leading order in G, given by equations (9.37,9.38). Introducing this expansion into the expression (9.86) we encounter the ratio of the propagating frequencies in the medium ω_j and the bare frequencies W_α. Just as we did in the previous section, we focus on the relevant case of ultrarelativistic species and approximate as in equation (9.59) $\omega_j(k) \sim W_\alpha(k) \sim k$, in which case we find the relation between the creation-annihilation operators for the flavor fields and those of the $1,2$ fields to be[197]

$$a_a(\vec{k},t) = \cos\theta_m a_1(\vec{k},t) + \sin\theta_m a_2(\vec{k},t) \quad ; \quad a_s(\vec{k},t) = \cos\theta_m a_2(\vec{k},t) - \sin\theta_m a_1(\vec{k},t) \tag{9.89}$$

leading to the simpler expressions for the active and sterile distributions,

$$N_a(k;t) = \mathrm{Tr}\rho_{i,S}(t)\Bigg[\quad \cos^2\theta_m a_1^\dagger(\vec{k},t)a_1(\vec{k},t) + \sin^2\theta_m a_2^\dagger(\vec{k},t)a_2(\vec{k},t) + \frac{1}{2}\sin 2\theta_m (a_1^\dagger(\vec{k},t)a_2(\vec{k},t) + a_2^\dagger(\vec{k},t)a_1(\vec{k},t))\Bigg] \tag{9.90}$$

$$N_s(k;t) = \mathrm{Tr}\rho_{i,S}(t)\Bigg[\quad \cos^2\theta_m a_2^\dagger(\vec{k},t)a_2(\vec{k},t) + \sin^2\theta_m a_1^\dagger(\vec{k},t)a_1(\vec{k},t) - \frac{1}{2}\sin 2\theta_m (a_1^\dagger(\vec{k},t)a_2(\vec{k},t) + a_2^\dagger(\vec{k},t)a_1(\vec{k},t))\Bigg] . \tag{9.91}$$

In the interaction picture of $\overline{H}_0$ the products $a_j^\dagger(\vec{k},t)a_j(\vec{k},t)$ are time independent and $a_1^\dagger(\vec{k},t)a_2(\vec{k},t) = a_1^\dagger(\vec{k},0)a_2(\vec{k},0)\ e^{i(\omega_1(k)-\omega_2(k))t}$. It is convenient to introduce the distribution functions and off-diagonal correlators

$$n_{11}(k,t) = \mathrm{Tr}\rho_{i,S}(t)a_1^\dagger(k,t)a_1(k,t) \quad , \quad n_{22}(k,t) = \mathrm{Tr}\rho_{i,S}(t)a_2^\dagger(k,t)a_2(k,t) \tag{9.92}$$

$$n_{12}(k,t) = \mathrm{Tr}\rho_{i,S}(t)a_1^\dagger(k,t)a_2(k,t) \quad , \quad n_{21}(k,t) = \mathrm{Tr}\rho_{i,S}(t)a_2^\dagger(k,t)a_1(k,t) = n_{12}^*(k,t) \tag{9.93}$$

In terms of these, the distribution functions for the active and sterile species in the *ultrarelativistic* limit becomes

$$N_a(k;t) = \cos^2\theta_m n_{11}(k;t) + \sin^2\theta_m n_{22}(k;t) + \frac{1}{2}\sin 2\theta_m \Big(n_{12}(k;t) + n_{21}(k;t)\Big) \tag{9.94}$$

$$N_s(k;t) = \sin^2\theta_m n_{11}(k;t) + \cos^2\theta_m n_{22}(k;t) - \frac{1}{2}\sin 2\theta_m \Big(n_{12}(k;t) + n_{21}(k;t)\Big) . \tag{9.95}$$

From eqn. (9.85) we obtain the following kinetic equations for $n_{ij}(k;t)$

$$\dot{n}_{11} = -\Gamma_1\Big[n_{11} - n_{eq,1}\Big] - \frac{\widetilde{\Gamma}}{2}\Big[n_{12} + n_{21}\Big] \tag{9.96}$$

$$\dot{n}_{22} = -\Gamma_2\Big[n_{22} - n_{eq,2}\Big] - \frac{\widetilde{\Gamma}}{2}\Big[n_{12} + n_{21}\Big] \tag{9.97}$$

$$\dot{n}_{12} = \Big[-i\Delta\omega - \frac{\Gamma_{aa}}{2}\Big]n_{12} - \frac{\widetilde{\Gamma}}{2}\Big[(n_{11} - n_{eq,1}) + (n_{22} - n_{eq,2})\Big] \tag{9.98}$$

$$\dot{n}_{21} = \Big[+i\Delta\omega - \frac{\Gamma_{aa}}{2}\Big]n_{21} - \frac{\widetilde{\Gamma}}{2}\Big[(n_{11} - n_{eq,1}) + (n_{22} - n_{eq,2})\Big] , \tag{9.99}$$

where $n_{eq,j} = n(\omega_j(k))$ are the equilibrium distribution functions for the corresponding propagating modes, and $\Delta\omega = (\omega_2(k) - \omega_1(k))$. As we have argued above, in perturbation theory $\Gamma_{aa}(k)/\Delta\omega(k) \ll 1$, which is the same statement as the approximation $\widetilde{\gamma} \ll 1$ as discussed for the effective action, and in this case the off diagonal contributions to the kinetic equations yield

perturbative corrections to the distribution functions and correlators. To leading order in this ratio we find the distribution functions,

$$n_{11}(t) = n_{eq,1} + \Big(n_{11}(0) - n_{eq,1}\Big)\ e^{-\Gamma_1 t} - \frac{\widetilde{\Gamma} e^{-\Gamma_1 t}}{2\Delta\omega}\Bigg[i\ n_{12}(0)\Big[e^{-i\Delta\omega t}\ e^{\frac{1}{2}(\Gamma_2-\Gamma_1)t} - 1\Big] + c.c.\Bigg] \tag{9.100}$$

$$n_{22}(t) = n_{eq,2} + \Big(n_{22}(0) - n_{eq,2}\Big)\ e^{-\Gamma_2 t} - \frac{\widetilde{\Gamma} e^{-\Gamma_2 t}}{2\Delta\omega}\Bigg[i\ n_{12}(0)\Big[e^{-i\Delta\omega t}\ e^{\frac{1}{2}(\Gamma_1-\Gamma_2)t} - 1\Big] + c.c.\Bigg] \tag{9.101}$$

and off-diagonal correlators

$$\begin{aligned} n_{12}(t) &= e^{-i\Delta\omega t}\ e^{-\frac{\Gamma_{aa}}{2}t}\left\{ n_{12}(0) + i\frac{\widetilde{\Gamma}}{2\Delta\omega}\Bigg[(n_{11}(0) - n_{eq,1})\Big[e^{i\Delta\omega t}\ e^{\frac{1}{2}(\Gamma_2-\Gamma_1)t} - 1\Big]\right. \\ &+ \left.(n_{22}(0) - n_{eq,2})\Big[e^{i\Delta\omega t}\ e^{\frac{1}{2}(\Gamma_1-\Gamma_2)t} - 1\Big]\Bigg]\right\} \end{aligned} \tag{9.102}$$

where

$$\frac{\widetilde{\Gamma}}{2\Delta\omega} = \frac{1}{2}\sin 2\theta_m \frac{\mathrm{Im}\Sigma_{aa}(k,k)}{2k(\omega_2(k) - \omega_1(k)} = \frac{1}{2}\sin 2\theta_m \widetilde{\gamma} \tag{9.103}$$

with $\widetilde{\gamma}$ defined in eqn. (9.41) and we have suppressed the momenta index for notational convenience.

9.4.1 Comparing the effective action and quantum master equation

We can now establish the equivalence between the time evolution of the distribution functions obtained from the effective action and the quantum master equation, however in order to compare the results we must first determine the initial conditions in equations (9.100-9.102). The initial values $n_{ij}(0)$ must be determined from the initial condition and depend on the initial density matrix. Two important cases stand out: i) an initial density matrix diagonal in the flavor basis or ii) diagonal in the $1-2$ basis of propagating eigenstates in the medium.

Initial density matrix diagonal in the flavor basis: the initial expectation values are obtained by inverting the relation between $\varphi_{1,2}$ and $\phi_{a,s}$. We obtain

$$n_{11}(0) = \langle a_1^\dagger(\vec{k}) a_1(\vec{k})\rangle(0) = \cos^2\theta_m N_a(0) + \sin^2\theta_m N_s(0) \tag{9.104}$$

$$n_{22}(0) = \langle a_2^\dagger(\vec{k}) a_2(\vec{k})\rangle(0) = \cos^2\theta_m N_s(0) + \sin^2\theta_m N_a(0) \tag{9.105}$$

$$n_{12}(0) = \langle a_1^\dagger(\vec{k}) a_2(\vec{k})\rangle(0) = \frac{1}{2}\sin 2\theta_m (N_a(0) - N_s(0)) \tag{9.106}$$

It is straightforward to establish the equivalence between the results obtained from the effective action and those obtained above from the quantum master equation as follows: i) neglect the second order frequency shifts ($\Omega_{1,2} \sim \omega_{1,2}$) and the perturbatively small corrections of order $\widetilde{\gamma}$, ii) insert the initial conditions (9.104-9.106) in the solutions (9.100-9.102), finally using the relations (9.94,9.95) for the active and sterile distribution functions we find precisely the results given by equations (9.63,9.64) obtained via the non-equilibrium effective action.

Initial density matrix diagonal in the $1-2$ basis: in this case

$$\begin{aligned} \langle a^\dagger_1(\vec{k}) a_1(\vec{k})\rangle(0) &= N_1(0) \\ \langle a^\dagger_2(\vec{k}) a_2(\vec{k})\rangle(0) &= N_2(0) \\ \langle a^\dagger_1(\vec{k}) a_2(\vec{k})\rangle(0) &= 0 \end{aligned} \tag{9.107}$$

with these initial conditions it is straightforward to obtain the result (9.67,9.68).

The fundamental advantage in the method of the effective action is that it highlights that the main ingredient is the *full propagator in the medium* and the emerging time scales for the time evolution of distribution functions and coherences are completely determined by the quasiparticle dispersion relations and damping rates.

9.4.2 Quantum kinetic equations: summary

Having confirmed the validity of the kinetic equations via two independent but complementary methods, we now summarize the quantum kinetic equations in a form amenable to numerical study. For this purpose it is convenient to define the hermitian combinations

$$n_R(t) = n_{12}(t) + n_{21}(t) \; ; \; n_I(t) = i(n_{12}(t) - n_{21}(t)) \tag{9.108}$$

in terms of which the quantum kinetic equations for the distribution functions and coherences become (suppressing the momentum label)

$$\dot{n}_{11} = -\Gamma_{aa} \cos^2\theta_m \Big[n_{11} - n_{eq,1}\Big] - \frac{\Gamma_{aa}}{4} \sin 2\theta_m \; n_R \tag{9.109}$$

$$\dot{n}_{22} = -\Gamma_{aa} \sin^2\theta_m \Big[n_{22} - n_{eq,2}\Big] - \frac{\Gamma_{aa}}{4} \sin 2\theta_m \; n_R \tag{9.110}$$

$$\dot{n}_R = -(\omega_2 - \omega_1) \; n_I - \frac{\Gamma_{aa}}{2} n_R - \frac{\Gamma_{aa}}{2} \sin 2\theta_m \Big[(n_{11} - n_{eq,1}) + (n_{22} - n_{eq,2})\Big] \tag{9.111}$$

$$\dot{n}_I = (\omega_2 - \omega_1) \; n_R - \frac{\Gamma_{aa}}{2} n_I \, , \tag{9.112}$$

with the active and sterile distribution functions related to the quantities above as follows

$$N_a(k;t) = \cos^2\theta_m n_{11}(k;t) + \sin^2\theta_m n_{22}(k;t) + \frac{1}{2}\sin 2\theta_m n_R(k;t) \quad (9.113)$$

$$N_s(k;t) = \sin^2\theta_m n_{11}(k;t) + \cos^2\theta_m n_{22}(k;t) - \frac{1}{2}\sin 2\theta_m n_R(k;t)\,. \quad (9.114)$$

In the perturbative limit when $\Gamma_{aa}\sin 2\theta_m/\Delta\omega \ll 1$ which as argued above is the correct limit in all but for a possible small region near an MSW resonance[198], the set of kinetic equations simplify to

$$\dot{n}_{11} = -\Gamma_{aa}\cos^2\theta_m\Big[n_{11} - n_{eq,1}\Big] \quad (9.115)$$

$$\dot{n}_{22} = -\Gamma_{aa}\sin^2\theta_m\Big[n_{22} - n_{eq,2}\Big] \quad (9.116)$$

$$\dot{n}_R = -\Big(\omega_2 - \omega_1\Big)\, n_I - \frac{\Gamma_{aa}}{2} n_R \quad (9.117)$$

$$\dot{n}_I = \Big(\omega_2 - \omega_1\Big)\, n_R - \frac{\Gamma_{aa}}{2} n_I\,. \quad (9.118)$$

In this case the active and sterile populations are given by (suppressing the momentum variable)

$$\begin{aligned} N_a(t) &= \cos^2(\theta_m)\Big[n_{eq}(\omega_1) + \Big(n_{11}(0) - n_{eq}(\omega_1)\Big)\, e^{-\Gamma_1 t}\Big] \\ &+ \sin^2(\theta_m)\Big[n_{eq}(\omega_2) + \Big(n_{22}(0) - n_{eq}(\omega_2)\Big)\, e^{-\Gamma_2 t}\Big] \\ &+ \sin(2\theta_m)\, e^{-\frac{\Gamma_{aa}}{2}t}\, \cos\left[(\omega_1 - \omega_2)t\right]\; n_{12}(0)\,. \end{aligned} \quad (9.119)$$

$$\begin{aligned} N_s(t) &= \sin^2(\theta_m)\Big[n_{eq}(\omega_1) + \Big(n_{11}(0) - n_{eq}(\omega_1)\Big)\, e^{-\Gamma_1 t}\Big] \\ &+ \cos^2(\theta_m)\Big[n_{eq}(\omega_2) + \Big(n_{22}(0) - n_{eq}(\omega_2)\Big)\, e^{-\Gamma_2 t}\Big] \\ &- \sin(2\theta_m)\, e^{-\frac{\Gamma_{aa}}{2}t}\, \cos\left[(\omega_1 - \omega_2)t\right]\; n_{12}(0)\,, \end{aligned} \quad (9.120)$$

where

$$\Gamma_1(k) = \Gamma_{aa}(k)\cos^2\theta_m \;\;;\;\; \Gamma_2(k) = \Gamma_{aa}(k)\sin^2\theta_m \quad (9.121)$$

and assumed that $n_{12}(0)$ is real as is the case when the initial density matrix is diagonal both in the flavor or $1,2$ basis,

$$n_{12}(0) = \begin{cases} \frac{1}{2}\sin 2\theta_m\; (N_a(0) - N_s(0)) & \text{diagonal in flavor basis} \\ 0 & \text{diagonal in } 1,2 \text{ basis} \end{cases} \quad (9.122)$$

It is clear that the evolution of the active and sterile distribution functions *cannot*, in general, be written as simple rate equations.

From the expressions given above for the quantum kinetic equations it is straightforward to generalize to account for the fermionic nature of neutrinos: the equilibrium distribution functions are replaced by the Fermi-Dirac distributions, and Pauli blocking effects enter in the explicit calculation of the damping rates.

9.5 TRANSITION PROBABILITIES AND COHERENCES

9.5.1 A "transition probability" in a medium

The concept of a transition probability as typically used in neutrino oscillations is not suitable in a medium when the description is not in terms of wave functions but density matrices. However, an equivalent concept can be provided as follows. Consider expanding the active and sterile fields in terms of creation and annihilation operators. In the ultrarelativistic limit the positive frequency components are obtained from the relation (9.89)and their expectation values in the reduced density matrix are given by

$$\varphi_{a,s}(\vec{k},t) \equiv \langle a_{a,s}(\vec{k},t)\rangle \,. \tag{9.123}$$

The kinetic equations for $\langle a_{1,2}(\vec{k})\rangle(t)$ are found to be

$$\frac{d}{dt}\langle a_1(\vec{k})\rangle(t) = \Big(-i\omega_1(k) - \frac{\Gamma_1(k)}{2}\Big)\langle a_1(\vec{k})\rangle(t) - \frac{\widetilde{\Gamma}}{2}\,\langle a_2(\vec{k})\rangle(t) \tag{9.124}$$

$$\frac{d}{dt}\langle a_2(\vec{k})\rangle(t) = \Big(-i\omega_2(k) - \frac{\Gamma_2(k)}{2}\Big)\langle a_2(\vec{k},t)\rangle - \frac{\widetilde{\Gamma}}{2}\,\langle a_1(\vec{k})\rangle(t)\,, \tag{9.125}$$

where $\widetilde{\Gamma}$ has been defined in eqn. (9.83). To leading order in $\widetilde{\Gamma}/\Delta\omega$ the solutions of these kinetic equations are

$$\langle a_1(\vec{k})\rangle(t) = \langle a_1(\vec{k})\rangle(0)\; e^{-i\omega_1 t}e^{-\frac{\Gamma_1}{2}t} - \frac{i\widetilde{\Gamma}}{2\Delta\omega}\langle a_2(\vec{k})\rangle(0)\Big[e^{-i\omega_2 t}e^{-\frac{\Gamma_2}{2}t} - e^{-i\omega_1 t}e^{-\frac{\Gamma_1}{2}t}\Big] \tag{9.126}$$

$$\langle a_2(\vec{k})\rangle(t) = \langle a_2(\vec{k})\rangle(0)\; e^{-i\omega_2 t}e^{-\frac{\Gamma_2}{2}t} + \frac{i\widetilde{\Gamma}}{2\Delta\omega}\langle a_1(\vec{k})\rangle(0)\Big[e^{-i\omega_1 t}e^{-\frac{\Gamma_1}{2}t} - e^{-i\omega_2 t}e^{-\frac{\Gamma_2}{2}t}\Big]\,. \tag{9.127}$$

The initial values $\langle a_{1,2}(\vec{k})\rangle(0)$ determine the initial values $\varphi_{a,s}(\vec{k};0)$, or alternatively, giving the initial values $\varphi_{a,s}(\vec{k};0)$ determines $\langle a_{1,2}(\vec{k})\rangle(0)$. Consider the case in which the initial density matrix is such that

$$\langle a_a(\vec{k},0)\rangle \equiv \varphi_a(\vec{k}) \neq 0 \;\;;\;\; \langle a_s(\vec{k},0)\rangle \equiv \varphi_s(\vec{k},0) = 0 \tag{9.128}$$

the initial values of $\langle a_{1,2}(\vec{k})\rangle(0)$ are obtained by inverting the relation (9.74) from which we find

$$\varphi_s(\vec{k},t) = -\frac{1}{2}\sin 2\theta_m(1-i\widetilde{\gamma})\Big[e^{-i\omega_1 t}e^{-\frac{\Gamma_1}{2}t} - e^{-i\omega_2 t}e^{-\frac{\Gamma_2}{2}t}\Big]\varphi_a(\vec{k},0)\,, \tag{9.129}$$

this result coincides with that found in ref.[197]. We can interpret the "transition probability" as

$$P_{a\to s}(\vec{k},t) = \left|\frac{\varphi_s(\vec{k},t)}{\varphi_a(\vec{k},0)}\right|^2 = \frac{1}{2}\sin^2 2\theta_m\,\left[e^{-\Gamma_1 t} + e^{-\Gamma_2 t} - 2\cos\Big(\big(\omega_2-\omega_1\big)t\Big)\,e^{-\frac{1}{2}(\Gamma_1+\Gamma_2)t}\right] \tag{9.130}$$

where we have neglected perturbative corrections of $\mathcal{O}(\widetilde{\gamma})$. This result coincides with that obtain in ref.[197] from the effective action, and confirms a similar result for neutrinos with standard model interactions[198]. We emphasize that this "transition probability" is *not* obtained from the time evolution of single particle wave functions, but from *expectation values in the reduced density matrix*: the initial density matrix features a non-vanishing expectation value of the active field but a vanishing expectation value of the sterile field, however, upon time evolution the density matrix develops an expectation value of the sterile field. The relation between the transition probability (9.130) and the time evolution of the distribution functions and coherences is now explicit, the first two terms in (9.130) precisely reflect the time evolution of the distribution functions n_{11}, n_{22} with time scales $1/\Gamma_{1,2}$ respectively, while the last, oscillatory term is the interference between the active and sterile components and is damped out on the decoherence time scale τ_{dec}. This analysis thus confirms the results in ref.[198].

9.5.2 Coherences

The time evolution of the off-diagonal coherence $\langle a_1^\dagger(\vec{k})a_2(\vec{k})\rangle(t)$ is determined by the kinetic equation (9.98), neglecting perturbatively small corrections of $\mathcal{O}(\widetilde{\gamma})$

$$\langle a_1^\dagger(\vec{k})a_2(\vec{k})\rangle(t) = \langle a_1^\dagger(\vec{k})a_2(\vec{k})\rangle(0)\; e^{i\Delta\omega t}e^{-\frac{\Gamma_{aa}}{2}t} \tag{9.131}$$

where we have used the relations (9.83) in the ultrarelativistic limit. Therefore, in perturbation theory, if the initial density matrix is off-diagonal in the $1-2$ basis (propagating modes in the medium) the off-diagonal correlations are exponentially damped out on the coherence time scale $\tau_{dec} = 2/\Gamma_{aa}(k)$. This coherence term and its hermitian conjugate are precisely the ones responsible for the oscillatory term in the transition probability (9.130). An important consequence of the damping of the off-diagonal coherences is that in perturbation theory the equilibrium density matrix is *diagonal in the basis of the propagating modes in the medium*. This result confirms the

arguments in ref.[199]. As can be seen from the expression of the transition probability (9.130) this is precisely the time scale for suppression of the *oscillatory* interference term. However, the transition probability is *not* suppressed on this coherence time scale, the first two terms in (9.130) reflect the fact that the *occupation* numbers build up on time scales $1/\Gamma_1; 1/\Gamma_2$ respectively and the interference term is exponentially suppressed on the decoherence time scale $\tau_{dec} = 2/(\Gamma_1 + \Gamma_2)$. For small mixing angle in the medium θ_m all of these time scales can be widely different.

It is noteworthy to compare the transition probability (9.129) with the distribution functions (9.119,9.120). The first two, non-oscillatory terms in (9.129) describe the same time evolution as the distribution functions n_{11}, n_{22} of the propagating modes in the medium, while the last, oscillatory term describes the interference between these. This confirms the results and arguments provided in ref.[198].

9.6 FROM THE QUANTUM MASTER EQUATION TO THE QKE FOR THE "POLARIZATION" VECTOR

The results of the previous section allows us to establish a correspondence between the quantum master equation (9.82) the quantum kinetic equations (9.109-9.112) and the quantum kinetic equation for a polarization vector often used in the literature[66, 71]. Following ref.[201], let us define the "polarization vector" with the following components,

$$P_0(\vec{k},t) = \langle a_a^\dagger(\vec{k},t)a_a(\vec{k},t) + a_s^\dagger(\vec{k},t)a_s(\vec{k},t)\rangle = N_a(k,t) + N_s(k,t) \tag{9.132}$$

$$P_x(\vec{k},t) = \langle a_a^\dagger(\vec{k},t)a_s(\vec{k},t) + a_s^\dagger(\vec{k},t)a_a(\vec{k},t)\rangle \tag{9.133}$$

$$P_y(\vec{k},t) = -i\langle a_a^\dagger(\vec{k},t)a_s(\vec{k},t) - a_s^\dagger(\vec{k},t)a_a(\vec{k},t)\rangle \tag{9.134}$$

$$P_z(\vec{k},t) = \langle a_a^\dagger(\vec{k},t)a_a(\vec{k},t) - a_s^\dagger(\vec{k},t)a_s(\vec{k},t)\rangle = N_a(k,t) - N_s(k,t) \tag{9.135}$$

where the creation and annihilation operators for the active and sterile fields are related to those that create and annihilate the propagating modes in the medium $1, 2$ by eqn. (9.89), and the angular brackets denote expectation values in the reduced density matrix $\rho_{S,i}$ which obeys the quantum master equation (9.82). In terms of the population and coherences n_{ij} the elements of the polarization vector are given by

$$P_0 = n_{11} + n_{22} \tag{9.136}$$

$$P_x = -\sin 2\theta_m \Big(n_{11} - n_{22}\Big) + \cos 2\theta_m n_R \tag{9.137}$$

$$P_y = -n_I \tag{9.138}$$

$$P_z = \cos 2\theta_m \Big(n_{11} - n_{22}\Big) + \sin 2\theta_m n_R \tag{9.139}$$

where $n_{R,I}$ are defined by equation (9.108). Using the quantum kinetic equations (9.109-9.112) we find

$$\frac{dP_0}{dt} = -\frac{\Gamma_{aa}}{2} P_z - \frac{\Gamma_{aa}}{2}\left[\Big(n_{11} - n_{eq,1}\Big) + \Big(n_{22} - n_{eq,2}\Big)\right] + \frac{\Gamma_{aa}}{2}\cos 2\theta_m \Big(n_{eq,1} - n_{eq,2}\Big) \tag{9.140}$$

$$\frac{dP_x}{dt} = -(\omega_2 - \omega_1)\cos 2\theta_m n_I - \frac{\Gamma_{aa}}{2} P_x - \frac{\Gamma_{aa}}{2}\sin 2\theta_m \Big(n_{eq,1} - n_{eq,2}\Big) \tag{9.141}$$

$$\frac{dP_y}{dt} = -(\omega_2 - \omega_1) n_R - \frac{\Gamma_{aa}}{2} P_y \tag{9.142}$$

$$\frac{dP_z}{dt} = -(\omega_2 - \omega_1)\sin 2\theta_m n_I - \frac{\Gamma_{aa}}{2} P_z - \frac{\Gamma_{aa}}{2}\left[\Big(n_{11} - n_{eq,1}\Big) + \Big(n_{22} - n_{eq,2}\Big)\right] \tag{9.143}$$

We now *approximate*

$$\Big(n_{eq,1} - n_{eq,2}\Big) \sim \frac{(\omega_2 - \omega_1)}{T}\, n'_{eq}(x) \sim 0\,, \tag{9.144}$$

thus neglecting the last terms in eqns. (9.140,9.141), introducing the vector $\vec{V}$ with components

$$\vec{V} = (\omega_2 - \omega_1)\,\Big(\sin 2\theta_m, 0, -\cos 2\theta_m\Big) \tag{9.145}$$

we find the following equations of motion for the polarization vector

$$\frac{d\vec{P}}{dt} = \vec{V} \times \vec{P} - \frac{\Gamma_{aa}}{2}\Big(P_x \hat{x} + P_y \hat{y}\Big) + \frac{dP_0}{dt}\hat{z} \tag{9.146}$$

This equation is exactly of the form

$$\frac{d\vec{P}}{dt} = \vec{V} \times \vec{P} - D\vec{P}_T + \frac{dP_0}{dt}\hat{z} \tag{9.147}$$

used in the literature[60, 66, 71, 77, 78], where D and $\vec{P}_T$ can be identified from eqn. (9.146).

Therefore the quantum kinetic equation for the polarization vector (9.146) is *equivalent* to the full set of quantum kinetic equations (9.109-9.112) or equivalently to equations (9.96-9.99)

under the approximation (9.144). Furthermore since the quantum kinetic equations (9.109-9.112) have been proven to be equivalent to the time evolution obtained from the effective action, we conclude that the kinetic equation for the polarization vector (9.147) is completely equivalent to the effective action and the quantum master equation under the approximations discussed above. This equivalence between the effective action, the kinetic equations obtained from quantum Master equation and the kinetic equations for the polarization vector makes explicit that the *fundamental* scales for decoherence and damping are determined by $\Gamma_{1,2}$, which are twice the damping rates of the quasiparticle modes. These are completely determined by the complex poles of the propagator in the medium. Furthermore the formulation in terms of the effective action, or equivalently the quantum master equation (9.82) provides more information: for example from both we can extract the transition probability $P_{a\to s}$ in the medium from expectation values of the field operators (or creation/annihilation operators) in the reduced density matrix, leading unequivocally to the expression (9.130) which indeed features the *two* relevant time scales. Furthermore it directly yields information on the off-diagonal coherences (9.131) which fall off on the decoherence time scale $\tau_{dec} = 2/\Gamma_{aa}$, thus elucidating that the reduced density matrix in equilibrium (the asymptotic long time limit) is *diagonal in the 1-2 basis*. While this information could be extracted from linear combinations of P_x, P_y it is hidden in the solution of the kinetic equation for the polarization, whereas it is exhibited clearly in the quantum kinetic equations (9.96-9.99) in the regime in which perturbation theory is applicable $|\Gamma_{aa}\sin 2\theta_m/(\omega_2 - \omega_1)| \ll 1$. In this regime, which as argued above is the most relevant, the set of quantum kinetic equations (9.115-9.118) combined with the relations (9.94-9.95) yield a much simpler and numerically amenable description of the time evolution of the populations and coherences: the active and sterile distribution functions are given by equations (9.119,9.120) and the off-diagonal coherence by eqn. (9.131). Therefore, while the kinetic equation for the polarization and the quantum kinetic equations (9.115-9.118) are equivalent and both are fundamentally consequences of the effective action or equivalently the quantum master equation, the study of sterile neutrino production in the early Universe does *not* implement any of these equivalent quantum kinetic formulations but instead assume a phenomenological approximate description in terms of a simple *rate equation*[20, 77, 78], which implies only one damping scale. Such a simple rate equation *cannot* describe accurately the time evolution of distribution functions and coherences which involve two different time scales (away from MSW resonances). In our view, part of the problem in this formulation is the time averaged transition probability introduced in ref.[77] which inputs the usual quantum mechanical vacuum transition probability but *damped by*

a simple exponential on the decoherence time scale, clearly in contradiction with the result (9.130) obtained from the *reduced quantum density matrix*. Within the kinetic formulation for the time evolution of the polarization vector $P_0, \vec{P}$, eqn. (9.146) it is not possible to extract the notion of a transition probability because the components of polarization vector are expectation values of *bilinear* operators in the reduced density matrix. Instead, the concept of active-sterile transition probability *can* be established in a medium via expectation values of the field operators (or their creation/annihilation operators) in the reduced density matrix es discussed in section (9.5.1).

9.7 CONCLUSIONS

Our goal is to study the non-equilibrium quantum kinetics of production of active and sterile neutrinos in a medium. We make progress towards that goal by studying a model of an active and a sterile *mesons* coupled to a bath in thermal equilibrium via couplings that model charged and current interactions of neutrinos. The dynamical aspects of mixing, oscillations, decoherence and damping are fairly robust and the results of the study can be simply modified to account for Pauli blocking effects of fermions. As already discussed in ref[197] this model provides a remarkably faithful description of the non-equilibrium dynamics of neutrinos.

We obtained the quantum kinetic equations for the active and sterile species via two independent but complementary methods. The first method obtains the non-equilibrium effective action for the active and sterile species after integrating out the bath degrees of freedom. This description provides a non-perturbative Dyson-like resummation of the self-energy radiative corrections, and the dynamics of the distribution functions is completely determined by the solutions of a Langevin equation with a noise term that obeys a generalized fluctuation-dissipation relation. The important ingredient in this description is the *full propagator*. The poles of the propagator correspond to two quasiparticle modes whose frequencies obey the usual dispersion relations of neutrinos in a medium with the corrections from the index of refraction (forward scattering), with damping rates (widths)

$$\Gamma_1 = \Gamma_{aa} \cos^2\theta_m \; ; \; \Gamma_2 = \Gamma_{aa} \sin^2\theta_m \, . \tag{9.148}$$

where Γ_{aa} is the interaction rate of the active species *in absence of mixing* (in the ultrarelativistic limit) and θ_m is the mixing angle *in the medium*. These *two damping* scales, along with the quasiparticle frequencies completely determine the evolution of the distribution functions. This is

one of the important aspects of the kinetic description in terms of the non-equilibrium effective action: *the dispersion relations and damping rates of the quasiparticle modes corresponding to the poles of the full propagator completely determine the non-equilibrium evolution of the distribution functions and coherences.*

We also obtained the quantum master equation for the *reduced* density matrix for the "neutrino degrees of freedom" by integrating (tracing) over the bath degrees of freedom taken to be in thermal equilibrium. An important aspect of the derivation consists in including the matter potential, or index of refraction from forward scattering to lowest order in the interactions in the unperturbed Hamiltonian. This method provides a re-arrangement of the perturbative expansion that includes self-consistently the index of refraction corrections and builds in the correct propagation frequencies in the medium. In this manner the the reduced density matrix (in the interaction picture) evolves in time *only through second order processes*. From the reduced density matrix we obtain the quantum kinetic equations for the distribution functions and coherences. These are *exactly the same as those obtained from the non-equilibrium effective action*. We also obtain the kinetic equation for coherences and introduce a generalization of the active-sterile transition probability by obtaining the time evolution of expectation values of the active and sterile *fields* in the reduced quantum density matrix. Within the realm of validity of the perturbative expansion the set of kinetic equations for the distribution functions and coherences are given by

$$\begin{aligned} \dot{n}_{11} &= -\Gamma_{aa}\cos^2\theta_m\Big[n_{11}-n_{eq,1}\Big] \;\; ; \;\; \dot{n}_{22} = -\Gamma_{aa}\sin^2\theta_m\Big[n_{22}-n_{eq,2}\Big] \\ \dot{n}_{12} &= \Big[-i\Big(\omega_2(k)-\omega_1(k)\Big)-\frac{\Gamma_{aa}}{2}\Big]n_{12} \;\; ; \;\; n_{21}=n^*_{12}\,, \end{aligned} \tag{9.149}$$

where $n_{eq,j} = n(\omega_j(k))$ are the equilibrium distribution functions for the corresponding propagating modes, $\omega_{1,2}(k)$ are the dispersion relations in the medium including the index of refraction, and the active and sterile distribution functions are given by

$$N_a(k;t) = \cos^2\theta_m n_{11}(k;t)+\sin^2\theta_m n_{22}(k;t)+\frac{1}{2}\sin 2\theta_m\Big(n_{12}(k;t)+n_{21}(k;t)\Big) \tag{9.150}$$

$$N_s(k;t) = \sin^2\theta_m n_{11}(k;t)+\cos^2\theta_m n_{22}(k;t)-\frac{1}{2}\sin 2\theta_m\Big(n_{12}(k;t)+n_{21}(k;t)\Big)\,. \tag{9.151}$$

The set of equations (9.149) provide a simple system of uncoupled rate equations amenable to numerical study, whose solution yields the active and sterile distribution functions via the relations (9.150,9.151), with straightforward modifications for fermions.

From the kinetic equations above, it is found that the coherences

$$n_{12} = \langle a_1^\dagger a_2 \rangle \tag{9.152}$$

which are off-diagonal (in the $1-2$ basis of propagating modes in the medium) expectation values in the reduced quantum density matrix are exponentially suppressed on a *decoherence* time scale $\tau_{dec} = 2/\Gamma_{aa}$ indicating that the equilibrium reduced density matrix is diagonal in the $1-2$ basis, confirming the arguments in ref.[199].

The generalization of the active-sterile transition probability in the medium via the *expectation value of the active and sterile fields in the reduced quantum density matrix* yields

$$P_{a\to s} = \frac{1}{2}\sin^2 2\theta_m \left[e^{-\Gamma_1 t} + e^{-\Gamma_2 t} - 2\cos\Big(\big(\omega_2 - \omega_1\big)t\Big)\, e^{-\frac{\Gamma_{aa}}{2}t} \right] \tag{9.153}$$

this result shows that the active-sterile transition probability depends on the *two damping time scales of the quasiparticle modes in the medium* which are also the time scales of kinetic evolution of the distribution functions, and confirms the results of refs.[198].

Finally, from the full set of quantum kinetic equations (9.115-9.118) and the approximation (9.144) we have obtained the set of quantum kinetic equations for the polarization vector, most often used in the literature,

$$\frac{d\vec{P}}{dt} = \vec{V}\times\vec{P} - \frac{\Gamma_{aa}}{2}\Big(P_x\hat{x} + P_y\hat{y}\Big) + \frac{dP_0}{dt}\hat{z} \tag{9.154}$$

where the relation between the components of the polarization vector $P_0, \vec{P}$ and the distribution functions and coherences is explicitly given by eqns. (9.132-9.135) (or equivalently (9.136-9.139)), and $\vec{V}$ is given by eqn. (9.145). Thus we have unambiguously established the direct relations between the effective action, quantum master equation, the full set of kinetic equations for population and coherences and the quantum kinetic equations in terms of the "polarization vector" most often used in the literature. These are all equivalent, but the effective action approach distinctly shows that the *two* independent fundamental damping scales are those associated with $\Gamma_{1,2}$, namely the damping rates of the quasiparticles in the medium, which are determined by the complex poles of the propagator. Furthermore in the regime of validity of perturbation theory, the set of kinetic equations (9.149) obtained from the quantum master equation yield a simple and clear understanding of the different time scales for the active and sterile distribution functions and a remarkably concise description of active and sterile production when combined with the relations (9.150,9.151). These simpler set of rate equations are hidden in the kinetic equation (9.154).

We have also argued that the simple phenomenological rate equation used in numerical studies of sterile neutrino production in the early Universe is *not* an accurate description of the non-equilibrium evolution, and trace its shortcomings to the time integral of an overly simplified description of the transition probability in the medium.

10.0 NEW INFLATION VS. CHAOTIC INFLATION, HIGHER DEGREE POTENTIALS AND THE RECONSTRUCTION PROGRAM IN LIGHT OF WMAP3

10.1 INTRODUCTION

Inflation provides a simple and robust mechanism to solve several outstanding problems of the standard Big Bang model [202, 203] becoming a leading paradigm in cosmology. Superhorizon quantum fluctuations amplified during inflation provide an explanation of the origin of the temperature anisotropies in the cosmic microwave background (CMB) and the seeds for large scale structure formation[204], as well as of tensor perturbations (primordial gravitational waves). Although there is a diversity of inflationary models, most of them predict fairly generic features: a gaussian, nearly scale invariant spectrum of (mostly) adiabatic scalar and tensor primordial fluctuations [204]. These features provide an excellent fit to the highly precise data provided by the Wilkinson Microwave Anisotropy Probe (WMAP) [205, 206, 207, 208] which begins to constrain inflationary models.

The combination of CMB [206, 207] and large scale structure data [209, 210] yield fairly tight constraints for the two dimensional marginalized contours of the tensor to scalar ratio r and the scalar index n_s. While $n_s = 1$ was excluded at the $95\% CL$ in [210] a most notable result that stems from the analysis of WMAP3 data is a confirmation that a scale invariant Harrison-Zeldovich spectrum is excluded at the 3σ level [207]. A combination of data from WMAP3 and large scale surveys distinctly favor $n_s < 1$ [211]. These latest bounds on the index of the power spectrum of scalar perturbations, and emerging bounds on the ratio of tensor to scalar fluctuations r begin to offer the possibility to discriminate different inflationary models. For example, the third year WMAP data disfavors the predictions for the scalar index and the tensor to scalar ratio from a monomial inflationary potential $\lambda\, \phi^4$ showing them to lie outside the 3σ contour, but the simple

monomial $m^2\ \phi^2/2$ yields a good fit to the data [207] and predicts a tensor to scalar ratio $r \sim 0.16$ within the range of forthcoming CMB observations.

Current and future CMB observations in combination with large scale structure surveys will yield tight constraints on the inflationary models, this motivates the exploration of clear predictions from the models and their confrontation with the data.

In distinction with the approach followed in [206, 207, 212] or studies of specific models[213], or statistical analysis combined with WMAP3 and LSS data[214, 215], we study the predictions for the power spectra of scalar fluctuations and the tensor to scalar ratio for *families* of new and chaotic inflationary models in the framework of the method presented in ref.[216]. This method relies on the effective field theory approach combined with a systematic expansion in $1/N_e$ where $N_e \sim 50$ is the number of e-folds before the end of inflation. The family of inflationary models that we study is characterized by effective field theories with potentials of the form

$$V(\phi) = V_0 - \frac{1}{2}\, m^2\, \phi^2 + \frac{\lambda}{2\,n}\, \phi^{2\,n} \quad , \quad \text{broken symmetry} \tag{10.1}$$

$$V(\phi) = \frac{1}{2}\, m^2\, \phi^2 + \frac{\lambda}{2\,n}\, \phi^{2\,n} \quad , \quad \text{unbroken symmetry} \ , \tag{10.2}$$

with $n = 2, 3, 4 \cdots$. For broken symmetry models with potentials of the form (10.1) there are two distinct regions: small and large field, corresponding to values of the inflaton field smaller or larger than the symmetry breaking scale respectively.

We implement the systematic expansion in $1/N_e$ where $N_e \sim 50$ is the number of e-folds before the end of inflation when wavelengths of cosmological relevance crossed the Hubble radius[216]. The $1/N_e$ expansion is a powerful and systematic tool that allows to re-cast the slow roll hierarchy as expansion in powers of $1/N_e$ [216]. This expansion allows us to implement a reconstruction program [217] which yields the scale of the inflaton field when modes of cosmological relevance today crossed the Hubble radius during inflation, and in the case of new inflation models also yields the *scale of symmetry breaking*.

We study the dependence of the observables (n_s, r and $dn_s/d\ln k$) on the degree of the inflaton potential ($2\,n$) for new and chaotic inflation and confront them with the WMAP3 data. This study shows in general that fourth degree potentials ($n = 2$) provide the best fit to the data. We find that new inflation fits the data on an appreciable wider range of the parameters while chaotic inflation does this in a much narrow range. Therefore, amongst the families of inflationary models studied, new inflation emerges as a leading contender in comparison with chaotic inflation. The present

analysis confirms the statement that within the framework of effective field theories with polynomial potentials, new inflation is a preferred model reproducing the present data [219, 220, 221].

10.2 EFFECTIVE FIELD THEORY, SLOW ROLL AND $1/N_E$ EXPANSIONS

In the absence of a fundamental microscopic description of inflation, an effective field theory approach, when combined with the slow roll expansion provides a robust paradigm for inflation with predictive power. The reliability of the effective field theory description hinges on a wide separation between the Hubble and Planck scales, and is validated by the bound from temperature fluctuations $H/M_{Pl} < 10^{-5}$ [216].

The slow roll expansion relies on the smallness of a hierarchy of the dimensionless ratios [203, 217, 222],

$$\epsilon_v = \frac{M_{Pl}^2}{2}\left[\frac{V^{'}(\phi)}{V(\phi)}\right]^2 \quad , \quad \eta_v = M_{Pl}^2\,\frac{V^{''}(\phi)}{V(\phi)} \quad , \quad \xi_v = M_{Pl}^4\,\frac{V'(\phi)\,V^{'''}(\phi)}{V^2(\phi)}\,. \tag{10.3}$$

The effective field theory expansion in H/M_{Pl} and the slow roll expansion are independent, the latter can be interpreted as an adiabatic expansion [216] wherein the derivatives of the inflationary potential are small.

The CMB data is consistently described within the slow roll expansion with inflationary potentials of the form [203, 216]

$$V(\phi) = M^4\,v\left(\frac{\phi}{M_{Pl}}\right)\,. \tag{10.4}$$

Within the slow roll approximation the number of e-folds before the end of inflation for which the value of the field is ϕ_{end} is given by

$$N\left[\phi(t)\right] = -\frac{1}{M_{Pl}^2}\int_{\phi(t)}^{\phi_{end}} V(\phi)\,\frac{d\phi}{dV}\,d\phi \quad . \tag{10.5}$$

It proves convenient to introduce N_e as the typical number of e-folds before the end of inflation during which cosmologically relevant wavelengths cross the Hubble radius during inflation, and ϕ_c as the value of the inflaton field corresponding to N_e

$$N_e = -\frac{1}{M_{Pl}^2}\int_{\phi_c}^{\phi_{end}} V(\phi)\,\frac{d\phi}{dV}\,d\phi\,. \tag{10.6}$$

The precise value of N_e is certainly near $N_e = 50$ [203, 218]. We will take the value $N_e = 50$ as a reference baseline value for numerical analysis, but from the explicit expressions obtained in

the systematic $1/N_e$ expansion below, it becomes a simple rescaling to obtain results for arbitrary values of N_e [see eq. (10.10) below].

The form of the potential eq.(10.4) and the above definition for the number of e-folds, suggests to introduce the following rescaled field variable [216]

$$\phi = \sqrt{N_e} M_{Pl}\, \chi \tag{10.7}$$

where the rescaled field χ is dimensionless. Furthermore, it is also convenient to scale N_e out of the potential and write

$$V(\phi) = N_e\, M^4\, w(\chi)\ . \tag{10.8}$$

With this definition, eq. (10.6) becomes

$$1 = -\int_{\chi_c}^{\chi_{end}} \frac{w(\chi)}{w'(\chi)}\, d\chi \tag{10.9}$$

where the prime stands for derivative with respect to χ, χ_{50} is the value of χ corresponding to N_e e-folds before the end of inflation, and χ_{end} is the value of χ at the end of inflation.

We emphasize that there is *no* dependence on N_e in the expression (10.9), therefore χ_c, χ_{end} only depend on the coupling g and the degree n. The slow roll parameters then become,

$$\epsilon_v = \frac{1}{2\, N_e} \left[\frac{w'(\chi_c)}{w(\chi_c)}\right]^2 \quad , \quad \eta_v = \frac{1}{N_e}\, \frac{w''(\chi_c)}{w(\chi_c)} \quad , \quad \xi_v = \frac{1}{N_e^2}\, \frac{w'(\chi_c)\, w'''(\chi_c)}{w^2(\chi_c)}\ . \tag{10.10}$$

It is clear from eqs.(10.9) and (10.10) that during the inflationary stage when wavelengths of cosmological relevance cross the horizon, it follows that $w(\chi_c), w'(\chi_c) \sim \mathcal{O}(1)$ leading to the slow roll expansion as a consistent expansion in $1/N_e$ [216].

The connection between the slow roll expansion and the expansion in $1/N_e$ becomes more explicit upon introducing a *stretched* dimensionless time variable τ and a dimensionless Hubble parameter h as follows [216]

$$\tau = \frac{M^2\, t}{\sqrt{N_e}\, M_{Pl}} \quad ; \quad h = \frac{M_{Pl}\, H}{\sqrt{N_e}\, M^2}\ . \tag{10.11}$$

In terms of τ, χ and h the Friedmann equation and the equation of motion for the inflaton become,

$$h^2(\tau) = \frac{1}{3}\left[\frac{1}{2\, N_e}\left(\frac{d\chi}{d\tau}\right)^2 + w(\chi)\right]\ ,$$

$$\frac{1}{N_e}\, \frac{d^2\chi}{d\tau^2} + 3\, h\, \frac{d\chi}{d\tau} + w'(\chi) = 0\ . \tag{10.12}$$

This equation of motion can be solved in a systematic expansion in $1/N_e$. The definition (10.7) also makes manifest that χ is a *slowly varying field*, since a change $\Delta\phi \sim M_{Pl}$ in the inflaton field implies a *small* change of the dimensionless field $\Delta\chi \sim 1/\sqrt{N_e}$.

In terms of these definitions, the CMB observables can be written manifestly in terms of the $1/N_e$ expansion. The amplitude of scalar perturbations is given by

$$\Delta^2_{\mathcal{R}} = \frac{N_e^2}{12\pi^2}\left(\frac{M}{M_{Pl}}\right)^4 \frac{w^3(\chi_c)}{[w'(\chi_c)]^2} \ , \tag{10.13}$$

and the spectral index n_s, the ratio of tensor to scalar perturbations r and the running of n_s with the wavevector $dn_s/d\ln k$ become

$$n_s = 1 - 6\,\epsilon_v + 2\,\eta_v \quad , \quad r = 16\,\epsilon_v \tag{10.14}$$

$$\frac{dn_s}{d\ln k} = -\frac{2}{N_e^2}\left\{\frac{w'(\chi_c)w'''(\chi_c)}{w^2(\chi_c)} + 3\left[\frac{w'(\chi_c)}{w(\chi_c)}\right]^4 - 4\,\frac{[w'(\chi_c)]^2\,w''(\chi_c)}{w^3(\chi_c)}\right\} . \tag{10.15}$$

The virtue of the $1/N_e$ expansion is that we can choose a reference baseline value for N_e, say $N_e = 50$ for numerical study, and use the scaling with N_e of the slow roll parameters given by eqs.(10.10), (10.14) and (10.15) to obtain their values for arbitrary N_e, namely

$$\begin{aligned} \epsilon_v[N_e] &= \epsilon_v[50]\,\frac{50}{N_e} \quad , \quad \eta_v[N_e] = \eta_v[50]\,\frac{50}{N_e} \quad , \quad r[N_e] = r[50]\,\frac{50}{N_e} \quad , \\ \frac{dn_s}{d\ln k}[N_e] &= \frac{dn_s}{d\ln k}[50]\left(\frac{50}{N_e}\right)^2 \quad , \quad n_s[N_e] = n_s[50] + (1 - n_s[50])\,\frac{N_e - 50}{N_e} \ . \end{aligned} \tag{10.16}$$

In what follows we will take $N_e = 50$ as representative of the cosmologically relevant case, however, the simple scaling relations (10.16) allow a straightforward extrapolation to other values.

The combination of WMAP and SDSS (LRG) data yields [207]

$$n_s = 0.958 \pm 0.016 \quad \text{(assuming } r = 0 \text{ with no running)} \tag{10.17}$$

$$r < 0.28 \ (95\%\,CL) \ \text{ no running} \tag{10.18}$$

$$r < 0.67 \ (95\%\,CL) \ \text{ with running} \ . \tag{10.19}$$

The running must be very small and of the order $\mathcal{O}(1/N_e^2) \sim 10^{-3}$ in slow roll for generic potentials[216]. Therefore, we can safely consider $dn_s/d\ln k = 0$ in our analysis. Figure 14 in ref.[207] and figure 2 in ref.[221] show that the preferred value of n_s slowly grows with the preferred value of r for $r > 0$. We find approximately that

$$\frac{\Delta n_s}{\Delta r} \simeq 0.12 \tag{10.20}$$

Therefore, for $r \sim 0.1$ the central value of n_s shifts from $n_s = 0.958$ ($r = 0$) to $n_s = 0.97$ ($r = 0.1$) as can be readily gleaned from the quoted figures in these references.

As a simple example that provides a guide post for comparison let us consider first the monomial potential

$$V(\phi) = \frac{\lambda}{2\,n}\,\phi^{2\,n}\,. \tag{10.21}$$

The case $n = 1$ yields a satisfactory fit to the WMAP data [206, 207]. For these potentials it follows that,

$$w(\chi) = \frac{\chi^{2\,n}}{2\,n} \quad ; \quad M^4 = \lambda\,N_e^{n-1}\,M_{Pl}^{2\,n}\;, \tag{10.22}$$

inflation ends at $\chi_{end} = 0$, and the value of the dimensionless field χ_c at N_e e-folds before the end of inflation is

$$|\chi_c| = 2\,\sqrt{n}\,. \tag{10.23}$$

These results lead to [203]

$$\epsilon_v = \frac{n}{2\,N_e} \quad , \quad \eta_v = \frac{2\,n-1}{2\,N_e} \tag{10.24}$$

$$n_s - 1 = -\frac{n+1}{N_e} \quad , \quad r = \frac{8\,n}{N_e} \quad , \quad \frac{dn_s}{d\ln k} = -\frac{n+1}{N_e^2}\,. \tag{10.25}$$

Taking $N_e = 50$ as a baseline, these yield

$$n_s - 1 = -2\,(n+1)\times 10^{-2}\,\left(\frac{50}{N_e}\right) \quad , \quad r = 0.16\,n\,\left(\frac{50}{N_e}\right) \quad , \quad \frac{dn_s}{d\ln k} = -4\,(n+1)\times 10^{-4}\,\left(\frac{50}{N_e}\right)^2\,. \tag{10.26}$$

10.3 FAMILY OF MODELS

We study the CMB observables $n_s, r, dn_s/d\ln k$ for families of new inflation and chaotic models determined by the following inflationary potentials.

$$V(\phi) \;=\; V_0 - \frac{1}{2}\,m^2\,\phi^2 + \frac{\lambda}{2\,n}\,\phi^{2\,n} \quad , \quad \text{broken symmetry} \tag{10.27}$$

$$V(\phi) \;=\; \frac{1}{2}\,m^2\,\phi^2 + \frac{\lambda}{2\,n}\,\phi^{2\,n} \quad , \quad \text{unbroken symmetry}\,. \tag{10.28}$$

Upon introducing the rescaled field χ given by eq. (10.7) we find that these potentials can be written as

$$V(\phi) = N_e\,m^2\,M_{Pl}^2\,w(\chi)\,, \tag{10.29}$$

where we recognize that

$$M^4 = m^2\ M_{Pl}^2\ . \tag{10.30}$$

Then, the family of potentials eqs.(10.27)-(10.28) are

$$w(\chi) = w_0 - \frac{1}{2}\,\chi^2 + \frac{g}{2\,n}\,\chi^{2\,n} \quad , \quad \text{broken symmetry} \tag{10.31}$$

$$w(\chi) = \frac{1}{2}\,\chi^2 + \frac{g}{2\,n}\,\chi^{2\,n} \quad , \quad \text{unbroken symmetry}\ . \tag{10.32}$$

where w_0 and g are dimensionless and related to V_0 and λ by

$$V_0 = w_0\ N_e\ m^2\ M_{Pl}^2 \quad , \quad \lambda = \frac{m^2\ g}{M_{Pl}^{2\,n-2}\ N_e^{n-1}}\ . \tag{10.33}$$

New inflation models described by the dimensionless potential given by eq. (10.31) feature a minimum at χ_0 which is the solution to the following conditions

$$w'(\chi_0) = w(\chi_0) = 0\ . \tag{10.34}$$

These conditions yield,

$$g = \frac{1}{\chi_0^{2\,n-2}} \quad , \quad w_0 = \frac{\chi_0^2}{2\,n}\ (n-1)\ , \tag{10.35}$$

χ_0 determines the scale of symmetry breaking ϕ_0 of the inflaton potential upon the rescaling eq.(10.7), namely

$$\phi_0 = \sqrt{N_e}\ M_{Pl}\ \chi_0\ . \tag{10.36}$$

It is convenient to introduce the dimensionless variable

$$x = \frac{\chi}{\chi_0} \tag{10.37}$$

Then, from eqs.(10.35) and (10.37), the family of inflation models eq.(10.31)-(10.32) take the form

$$w(\chi) = \frac{\chi_0^2}{2\,n}\ \left[n\ (1-x^2) + x^{2\,n} - 1\right] \quad , \quad \text{broken symmetry}\ , \tag{10.38}$$

$$w(\chi) = \frac{\chi_0^2}{2\,n}\left[n\ x^2 + x^{2\,n}\right] \quad , \quad \text{unbroken symmetry}\ . \tag{10.39}$$

In terms of the variable x, the small and large field regions for the potential eq.(10.38) correspond to $x < 1$ and $x > 1$, respectively. The form of the dimensionless potentials $w(x)$ for both families are depicted in fig. 10.1. The left panel in this figure shows the new (small field) or chaotic (large field) behavior of the broken symmetry potential eq.(10.38) depending on whether the initial value of the inflaton is smaller or larger than the minimum of the potential $x = 1$.

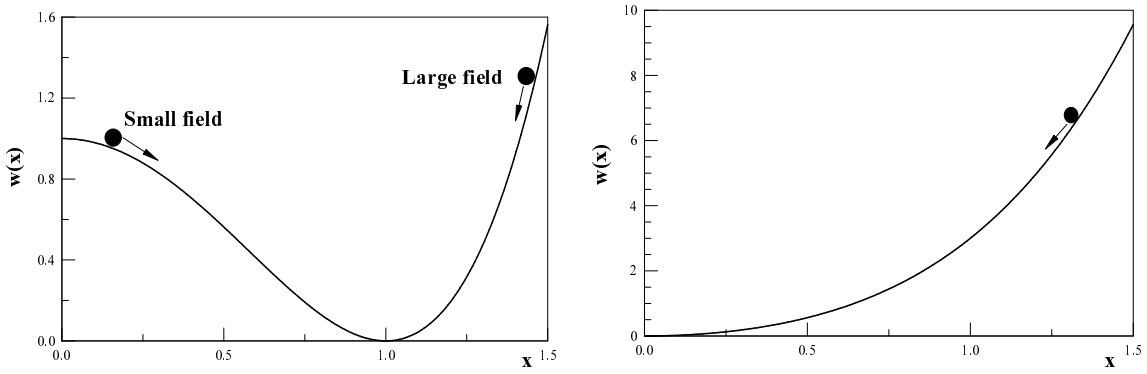

Figure 10.1: Left panel: broken symmetry potential for for $n = 2$, small and large field cases. Right panel: unbroken symmetry potential for $n = 2$, large field inflation.

10.4 BROKEN SYMMETRY MODELS

Inflation ends when the inflaton field arrives to the minimum of the potential. For the new inflation family of models eq.(10.38) inflation ends for

$$\chi_{end} = \chi_0 \ . \tag{10.40}$$

In terms of the dimensionless variable x, the condition eq.(10.9) becomes

$$\frac{2\,n}{\chi_0^2} = I_n(X) \quad , \quad X = \frac{\chi_{50}}{\chi_0} \equiv x_c \ , \tag{10.41}$$

where

$$I_n(X) = \int_X^1 \frac{dx}{x}\ \frac{n\,(1-x^2) + x^{2\,n} - 1}{1 - x^{2\,n-2}} = \int_X^1 \frac{n - \sum_{m=0}^{n-1} x^{2m}}{\sum_{m=0}^{n-2} x^{2m}}\ \frac{dx}{x} \ . \tag{10.42}$$

This integral can be computed in closed form in terms of hypergeometric functions [224] which can be reduced to a finite sum of elementary functions[225].

For a fixed given value of X, the value of χ_0 and therefore of the dimensionless coupling g is determined by the equation (10.41). Once we obtain this value, the CMB observables eqs. (10.14)-(10.15) are obtained by evaluating the derivatives of $w(\chi)$ at the value $\chi = \chi_{50} = \chi_0\ X$ with the corresponding value of the coupling g. Thus, a study of the range of possible values for $n_s,\ r,\ dn_s/d\ln k$ is carried out by exploring the relationship between these spectral indices as a

function of X. For this study we choose the baseline value $N_e = 50$ from which the indices can be obtained for arbitrary value of N_e by the relation (10.16).

While the dependence of χ_0 and g upon the variable X must in general be studied numerically, their behavior in the relevant limits, $X \to (0,\ 1)$ for small field inflation and $X >> 1$ for large field inflation can be derived from eqs.(10.41)-(10.42).

For small field inflation and $X \to 0$ the lower limit of the integral dominates leading to

$$\chi_0^2 \overset{X\to 0}{=} \frac{2\,n}{n-1}\,\frac{1}{\log\frac{1}{X}} \quad , \quad g \overset{X\to 0}{=} \left(\frac{n-1}{2\,n}\,\log\frac{1}{X}\right)^{n-1} \quad , \tag{10.43}$$

thus, as $X \to 0$ these are *strongly coupled theories*. This result has a clear and simple interpretation: for $N_e = 50$ to be the number of e-folds between $x = X$ and $x = 1$ the coupling g must be large and the potential must be steep, otherwise there would be many more e-folds in such interval.

For small field inflation and $X \to 1^-$ the integral $I_n(X)$ obviously vanishes and

$$\chi_0^2 \overset{X\to 1^-}{=} \left(\frac{2}{1-X}\right)^2\left[1+\frac{2\,n-1}{9}\,(X-1)+\mathcal{O}(X-1)^2\right] \quad , \quad g \overset{X\to 1^-}{=} \left[\frac{1}{2}\,(1-X)\right]^{2\,(n-1)} \to 0\,, \tag{10.44}$$

thus, as $X \to 1^-$, these are a *weakly coupled family of models*.

For large field inflation and $X \gg 1$, the integral $I_n(X)$ is dominated by the term with the highest power, namely $x^{2\,n}$, leading to the behavior

$$\chi_0^2 \overset{X\gg 1}{=} \frac{4\,n}{X^2} \quad , \quad g \overset{X\gg 1}{=} \left(\frac{X^2}{4\,n}\right)^{n-1} \quad , \tag{10.45}$$

which leads to a strongly coupled regime. The results of a numerical analysis are depicted in fig. 10.2.

Before we proceed with a numerical study of the CMB indices and the tensor to scalar ratio, we can extract interesting and relevant information by focusing on the region $X \sim 1$ which as discussed above corresponds to a weakly coupled family for broken symmetry potentials. This is the region near the *minimum* of the potential and the integral $I_n(X)$ can be evaluated simply by expanding $w(\chi)$ and its derivative near the minimum. To leading order in $(X-1)$ the condition (10.41) leads to eq.(10.44) and

$$(\chi_c - \chi_0)^2 = 4 \quad \text{or} \quad |\chi_c - \chi_0| = 2\,. \tag{10.46}$$

This is precisely eq.(10.23) for $n = 1$ upon the shift $\chi_c \to \chi_c - \chi_0$. Namely, eq.(10.46) is the condition eq.(10.23) for the quadratic monomial potential with minimum at $\chi = \chi_0$ instead of

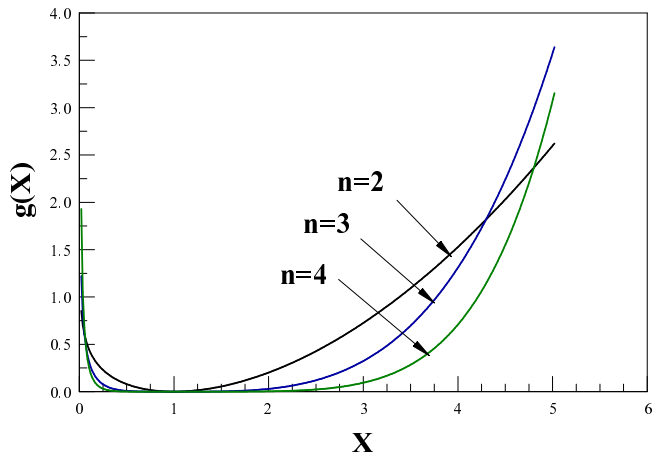

Figure 10.2: The coupling g as a function of X, for the degrees of the new inflation potential $n = 2,\ 3,\ 4$. For $X \to 1$, g vanishes as $\left[\frac{1-X}{2}\right]^{2\,(n-1)}$. The point $X = 1,\ g = 0$ corresponds to the monomial $m^2\ \phi^2/2$. g increases both for $X \to 0$ and for large X as, $\left(\log \frac{1}{X}\right)^{n-1}$ and $\left(\frac{X^2}{4\,n}\right)^{n-1}$, respectively.

$\chi = 0$ as in eq.(10.22). This is clearly a consequence of the fact that near the minimum $X = 1$ the potential is quadratic, therefore for $X \sim 1$ the quadratic monomial is an excellent approximation to the family of higher degree potentials and more so because $g \sim 0$. For $X \sim 1$ we find to leading order in $(X - 1)$ the values:

$$\epsilon_v = \eta_v = 0.01\left(\frac{50}{N_e}\right) \quad , \quad n_s = 0.96{+}0.04\left(\frac{N_e - 50}{N_e}\right) \quad , \quad r = 0.16\left(\frac{50}{N_e}\right) \quad , \quad \frac{dn_s}{d\ln k} = -0.0008\left(\frac{50}{N_e}\right)^2 . \tag{10.47}$$

The fact that the potential eq.(10.38) is quadratic around the minimum $X = 1$ explains that we have in this limit identical results for new inflation with the potential eq.(10.38) than with chaotic inflation with the monomial potential $m^2\ \phi^2/2$.

As observed in [207] these values of $r,\ n_s$ for $N_e \sim 50$ yield a good fit to the available CMB data.

The results of the numerical analysis for $\epsilon_v,\ \eta_v,\ n_s,\ r$ and $dn_s/d\ln k$ for the baseline value $N_e = 50$ are depicted in fig. 10.3, 10.4, 10.5 and 10.6 respectively.

The vertical dashed line in fig. 10.4 at $X \sim 0.2$ determines the lower limit of X for which n_s is consistent with the WMAP data for $r = 0$. For large values of $X,\ n_s$ approaches asymptotically

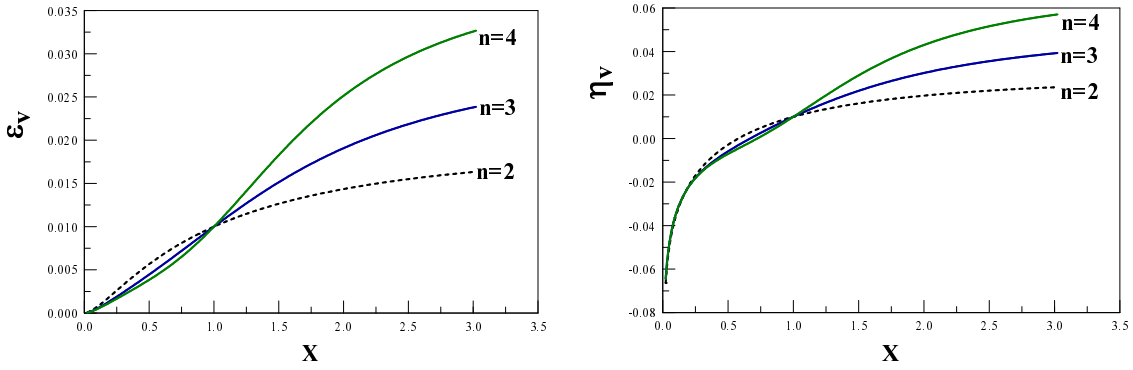

Figure 10.3: Slow roll parameters as a function of X for $N_e = 50$. Left panel ϵ_v, right panel η_v, for new inflation with the degrees of the potential $n = 2, 3, 4$. The results for arbitrary values of N_e are obtained by multiplying by the factor $\frac{50}{N_e}$.

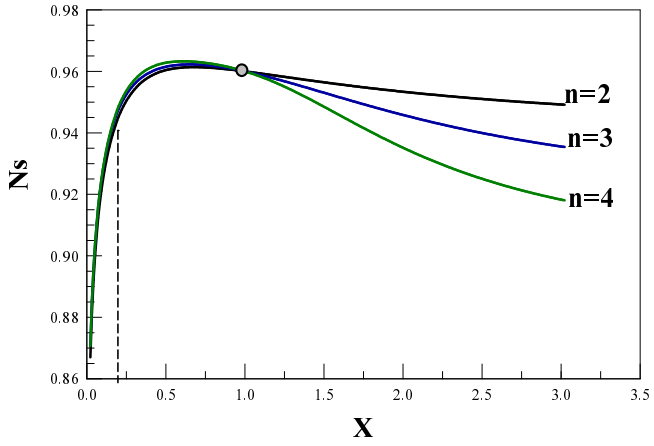

Figure 10.4: Scalar spectral index n_s for the degrees of the potential $n = 2, 3, 4$ for new inflation with $N_e = 50$. The vertical line delimits the smallest value of n_s (for $r = 0$) [207]. The grey dot at $n_s = 0.96,\ X = 1$ corresponds to the value for the monomial potential $n = 1,\ m^2\ \phi^2/2$. Notice that the small field behavior is n independent. For arbitrary N_e the result follows directly from the $N_e = 50$ value by using Eq. (9.16).

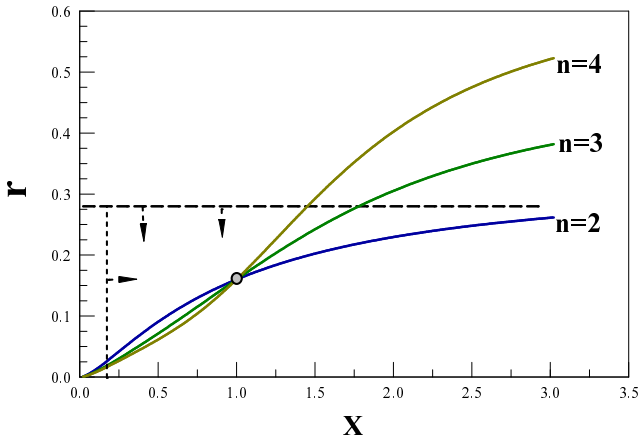

Figure 10.5: Tensor to scalar ratio r vs. X for the degrees of the potential $n = 2,\ 3,\ 4$ for new inflation with $N_e = 50$. The horizontal dashed line corresponds to the upper limit $r = 0.28\ (95\%CL)$ from WMAP3 without running. The vertical dashed line determines the minimum value of X, $X \sim 0.2$, consistent with the WMAP limits for n_s as in fig. 10.4. The grey dot at $X = 1,\ r = 0.16$ corresponds to the value for the monomial potential $m^2\ \phi^2/2$. The small field limit is nearly independent of n. For arbitrary N_e the result follows directly from the $N_e = 50$ value by using Eq. (9.16).

the values for the monomial potentials $\phi^{2\,n}$ given by eq. (10.26). For the larger degrees n, the asymptotic behavior of n_s and r settles at larger values of X, this is a consequence of the larger region in which the coupling is small as observed in fig. 10.2 for larger degrees n. The horizontal dashed lines with vertical downward arrows in fig. 10.5 determines the upper bound from WMAP [207] given by eq. (10.19) *without* running, since from fig. 10.6 the values of $dn_s/d\ln k$ for these models are negligible. The vertical dashed line with the right-pointing arrow in fig. 10.5 determines the values of X for which n_s are consistent with the WMAP data (see also fig. 10.4).

From these figures we see that unlike the case of a pure monomial potential $\lambda\,\phi^{2\,n}$ with $n \geq 2$, there is a **large** region of field space within which the new inflation models given by eq.(10.27) are **consistent** with the bounds from marginalized WMAP3 data and the combined WMAP3 + LSS data [207].

Fig. 10.7 displays r vs n_s for the values $n = 2, 3, 4$ in new inflation and indicate the trend with

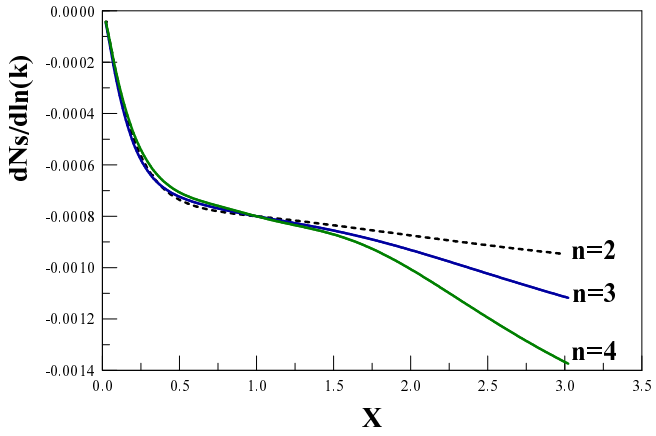

Figure 10.6: Running of the scalar index $dn_s/d\ln k$ vs. X for the degrees of the potential $n = 2, 3, 4$ respectively for new inflation with $N_e = 50$. The small field behavior is independent of n. For arbitrary N_e the result follows directly from the $N_e = 50$ value by using Eq. (9.16).

n. While r is a monotonically increasing function of X, n_s features a *maximum* as a function of X, hence r becomes a **double-valued** function of n_s. The grey dot at $r = 0.16$, $n_s = 0.96$ corresponds to the monomial potential $m^2\ \phi^2/2$ for $N_e = 50$. Values below the grey dot along the curve in fig. 10.7 correspond to small fields $X < 1$ while values above it correspond to large fields $X > 1$. We see from figs. 10.5 and 10.7 that *large fields systematically lead to larger values of* r. Models that fit the WMAP data to 95% CL are within the tilted box. The tilt accounts for the growth of the preferred value of n_s with r [207] according to eq. (10.20).

Fig. 10.8 displays the running of the scalar index vs. n_s for the different members of the family of new inflation showing clearly that running is all but negligible in the entire range of values consistent with the WMAP data. This was expected since the running in slow-roll is of the order $\sim \frac{1}{N_e^2} \simeq 4 \times 10^{-4}$ [see eq.(10.15)] [216].

We note that $dn_s/d\ln k$ is a monotonically *decreasing* function of X approaching asymptotically the values for the monomials $\phi^{2\,n}$ given by eq. (10.26). $X \sim 0.2$ which is the *minimum value* of X consistent with the bounds from WMAP on n_s (see fig. 10.4).

10.4.1 Field reconstruction

The above analysis suggests to study the *inverse problem*, namely, for a given member of the family labeled by n, we may ask what is the value ϕ_c of the field at Hubble crossing and what is the scale ϕ_0 of symmetry breaking of the potential which are consistent with the CMB+LSS data. This is tantamount to the program of reconstruction of the inflaton potential advocated in ref. [217] and is achieved as follows: eq.(10.41) yields $\chi_0 = \chi_0[X]$ from which we obtain $\chi_c = \chi_0\, X$. These results are then input into the expression for n_s by evaluating the potential $w(\chi)$ and its derivatives at the value of χ_c. This yields $n_s = n_s[\chi_c]$ which is then inverted to obtain $\chi_c = \chi_c[n_s]$ and thus ϕ_c.

In the region $X \sim 1$ corresponding to the weakly coupled case, this reconstruction program can be carried out as a systematic series in

$$\Delta \equiv X - 1 = \frac{\chi_{50}}{\chi_0} - 1 \,, \tag{10.48}$$

by expanding the inflationary potential and its derivatives in a power series in x around $x = 1$ in the integrand of $I_n(X)$ [eq. (10.42)]. For $X = 1$ the value of the scalar index n_s is determined by the simple monomial $m^2\ \phi^2/2$ which from eq. (10.25) for $n = 1$ is given by $n_s - 1 = -2/N_e$. Therefore, in terms of n_s, the actual expansion parameter is $n_s - 1 + 2/N_e$.

We obtain n_s to first order in Δ from eqs.(10.10), (10.14), (10.38), (10.44) and (10.48) with the result,

$$n_s - 1 = -\frac{2}{N_e}\left[1 + \frac{2\,n-1}{18}\,\Delta + \mathcal{O}(\Delta^2)\right]$$

then, by inverting this equation we find:

$$\Delta(n_s, n) = X - 1 = -\frac{9N_e}{2\,n-1}\left(n_s - 1 + \frac{2}{N_e}\right) + \mathcal{O}\left(\left[n_s - 1 + \frac{2}{N_e}\right]^2\right) \,, \tag{10.49}$$

and from eqs. (10.44) and (10.49) we find,

$$\chi_0(n_s, n) = \frac{2\,(2\,n-1)}{9\,N_e\left|n_s - 1 + \frac{2}{N_e}\right|}\left[1 - \frac{N_e}{2}\left(n_s - 1 + \frac{2}{N_e}\right)\right] + \mathcal{O}\left(\left[n_s - 1 + \frac{2}{N_e}\right]\right) \tag{10.50}$$

The leading order ($\propto 1/\Delta$) of this result for $\chi_0(n_s, n)$ can be simply cast as eq.(10.46): this is recognized as the condition to have 50 e-folds for the quadratic monomial centered in the broken symmetry minimum [see discussion below eq. (10.46)].

Finally, the value of the (dimensionless) field χ_c at Hubble crossing is determined from $\chi_c(n_s, n) = \chi_0\,[1 + \Delta(n_s, n)]$ from which we obtain

$$\chi_c = \frac{2\,(2\,n-1)}{9\,N_e\left|n_s - 1 + \frac{2}{N_e}\right|}\left[1 - \frac{(2\,n+17)\,N_e}{2\,(2\,n-1)}\left(n_s - 1 + \frac{2}{N_e}\right)\right] + \mathcal{O}\left(\left[n_s - 1 + \frac{2}{N_e}\right]\right) \,. \tag{10.51}$$

The coupling constant g can be also expressed in terms of n_s in this regime with the result,

$$g = \left[\frac{9\,N_e\left|n_s - 1 + \frac{2}{N_e}\right|}{2\,(2\,n-1)}\right]^{2\,n-2} \to 0\ ,$$

which exhibits the weak coupling character of this limit.

This analysis shows that the region in field space that corresponds to the region in n_s that *best fits the WMAP data* can be systematically reconstructed in an expansion in $n_s - 1 + 2/N_e$. This is yet another bonus of the $1/N_e$ expansion. Although the above analysis can be carried out to an arbitrary order in $n_s - 1 + 2/N_e$, it is more convenient to perform a numerical study of the region outside from $X \sim 1$ to find the values of χ_c and χ_0 as a function of n_s for fixed values of $n,\ N_e$. Figures 10.9 and 10.10 display $\chi_c,\ \chi_0$ as a function of n_s with $N_e = 50$ for different values of n for the small field region $X < 1$ and the large field region $X > 1$ respectively. The point $X = 1$ is a degeneracy point and corresponds to the quadratic monomial as discussed above.

Finally, the values for the dimensionful field ϕ are given by $\phi_c = \sqrt{N_e}\ M_{Pl}\ \chi_c,\ \phi_0 = \sqrt{N_e}\ M_{Pl}\ \chi_0$. Figures 10.7, 10.9 and 10.10 lead to the conclusion that for the range of CMB parameters $r < 0.1$ and $n_s \leq 0.96$, the typical value of the *symmetry breaking scale* is $\phi_0 \sim 10\ M_{Pl}$ and the value of the inflaton field at which cosmologically relevant wavelengths crossed the Hubble radius during new inflation is $\phi_c \sim M_{Pl}$ with a weak dependence on n. For $0.1 < r < 0.16$ we have $|\phi_c - \phi_0| \sim 15\ M_{Pl}$.

We obtain for the coupling g in the $X \to 0$ limit which is a strong coupling regime [see eq.(10.43)] where $n_s \ll 1$,

$$g = \left[\frac{N_e}{4}\ \left(1 - \frac{1}{n}\right)(1 - n_s)\right]^{n-1}\ .$$

Finally, we have the $X \to \infty$ limit which is also a strong coupling limit [see eq.(10.45)] where $n_s \to 1 - (n+1)/N_e$ and we find,

$$\chi_0^2 = (4\,n)^2\left[\frac{N_e(1-n_s) - (n+1)}{4\,n(n-1) + 3\,\left(1 + \frac{1}{n-2}\right)}\right]^{\frac{1}{n-1}} \to 0$$
$$g = \frac{4\,n(n-1) + 3\,\left(1 + \frac{1}{n-2}\right)}{(4\,n)^{n-1}\ [N_e(1-n_s) - (n+1)]} \to \infty\ . \tag{10.52}$$

10.5 CHAOTIC INFLATION MODELS

We now turn to the study of the family of chaotic inflationary potentials given by eq. (10.39). Taking that the end of inflation corresponds to $x = 0$, the condition eq.(10.9) now becomes

$$\frac{2\,n}{\chi_0^2} = J_n(X) = \int_0^X \frac{n + x^{2\,n-2}}{1 + x^{2\,n-2}}\; x\; dx\,. \tag{10.53}$$

Again, this integral can be computed in closed form in terms of hypergeometric functions [224] which can be reduced to a finite sum of elementary functions[225]. For general values of X the integral will be studied numerically, but the small X region can be studied by expanding the integrand in powers of $x^{2\,n-2}$, with the result

$$1 = \frac{\chi_0^2\, X^2}{4}\left[1 - \frac{n-1}{n^2}\; X^{2\,n-2} + \mathcal{O}(X^{4\,n-4})\right]\,. \tag{10.54}$$

For small X and recalling that $X = \chi_c/\chi_0$ this relation yields

$$|\chi_c| = 2\left[1 + \frac{n-1}{2\,n^2}\; X^{2\,n-2} + \mathcal{O}(X^{4\,n-4})\right] \tag{10.55}$$

which is again, at dominant order the relation for the quadratic monomial potential eq.(10.23) for $n = 1$. This must be the case because the small field limit is dominated by the quadratic term in the potential. For small fields, $\chi_0 \approx 2/X$ and the coupling g vanishes as,

$$g(X) \overset{X\to 0}{=} \left(\frac{X}{2}\right)^{2\,n-2}\,. \tag{10.56}$$

The coupling as a function of X is shown in fig. 10.11.

The dependence of $\epsilon_v,\ \eta_v$ in the full range of X for several representative values of n is studied numerically: these results are displayed in fig. 10.12. In the small X regime, we obtain from eqs. (10.10), (10.39) and (10.54) the expressions,

$$\epsilon_v = \frac{1}{2\,N_e}\left[1 + \frac{(2\,n-1)(n-1)}{n^2}\; X^{2\,n-2} + \mathcal{O}\left(X^{4\,n-4}\right)\right] \tag{10.57}$$

$$\eta_v = \frac{1}{2\,N_e}\left[1 + \frac{(2\,n-1)(n^2-1)}{n^2} X^{2\,n-2} + \mathcal{O}\left(X^{4\,n-4}\right)\right] \tag{10.58}$$

As $X \to 0$, ϵ_v and η_v tend to the result from the quadratic monomial potential, namely $\epsilon_v = \eta_v = 1/[2\,N_e]$ as must be the case because the quadratic term dominates the potential for $X \ll 1$.

Figures 10.13, 10.14 display $n_s,\ r$ as functions of X for $N_e = 50$ respectively. The horizontal dashed lines in these figures delimit the WMAP band of 95% CL from ref. [207]. For $X \to 0$, $n_s \to 0.96$ and $r \to 0.16$ which are the values from the quadratic monomial $m^2\,\phi^2/2$.

For $X \gg 1$, the values of $n_s,\ r$ for the monomial potentials $\phi^{2\,n}$ are attained asymptotically, namely, (for $N_e = 50$): $n_s - 1 = -2\,(n+1) \times 10^{-2},\ r = 0.16\,n$.

Comparing figs. 10.13, 10.14 to those for the new inflation case, (figs. 10.4 and 10.5), we note that the range in which the chaotic family provide a good fit to the WMAP data is *very much smaller* than for new inflation. Fig. 10.13 shows that in chaotic inflation *only* for $n = 2$ the range of n_s is allowed by the WMAP data in a fairly extensive range of values of X, whereas for $n = 3,\ 4$ (and certainly larger), there is a *relatively small* window in field space for $X < 1$ which satisfies the data for n_s and r simultaneously.

The tensor to scalar ratio r in chaotic inflationary models is *larger* than 0.16 for all values of X, approaching asymptotically for large X the value $r = 0.16\,n$ associated to the monomial potentials $\phi^{2\,n}$.

Fig. 10.15 displays $dn_s/d\ln k$ as a function of X, while the running is again negligible, it is *strikingly different* from the new inflation case. *Again* this figure, in combination with those for n_s and r as functions of X distinctly shows that **only** $n = 2$ in chaotic inflation is compatible with the bounds from the WMAP data, while for $n = 3, 4$ only a *small window* for $X < 1$ is allowed by the data. We see from fig. 10.15 that $dn_s/d\ln k$ takes negative as well as positive values for chaotic inflation, in contrast with new inflation where $dn_s/d\ln k < 0$.

The fact that the combined bounds on $n_s,\ r$ and $dn_s/d\ln k$ from the WMAP3 data [207] provide much more stringent constraints on chaotic models is best captured by displaying r as a function of n_s in fig. 10.16. The region allowed by the WMAP data lies within the tilted box delimited by the vertical and horizontal dashed lines that represent the $95\%CL$ band.

A complementary assessment of the allowed region for this family of effective field theories is shown in fig. 10.17 which distinctly shows that **only** the $n = 2$ case of chaotic inflation is allowed by the WMAP3 data.

10.5.1 Field reconstruction

The reconstruction program proceeds in the same manner as in the case of new inflation: the first step is to obtain $\chi_0(X)$ from eq.(10.53). Then ϵ_v and η_v are obtained as a function of X which yields $n_s(X)$. Inverting this relation we find $X = X(n_s)$ and finally $\chi_c(n_s) = \chi_0\ X(n_s)$. While this program must be carried out numerically, we can gain important insight by focusing on the small X region and using eq.(10.54).

From eqs. (10.14), (10.57) and (10.58) we find

$$n_s - 1 + \frac{2}{N_e} = X^{2\,n-2}\ \frac{(2\,n-1)(n-1)(n-2)}{n^2\,N_e} + \mathcal{O}\Big(X^{4n-4}\Big) \tag{10.59}$$

As $X \to 0$ it follows that $n_s \to 1 - 2/N_e$ which is the value for the scalar index for the quadratic monomial potential $m^2\phi^2/2$. However, for $n > 2$ this limit is approached from above, namely for $n > 2$ it follows that $n_s > 1 - 2/N_e$. The small X region corresponds to small departures of n_s from the value determined by the quadratic monomial $1 - 2/N_e$ but always larger than this value for $n > 2$. In the small field limit we reconstruct the value of χ_c in an expansion in $n_s - 1 + 2/N_e$. The leading order in this expansion is obtained by combining eqs. (10.55) and (10.59), we obtain

$$|\chi_c| = 2\left[1 + \frac{\left(n_s - 1 + \frac{2}{N_e}\right)N_e}{2\,(2\,n-1)\,(n-2)}\right] + \mathcal{O}\left(\left[n_s - 1 + 2/N_e\right]^2\right) \tag{10.60}$$

Obviously, this leading order term is singular at $n = 2$, this is a consequence of the result eq.(10.59) which entails that for $n = 2$ the expansion must be pursued to higher order, up to X^{4n-4}.

We find from eqs. (10.14), (10.57) and (10.58) for $n = 2$,

$$n_s - 1 + \frac{2}{N_e} = -\frac{17}{24\,N_e}\ X^4 + \mathcal{O}\Big(X^6\Big) \quad , \quad n = 2\,, \tag{10.61}$$

therefore,

$$|\chi_c| = 2\left[1 + \sqrt{\frac{3\,N_e}{136}\left(1 - \frac{2}{N_e} - n_s\right)}\right] + \mathcal{O}\left(n_s - 1 + \frac{2}{N_e}\right) \quad , \quad n = 2\,. \tag{10.62}$$

We see that the derivative of χ_c with respect to n_s is singular for $n = 2$ at $n_s = 1 - \frac{2}{N_e}$. We note that for $n = 2$ there is a sign change with respect to the cases $n > 2$ and $n_s - 1 + 2/N_e \leq 0$ as determined by eq. (10.61).

Fig. 10.18 shows χ_c as a function of n_s for $n = 2,\ 3,\ 4$ for $N_e = 50$. The case $n = 2$ clearly shows the singularity in the derivative $\partial\chi_c/\partial n_s$ at $n_s = 1 - 2/N_e = 0.96$ [see eq.(10.62)].

Combining fig. 10.18 with fig. 10.16 it is clear that there is a small window in field space within which chaotic models provide a good fit to the WMAP3 data, for $N_e = 50$ we find:

$$\begin{aligned}
n = 2 \ &: \quad 0.95 \lesssim n_s \leq 0.960\ ,\ 2.0 \leq |\chi_c| \lesssim 2.25 \\
n = 3 \ &: \quad 0.96 \leq n_s \lesssim 0.965\ ,\ 2.0 \leq |\chi_c| \lesssim 2.15 \\
n = 4 \ &: \quad 0.96 \leq n_s \leq 0.975\ ,\ 2.0 \leq |\chi_c| \lesssim 2.10\ .
\end{aligned} \tag{10.63}$$

Restoring the dimensions via eq. (10.7) these values translate into a narrow region of width $\Delta\phi \lesssim 1.5\,M_{Pl}$ around the scale $|\phi_c| \sim 15\ M_{Pl}$.

Therefore, the joint analysis for $n_s,\ r,\ dn_s/d\ln k$ distinctly reveals that: (i) chaotic models favor *larger* values of r thus, larger tensor amplitudes, and (ii) feature *smaller* regions in field space consistent with the CMB and large scale structure data. *Only* the case $n = 2$ features a larger region of consistency with the combined WMAP3 data.

10.6 CONCLUSIONS

The fact that current observations of the CMB and LSS are already placing constraints on inflationary models which will undoubtedly become more stringent with forthcoming observations, motivates a study of the predictions for the CMB power spectra from different inflationary scenarios. We perform a systematic study of *families* of single field new and chaotic inflation slow roll models characterized by effective field theories with potentials of the form

$$V(\phi) = V_0 - \frac{1}{2}\, m^2\, \phi^2 + \frac{\lambda}{2\,n}\, \phi^{2n} \quad , \quad \text{broken symmetry} \tag{10.64}$$

$$V(\phi) = \frac{1}{2}\, m^2\, \phi^2 + \frac{\lambda}{2\,n}\, \phi^{2\,n} \quad , \quad \text{unbroken symmetry} \ . \tag{10.65}$$

Unlike the approach followed in [206, 207] based on the inflationary flow equations[212], or more recent studies which focused on specific inflationary models [213], or on statistical analysis of models [214], we implement an expansion in $1/N_e$ where $N_e \sim 50$ is the number of e-folds before the end of inflation when wavelengths of cosmological relevance today cross the Hubble radius during inflation. We provide an analysis of the dependence of CMB observables ($n_s,\ r$ and $dn_s/d\ln k$) with n and establish the region in field space within which these families provide a good agreement with the WMAP3 data combined with large scale surveys.

For new inflation models with potentials eq.(10.64) there are two distinct regions corresponding to values of the inflaton field smaller (small field) or larger (large field) than the symmetry breaking scale. For this family we find a **wide range** in the $r - n_s$ plane in which the different members $n = 2,\ 3,\ 4...$ are allowed by the data both for small and large fields with negligible running of the scalar index:

$$-4\ (n+1) \times 10^{-4} \leq dn_s/d\ln k \leq -2 \times 10^{-4} \ .$$

For $N_e = 50$ the values $n_s = 0.96, r = 0.16$ which are those determined by the simple monomial potential $m^2\ \phi^2/2$ determine a divide and a degeneracy point in the field and parameter space. Small field regions yield $r < 0.16$ while large field regions correspond to $r > 0.16$.

The $1/N_e$ expansion also provides a powerful tool to implement a *reconstruction program* that allows to extract the value of the field N_e e-folds before the end of inflation, and in the case of new inflationary models, the symmetry breaking scale.

We find that the region of field space favored by the WMAP3 data can be explored in a systematic expansion in $n_s - 1 + 2/N_e$. An analytic and numerical study of this region lead us to conclude that if forthcoming data on tensor modes favors $r < 0.16$ then new inflation **is favored**, and we **predict** for $r < 0.1$ that (i) the **symmetry breaking scale** is

$$\phi_0 \sim 10\ M_{Pl}\ ,$$

and (ii) the value of the field when cosmologically relevant wavelengths cross the Hubble radius is $|\phi_c| \sim M_{Pl}$.

The family of chaotic inflationary models characterized by the potentials eq.(10.65) feature tensor to scalar ratios $r \geq 0.16$ (for $N_e = 50$), with the minimum, $r = 0.16$ obtained in the limit of small inflaton amplitude and corresponds to the monomial potential $m^2\ \phi^2/2$ which is again a degeneracy point for this family of models.

The combined marginalized data from WMAP3 [207] yields a very small window within which chaotic models are allowed by the data, the largest region of overlap with the (r, n_s) WMAP3 data corresponds to $n = 2$ and the width of the region decreases with larger n. The typical scale of the field at Hubble crossing for these models is $|\phi_c| \sim 15\ M_{Pl}$ (for $N_e = 50$). Some small regions in field space consistent with the WMAP3 data feature peaks in the running of the scalar index but in the region consistent with the WMAP3 data in chaotic inflation the running is again negligible. If future observations determine a tensor to scalar ratio $r < 0.16$, such bound will, all by itself, **rule out** the large family of chaotic inflationary models of the form (10.65) for any n.

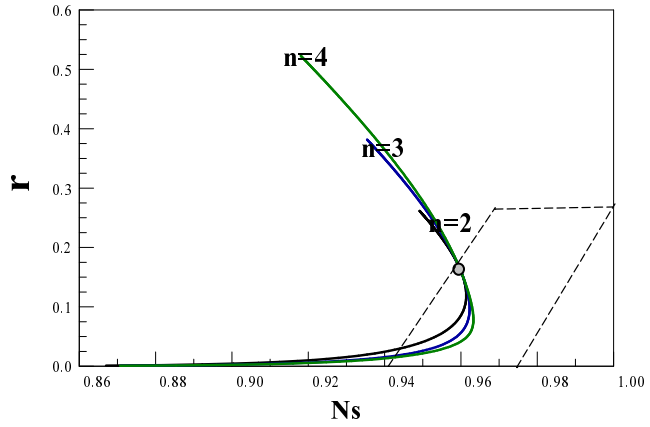

Figure 10.7: Tensor to scalar ratio r vs. n_s for degrees of the potential $n = 2,\, 3,\, 4$ respectively for new inflation with $N_e = 50$. r turns to be a **double-valued** function of n_s exhibiting a maximum value for n_s. The values inside the box between the dashed lines correspond to the WMAP3 marginalized region of the $r - n_s$ plane with $(95\% CL):\ r < 0.28,\ 0.942 + 0.12\, r \leq n_s \leq 0.974 + 0.12\, r$, see eq.(10.20). The grey dot corresponds to the values for the monomial potential $m^2\phi^2/2$ and the value $X = 1:\ r = 0.16,\ n_s = 0.96$.

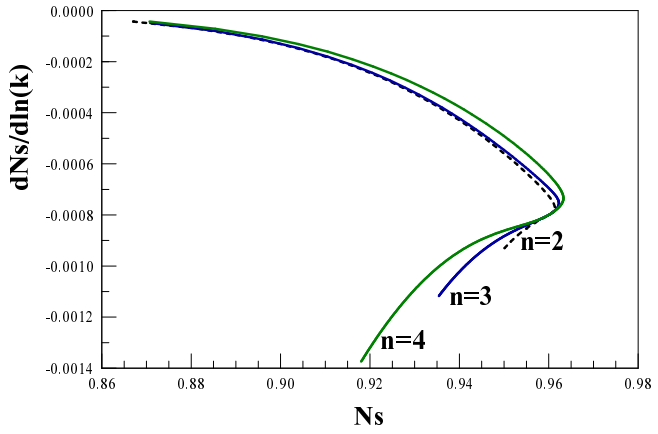

Figure 10.8: Running of the scalar index $dn_s/d\ln k$ vs. n_s for degrees of the potential $n = 2,\, 3,\, 4$ respectively for new inflation with $N_e = 50$. The values for arbitrary N_e follow directly from the $N_e = 50$ value by using Eq. (9.16).

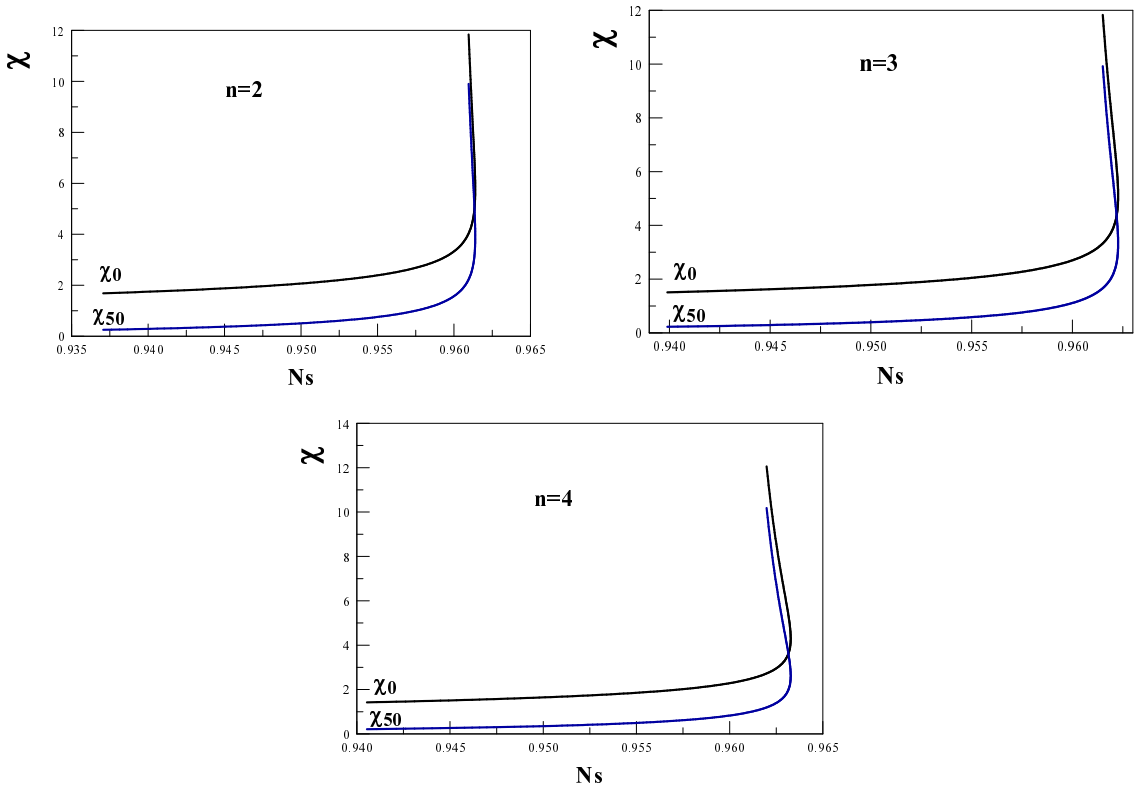

Figure 10.9: Reconstruction program for broken symmetry potentials with $N_e = 50$, small field case $X < 1$. $\chi_{50} \equiv \chi_c$ and χ_0 vs. n_s for degrees of the potential $n = 2, 3, 4$, respectively. These values of χ_c, n_s correspond to the region $r < 0.16$.

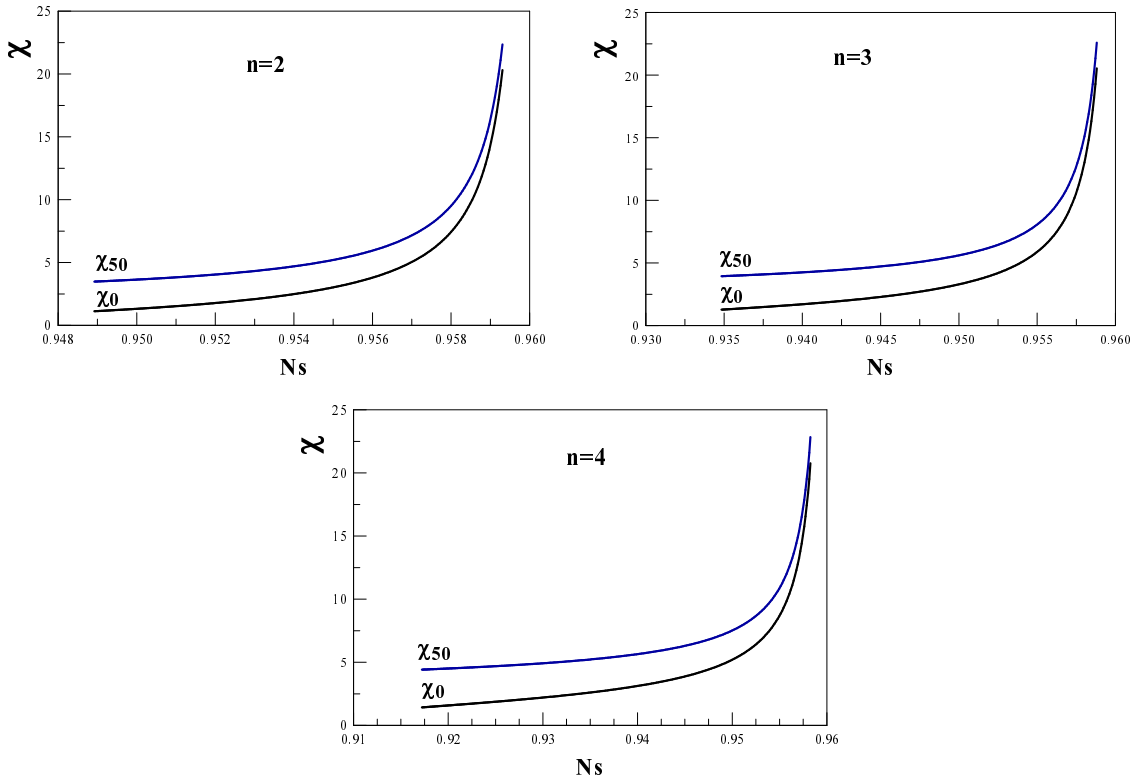

Figure 10.10: Reconstruction Program for broken symmetry potentials with $N_e = 50$, large field case $X > 1$. $\chi_{50} \equiv \chi_c$ and χ_0 vs. n_s for degrees of the potential $n = 2, 3, 4$, respectively. These values of χ, n_s correspond to the region $r > 0.16$.

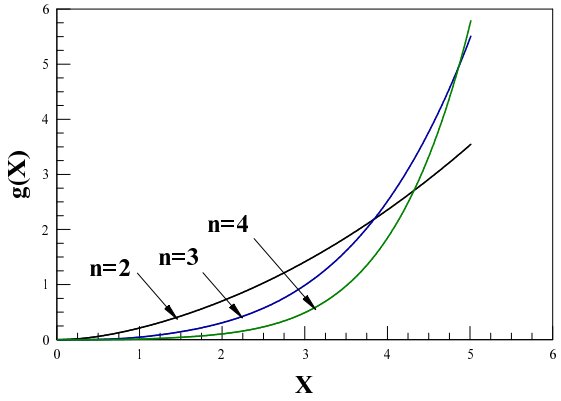

Figure 10.11: Coupling g as a function of X for $N_e = 50$, for $n = 2, 3, 4$ for chaotic inflation. g turns to be a monotonically increasing function of X. g vanishes for $X \to 0$ as $\left(\frac{X}{2}\right)^{2n-2}$ in sharp contrast with new inflation where g strongly increases for $X \to 0$.

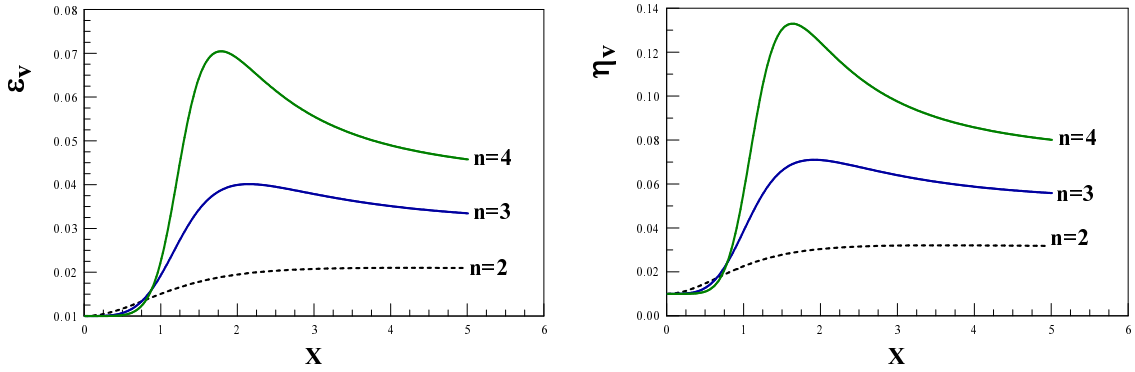

Figure 10.12: Left panel ϵ_v, right pannel η_v as a function of X for $N_e = 50$, for chaotic inflation with degrees of the potential $n = 2, 3, 4$. The small X behavior is n independent.

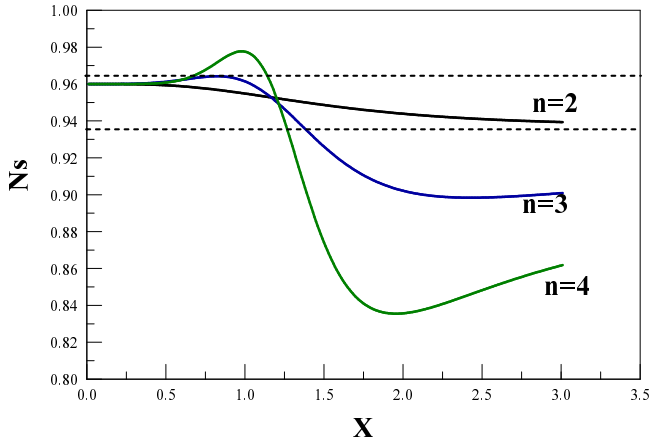

Figure 10.13: Scalar spectral index n_s for degrees of the potential $n = 2, 3, 4$ respectively for chaotic inflation with $N_e = 50$. For $X \to 0$, n_s reaches for all n the value $n_s = 0.96$ corresponding to the monomial potential $m^2\phi^2/2$.

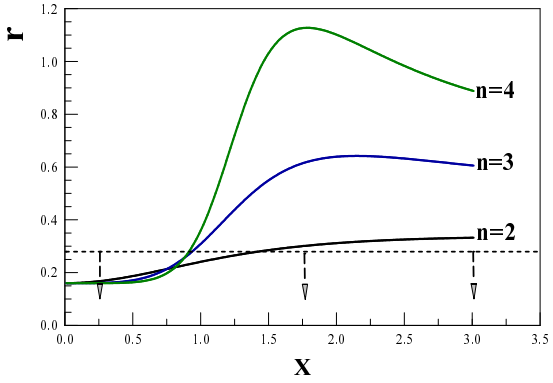

Figure 10.14: Tensor to scalar ratio r vs. X for degrees of the potential $n = 2, 3, 4$ respectively for chaotic inflation with $N_e = 50$. The horizontal dashed lines with the downward arrows delimit the region of 95% CL given by WMAP3 with no running $r < 0.28$.

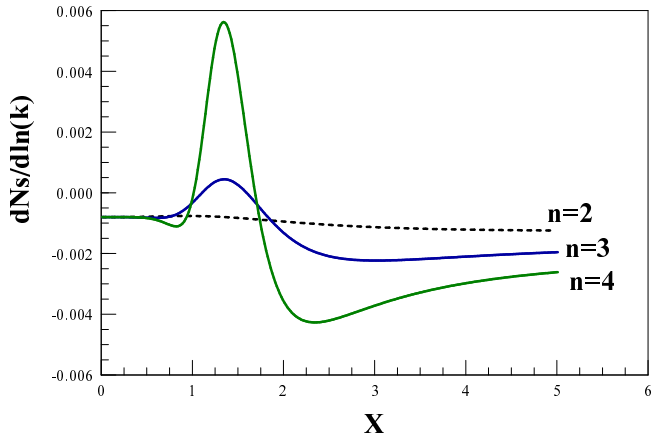

Figure 10.15: Running of the scalar index $dn_s/d\ln k$ vs. X for degrees of the potential $n = 2,\ 3,\ 4$ respectively for chaotic inflation with $N_e = 50$. The $X \to 0$ behavior is n independent. $dn_s/d\ln k$ features a maximun value that gets stronger with increasing n. For chaotic inflation $dn_s/d\ln k$ takes negative as well as positive values, in contrast with new inflation where $dn_s/d\ln k < 0$.

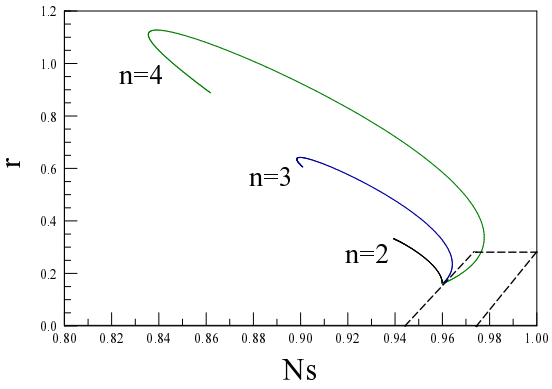

Figure 10.16: Tensor to scalar ratio r vs. n_s for degrees of the potential $n = 2,\ 3,\ 4$ respectively for chaotic inflation with $N_e = 50$. The range of 95% CL as determined by WMAP3 [207] is within the tilted box delimited by : $r < 0.28,\ 0.942 + 0.12\,r \leq n_s \leq 0.974 + 0.12\,r$, see Eq. (9.20).

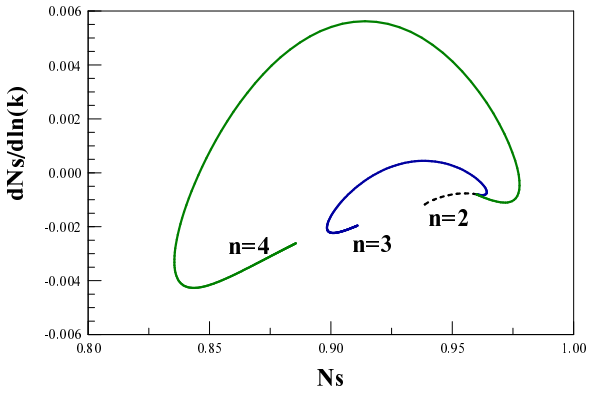

Figure 10.17: Running of the scalar index $dn_s/d\ln k$ vs. n_s for degrees of the potential $n = 2$, 3, 4 respectively for chaotic inflation with $N_e = 50$.

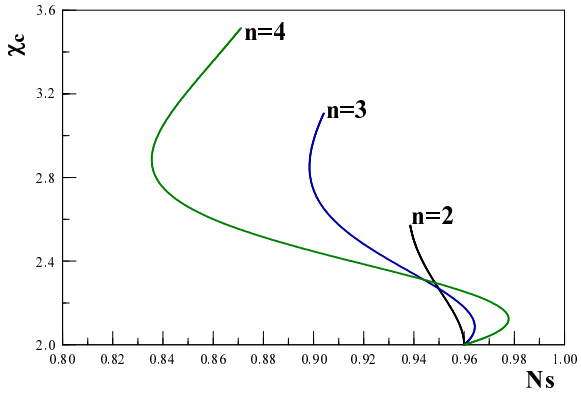

Figure 10.18: Reconstruction program for chaotic inflation with $N_e = 50$ χ_c vs. n_s for $n = 2$, 3, 4 respectively.

11.0 EXTENDED SUMMARY OF MAIN RESULTS

In this last chapter, we give a summary to each of the previous chapters. The main ideas and results in each chapter are highlighted.

Oscillations and Evolution of a Hot and Dense Gas of Flavor Neutrinos: a Free Field Theory Study

In this thesis, we first study the time evolution of the distribution functions for hot and/or dense gases of two flavor Dirac neutrinos as a consequence of flavor mixing and dephasing, in the absence of weak interactions. This is achieved by obtaining the time evolution of the flavor density matrix directly from quantum field theory at finite temperature and density. The dynamics of neutrino oscillations features a hierarchy of time scales. The shorter time scales are associated with the interference between particle and *antiparticle* states, while the longer time scales emerge from the interference between particle states (or antiparticle states) of different masses. In the degenerate case, an initial flavor asymmetry will relax towards an asymptotic limit via dephasing resulting from the oscillations between flavor modes that are not Pauli blocked, with a power law proportional to the inverse of time. The distribution function for flavor neutrinos and antineutrinos as well as off-diagonal densities are obtained. In the nearly degenerate or relativistic case, as is likely to prevail in the early universe as well as in core collapse supernovae, the time scales are widely separated. This allows to describe the dynamics on the longer time scales in terms of an "effective" (free) theory. In this effective description, the Heisenberg creation and annihilation field operators for flavor neutrinos and antineutrinos obey the familiar Bloch type equations and the spinor structure is common to both flavors as well as the mass eigenstates. This effective description allows to obtain in a simple manner the dynamics of the distribution functions, off diagonal correlation functions and the non-equilibrium propagators, all of which must be understood as an average over the shoter time scales and valid only on the longer scales.

Neutrino Oscillations in the Early Universe

We study neutrino oscillations in the early universe by implementing finite-temperature field theory. Particularly, we are interested in the temperature regimes $m_e \ll T \ll m_\mu$ and $m_\mu \ll T \ll M_W$, which are relevant for Big Bang Nucleosynthesis (BBN). We focus on two flavors of Dirac neutrinos; however, the formulation is general. The propagation of neutrinos is determined by the *effective* Dirac equation which includes the self-energy corrections. We obtain the equations of motion for neutrino of both chirality and helicity in the medium, allowing for CP asymmetry. An expansion of the self-energy in terms of the neutrino frequency ω and momentum k is carried out to lowest order in ω/M_W and k/M_W. It is found that contributions non-local in space-time to the self-energy dominate over the asymmetry for $T \gtrsim 3 - 5\,\mathrm{MeV}$ if the lepton and neutrino asymmetries are of the same order as the observed baryon asymmetry. We find a new contribution which cannot be interpreted as the usual effective potential. The medium dispersion relations and mixing angles are found to be both energy and helicity dependent, and a resonance like the Mikheyev-Smirnov-Wolfenstein (MSW) resonance is realized. The oscillation time scale in the medium is longer as compared to that in the vacuum near a resonance, but much shorter for off resonance high energy neutrinos for which the medium mixing angle becomes vanishingly small. The equations of motion reduce to the familiar form of vacuum oscillation formulae for negative helicity ultrarelativistic neutrinos, but include consistently both the mixing angle and the oscillation frequencies in the medium. These equations of motion also allow to study the dynamics of right-handed neutrinos.

Space-Time Propagation of Neutrino Wave-Packets at High Temperature and Density

For a deeper study of neutrinos oscillations in the early universe, we investigate the space-time evolution of "flavor" neutrino wave-packets at finite temperature and density prior to BBN. There is a rich hierarchy of time scales associated with coherence, transverse and longitudinal dispersions. For relativistic neutrinos, the time scale of longitudinal dispersion is much longer than that of transverse dispersion by the enormous Lorentz dilation factor. There exists a coherence time limit beyond which the two mass eigenstates cease to overlap and so neutrino oscillation is exponentially suppressed. But a novel phenomenon of "frozen coherence" can occur if the longitudinal dispersion catches up with the progressive separation between the two mass eigenstates in the medium, before the coherence time limit has been reached. Near a resonance, the coherence time scale is enhanced

by a factor $1/\sin 2\theta$ compared to the vacuum. Collisional relaxation via charged and neutral currents occurs on time scales much shorter than the coherence time scale. However, the transverse dispersion occurs at a much shorter scale than all other possible time scales in the medium, resulting in a large suppression in the transition probabilities from electron-neutrino to muon-neutrino, on a time scale much shorter than the Hubble time. This indicates that neutrino wave-packets produced just prior to BBN will cease to oscillate rapidly, without distorting the electron-neutrino abundance, and hence without affecting the correct neutron-to-proton ratio for the observed mass fraction of Helium-4 due to BBN.

Charged Lepton Mixing and Oscillations from Neutrino Mixing in the Early Universe

Charged lepton non-conserving processes are highly suppressed in the vacuum due to the smallness of neutrino masses. This motivates us to explore the possibility of large charged lepton mixing, for two generations e and μ, as a consequence of neutrino mixing in the temperature regime $m_\mu \ll T \ll M_W$ in the early universe. We state the general criteria for charged lepton mixing, critically re-examine aspects of neutrino equilibration and provide arguments to suggest that neutrinos may equilibrate as mass eigenstates in the temperature regime prior to flavor equalization. We assume this to be the case, and that neutrino mass eigenstates are in equilibrium with different chemical potentials. Charged lepton self-energies are obtained to leading order for both electromagnetic and weak interactions. We find that it is the off-diagonal elements in the charged-current self-energy that are responsible for the charged lepton mixing. For a large lepton asymmetry in the neutrino sector, there could be a resonant charged lepton mixing in the temperature range $T \sim 5\,\mathrm{GeV}$. In this regime, the electromagnetic damping rate is of the same order as the charged lepton oscillation frequency, suggesting a substantial transition probability during equilibration. This is a novel phenomenon that has not been recognized, without invoking Grand Unification Theory (GUT) or Supersymmetry (SUSY) models.

Sterile Neutrino Production via Active-Sterile Oscillations: the Quantum Zeno Effect

Motivated by the importance of sterile neutrinos in astrophysics and cosmology, we study their production in the early universe via active-sterile oscillations. We provide a quantum field theoretical reassessment of the quantum Zeno suppression on the active-to-sterile transition probability

$P_{a\to s}(t)$ and its time average. In analogy with the neutral kaon system, we point out that there are *two* different relaxation rates Γ_1 and Γ_2, corresponding to the propagating modes in the medium. We find that the *complete* conditions for quantum Zeno suppression on $P_{a\to s}(t)$ are: (i) the active neutrino scattering rate being much larger than the oscillation frequency, and (ii) the two relaxation rates of the propagating modes being approximately equal. Condition (ii) has been missing in the literature. For keV sterile neutrinos with $\sin 2\theta \lesssim 10^{-3}$, we find that these conditions for quantum Zeno suppression are fulfilled only near an MSW resonance at $T_{MSW} \sim 215\,\mathrm{MeV}$. Far away from the resonance, either at high or low temperatures, there is a wide hierarchy between the two relaxation rates of the propagating modes in the medium. We show that even for the case with the active neutrino scattering rate being much larger than the oscillation frequency, which is usually taken to indicate quantum Zeno suppression in the literature, the transition probability could still be substantial on time scales much longer than the decoherence time scale, if the two relaxation rates are widely separated. While the oscillatory term in $P_{a\to s}(t)$ is suppressed on the decoherence time scale, at very high or low temperature, this is not the relevant time scale for the suppression of the transition probability, but either $1/\Gamma_1$ or $1/\Gamma_2$ whichever is longer.

Particle Abundance in a Thermal Plasma: Quantum Kinetics versus Boltzmann Equation

We study the abundance of a particle species in a thermalized plasma by introducing a quantum kinetic description based on the non-equilibrium effective action. A stochastic interpretation of quantum kinetics in terms of a Langevin equation emerges naturally. We consider a particle species that is stable in the vacuum and interacts with heavier particles that constitute a thermal bath in equilibrium. Asymptotic theory suggests a definition of a fully renormalized single-particle distribution function. Its real time dynamics is completely determined by the non-equilibrium effective action which furnishes a Dyson-like resummation of the perturbative expansion. The distribution function reaches thermal equilibrium on a time scale $\sim 1/2\,\Gamma_k(T)$, with $\Gamma_k(T)$ being the quasiparticle relaxation rate. The equilibrium distribution function depends on the full spectral density as a consequence the fluctuation-dissipation relation. Such dependence leads to off-shell contributions to the particle abundance. A specific model of a bosonic field Φ in interaction with two thermalized heavier bosonic fields χ_1 and χ_2 is studied. The decay of the heaviest particle and the corresponding recombination processes lead to a width in the spectral function for the particle Φ and off-shell corrections to the particle abundance. We find substantial departures from the

usual Bose-Einstein prediction in both high temperature limit, and the low temperature but large momentum limit. In the latter case, the particle abundance is exponentially suppressed but larger than the Bose-Einstein result. We obtain the Boltzmann equation in renormalized perturbation theory and point out the origin of the different results. We argue that the corrections to the abundance of cold dark matter candidates are observationally negligible, and that recombination erases any possible spectral distortions on the CMB.

Non Equilibrium Dynamics of Mixing, Oscillations and Equilibration: a Model Study

Armed with the powerful non-equilibrium field theory methods, we proceed to examine the interplay between neutrino mixing, oscillations and equilibration in a thermal medium. The non-equilibrium dynamics is studied in a field theory of flavored neutral mesons that effectively models two flavors of mixed neutrinos, in interaction with other mesons that represent a thermal bath of hadrons or quarks and charged leptons. This model describes the general features of neutrino mixing and relaxation via charged currents in a medium. The reduced density matrix and the non-equilibrium effective action that describe the propagation of neutrinos are obtained by integrating out the bath degrees of freedom. We obtain the dispersion relations, mixing angles and relaxation rates of the "neutrino" quasiparticles. The dispersion relations and mixing angles are of the same form as those of neutrinos in the medium, and the relaxation rates are given by $\Gamma_1(k) = \Gamma_{ee}(k)\cos^2\theta_m(k) + \Gamma_{\mu\mu}(k)\sin^2\theta_m(k)$; $\Gamma_2(k) = \Gamma_{\mu\mu}(k)\cos^2\theta_m(k) + \Gamma_{ee}(k)\sin^2\theta_m(k)$ where $\Gamma_{\alpha\alpha}(k)$ are the relaxation rates of the flavor fields without mixing, and $\theta_m(k)$ is the mixing angle in the medium. The long time dynamics is approximately described by an effective Weisskopf-Wigner non-hermitian Hamiltonian. At long time, namely, $t >> \Gamma_{1,2}^{-1}$, the two-point function of the "neutrino" fields becomes time-translational invariant, reflecting the approach to equilibrium. The equilibrium density matrix is found to be nearly diagonal in the basis of eigenstates of an effective Hamiltonian that includes self-energy corrections in the medium, with perturbatively small off-diagonal elements.

Production of a Sterile Species: Quantum Kinetics

We investigate the production of a sterile species from active-sterile neutrino mixing in a thermalized medium, within the effective model developed in Chapter 8. The quantum kinetic equations for the distribution functions and coherences are derived from two independent but complementary

methods, namely the non-equilibrium effective action obtained by integrating out the "bath degrees of freedom" and the quantum master equation for the reduced density matrix. The set of kinetic equations derived via these two different techniques are shown to be identical up to the leading order in perturbative quantities. We show that if the initial density matrix is off-diagonal in the basis of the propagating modes in the medium, the off-diagonal coherences are damped out on the decoherence time scale. The damping of these off-diagonal coherences leads to an equilibrium reduced density matrix diagonal in the basis of propagating modes in the medium. The "neutrino" distribution functions reach equilibrium on the relaxation time scales $1/\Gamma_1$ and $1/\Gamma_2$ associated with the quasiparticle modes in the medium. Away from the MSW resonance, the time scales $1/\Gamma_1$ and $1/\Gamma_2$ are widely separated, which precludes the kinetic description of active-sterile production in terms of a simple rate equation that is commonly used in the literature. We derive explicitly the usual quantum kinetic equations in terms of the "polarization vector" and show their equivalence to those obtained from the non-equilibrium effective action and quantum master equation. However, while the notion of active-to-sterile transition probability $P_{a\to s}(t)$ is well-defined in the non-equilibrium effective action and quantum master equation approaches, it is not possible to extract $P_{a\to s}(t)$ from the components of the "polarization vector" because they are expectation values of *bilinear* operators in the reduced density matrix.

New Inflation vs. Chaotic Inflation, Higher Degree Potentials and the Reconstruction Program in Light of WMAP3

The CMB power spectra are studied for different *families* of single-field new and chaotic inflation models in the effective field theory approach to inflation. We implement a systematic expansion in $1/N_e$ where $N_e \sim 50$ is the number of e-foldings before the end of inflation. We study the dependence of the observables (n_s, r and $dn_s/d\ln k$) on the degree of the inflaton potential ($2\,n$) and confront them to the WMAP3 and large scale structure (LSS) data. This shows in general that fourth degree potentials ($n = 2$) provide the best fit to the data, and the window of consistency with the WMAP3 and LSS data narrows with growing n. New inflation yields a good fit to the r and n_s data in a wide range of field and parameter space. Small field inflation yields $r < 0.16$ while large field inflation yields $r > 0.16$ (for $N_e = 50$). All members of the new inflation family predict a small but negative running $-4\,(n+1) \times 10^{-4} \leq dn_s/d\ln k \leq -2 \times 10^{-4}$. (The values of r, n_s, $dn_s/d\ln k$ for arbitrary N_e follow by a simple rescaling from the $N_e = 50$ values). A reconstruction program is carried out, suggesting quite generally that for n_s consistent with the WMAP3 and LSS data

and $r < 0.1$, the symmetry breaking scale for new inflation is $|\phi_0| \sim 10\ M_{Pl}$, while the field scale at Hubble crossing is $|\phi_c| \sim M_{Pl}$. The family of chaotic models feature $r \geq 0.16$ (for $N_e = 50$), where the minimum value $r = 0.16$ corresponds to small amplitude of the inflaton and coincides with the value obtained from the monomial $m^2\phi^2/2$. Only a restricted subset of chaotic models are consistent with the combined WMAP3 bounds on $r,\ n_s,\ dn_s/d\ln k$ with a narrow window in field amplitude around $|\phi_c| \sim 15\ M_{Pl}$. We conclude that a measurement of $r < 0.16$ (for $N_e = 50$) distinctly rules out a large class of chaotic scenarios and favors small field new inflationary models. As a general consequence, new inflation emerges more favored than chaotic inflation.

APPENDIX A

REAL-TIME PROPAGATORS AND SELF-ENERGIES

A.1 FERMIONS

Consider a generic fermion field $f(\vec{x},t)$ of mass m_f. The Wightmann and Green's functions at finite temperature are given as

$$i\,S^{>}_{\alpha,\beta}(\vec{x}-\vec{x}',t-t') = \langle f_\alpha(\vec{x},t)\overline{f}_\beta(\vec{x}',t')\rangle = \frac{1}{V}\sum_{\vec{p}} e^{i\vec{p}\cdot(\vec{x}-\vec{x}')}\; iS^{>}_{\alpha,\beta}(\vec{p},t-t'), \tag{A.1}$$

$$i\,S^{<}_{\alpha,\beta}(\vec{x}-\vec{x}',t-t') = -\langle \overline{f}_\beta(\vec{x}',t')f_\alpha(\vec{x},t)\rangle = \frac{1}{V}\sum_{\vec{p}} e^{i\vec{p}\cdot(\vec{x}-\vec{x}')}\; i\,S^{<}_{\alpha,\beta}(\vec{p},t-t'), \tag{A.2}$$

where α,β are Dirac indices and V is the quantization volume.

The real-time Green's functions along the forward $(+)$ and backward $(-)$ time branches are given in terms of these Wightmann functions as

$$\begin{aligned}\langle f^{(+)}_\alpha(\vec{x},t)\overline{f}^{(+)}_\beta(\vec{x}',t')\rangle &= i\,S^{++}(\vec{x}-\vec{x}',t-t') \\ &= i\,S^{>}(\vec{x}-\vec{x}',t-t')\,\Theta(t-t') + i\,S^{<}(\vec{x}-\vec{x}',t-t')\,\Theta(t'-t)\;, \qquad \text{(A.3)}\\ \langle f^{(+)}_\alpha(\vec{x},t)\overline{f}^{(-)}_\beta(\vec{x}',t')\rangle &= i\,S^{+-}(\vec{x}-\vec{x}',t-t') = i\,S^{<}(\vec{x}-\vec{x}',t-t')\;. \qquad \text{(A.4)}\end{aligned}$$

At finite temperature T, it is straightforward to obtain these correlation functions by expanding the free fermion fields in terms of Fock creation and annihilation operators and massive spinors. In a CP asymmetric medium, the chemical potential μ_f for the fermion f is non-zero. Particles and anti-particles obey the following Fermi-Dirac distribution functions respectively

$$N_f(p_0) = \frac{1}{e^{(p_0-\mu_f)/T}+1} \quad , \quad \bar{N}_f(p_0) = \frac{1}{e^{(p_0+\mu_f)/T}+1}\;. \tag{A.5}$$

The fermionic propagators are conveniently written in a dispersive form

$$i\, S^{>}_{\alpha,\beta}(\vec{p}, t-t') = \int_{-\infty}^{\infty} dp_0\, \rho^{>}_{\alpha,\beta}(\vec{p}, p_0)\, e^{-ip_0(t-t')}\,, \tag{A.6}$$

$$i\, S^{<}_{\alpha,\beta}(\vec{p}, t-t') = \int_{-\infty}^{\infty} dp_0\, \rho^{<}_{\alpha,\beta}(\vec{p}, p_0)\, e^{-ip_0(t-t')}\,, \tag{A.7}$$

where we have

$$\rho^{>}_{\alpha,\beta}(\vec{p}, p_0) = \frac{\gamma^0\, p_0 - \vec{\gamma}\cdot\vec{p} + m_f}{2p_0}\, [1 - N_f(p_0)]\, \delta(p_0 - \omega_p) + \frac{\gamma^0\, p_0 - \vec{\gamma}\cdot\vec{p} + m_f}{2p_0}\, \bar{N}_f(-p_0)\, \delta(p_0 + \omega_p)\,, \tag{A.8}$$

$$\rho^{<}_{\alpha,\beta}(\vec{p}, p_0) = \frac{\gamma^0\, p_0 - \vec{\gamma}\cdot\vec{p} + m_f}{2p_0}\, N_f(p_0)\, \delta(p_0 - \omega_p) + \frac{\gamma^0\, p_0 - \vec{\gamma}\cdot\vec{p} + m_f}{2p_0}\, [1 - \bar{N}_f(-p_0)]\, \delta(p_0 + \omega_p)\,, \tag{A.9}$$

with $\omega_p = \sqrt{|\vec{p}|^2 + m_f^2}$. Using the relation $\bar{N}_f(-p_0) = 1 - N_f(p_0)$, we can write

$$\rho^{>}_{\alpha,\beta}(\vec{p}, p_0) = [1 - N_f(p_0)]\, \rho^{f}_{\alpha,\beta}(\vec{p}, p_0)\,, \tag{A.10}$$

$$\rho^{<}_{\alpha,\beta}(\vec{p}, p_0) = N_f(p_0)\, \rho^{f}_{\alpha,\beta}(\vec{p}, p_0)\,, \tag{A.11}$$

where the free fermionic spectral density $\rho^f(\vec{p}, p_0)$ is given by

$$\rho^f(\vec{p}, p_0) = \frac{\not{p}_+}{2\omega_p}\, \delta(p_0 - \omega_p) + \frac{\not{p}_-}{2\omega_p}\, \delta(p_0 + \omega_p)\,, \tag{A.12}$$

$$\not{p}_\pm = \gamma^0\, \omega_p \mp \vec{\gamma}\cdot\vec{p} \pm m_f\,. \tag{A.13}$$

A.2 VECTOR BOSONS

Consider a generic real vector boson field $A_\mu(\vec{x}, t)$ of mass M. In unitary gauge, it can be expanded in terms of Fock creation and annihilation operators of *physical* states with three polarizations as

$$A^\mu(\vec{x}, t) = \frac{1}{\sqrt{V}} \sum_\lambda \sum_{\vec{k}} \frac{\epsilon^\mu_\lambda(\vec{k})}{\sqrt{2\, W_k}} \left[a_{\vec{k},\lambda}\, e^{-iW_k\, t}\, e^{i\vec{k}\cdot\vec{x}} + a^\dagger_{\vec{k},\lambda}\, e^{iW_k\, t}\, e^{-i\vec{k}\cdot\vec{x}} \right] \quad ; \quad k^\mu\, \epsilon_{\mu,\lambda}(\vec{k}) = 0\,, \tag{A.14}$$

where $W_k = \sqrt{|\vec{k}\,|^2 + M^2}$ and k^μ is *on-shell* $k^\mu = (W_k, \vec{k})$. The three polarization vectors are such that

$$\sum_{\lambda=1}^{3} \epsilon^\mu_\lambda(\vec{k})\, \epsilon^\nu_\lambda(\vec{k}) = P^{\mu\nu}(\vec{k}) = -\left(g^{\mu\nu} - \frac{k^\mu k^\nu}{M^2} \right)\,. \tag{A.15}$$

It is now straightforward to compute the Wightmann functions of the vector bosons in a state in which the physical degrees of freedom are in thermal equilibrium at temperature T. These are given by

$$\langle A_\mu(\vec{x},t)A_\nu(\vec{x}',t')\rangle = i\,G^{>}_{\mu,\nu}(\vec{x}-\vec{x}',t-t'), \tag{A.16}$$

$$\langle A_\nu(\vec{x}',t')A_\mu(\vec{x},t)\rangle = i\,G^{<}_{\mu,\nu}(\vec{x}-\vec{x}',t-t'), \tag{A.17}$$

where $G^{<,>}$ can be conveniently written as spectral integrals in the form

$$i\,G^{>}_{\mu,\nu}(\vec{x}-\vec{x}',t-t') = \frac{1}{V}\sum_{\vec{k}} e^{i\vec{k}\cdot(\vec{x}-\vec{x}')}\int_{-\infty}^{\infty} dk_0\; e^{-ik_0(t-t')}\;[1+N_b(k_0)]\;\rho_{\mu\nu}(k_0,\vec{k}), \tag{A.18}$$

$$i\,G^{<}_{\mu,\nu}(\vec{x}-\vec{x}',t-t') = \frac{1}{V}\sum_{\vec{k}} e^{i\vec{k}\cdot(\vec{x}-\vec{x}')}\int_{-\infty}^{\infty} dk_0\; e^{-ik_0(t-t')}\;N_b(k_0)\;\rho_{\mu\nu}(k_0,\vec{k})\;, \tag{A.19}$$

where

$$N_b(k_0) = \frac{1}{e^{k_0/T}-1}\;, \tag{A.20}$$

and the spectral density is given by

$$\rho_{\mu\nu}(k_0,\vec{k}) = \frac{1}{2W_k}\left[P_{\mu\nu}(\vec{k})\;\delta(k_0-W_k) - P_{\mu\nu}(-\vec{k})\;\delta(k_0+W_k)\right]\;. \tag{A.21}$$

In terms of these Wightmann functions, the real-time correlation functions along the forward and backward time branches are given by

$$\langle A^{(+)}_\mu(\vec{x},t)A^{(+)}_\nu(\vec{x}',t')\rangle = iG^{>}_{\mu,\nu}(\vec{x}-\vec{x}',t-t')\;\Theta(t-t') + i\,G^{<}_{\mu,\nu}(\vec{x}-\vec{x}',t-t')\;\Theta(t'-t), \tag{A.22}$$

$$\langle A^{(+)}_\mu(\vec{x},t)A^{(-)}_\nu(\vec{x}',t')\rangle = i\,G^{<}_{\mu,\nu}(\vec{x}-\vec{x}',t-t')\;. \tag{A.23}$$

For the charged vector bosons, the correlation functions can be found simply from those of the real vector boson fields described above by writing the charged fields as linear combinations of *two* real fields $A^{1,2}$, namely

$$W^{\pm}_\mu(\vec{x},t) = \frac{1}{\sqrt{2}}[A^1_\mu(\vec{x},t) \pm iA^2_\mu(\vec{x},t)]\;. \tag{A.24}$$

It is straightforward to find the correlation function

$$\langle W^{+}_\mu(\vec{x},t)W^{-}_\mu(\vec{x}',t')\rangle = G^{>}_{\mu\nu}(\vec{x}-\vec{x}',t-t')\;, \tag{A.25}$$

and similarly for the other necessary Wightmann and Green's functions.

A.3 RETARDED SELF-ENERGIES FOR CHARGED AND NEUTRAL CURRENT INTERACTIONS

The diagrams for the one-loop retarded self-energy from charged current interactions are displayed in Fig. (A1).

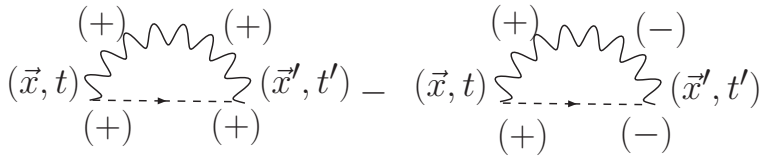

Figure A1: Retarded self-energy for charged current interactions. The wiggly line is a charged vector boson and the dashed line a lepton. The labels $(\pm)$ correspond to the forward $(+)$ and backward $(-)$ time branches. The corresponding propagators are $i\,S^{\pm,\pm}(\vec{x}-\vec{x}',t-t')$ and $i\,G^{\pm\pm}_{\mu\nu}(\vec{x}-\vec{x}',t-t')$ for leptons and charged bosons respectively.

A straightforward calculation yields for the charged current contribution the following result

$$\Sigma^{CC}_{ret}(\vec{x}-\vec{x}',t-t') = \frac{ig^2}{2}\,R\,\gamma^\mu\left[i\,S^{++}(\vec{x}-\vec{x}',t-t')\,i\,G^{++}_{\mu\nu}(\vec{x}-\vec{x}',t-t') - i\,S^{<}(\vec{x}-\vec{x}',t-t')\,i\,G^{<}_{\mu\nu}(\vec{x}-\vec{x}',t-t')\right]\,\gamma^\nu\,L\,, \tag{A.26}$$

with

$$R=\frac{1+\gamma^5}{2}\quad,\quad L=\frac{1-\gamma^5}{2}\,.$$

A similar result is obtained for the neutral current contribution to the self-energy by simply replacing $g/\sqrt{2}\to g/2\cos\theta_w$ and $M_W\to M_Z=M_W/\cos\theta_w$.

Using the representation of the fermion and vector boson propagators given above the retarded self-energy (A.26) can be written as

$$\Sigma_{ret}(\vec{x}-\vec{x}',t-t')=\frac{i}{V}\sum_{\vec{k}}\int_{-\infty}^{\infty}dk_0\,R\left[\overline{\Sigma}_W(\vec{k},k_0)+\overline{\Sigma}_Z(\vec{k},k_0)\right]\,L\,e^{i\vec{k}\cdot(\vec{x}-\vec{x}')}\,e^{-ik_0(t-t')}\,\Theta(t-t') \tag{A.27}$$

The contributions from charged and neutral vector bosons are given by

$$\overline{\Sigma}_W(\vec{k},k_0) = \frac{g^2}{2}\int\frac{d^3q}{(2\pi)^3}\int dp_0\int dq_0\,\delta(p_0+q_0-k_0)\,\gamma^\mu\,\rho^f(\vec{k}-\vec{q},p_0)\,\rho^W_{\mu\nu}(\vec{k})(\vec{q},q_0)\,\gamma^\nu\,[1-N_f(p_0)+N_b(q_0)]\,, \tag{A.28}$$

$$\overline{\Sigma}_Z(\vec{k},k_0) \;=\; \frac{g^2}{4\,\cos^2\theta_w}\int\frac{d^3q}{(2\pi)^3} \int dp_0\int dq_0\;\delta(p_0+q_0-k_0)\;\gamma^\mu\;\rho^f(\vec{k}-\vec{q},p_0)\;\rho^Z_{\mu\nu}(\vec{q},q_0)\;\gamma^\nu\;[1-N_f(p_0)+N_b(q_0)]\;, \tag{A.29}$$

where $\rho_{W,Z}(\vec{q},q_0)$ are the vector boson spectral densities given by eq.(A.21) with $M\equiv M_{W,Z}$ respectively. It is clear that $\overline{\Sigma}_{W,Z}(\vec{k},k_0)$ corresponds to a vector-like theory.

Using the integral representation of the function $\Theta(t-t')$, the retarded self-energy can be written in the following simple dispersive form

$$\Sigma_{ret}(\vec{x}-\vec{x}',t-t') = \frac{1}{V}\sum_{\vec{k}}\int_{-\infty}^{\infty}\frac{d\omega}{2\pi}\;e^{i\vec{k}\cdot(\vec{x}-\vec{x}')}\;e^{-i\omega(t-t')}\;R\;\left[\Sigma_W(\vec{k},\omega)+\Sigma_Z(\vec{k},\omega)\right]\;L\;, \tag{A.30}$$

$$\Sigma_{W,Z}(\vec{k},\omega) = \int dk_0\;\frac{\overline{\Sigma}_{W,Z}(\vec{k},k_0)}{k_0-\omega-i\epsilon}, \tag{A.31}$$

where $\epsilon\to 0^+$. Hence, from the above expression, we identify

$$\overline{\Sigma}_{W,Z}(\vec{k},\omega) = \frac{1}{\pi}\;Im\,\Sigma_{W,Z}(\vec{k},\omega)\;. \tag{A.32}$$

Furthermore, since $R\,(\pm m_f)\,L=0$, the factor $\pm m_f$ in the free fermionic spectral density defined in Eqns. (A.12) and (A.13) can be ignored when we compute $R\,\left[\overline{\Sigma}_W(\vec{k},\omega)+\overline{\Sigma}_Z(\vec{k},\omega)\right]\,L$. The signature of the the fermion mass m_f is only reflected in the factors of ω_p in the spectral density. Ignoring the factor m_f from now on, the fermionic spectral density is proportional to the γ matrices only and does not feature the identity matrix or γ^5. Therefore, there is the following simplification

$$R\,\left[\overline{\Sigma}_W(\vec{k},\omega)+\overline{\Sigma}_Z(\vec{k},\omega)\right]\,L = \left[\overline{\Sigma}_W(\vec{k},\omega)+\overline{\Sigma}_Z(\vec{k},\omega)\right]\,L\;. \tag{A.33}$$

APPENDIX B

CALCULATION OF THE IMAGINARY PART OF THE SELF-ENERGY

The imaginary part of the self-energy is given in the text, eqn. (7.148).

Integrating over dp_0, dq_0 and then performing the transformation $\vec{p} \to -\vec{p}-\vec{k}$ in all the integrals involving $n(\omega^{(2)}_{\vec{p}+\vec{k}})$, we can write

$$\mathrm{Im}\widetilde{\Sigma}^R(\omega,\vec{k}) = \sigma_0 + \sigma_I + \sigma_{II} + (\sigma^{(1)}_{III} - \sigma^{(2)}_{III}) + (\sigma^{(1)}_{IV} - \sigma^{(2)}_{IV}) \tag{B.1}$$

where

$$\sigma_0 = \frac{g^2}{32\pi^2}\,\mathrm{sign}(\omega)\int \frac{d^3\vec{p}}{\omega^{(1)}_{\vec{p}}\omega^{(2)}_{\vec{p}+\vec{k}}}\,\delta(\,|\omega| - \omega^{(1)}_{\vec{p}} - \omega^{(2)}_{\vec{p}+\vec{k}}\,), \tag{B.2}$$

$$\sigma_I = \frac{g^2}{32\pi^2}\,\mathrm{sign}(\omega)\int \frac{d^3\vec{p}}{\omega^{(1)}_{\vec{p}}\omega^{(2)}_{\vec{p}+\vec{k}}}\,n(\omega^{(1)}_{\vec{p}})\,\delta(\,|\omega| - \omega^{(1)}_{\vec{p}} - \omega^{(2)}_{\vec{p}+\vec{k}}\,), \tag{B.3}$$

$$\sigma_{II} = \frac{g^2}{32\pi^2}\,\mathrm{sign}(\omega)\int \frac{d^3\vec{p}}{\omega^{(2)}_{\vec{p}}\omega^{(1)}_{\vec{p}+\vec{k}}}\,n(\omega^{(2)}_{\vec{p}})\,\delta(\,|\omega| - \omega^{(2)}_{\vec{p}} - \omega^{(1)}_{\vec{p}+\vec{k}}\,), \tag{B.4}$$

$$\sigma^{(1)}_{III} = \frac{g^2}{32\pi^2}\int \frac{d^3\vec{p}}{\omega^{(1)}_{\vec{p}}\omega^{(2)}_{\vec{p}+\vec{k}}}\,n(\omega^{(1)}_{\vec{p}})\,\delta(\,\omega + \omega^{(1)}_{\vec{p}} - \omega^{(2)}_{\vec{p}+\vec{k}}\,)\,; \quad \sigma^{(2)}_{III} = \sigma^{(1)}_{III}(\omega \to -\omega), \tag{B.5}$$

$$\sigma^{(1)}_{IV} = \frac{g^2}{32\pi^2}\int \frac{d^3\vec{p}}{\omega^{(2)}_{\vec{p}}\omega^{(1)}_{\vec{p}+\vec{k}}}\,n(\omega^{(2)}_{\vec{p}+\vec{k}})\,\delta(\,\omega + \omega^{(2)}_{\vec{p}} - \omega^{(1)}_{\vec{p}+\vec{k}}\,)\,; \quad \sigma^{(2)}_{IV} = \sigma^{(1)}_{IV}(\omega \to -\omega). \tag{B.6}$$

Obviously, σ_0 represents the zero temperature contribution. Note that σ_{II} and $\sigma^{(1)}_{IV}$ can be obtained by exchanging M_1 and M_2 in σ_I and $\sigma^{(1)}_{III}$ respectively. Thus, we will only outline the main steps in computing σ_0, σ_I and $\sigma^{(1)}_{III}$ in this appendix. First of all, let $\omega_p = \omega^{(1)}_{\vec{p}}$ and $z = \omega^{(2)}_{\vec{p}+\vec{k}}$.

Then, we have

$$\sigma_0 + \sigma_I = \frac{g^2}{16\pi k}\text{sign}(\omega)\int_{M_1}^{\infty}[\,1+n(\omega_p)\,]\,d\omega_p\int_{z^-}^{z^+}\delta(\,|\omega|-\omega_p-z\,)\,dz \tag{B.7}$$

where

$$z^{\pm} = \sqrt{(p\pm k)^2+M_2^2} \tag{B.8}$$

$$= \sqrt{\omega_p^2 \pm 2k\sqrt{\omega_p^2-M_1^2}+k^2-(M_1^2-M_2^2)}. \tag{B.9}$$

Without loss of generality we can assume that $M_1 > M_2$ for convenience. For the integral to be non-vanishing, we require that

$$z^- < z = |\omega| - \omega_p < z^+. \tag{B.10}$$

Squaring both sides twice properly, these two inequalities can be reduced to $f(\omega_p) < 0$ where

$$f(\omega_p) = 4(|\omega|^2-k^2)\omega_p^2 - 4|\omega|(|\omega|^2-a)\omega_p + (|\omega|^2-a)^2 + 4kM_1^2 \tag{B.11}$$

and $a = k^2-(M_1^2-M_2^2)$. Notice that the graph $f(\omega_p)$ against ω_p represents a conic with positive y-intercept. Solving $f(\omega_p)=0$ for ω_p, we obtain

$$\omega_p \equiv \omega_p^{\pm} = \frac{|\omega|(|\omega|^2-a) \pm k\sqrt{(|\omega|^2-a)^2-4(|\omega|^2-k^2)M_1^2}}{2(|\omega|^2-k^2)}. \tag{B.12}$$

There are two possibilities: (i) $|\omega|^2-k^2>0$, (ii) $k^2-|\omega|^2>0$. For $k^2-|\omega|^2>0$, graphs with $f(\omega_p)$ against ω_p show that condition (B.10) can be satisfied only if $\omega_p > \omega_p^-$ but algebraic calculation indicates that $|\omega|-\omega_p^- < 0$. Thus, condition (B.10) can never be satisfied and this solution should be ignored. For $|\omega|^2-k^2>0$, we have $|\omega|^2-a>0$.

A detailed analysis of $f(\omega_p)$ as well as $z^{\pm}$ and $|\omega|-\omega_p$ as functions of ω_p reveals that that condition (B.10) can always be satisfied for $\omega_p^- < \omega_p < \omega_p^+$ and $|\omega| > \sqrt{k^2+M_2^2}+M_1$. For the discriminant in $\omega_p^{\pm}$ to be positive, we require that $|\omega| > \sqrt{k^2+(M_1+M_2)^2}$ or $|\omega| < \sqrt{k^2+(M_1-M_2)^2}$. Since $\sqrt{k^2+M_2^2}+M_1 > \sqrt{k^2+(M_1-M_2)^2}$, we can only pick up $|\omega| > \sqrt{k^2+(M_1+M_2)^2}$. As a result, we conclude that

$$\sigma_0 = \frac{g^2}{16\pi k}\,\mathrm{sign}(\omega)\,\Theta[\,|\omega|^2 - k^2 - (M_1+M_2)^2\,]\,(\omega_p^+ - \omega_p^-), \tag{B.13}$$

$$\sigma_I = \frac{g^2}{16\pi k\beta}\,\mathrm{sign}(\omega)\,\Theta[\,|\omega|^2 - k^2 - (M_1+M_2)^2\,]\,\ln\left(\frac{1-e^{-\beta\omega_p^+}}{1-e^{-\beta\omega_p^-}}\right). \tag{B.14}$$

Now, we proceed to compute $\sigma_{III}^{(1)}$:

$$\sigma_{III}^{(1)} = \frac{g^2}{16\pi k}\int_{M_1}^{\infty} n(\omega_p)\,d\omega_p \int_{z^-}^{z^+} \delta(\,\omega+\omega_p - z\,)\,dz. \tag{B.15}$$

For the integral to be non-vanishing, we require that

$$z^- < z = \omega + \omega_p < z^+ \tag{B.16}$$

which can be reduced to $g(\omega_p) < 0$ where

$$g(\omega_p) = 4(\omega^2-k^2)\omega_p^2 + 4\omega(\omega^2-a)\omega_p + (\omega^2-a)^2 + 4km_1^2. \tag{B.17}$$

Solving $g(\omega_p) = 0$ for ω_p, we obtain

$$\omega_p \equiv \xi_p^{\pm}(\omega) = \frac{-\omega(\omega^2-a) \pm k\sqrt{(\omega^2-a)^2 - 4(\omega^2-k^2)M_1^2}}{2(\omega^2-k^2)} \tag{B.18}$$

First, note that $z^{\pm} \to \omega_p \pm k$ as $\omega_p \to \infty$. Then, drawing graphs with $g(\omega_p)$ against ω_p and diagrams with $z^{\pm}$ and $\omega+\omega_p$ against ω_p, we observe that condition (B.16) is always satisfied for $k^2-\omega^2 > 0$ with $\omega_p > \xi_p^-(\omega)$. For $\omega^2 - k^2 > 0$, we have $|\omega|^2 - a > 0$ and graphs with $g(\omega_p)$ against ω_p show that condition (B.16) can be satisfied only if $\omega < 0$ and $\xi_p^- < \omega_p < \xi_p^+$. Moreover, an algebraic calculation indicates that both $\omega + \xi_p^- < 0$ and $\omega + \xi_p^+ < 0$ unless $\omega^2 - k^2 < M_1^2 - M_2^2$. Additionally, for the discriminant in $\xi_p^{\pm}$ to be positive, we require that $\omega^2 - k^2 > (M_1+M_2)^2$ or $\omega^2 - k^2 < (M_1-M_2)^2$. The condition $\omega^2 - k^2 > (M_1+M_2)^2$ contradicts $\omega^2 - k^2 < M_1^2 - M_2^2$. Hence, we must take $\omega^2 - k^2 < (M_1-M_2)^2$. Graphs of $z^{\pm}$ and $\omega+\omega_p$ against ω_p confirm that condition (B.16) is always satisfied for $0 < \omega^2 - k^2 < (M_1-M_2)^2$. As a result, we have

$$\begin{aligned}\sigma_{III}^{(1)} - \sigma_{III}^{(2)} &= \frac{g^2}{16\pi k\beta}\,\Theta(k^2-\omega^2)\ln\left(\frac{1-e^{-\beta\xi_p^-(-\omega)}}{1-e^{-\beta\xi_p^-(\omega)}}\right) \\ &\quad + \frac{g^2}{16\pi k\beta}\,\mathrm{sign}(\omega)\,\Theta(\omega^2-k^2)\,\Theta[\,k^2+(M_1-M_2)^2-\omega^2\,]\ln\left(\frac{1-e^{-\beta\omega_p^-}}{1-e^{-\beta\omega_p^+}}\right)\end{aligned} \tag{B.19}$$

where $\omega_p^{\pm}$ are the roots given by (B.12). For $k^2 - \omega^2 > 0$ and $\omega > 0$, $\xi_p^-(-\omega) = |\omega_p^-|$ and $\xi_p^-(\omega) = |\omega_p^+|$. For $k^2 - \omega^2 > 0$ and $\omega < 0$, $\xi_p^-(-\omega) = |\omega_p^+|$ and $\xi_p^-(\omega) = |\omega_p^-|$. Therefore, we conclude that

$$\sigma_{III}^{(1)} - \sigma_{III}^{(2)} = \frac{g^2}{16\pi k\beta}\,\mathrm{sign}(\omega)\,\Theta[\,k^2 + (M_1 - M_2)^2 - \omega^2\,]\ln\left(\frac{1 - e^{-\beta|\omega_p^-|}}{1 - e^{-\beta|\omega_p^+|}}\right). \tag{B.20}$$

Finally, to obtain $\sigma_{IV}^{(1)} - \sigma_{IV}^{(2)}$, we simply need to exchange M_1 and M_2 in $\sigma_{III}^{(1)} - \sigma_{III}^{(2)}$.

APPENDIX C

A SIMPLER CASE

Consider for simplicity the case of one scalar field. The solution of the Langevin equation is given by

$$\Psi_{\vec{k}}(t) = \dot{g}(k;t)\,\Psi^0_{\vec{k}} + g(k;t)\,\Pi^0_{\vec{k}} + \int_0^t g(k;t')\;\xi_{\vec{k}}(t-t')dt'\,, \tag{C.1}$$

where the dot stands for derivative with respect to time. In the Breit-Wigner approximation and setting $Z_k = 1$

$$g(k;t) = \frac{\sin[\Omega(k)\,t]}{\Omega(k)}\,e^{-\frac{\Gamma(k)}{2}t}\,. \tag{C.2}$$

where $\Omega(k)$ is the position of the quasiparticle pole (dispersion relation) and its width is given by

$$\Gamma(k) = \frac{\Sigma_I(\Omega(k))}{\Omega(k)} \tag{C.3}$$

The particle number is given by

$$N(k,t) = \frac{1}{2W(k)}\left[\langle\dot{\Psi}(\vec{k},t)\dot{\Psi}(-\vec{k},t)\rangle + W^2(k)\langle\Psi(\vec{k},t)\Psi(-\vec{k},t)\rangle\right] - \frac{1}{2} \tag{C.4}$$

where $W(k)$ is the bare frequency. Taking the initial density matrix of the field Ψ to be that corresponding to a free-field with arbitrary non-equilibrium initial distribution function $N(k;0)$ and carrying out both averages, over the initial density matrix for the field and of the quantum noise and using that the average of the latter vanishes, we find

$$N(k;t) = N_1(k;t) + N_2(k;t) - \frac{1}{2} \tag{C.5}$$

with

$$N_1(k;t) = \frac{1+2N(k;0)}{4\,W^2(k)}\left[(\ddot{g}(k;t))^2 + 2W^2(k)(\dot{g}(k;t))^2 + W^4(k)g^2(k;t)\right] \tag{C.6}$$

$$N_2(k;t) = \frac{1}{2W^2(k)}\int\frac{d\omega}{2\pi}\,\Sigma_I(k;\omega)\,[1+2n(\omega)]\;\left[W^2(k)\big|h(\omega,t)\big|^2 + \big|f(\omega,t)\big|^2\right] \tag{C.7}$$

where

$$\tag{C.8}$$

$$h(\omega,t) = \int_0^t e^{-i\omega t'} g(k;t')dt' \tag{C.9}$$

$$f(\omega,t) = \int_0^t e^{-i\omega t'} \dot{g}(k;t')dt' \tag{C.10}$$

The terms $N_1(k;t); N_2(k;t)$ have very different origins: the term $N_1(k;t)$ depends on the initial condition and originates in the first two terms in (9.28) namely those *independent of the noise*, which survive upon taking the average over the noise. The term $N_2(k;t)$ is independent of the initial conditions and is solely determined by the correlation function of the noise term and is a consequence of the fluctuation dissipation relation. Using the expression (C.2) we find

$$N_1(k;t) = \left[\frac{1}{2} + N(k;0)\right] e^{-\Gamma(k)t} \left[1 + \sin^2(\Omega(k)t) \left(\frac{\Omega^2(k) - W^2(k)}{2W(k)\Omega(k)}\right)^2 + \mathcal{O}\left(\frac{\Gamma^2(k)}{\Omega^2(k)}\right)\right] \tag{C.11}$$

where the neglected terms of order $\Gamma^2(k)/\Omega^2(k) \ll 1$ are perturbatively small. The oscillatory term in (C.11) averages out on a short time scale $1/\Omega(k) \ll 1/\Gamma(k)$ and we can replace (C.11) by its average over this short time scale yielding

$$N_1(k;t) \approx \left[\frac{1}{2} + N(k;0)\right] e^{-\Gamma(k)t} \left[1 + \frac{1}{2}\left(\frac{\Omega^2(k) - W^2(k)}{2W(k)\Omega(k)}\right)^2 + \mathcal{O}\left(\frac{\Gamma^2(k)}{\Omega^2(k)}\right)\right] \tag{C.12}$$

In perturbation theory $\Omega^2(k) - W^2(k)/2W(k)\Omega(k) \ll 1$, can be neglected to leading order in perturbative quantities, thus we obtain

$$N_1(k;t) \approx \left[\frac{1}{2} + N(k;0)\right] e^{-\Gamma(k)t}\,. \tag{C.13}$$

Using the fact that $\Sigma_I(\omega) = -\Sigma_I(-\omega)$ we can perform the integrals in $N_2(k;t)$ in the narrow width (Breit-Wigner) approximation by using eqn. (C.3), with the result

$$N_2(k;t) \simeq Z_k^2 \left[\frac{W^2(k) + \Omega^2(k)}{2W(k)\Omega(k)}\right] \left[\frac{1}{2} + n(\Omega(k))\right] \left(1 - e^{-\Gamma(k)t}\right) + \mathcal{O}\left(\frac{\Gamma^2(k)}{\Omega^2(k)}\right) \tag{C.14}$$

Replacing in perturbation theory

$$Z_k \approx 1 \;\; ; \;\; \frac{W^2(k) + \Omega^2(k)}{2W(k)\Omega(k)} \approx 1 \tag{C.15}$$

we find

$$N(k;t) = n(\Omega(k)) + (N(k;0) - n(\Omega(k)))\; e^{-\Gamma(k)t} \tag{C.16}$$

which is the solution of the usual kinetic equation

$$\frac{dN(k;t)}{dt} = -\Gamma(k)\left(N(k;t) - N_{eq}(k)\right) \tag{C.17}$$

where

$$N_{eq}(k) = n(\Omega(k)) \tag{C.18}$$

It is important to highlight the series of approximations that led to this result: i) the narrow width (Breit-Wigner) approximation, ii) $Z_k \sim 1$, iii) $\Omega^2(k) \sim W^2(k)$, iv) $\Gamma(k)/\Omega(k) \ll 1$, these approximations are all warranted in perturbation theory. Clearly including perturbative corrections lead to perturbative departures of the usual kinetic equation and of the equilibrium distribution function.

APPENDIX D

QUANTUM MASTER EQUATION

Taking the trace over the bath variables with the factorized density matrix (9.78), the double commutator in equation (9.79) becomes

$$
\begin{aligned}
-\sum_{\vec{k}} \int_0^t dt' \qquad & \Big\{ \phi_a(t)\phi_a(t')\rho_{S,i}(t)\ \mathrm{Tr}_B \rho_B(0)\mathcal{O}(t)\mathcal{O}(t') \\
& +\rho_{S,i}(t)\phi_a(t')\phi_a(t)\ \mathrm{Tr}_B \rho_B(0)\mathcal{O}(t')\mathcal{O}(t) \\
& -\phi_a(t)\rho_{S,i}(t)\phi_a(t')\ \mathrm{Tr}_B \rho_B(0)\mathcal{O}(t')\mathcal{O}(t) \\
& -\phi_a(t')\rho_{S,i}(t)\phi_a(t)\ \mathrm{Tr}_B \rho_B(0)\mathcal{O}(t)\mathcal{O}(t') \Big\} . \qquad \text{(D.1)}
\end{aligned}
$$

We suppressed the momentum index to simplify notation but used the fact that translational invariance of the bath implies that the correlation functions are diagonal in momentum. The bath correlation functions were given in ref.[197] (see section 3-B in this reference) and we just summarize these results:

$$
\mathrm{Tr}_B \rho_B(0)\mathcal{O}(t)\mathcal{O}(t') = \frac{1}{\pi}\int_{-\infty}^{\infty} d\omega\ \mathrm{Im}\widetilde{\Sigma}_{aa}(k;\omega)[1+n(\omega)]\ e^{-i\omega(t-t')} \qquad \text{(D.2)}
$$

$$
\mathrm{Tr}_B \rho_B(0)\mathcal{O}(t')\mathcal{O}(t) = \frac{1}{\pi}\int_{-\infty}^{\infty} d\omega\ \mathrm{Im}\widetilde{\Sigma}_{aa}(k;\omega)\ n(\omega)\ e^{-i\omega(t-t')} \qquad \text{(D.3)}
$$

where we used the property $\mathrm{Im}\widetilde{\Sigma}_{aa}(k;\omega) = -\mathrm{Im}\widetilde{\Sigma}_{aa}(k;-\omega)$[197]. The self energy $\widetilde{\Sigma}$ is obtained from the discontinuity across the $W-\chi$ lines in the diagram in fig. (9.2) and is the same quantity that enters in the non-equilibrium effective action, and $n(\omega)$ is the equilibrium distribution function. The active field ϕ_a is related to the fields that create and annihilate the propagating modes in the medium $\varphi_{1,2}$ as in eq. (9.87), hence terms of the form

$$
\phi_a(t)\phi_a(t') = \cos^2\theta_m \varphi_1(t)\varphi_1(t') + \sin^2\theta_m \varphi_2(t)\varphi_2(t') + \frac{1}{2}\sin 2\theta_m \big(\varphi_1(t)\varphi_2(t') + \varphi_2(t)\varphi_1(t')\big) , \qquad \text{(D.4)}
$$

and all other terms in (D.1) are written accordingly. The next step requires writing these fields in terms of creation and annihilation operators in the interaction picture of $\overline{H}_0$, their expansion is shown in eqn. (9.88). The resulting products of creation and annihilation operators all feature phases which are re-arranged to depend separately on the variable t and $t-t'$, for example

$$a_j a_j \; e^{2i\omega_j t} \; e^{-i\omega_j (t-t')} \quad ; \quad a_j^\dagger a_j \; e^{i\omega_j (t-t')} \quad ; \quad a_i^\dagger a_j \; e^{i(\omega_i-\omega_j)t} \; e^{i\omega_j (t-t')} \quad , \text{etc.} . \tag{D.5}$$

The exponentials that depend on $t-t'$, such as $e^{\pm i\omega_j (t-t')}$ are combined with the exponentials in (D.2,D.3) and the integral in t' in (D.1) is written as an integral in $\tau = t-t'$. The Wigner-Weisskopf approximation for the resulting integral yields eqn. (9.81). After performing the time integral the terms of the form $a_j^\dagger a_j$ do not feature any phase, whereas terms of the form $a_i a_j$ (and their hermitian conjugate) feature terms of the form $e^{\pm i(\omega_i+\omega_j)t}$, all of these rapidly oscillating terms average out and are neglected in the "rotating wave approximation"[200], which is tantamount to time-averaging these rapidly varying terms. The remaining terms can be gathered together into two different type of contributions, diagonal and off-diagonal in the $1-2$ indices. The diagonal contributions do not feature explicit time dependence while the off-diagonal one features an explicit time dependence of the form $e^{\pm i(\omega_1-\omega_2)t}$.

Diagonal: The diagonal contributions are

$$\begin{aligned}
\frac{d\rho_{S,i}}{dt} \;=\; \sum_{j=1,2} \sum_{\vec{k}} \Bigg\{ & -i\Delta\omega_j(k) \big[a_j^\dagger(\vec{k}) a_j(\vec{k}), \rho_{S,i}(t) \big] \\
& - \frac{\Gamma_j(k)}{2} \Bigg[\Big(1 + n(\omega_j(k)) \Big) \Big(\rho_{S,i} a_j^\dagger(\vec{k}) a_j(\vec{k}) + a_j^\dagger(\vec{k}) a_j(\vec{k}) \rho_{S,i} - 2 a_j(\vec{k}) \rho_{S,i} a_j^\dagger(\vec{k}) \Big) \\
& + n(\omega_j(k)) \Big(\rho_{S,i} a_j(\vec{k}) a_j^\dagger(\vec{k}) + a_j(\vec{k}) a_j^\dagger(\vec{k}) \rho_{S,i} - 2 a_j^\dagger(\vec{k}) \rho_{S,i} a_j(\vec{k}) \Big) \Bigg] \Bigg\}
\end{aligned} \tag{D.6}$$

where the second order frequency shifts $\Delta\omega_j(k)$ and the widths $\Gamma_j(k)$ are given in equations (9.35-9.40).

Off diagonal: The full expression for the off-diagonal contributions is lengthy and cumbersome and we just quote the result for the real part of the quantum master equation, neglecting the imaginary part which describes a second order shift to the oscillation frequencies of the off-diagonal coherences.

$$
\begin{aligned}
\frac{d\rho_{S,i}}{dt} &= \sum_{\vec{k}} \Bigg\{ -\frac{\widetilde{\Gamma}_1(k)}{2}\Bigg[\Big(1+n(\omega_1(k))\Big)\Big(a_2^\dagger(k;t)a_1(k;t)\rho_{S,i} + \rho_{S,i}a_1^\dagger(k;t)a_2(k;t) - a_2(k;t)\rho_{S,i}a_1^\dagger(k;t) \\
&\quad -a_1(k;t)\rho_{S,i}a_2^\dagger(k;t)\Big) + n(\omega_1(k))\Big(a_2(k;t)a_1^\dagger(k;t)\rho_{S,i} + \rho_{S,i}a_1(k;t)a_2^\dagger(k;t) - a_2^\dagger(k;t)\rho_{S,i}a_1(k;t) \\
&\quad -a_1^\dagger(k;t)\rho_{S,i}a_2(k;t)\Big)\Bigg] \\
&\quad -\frac{\widetilde{\Gamma}_2(k)}{2}\Bigg[\Big(1+n(\omega_2(k))\Big)\Big(a_1^\dagger(k;t)a_2(k;t)\rho_{S,i} + \rho_{S,i}a_2^\dagger(k;t)a_1(k;t) - a_1(k;t)\rho_{S,i}a_2^\dagger(k;t) \\
&\quad -a_2(k;t)\rho_{S,i}a_1^\dagger(k;t)\Big) + n(\omega_2(k))\Big(a_1(k;t)a_2^\dagger(k;t)\rho_{S,i} + \rho_{S,i}a_2(k;t)a_1^\dagger(k;t) - a_1^\dagger(k;t)\rho_{S,i}a_2(k;t) \\
&\quad -a_2^\dagger(k;t)\rho_{S,i}a_1(k;t)\Big)\Bigg]\Bigg\} \qquad \text{(D.7)}
\end{aligned}
$$

where the interaction picture operators

$$
a_j(k;t) = a_j(k;0)\ e^{-i\omega_j t} \qquad \text{(D.8)}
$$

and

$$
\widetilde{\Gamma}_j(k) = \frac{1}{2}\sin 2\theta_m\ \frac{\mathrm{Im}\widetilde{\Sigma}_{aa}(k;\omega_j(k))}{\sqrt{\omega_1(k)\omega_2(k)}}\ \ ; j = 1,2\,. \qquad \text{(D.9)}
$$

BIBLIOGRAPHY

[1] C. Giunti and M. Lavede, hep-ph/0310238; S.M. Bilenky, C. Giunti, J.A. Grifols, E. Masso, Phys.Rept. **379**, 69 (2003); C. Giunti, Found. Phys. Lett. **17**, 103 (2004); S. M. Bilenky and C. Giunti, Int. J. Mod. Phys. **A16**, 3931 (2001).

[2] A. Yu. Smirnov, hep-ph/0311259; hep-ph/0306075 ; hep-ph/0305106; hep-ph/0305106.

[3] S. M. Bilenky, hep-ph/0402153; W.M. Alberico, S.M. Bilenky, hep-ph/0306239; S. M. Bilenky, hep-ph/0210128

[4] W. C. Haxton, nucl-th/9901076, Wick C. Haxton, Barry R. Holstein, Am.J.Phys. **68**, 15 (2000).

[5] W. Grimus, hep-ph/0307149.

[6] B. Pontecorvo, Zh. Eksp. Toer. Fiz. **34**,247 [Sov. Phys. JETP **7**,172 (1958)]; Zh. Eksp. Toer. Fiz. **53**, 1717 [Sov. Phys. JETP **26**, 984 (1968)]; Z. Maki, M. Nakazawa and S. Sakata, Prog. Theor. Phys. **28**, 870 (1962).

[7] S. M. Bilenky and B. Pontecorvo, Phys. Rept. **41**, 225 (1978).

[8] D. N. Spergel *et. al.* (WMAP collaboration), Astrophys.J.Suppl. **148** , 175 (2003).

[9] C. W. Kim and A. Pevsner, *Neutrinos in Physics and Astrophysics*, (Harwood Academic Publishers, Chur, Switzerland, 1993).

[10] R. N. Mohapatra and P. B. Pal, *Massive Neutrinos in Physics and Astrophysics*, (World Scientific, Singapore, 1998).

[11] M. Fukugita and T. Yanagida, *Physics of Neutrinos and Applications to Astrophysics*, (Springer-Verlag Berlin Heidelberg 2003).

[12] G. G. Raffelt, *Stars as Laboratories for Fundamental Physics*, (The University of Chicago Press, Chicago, 1996).

[13] T. K. Kuo and J. Pantaleone, Rev. of Mod. Phys. **61**, 937 (89).

[14] A. D. Dolgov, Surveys High Energ.Phys. **17**, 91, (2002); Phys.Rept. **370**, 333 (2002); Nuovo Cim. **117 B**, 1081, (2003); hep-ph/0109155 (talk at XV Rencontres de Physique de La Vallee d'Aoste, March, 2001); A.D. Dolgov, S.H. Hansen, S. Pastor, S.T. Petcov, G.G. Raffelt, D.V. Semikoz, Nucl.Phys. B632 (2002) 363-382.

[15] C. Athanassopoulos *et.al.* (LSND collaboration), Phys.Rev.Lett. **81**, 1774 (1998).

[16] A. Aguilar *et.al.* (LSND collaboration), Phys.Rev. **D64** , 112007 (2001).

[17] S. Dodelson and L. M. Widrow, Phys. Rev. Lett. **72**, 17 (1994).

[18] T. Asaka, M. Shaposhnikov, A. Kusenko, Phys. Lett. **B 638**, 401 (2006).

[19] X. Shi, G. M. Fuller, Phys. Rev. Lett. **83**, 3120 (1999).

[20] K. Abazajian, G. M. Fuller, M. Patel, Phys. Rev. **D64**, 023501 (2001).

[21] S. H. Hansen, G. Mangano, A. Melchiorri, G Miele and O. Pisanti, Phys. Rev. **D65**, 023511 (2001).

[22] K. Abazajian, G. M. Fuller, Phys. Rev. **D66**, 023526 (2002).

[23] K. Abazajian, Phys. Rev. **D73**, 063506 (2006), *ibid*, 063513 (2006).

[24] P. Biermann, A. Kusenko, Phys. Rev. Lett. **96**, 091301 (2006).

[25] K. Abazajian, S. M. Koushiappas, Phys. Rev. **D74** 023527 (2006).

[26] A. D. Dolgov, Phys. Rept. **370**, 333 (2002); Surveys High Energ.Phys. **17** 91 (2002).

[27] J. Lesgourgues, S. Pastor, Phys.Rept. **429** 307, (2006).

[28] S. Hannestad, arXiv:hep-ph/0602058.

[29] P. L. Biermann, F. Munyaneza, astro-ph/0702173, astro-ph/0702164, F. Munyaneza, P. L. Biermann, astro-ph/0609388, J. Stasielak, P. L. Biermann, A. Kusenko Astrophys.J. **654**, 290 (2007).

[30] M. Shaposhnikov, astro-ph/0703673.

[31] G. Raffelt, G. Sigl, Astropart.Phys. **1**, 165 (1993).

[32] J. Hidaka, G. M. Fuller, astro-ph/0609425.

[33] C. J. Smith, G. M. Fuller, C. T. Kishimoto, K. Abazajian, astro-ph/0608377.

[34] C. T. Kishimoto, G. M. Fuller, C. J. Smith, Phys.Rev.Lett. **97** , 141301 (2006).

[35] A. Kusenko, G. Segre, Phys. Rev. **D59**, 061302, (1999).

[36] G. M. Fuller, A. Kusenko, I. Mociouiu, S. Pascoli, Phys. Rev. **D68**, 103002 (2003).

[37] A. Kusenko, hep-ph/0703116.

[38] A. A. Aguilar-Arevalo *et.al.* (MiniBooNE collaboration) arXiv:0704.1500 [hep-ex].

[39] M. Maltoni, T. Schwetz, arXiv:0705.0107 [hep-ph].

[40] K. Abazajian, G. M. Fuller, W. H. Tucker, Astrop. J. **562**, 593 (2001).

[41] A. Boyarsky, A Neronov, O Ruchayskiy, M. Shaposhnikov, Mon.Not.Roy.Astron.Soc. **370**, 213 (2006); JETP Lett. **83** , 133 (2006); Phys.Rev. **D74**, 103506 (2006); A. Boyarsky, A. Neronov, O. Ruchayskiy, M. Shaposhnikov, I. Tkachev, astro-ph/0603660; A. Boyarsky, J. Nevalainen, O. Ruchayskiy, astro-ph/0610961; A. Boyarsky, O. Ruchayskiy, M. Markevitch, astro-ph/0611168.

[42] S. Riemer-Sorensen, K. Pedersen, S. H. Hansen, H. Dahle, arXiv:astro-ph/0610034; S. Riemer-Sorensen, S. H. Hansen and K. Pedersen, Astrophys. J. **644** (2006) L33 (arXiv:astro-ph/0603661).

[43] K. N. Abazajian, M. Markevitch, S. M. Koushiappas, R. C. Hickox, astro-ph/0611144.

[44] F. Bezrukov, M. Shaposhnikov, hep-ph/0611352.

[45] A. de Gouvea, hep-ph/0411274, TASI lectures on neutrino physics.

[46] M. Prakash, J. M. Lattimer, R. F. Sawyer, R. R. Volkas, Ann.Rev.Nucl.Part.Sci. **51**, 295 (2001); S. Reddy, M. Prakash, J. M. Lattimer, Phys.Rev. **D58**, 013009 (1998)

[47] M. Prakash, J.M. Lattimer, J.A. Pons, A.W. Steiner, S. Reddy, Lect.Notes Phys. **578**, 364 (2001), S. Reddy, M. Prakash, nucl-th/9508009.

[48] D. G. Yakovlev, A. D. Kaminker, O. Y. Gnedin, P. Haensel, Phys.Rept. **354**, 1 (2001).

[49] M. Barkovich, J. C. D'Olivo, R. Montemayor, hep-ph/0503113.

[50] L. Wolfenstein, Phys. Rev. **D17**, 2369 (1978); Phys. Rev. **D20**, 2634 (1979); Phys. Lett. **B194** 197 (1987).

[51] S. P. Mikheyev and A. Yu Smirnov, , Yad. Fiz.**42**, 1441 (1985) (Sov. J. Nucl. Phys. **42**, 913 (1985)); Nuovo Cimento **C9**, 17 (1986); Zh. Eksp. Toer. Fiz. **91**, 7 (1986) (Sov. Phys. JETP **64**, 4 (1986)).

[52] M. Fukugita and T. Yanagida, Phys. Lett. **B174**, 45 (1986).

[53] W. Buchmuller, R. D. Peccei and T. Yanagida, hep-ph/0502169.

[54] W. Buchmuller, P. Di Bari and M. Plumacher, New J. Phys. **6**,105 (2004); Annals Phys. **315** , 305 (2005); Nucl. Phys. **B665**, 445 (2003); W. Buchmuller, Acta Phys. Polon. **B32** , 3707 (2001); Lect. Notes Phys. **616**, 39 (2003).

[55] G. M. Fuller, W. C. Haxton, G. C. McLaughlin Phys.Rev.**D59**, 085005 (1999); J. Pantaleone, Phys.Lett. **B342**, 250 (1995); B. Jegerlehner, F. Neubig, G. Raffelt, Phys.Rev.**D54**, 1194 (1996).

[56] H. A. Bethe, Phys. Rev. Lett. **56**, 1305 (1986).

[57] D. Notzold and G. Raffelt, Nucl. Phys. **B307**, 924 (1988).

[58] K. Enqvist, K. Kainulainen, J. Maalampi, Nucl. Phys. **B349**, 754 (1991); Phys. Lett. **B244**, 186 (1990); K. Enqvist, K. Kainulainen, M. Thompson, Nucl. Phys. **B373**, 498 (1992).

[59] R. Barbieri and A. Dolgov, Nucl. Phys. **B 349**, 743 (1991).

[60] R. A. Harris, L. Stodolsky, Phys. Lett. **B116**, 464 (1982); L. Stodolsky, Phys.Rev. **D36**:2273, (1987).

[61] J. Cline, Phys. Rev. Lett. **68**, 3137 (1992).

[62] P. Mannheim, Phys. Rev. **D37**, 1935 (1988).

[63] G. Raffelt, G. Sigl, L. Stodolsky, Phys. Rev. Lett. **70**, 2363 (1993); Phys. Rev. **D45**, 1782 (1992).

[64] G.Sigl and G.Raffelt, Nucl.Phys.**B 406**, 423 (1993).

[65] G. Raffelt, G. Sigl and L. Stodolsky, Phys. Rev. **D45**, 1782 (1992); Phys. Rev. Lett. **70**, 2363 (1993); G. Sigl and G. Raffelt, Nucl. Phys. **B 406**, 423 (1993).

[66] B. H. J. McKellar and M. J. Thompson, Phys. Rev. **D49**, 2710 (1994).

[67] J. Pantaleone, Phys. Lett. **342**, 250 (1995); J. Pantaleone, Phys.Rev.**D46**, 510 (1992) .

[68] G.Sigl, Phys.Rev. **D51**, 4035 (1995).

[69] V. A. Kostelecky, J. Pantaleone and S. Samuel, Phys. Lett. **B315**, 46 (1993); V. Kostelecky and S. Samuel, Phys. Lett. **B318**, 127 (1993); V. Kostelecky and S. Samuel, Phys. Rev. **D49**, 1740 (1994); V. Kostelecky and S. Samuel, Phys. Rev. **D52**, 3184 (1995).

[70] C. Lunardini and A. Y. Smirnov, Phys. Rev. **D64**, 073006 (2001).

[71] Y. Y. Y. Wong, Phys. Rev. **D66**, 025015 (2002); AIP Conf.Proc. **655**, 240 (2003).

[72] K. N. Abazajian, J. F. Beacom and N. F. Bell, Phys. Rev. **D 66**, 013008 (2002).

[73] N. F. Bell, R. R. Volkas, Y. Y. Y. Wong, Phys. Rev. **D59**, 113001 (1999), N. F. Bell, R. Foot, R. R. Volkas, Phys.Rev. **D58**, 105010 (1998); N. F. Bell, hep-ph/0311283.

[74] A. Friedland and C. Lunardini, Phys. Rev. **68**, 013007 (2003).

[75] P. Strack and A. Burrows, Phys.Rev. **D71**, 093004 (2005); P. Strack, hep-ph/0505056 (Master's Thesis).

[76] K. Kainulainen, Phys. Lett. **B244**, 191 (1990).

[77] R. Foot, R. R. Volkas, Phys. Rev. **D55**, 5147 (1997).

[78] P. Di Bari, P. Lipari, M. Lusignoli, Int. J. Mod. Phys. **A15**, 2289 (2000).

[79] J. Lykken, O. Mena and S. Razzaque, arXiv: 0705.2029 [hep-ph].

[80] D. Hooper, D. Morgan and E. Winstanley, Phys. Rev. **D72**, 065009 (2005) [arXiv: hep-ph/0506091].

[81] U. Jacob and T. Piran, Nature Phys. **3**, 87-90 (2007) [arXiv: hep-ph/0607145].

[82] J. Ahrens *et al.* [The IceCube Collaboration], Nucl. Phys. Proc. Suppl. **118**, 388 (2003) [arXiv: astro-ph/0209556].

[83] J. Schwinger, J. Math. Phys. **2**, 407 (1961); K. T. Mahanthappa, Phys. Rev. **126**, 329 (1962); P. M. Bakshi and K. T. Mahanthappa, J. Math. Phys. **41**, 12 (1963); L. V. Keldysh, JETP **20**, 1018 (1965); K. Chou, Z. Su, B. Hao And L. Yu, Phys. Rep. **118**, 1 (1985); A. Niemi and G. Semenoff, Ann. of Phys. (NY) **152**, 105 (1984); N. P. Landsmann and C. G. van Weert, Phys. Rep. **145**, 141 (1987); E. Calzetta and B. L. Hu, Phys. Rev. **D41**, 495 (1990); *ibid.* **D37**, 2838 (1990); J. P. Paz, Phys. Rev. **D41**, 1054 (1990); *ibid.* **D42**, 529 (1990).

[84] R. D. Jordan, Phys. Rev. **D33**, 444 (1986).

[85] D. Boyanovsky, H. J. de Vega and R. Holman, Proceedings of the Second Paris Cosmology Colloquium, Observatoire de Paris, June 1994, pp. 127-215, H. J. de Vega and N. Sanchez, Editors World- Scientific, 1995; Advances in Astrofundamental Physics, Erice Chalonge Course, N. Sanchez and A. Zichichi Editors, World Scientific, 1995; D. Boyanovsky, H. J. de Vega, R. Holman, D.-S. Lee and A. Singh, Phys. Rev. **D51**, 4419 (1995); D. Boyanovsky, H. J. de Vega, R. Holman and J. Salgado, Phys. Rev. **D54**, 7570 (1996). D. Boyanovsky, H. J. de Vega, C. Destri, R. Holman and J. Salgado, Phys. Rev. **D57**, 7388 (1998).

[86] D. Boyanovsky, H. J. de Vega and R. Holman, Proceedings of the Second Paris Cosmology Colloguium, Observatoire de Paris, June 1994, pp. 127-215, H. J. de Vega and N. Sanchez, Editors World Scientific, 1995; Advances in Astrofundamental Physics, Erice Chalonge Course, N. Sanchez and A. Zichichi Editors, World Scientific, 1995; D. Boyanovsky, H. J. de Vega, R. Holman and D.-S. Lee, Phys. Rev. **D52**, 6805 (1995).

[87] S. Y.-Wang, D. Boyanovsky, H. J. de Vega, D.-S. Lee and Y. J. Ng, Phys. Rev. **D61**, 065004 (2000); D. Boyanovsky, H. J. de Vega, D.-S.Lee, Y.J. Ng and S.-Y. Wang, Phys. Rev. **D59**, 105001 (1999).

[88] D. Boyanovsky, I.D. Lawrie, D.S. Lee, Phys.Rev. **D54**, 4013 (1996); S. M. Alamoudi, D. Boyanovsky, H. J. de Vega, R. Holman, Phys.Rev. **D59**, 025003 (1998); D. Boyanovsky, H.J. de Vega, S.-Y. Wang, Phys.Rev. **D61**, 065006 (2000).

[89] M. Blasone and G. Vitiello, Phys.Rev. **D60**, 111302 (1999); M. Blasone, G. Vitiello, Annals of Physics **244**,283 (1995); Erratum-ibid. **249**, 363 (1996); E. Alfinito, M. Blasone, A. Iorio, G. Vitiello, Phys.Lett. **B362**, 91 (1995); E.Alfinito, M.Blasone, A.Iorio, G.Vitiello, Acta Phys.Polon. **B27** , 1493 (1996); M.Blasone, P.A.Henning, G.Vitiello, hep-ph/9605335; M. Blasone, P. P. Pacheco, H. W. C. Tseung, Phys.Rev. **D67**073011(2003), and references therein.

[90] K. Fujii, C. Habe and T. Yabuki, Phys. Rev. **D64**, 013011 (2001), Phys. Rev. **D59**, 113003 (1999); K. Fujii and T. Shimomura, hep-ph/0402274.

[91] C-R. Ji and Y. Mischchenko, Phys. Rev. **D65**, 096015 (2002); hep-ph/0403073.

[92] K. Eguchi *et.al.* (KamLAND collaboration), Phys. Rev. Lett.**90**, 021802 (2003).

[93] J. C. D' Olivo and J. F. Nieves, Int. Jour. of Mod. Phys. **A11**, 141 (1996).

[94] J. Pantaleone, Phys. Lett. **B287**, 128 (1992), Phys. Rev. **D46**, 510 (1992).

[95] D. Boyanovsky and C. M. Ho, Phys. Rev. **D69**, 125012 (2004).

[96] M. E. Peskin and D. V. Schroeder, *An introduction to Quantum Field Theory*, Advanced Book Program, Addison-Wesley Pub. Co, Reading, Massachusetts, 1995.

[97] J. C. D'Olivo, J. F. Nieves and M. Torres, Phys. Rev. **D46**, 1172 (1992); E. S. Tututi, M. Torres and J. C. D'Olivo, Phys. Rev. **D66**, 043001 (2002).

[98] B. Kayser, Phys. Rev. **D24**, 110 (1981).

[99] J. Rich, Phys. Rev. **D48**, 4318 (1993).

[100] C. Giunti, C. W. Kim and U. W. Lee, Phys. Rev. **D44**, 3635 (1991).

[101] C. Giunti, C. W. Kim and U. W. Lee, Phys. Lett. **B274**, 87 (1992).

[102] C. Giunti and C. W. Kim, Phys. Rev. **D58**, 017301 (1998).

[103] K. Kiers, S. Nussinov and N. Weiss, Phys. Rev. **D53**, 537 (1996).

[104] C. Giunti, C. W. Kim, J. A. Lee and U. W. Lee, Phys. Rev. **D48**, 4310 (1993).

[105] C. Giunti, JHEP 11, 017 (2002).

[106] W. Grimus, P. Stockinger and S. Mohanty, Phys. Rev. **D59**, 013011 (1998).

[107] C. Y. Cardall, Phys. Rev. **D61**, 073006 (2000).

[108] M. Beuthe, Phys. Rept. 375, 105 (2003).

[109] A. D. Dolgov, O. V. Lychkovskiy, A. A. Mamonov, L. B. Okun, M. V. Rotaev and M.G. Schepkin, Nucl.Phys.**B729**,79 (2005); A. D. Dolgov, O. V. Lychkovskiy, A. A. Mamonov, L. B. Okun, and M.G. Schepkin, Eur.Phys.J.**C44**,431 (2005).

[110] C. Lunardini and A. Yu. Smirnov, Phys. Rev. **D64**, 073006 (2001).

[111] A. D. Dolgov, S. H. Hansen, S. Pastor, S. T. Petcov, G. G. Raffelt and D. V. Semikoz, Nucl. Phys. **B632**, 363 (2002).

[112] K. Abazajian, J. F. Beacom and N. F. Bell, Phys. Rev. **D66**, 013008 (2002).

[113] C. M. Ho, D. Boyanovsky and H. J. de Vega, Phys. Rev. **D72**, 085016 (2005).

[114] A. E. Bernardini, Europhys. Lett. **73**, 157 (2006); A. E. Bernardini and S. De Leo, Phys. Rev. **D71**, 076008 (2005); Eur. Phys. J. C. **37**, 471 (2004).

[115] E. W. Kolb and M. S. Turner, *The Early Universe*, (Westview Press, 1990)

[116] B. W. Lee and R. Shrock, Phys. Rev. **D16**, 1444, 1977.

[117] S. T. Petcov, Yad. Fiz. **25**, 641 [Sov. J. Nucl. Phys. **25**, 340] (1977).

[118] S. M. Bilenky and S. T. Petcov, Rev. of Mod. Phys. **59**, 671 (1987).

[119] J. P. Kneller, R. J. Scherrer, G. Steigman and T. P. Walker, Phys. Rev. **D64**, 123506 (2001).

[120] C. Giunti, hep-ph/0409230; A.D.Dolgov, A.Yu.Morozov, L.B.Okun, M.G.Schepkin, Nucl.Phys. **B502**3 (1997); Y. Srivastava, A. Widom and E. Sassaroli, Eur. Phys. J. **C2**, 769 (1998); Y. N. Srivastava and A. Widom, hep-ph/9707268.

[121] C. P. Slichter, *Principles of Magnetic Resonance*, (Springer-Verlag, Berlin, Heidelberg, 1978).

[122] L. Stodolsky, Phys. Rev. **D36**, 2273 (1987); R. A. Harris, L. Stodolsky, Phys. Lett. **B116**, 464 (1982); R. A. Harris and L. Stodolsky, Phys. Lett. **B78**, 313 (1978).

[123] A. Manohar, Phys. Lett. **B186**, 370 (1987).

[124] A. Dolgov, Yad. Fiz. **33**, 1309 (1981)[Sov. J. Nucl. Phys.**33**, 700 (1981)].

[125] G. Raffelt, G. Sigl and L. Stodolsky, Phys. Rev. Lett. **70**, 2363 (1993); Phys. Rev. **D45**, 1782 (1992).

[126] G. Sigl and G. Raffelt, Nucl. Phys. **B406**, 423 (1993).

[127] J. H. Field, hep-ph/0303241; hep-ph/0503034.

[128] Y. F. Li and Q. Y. Liu, hep-ph/0604069.

[129] D. Boyanovsky, C. M. Ho, Phys.Rev. **D69**,125012 (2004).

[130] K. Abazajian, G.M. Fuller, M. Patel, Phys.Rev. **D64** (2001) 023501.

[131] R. Foot and R. R. Volkas, Phys. Rev. **D55**, 5147 (1997).

[132] E. Braaten and R. Pisarski, Nucl. Phys. **B337**,569 (1990); **B339**,310 (1990); R. Pisarski, Phys. Rev. Lett. **63**, 1129 (1989); Nucl. Phys. **A525**, 175 (1991).

[133] M. Le Bellac, *Thermal Field Theory*, (Cambridge University Press, Cambridge, England, 1996).

[134] J.-P. Blaizot and E. Iancu, Phys. Rev. Lett. **76**, 3080 (1996); Phys. Rev. **D55**, 973 (1997); **56**, 7877 (1997).

[135] S.-Y. Wang, D. Boyanovsky, H. J. de Vega and D.-S. Lee, Phys. Rev. **D62**, 105026 (2000); D. Boyanovsky, H. J. de Vega, S.-Y. Wang, Phys.Rev. **D67**, 065022 (2003); D. Boyanovsky, H. J. de Vega, Annals Phys. **307**, 335 (2003).

[136] B. Misra, E. C. C. Sudarshan, J. Math. Phys. **18**, 756 (1977).

[137] R. R. Volkas, Y. Y. Y. Wong, Phys. Rev. **D62**, 093024 (2000); K. S. M. Lee, R. R. Volkas, Y. Y. Y. Wong, *ibid* 093025 (2000).

[138] T. Asaka, M. Laine and M. Shaposhnikov, JHEP 0606 (2006) 053; JHEP 0701 (2007) 091.

[139] See the recent review by R. Fleischer, hep-ph/0608010.

[140] For a thorough pedagogical description see: A. Seiden, *Particle Physics: A comprehensive Introduction*, Addison Wesley, (San Francisco, 2004).

[141] J. Schwinger, J. Math. Phys. **2**, 407 (1961).

[142] K. T. Mahanthappa, Phys. Rev. **126**, 329 (1962); P. M. Bakshi and K. T. Mahanthappa, J. Math. Phys. **41**, 12 (1963).

[143] L. V. Keldysh, JETP **20**, 1018 (1965).

[144] See also the following reviews: K. Chou, Z. su, B. Hao and L. Yu, Phys. Rept. **118**, 1 (1985); A. Niemi and G. Semenoff, Ann. Phys. (NY), **152**, 105 (1984); N. P. Landsmann and C. G. van Weert, Phys. Rept. **145**, 141 (1985); J. Rammer and H. Smith, Rev. of Mod. Phys. **58**, 323 (1986).

[145] C. M. Ho, D. Boyanovsky, H. J. de Vega, Phys.Rev. **D72** , 085016 (2005); C. M. Ho, D. Boyanovsky, Phys.Rev. **D73**, 125014 (2006).

[146] D. Boyanovsky and C. M. Ho, arXiv: hep-ph/0610036.

[147] A. Fetter and D. Walecka, *Quantum Theory of Many Particle Systems*, (McGraw-Hill, San Francisco 1971); G. D. Mahan, *Many Particle Physics*, (Plenum Press, New York, 1990).

[148] J. I. Kapusta, *Finite Temperature Field Theory*, (Cambridge Monographs on Mathematical Physics, Cambridge University Press 1989); M. Le Bellac, *Thermal Field Theory* (Cambridge Monographs on Mathematical Physics, Cambridge University Press 1996).

[149] H. A. Weldon, Phys. Rev. **D26**, 2789 (1982); Phys. Rev. **D28**, 2007 (1983); Phys. Rev. **D40**, 2410 (1989).

[150] D. Boyanovsky, C. M. Ho, Astropart.Phys. 27 (2007) 99.

[151] D. Boyanovky, C. M. Ho, in preparation.

[152] E. W. Kolb and M. S. Turner, *The Early Universe*, (Addison-Wesley, Redwood City, 1990).

[153] J. Bernstein *Kinetic theory in the expanding Universe* (Cambridge Monographs on Mathematical Physics, Cambridge University Press, Cambridge, 1988).

[154] W. Buchmuller, in the proceedings of *Particles, Strings and Cosmology (PASCOS'01)* (Eds. Paul Frampton and Jack Ng. ; Rinton Press, Princeton, N.J., 2001); W. Buchmuller and M. Plumacher, Phys.Lett. **B511**,74 (2001); W, Buchmuller and S. Fredenhagen, Phys.Lett. **B483**, 217 (2000), and references therein.

[155] Sh. Matsumoto and M. Yoshimura, Phys.Rev. **D61** 123508 (2000); Phys.Rev. **D61** 123509 (2000); Phys. Rev. **D59**, 123511 (1999). I. Joichi, Sh. Matsumoto and M. Yoshimura, Phys. Rev. **D 58** 043507 (1998); Prog. Theor. Phys. **98** 9 (1997).

[156] M. Srednicki, Phys. Rev. **D62**, 023505 (2000); A. Singh and M. Srednicki, Phys. Rev. **61**, 023509 (1999); M. Srednicki, hep-ph-0005174 (2000).

[157] E. Braaten and Y. Jia, Phys. Rev. **63**, 096009 (2001).

[158] P. Bucci and M. Pietroni, Phys. Rev. **D63**, 045026 (2001); hep-ph/0111375 (2001).

[159] L. P. Kadanoff and G. Baym *Quantum Statistical Mechanics*, (W. A. Benjamin, New York, 1962).

[160] W. Botermans and R. Malfliet, Phys. Rept. **198** 115, (1990); P. Danielewicz, Ann. Phys. (N.Y.) **152**, 239 (1984); S. Ochs and U. W. Heinz, Annals of Phys (N.Y.) **266**, 351 (1998), H.-T. Elze and U. W. Heinz, Phys.Rept.**183**, 81 (1989).

[161] E. Calzetta and B. L. Hu, Phys. Rev. **D37**, 2878 (1988).

[162] D. Boyanovsky, I.D. Lawrie and D.S. Lee, Phys.Rev. **D54** 4013 (1996).

[163] D. Boyanovsky, H.J. de Vega and S.-Y. Wang, Phys.Rev. **D61** 065006 (2000); Phys.Rev. **D67** 065022 (2003); S.-Y. Wang, D. Boyanovsky, H. J. de Vega and D.-S. Lee, Phys.Rev. **D62** 105026 (2000); D. Boyanovsky and H. J. de Vega Ann. of Phys. **307**, 335 (2003).

[164] R.P Feynman and F. L. Vernon, Ann. Phys. (N.Y.) **24**, 118 (1963).

[165] A. O. Caldeira and A. J. Leggett, Physica **A 121**, 587 (1983).

[166] H. Grabert, P. Schramm and G.-L. Ingold, Phys. Rept. **168**, 115 (1988); A. Schmid, J. Low Temp. Phys. **49**, 609 (1982).

[167] D. Boyanovsky and H. J. de Vega, arXiv:hep-ph/0311156 (to appear in Nucl. Phys. A).

[168] S. M. Alamoudi, D. Boyanovsky, H. J. de Vega and R. Holman,Phys.Rev. **D59** 025003 (1998); S. M. Alamoudi, D. Boyanovsky and H. J. de Vega, Phys. Rev. **E60**, 94, (1999).

[169] J. Yokoyama, hep-ph/0406072 (2004).

[170] P.C. Martin, E.D. Siggia and H. A. Rose, Phys. Rev.**A8**, 423 (1973).

[171] J. I. Kapusta, *Finite temperature field theory*, (Cambridge Monographs on Mathematical Physics, Cambridge University Press, Cambridge, 1989).

[172] M. Le Bellac, *Thermal Field Theory*, (Cambridge University Press, Cambridge, England, 1996).

[173] E. Braaten and R.D. Pisarski, Nucl. Phys. **B337**, 569 (1990); **B339**, 310 (1990); R.D. Pisarski, Physica A **158**, 146 (1989); Phys. Rev. Lett. **63**, 1129 (1989); Nucl. Phys. **A525**, 175 (1991).

[174] D. Boyanovsky, M. D'attanasio, H.J. de Vega, R. Holman and D.-S.Lee, Phys.Rev. **D52** 6805 (1995).

[175] D. Boyanovsky and H. J. de Vega, Phys.Rev. **D65**, 085038 (2002).

[176] G. Raffelt, G. Sigl and L. Stodolsky, Phys. Rev. Lett. **70**, 2363 (1993); Phys. Rev. **D45**, 1782 (1992).

[177] B. H. J. McKellar, M. J. Thompson, Phys. Rev. **D49**, 2710 (1994).

[178] K. Enqvist, K. Kainulainen, J. Maalampi, Nucl. Phys. **B349**, 754 (1991).

[179] C. Giunti, C. W. Kim, J. A. Lee, U. W. Lee, Phys. Rev. **D48**, 4310 (1993); J. Rich, Phys. Rev. **D 48**, 4318 (1993).

[180] C. Giunti, Eur.Phys.J. **C39** 377 (2005); C. Giunti, hep-ph/0301231, hep-ph/0608070.

[181] C. Y. Cardall, hep-ph/0107004.

[182] D. Boyanovsky and C. M. Ho, Astropart.Phys. 27 (2007) 99.

[183] G. Steigman, hep-ph/0309347; J. P. Kneller, G. Steigman, New J.Phys. **6** 117 (2004) 117; G. Steigman, Phys.Scr. **T121**, 142 (2005); Int.J.Mod.Phys. **E15** 1 (2006); astro-ph/0307244; K. A. Olive, G. Steigman, T. P. Walker, Phys.Rept. **333** 389 (2000); K. A. Olive, G. Steigman, Phys.Lett. **B354**, 357 (1995).

[184] A.D. Dolgov, O.V. Lychkovskiy, A.A. Mamonov, L.B. Okun, M.V. Rotaev, M.G. Schepkin, Nucl.Phys. **B729** 79 (2005).

[185] M. Binger and C.-R. Ji, Phys.Rev. **D60**, 056005 (1999); C-R. Ji and Y. Mishchenko, Phys. Rev. **D64** , 076004(2001).

[186] D. Boyanovsky, K. Davey and C. M. Ho, Phys. Rev.**D71**, 023523 (2005); D. Boyanovsky and H. J. de Vega, Nucl.Phys.**A747**,564 , (2005).

[187] S. Pastor, G. G. Raffelt., D. V. Semikoz, Phys.Rev.**D65**, 053011, (2002).

[188] L. Maiani, M. Testa, Annals Phys. **263**, 353 (1998).

[189] C. M. Ho, D. Boyanovsky, H. J. de Vega, Phys.Rev. **D72**, 085016 (2005); C. M. Ho, D. Boyanovsky, Phys.Rev. **D73**, 125014 (2006).

[190] G. Raffelt and G. Sigl, Astroparticle Physics **1**, 165, (1993).

[191] V. Weisskopf and E. Wigner, Z. Phys. **63**, 54 (1930); Z. Phys. **65**, 18 (1930);

[192] G. V. Dass and W. Grimus, Phys.Lett.**B521**, 267 (2001); hep-ph/0203043; R.A. Bertlmann, W. Grimus, Phys.Rev.**D64**,056004 (2001).

[193] M. Beuthe, G. Lopez Castro, J. Pestieau, Int.J.Mod.Phys. **A13**, 3587 (1998); M. Beuthe, Phys.Rept. **375**, 105 (2003).

[194] K. N. Abazajian, G. M. Fuller, Phys.Rev. **D66** 023526 (2002) .

[195] R. Fleischer, arXiv:hep-ph/0608010

[196] M. Beuthe, Phys.Rept. **375** 105 (2003); M. Beuthe, G. Lopez Castro, J. Pestieau, Int.J.Mod.Phys. **A13**, 3587 (1998).

[197] D. Boyanovsky, C. M. Ho, Phys. Rev. **D75**, 085004 (2007).

[198] D. Boyanovsky, C. M. Ho, arXiv: hep-ph/0612092.

[199] D. Boyanovsky, C. M. Ho, Astropart.Phys. **27**, 99 (2007).

[200] M. O. Scully and M. S. Zubairy, *Quantum Optics* (Cambridge University Press, Cambridge, 1997); P. Meystre and M. Sargent III, *Elements of Quantum Optics* (3rd Edition), (Springer Verlag, Berlin, 1998); C. W. Gardiner and P. Zoller, *Quantum Noise* (3rd Ed. Springer, Berlin, Heidelberg, 2004).

[201] D. Boyanovsky and C. M. Ho, Phys. Rev. **D69**, 125012 (2004). The components of the polarization vector P_x, P_y, P_z are the expectation values of S_y, S_x, S_z of this reference respectively in the quantum master equation.

[202] D. Kazanas, Astrophys. J **241**, L59 (1980). A. Guth, Phys. Rev. **D23**, 347 (1981); astro-ph/0404546 (2004). K. Sato, Mon. Not. R. Astron. Soc. **195**, 467 (1981).

[203] E. W. Kolb and M. S. Turner, *The Early Universe* Addison Wesley, Redwood City, C.A. 1990. P. Coles and F. Lucchin, *Cosmology*, John Wiley, Chichester, 1995. A. R. Liddle and D. H. Lyth, *Cosmological Inflation and Large Scale Structure*, Cambridge University Press, 2000. S. Dodelson, *Modern Cosmology*, Academic Press, 2003. D. H. Lyth , A. Riotto, Phys. Rept. **314**, 1 (1999).

[204] V. F. Mukhanov , G. V. Chibisov, Soviet Phys. JETP Lett. **33**, 532 (1981); V. F. Mukhanov, H. A. Feldman , R. H. Brandenberger, Phys. Rept. **215**, 203 (1992). S. W. Hawking, Phys. Lett. **B115**, 295 (1982). A. H. Guth , S. Y. Pi, Phys. Rev. Lett. **49**, 1110 (1982). A. A. Starobinsky, Phys. Lett. **B117**, 175 (1982). J. M. Bardeen, P. J. Steinhardt , M. S. Turner, Phys. Rev. **D28**, 679 (1983).

[205] C. L. Bennett *et.al.* (WMAP collaboration), Ap. J. Suppl. **148**, 1 (2003). A. Kogut *et.al.* (WMAP collaboration), Ap. J. Suppl. **148**, 161 (2003). D. N. Spergel *et. al.* (WMAP collaboration), Ap. J. Suppl. **148**, 175 (2003).

[206] H. V. Peiris *et.al.* (WMAP collaboration), Ap. J. Suppl.**148**, 213 (2003).

[207] D. N. Spergel *et. al.* (WMAP collaboration), astro-ph/0603449.

[208] L. Page, *et. al.* (WMAP collaboration), astro-ph/0603450. G. Hinshaw,*et. al.* (WMAP collaboration), astro-ph/0603451. N. Jarosik, *et. al.* (WMAP collaboration), astro-ph/0603452.

[209] M. Tegmark *et.al.* Phys. Rev **D69**,103501, (2004) D. J. Eisenstein *et.al.* ApJ. **633**, 560 (2005) U. Seljak et al., Phys. Rev. D71, 103515 (2005).

[210] A. G. Sánchez *et. al.*, Mon. Not. Roy. Astron. Soc. **366**, 189 (2006). S. Cole *et.al.* Mon. Not. Roy. Astron. Soc. **362**, 505 (2005).

[211] A. G. Sanchez and C. M. Baugh, astro-ph/0612743.

[212] M. B. Hoffman and M. S. Turner, Phys. Rev. **64**, 023506 (2001). W. H. Kinney, Phys. Rev. **D66**,083508 (2002).

[213] C. Savage, K. Freese and W. H. Kinney, Phys. Rev. **D 74**, 123511 (2006); L. Alabidi and D. H. Lyth, astro-ph/0510441, astro-ph/0603539; J. Martin and C. Ringeval, JCAP **0608** (2006) 009.

[214] W. H. Kinney, E. W. Kolb, A. Melchiorri and A. Riotto, Phys.Rev. D74 (2006) 023502.

[215] F. Finelli, M. Rianna, N. Mandolesi, JCAP **0612**, 006 (2006). H. Peiris, R. Easther, JCAP **0610**, 017 (2006); JCAP **0607**, 002 (2006); R. Easther, H. Peiris, JCAP **0609**, 010 (2006). S. M. Leach, A. R Liddle, Phys.Rev. **D68**, 123508 (2003); Mon.Not.Roy.Astron.Soc. **341**, 1151 (2003).

[216] D. Boyanovsky, H. J. de Vega and N. G. Sanchez, Phys. Rev. **D73**, 023008 (2006). See also ref. [223].

[217] J. Lidsey, A. Liddle, E. Kolb, E. Copeland, T. Barreiro and M. Abney, Rev. of Mod. Phys. **69**, 373, (1997).

[218] W. H. Kinney, A. Riotto, JCAP **0603**, 0.11 (2006); M. Giovannini, arXiv:astro-ph/0703730.

[219] D. Cirigliano, H. J. de Vega and N. G. Sanchez, Phys. Rev. **D71**, 103518 (2005);

[220] H. J. de Vega and N. G. Sanchez, Phys. Rev. **D74**, 063519 (2006).

[221] C. Destri, H. J. de Vega, N. G. Sanchez, arXiv:astro-ph/0703417

[222] A. R. Liddle, P. Parsons , J. D. Barrow, Phys. Rev. **D50**, 7222 (1994).

[223] G. Mangano, G. Miele, C. Stornaiolo, Mod.Phys.Lett.A10, 1977 (1995).

[224] I. S. Gradshteyn and I. M. Ryshik, Table of Integrals, Series and Products, Academic Press, 1980.

[225] A. P. Prudnikov, Yu. A. Brichkov, O, I. Marichev, Integrals and Series, vol. 3, Nauka, Moscow, 1986.